Chemical Transformations of Phosphine and Phosphido Ruthenium Complexes

Yong-Shen Han

June 2020

A thesis submitted for the degree of Doctor of Philosophy of

The Australian National University

Australian National University

Author's Declaration

This thesis is an account of work conducted at the Research School of Chemistry, Australian National University between June 2014 and June 2020. Except where due reference has been made all work in this thesis is my own.

Yong-Shen Han

June 2020

Acknowledgements

Completing this thesis and the work it contains has been one of the most difficult things I have done in my life, and it has been a long, draining process. So very many people have helped me along the way and I would like to thank them here.

First, I would like to thank my supervisor, Tony Hill, for his patience, wisdom and compassion. He is fundamentally a good person, and my faith in him and his guidance carried me through to completion.

I would also like to extend a thank you to Tony and his partner, Mark, for all of their kindness and hospitality. It was lovely to feel like part of the family.

Next, I would like to thank all the members of the Hill group during my time as a PhD student. Annie and Caitlin have been fantastic friends and role models. I couldn't have asked for better people to share the journey and fun times with than Kathy and Richie; thanks to Kathy for all the long discussions and reflections and to Richie for always keeping things fun. Manab and Stephen were incredibly supportive at the beginning, and the immaculate lab was certainly missed once Stephen retired. Ben made such a positive impact on arrival and his advice on all things at the end has been greatly appreciated. Thanks to Harry, Steve, Chee Sheng, Ryan, Liam and Lachlan for creating such an excellent group atmosphere at the end of my PhD – I hope I was able to help you as much as you all helped me. Thank you to Tim, Jane, Takao, Richard, Kedar and Anders for their contributions to the group and for being part of the journey.

There have been a bunch of supportive people in the RSC community. Thank you to Mark and Geoff for having faith in my teaching ability and giving me some of the most enjoyable and rewarding experiences of my PhD. Thanks to Chris in NMR and Anitha and Joe from mass spectroscopy for the always-reliable support. I am grateful to Anthony Willis and Jas Ward for their patience in teaching me crystallography and to Manab, Nick White, Ben and Michael Gardiner for their additional guidance. I really appreciated the support and kindness from Gottfried at the end. I would like to thank Russ and Nick for providing excellent advice and for

being great friends. Eleanor, thank you for working together for some of my proudest acheivements during my PhD and for being a friend when I felt like I had no one else to turn to.

Thank you to Josef, Andrew and Libby at the ANU Counselling service for making me a stronger person. I would like to take a moment to encourage anyone reading this not to be afraid to seek support – these three people have been crucial to the completion of my PhD.

Natalie, words cannot express how lucky I am to have your love and support.

Finally, I would like to thank my family – my mother, father and sister. Throughout my life you have all given so much to make sure I have had every opportunity available to me. I am eternally grateful, and everything I have and will accomplish is thanks to you.

Abstract

Primary phosphine chemistry is far less developed than that of higher-substituted phosphines. One of the main reasons for this disparity is that primary phosphines are reputedly difficult to work with, being notoriously toxic, malodorous and air-sensitive. Additionally, the phosphorus lone pair on primary phosphines is less basic and nucleophilic than in the corresponding secondary or tertiary phosphines. Despite these limitations, primary phosphines are a desirable class of molecule for study on account of the two P–H bonds which provide ample opportunity for further functionalisation.

Phosphido (PR_2) groups provide an interesting avenue into phosphorus-based chemistry. As a ligand the phosphorus atom may generally either be pyramidal and nucleophilic, or planar and electrophilic. In the case of a PR_2 ligand with a pyramidal phosphorus atom the phosphorus lone pair can experience enhanced nucleophilicity and basicity due to a π interaction with a filled metal d orbital. The work described in this thesis involves endeavours to exploit the increased phosphorus-based reactivity of phosphido complexes for the potential derivatisation of primary phosphines.

Initial efforts focused on the conveniently-available starting material $[RuCl(PPh_3)_2(Tp)]$ and its substitution reactions with cyclohexylphosphine (PH_2Cy). The substitution of one neutral triphenylphosphine ligand was achieved but full conversion to the bis(cyclohexylphosphine) complex $[RuCl(PH_2Cy)_2(Tp)]$ was not observed, even under forcing conditions. Attempted substitution of the chloride with one equivalent of cyclohexylphosphine resulted in mixtures of $[RuCl(PPh_3)(PH_2Cy)(Tp)]$, $[Ru(PPh_3)(PH_2Cy)_2(Tp)]^+$ and the starting material $[RuCl(PPh_3)_2(Tp)]$. Direct formation of the cation $[Ru(PPh_3)(PH_2Cy)_2(Tp)]^+$ was achieved when an excess of cyclohexylphosphine was used. Substitution chemistry was also conducted on the complex bearing the bidentate ligand 1,1'-bis(diphenylphosphino)ferrocene (dppf), $[RuCl(dppf)(Tp)]$, to form $[Ru(PH_2Cy)(dppf)(Tp)]^+$. The deprotonation of $[RuCl(PPh_3)(PH_2Cy)(Tp)]$ resulted in the cyclometallation of the triphenylphosphine ligand, and experiments were conducted to gain insight into this process. Deprotonating the cations $[Ru(PPh_3)(PH_2Cy)_2(Tp)]^+$ and $[Ru(PH_2Cy)(dppf)(Tp)]^+$ appeared to form the respective

phosphido complexes, but the products were extremely basic and were not isolated. The *in situ* reactivity of the putative [Ru(PHCy)(dppf)(Tp)] with $AuCl(SMe_2)$ was also investigated.

It was predicted that the introduction of the π-acidic co-ligand CO would mitigate the high basicity of the phosphorus lone pair, yielding a more conveniently-handled phosphido complex. Beginning from the acetonitrile-substituted octahedral cation $[RuCl(NCMe)(CO)(PPh_3)_2(PH_2Cy)]^+$ the new cationic complexes $[RuCl(CO)_2(PPh_3)_2(PH_2Cy)]^+$, $[RuCl(CO)(CNMes)(PPh_3)_2(PH_2Cy)]^+$, $[Ru(CO)(PPh_3)_2(PH_2Cy)(S_2CNEt_2)]^+$ and $[Ru(CO)(PPh_3)(PH_2Cy)(Tp)]^+$ (Tp = hydrotris(pyrazolyl)borate) were obtained. The cation $[Ru(CO)(PPh_3)(PH_2Cy)(Tp)]^+$ could also be synthesised using $[RuH(CO)(PPh_3)(Tp)]$ as the precursor. The attempted deprotonation of $[RuCl(CO)_2(PPh_3)_2(PH_2Cy)]^+$ and $[Ru(CO)(PPh_3)_2(PH_2Cy)(S_2CNEt_2)]^+$ resulted in an intractable mixture of products while the deprotonation of $[Ru(CO)(PPh_3)(PH_2Cy)(Tp)]^+$ successfully yielded a phosphido complex amenable to study. The ambiphilic nature of phosphido complexes was also demonstrated through the synthesis of the complexes $[Ru(L)(CO)(PPh_3)_2\{PH(OMe)Cy\}]$ (L = CO, CNMes). The reactivity of these complexes bearing the unusual PH(OMe)Cy ligand was also investigated, primarily focused on ligand substitution and the behaviour of the Ru(0) centre.

Work was undertaken to gain further understanding of the properties of the phosphido complex [Ru(CO)(PPh$_3$)(PHCy)(Tp)]. The complex was obtained as a mixture of two diastereomers and the kinetics of the exchange process were investigated by NMR spectroscopy. Treating [Ru(CO)(PPh$_3$)(PHCy)(Tp)] with MeI resulted in a mixture of the cations $[Ru(CO)(PPh_3)(PH_2Cy)(Tp)]^+$, $[Ru(CO)(PPh_3)(PHMeCy)(Tp)]^+$ and $[Ru(CO)(PPh_3)(PMe_2Cy)(Tp)]^+$. The di(methyl)phosphine complex could be obtained directly from the reaction of $[Ru(CO)(PPh_3)(PH_2Cy)(Tp)]^+$ with excess base and MeI. The addition of borane dimethylsulfide complex to [Ru(CO)(PPh$_3$)(PHCy)(Tp)] resulted in the formation of $[Ru(CO)(PPh_3)\{PH(BH_3)Cy\}(Tp)]$. This product could also be obtained from the reaction of $[Ru(CO)(PPh_3)(PH_2Cy)(Tp)]^+$ with $NaBH_4$. The carbon disulfide adduct $[Ru(CO)(PPh_3)\{PH(CS_2)Cy\}(Tp)]$ formed upon the addition of carbon disulfide to [Ru(CO)(PPh$_3$)(PHCy)(Tp)]. This adduct formation is reversible, and the product could only be isolated as $[Ru(CO)(PPh_3)\{PH(CS_2Me)Cy\}(Tp)]^+$ following methylation.

The reaction between [Ru(CO)(PPh_3)(PHCy)(Tp)] and an appropriate chalcogen source resulted in the formation of the complexes [Ru(CO)(PPh_3){PH(E)Cy}(Tp)] (E = O, S, Se, Te). Only the sulfide and selenide products were isolated and fully characterised, while evidence for the formation of the oxide and telluride complexes was obtained. The sulfide and selenide products are nucleophilic at the chalcogen atom, reacting with MeOTf to give the cations $[Ru(CO)(PPh_3)\{PH(EMe)Cy\}(Tp)]^+$ (E = S, Se). Additionally, the sulfide complex may be reversibly protonated to give $[Ru(CO)(PPh_3)\{PH(EH)Cy\}(Tp)]^+$. The cationic complex $[Ru(CO)(PPh_3)\{PH(SMe)Cy\}(Tp)]^+$ reacts with base to give the transient phosphido complex [Ru(CO)(PPh_3){P(SMe)Cy}(Tp)]. The *in situ* reactivity of this phosphido complex was explored with the electrophiles MeI, $BH_3.SMe_2$ and elemental sulfur.

Table of Contents

List of Abbreviations

Ac	acetyl; $C(O)CH_3$
acac	acetylacetonate; $\{MeC(O)CHC(O)Me\}^-$
ADEQUATE	Adequate DoublE QUAntum Transfer Experiment
ATR	Attenuated Total Reflectance
ca.	*circa*; approximately
cf.	*confer*; compare(d) with
Cp	cyclopentadienyl; $C_5H_5^-$
Cp*	pentamethylcyclopentadienyl; $C_5Me_5^-$
δ_A	chemical shift of nucleus A in parts per million
DBU	1,8-diazabicyclo[5.4.0]undec-7-ene
depe	1,2-bis(diethylphosphino)ethane
DMF	*N,N*-dimethylformamide
dmpe	1,2-bis(dimethylphosphino)ethane
DMSO	dimethyl sulfoxide
dppm	bis(diphenylphosphino)methane
dppe	1,2-bis(diphenylphosphino)ethane
dppf	1,1'-bis(diphenylphosphino)ferrocene
η^n	n-*hapto* coordination
e.g.	*exempli gratia*; for example
e.s.d.	estimated standard deviation
Et	ethyl; CH_2CH_3
Et_2O	diethyl ether
ESI	Electrospray Ionisation
EtOH	ethanol
EXSY	EXchange SpectroscopY
HMBC	Heteronuclear Multiple Bond Correlation (spectroscopy)
HOMO	Highest Occupied Molecular Orbital
HSQC	Heteronuclear Single Quantum Coherence (spectroscopy)
i.e.	*id est*; that is

IMes	1,3-dimesitylimidazol-2-ylidene
^{i}Pr	isopropyl; $CH(CH_3)_2$
IR	infrared (spectroscopy)
Is	isityl; 2,4,6-tris(isopropyl)phenyl
κ^n	n-dentate coordination
LUMO	Lowest Unoccupied Molecular Orbital
$^{n}J_{AB}$	n-bond coupling constant between nuclei A and B
μ_n	bridging n centres
Me	methyl; CH_3
m/z	mass-to-charge ratio
Mes	mesityl; 2,4,6-trimethylphenyl
Mes*	super mesityl; 2,4,6-tris(*tert*-butyl)phenyl
MS	mass spectrometry/spectrum
n.b.	*nota bene*; note well
NMR	Nuclear Magnetic Resonance (spectroscopy)
^{n}Bu	*n*-butyl; $CH_2CH_2CH_2CH_3$
ppm	parts per million
pz	pyrazolyl; $C_3H_3N_2$
r.t.	room temperature
SOMO	Singularly-Occupied Molecular Orbital
^{t}Bu	*tert*-butyl; $C(CH_3)_3$
Tf	triflyl, trifluoromethylsulfonyl; SO_2CF_3
THF	tetrahydrofuran
tol	tolyl, methylphenyl; $C_6H_4CH_3$
Tp	hydrotris(pyrazolyl)borate
Ts	tosyl, *para*-toluenesulfonyl
Xy	2,6-xylyl; 2,6-dimethylphenyl

CHAPTER 1
Introduction

Chapter 1: Introduction

The chemistry of phosphorus is extensive and varied, and it has found diverse interest in the traditionally-defined disciplines of inorganic, organic and biological chemistry.[1] The goals of this thesis are to further expand the broad field of phosphorus chemistry with a particular focus on primary phosphine transition metal complexes and their phosphido[†] derivatives. As such, the first objective of this chapter is to provide an overview of primary phosphines and the chemistry that arises from their interaction with metal complexes. Secondly, the properties of phosphido ligands are discussed, highlighting the distinctive properties which make them desirable for study. This will include background on their syntheses and an overview of the reactivity of phosphido complexes with one or more P–H bonds.

1.1 Primary Phosphines

1.1.1 Properties of Primary Phosphines

Phosphines (PR_3) are ubiquitous as ligands in organometallic chemistry. Coordination occurs through the phosphorus lone pair, while modifying the substituents at phosphorus allows for the variation of steric and electronic properties. As a result, phosphines have been extensively studied as support ligands for all manner of transition metal-mediated processes, the most celebrated being palladium-catalysed cross-coupling and rhodium-catalysed hydroformylation reactions.[2-3] Phosphines have also played a key role in the Nobel Prize-winning work of Grubbs on olefin metathesis,[4] and of Noyori[5] and Knowles[6] in asymmetric hydrogenation. The latter works are notable in that they utilise the chirality of phosphine ligands to impose enantioselectivity on the product distribution of catalytic reactions.

[†] An important note should be made about the at times confusing nomenclature of phosphorus-containing molecules. Traditionally, 'phosphide' may refer to either P^{3-} or PR_2^-. Correspondingly, 'phosphido' may refer to either of these species acting as a ligand. To clear up confusion IUPAC recommends the terms 'phosphanide' and 'phosphanido' as terms for PR_2^-, which are directly derived from the preferred term 'phosphane' for PR_3 (traditionally, 'phosphine') molecules. However, despite these recommendations the traditional terms 'phosphine', 'phosphide' and 'phosphido' continue to see popular (indeed, overwhelming majority) usage in reference to the organophosphorus compounds. As such, this thesis maintains alignment with the most prominent use of the terms, and 'phosphido' will generally refer to the ligand 'PR_2^-'. Any deviations from this nomenclature will be clearly indicated with accompanying line formulae and schemes.

An overwhelming majority of studies focus on tertiary phosphines (with three non-hydrogen substituents on phosphorus), while there are far fewer investigations into the lower-substituted primary phosphines (PH_2R, Figure 1.1). The reduced attention on primary phosphines arises from their notoriety for being air sensitive, potentially pyrophoric, highly toxic, volatile and malodorous.[7-8] The decomposition of primary phosphines in air occurs exothermically *via* a three-step oxidation to the corresponding phosphonate (Scheme 1.1). Generally, the increased sensitivity of primary phosphines compared to their tertiary counterparts is attributed to presence of exposed, polar P–H, rather than P–C, bonds. An additional factor contributing to the lower stability of primary *versus* tertiary phosphines is the reduced steric protection around the phosphorus centre.[7]

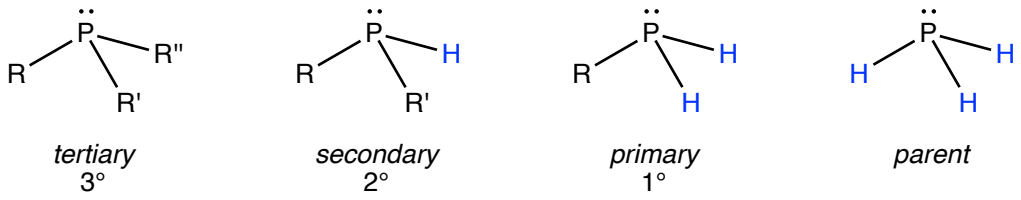

Figure 1.1. Various substitutions of phosphine

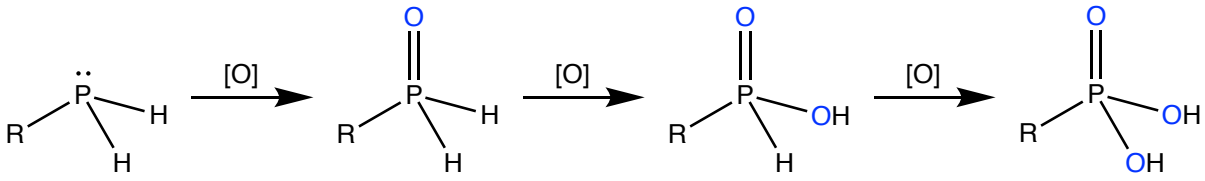

Scheme 1.1. Oxidation of primary phosphines

Another factor that reduces the desirability of research into primary phosphines is that the phosphorus lone pair is less basic and nucleophilic than in the higher-substituted equivalents. As a result, they are both less reactive and form metal complexes with weaker M–P bonds.[9] The reduced reactivity of the lone pair has been attributed to the smaller substituent cone angle of primary (*ca*. 90°) *versus* tertiary (*ca*. 108°) phosphines, with the different geometry resultubg in poorer orbital overlap in the phosphorus-substituent bond. The excess electron density from the poorer overlap is redistributed to the phosphorus lone pair, resulting in an overall increase in s character for this orbital. The geometric difference was highlighted as an important aspect; inductive effects alone did not account for the difference in the lone pair energy between primary and tertiary phosphines.[10] Comparably, the larger inter-substituent angles have been suggested to enhance the phosphine basicity for sterically cumbersome phosphines.[11]

Research has been conducted into producing primary phosphines which are air stable so that experiments with them are more convenient to conduct.[7-8] The majority of examples employ a large amount of steric bulk to impart stability onto the phosphorus centre. For example, mesitylphosphine (mesityl = Mes = 2,4,6-trimethylphenyl) is recognised as being moderately stable. Increasing the bulk by varying the substituents on the aryl ring (*e.g.* PH_2Mes^*; Mes* = 'super mesityl' = 2,4,6-tris(*tert*-butyl)phenyl) results in a marked improvement in stability. Bulky substituents such as tryptycenyl and triphenylmethyl ('trityl') groups have also been used to generate air- and moisture-stable primary phosphines.

Stabilisation of primary phosphines has also been achieved by reducing the activity of the lone pair. This has been demonstrated in systems featuring extended π-conjugation in the carbon backbone of the primary phosphine. Increasing the degree of conjugation increases the air stability of the phosphine. For example, the stability of a set of primary phosphines was found to follow the order phenylphosphine < 5,6,7,8-tetrahydro-2-naphthylphosphine < 2-naphthylphosphine < 2-phosphanyl-1,1'-binaphthyl (Figure 1.2).[12] The role of conjugation in providing stability to these phosphines was investigated computationally[13] and it was found that stability was directly linked to the amount of phosphorus character in the HOMO of the molecule. That is, as conjugation increases the lone pair on phosphorus is no longer the most active nucleophilic site. Additionally, phosphines with increased π-conjugation were also found to have increased energies for the SOMO of the corresponding radical cation. Access to this radical species is believed to play a key part in one mechanism for phosphine oxidation.[8] The series of ferrocenyl phosphines $[Fe\{C_5H_4(CH_2)_nPH_2\}(Cp)]$ (n = 0, 1, 2) are also reported to be relatively air-stable.[14-17] Although the origins of this stability are unclear,[17] they presumably involve a combination of steric and electronic stabilisation.

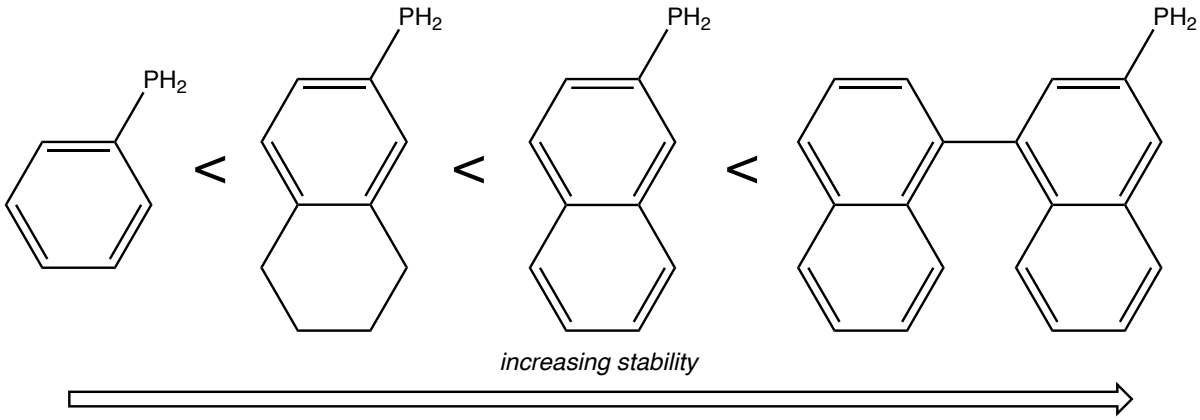

Figure 1.2. Primary phosphines stabilised through conjugation

1.1.2 Reactivity of Primary Phosphines and Metal Complexes

The distinguishing feature that makes primary phosphines desirable for study is the presence of two functionalisable P−H bonds. As a result, primary phosphines can act as a versatile synthon and an illustration of the types of reactions that they can undergo is shown in Scheme 1.2.[8, 18] Compounds derived from primary phosphines have been used in fields as diverse as asymmetric catalysis, carbohydrate research, macrocyclic synthesis, medicinal chemistry and polymer science.[8]

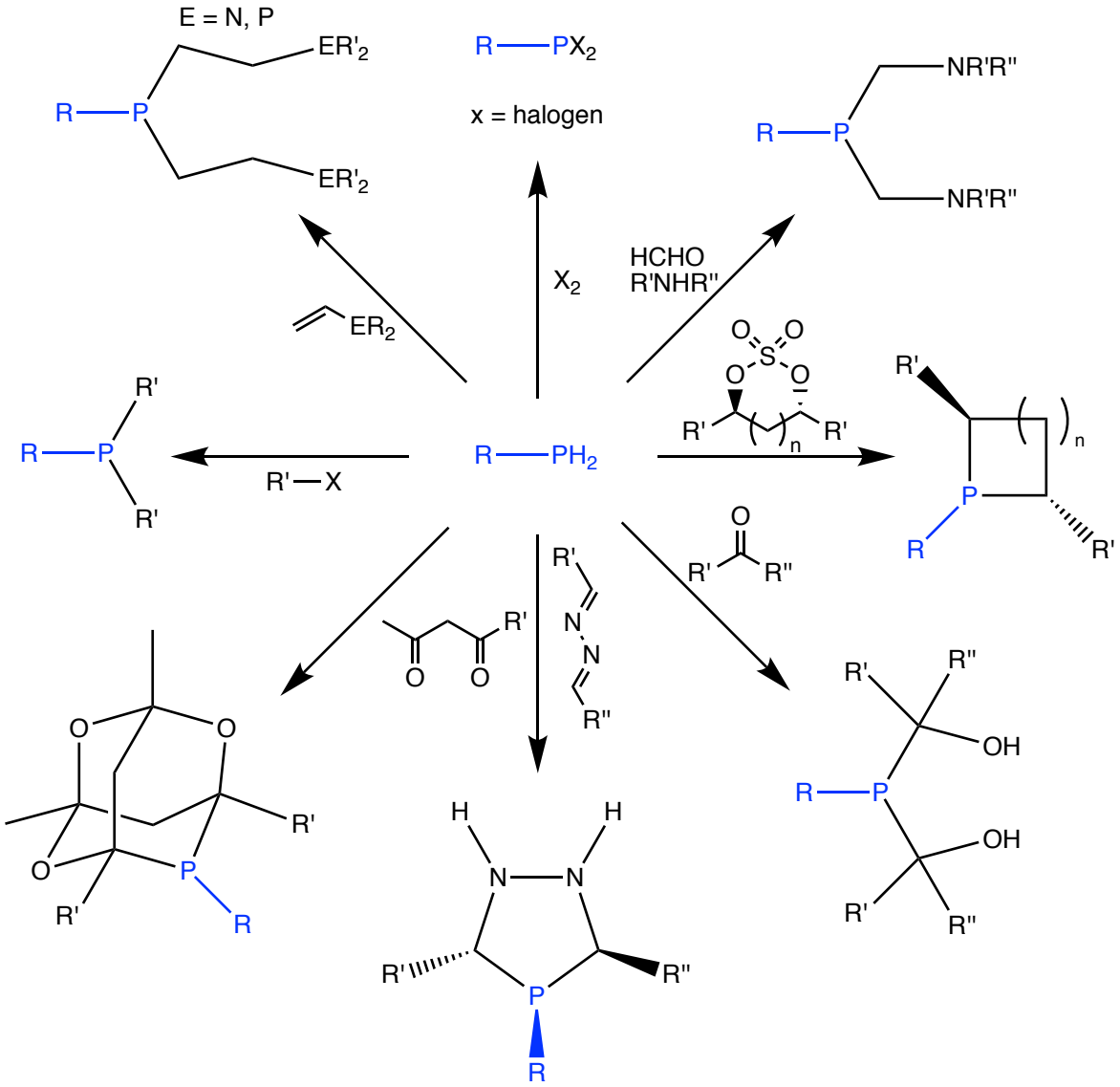

Scheme 1.2. Illustrative reactions of primary phosphines

A wide range of metal complexes with primary phosphine ligands are known, and they have been summarised in previous reviews.[7-8] As a result, only examples which lead to interesting or unusual reactivity will be discussed here. In general, discussions involving transition metal phosphido complexes are reserved for later in this chapter (Section 1.2.3).

One area to which primary phosphines have contributed is the synthesis of stable terminal phosphinidene complexes. These complexes were only an aspiration for organometallic chemists[19] until Lappert's seminal report in 1987.[20] While Lappert's approach relied on the reaction between low-valent metal complexes and dihalophosphines (Scheme 1.3), the use of primary phosphines and their derivatives have since proved to serve as another viable route.

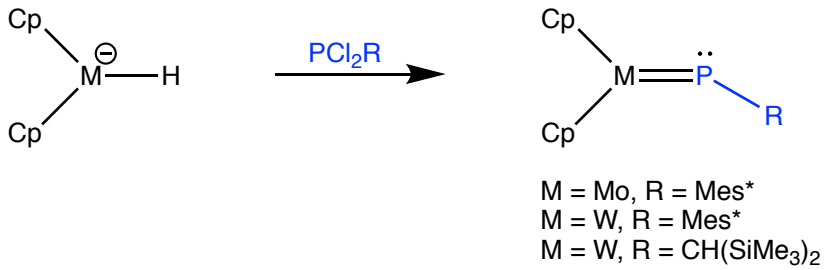

Scheme 1.3. Lappert's synthesis of terminal phosphinidene complexes

Schrock reported the first use of a primary phosphine derivative to obtain a stable terminal phosphinidene complex.[21] Treating the complex $[TaCl_2(N_3N)]$ ($N_3N = (Me_3SiNCH_2CH_2)_3N$) with two equivalents of a lithium phosphide, LiPHR (R = Ph, Cy, ^{t}Bu), yields the phosphinidene complexes $[Ta(=PR)(N_3N)]$ (R = Ph, Cy, ^{t}Bu) (Scheme 1.4). This work was significant for several reasons. Firstly, previous terminal phosphinidene complexes were stabilised through the use of a bulky substituent (*e.g.* Mes) at phosphorus, whereas Schrock's work used smaller substituents and provided the steric bulk through the co-ligand N_3N. The complexes $[Ta(=PR)(N_3N)]$ (R = Ph, Cy, ^{t}Bu) were also the first isolated examples of nucleophilic phosphinidene complexes; previous examples had all been electrophilic at phosphorus. As a result of their nucleophilicity the complexes $[Ta(=PR)(N_3N)]$ could be used to efficiently serve as phospha-Wittig reagents through their reactions with aldehydes to afford phosphaalkenes and the oxotantalum complex $[Ta(O)(N_3N)]$. Finally, by conducting the same reaction with the Mo and W analogues, the terminal phosphido complexes $[M(\equiv P)(N_3N)]$ (M = Mo, W) were synthesised (Scheme 1.5).[22] Along with Cummins' simultaneous report[23] this was the first example of a metal-phosphorus triple bond. While the approach was successfully extended to form the arsenide complex $[Mo(\equiv As)(N_3N)]$, the mechanism for the formation of the metal-pnictogen triple bond remains unclear.[24]

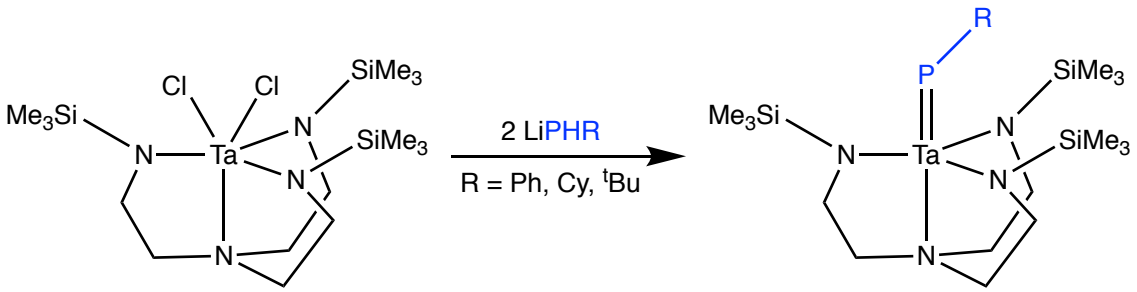

Scheme 1.4. Schrock's synthesis of terminal phosphinidene complexes

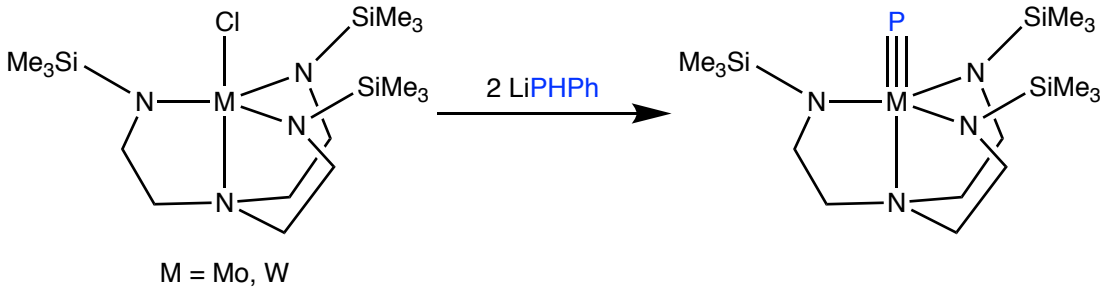

Scheme 1.5. Schrock's synthesis of terminal phosphide complexes

Phosphinidene formation has also been observed *via* the direct addition of a primary phosphine to a metal complex. The addition of PH_2Ph, or its congeners NH_2Ph and AsH_2Ph, to $[Ta(silox)_3]$ (silox = OSi^tBu_3) results in the formation of the pnictinidene complexes $[Ta(=EPh)(silox)_3]$ (E = N, P, As) (Scheme 1.6). A two-step process occurs, in which the first step is oxidative addition of the E–H bond to the metal centre to form $[TaH(EHPh)(silox)_3]$ (E = N, P, As). These intermediates can be observed spectroscopically, but cannot be isolated before the overall loss of H_2 occurs to give the pnictinidene complexes.[25]

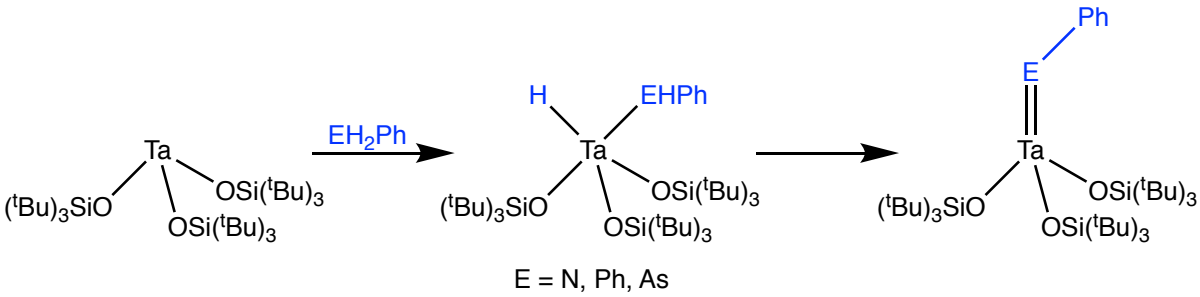

Scheme 1.6. Pnictinidene formation upon addition of a primary pnictane

Lammertsma demonstrated that phosphinidene complexes could be obtained directly from primary phosphine metal complexes.[26] This work was conducted on the complexes $[IrCl_2(PH_2R)(Cp^*)]$ (R = Mes, Is, Mes*; Is = isityl = 2,4,6-tris(isopropyl)phenyl), which underwent dehydrohalogenation in the presence of an extraneous ligand to give the

phosphinidene complexes [Ir(=PR)(L)(Cp*)] (R = Mes, Is, Mes*, L = PPh_3; R = Mes*, L = PH_2Mes, PMe_3, $P(OMe)_3$, $AsPh_3$, CN^tBu, CNXy, CO) (Scheme 1.7). The extraneous ligand is required to provide stability to the complex, in contrast to the isolable 'pogo-stick' complex [Ir(≡N^tBu)(Cp*)] reported by Bergman[27]; attempts to obtain the transient intermediate [Ir(≡PR)(Cp*)] were unsuccessful and led to mixtures of unidentifiable products. Additionally, the reaction was unsuccessful with an unsubstituted phenyl substituent at phosphorus, highlighting the importance of steric bulk to the process. When the method was extended to rhodium the stability of the phosphinidene complexes [Rh(=PR)(PPh_3)(Cp*)] (R = Mes, Is, Mes*) were significantly reduced for the mesityl compared to the isityl phosphorus substituent.[28] This further emphasises the importance of steric bulk to the stability of these systems. Ruthenium and osmium phosphinidene complexes were also subsequently accessed by the same method.[29]

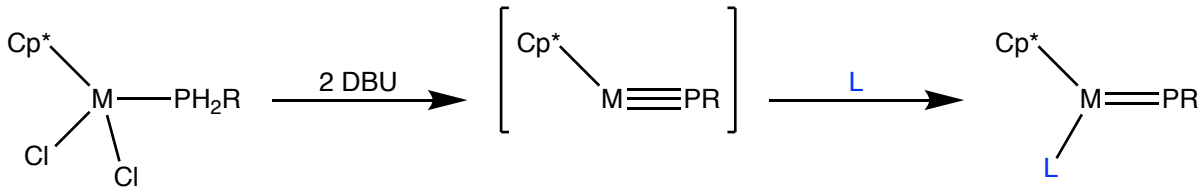

M = Rh, L = PPh_3, R = Mes, Is, Mes*
M = Ir, L = PPh_3, R = Mes, Is, Mes*
M = Ir, L = PH_2Mes, PMe_3, $P(OMe)_3$, $AsPh_3$, CN^tBu, CNXy, CO, R = Mes*

Scheme 1.7. Phosphinidene formation via *double deprotonation of a primary phosphine complex*

Mindiola reported the final major pathway to date for obtaining terminal phosphinidene complexes from primary phosphines and their derivatives.[30] This pathway involved the α-H-migration from a phosphido to a carbene co-ligand in [Ti(=CH^tBu)(PHR)(Nacnac)] (R = Cy, Is, Mes*; Nacnac = [Ar]NC(Me)CHC(Me)N[Ar], Ar = 2,6-$^iPr_2C_6H_3$) to form the intermediate [Ti(=PR)(CH_2^tBu)(Nacnac)] (R = Cy, Is, Mes*) (Scheme 1.8). The phosphinidene intermediate could only be isolated for the bulky Mes* substituent, while it was transiently observed for the Is group and not seen for the Cy group. For the smaller Cy and Is substituents, the ultimate product was the 3-phosphinoamido complex [Ti(=NAr)(OEt_2){(Ar)NC(Me)CHC(Me)P(R)}] (R = Cy, Is; Ar = 2,6-$^iPr_2C_6H_3$) (Scheme 1.8). The α-H-migration approach to terminal phosphinidene complexes was also extended to vanadium[31] and niobium[32] complexes.

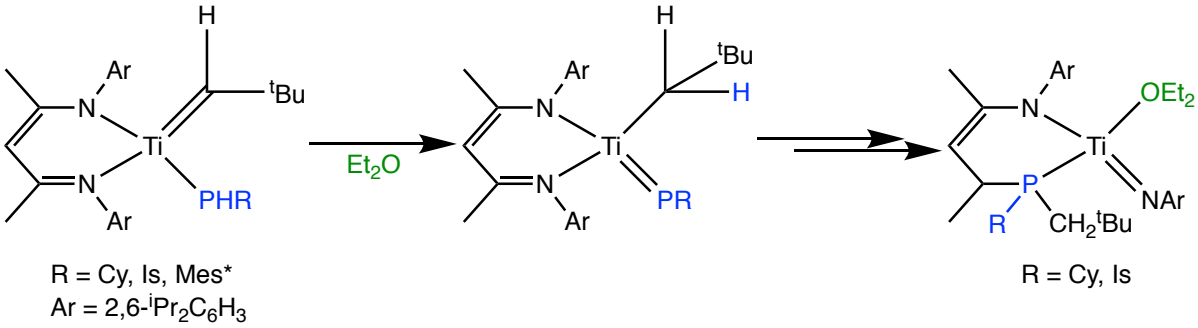

Scheme 1.8. Phosphinidene formation via *α-H-migration*

Another application of the interaction of primary phosphines with transition metals is the formation of P−P bonds. Hey first demonstrated this process *via* the addition of PH_2Ph to either $[ZrCl(CH_3)(Cp)_2]$ or $[Zr(CH_3)_2(Cp)_2]$ to give the triphosphinato ($P_3R_3^{2-}$) complex $[Zr(\kappa^2\text{-}P_3Ph_3)(Cp)_2]$ (Scheme 1.9).[33] The same product was observed upon the addition of two equivalents of LiPHPh to $[ZrCl_2(Cp)_2]$. This work served as an extension of previously-reported secondary phosphide chemistry.[34] Jones further elaborated upon the theme by reporting that the product was affected by both the phosphorus and the cyclopentadienyl substituents.[35] For the bulky ^{t}Bu phosphorus substituent the bridged-phosphido complex $[Zr(\mu\text{-}PH^tBu)(Cp)_2]_2$ (Figure 1.3b) and the terminal bisphosphido complex $[Zr(PH^tBu)_2(Cp)_2]$ (Figure 1.3c) are formed in addition to the triphosphinato complex (Figure 1.3a). When there are two trimethylsilyl substituents on each Cp ring (*i.e.* $C_5H_3(SiMe_3)_2$) in addition to a ^{t}Bu group on phosphorus a mixture of the bisphosphido complex $[Zr(PH^tBu)_2\{\eta^5\text{-}C_5H_3(SiMe_3)\}_2]$ (Figure 1.3d) and the biphosphinato ($P_2R_2^{2-}$) complex $[Zr(\kappa^2\text{-}P_2{}^tBu_2)\{\eta^5\text{-}C_5H_3(SiMe_3)\}_2]$ (Figure 1.3e) is formed. Stephan then demonstrated that for the bulky Mes phosphorus substituent, the bisphosphido complex $[Zr(PHMes)_2(Cp)_2]$ (Figure 1.3f) was the only product.[36] Further work was conducted by Stephan, implicating a phosphinidene intermediate and the importance of P−H activation of a primary phosphine in the formation of the bi- and triphosphinato structures.[36-38] Stephan[39-40] and Waterman[41-42] extended this work to the catalytic dehydrocoupling reactions of primary phosphines with a variety of main group hydrides.

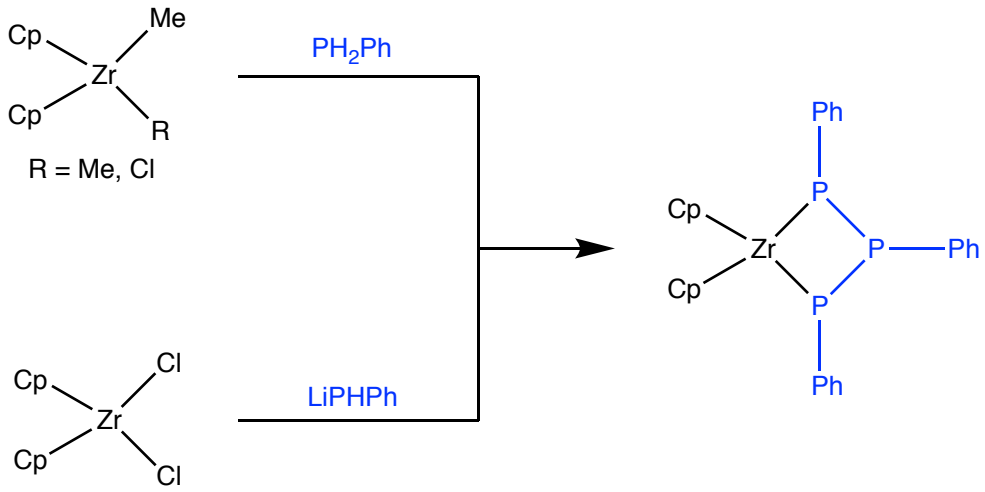

Scheme 1.9. Dehydrocoupling of primary phosphines and phosphides

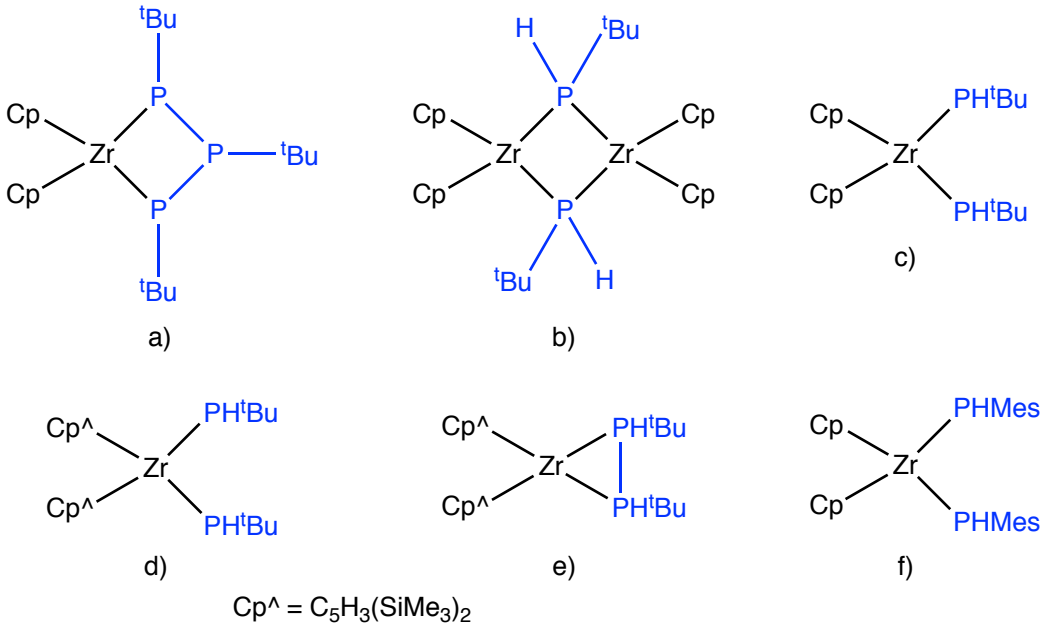

Figure 1.3. Substituent effect on primary phosphine zirconocene derivatives

Primary phosphine complexes may also serve as reagents in hydrophosphination reactions. The first example of transition metal-mediated hydrophosphination was reported by Huttner.[43] Expanding upon the established reactivity of primary phosphine addition to alkynes, Huttner reported that the metal complex $[Mn(CO)_2(PH_2Ph)(Cp)]$ underwent stereospecific addition to carbon-carbon triple bonds. Specifically, the product of *trans* addition was exclusively observed with phenylacetylene and diphenylacetylene (Scheme 1.10). Pringle established catalytic hydrophosphination with the report of platinum-catalysed addition of PH_3 (and $PH(CH_2CH_2CN)_2$) to acrylonitrile.[44-45] The mechanism involves oxidative

addition of a P–H bond to form an intermediate reactive phosphido complex, a recurring theme in subsequent hydrophosphination catalysis research.[46-49]

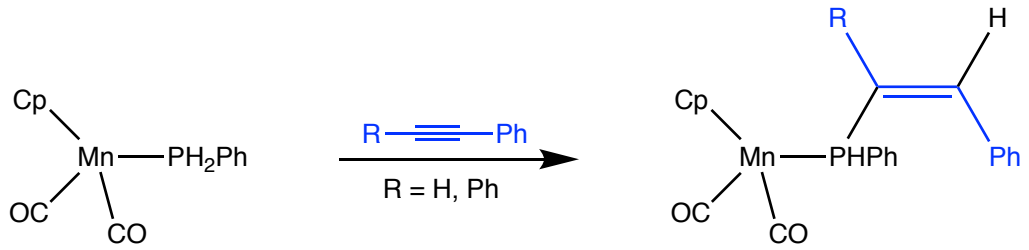

Scheme 1.10. Stereospecific hydrophosphination with a primary phosphine manganese complex

1.2 Terminal Phosphido Complexes

Phosphido groups (PR_2^-) effectively have two electron pairs available for bonding with one or two metals. As such they have found considerable application as bridging ligands for the formation of metal clusters.[50-55] The work in this thesis, however, primarily focuses on terminal phosphido ligands and this will be the main emphasis of discussion.

1.2.1 Synthesis of Terminal Phosphido Complexes

The first example of a terminal phosphido transition metal complex was reported in 1968.[56] The phosphido complexes $[Fe(CO)_2\{P(C_6F_5)_2\}(Cp)]$ and $[Mo(CO)_3\{P(C_6F_5)_2\}(Cp)]$ (in addition to their arsenido analogues) were prepared from the reaction between $PCl(C_6F_5)_2$ (arsenido analogues from $AsCl(C_6F_5)_2$) and the anions $[Fe(CO)_2(Cp)]^-$ or $[Mo(CO)_3(Cp)]^-$, respectively (Scheme 1.11). This route, based on the substitution of a halide by a nucleophilic organometallic fragment, is one of the most frequently-reported approaches to obtain terminal phosphido complexes.

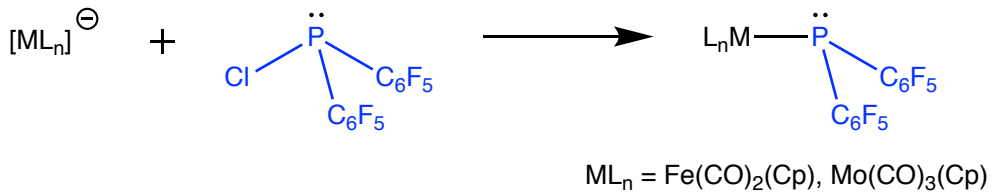

Scheme 1.11. Terminal phosphido complex formation via phosphorus halide substitution

An alternative route to terminal phosphido transition metal complexes was reported a year later.[57] Following investigations into the use of $PH(C_6F_5)_2$ as a ligand, Green and Stone reported that the complexes $[M(CO)_5\{PH(C_6F_5)_2\}]$ (M = Cr, Mo) reacted with ^nBuLi to form the new anionic phosphido complexes $[M(CO)_5\{P(C_6F_5)_2\}]^-$ (M = Cr, Mo) (Scheme 1.12). Further reactions with these complexes proceeded in low yields, leading to the authors describing them as having 'little value as synthetical reagents'. However, the report was essential to establishing the deprotonation of non-tertiary phosphine metal complexes as a major route to terminal phosphido complexes.

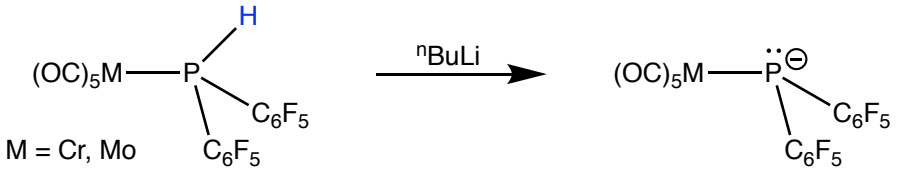

Scheme 1.12. Terminal phosphido complex formation via *P–H bond deprotonation*

A closely related pathway to the deprotonation of non-tertiary phosphine metal complexes is the deprotonation of metal hydride complexes bearing a halophosphine ligand. Malisch demonstrated this route through the deprotonation of $[WH(CO)_2\{PCl(O_2C_2Me_4)\}(Cp)]$ to yield the planar phosphido complex (see Section 1.2.2) $[W(CO)_2\{P(O_2C_2Me_4)\}(Cp)]$ (Scheme 1.13).[58] The same product could be obtained in a comparable 'umpolung' manner from the deprotonation of $[WCl(CO)_2\{PH(O_2C_2Me_4)\}(Cp)]$,[59] illustrating the close relationship between the two methods. No other reports utilising this metal hydride deprotonation approach are known.

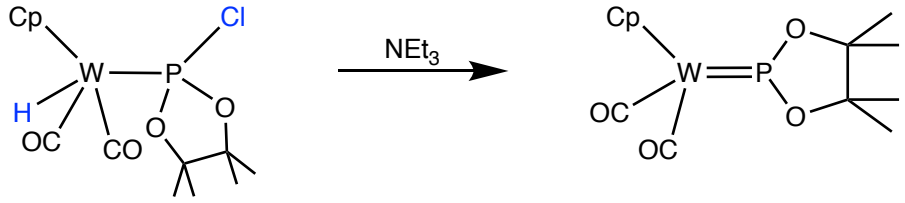

Scheme 1.13. Terminal phosphido complex formation via *metal hydride deprotonation*

Another common method of accessing terminal phosphido complexes is *via* the use of a metal phosphide salt to achieve substitution at a metal-nucleofuge bond. This approach was first utilised by Haines during investigations into bridged iron species. *En route* to the phosphido-bridged dinuclear species $[(\mu\text{-}PPh_2)\{Fe(CO)_4\}\{Fe(CO)_2(Cp)\}]$, the phosphido complex $[Fe(CO)_2(PPh_2)(Cp)]$ was obtained from the addition of $LiPPh_2$ to $[FeCl(CO)_2(Cp)]$ (Scheme

1.14).[60] The use of phosphide salts had previously been reported, but more generally towards the direct syntheses of phosphido-bridged clusters.[34]

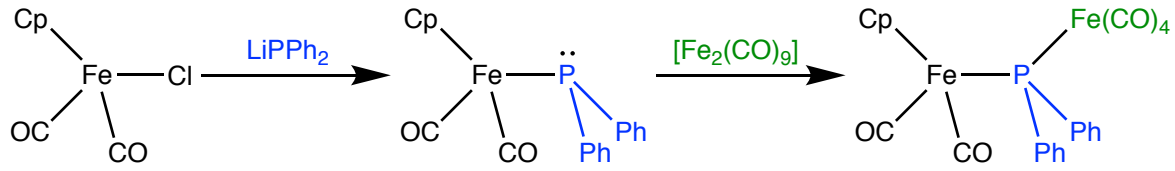

Scheme 1.14. Terminal phosphido complex formation using lithium phosphide salts

Terminal phosphido complexes have also been obtained through the oxidative addition of P–H bonds to metal complexes, as first reported by Schunn in 1973.[61] While investigating the coordination chemistry of PH_3 Schunn reported that the kinetic product with $[Ir(dppe)_2]^+$ (dppe = 1,2-bis(diphenylphosphino)ethane) was the expected complex $[Ir(PH_3)(dppe)_2]^+$, but upon warming the mixture from −78°C to room temperature the phosphido complex *cis*-$[IrH(PH_2)(dppe)_2]^+$ was formed (Scheme 1.15). The isomer *trans*-$[IrH(PH_2)(dppe)_2]^+$ was obtained when $[Ir(CO)(dppe)_2]^+$ was used as the precursor (Scheme 1.15). The oxidative addition was reversible for the *cis* isomer, reforming $[Ir(dppe)_2]^+$ upon heating under vacuum. With the notable exception of hydrophosphination catalysts,[45, 62-63] direct oxidative addition is less commonly used to synthesise terminal phosphido complexes due to the more restrictive conditions required (*i.e.* vacant coordination site, low-valent metal) compared to other routes.

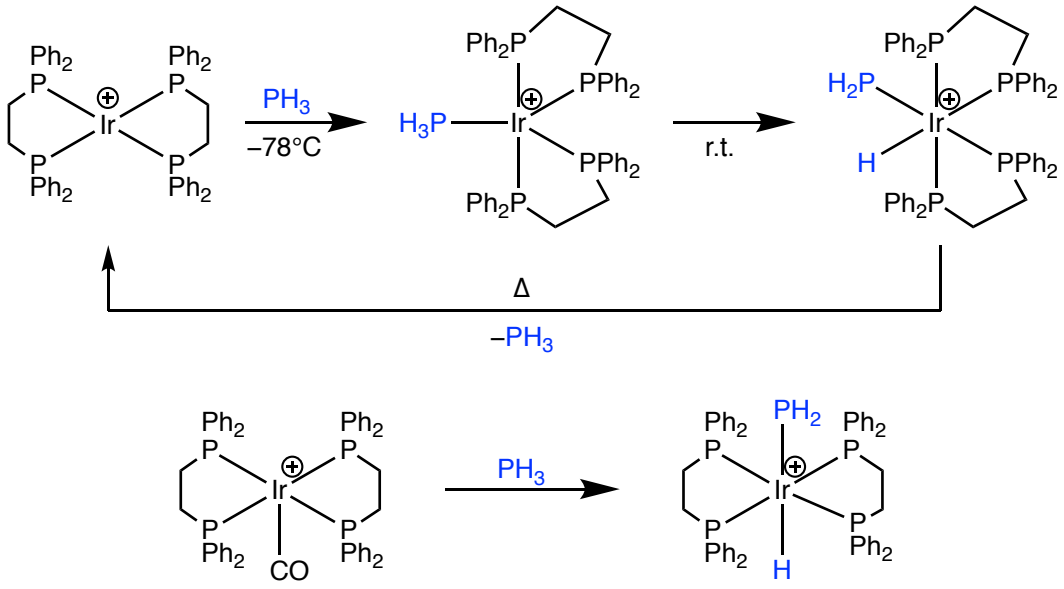

Scheme 1.15. Oxidative addition of P–H bonds to form terminal phosphido complexes

An extension to the oxidative addition approach was reported by Bergman.[64] Bergman studied the addition of the hydrogen-heteroatom bonds in the molecules HX (X = OAr, SC_6H_4Me-4, NHPh, PHPh) to the ruthenium(0) ethylene complexes $[Ru(PMe_3)_4(C_2H_4)]$ and $[Ru(C_2H_4)(dmpe)_2]$ (dmpe = 1,2-bis(dimethylphosphino)ethane). For the PMe_3 complex, the products were the hydrides $[RuH(X)(PMe_3)_4]$ (X = OAr, SC_6H_4Me-4, NHPh, PHPh) and ethylene (Scheme 1.16). Initially it would appear that a process involving ethylene dissociation followed by oxidative addition had occurred. However, the reaction between $[Ru(C_2H_4)(dmpe)_2]$ and HSC_6H_4Me-4 or PH_2Ph produced the ethyl complexes $[Ru(Et)(X)(dmpe)_2]$ (X = SC_6H_4Me-4, PHPh). The hydride complexes $[RuH(X)(dmpe)_2]$ (X = SC_6H_4Me-4, PHPh) were obtained after thermolysis of the ethyl products (Scheme 1.16). These results indicate that the key step may not be direct oxidative addition of the H-X bond to the metal centre, and that the hydride ligand is instead ultimately the product of ethyl β-hydride elimination.

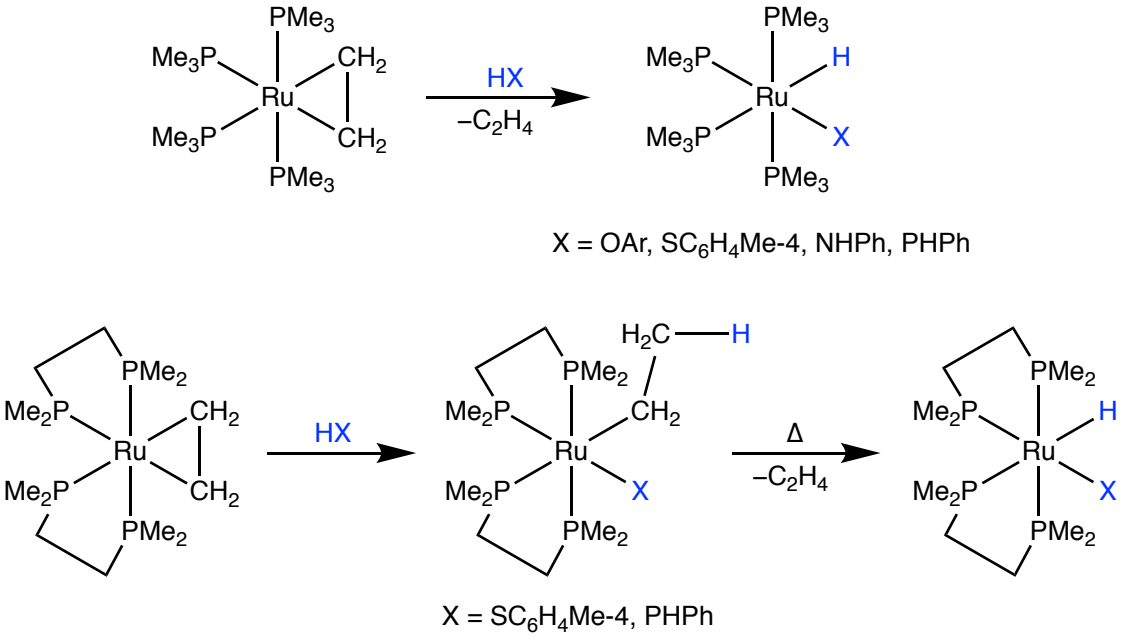

Scheme 1.16. Bergman's oxidative addition to ethylene complexes

A relatively recent method to obtain what might be loosely described as terminal phosphido complexes is the coordination of a carbene-phosphinidene to a metal. The first example of this was reported by Lavoie in 2014, in which the carbene-phosphinidene IMes=PPh[65] (IMes = 1,3-dimesitylimidazol-2-ylidene) substituted PPh_3 from $[RuCl_2(PPh_3)_2(=CHPh)]$ (Scheme 1.17).[66] The product, $[RuCl_2(PPh_3)\{PPh(IMes)\}(=CHPh)]$, may be described by a number of canonical forms (Figure 1.4). Importantly, one of these may be viewed as a phosphido

complex in which the imidazole ring is a singly-bonded phosphorus substituent. This bond description is particularly important upon inspection of the crystallographic structural data, which show a pyramidal phosphorus atom (angle sum of 315.5(2)°) and comparable P−Ph and P−IMes bond lengths of 1.843(2) and 1.847(2) Å, respectively. These values disagree with, for example, the corresponding metrics for the phosphaalkene complex [RuCl(I)(CO)(PPh_3)$_2${P(Me)=CH^{t}Bu}] (angle sum 360°; P−C: 1.80(1) Å, P=C: 1.657(9) Å),[67] indicating that the phosphaalkene canonical form does not contribute significantly to the solid-state structure of [$RuCl_2(PPh_3)${PPh(IMes)}(=CHPh)].

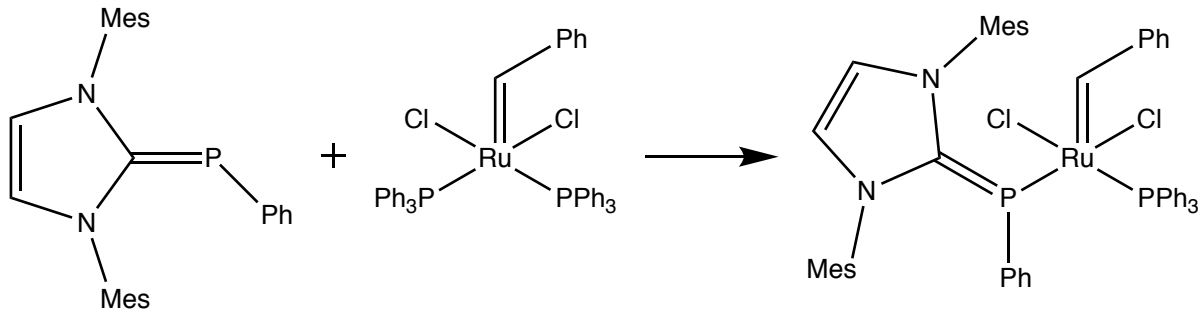

Scheme 1.17. Synthesis of a base-stabilised terminal phosphido complex using a carbene-phosphinidene

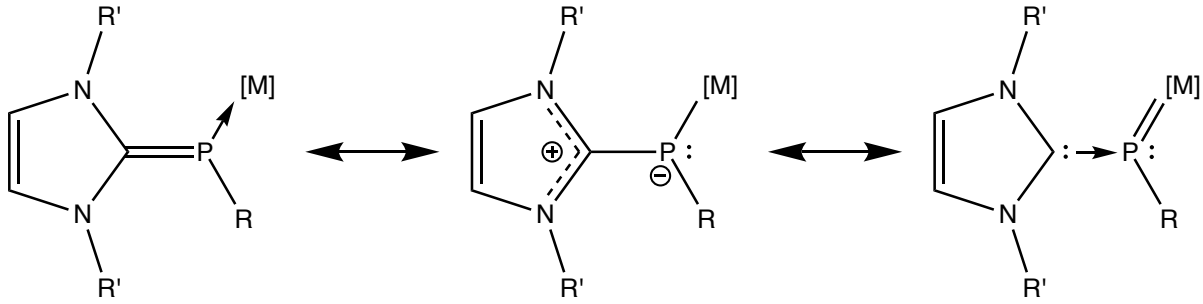

Figure 1.4. Resonance forms of a metal-coordinated carbene-phosphinidene

The cleavage of diphosphine bonds has been used to access a terminal phosphido complex. Dobbie obtained the iron complex [$Fe(CO)_2${$P(CF_3)_2$}(Cp)] from the addition of $P_2(CF_3)_4$ to the dimer [$Fe(CO)_2(Cp)]_2$ (Scheme 1.18).[68] This method served as an extension to previously-reported arsenic chemistry,[69] and had also been successfully applied to the synthesis of phosphido-bridged species.[56]

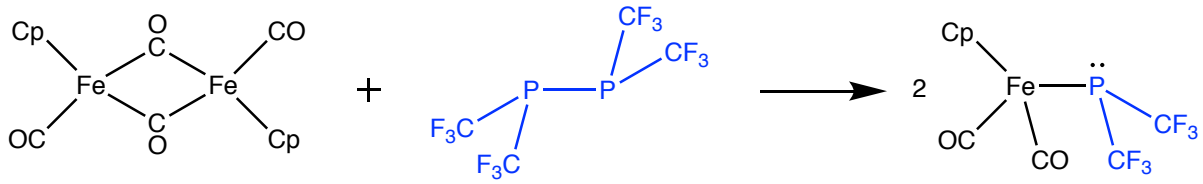

Scheme 1.18. Terminal phosphido complex formation via *cleavage of a diphosphine bond*

A unique case of terminal phosphido complex synthesis was reported by Hillhouse.[70] The complex [$HfH_2(Cp^*)_2$] reacts with the phosphines PHRR' (R = R' = Ph; R = H, R' = Ph; R = H, R' = Cy) *via* H_2 extrusion to give the phosphido complexes [$HfH(PRR')(Cp^*)_2$] (R = R' = Ph; R = H, R' = Ph; R = H, R' = Cy) (Scheme 1.19). This process was presumed to occur in a concerted (s-metathesis) fashion due to the unavailability of oxidative addition/reductive elimination pathways for Hf^{IV}, in direct analogy to the formation of the related amido complexes.[71-73] Accordingly the mechanism is distinct from those previously mentioned.

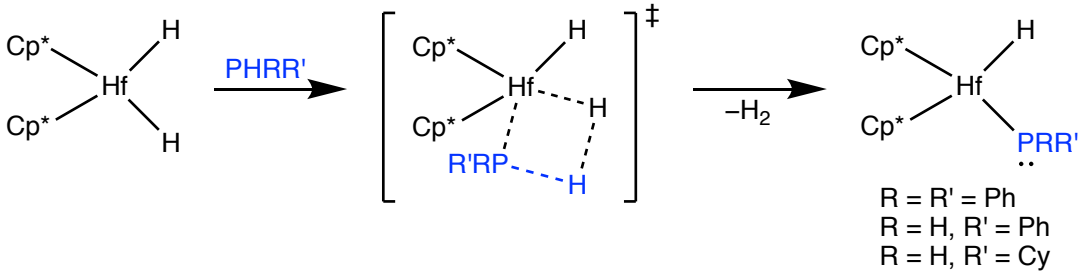

Scheme 1.19. Hillhouse's terminal phosphido complex synthesis via *H_2 extrusion*

1.2.2 Properties of Terminal Phosphido Ligands

Terminal phosphido ligands have a range of properties, particularly with respect to reactivity, that make them desirable for study. One of their main features is their ability to adopt one of two potential bonding modes with distinct behaviours: a pyramidal, one valence electron donor or a planar, three valence electron donor (Figure 1.5).[‡] For the pyramidal case, pronounced reactivity of the phosphorus lone pair towards electrophiles has been demonstrated. Additionally, the inversion barrier for the phosphido phosphorus atom is much lower than the corresponding non-metal-substituted phosphines and this has led to their application in asymmetric synthesis.

[‡] The formal valence bond description for the planar phosphido ligand should be a single and arrow bond, as shown in Figure 1.5, symbolising the 3-electron nature of this interaction. For simplicity, however, the shorthand of a metal-phosphorus double bond is also commonly used and this abbreviation is applied throughout this thesis. Such a shorthand also serves to represent the additional complexities surrounding the exact electronic nature of this interaction (*vide infra*) in a broad manner.

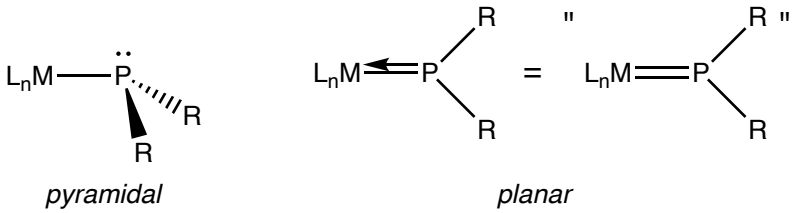

Figure 1.5. Potential bonding modes of a terminal phosphido complex

The two binding modes for the PR_2 ligand are distinguished by the behaviour of the phosphorus lone pair. In the pyramidal case the lone pair does not participate in bonding with the metal centre, and the phosphorus atom is nucleophilic. This type of bonding is more commonly observed for the more electron-rich (high d-occupancy) late transition metals, in which interaction with the lone pair is not required to satisfy electron-counting requirements. Indeed, interaction between the lone pair and metal centre may be destabilising (*vide infra*). Complexes with a pyramidal PR_2 group have also been considered as metallophosphines *i.e.* a phosphine with a metal substituent. For the planar bonding mode the phosphorus lone pair acts as a donor towards the metal centre. Accordingly, this form is more commonly observed for electron-deficient early transition metals. The planar mode is generally electrophilic at phosphorus, in which case it may also be considered as a phosphenium complex. Interconversion between pyramidal and planar forms may have an impact on the lability of co-ligands (*cf.* S_N1_{CB} mechanism).[74]

Examples of ambiphilic phosphido complexes, implicitly displaying both nucleophilic and electrophilic reactivity, were reported by Roper.[75-77] The salts $[OsCl(CO)_2(PPh_3)_2(PH_2R)]ClO_4$ (R = H, Ph, Me, CMe_3) may all be deprotonated to give the nucleophilic phosphido complexes $[OsCl(CO)_2(PPh_3)_2(PHR)]$ (Scheme 1.20). Alternatively, when deprotonation is conducted with excess base and methanol as the solvent, the products $[Os(CO)_2(PPh_3)_2\{PH(OMe)R\}]$ (R = Ph, Me, CMe_3) are formed. Roper also demonstrated that the phosphido complex $[OsCl(CO)_2(PPh_3)_2(PHPh)]$ reacts with methoxide in methanol to give $[Os(CO)_2(PPh_3)_2\{PH(OMe)Ph\}]$. As such, the phosphido complex is an intermediate in the formation of the complexes $[Os(CO)_2(PPh_3)_2\{PH(OMe)R\}]$, and a mechanism involving a labile chloride and donation of the phosphorus lone pair to form a planar, electrophilic intermediate was proposed (Scheme 1.20). A similar process led to the formation of the complexes $[M(CO)_2(PPh_3)_2\{PH_2(OR)\}]$ (M = Ru, Os; R = Me, Et, ^{i}Pr); the reaction of the acetato complexes

$[M(O_2CMe)(CO)_2(PPh_3)_2(PH_2)]$ (M = Ru, Os) with $HClO_4$ and the appropriate alcohol led to the formation of the cations $[MH(CO)_2(PPh_3)_2\{PH_2(OR)\}]^+$ (M = Ru, Os; R = Me, Et, ^{i}Pr), which were deprotonated to form $[M(CO)_2(PPh_3)_2\{PH_2(OR)\}]$ (M = Ru, Os; R = Me, Et, ^{i}Pr) (Scheme 1.21).[77]

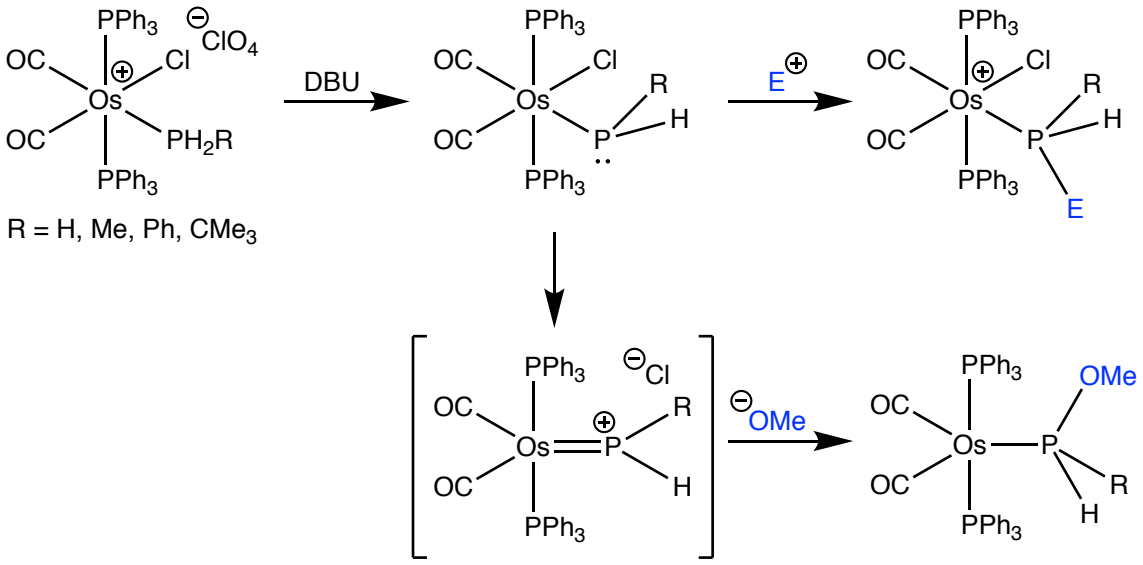

Scheme 1.20. Roper's ambiphilic phosphido complexes

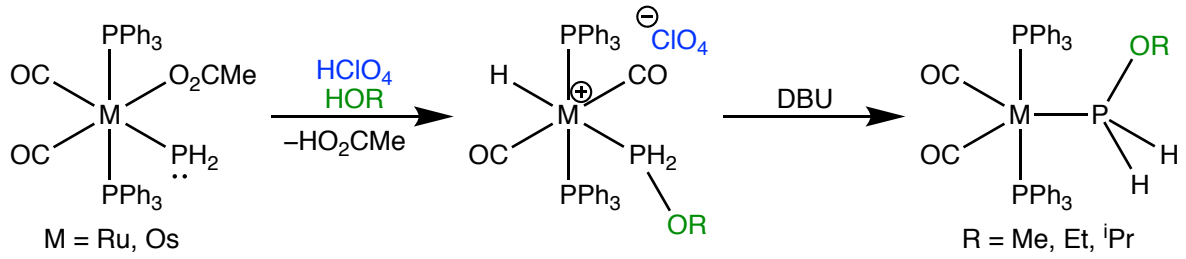

Scheme 1.21. Formation of $PH_2(OR)$ (R = Me, Et, ^{i}Pr) complexes from phosphido complexes with acyl co-ligands

While the planar PR_2 ligand is generally found to be electrophilic at phosphorus,[78-79] examples of planar, nucleophilic PR_2 ligands have also been reported.[80] As a result of this ambiphilic behaviour an analogy between electrophilic and nucleophilic planar PR_2 ligands and Fischer- and Schrock-type carbenes has been drawn.[81] At the core of this comparison is the fact that Fischer carbenes are electrophilic and commonly have heteroatomic substituents, while Schrock carbenes are generally nucleophilic and contain H, alkyl or aryl groups. It has been argued that the similar characteristics arise from analogous orbital energies of donor atom frontier orbitals. For Fischer carbenes the gap between the p_π and $sp^2{}_\sigma$ orbitals is large,

meaning the carbon atom has a vacant p_π orbital available for nucleophilic attack. In contrast, for Schrock carbenes the orbital gap is much smaller, leading to near-degenerate orbitals and a more-accessible triplet state (Figure 1.6). The presence of electron density in the p_π orbital renders the carbon atom nucleophilic. In a similar fashion, electrophilic planar PR_2 fragments have a large SOMO-HOMO gap, leading to a high-energy electron. The phosphorus atom may then be easily oxidised to form a cationic fragment with a vacant orbital for nucleophilic attack. For the nucleophilic planar PR_2 ligand, a reduction in the SOMO-HOMO gap leads to near-degeneracy of the orbital energies. This allows access to the commonly-accepted bonding description of phosphido ligands in which the SOMO is the metal-phosphorus bonding orbital and the HOMO is a lone pair on phosphorus (Figure 1.7).

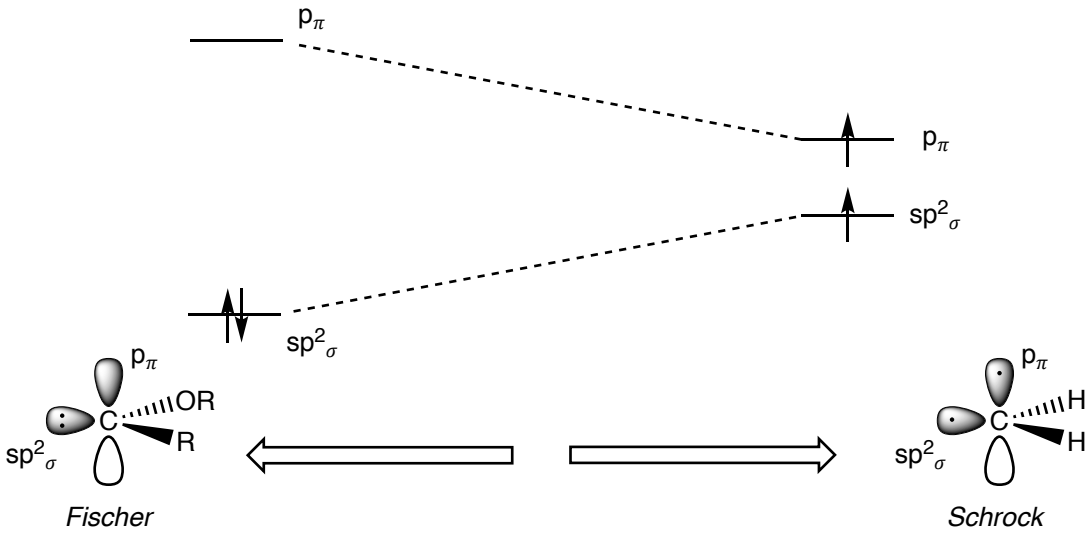

Figure 1.6. Frontier molecular orbital diagram for singlet and triplet carbenes

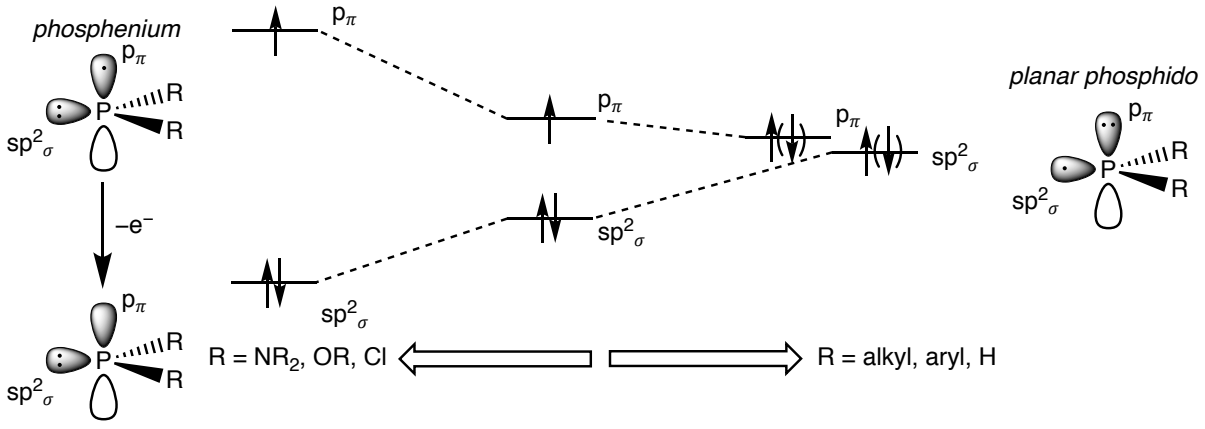

Figure 1.7. Frontier molecular orbital diagram for PR_2 ligand

An important property of pyramidal phosphido complexes ('metallophosphines') is that the phosphorus atom exhibits increased nucleophilicity compared to conventional phosphines. The increased reactivity was first reported in 1973 by Dobbie, who produced the chalcogenophosphonyl complexes $[Fe(CO)_2\{P(E)(CF_3)_2\}(Cp)]$ (E = O, S, Se) from the reaction of the phosphido complex $[Fe(CO)_2\{P(CF_3)_2\}(Cp)]$ with an appropriate chalcogen source (Scheme 1.22). The formation of $[Fe(CO)_2\{P(S)(CF_3)_2\}(Cp)]$ and $[Fe(CO)_2\{P(Se)(CF_3)_2\}(Cp)]$ occurred at 60°C and room temperature, respectively. In comparison, temperatures in excess of 150°C were required for the addition of sulfur to fluorocarbyl phosphines and the addition of selenium had only been observed for $P_2(CF_3)_4$ at temperatures over 80°C.[68]

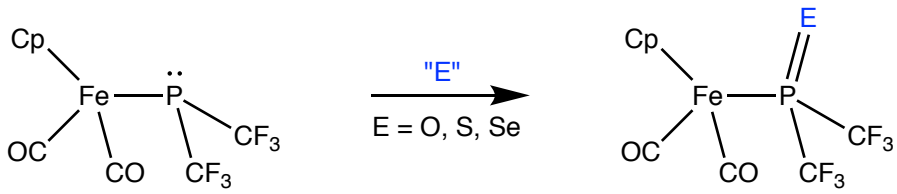

Scheme 1.22. Reaction of a phosphido complex to form chalcogen adducts

The seminal work towards understanding the enhanced reactivity of pyramidal phosphido ligands was conducted by Gladysz.[82-83] This phenomenon was attributed to repulsive π interactions between a filled transition metal d orbital and the phosphorus lone pair, resulting in the destabilisation of the latter (Figure 1.8). The repulsion was observed in the molecular structures of the rhenium complexes $[Re(NO)(PPh_3)(PR_2)(Cp)]$ (R = Ph, ^{t}Bu), in which the Re–PR_2 distance was longer than the Re–PPh_3 distance (Δ_{ReP} = 0.103(4) Å, PPh_2; 0.169(6) Å, P^tBu_2). The increased phosphorus reactivity of $[Re(NO)(PPh_3)(PPh_2)(Cp)]$ was also noted through its reaction with weakly-electrophilic CH_2Cl_2 and its rapid oxidation to $[Re(NO)(PPh_3)\{P(O)Ph_2\}(Cp)]$ compared to the non-metal-substituted PPh_3. Gladysz's report was also supplemented by computational investigations into the analogue $[Re(NO)(PH_3)(PH_2)(Cp)]$. Specifically, the energies of conformers resulting from rotation about the Re–PH_2 bond were calculated. Two energetic minima were found in this calculation that directly corresponded to conformations in which the phosphorus lone pair was orthogonal to the frontier Re d_π orbital.

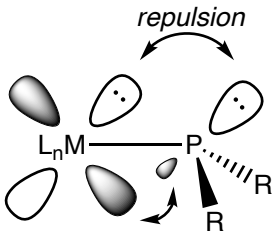

Figure 1.8. Metal d to phosphorus p interactions in terminal phosphido ligands

In an application of this principle, Gladysz trialled the complexes [Re(NO)(PPh$_3$)(PR$_2$)(Cp)] (R = Ph, ^{t}Bu, Me), [Ru(PEt$_3$)$_2$(PR$_2$)(Cp)] (R = Ph, ^{t}Bu, Cy) and [Ru(PR$_2$)(depe)(Cp)] (R = Ph, ^{t}Bu; depe = 1,2-bis(diethylphosphino)ethane) (Figure 1.9) as a support ligand for cross-coupling reactions.[84-86] Gladysz's reasoning was that the most successful phosphines utilised for palladium-mediated cross coupling reactions were those that were both highly basic (hence strongly bound) and sterically large. The complex [Ru(P^{t}Bu$_2$)(depe)(Cp)] gave a catalyst of comparable activity to the benchmark organophosphine P^{t}Bu$_3$, while all other phosphido complexes trialled gave palladium catalysts with a lower activity than this standard.

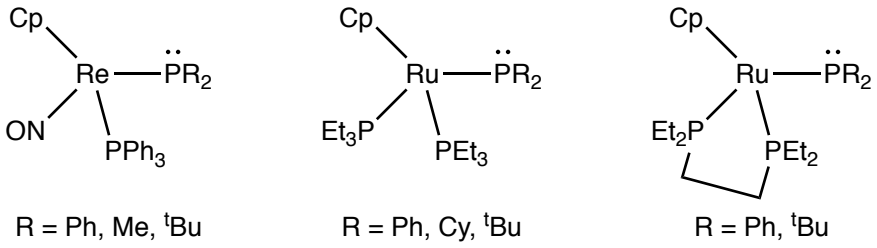

Figure 1.9. Terminal phosphido complexes trialled as ligands for cross-coupling reactions

Pyramidal phosphido complexes have lower phosphorus inversion (Scheme 1.23) barriers than free phosphines. The lower inversion barrier was first noted by Malisch in the complex [W(CO)$_2$(PMe$_3$)(P^{i}Pr$_2$)(Cp)].[87] The complex had a measured phosphorus inversion barrier of 60.2 kJ mol^{-1}, much lower than the typical range of 134−226 kJ mol^{-1} reported for free phosphines.[88] Malisch eliminated the possibility that configuration inversion was a metal-centred process by synthesising the derivatives [W(CO)$_2$(PMe$_3$){PR^{i}Pr$_2$}(Cp)]$^+$ (R = H, Me, Br) and [W(CO)$_2$(PMe$_3$){P(S)^{i}Pr$_2$}(Cp)] which did not show any temperature-dependent NMR spectra. Gladysz further expanded the study of pyramidal phosphido ligand inversion barriers with the complexes [Re(NO)(PPh$_3$)(PRR')(Cp)] (R = H, R' = Ph; R = R' = *p*-tolyl).[89] A phosphorus inversion barrier of 48.4(4) kJ mol^{-1} was measured for [Re(NO)(PPh$_3$)(PHPh)(Cp)], although rotation about the Re−P bond could not be ruled out as the dynamic process responsible for this barrier. However, the complex [Re(NO)(PPh$_3$){P(*p*-tol)$_2$}(Cp)] contains diastereotopic tolyl

groups which cannot be exchanged by rotation, and a comparable phosphorus inversion barrier of 54.4(4) kJ mol^{-1} was measured. Gladysz excluded the possibility of a rhenium-centred inversion through the synthesis of S_{Re}-[Re(NO)(PPh_3){P(*p*-tol)$_2$}(Cp)] and observing that it was configurationally stable.

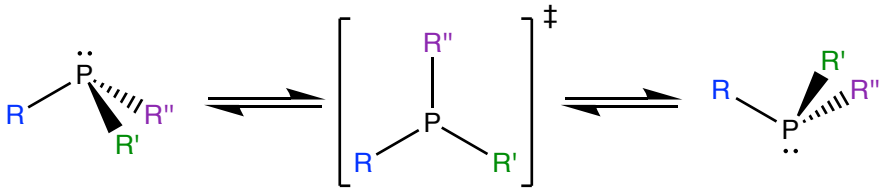

Scheme 1.23. Phosphorus inversion

The mechanism of inversion was investigated computationally by Marynick.[90] For early, electron-deficient transition metal complexes inversion involves a planar phosphido intermediate with metal-ligand π bonding (Scheme 1.24). Thus, the lowered barrier to inversion is a result of an energetically-favourable intermediate. A different effect lowers the phosphorus inversion barrier for middle and late transition metal phosphido complexes. The aforementioned π interaction is unfavourable because they are electron-rich (high d-occupancies), and a low-energy intermediate is not accessible. Instead, the repulsive interaction between the metal and the phosphorus lone pair serves to destabilise the pyramidal ground state, in turn reducing the barrier to inversion.

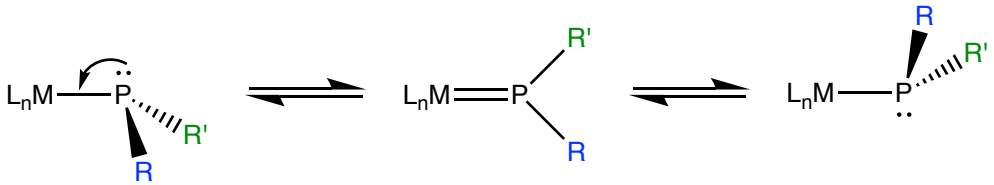

Scheme 1.24. Phosphorus inversion mechanism for early transition metal terminal phosphido complexes

Rapid phosphorus inversion in phosphido complexes has been used advantageously for the stereoselective synthesis of phosphines. Wild first demonstrated this approach through the use of a stereoactive co-ligand to effect the stereoselective alkylation of iron phosphido complexes.[91-93] Bergman and Toste extended this stereoselective alkylation into a catalytic ruthenium-centred process.[94-95] Further efforts by Glueck allowed for the palladium- or platinum-catalysed asymmetric synthesis of P-chiral phosphines *via* a phosphido intermediate.[63] The salient point of all these approaches is that the phosphorus undergoes

rapid conversion while the stereoactive co-ligand imposes a thermodynamic preference for a single configuration, leading to stereoselectivity (Scheme 1.25).

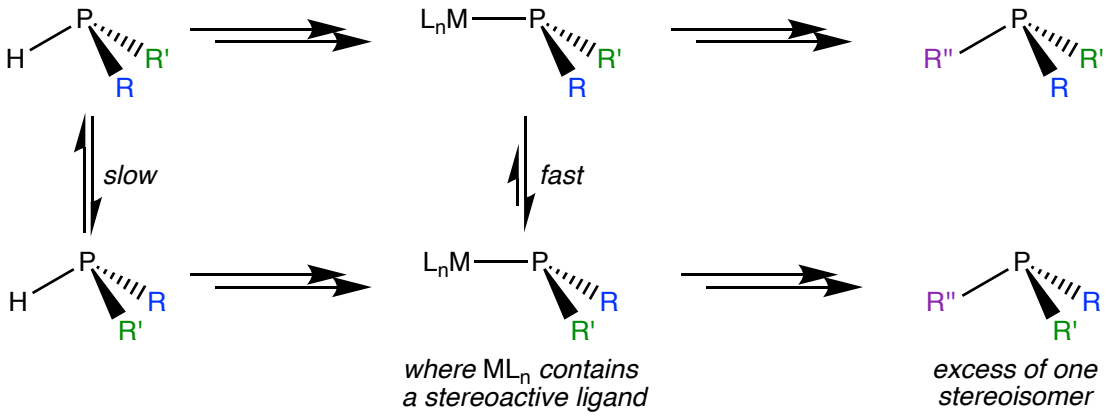

Scheme 1.25. Generalised method for stereoselective synthesis of phosphines using a terminal phosphido intermediate

Phosphido ligands bear a strong resemblance to their lighter amido counterparts, but differences in behaviour are observed. In studies investigating the role of α-hydrogen migration in the formation of carbene ligands, Schrock synthesised the amido-carbyne complex [$WCl_2(PEt_3)_2$(NHPh)(CCMe)] and its phosphido analogue [$WCl_2(PEt_3)_2$(PHPh)(CCMe)]. The amido complex underwent hydrogen migration when heated to form the imido-carbene complex [$WCl_2(PEt_3)_2$(NPh)(CHCMe)], while no conversion was observed for the heavier phosphido congener (Scheme 1.26). Schrock reasoned that given the higher acidity of P–H *versus* N–H bonds, the only factor that apparently prevented hydrogen migration from the phosphido group to the carbyne was the longer W–P bond in comparison to the W–N bond.[96]

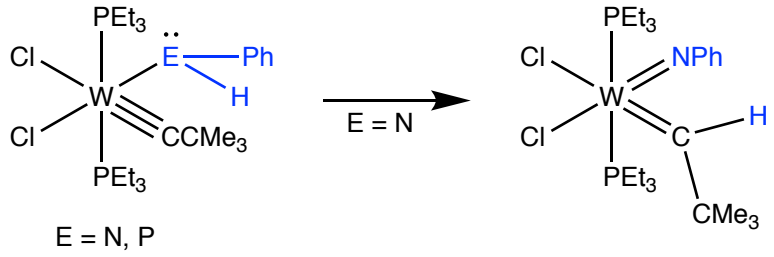

Scheme 1.26. Hydrogen migration for an amido, but not phosphido, complex

1.2.3 Reactivity of Primary Phosphido Complexes

In direct correlation to the number of studies conducted on their phosphine counterparts, reports on chemistry involving phosphido ligands with one or two P–H bonds are far fewer than those concerning phosphido ligands with no P–H bonds. Nevertheless, a range of these

complexes is known and a number have been discussed in previous sections. This section will focus on reports that have not already been covered, and that have investigated the reactivity of primary or parent phosphido complexes.

Acyl-phosphido complexes of the type $[OsCl(CO)_2(PPh_3)_2\{PH(C[O]R)\}]$ (R = CF_3, ^tBu, Me, CO_2Et, Ph, *p*-$C_6H_4NO_2$) were formed *via* the reaction of the phosphido complex $[OsCl(CO)_2(PPh_3)_2(PH_2)]$ with the appropriate acid chloride or anyhydride.[97] The complex $[OsCl(CO)_2(PPh_3)_2\{PH(C[O]CF_3)\}]$ further reacted with sodium hydride to furnish the bidentate phosphaalkenyl complex $[Os(CO)_2(PPh_3)_2\{\kappa^2\text{-}P,O\text{-}PC(CF_3)O\}]$ (Scheme 1.27). The phosphorus atom in this phosphaalkenyl complex is nucleophilic, and can react with electrophiles such as MeI, $Fe_2(CO)_9$ and AuI. Through this work Roper demonstrated the utility of combining the functionalisability of P−H bonds with the reactivity of phosphido complexes, as well as the stepwise reactivity of the phosphorus atom.

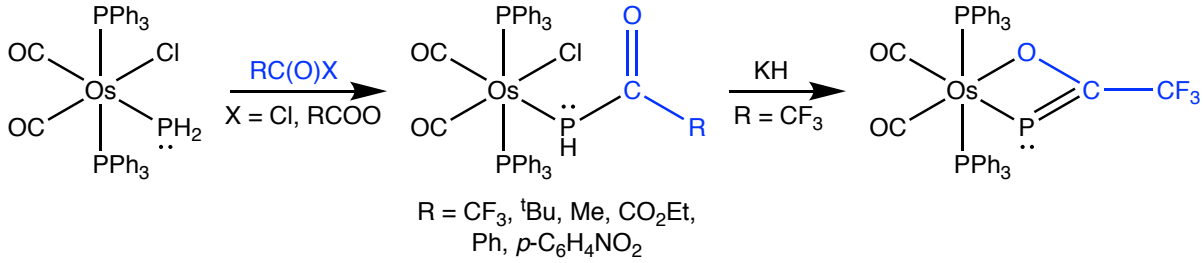

Scheme 1.27. Synthesis and reactivity of acyl-phosphido complexes

Following the deprotonation of the complexes $[WCl(CO)_2(PH_2Mes)(L)]$ (L = Cp, Cp*) the expected products $[W(CO)_2(PHMes)(L)]$ (L = Cp, Cp*) could not be observed, even at −78°C. Instead, spontaneous rearrangement occurred to give the phosphinidene-bridged bimetallic complexes $[(\mu\text{-}PMes)\{W(CO)_2(L)\}\{W(CO)_2(PH_2Mes)(L)\}]$ (L = Cp, Cp*) (Scheme 1.28). This rearrangement involves dimerisation to form $[(\mu\text{-}PHMes)_2\{W(CO)_2(L)\}_2]$ followed by hydrogen migration, and can be prevented by the addition of PMe_3 resulting in the isolation of $[W(CO)_2(PMe_3)(PHMes)(L)]$ (L = Cp, Cp*). The Cp*-substituted dimer rearranges above −40°C with loss of PH_2Mes to yield the symmetrical structure $[W_2(CO)_4(Cp^*)_2(\mu\text{-}PMes)]$.[98]

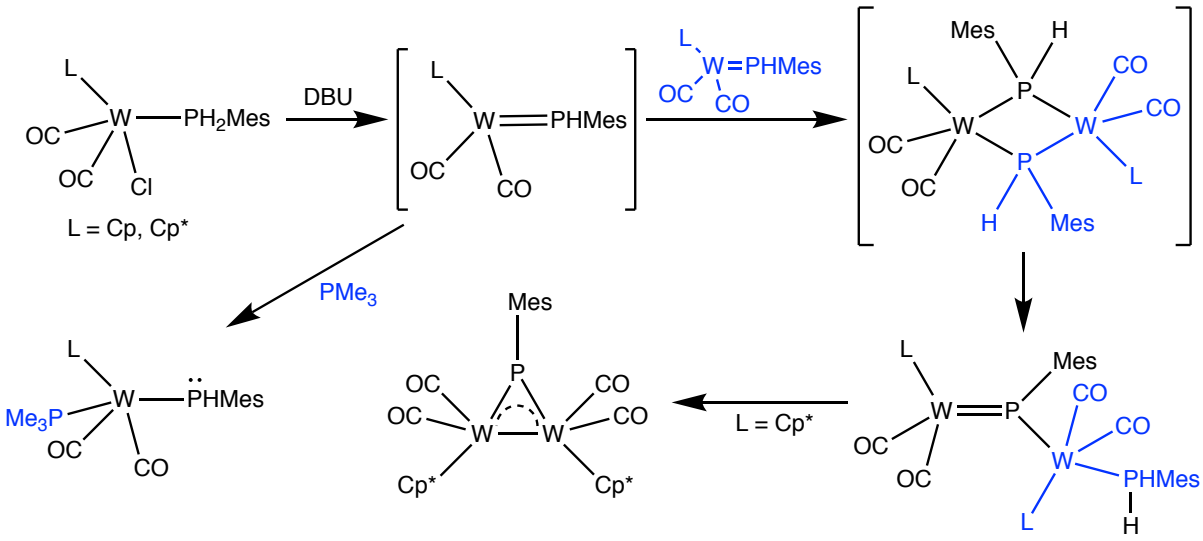

Scheme 1.28. Deprotonation and subsequent reactivity of [WCl(CO)$_2$(PH$_2$Mes)(L)] (L = Cp, Cp)*

Stephan reported an improved synthesis of the terminal phosphinidene complex [Zr(PMe$_3$)(PMes*)(Cp)$_2$] *via* an intermediate primary phosphido complex (Scheme 1.29). The key difference was the use of [ZrCl(Me)(Cp)$_2$] as the precursor[99] rather than [Zr(Cl$_2$)(Cp)$_2$] or [ZrCl(PHMes*)(Cp)$_2$].[38, 100] The intermediate [ZrMe(PHMes*)(Cp)$_2$] was formed following the reaction with LiPHMes*, and this complex was unstable with respect to the loss of methane. Thus, when the elimination was conducted in the presence of PMe$_3$ the complex [Zr(PMe$_3$)(PMes*)(Cp)$_2$] was obtained (Scheme 1.29). Further research on the intermediate phosphido complex [ZrMe(PHMes*)(Cp)$_2$] and its less bulky analogue [ZrMe(PHMes)(Cp)$_2$] demonstrated the extreme reactivity of these species. The larger species, [ZrMe(PHMes*)(Cp)$_2$], underwent insertion reactions with benzophenone, acetone, cyclohexanone and benzonitrile, with the zirconium-phosphorus bond adding across the C–X (X = O, N) π-bond in each case. Insertion with acetone was observed for the smaller complex [ZrMe(PHMes)(Cp)$_2$] (Scheme 1.29), but it was otherwise unstable and underwent a rearrangement reaction to form the symmetrical phosphinidene-bridged species [Zr$_2$Me$_2$(μ-PMes)(Cp)$_4$] (Scheme 1.30). The addition of PH$_2$Mes to the phosphinidene-bridged species with heating (110°C) resulted in C–H activation of one Cp ring and the formation of a new phosphido-bridged species (Scheme 1.30).

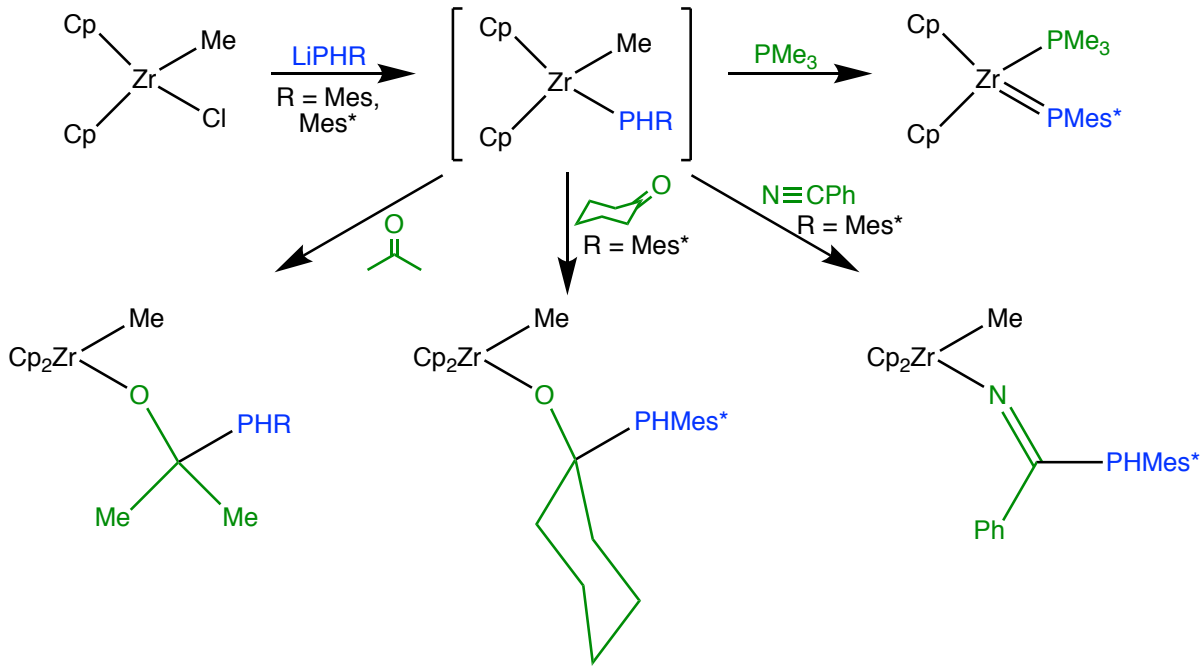

Scheme 1.29. Reactivity of $[Zr(Me)(PHR)(Cp)_2]$ (R = Mes, Mes)*

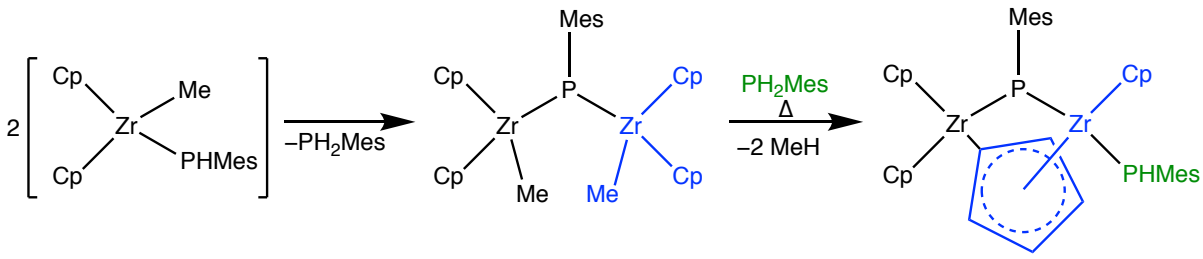

Scheme 1.30. C–H activation of a Cp ring in $[Zr_2Me_2(\mu\text{-}PHMes)(Cp)_4]$

Another example of insertion into the metal-phosphorus bond was reported for the complex $[Zr(PHPh)(N_3N)]$ (N_3N = $N(CH_2CH_2NSiMe_3)_3$).[101] Upon the addition of benzylisocyanide, 1,1-insertion occurs to form the imine-containing $[Zr\{C(=NCH_2Ph)(PHPh)\}(N_3N)]$. This product is unstable and undergoes rearrangement to the phosphaalkene-containing complex $[Zr\{N(CH_2Ph)(CH=PPh)\}(N_3N)]$ (Scheme 1.31). Rearrangement was observed at −30°C in the absence of light and was greatly accelerated in solution, with polar solvents such as Et_2O having the most pronounced effect.

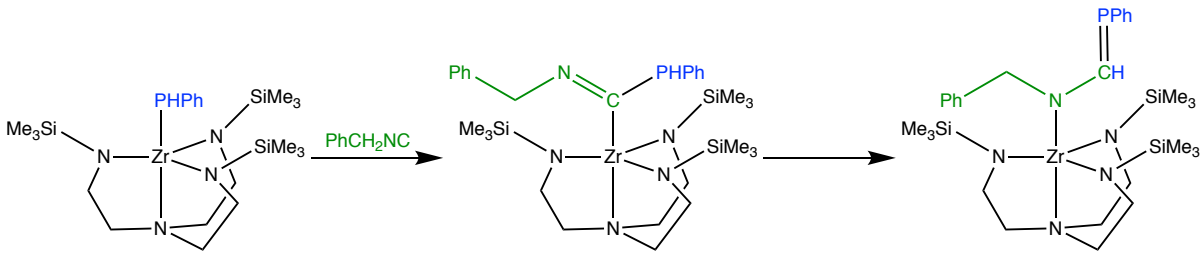

Scheme 1.31. Benzonitrile insertion into a Zr–P bond

Cases in which overall insertion into the P−H bond occurs have also been reported. The iron complex $[Fe(CO)_2(PHMes)(Cp)]$ reacts with the organoisothiocyanates SCNR (R = Me, Et, Ph) to give the thioamide-substituted phosphido complexes $[Fe(CO)_2\{P(Mes)(C[S]NHR)\}(Cp)]$ (R = Me, Et, Ph) (Scheme 1.32).[102] The phosphorus atom in these complexes remains reactive and undergoes methylation and sulfur oxidation. When the phosphorus substituent is a *tert*-butyl group rather than a mesityl group a second organoisothiocyanate addition occurs with formation of a metallacycle *via* nucleophilic addition of the nitrogen to a carbonyl ligand (Scheme 1.33).[103] In closely related chemistry the primary phosphine complex salts $[Fe(CO)_2(PH_2R)(Cp)]BF_4$ (R = ^{t}Bu, Ph, Mes) react with ethyl diazoacetate to yield either $[Fe(CO)_2\{PHR(NHN{=}CHCO_2Et)\}(Cp)]BF_4$ or $[Fe(CO)_2\{PR(NHN{=}CHCO_2Et)_2\}(Cp)]BF_4$ (R = ^{t}Bu, Ph, Mes) depending on stoichiometry (Scheme 1.34). Ethyl diazoacetate is presumed to serve as a base and the implied intermediate is a phosphido complex.[104]

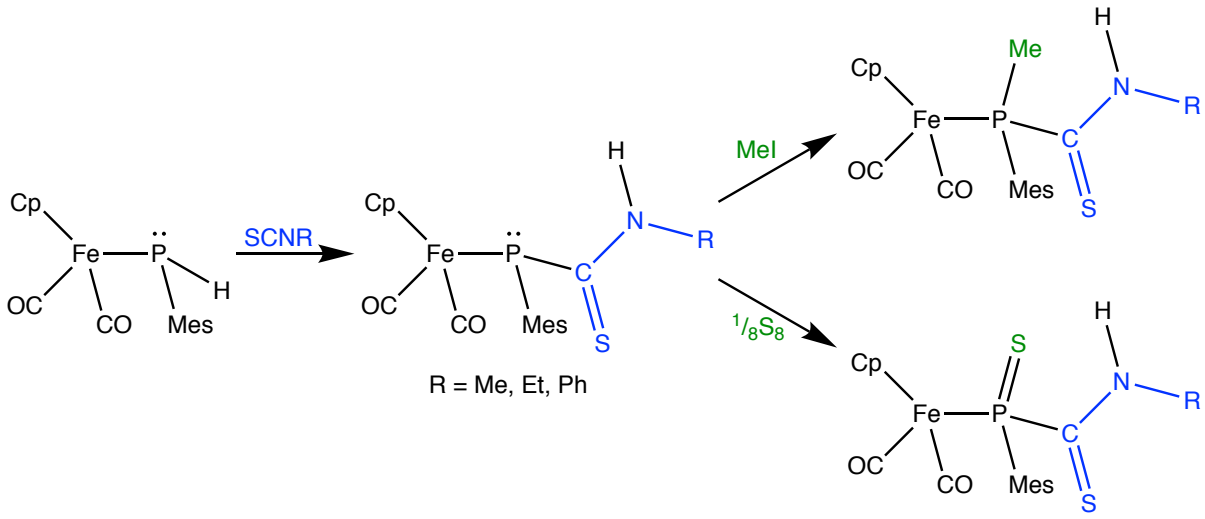

Scheme 1.32. Insertion into the P−H bond of a primary phosphido complex

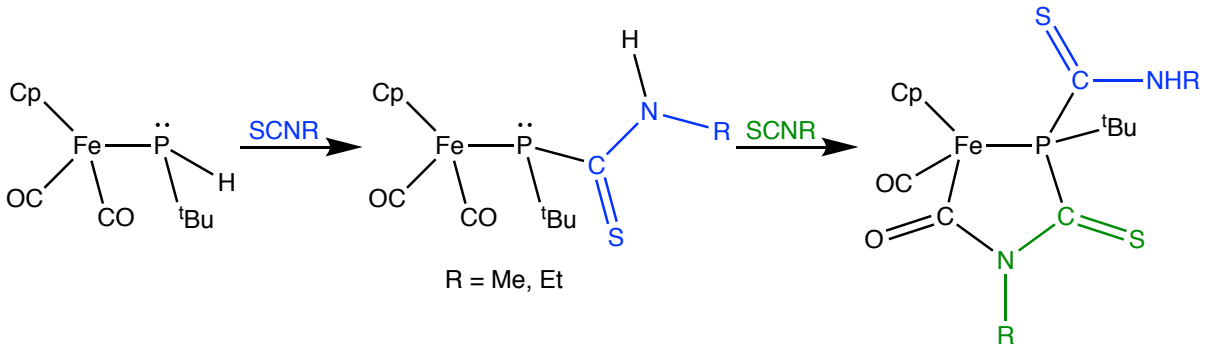

Scheme 1.33. Stepwise reactivity of organoisothiocyanates with $[Fe(CO)_2(PH^tBu)(Cp)]$

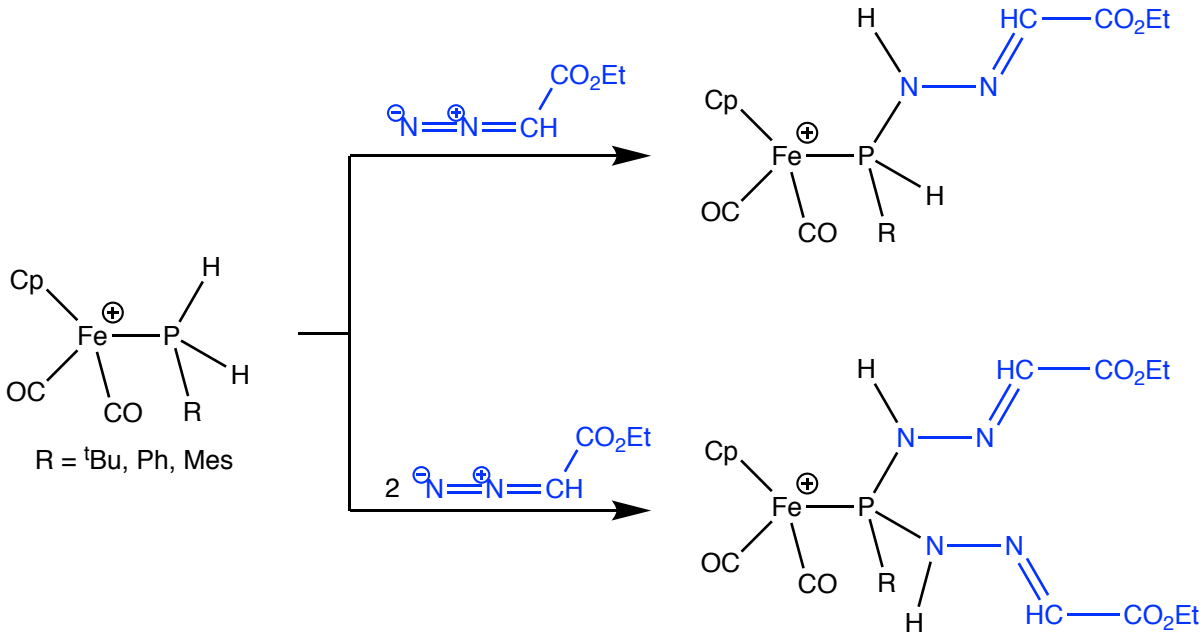

Scheme 1.34. Reaction of ethyl diazoacetate with primary phosphine iron complexes

Hillhouse has demonstrated interesting transformations of primary phosphido ligands to terminal phosphinidene ligands. The Ni(I) complex [Ni(dtbpe)(PHAr)] (dtbpe = 1,2-bis(di-*tert*-butylphosphino)ethane, Ar = 2,6-dimesitylphenyl), obtained from [Ni(μ-Cl)(dtbpe)]$_2$ and two equivalents of LiPHAr, can undergo one-electron oxidation to give the planar phosphido cation [Ni(=PHAr)(dtbpe)]$^+$. Deprotonation with NaN(SiMe$_3$)$_2$ results in the nickel phosphinidene complex [Ni(PAr)(dtbpe)] (Scheme 1.35).[105] A more facile route was reported later by Hillhouse, involving a free radical hydrogen-atom abstraction process.[106]

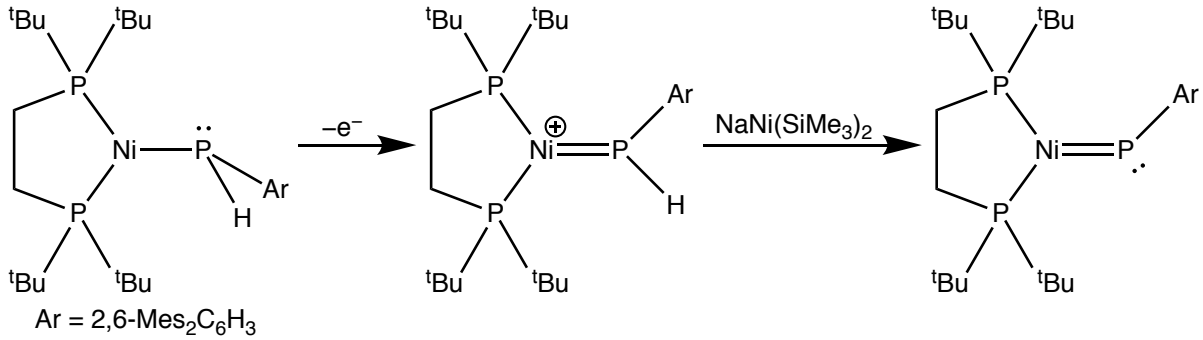

Scheme 1.35. Synthesis of a terminal phosphinidene complex via *oxidation and deprotonation of a nickel phosphido complex*

Cummins has also implicated a primary phosphido complex as a key intermediate en route to a terminal phosphinidene complex.[107] The phosphinidene complex [Ta{N(CH$_2$^{t}Bu)Ar}$_3$(PPh)] (Ar = 3,5-Me$_2$C$_6$H$_3$) was initially obtained from [TaH{N(CH$_2$^{t}Bu)Ar}$_2${η^2-ArNCH^{t}Bu}] and PH$_2$Ph,

but in low *in situ* yield. A modified procedure was developed which utilised the halide [TaCl{N(CH$_2$^{t}Bu)Ar}$_2${η^2-ArNCH^{t}Bu}] and 1.5 equivalents of LiPHR (R = Cy, Ph), yielding the complexes [Ta{N(CH$_2$^{t}Bu)Ar}$_3$(PR)] (R = Cy, Ph) (Scheme 1.36). A phosphido complex was postulated to be an intermediate for the formation of both phosphinidene complexes, and was directly isolated for the phenyl substituent. Treatment of this intermediate with additional LiPHPh gave the aforementioned phenylphosphinidene complex, indicating the overall transfer of the phosphorus H atom to the α-carbon of the adjacent three-membered ring (Scheme 1.36).

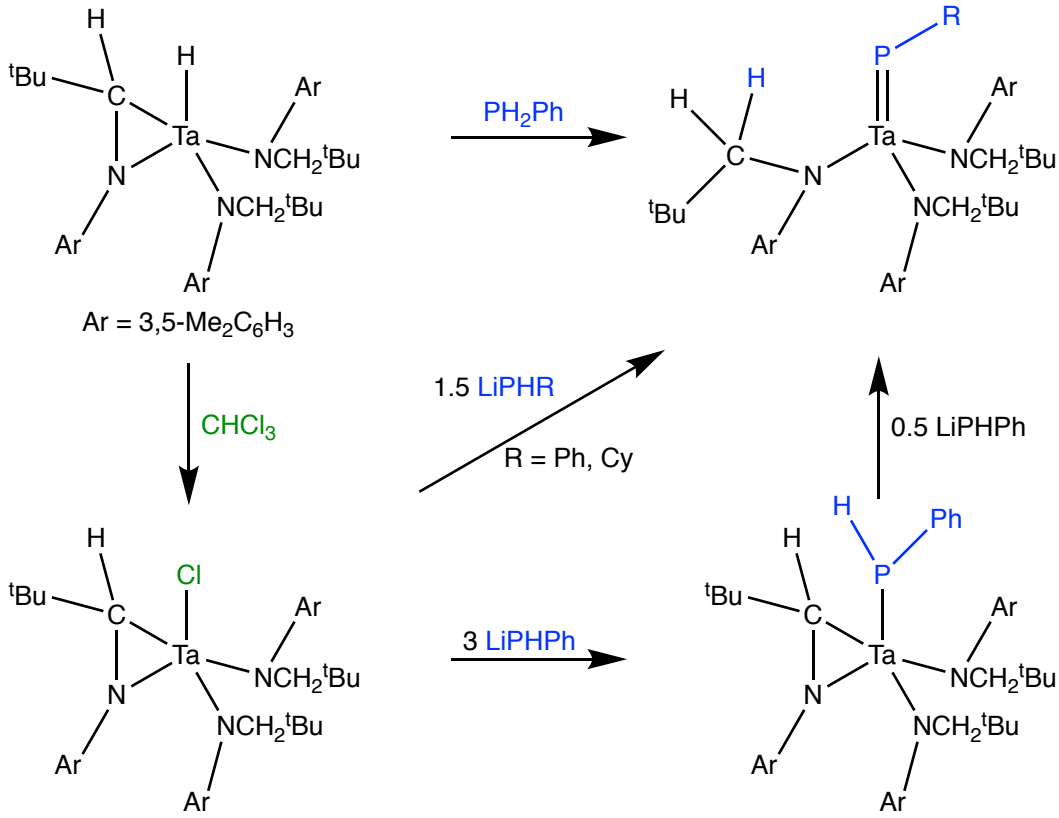

Scheme 1.36. Cummins' synthesis of a terminal phosphinidene complex via *a primary phosphido intermediate*

Chen reported the use of a primary phosphido complex to form a phosphinidene-bridged species.[108] Initially, the diketiminate-substituted complex [ScMe{PH(Ar)}{MeC(NAr)CHC(NAr)Me}] (Ar = 2,6-^{i}Pr$_2$C$_6$H$_3$) was observed to undergo methane elimination to give a mixture of [Sc$_2$(μ-CH$_2$)(μ-PAr){MeC(NAr)CHC(NAr)Me}$_2$] and [Sc(PHAr)$_2${MeC(NAr)CHC(NAr)Me}]. The dinuclear methylidene- and phosphinidene-bridged complex could be directly obtained from the reaction between [ScMe{PH(Ar)}{MeC(NAr)CHC(NAr)Me}] and [ScMe$_2${MeC(NAr)CHC(NAr)Me}] (Scheme 1.37).

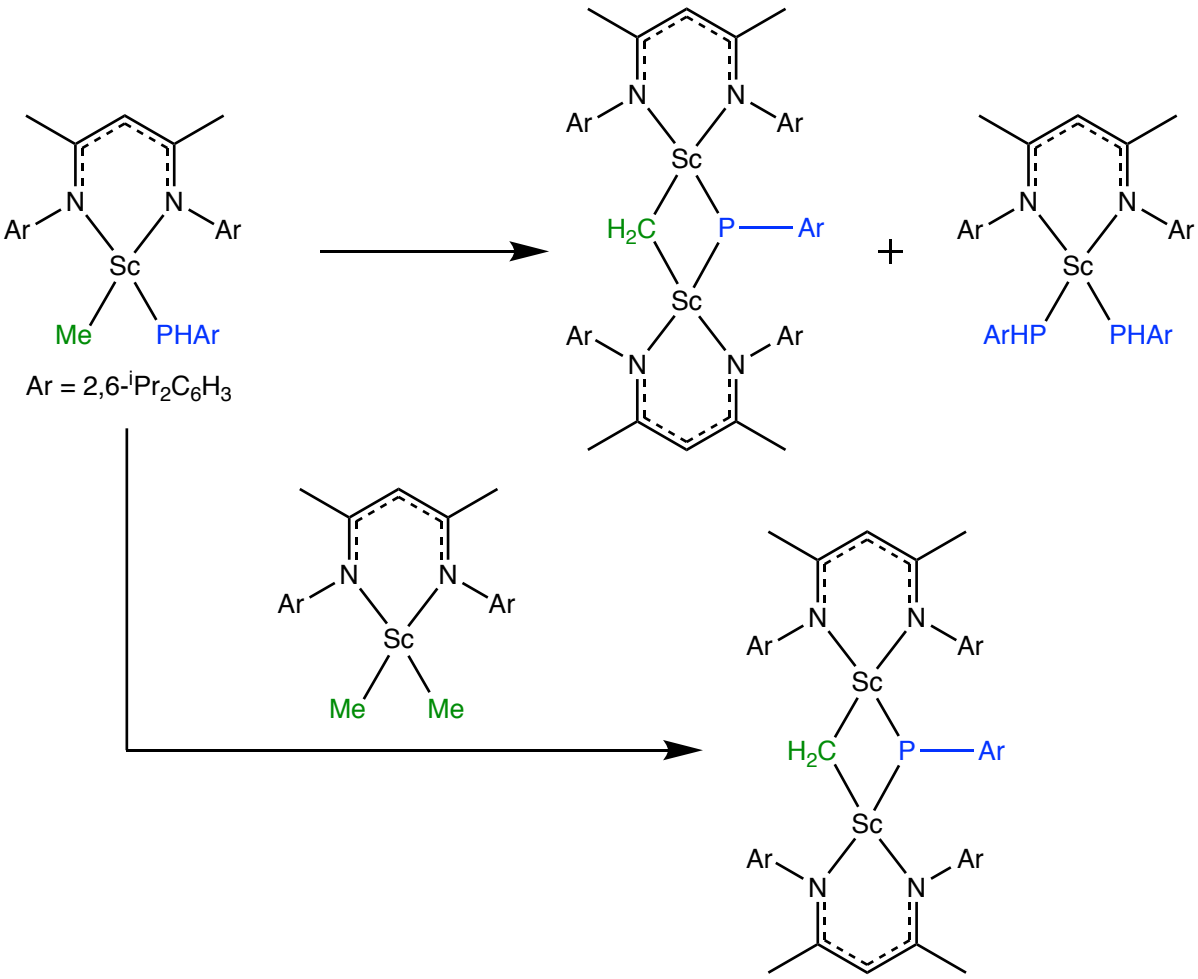

Scheme 1.37. Decomposition and reactivity of a scandium phosphido species

Primary phosphido rare-earth metal complexes have been shown to react with $O{=}PPh_3$. The complexes [M(Me)(PHAr)(L)] (L = MeC{N(2,6-$^{i}Pr_2C_6H_3$)}CHC(Me)($NCH_2CH_2NMe_2$); M = Sc, Lu; Ar = 2,4,6-$^{t}Bu_3C_6H_2$, 2,6-$^{i}Pr_2C_6H_3$, 2,6-$Me_2C_6H_3$) form the products [M(Ph){κ^2-$CH_2P(O)Ph_2$}(L)] upon the additon of $O{=}PPh_3$ (Scheme 1.38).[109] The elimination of a primary phosphine was observed, rather than the expected elimination of methane. Additionally, a P–C(aryl) bond has been broken in favour of a P–C(alkyl) bond. The likely mechanism proposed by the authors involves $O{=}PPh_3$ coordination to the metal centre followed by nucleophilic attack of the methyl group to the phosphorus atom with the attendant shift of a phenyl group to the metal centre. The phosphido group then abstracts hydrogen from the $O{=}PMePh_2$ ligand to give free phosphine and the newly-formed bidentate ligand (Scheme 1.38).

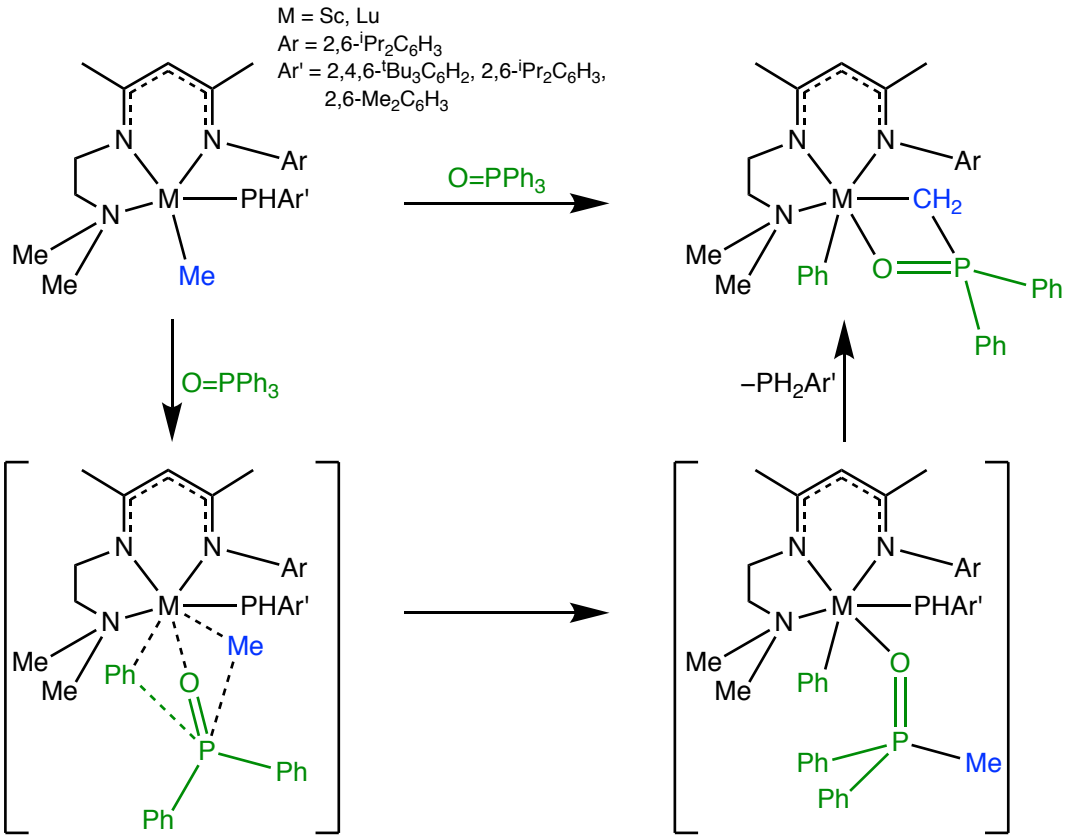

Scheme 1.38. Reaction of primary phosphido rare-earth complexes with triphenylphosphine oxide

As previously discussed, the coordination of a carbene-stabilised phosphinidene presents a relatively new method towards the synthesis of a phosphido-type product. Following the synthesis of the N-heterocyclic carbene-stabilised parent phosphinidene[110-112] only one study has been undertaken into the reactivity of its metal complexes. In an attempt to establish the reactivity of the phosphorus lone pair in [W(CO)$_5${PH(IMes)}] through the addition of excess [W(CO)$_5$(THF)] a clean product could not be obtained; only mixtures of mono- and bimetallic species were observed (Scheme 1.39).[113]

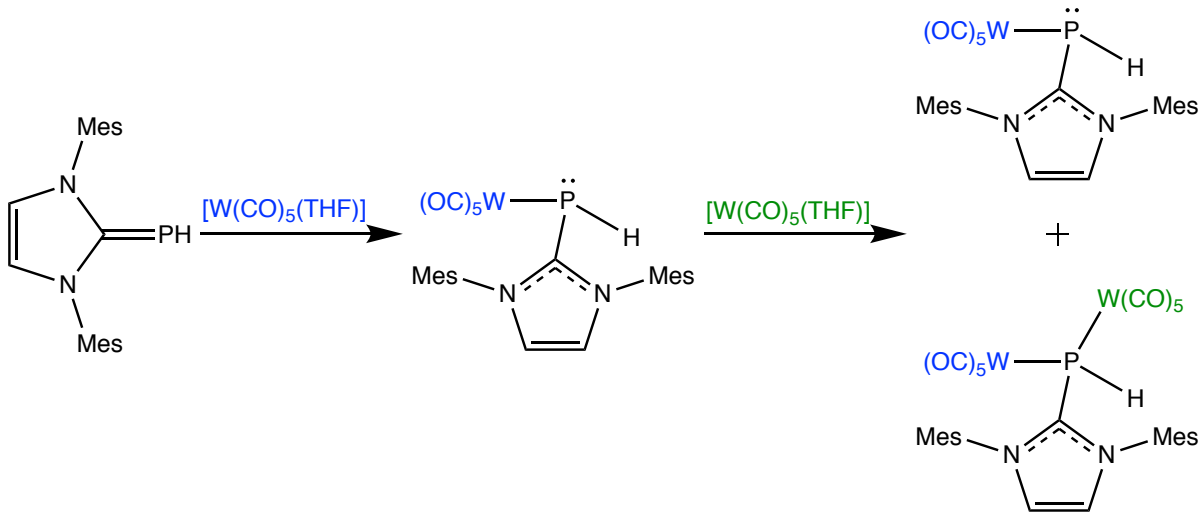

Scheme 1.39. Attempted formation of carbene-phosphinidene-bridged dimers

An interesting example of intramolecular reactivity displayed by a phosphido complex was reported by Smith.[114] The tris(carbene)borate-substituted complex [Fe(PHPh){κ^3-B(Ph)(MesIm)$_3$}] (MesIm = *N'*-mesityl-*N*-imidazolyl) spontaneously undergoes C–H activation of one mesityl group to give a new hydride complex in which the phosphorus atom is bonded to the mesityl ring to form a new metallacycle (Scheme 1.40). Isotopic labelling showed that the metal hydride originates from the phosphorus atom. Furthermore, computational investigation indicated that the most likely intermediate was an arrested α-hydride-migration product in which the phosphorus atom is highly nucleophilic. The accentuated reactivity of the phosphorus allows it to undergo a C–H insertion reaction. Further C–H activation occurs upon heating, with an overall loss of H_2 (Scheme 1.40).

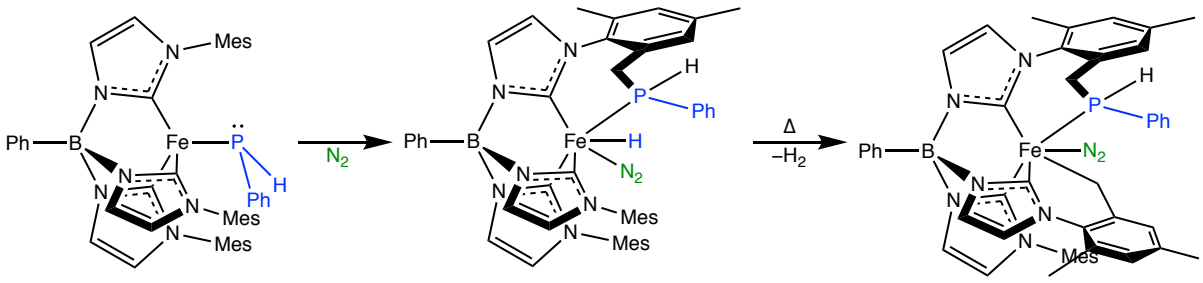

Scheme 1.40. Smith's intramolecular reactivity of a phosphido complex

1.3 Project Aims

Primary phosphines have an established synthetic utility, but they have remained relatively understudied compared to other phosphines. The factors that limit their prevalence, lower reactivity and higher instability, may all be ameliorated upon coordination to a metal centre. Indeed, by accessing phosphido complexes derived from primary phosphines the special properties of the terminal phosphido ligand may then be exploited for further chemistry. Therefore, the work detailed in this thesis aims to synthesise new primary phosphine complexes with the goal of obtaining their respective phosphido complexes. The properties and reactivities of the phosphido complexes may then be studied with the overarching objective of developing unique phosphorus-based architectures.

Firstly, ruthenium phosphine and phosphido complexes bearing the hydrotris(pyrazolyl)borate ligand were pursued (Chapter 2). Next, octahedral complexes bearing the π-acidic CO ligand were studied with the goal of mitigating the reactivity observed for the phosphido complex phosphorus lone pair. Studies in this area also led to complexes bearing the unusual PH(OMe)Cy. This ligand is unstable in its free state, and further investigations into these complexes were undertaken (Chapter 3). The synthesis of a new phosphido complex which was relatively amenable to experimental investigation is detailed in Chapter 4. Investigations into the dynamic behaviour of the phosphido complex and its reactions with selected electrophiles are also included in the same chapter. Finally, research into adduct formation of the new phosphido complex with chalcogens and the reactivity of the chalcogenide products are discussed in Chapter 5.

CHAPTER 2
Complexes Derived From [RuCl(PPh$_3$)$_2$(Tp)]

Chapter 2: Complexes Derived From [RuCl(PPh$_3$)$_2$(Tp)]

2.1 Introduction

Molecules bearing tris(pyrazolyl)borate ligands (Figure 2.1) were deemed desirable as a starting point to begin research into primary phosphine complexes and their phosphido derivatives. Such ligands coordinate facially to a metal centre through the three pyrazolyl rings, essentially rendering these coordination sites inert. Reactivity may then be directed towards the three remaining sites. Consequently, tris(pyrazolyl)borate ligands have found significant utility as support ligands and their use has been well documented.[115-118]

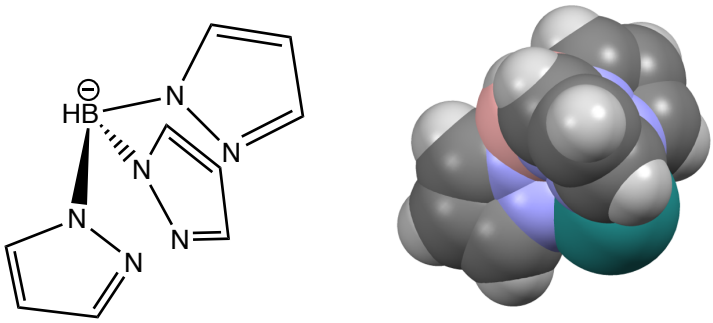

Figure 2.1. The parent tris(pyrazolyl)borate ligand, hydrotris(pyrazolyl)borate (left) and a space-filling representation of its coordination to a metal centre (right)

Gunnoe demonstrated the capability of tris(pyrazolyl)borate ligands to support low-coordinate Group 15-transition metal chemistry through his work on amine and amido complexes (Scheme 2.1).[119-124] Complexes of the type [Ru(NH$_2$R)(CO)(PPh$_3$)(Tp)]$^+$ (R = H, Ph, ^{t}Bu; Tp = hydrotris(pyrazolyl)borate) and [Ru(NH$_2$R)(L)$_2$(Tp)]$^+$ (R = H, Ph, ^{t}Bu; L = PMe$_3$, P(OMe)$_3$, CO) and their corresponding conjugate base amido complexes were studied. Gunnoe was able to demonstrate that the π-electron repulsion between the filled (d^6) metal d orbitals and the lone pair of the heteroatom observed for phosphido complexes (See Section 1.2.2) was also present in amido complexes. The interaction results in the significant basicity of the nitrogen lone pair, such that the amido complexes are sufficiently basic to deprotonate phenylacetylene and 1,4-cyclohexadiene.

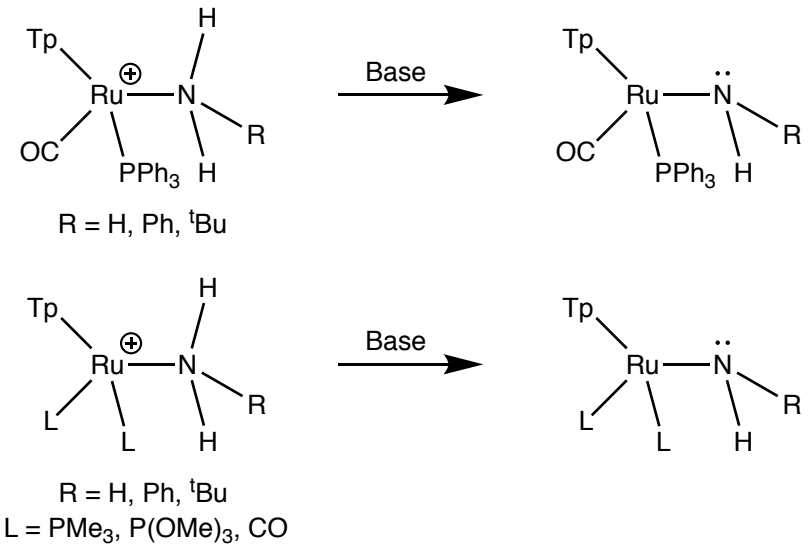

Scheme 2.1. Gunnoe's amine and amido complexes

The complex [RuCl(PPh$_3$)$_2$(Tp)] was chosen as the initial starting material[125] because the synthesis of this complex on a large scale is well-established and it provides multiple avenues into further functionalisation.[126] Specifically, the presence of both PPh$_3$ and Cl ligands provide potentially-labile groups to access new complexes *via* substitution.

Of the wide variety of primary phosphines available, cyclohexylphosphine (PH$_2$Cy) was selected for this work. It was expected that the cyclohexyl substituent could provide sufficient steric bulk to facilitate low-coordinate phosphorus chemistry (see Section 1.1.1). Additionally, the cyclohexyl resonances should appear in the low frequency alkyl region of the ^{1}H and ^{13}C{^{1}H} NMR spectra. This positions them separately from the aromatic resonances of the expected Tp and PPh$_3$ co-ligands, decluttering the spectra and allowing for more straightforward characterisation.

The work presented in this chapter focuses on ruthenium cyclohexylphosphine complexes derived from [RuCl(PPh$_3$)$_2$(Tp)]. The substitution chemistry of [RuCl(PPh$_3$)$_2$(Tp)] with PH$_2$Cy was investigated with the goal of synthesising a library of new compounds. Deprotonation reactions of each of the cyclohexylphosphine complexes were then explored with the ultimate goal of obtaining a convenient primary phosphido complex precursor which can serve as a springboard into in-depth reactivity studies.

2.2 Substitution Reactions

2.2.1 Synthesis of [RuCl(PPh$_3$)(PH$_2$Cy)(Tp)]

Substitution of PPh_3 in $[RuCl(PPh_3)_2(Tp)]$ for PH_2Cy was the first experiment conducted. In order to favour substitution of the neutral ligand, rather than ionisation of the halide, the reaction was conducted in the non-polar solvent toluene. Thus, a toluene solution of $[RuCl(PPh_3)_2(Tp)]$ and PH_2Cy was stirred at room temperature to furnish $[RuCl(PPh_3)(PH_2Cy)(Tp)]$ as a yellow solid in 83% yield (Scheme 2.2).

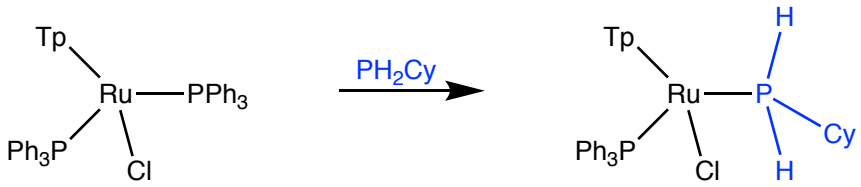

Scheme 2.2. Synthesis of [RuCl(PPh$_3$)(PH$_2$Cy)(Tp)]

The ^{1}H NMR data agreed with the formation of $[RuCl(PPh_3)(PH_2Cy)(Tp)]$. Each pyrazolyl ring is *trans* to a unique group, rendering them inequivalent and resulting in the observation of nine distinct resonances. The asymmetry at the ruthenium centre also manifested in the appearance of two distinct P–H resonances. These two hydrogen atoms are diastereotopic,[127] and therefore appear as separate signals at δ_H 4.32 and 3.89. Both resonances showed a one-bond coupling to phosphorus of 328 Hz, but the smaller couplings (to the geminal H, $^2J_{HH}$; to PPh_3, $^3J_{PH}$; and to the H at the 1 position of the Cy ring, $^3J_{HH}$) could not be resolved (^{1}H nuclei observed at 400.1 MHz). The appearance of a multiplets in the region 1.54–0.59 ppm indicated the introduction of the cyclohexyl group. No resonances in this region were sufficiently separated to be assigned. Multiplets between 7.33–7.23 ppm were observed for the PPh_3 group.

In general, the $^{13}C\{^1H\}$ NMR data were in good agreement with the ^{1}H NMR data. As in the ^{1}H spectrum, nine pyrazolyl resonances were observed. Additionally, six separate cyclohexyl resonances were present due to the asymmetric nature of the molecule. Finally, there were four phenyl signals due to the PPh_3 group. The *ipso*, *ortho* and *meta* positions relative to the phosphorus substituent all displayed J_{PC} coupling.

The $^{31}P\{^1H\}$ NMR spectrum of [RuCl(PPh$_3$)(PH$_2$Cy)(Tp)] contained two mutually-coupled doublets ($^2J_{PP}$ = 32 Hz) at δ_P 49.3 and 15.1. The latter resonance is due to the PH$_2$Cy group, as it appears as a triplet with a $^1J_{PH}$ of 327 Hz in the ^{31}P NMR spectrum.

2.2.2 Synthesis of [RuCl(PH$_2$Cy)$_2$(Tp)]

Following the successful synthesis of [RuCl(PPh$_3$)(PH$_2$Cy)(Tp)], the synthesis of [RuCl(PH$_2$Cy)$_2$(Tp)] was pursued to determine if the substitution of both PPh$_3$ ligands from [RuCl(PPh$_3$)$_2$(Tp)] for PH$_2$Cy was possible (Scheme 2.3). Stirring a toluene solution of [RuCl(PPh$_3$)$_2$(Tp)] with two equivalents of PH$_2$Cy at room temperature for 5 days resulted only in the formation of [RuCl(PPh$_3$)(PH$_2$Cy)(Tp)]. To promote the second substitution the mixture was heated under reflux in toluene. After 96 hours of heating, only trace amounts of [RuCl(PPh$_3$)(PH$_2$Cy)(Tp)] were detected in an aliquot of the reaction mixture. However, upon workup the product still contained *ca*. 6% [RuCl(PPh$_3$)(PH$_2$Cy)(Tp)] as estimated by $^{31}P\{^1H\}$ NMR spectroscopy, a higher percentage than observed in the reaction mixture. The increased proportion of [RuCl(PPh$_3$)(PH$_2$Cy)(Tp)] following workup is expected to be due to the loss of other products and indicates the difficulty of resolving mixtures [RuCl(PPh$_3$)(PH$_2$Cy)(Tp)] and [RuCl(PH$_2$Cy)$_2$(Tp)].

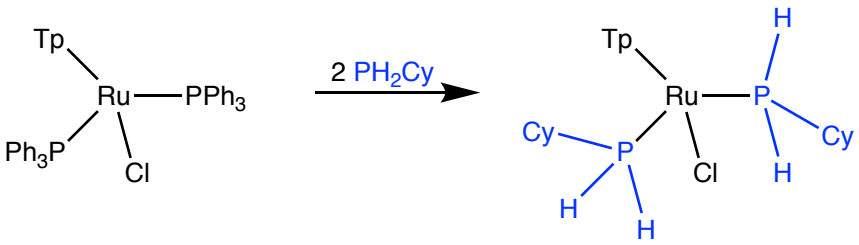

Scheme 2.3. Synthesis of [RuCl(PH$_2$Cy)$_2$(Tp)]

The substitution of the second PPh$_3$ group was clearly indicated in the spectral data. A single $^{31}P\{^1H\}$ NMR resonance at δ_P 9.6 was observed, indicating the presence of only one phosphorus environment. This resonance split into an apparent triplet ($^1J_{PH}$ = 326 Hz) in the absence of ^1H decoupling, demonstrating that it arises from a PH$_2$ group. Additionally, no aromatic PPh$_3$ resonances were observed in either the ^1H or $^{13}C\{^1H\}$ NMR spectra. Finally, the correct isotopic distribution was observed at *m/z* 582.1303 in the high resolution ESI mass

spectrum, in good agreement with the calculated value of 582.1302 for $C_{21}H_{36}{}^{11}B^{35}ClN_6P_2{}^{102}Ru$ (*i.e.* $[RuCl(PH_2Cy)_2(Tp)]^+$).

Introducing a second PH_2Cy ligand results in an increased symmetry (time-averaged C_S) in $[RuCl(PH_2Cy)_2(Tp)]$ compared to $[RuCl(PPh_3)(PH_2Cy)(Tp)]$. A mirror plane bisects the P−Ru−P angle in $[RuCl(PH_2Cy)_2(Tp)]$, and this phenomenon is inferred spectroscopically. There are only two sets of pyrazolyl resonances in the ^1H and $^{13}C\{^1H\}$ NMR spectra. The two sets appear in a 2:1 ratio for the two rings *trans* to PH_2Cy compared to the one ring *trans* to the Cl. Despite the mirror plane, the P−H atoms are chemically inequivalent and symmetry-equivalent pairs are related *via* reflection in this plane. Accordingly, there are two doublets at δ_H 4.62 ($^1J_{PH}$ = 324 Hz) and 4.30 ($^1J_{PH}$ = 316 Hz) in the ^1H NMR spectrum. In a similar manner, each carbon of the cyclohexyl ring is in a unique environment and there are six cyclohexyl resonances in the $^{13}C\{^1H\}$ NMR spectrum.

2.2.3 Synthesis of $[Ru(PPh_3)(PH_2Cy)_2(Tp)]PF_6$

In addition to the substitution of neutral PPh_3 from $[RuCl(PPh_3)_2(Tp)]$, the substitution of Cl to form a cationic complex was also explored. Cationic complexes were deemed desirable as this would be expected to make the subsequent deprotonation more favourable.

Conditions for the reaction were adapted from the work of Sun and Simpson, who reported the substitution of Cl for PMe_3 from the neutral complex $[RuCl(CO)(PPh_3)(Tp)]$.[128] The addition of one equivalent of PH_2Cy to a mixture of $[RuCl(PPh_3)_2(Tp)]$ and $NaPF_6$ in MeOH resulted in the formation of a mixture of $[RuCl(PPh_3)_2(Tp)]$, $[RuCl(PPh_3)(PH_2Cy)(Tp)]$ and *bis*-substituted product $[Ru(PPh_3)(PH_2Cy)_2(Tp)]PF_6$ (Scheme 2.4). No $^{31}P\{^1H\}$ NMR resonances which could be attributed to $[Ru(PPh_3)_2(PH_2Cy)(Tp)]PF_6$ were detected. This observation implies that, even in a polar solvent, the substitution of Cl is slow compared to PPh_3. Additionally, the rate of Cl substitution is faster for $[RuCl(PPh_3)(PH_2Cy)(Tp)]$ than for $[RuCl(PPh_3)_2(Tp)]$. The reason for this difference in substitution rate could be the reduced steric bulk in $[RuCl(PPh_3)(PH_2Cy)(Tp)]$ which contains one PPh_3 group instead of two (%V_{buried} for 3.5 Å radius sphere[129] PH_2Cy: 20.3; PPh_3: 26.2). The salt $[Ru(PPh_3)(PH_2Cy)_2(Tp)]PF_6$ could be directly obtained in 75% yield through the use of excess PH_2Cy (Scheme 2.5).

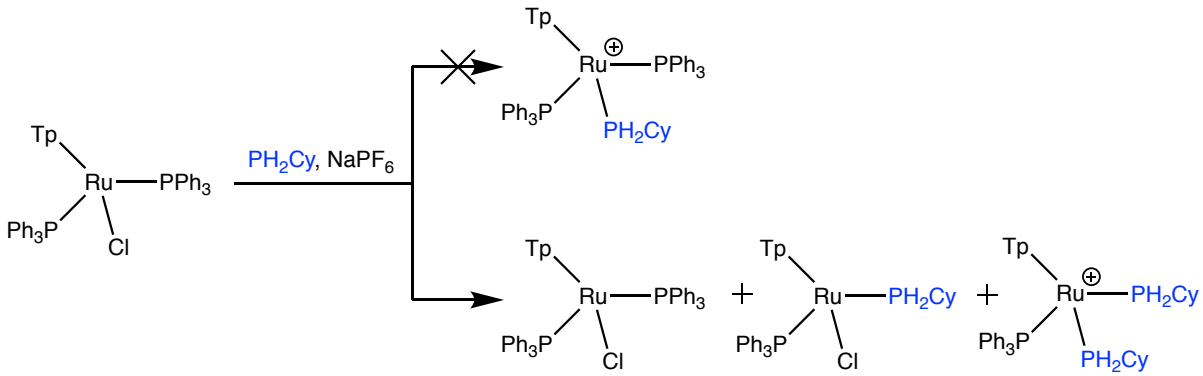

Scheme 2.4. Attempted synthesis of $[Ru(PPh_3)_2(PH_2Cy)(Tp)]^+$

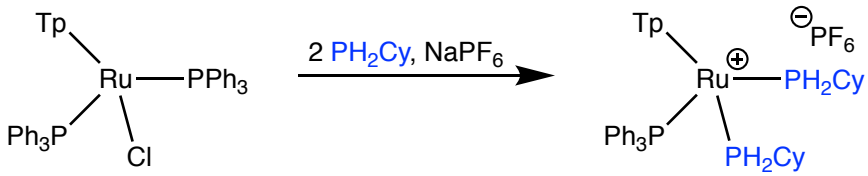

Scheme 2.5. Synthesis of $[Ru(PPh_3)(PH_2Cy)_2(Tp)]PF_6$

The resonances for $[Ru(PPh_3)(PH_2Cy)_2(Tp)]^+$ were easily identified in the $^{31}P\{^1H\}$ NMR spectrum. The PPh_3 group appeared as a triplet at δ_P 44.9, coupled to the phosphorus nuclei of two equivalent PH_2Cy groups. These PH_2Cy groups gave rise to a doublet at δ_P 3.8, which further split into a triplet with $^1J_{PH}$ = 337 Hz in the absence of ^1H decoupling. A septet at δ_P −143.4 was present for the PF_6^- anion.

As for C_S-symmetric $[RuCl(PH_2Cy)_2(Tp)]$ above, the $[Ru(PPh_3)(PH_2Cy)_2(Tp)]^+$ cation contains a plane of symmetry which bisects the CyH_2P−Ru−PH_2Cy angle. The symmetry renders two of the three pyrazolyl rings equivalent and is apparent in both the ^1H and $^{13}C\{^1H\}$ NMR spectra, with the corresponding resonances appearing in a 2:1 ratio. Additionally, each carbon in a cyclohexyl ring becomes inequivalent and symmetry-equivalent pairs occur between the two rings. Accordingly, six carbon resonances for the cyclohexyl rings are observed in the $^{13}C\{^1H\}$ NMR spectrum.

Curiously, virtual coupling is observed for the cyclohexyl resonances in the $^{13}C\{^1H\}$ NMR spectrum (Figure 2.2). Virtual coupling is a phenomenon in which a nucleus which would ordinarily couple to two nuclei with very different *J* values couples to them as if they were

identical. Such a phenomenon arises when the two chemically equivalent, but magnetically inequivalent, nuclei in question are strongly coupled to each other. While virtual coupling is usually observed in *trans*-disposed phosphines which are strongly coupled through a shared metal orbital (typically 200-300 Hz for *trans*-RuP$_2$ but 20-30 Hz for *cis*-RuP$_2$), *cis* virtual coupling is still known.[130] In this case the 1, 2 and 6 carbons of the cyclohexyl ring couple to the PH$_2$Cy phosphorus atoms as if they were equivalent, appearing as apparent triplets at δ_C 29.8 (1), 27.1 (2 or 6) and 26.8 (2 or 6) in the spectrum. Focusing on the signal at δ_C 29.8, the resonance shows a reduced-intensity central peak characteristic of virtual coupling.[131] Also present are two low-intensity peaks either side of the signal, a phenomenon commonly observed during virtual coupling[131] as well as other higher-order patterns. Another feature of virtual coupling is that the *J* value measured from the observed multiplet is the average of the individual constants between the nuclei. As such, the observed J_{PC} values of 14 and 5 Hz are much reduced from the corresponding values in [RuCl(PPh$_3$)(PH$_2$Cy)(Tp)] (26 and 10 Hz, respectively).

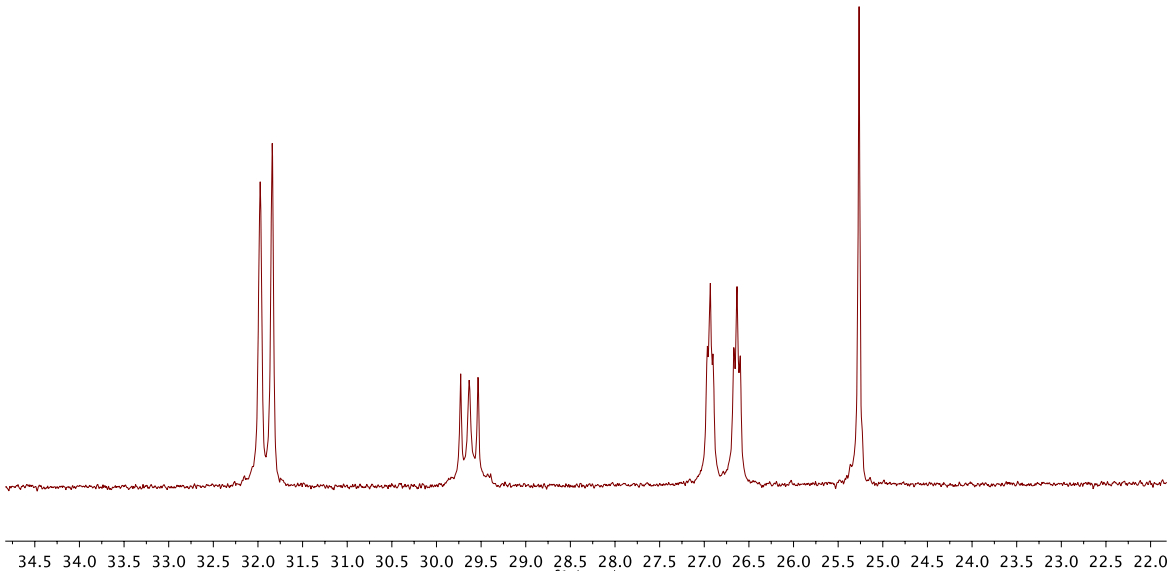

Figure 2.2. Cyclohexyl $^{13}C\{^1H\}$ NMR resonances of [Ru(PPh$_3$)(PH$_2$Cy)$_2$(Tp)]$^+$

Crystals of [Ru(PPh$_3$)(PH$_2$Cy)(Tp)]PF$_6$ were grown by vapour diffusion of Et$_2$O into a CH$_2$Cl$_2$ solution of the compound. The molecular structure of the cation (Figure 2.3) shows the presence of two PH$_2$Cy ligands and one PPh$_3$ ligand at the Ru centre. The PH$_2$Cy groups have shorter Ru−P distances (2.2899(8) and 2.2900(8) Å) compared to the PPh$_3$ ligand (2.3441(7) Å). The discrepancy likely arises from the reduced steric bulk of the primary *versus* tertiary

phosphine, with a small contribution due to the difference in basicities (Calculated Tolman Electronic Parameters:[132] PH_2Cy = 2072.8, PPh_3 = 2069.0). Additionally, the P−Ru−P angle is much smaller between the PH_2Cy groups (65.16(3)°) compared to those between PH_2Cy and PPh_3 (96.12(3)° and 95.69(3)°). The Ru−N bond lengths are equal within statistical significance (2.155(2), 2.158(2) and 2.146(2) Å), implying that there is no major *trans* influence difference between PH_2Cy and PPh_3. Three of the P−H hydrogen atoms are close to fluorine atoms of the PF_6 atom (Figure 2.4). These H···F distances range from 2.510−2.916 Å ($\Sigma_{\text{van der Waals radii}}$ = 2.57 Å).

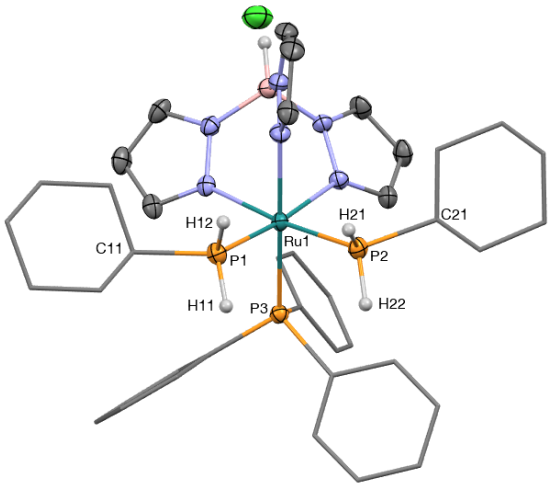

Figure 2.3. Molecular structure of [Ru(PPh$_3$)(PH$_2$Cy)$_2$(Tp)]$^+$ in a crystal of [Ru(PPh$_3$)(PH$_2$Cy)$_2$(Tp)]PF$_6$ (50% displacement ellipsoids, hexafluorophosphate anion and most H atoms omitted, phenyl and cyclohexyl rings simplified). Selected bond lengths (Å) and angles (°): Ru1−P1 2.2899(8), Ru1−P2 2.2900(8), Ru1−P3 2.3441(7), P1−C11 1.837(3), P2−C21 1.844(3), P1−H11 1.28(3), P1−H12 1.31(3), P2−H21 1.32(3), P2−H22 1.26(3), P1−Ru1−P2 85.16(3), P1−Ru1−P3 96.12(3), P2−Ru1−P3 95.69(3), H11−P1−H12 95(2), H21−P2−H22 97(2).

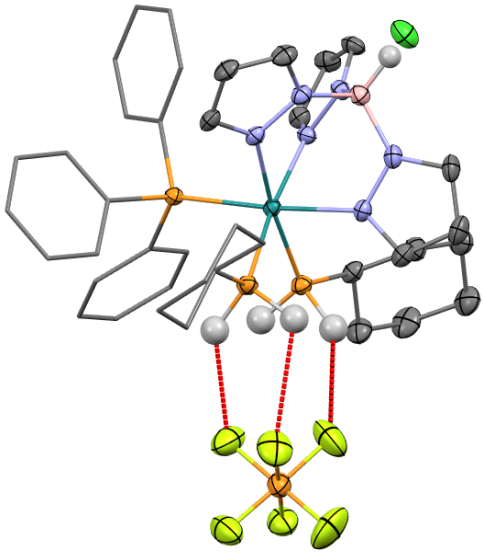

Figure 2.4. H···F interactions (red) in a crystal of [Ru(PPh$_3$)(PH$_2$Cy)$_2$(Tp)]PF$_6$

An interesting feature of the molecular structure is that the fourth substituent at boron is disordered between an H atom and a Cl atom in an 89:11 ratio. Upon closer inspection of the $^{31}P\{^1H\}$ NMR spectrum resonances for [Ru(PPh$_3$)(PH$_2$Cy)$_2$(^{Cl}Tp)]$^+$ (^{Cl}Tp = ClB(pz)$_3$) were present at δ_P 44.1 and 3.3. These resonances were estimated to comprise approximately 6% of the mixture by integration. A peak for [Ru(PPh$_3$)(PH$_2$Cy)$_2$(^{Cl}Tp)]$^+$ at *m/z* 842.2 was also present in the ESI mass spectrum, although its intensity was 1% of the [Ru(PPh$_3$)(PH$_2$Cy)$_2$(Tp)]$^+$ base peak. The sample also returned satisfactory elemental analysis results, suggesting a high level of bulk purity.

The presence of [Ru(PPh$_3$)(PH$_2$Cy)$_2$(^{Cl}Tp)]$^+$ is likely due to contamination of the original sample of [RuCl(PPh$_3$)$_2$(Tp)] with [RuCl(PPh$_3$)$_2$(^{Cl}Tp)]. The preparation of [RuCl(PPh$_3$)$_2$(Tp)] is known to produce the side product [RuH(PPh$_3$)$_2$(^{Cl}Tp)], which in turn reacts with CH_2Cl_2 or $CHCl_3$ to generate [RuCl(PPh$_3$)$_2$(^{Cl}Tp)].[133] Further investigation into the formation of [RuH(PPh$_3$)$_2$(^{Cl}Tp)] showed that the chlorination of boron occurs before complete tridentate coordination of Tp, and that the fully-closed TpRu cage is chemically robust. Therefore, it is unlikely that [Ru(PPh$_3$)(PH$_2$Cy)$_2$(^{Cl}Tp)]$^+$ forms in the latter stages of the synthesis of [Ru(PPh$_3$)(PH$_2$Cy)$_2$(Tp)]PF$_6$.

2.2.4 Synthesis of [Ru(PH$_2$Cy)(dppf)(Tp)]PF$_6$

While the synthesis of [Ru(PPh$_3$)(PH$_2$Cy)$_2$(Tp)]PF$_6$ presents a primary phosphine-containing, cationic complex, the presence of two PH$_2$Cy groups may complicate the intended deprotonation. Obtaining a cationic complex only containing a single PH$_2$Cy ligand was still desirable, so the introduction of bidentate ligands to provide coordinative stability was investigated.

The reaction of [RuCl(PPh$_3$)$_2$(Tp)] with a range of bidentate phosphines has been reported to yield the complexes [RuCl(L^2)(Tp)] (L^2 = dppm, dppe, dppf; dppm = 1,2-bis(diphenylphosphino)methane, dppf = 1,1'-bis(diphenylphosphino)ferrocene) (Scheme 2.6).[134] Of these three complexes the dppm and dppe variants were reported to be insoluble in a range of solvents, so the dppf complex was chosen for study.

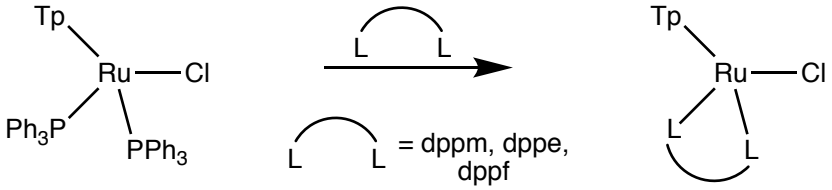

Scheme 2.6. The reaction of [RuCl(PPh$_3$)$_2$(Tp)] with bidentate phosphines

In conditions analogous to the synthesis of [Ru(PPh$_3$)(PH$_2$Cy)$_2$(Tp)]PF$_6$, stirring a mixture of [RuCl(dppf)(Tp)], NaPF$_6$ and PH$_2$Cy in MeOH gave [Ru(PH$_2$Cy)(dppf)(Tp)]PF$_6$ in 61% yield (Scheme 2.7). The salt [Ru(PH$_2$Cy)(dppf)(Tp)]PF$_6$ was identified in the ^{31}P{^{1}H} NMR spectrum *via* a doublet at δ_P 41.6 and a triplet at δ_P 19.8 ($^2J_{PP}$ = 28 Hz). A septet at δ_P −143.4 was also present for the PF_6^- anion. The resonance at δ_P 19.8 appears as a triplet ($^1J_{PH}$ = 340 Hz) in the ^{31}P NMR spectrum, consistent with the presence of one PH$_2$Cy group.

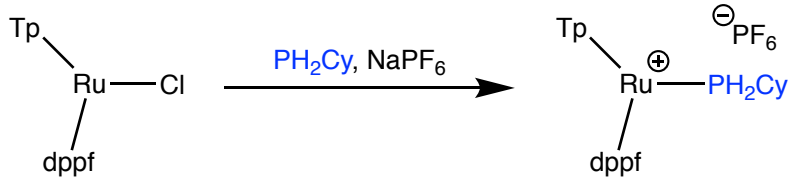

Scheme 2.7. Synthesis of [Ru(PH$_2$Cy)(dppf)(Tp)]PF$_6$

The plane of symmetry in [Ru(PH$_2$Cy)(dppf)(Tp)]$^+$ bisects the Ph$_2$P–Ru–PPh$_2$ angle, and contains the phosphorus atom of the PH$_2$Cy group. This symmetry is evident in the NMR spectra, with only one P–H ^{1}H NMR resonance at δ_H 3.08 ($^1J_{PH}$ = 340 Hz). There are four

cyclohexyl $^{13}C\{^1H\}$ NMR resonances, further indicating the presence of symmetry-equivalent groups. A distinct 2:1 ratio of the pyrazolyl resonances in both the ^1H and $^{13}C\{^1H\}$ NMR is also observed.

While the symmetry results in a reduced number of resonances due to the PH_2Cy group, there are an increased number of resonances for the dppf ligand. The two phenyl substituents at each phosphorus atom of the dppf are inequivalent, resulting in two sets of phenyl resonances in the $^{13}C\{^1H\}$ NMR spectrum. Similarly, each carbon in the cyclopentadienyl ring gives rise to a distinct $^{13}C\{^1H\}$ NMR resonance. The resonance of the cyclopentadienyl carbon directly bound to phosphorus interestingly displays virtual coupling to the other dppf phosphorus atom, appearing as a triplet with an apparent J_{PC} of 24 Hz.

An X-ray diffraction study confirmed the molecular structure of $[Ru(PH_2Cy)(dppf)(Tp)]^+$ (Figure 2.5). The molecular structure shows the coordination of a single PH_2Cy group to the ruthenium centre, in addition to the dppf and Tp ligands. The Ru−PH_2Cy distance (2.3115(5) Å) is shorter than the two Ru−PPh_2 distances (2.3526(5) and 2.3751(5) Å), likely due to the much smaller steric bulk of the primary phosphine. There is a 0.0225 Å (45 e.s.d.) difference in the Ru−PPh_2 bond lengths. This difference probably arises from packing effects, with the PPh_2 closer to the cyclohexyl group having the longer Ru−P distance to minimise steric interactions (Figure 2.6). The Ru−N distances (2.1381(15), 2.1356(16) and 2.1376(16) Å) are equal within statistical variance, suggesting that the *trans* influences of PH_2Cy and dppf are comparable.

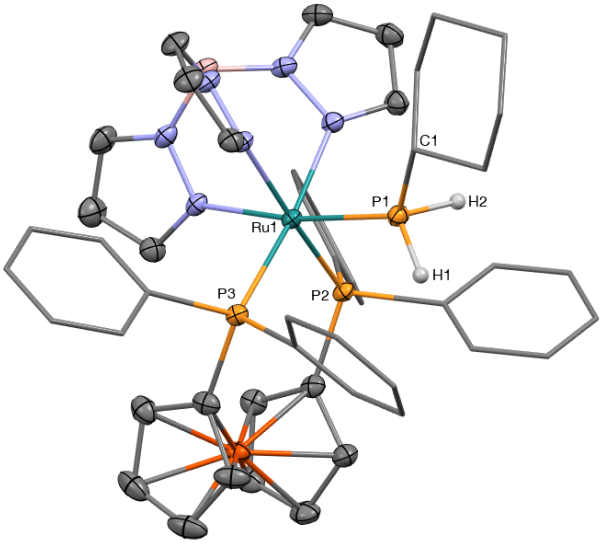

Figure 2.5. Molecular structure of [Ru(PH$_2$Cy)(dppf)(Tp)]$^+$ in a crystal of [Ru(PH$_2$Cy)(dppf)(Tp)]PF$_6$ (50% displacement ellipsoids, hexafluorophosphate anion and most H atoms omitted, phenyl and cyclohexyl rings simplified). Selected bond lengths (Å) and angles (°): Ru1–P1 2.3115(5), Ru1–P2 2.3526(5), Ru1–P3 2.3751(5), P1–C1 1.847(2), P1–H1 1.28(3), P1–H2 1.32(2), P1–Ru1–P2 94.319(17), P1–Ru1–P3 94.381(17), P2–Ru1–P3 98.161(16), H11–P1–H12 97.9(15).

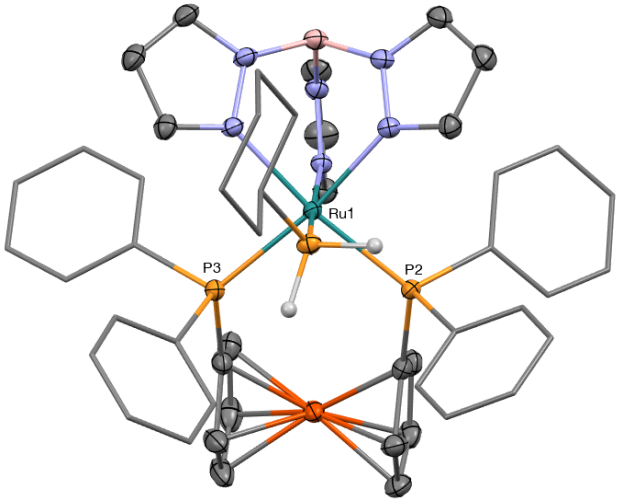

Figure 2.6. Alternative perspective of the molecular structure of [Ru(PH$_2$Cy)(dppf)(Tp)]$^+$ in a crystal

2.2.5 Attempted Synthesis of [Ru(PH$_2$Cy)(dppf)(Tp)]PF$_6$ from [Ru(NCMe)(dppf)(Tp)]PF$_6$

An alternative route to [Ru(PH$_2$Cy)(dppf)(Tp)]PF$_6$ was also investigated (Scheme 2.8). This route involved abstraction of the chloride from [RuCl(dppf)(Tp)]PF$_6$ in the presence of acetonitrile to form [Ru(NCMe)(dppf)(Tp)]PF$_6$. The acetonitrile ligand should then prove

labile, providing access to [Ru(PH$_2$Cy)(dppf)(Tp)]PF$_6$ and other complexes *via* ligand substitution.

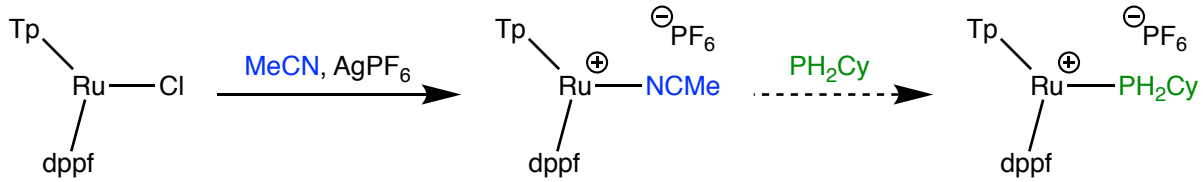

Scheme 2.8. Proposed alternative route to [Ru(PH$_2$Cy)(dppf)(Tp)]PF$_6$

Stirring a mixture of [RuCl(dppf)(Tp)] with AgPF$_6$ in MeCN resulted in the formation of a colourless precipitate. Filtration of the mixture, removal of solvent from the filtrate and recrystallisation of the residue resulted in the isolation of [Ru(NCMe)(dppf)(Tp)]PF$_6$ in 75% yield. The replacement of Cl with NCMe results in a *ca*. 10 ppm higher frequency shift of the dppf ^{31}P{^{1}H} NMR resonance from δ_P 35.7 to δ_P 45.2.

The characteristic 2:1 ratio of the pyrazolyl resonances is maintained in the ^{1}H and ^{13}C{^{1}H} NMR resonances. Additionally, the symmetry of the dppf fragment remains analogous to its symmetry in [Ru(PH$_2$Cy)(dppf)(Tp)]PF$_6$. Five separate ^{13}C{^{1}H} NMR resonances are observed for the cyclopentadienyl rings as well as two sets of phenyl resonances. The *ipso*, *ortho* and *meta* carbons of the phenyl ring and all of the Cp ^{13}C{^{1}H} NMR signals all appear as virtual triplets, showing virtual coupling to the remote ^{31}P nucleus.

The molecular structure of [Ru(NCMe)(dppf)(Tp)]$^+$ was determined by X-ray crystallography (Figure 2.7). The Ru–NCMe distance of 2.031(2) Å is in good agreement with the reported average of 2.090(37) Å for Ru(II) nitrile complexes.[135] While there is a difference in the Ru–P bond lengths (0.0079 Å, 9 e.s.d.) it is much less pronounced than for [Ru(PH$_2$Cy)(dppf)(Tp)]$^+$ (0.0225 Å, 45 e.s.d.). The Ru–N distances for the pyrazolyl rings *trans* to phosphorus are 0.060 Å longer than the group *trans* to MeCN, signifying the greater *trans* influence of P *versus* N.

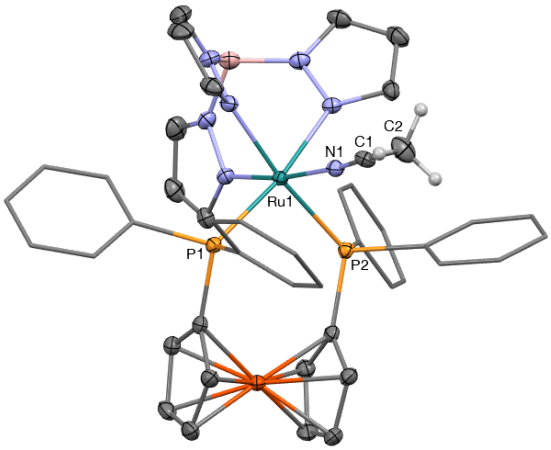

Figure 2.7. Molecular structure of [Ru(NCMe)(dppf)(Tp)]+ in a crystal of [Ru(NCMe)(dppf)(Tp)]PF$_6$.(MeCN) (50% displacement ellipsoids, acetonitrile solvate, hexafluorophosphate anion and most H atoms omitted, phenyl and cyclohexyl rings simplified). Selected bond lengths (Å) and angles (°): Ru1–P1 2.3438(8), Ru1–P2 2.3517(8), Ru1–N1 2.031(2), N1–C1 1.135(4), C1–C2 1.454(4), P1–Ru1–P2 99.36(3), P1–Ru1–N1 92.90(7), P2–Ru1–N1 92.84(7), N1–C1–C2 178.1(3).

Substitution of the MeCN ligand in [Ru(NCMe)(dppf)(Tp)]PF$_6$ for PH$_2$Cy was investigated (Scheme 2.8). When using a 15:1 CH$_2$Cl$_2$/MeCN mixture as the solvent, no reaction between [Ru(NCMe)(dppf)(Tp)]PF$_6$ and one equivalent of PH$_2$Cy was observed after heating under reflux for one week. With THF as the solvent, the reaction proceeded to approximately 40% completion after 16 hours of heating under reflux, as estimated by ^{31}P{^{1}H} NMR spectroscopy. After 4 days of heating the reaction had progressed to 95% complete. However, no further change was observed following a further 24 hours (5 days total) of heating.

The above observations indicate that the lability of the MeCN ligand in [Ru(NCMe)(dppf)(Tp)]PF$_6$ is not as high as expected. Indeed, further consultation of the literature showed that MeCN is similarly substitutionally inert from the cationic tris(acetonitrile) complex [Ru(NCMe)$_3$(Tp)]$^+$.[136] The rate of MeCN substitution for CD$_3$CN was measured to be eight orders of magnitude slower for [Ru(NCMe)$_3$(Tp)]$^+$ than for its Cp analogue [Ru(NCMe)$_3$(Cp)]$^+$. The reduced rate of substitution was explained by the increased electron-donating ability of Tp compared to Cp. This leads to a more electron-rich Ru centre, which in turn allows for more backbonding into the π* orbital of the acetonitrile ligand. While nitriles are not ordinarily considered important π-acceptors, it was argued that the increased

backbonding creates a sufficiently stronger Ru−NCMe bond to significantly inhibit the dissociative substitution mechanism.

Modifying the stoichiometry of the reaction between [Ru(NCMe)(dppf)(Tp)]PF$_6$ and PH$_2$Cy may have driven the reaction to completion. However, the extended reaction time and slow kinetics, in combination with similarly reported behaviour of [Ru(NCMe)$_3$(Tp)]$^+$, indicated that this route was not as facile as desired. Accordingly, further studies into the chemistry of [Ru(NCMe)(dppf)(Tp)]PF$_6$ were not pursued.

2.3 Deprotonation Reactions of Primary Phosphine Complexes

2.3.1 Deprotonation of [RuCl(PPh$_3$)(PH$_2$Cy)(Tp)]

Following the synthesis of the primary phosphine ruthenium complexes [RuCl(PPh$_3$)(PH$_2$Cy)(Tp)], [Ru(PPh$_3$)(PH$_2$Cy)$_2$(Tp)]PF$_6$ and [Ru(PH$_2$Cy)(dppf)(Tp)]PF$_6$, their deprotonation reactions to form phosphido complexes were investigated. The first of these complexes studied was [RuCl(PPh$_3$)(PH$_2$Cy)(Tp)].

Treating [RuCl(PPh$_3$)(PH$_2$Cy)(Tp)] with one equivalent of ^{n}BuLi or excess KH gave a major product with ^{31}P{^{1}H} NMR doublets ($^2J_{PP}$ = 36 Hz) at δ_P 16.9 and −4.8. Importantly, the resonance at δ_P 16.9 appeared as a triplet with $^1J_{PH}$ = 316 Hz in the absence of ^{1}H-decoupling. Therefore, this resonance is due to an intact PH$_2$Cy group following the reaction with a base. Indeed, the chemical shift is also relatively unchanged from [RuCl(PPh$_3$)(PH$_2$Cy)(Tp)] (δ_P 16.6). Instead, the change has occurred for the PPh$_3$ group, which has shifted to lower frequency from δ_P 49.7 to δ_P −4.8.

Instead of the phosphido complexes [RuCl(PPh$_3$)(PHCy)(Tp)]$^-$ or [Ru(PPh$_3$)(PHCy)(Tp)], the cyclometallated product [Ru(PH$_2$Cy)(κ^2-C$_6$H$_4$PPh$_2$-2)(Tp)] was obtained (Scheme 2.9). However, the ESI-MS data were inconclusive for the identification of the product. A peak for [M + H]$^+$ was observed, but this is exactly the same formulation and *m/z* as the [M – Cl]$^+$ ion observed for the starting material [RuCl(PH$_2$Cy)(PPh$_3$)(Tp)]. Stronger evidence comes from the high-frequency shift of the aryl phosphine resonance in the ^{31}P{^{1}H} NMR spectrum, which is characteristic of *ortho*-metallated phosphine complexes[137] with phosphines in four-

membered rings.[138] Cyclometallation was also observed for the related complex [Ru(PPh$_3$)(PCy$_2$)(η^5-indenyl)] with a similar shift to lower frequency in the ^{31}P{^{1}H} NMR resonance.[80] Further evidence was gained from the lack of reaction of the product with H_2O, indicating that a reaction more complex than a simple deprotonation to generate a strongly-basic phosphide had occurred.

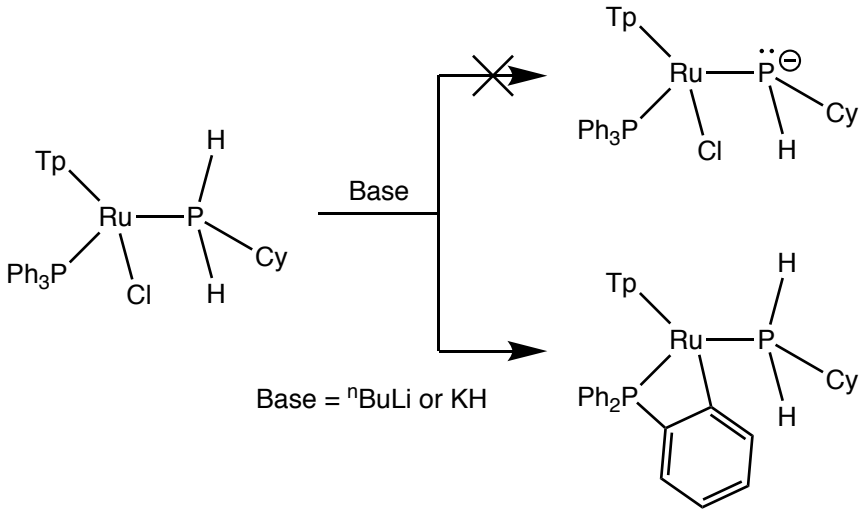

Scheme 2.9. Deprotonation of [RuCl(PPh$_3$)(PH$_2$Cy)(Tp)]

The cyclometallation was evident in the ^{13}C{^{1}H} NMR spectrum by a high frequency resonance at δ_C 173.9 for the metal-bound carbon. The resonance was an overlapping doublet of doublets, showing coupling to both phosphine phosphorus nuclei with an apparent $^2J_{PC}$ of 13 Hz. In addition, four more resonances were observed for the bridging phenylene group in the 1D ^{13}C{^{1}H} NMR spectrum, with the fifth obscured by solvent (C_6D_6) and only observed in 2D ^{1}H–^{13}C HSQC and HMBC NMR experiments.

Based on the fixed geometry of the newly-formed ring, the two remaining phenyl groups are expected to be distinct – one on the same face as cyclohexylphosphine and the other on the same face as a pyrazolyl ring. The different rings could not be distinguished by NMR however, with cluttered aromatic regions in both ^{1}H and ^{13}C{^{1}H} spectra and residual C_6D_6 signals obfuscating the definitive assignment of the remaining resonances. Notably, the most distinct ^{13}C{^{1}H} NMR resonance is that of the *ipso* carbon with its large $^1J_{PC}$ and only one signal is observed for the two rings. Whether this is due to the coincidence of two signals or if a second, undetected resonance is present is uncertain.

The C_1 symmetry at the ruthenium centre is the same as in [RuCl(PPh$_3$)(PH$_2$Cy)(Tp)], with a different group *trans* to each pyrazolyl ring. Correspondingly, there are three sets of pyrazolyl resonances in the $^{13}C\{^1H\}$ NMR spectrum. Three sets of ^1H NMR pyrazolyl resonances can also be seen, but three of these overlap with those for the phenyl rings. The asymmetric metal centre is also reflected in the NMR data of the PH$_2$Cy group. The diastereotopic P–H hydrogen atoms give rise to two separate ^1H NMR resonances at δ_H 4.37 and 4.18, and six separate $^{13}C\{^1H\}$ NMR signals are present for the cyclohexyl group.

The most likely mechanism of formation of [Ru(PH$_2$Cy)(κ^2-C$_6$H$_4$PPh$_2$-2)(Tp)] is *via* a planar Ru=P intermediate (Scheme 2.10) as observed for the related complexes [Ru(PPh$_3$)(PR$_2$)(η^5-indenyl)] (R = Cy, ^{i}Pr, Et).[80, 139-141] According to the commonly-accepted cyclometallation pathway, [137] the next step is oxidative addition of the C–H bond to the metal followed by hydrogen migration to the phosphorus atom. No evidence for the cyclometallated hydride intermediate was observed.

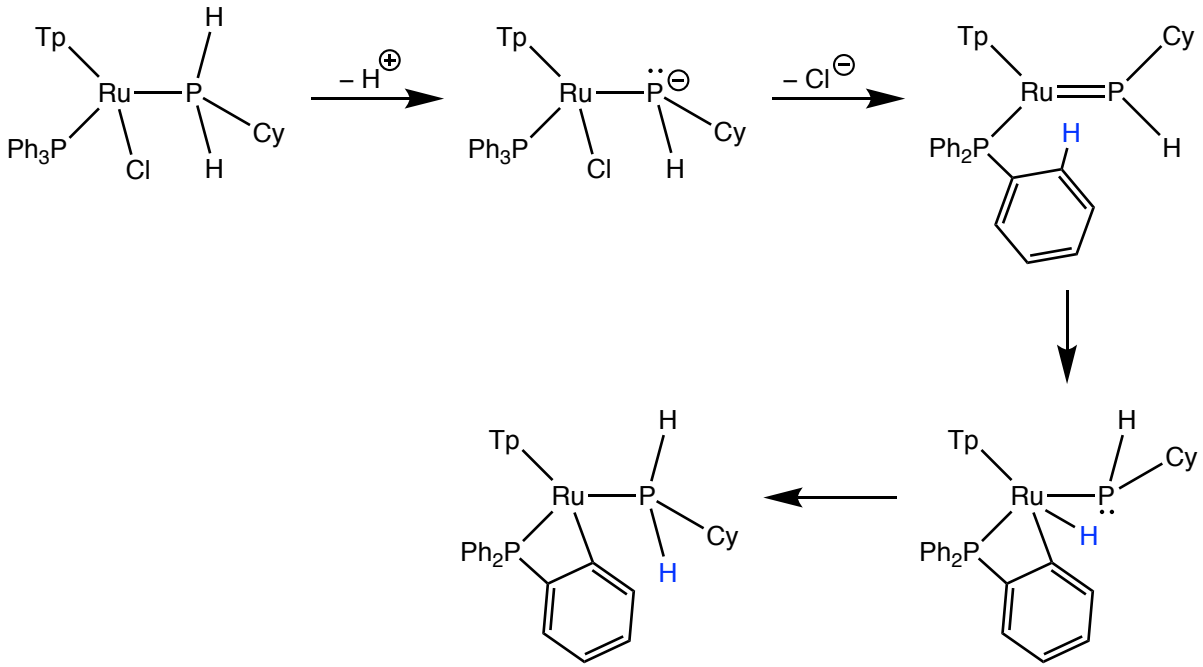

Scheme 2.10. Proposed mechanism of formation for [Ru(PH$_2$Cy)(κ^2-C$_6$H$_4$PPh$_2$-2)(Tp)] via *an oxidative addition pathway*

Another potential mechanism for the formation of [Ru(PH$_2$Cy)(κ^2-C$_6$H$_4$PPh$_2$-2)(Tp)] is *via* a [2 + 2] cycloaddition of the C−H phenyl bond across the planar R=P intermediate (Scheme 2.11). Cycloaddition reactions were reported for the indenyl analogues with alkenes and alkynes,[139-141] and similar reactivity cannot be explicitly ruled out for this system based on the available data. A concerted process for C−H activation would be unusual for a late transition metal system but there are an increasing number of σ-metathesis-type reactions for electron-rich metals, and also for those where non-innocent ligands (such as the phosphido ligand in this case) are involved.[142]

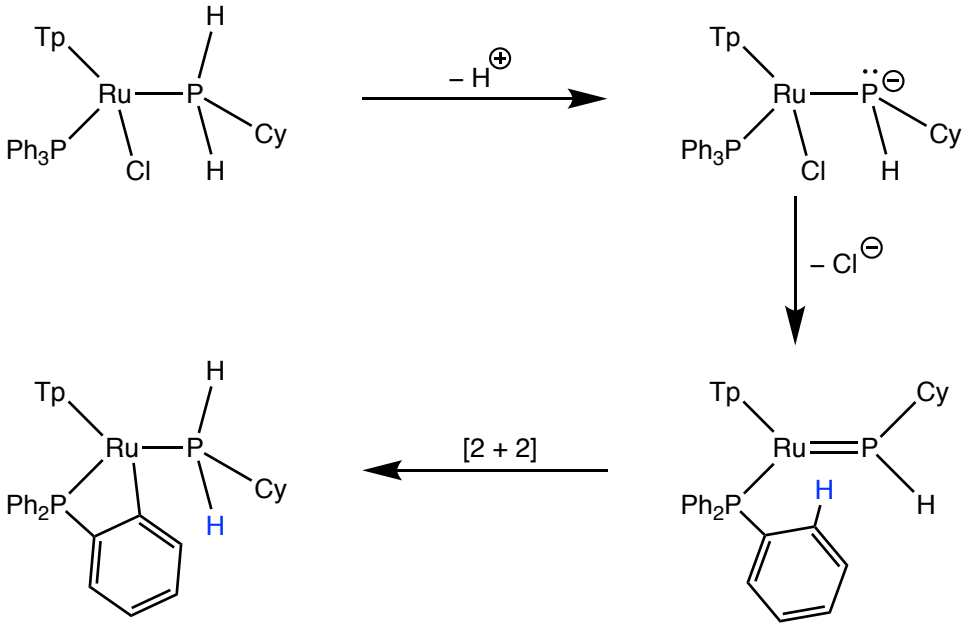

Scheme 2.11. Proposed mechanism of formation for [Ru(PH$_2$Cy)(κ^2-C$_6$H$_4$PPh$_2$-2)(Tp)] via *a concerted [2 + 2] cycloaddtion pathway*

In contrast to the deprotonation of [RuCl(PPh$_3$)(PH$_2$Cy)(Tp)], the planar phosphido intermediate is isolated for each of the indenyl complexes [Ru(PPh$_3$)(PR$_2$)(η^5-indenyl)] (R = Cy, ^{i}Pr, Et) and the cyclometallation step is much slower. The different kinetic behaviour probably arises from increased electron-donating ability of the Tp *versus* indenyl ligand, which would increase electron density at the metal and result in a much more reactive ruthenium centre. Thus, while extended time periods or heating are required for the transformation of [Ru(PPh$_3$)(PR$_2$)(η^5-indenyl)] (R = Cy, ^{i}Pr, Et) to [Ru(PHR$_2$)(κ^2-C$_6$H$_4$PPh$_2$-2)(η^5-indenyl)] (R = Cy, ^{i}Pr, Et), the intermediate [Ru(PPh$_3$)(PHCy)(Tp)] is not observed during its rapid cyclometallation to [Ru(PH$_2$Cy)(κ^2-C$_6$H$_4$PPh$_2$-2)(Tp)].

Further evidence that the formation of [Ru(PH$_2$Cy)(κ^2-C$_6$H$_4$PPh$_2$-2)(Tp)] occurs *via* a planar phosphido intermediate was gained by investigating the reaction of [RuCl(PPh$_3$)$_2$(Tp)] with ^{n}BuLi. If the H atom in the *ortho* position of the phenyl ring is sufficiently acidic to be directly deprotonated in [RuCl(PPh$_3$)(PH$_2$Cy)(Tp)] then it is likely to behave similarly in the closely-related complex [RuCl(PPh$_3$)$_2$(Tp)]. No substantial change was observed upon the addition of ^{n}BuLi to [RuCl(PPh$_3$)$_2$(Tp)] (Scheme 2.12). A singlet at δ_P 67.4 and two doublets ($^2J_{PP}$ = 32 Hz) at δ_P 69.2 and 61.3 in the ^{31}P{^{1}H} spectrum of the reaction mixture were purportedly due to the compounds [RuH(PPh$_3$)$_2$(Tp)][143-144] (comprising *ca*. 2%) and [RuH(H$_2$C=CHEt)(PPh$_3$)$_2$(Tp)] (comprising *ca*. 4%), respectively. These compounds are expected to arise from the substitution of Cl from [RuCl(PPh$_3$)$_2$(Tp)] to form [Ru(^{n}Bu)(PPh$_3$)$_2$(Tp)], followed by β-hydride elimination to give [RuH(H$_2$C=CHEt)(PPh$_3$)$_2$(Tp)] and subsequent 1-butene dissociation to produce [RuH(PPh$_3$)$_2$(Tp)] (Scheme 2.13). The formation of these two products was further supported by the presence of low frequency ^{1}H NMR resonances at δ_H −13.16 (triplet, $^2J_{PH}$ = 28 Hz, [RuH(PPh$_3$)$_2$(Tp)]) and −13.66 (doublet of doublets, $^2J_{PH}$ = 24 Hz, $^2J_{PH}$ = 35 Hz, [RuH(H$_2$C=CHEt)(PPh$_3$)$_2$(Tp)]). The relative lack of reactivity of [RuCl(PPh$_3$)$_2$(Tp)] compared to [RuCl(PPh$_3$)(PH$_2$Cy)(Tp)] highlights the importance of the PH$_2$Cy group to the ultimate formation of [Ru(PH$_2$Cy)(κ^2-C$_6$H$_4$PPh$_2$-2)(Tp)] and is consistent with P−H deprotonation being the most likely first step in the process.

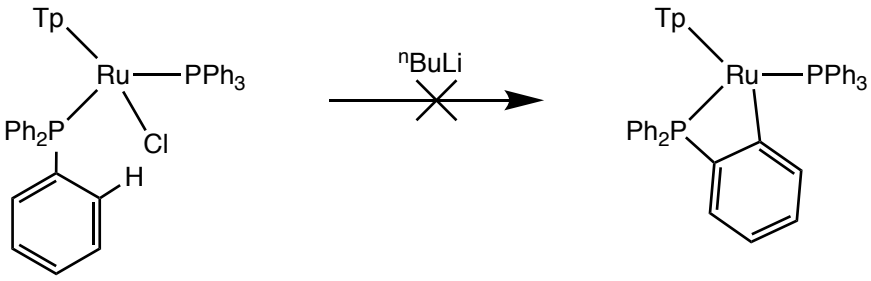

Scheme 2.12. Attempted reaction of [RuCl(PPh$_3$)$_2$(Tp)] with ^{n}BuLi

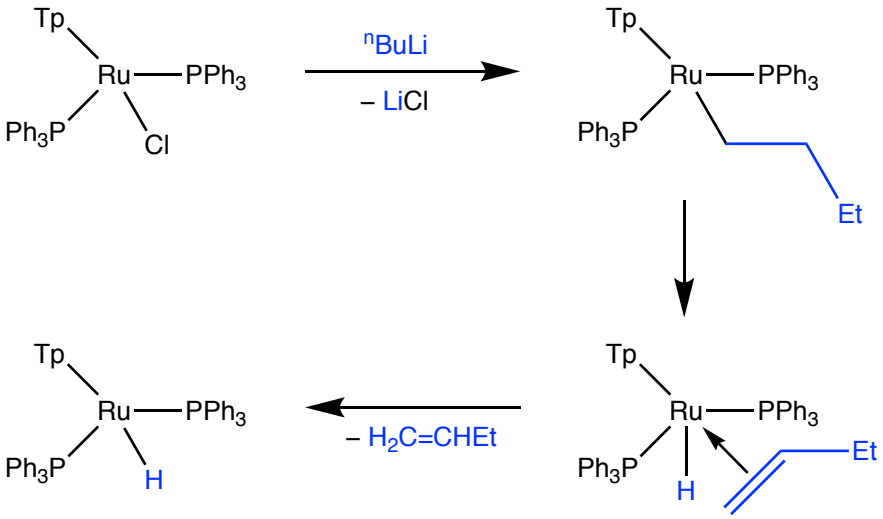

Scheme 2.13. Formation of [RuH(H$_2$C=CHEt)(PPh$_3$)$_2$(Tp)] and [RuH(PPh$_3$)$_2$(Tp)]

The satisfactory purification of [Ru(PH$_2$Cy)(κ^2-C$_6$H$_4$PPh$_2$-2)(Tp)] was not successfully achieved. The complex is thermally unstable and undergoes slow decomposition, even in anaerobic conditions. When this process is accelerated by heating a toluene solution under reflux for 3 days, the solution turns blue and over 40 resonances are observed in the corresponding ^{31}P{^{1}H} NMR spectrum. Among these resonances those for PPh$_3$ and O=PPh$_3$ can be identified, although they do not comprise significantly more of the mixture than any other resonance.

Several reactions of [Ru(PH$_2$Cy)(κ^2-C$_6$H$_4$PPh$_2$-2)(Tp)] were investigated. Overall, [Ru(PH$_2$Cy)(κ^2-C$_6$H$_4$PPh$_2$-2)(Tp)] arises from a formal dehydrohalogenation reaction of [RuCl(PPh$_3$)(PH$_2$Cy)(Tp)]. This process is reversible, and the addition of HCl to [Ru(PH$_2$Cy)(κ^2-C$_6$H$_4$PPh$_2$-2)(Tp)] results in the reformation of [RuCl(PPh$_3$)(PH$_2$Cy)(Tp)] (Scheme 2.14). However, as previously mentioned, there is no reaction upon the addition of H$_2$O to [Ru(PH$_2$Cy)(κ^2-C$_6$H$_4$PPh$_2$-2)(Tp)] (Scheme 2.15). Hence, H$_2$O is not sufficiently acidic to break the Ru−C bond.

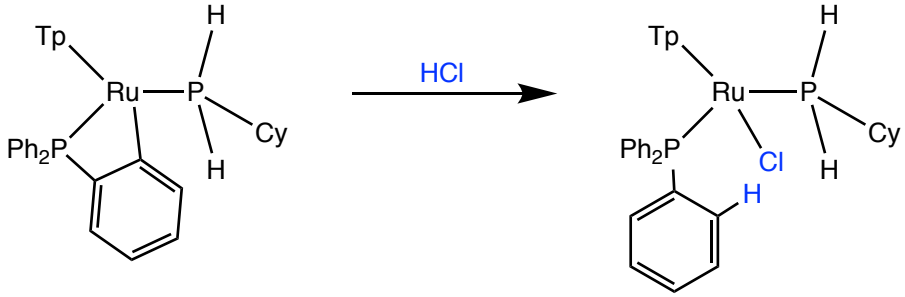

Scheme 2.14. Reaction of [Ru(PH$_2$Cy)(κ^2-C$_6$H$_4$PPh$_2$-2)(Tp)] with HCl

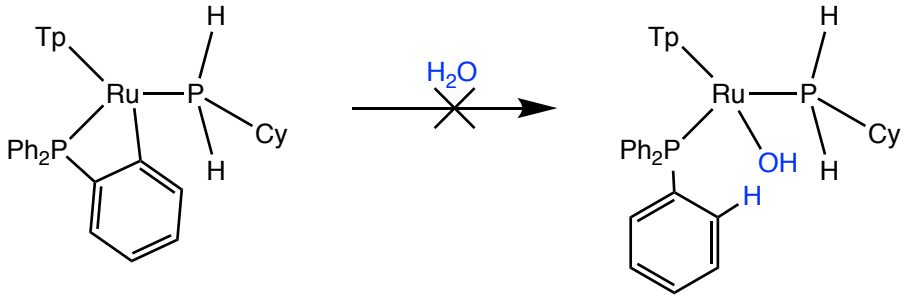

Scheme 2.15. Lack of reaction of [Ru(PH$_2$Cy)(κ^2-C$_6$H$_4$PPh$_2$-2)(Tp)] with H$_2$O

The cyclometallated complex [Co(PMe$_3$)$_3$(κ^2-C$_6$H$_4$PPh$_2$-2)] has been reported to undergo CO insertion (and PMe$_3$ substitution) to form the acyl complex [Co(CO)(PMe$_3$)$_2${κ^2-C(O)C$_6$H$_4$PPh$_2$-2}].[145] In the same report the unusual monodentate coordination of the C$_6$H$_4$PPh$_2$-2 fragment in the complex [NiCl(C$_6$H$_4$PPh$_2$-2)(PMe$_3$)$_2$] was also described. In this case the PMe$_3$ ligands appear to be too strongly bound to allow coordination of the PPh$_2$ fragment, coupled with the preference for d^8-square planar coordination by nickel(II). Based on these two results, the reaction of [Ru(PH$_2$Cy)(κ^2-C$_6$H$_4$PPh$_2$-2)(Tp)] with small, strongly-binding ligands such as CO or PMe$_3$ might prove intriguing. The reaction might be anticipated to either result in insertion into the Ru–C bond, or in ring-opening substitution of the PPh$_2$ moiety. No change, however, was observed in the reaction between [Ru(PH$_2$Cy)(κ^2-C$_6$H$_4$PPh$_2$-2)(Tp)] and CO or PMe$_3$ (Scheme 2.16), demonstrating the robust nature of the coordinatively-saturated cyclometallated structure with no apparent dissociative pathways available.

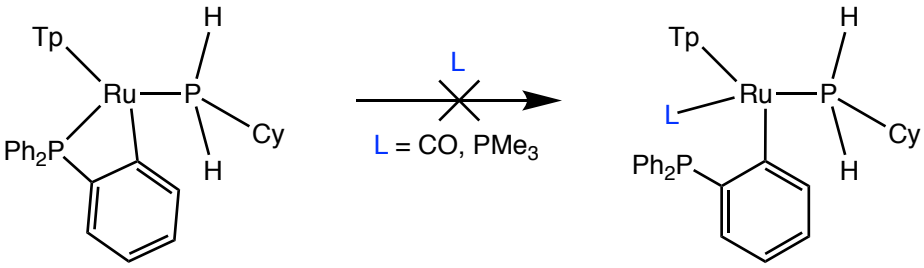

Scheme 2.16. Lack of reaction of [Ru(PH$_2$Cy)(κ^2-C$_6$H$_4$PPh$_2$-2)(Tp)] with CO or PMe$_3$

The complex [Ru(PH$_2$Cy)(κ^2-C$_6$H$_4$PPh$_2$-2)(Tp)] still retains a primary phosphine with two potentially reactive P–H bonds. Treatment of [Ru(PH$_2$Cy)(κ^2-C$_6$H$_4$PPh$_2$-2)(Tp)] with one equivalent of ^{n}BuLi (or, correspondingly, treatment of [RuCl(PPh$_3$)(PH$_2$Cy)(Tp)] with two equivalents of ^{n}BuLi) results in the formation of the putative phosphido complex anion [Ru(PHCy)(κ^2-C$_6$H$_4$PPh$_2$-2)(Tp)]$^-$ (Scheme 2.17). The product was identified by ^{31}P{^{1}H} NMR

spectroscopy *via* two doublets at δ_P −2.8 and –48.8. The resonance at δ_P −48.8 was identified as the resonance for the PHCy group due to its appearance as a doublet ($^1J_{PH}$ = 182 Hz) in the absence of ^{1}H-decoupling. An high-frequency shift (*ca*. 68 ppm) of the cyclohexylphosphine resonance from [Ru(PH$_2$Cy)(κ^2-C$_6$H$_4$PPh$_2$-2)(Tp)] is appropriate for the deprotonation and localisation of negative charge at phosphorus. Additionally, the reduction in the J_{PH} concurs with the change from four-coordinate to three-coordinate phosphorus. Such a change arises from phosphorus lone pairs having significant s-character, and the subsequent redistribution of this s-character into bonding orbitals for four-coordinate phosphorus.[146] Unfortunately, the anionic phosphido complex was found to be extremely basic and further purification and characterisation was not successfully achieved. The precursor was recovered in all attempts.

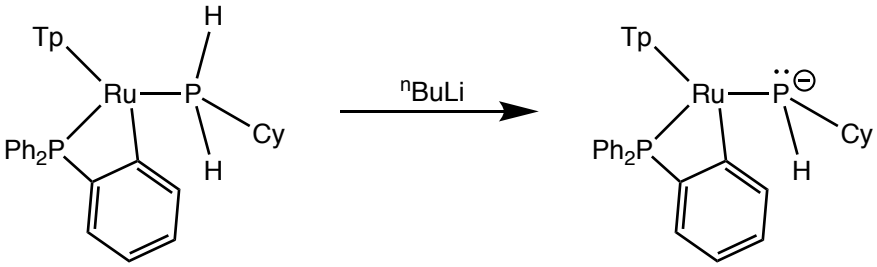

Scheme 2.17. Formation of [Ru(PHCy)(κ^2-C$_6$H$_4$PPh$_2$-2)(Tp)]$^-$

2.3.2 Deprotonation of [Ru(PPh$_3$)(PH$_2$Cy)$_2$(Tp)]PF$_6$

Investigations into the deprotonation of the cationic complex [Ru(PPh$_3$)(PH$_2$Cy)$_2$(Tp)]$^+$ to form [Ru(PPh$_3$)(PH$_2$Cy)(PHCy)(Tp)] were also conducted (Scheme 2.18). It was anticipated that the deprotonation of a cationic precursor should yield a neutral phosphido complex which might prove easier to handle than an anionic phosphido complex. The addition of one equivalent of ^{n}BuLi to [Ru(PPh$_3$)(PH$_2$Cy)$_2$(Tp)]PF$_6$ resulted in a mixture of products as determined by ^{31}P{^{1}H} NMR spectroscopy.

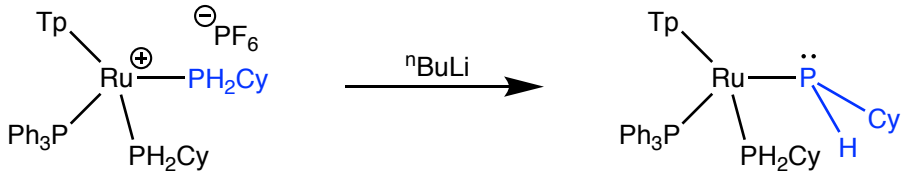

Scheme 2.18. Deprotonation of [Ru(PPh$_3$)(PH$_2$Cy)$_2$(Tp)]PF$_6$

The deprotonation of [Ru(PPh$_3$)(PH$_2$Cy)$_2$(Tp)]$^+$ to form [Ru(PPh$_3$)(PH$_2$Cy)(PHCy)(Tp)] results in the formation of adjacent Ru and P stereocentres. Accordingly, there are two possible diastereomers (four isomers total, Figure 2.8) of [Ru(PPh$_3$)(PH$_2$Cy)(PHCy)(Tp)] and two sets of NMR resonances would be expected. For each diastereomer there are three phosphorus environments: PPh$_3$, PH$_2$Cy and PHCy. The ^{31}P{^{1}H} NMR resonances for these three isomers are expected to be doublet of doublets as a result of coupling to the other two ^{31}P nuclei bound to ruthenium.

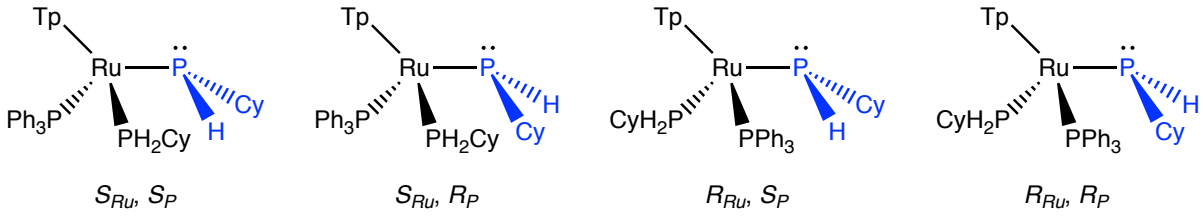

S_{Ru}, S_P S_{Ru}, R_P R_{Ru}, S_P R_{Ru}, R_P

Figure 2.8. Possible isomers of [Ru(PPh$_3$)(PH$_2$Cy)(PHCy)(Tp)]

Six ^{31}P{^{1}H} NMR resonances could be identified which could be due to the two diastereomers of [Ru(PPh$_3$)(PH$_2$Cy)(PHCy)(Tp)] following the deprotonation reaction with ^{n}BuLi (Figure 2.9). These resonances were at δ_P 55.2 (*blue*), 48.6 (*blue*), 23.8 (*red*), 11.5 (*red*), −17.0 (*green*) and −32.0 (*green*) and the respective compounds comprised *ca*. 75% of the mixture. Generally, the $^2J_{PP}$ values for these signals were not well resolved. The ^{31}P NMR data did, however, provide further insights. The resonances at δ_P 23.8 and 11.5 (*red*) appeared as triplets with $^1J_{PH}$ of 326 and 321 Hz, respectively. Based on these observations, these resonances are for the PH$_2$Cy groups of the two diastereomers of [Ru(PPh$_3$)(PH$_2$Cy)(PHCy)(Tp)]. The low frequency signals at δ_P −17.0 and −32.0 (*green*) are doublets in the ^{31}P NMR spectrum, with $^1J_{PH}$ of 172 and 174 Hz, respectively. The splitting and coupling values of these signals leads to their assignment as the PHCy resonances, and their low frequency position signifies that deprotonation at phosphorus has occurred.

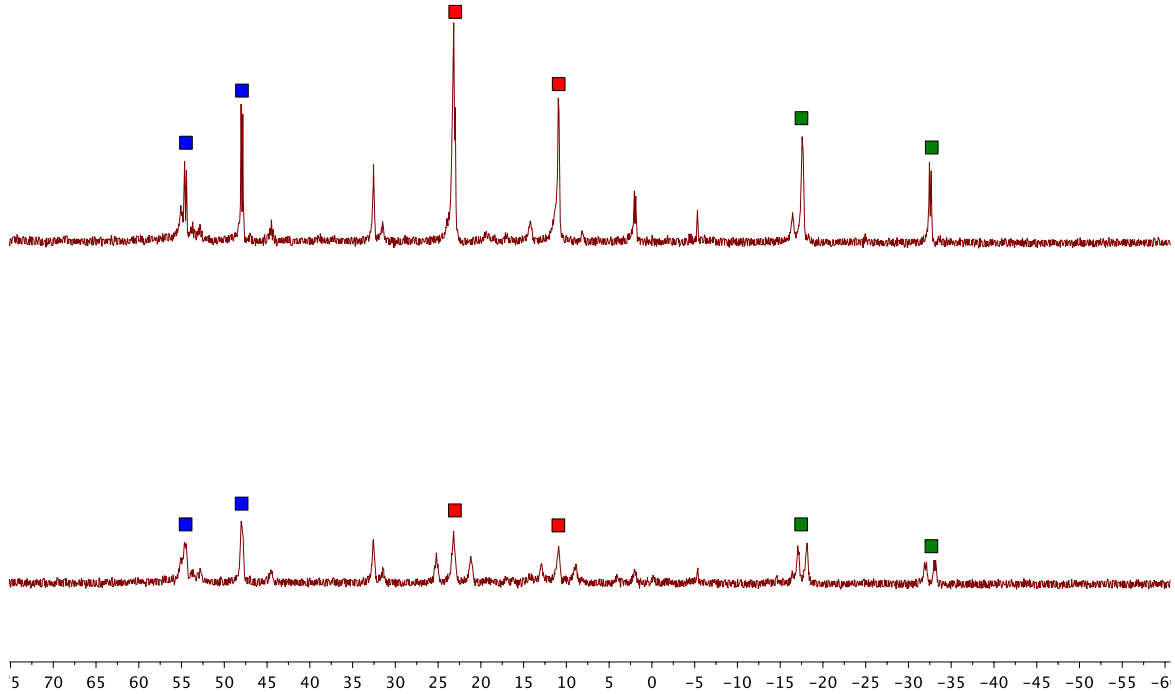

Figure 2.9. $^{31}P\{^1H\}$ (top) and ^{31}P (bottom) NMR spectra following the reaction of [Ru(PPh$_3$)(PH$_2$Cy)$_2$(Tp)]PF$_6$ with ^{n}BuLi

The product [Ru(PPh$_3$)(PH$_2$Cy)(PHCy)(Tp)] was extremely basic and could not be further purified for full characterisation. An NMR sample of [Ru(PPh$_3$)(PH$_2$Cy)(PHCy)(Tp)] in C_6D_6 prepared under a N_2 atmosphere was observed after 15 hours to have converted completely to [Ru(PPh$_3$)(PH$_2$Cy)$_2$(Tp)]$^+$, presumably due to adventitious H_2O. During the attempted purification of [Ru(PPh$_3$)(PH$_2$Cy)(PHCy)(Tp)] it was extracted into toluene to separate it from ionic by-products. However, following cannula filtration of the mixture through a glass sinter the filtrate was found to contain [Ru(PPh$_3$)(PH$_2$Cy)$_2$(Tp)]$^+$ as the major product by $^{31}P\{^1H\}$ NMR spectroscopy. As a cationic species, [Ru(PPh$_3$)(PH$_2$Cy)$_2$(Tp)]$^+$ would not be highly soluble in toluene and would have been expected to be excluded in the filtration step. Therefore, reprotonation must have occurred during the filtration, during the removal of solvent *in vacuo* or else during the preparation of the NMR sample. While it is not clear at which stage reprotonation happened, it became clear that [Ru(PPh$_3$)(PH$_2$Cy)(PHCy)(Tp)] was too basic to handle conveniently. As such, efforts were focused in other directions.

2.3.3 Deprotonation of [Ru(PH$_2$Cy)(dppf)(Tp)]PF$_6$

The salt [Ru(PH$_2$Cy)(dppf)(Tp)]PF$_6$ provides a further example of a cationic primary phosphine complex for deprotonation studies. Additionally, the presence of the bidentate dppf ligand obviates the formation of diastereomers upon deprotonation which should simplify the analysis of the products. The treatment of [Ru(PH$_2$Cy)(dppf)(Tp)]PF$_6$ with either one equivalent of ^{n}BuLi or excess KH resulted in the formation of [Ru(PHCy)(dppf)(Tp)] (Scheme 2.19).

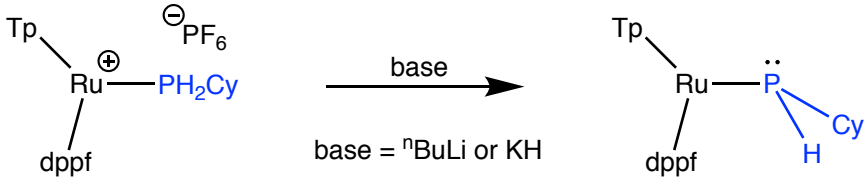

Scheme 2.19. Deprotonation of [Ru(PH$_2$Cy)(dppf)(Tp)]PF$_6$

The phosphido complex [Ru(PHCy)(dppf)(Tp)] was observed by ^{31}P{^{1}H} NMR spectroscopy. The two PPh$_2$ groups in [Ru(PHCy)(dppf)(Tp)] are diastereotopic, meaning that three ^{31}P{^{1}H} NMR signals were seen. These signals appear at δ_P 35.6, 24.8 and 2.2, and the $^2J_{PP}$ splittings are not well-resolved. The last of these is the PHCy resonance, which is a doublet in the ^{31}P NMR spectrum with a $^1J_{PH}$ of 169 Hz.

Similar to [Ru(PPh$_3$)(PH$_2$Cy)(PHCy)(Tp)], [Ru(PHCy)(dppf)(Tp)] was found to be extremely basic. As such, its handling was difficult and its satisfactory purification was not achieved. Indeed, removal of the solvent *in vacuo* and NMR analysis of the resultant residue showed that approximately 50% of the product had reverted to [Ru(PH$_2$Cy)(dppf)(Tp)]$^+$.

2.3.4 Reaction of [Ru(PHCy)(dppf)(Tp)] with [AuCl(SMe$_2$)]

In an attempt to establish the formation of [Ru(PHCy)(dppf)(Tp)] *via* its reactivity, its reaction with the AuCl source [AuCl(SMe$_2$)] was investigated. The salt [Ru(PH$_2$Cy)(dppf)(Tp)]PF$_6$ was deprotonated with KH in THF and the reaction mixture subjected to cannula filtration. The complex [AuCl(SMe$_2$)] was added to the filtrate which immediately turned black. Removal of the solvent from the mixture and ^{31}P{^{1}H} NMR spectroscopy of the resultant residue revealed peaks which were consistent with the formation of [Ru{PH(AuCl)Cy}(dppf)(Tp)] (Scheme 2.20). There were three resonances in total, the same number as seen for the precursor

[Ru(PHCy)(dppf)(Tp)]. The resonances were all doublets of doublets, each coupling to the other two ^{31}P nuclei, and appeared at δ_P 37.7, 33.2 and −10.0. The PHCy resonance is the latter of these, meaning that coordination to Au results in a *ca*. 12 ppm shift to lower frequency. A $^1J_{PH}$ of 300 Hz was measured in the ^{31}P NMR spectrum, the increase being in good agreement with an increased phosphorus coordination number. One other ^{31}P{^{1}H} NMR resonance, a singlet at δ_P 35.4, was observed and estimated to comprise 20% of the mixture but its source could not be identified.

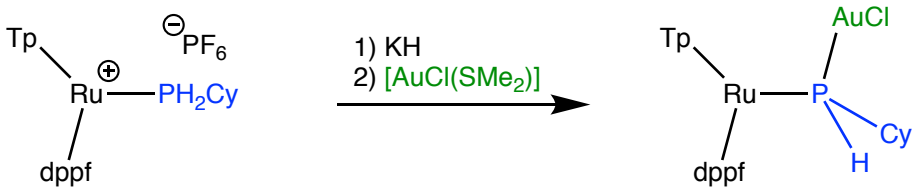

Scheme 2.20. In situ *reaction of [Ru(PHCy)(dppf)(Tp)] with [AuCl(SMe$_2$)]*

Despite the relatively clean formation of [Ru{PH(AuCl)Cy}(dppf)(Tp)] in the reaction mixture, its purification was not straightforward and was not successfully achieved. The residue from the reaction mixture was extracted with toluene to isolate the neutral components of the mixture. Solvent was removed *in vacuo* and ^{31}P{^{1}H} NMR analysis of the resulting residue showed that *ca*. 10% of the mixture had decomposed with the appearance of *ca*. 8 new resonances. Single crystals grown from this mixture revealed two different structures: [Ru{PH(AuCl)Cy}(dppf)(Tp)] and [{RuCl(Tp)}Au(μ-PHCy)(μ-*P,P'*-dppf)]$_2$.

Crystals grown from a CH_2Cl_2/*n*-hexane mixture revealed the molecular structure of the desired product, [Ru{PH(AuCl)Cy}(dppf)(Tp)] (Figure 2.10). The formation of the P−Au bond can be clearly seen, with a bond distance of 2.2725(13) Å. This bond distance is in good agreement with those previously reported for P−Au bonds with a two-coordinate Au atom.[135] The P−Au−Cl angle of 175.29(6)° is nearly linear, as is expected for Au(I) complexes. The Ru−PHCy distance of 2.3798(13) Å is longer than the corresponding distance in [Ru(PH_2Cy)(dppf)(Tp)]$^+$ (2.3115(5) Å). Two possible reasons for the longer bond length are the increased steric bulk of AuCl *versus* H and a change in Ru−P bond order when the phosphorus atom is acting as a bridging rather than a terminal ligand.

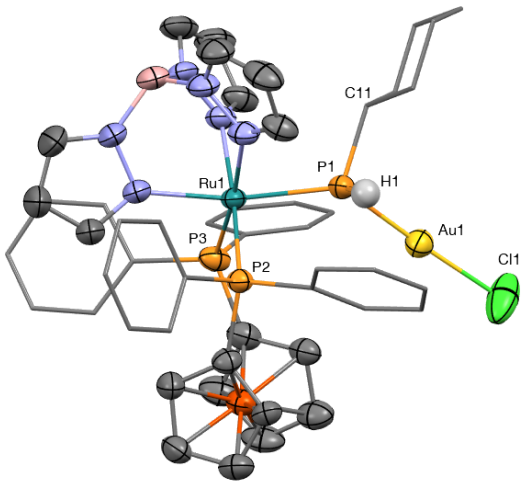

Figure 2.10. Molecular structure of S_P-[Ru{PH(AuCl)Cy}(dppf)(Tp)] in a crystal (50% displacement ellipsoids, most H atoms omitted, phenyl and cyclohexyl rings simplified). Selected bond lengths (Å) and angles (°): Ru1–P1 2.3798(13), Ru1–P2 2.3770(12), Ru1–P3 2.3435(13), Au1–P1 2.2725(13), Au1–Cl1 2.3114(18), P1–C11 1.878(5), P1–Ru1–P2 93.61(4), P1–Ru1–P3 100.76(5), P2–Ru1–P3 96.88(4), P11–Au1–Cl1 175.29(6), Ru1–P1–Au1 134.78(6), Ru1–P1–C11 113.43 (18). Molecule crystallised in the centrosymmetric $P2_1/n$ space group – enantiomer present in unit cell.

When single crystals were obtained from a benzene/hexane solvent mixture a different molecular structure was obtained. The structure determined from X-ray diffraction was a centrosymmetric metallamacrocyclic dimer resulting from the rearrangement of [Ru{PH(AuCl)Cy}(dppf)(Tp)] into [{RuCl(Tp)}Au(μ-PHCy)(μ-*P,P'*-dppf)]$_2$ (Figure 2.11, Scheme 2.21). While the mechanism of the dimerisation is not known, the steps that must have taken place can be identified. To form the dimer, the bidenticity of the dppf ligand has opened and one phosphine arm has replaced the chloride at gold. This chloride ends up coordinated to the Ru centre.

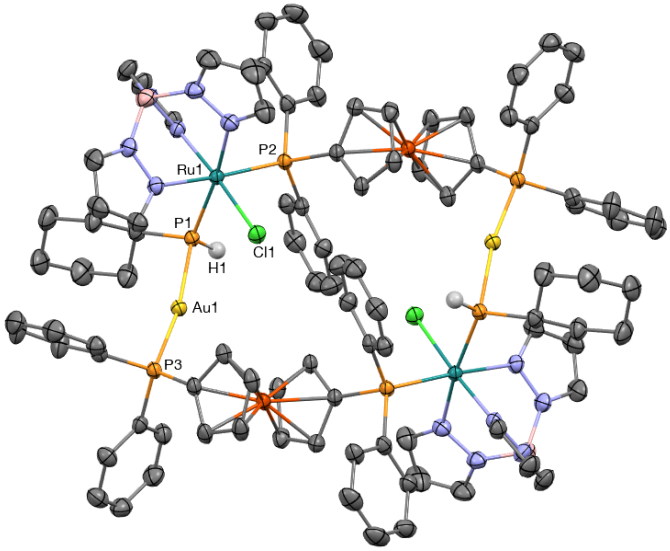

Figure 2.11. Molecular structure of [{RuCl(Tp)}Au(μ-PHCy)(μ-P,P'-dppf)]$_2$ in a crystal of [{RuCl(Tp)}Au(μ-PHCy)(μ-P,P'-dppf)]$_2$.2(C_6H_6) (50% displacement ellipsoids, two benzene solvates and most H atoms omitted, phenyl and cyclohexyl rings simplified). Selected bond lengths (Å) and angles (°): Ru1–P1 2.3228(6), Ru1–P2 2.2830(6), Ru1–Cl1 2.4380(6), Au1–P1 2.3177(6), Au1–P3 2.2851(6), P1–C11 1.863(3), P1–H1 1.29(3), P1–Ru1–P2 95.85(2), P1–Au1–P3 169.77(2), Ru1–P1–Au1 112.83(3), Ru1–P1–C11 119.02(9), Au1–P1–C11 102.33(9).

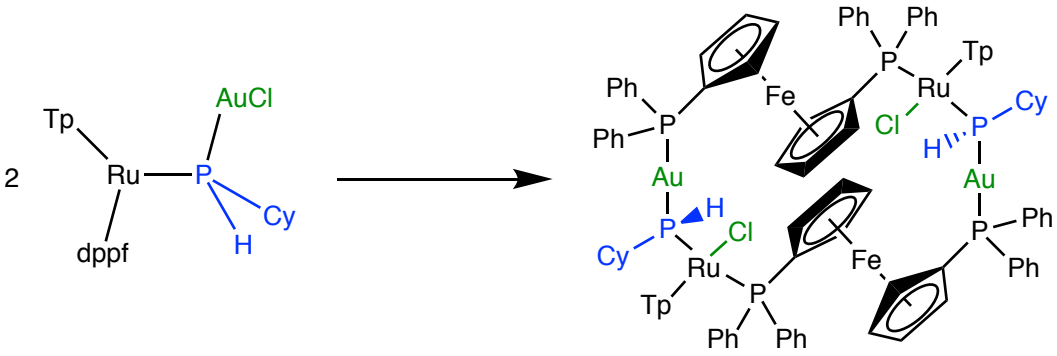

Scheme 2.21. Rearrangement of [Ru{PH(AuCl)Cy}(dppf)(Tp)]

Analysing the molecular structure of [{RuCl(Tp)}Au(μ-PHCy)(μ-*P,P'*-dppf)]$_2$ provides some interesting information, particularly in comparison with the structure of [Ru{PH(AuCl)Cy}(dppf)(Tp)]. The [{RuCl(Tp)}Au(μ-PHCy)(μ-*P,P'*-dppf)]$_2$ molecule is situated on a crystallographic inversion centre and only one half of the dimer is present in the asymmetric unit cell. There are smaller Ru–P distances in the dimer compared to the monomer (Ru–PHCy: 0.057 Å, 44 e.s.d. shorter; Ru–PPh$_2$: 0.061 Å, 47 e.s.d. shorter), likely due to reduced steric bulk of a Cl *versus* a PPh$_2$ group at the metal centre. The P–Au–P angle of 169.77(2)° is smaller than the P–Au–Cl angle of 175.29(6)° in [Ru{PH(AuCl)Cy}(dppf)(Tp)], suggesting a small degree

of strain within the ring of the dimer. Also within the Au coordination sphere, the Au−PHCy distance is 0.045 Å (35 e.s.d.) longer in the dimer, implying that dppf exerts a greater *trans* influence than Cl. As discussed previously, the bidentate coordination of the dppf ligand has opened to allow for dimer formation and the angle between the two vectors defined by the P−C_5H_4 bonds is now 162.6° compared to 30.5° in the monomer.

To gain further understanding into the behaviour of [{RuCl(Tp)}Au(μ-PHCy)(μ-*P,P'*-dppf)]$_2$ the crystals were redissolved in C_6D_6 and the $^{31}P\{^1H\}$ NMR spectrum acquired. In addition to the resonances for [Ru{PH(AuCl)Cy}(dppf)(Tp)] and the singlet at δ_P 35.4 (*vide supra*) there were two new singlets at δ_P 27.5 and 0.0. There were also broad resonances with a low signal-to-noise ratio at δ_P 54.6, 44.6 and 41.2. None of these new signals could be confidently assigned to the dimer [{RuCl(Tp)}Au(μ-PHCy)(μ-*P,P'*-dppf)]$_2$. Importantly, the resonances for [Ru{PH(AuCl)Cy}(dppf)(Tp)] should be distinct from those for [{RuCl(Tp)}Au(μ-PHCy)(μ-*P,P'*-dppf)]$_2$ and the two are unlikely to be mistaken for each other. The distinguishing feature is that each P atom is bound to the one Ru centre in [Ru{PH(AuCl)Cy}(dppf)(Tp)] whereas the two dppf phosphine arms in [{RuCl(Tp)}Au(μ-PHCy)(μ-*P,P'*-dppf)]$_2$ coordinate to different metals. As a result, there should be different coupling behaviour for the phosphorus nuclei in the monomer compared to the dimer (Figure 2.12). Each phosphorus nucleus in [Ru{PH(AuCl)Cy}(dppf)(Tp)] is coupled to two other phosphorus nuclei and accordingly each $^{31}P\{^1H\}$ NMR resonance is observed as a doublet of doublets. In contrast, only the PHCy phosphorus atom in the dimer [{RuCl(Tp)}Au(μ-PHCy)(μ-*P,P'*-dppf)]$_2$ couples to two other phosphorus nuclei (expected to appear as a doublet of doublets) while each of the two dppf phosphorus nuclei only couple to the one PHCy phosphorus atom (resulting in two doublets).

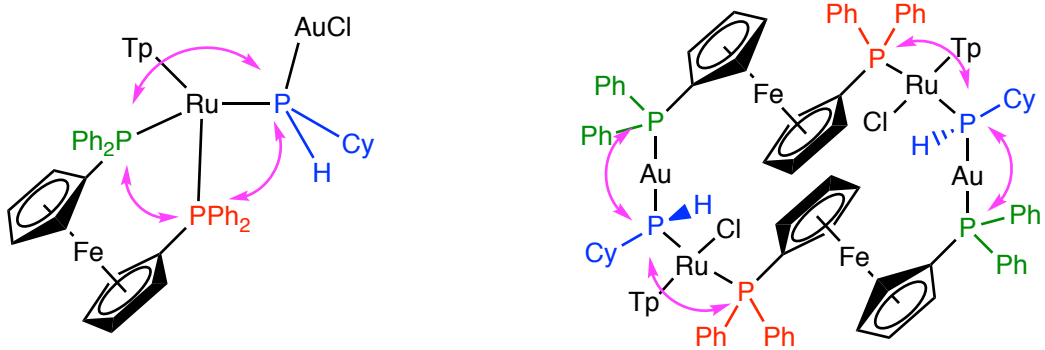

Figure 2.12. Coupling relationships (purple) between phosphorus nuclei in [Ru{PH(AuCl)Cy}(dppf)(Tp)] and [{RuCl(Tp)}Au(μ-PHCy)(μ-P,P'-dppf)]$_2$

The presence of [Ru{PH(AuCl)Cy}(dppf)(Tp)] in the $^{31}P\{^1H\}$ NMR spectrum acquired from the crystals of [RuAu(Cl)(μ-PHCy)(μ-dppf)(Tp)]$_2$ has some interesting implications. It is unclear if the crystal from which the molecular structure was determined was representative of the entire sample. Therefore, it is also uncertain if [Ru{PH(AuCl)Cy}(dppf)(Tp)] is always present as part of a mixture with [{RuCl(Tp)}Au(μ-PHCy)(μ-*P,P'*-dppf)]$_2$ or if the dimer reverts back to the monomer in solution. The latter possibility might imply that isolation of the dimer is a kinetic, albeit entropically-disfavoured, crystallisation phenomenon. A further feature to consider is that dppf is generally a robust chelate, and the d^6-octahedral geometry might be expected to render [Ru(PHCy)(dppf)(Tp)] somewhat inert towards ligand redistribution. Accordingly, the facile, requisite de-chelation of the dppf ligand provides circumstantial support for the co-ligand labilisation that arises from inclusion of the phosphido ligand and bears parallels to the familiar S_N1_{CB} mechanism for amine co-ligand substitution.[147]

Overall, the phosphido complex [Ru(PHCy)(dppf)(Tp)] was extremely basic and difficult to handle. Furthermore, while its reaction with [AuCl(SMe$_2$)] did produce the desired product, [Ru{PH(AuCl)Cy}(dppf)(Tp)], purification and handling was not straightforward and other unexpected products formed. As a result, studies were refocused towards the synthesis of a phosphido complex which was much more amenable to study.

2.4 Summary

The substitution reactions of [RuCl(PPh$_3$)$_2$(Tp)] with PH$_2$Cy were studied. When the substitution was conducted in toluene the replacement of one PPh$_3$ was found to be relatively facile, occurring at room temperature to give [RuCl(PPh$_3$)(PH$_2$Cy)(Tp)]. The replacement of the second PPh$_3$ ligand to give [RuCl(PH$_2$Cy)$_2$(Tp)] was much more difficult and did not proceed to completion after extended heating.

When substitution was conducted with one equivalent of PH$_2$Cy in MeOH in the presence of NaPF$_6$ a mixture of products formed. Analysis of the reaction mixture showed the presence of [RuCl(PPh$_3$)$_2$(Tp)], [RuCl(PPh$_3$)(PH$_2$Cy)(Tp)] and [Ru(PPh$_3$)(PH$_2$Cy)$_2$(Tp)]$^+$. This observation shows that even in polar conditions the substitution of PPh$_3$ is much more facile than the substitution of Cl. The relief of steric strain through the replacement of a bulky PPh$_3$ group is

likely the dominant reason for the selectivity. Additionally, the replacement of Cl from [RuCl(PPh$_3$)(PH$_2$Cy)(Tp)] is much more favourable than from [RuCl(PPh$_3$)$_2$(Tp)]. As a result, [Ru(PPh$_3$)(PH$_2$Cy)$_2$(Tp)]$^+$ is present while there was no evidence for the formation of [Ru(PPh$_3$)$_2$(PH$_2$Cy)(Tp)]$^+$. Conducting the substitution reaction with two equivalents of PH$_2$Cy cleanly produces the bis-substituted product [Ru(PPh$_3$)(PH$_2$Cy)$_2$(Tp)]PF$_6$.

To target a cationic Tp complex bearing a single PH$_2$Cy ligand the use of bidentate ligands was explored. Previous studies had shown that the solubility of the complex [RuCl(dppf)(Tp)] made it a convenient starting material, so it was chosen for this work. The addition of one equivalent of PH$_2$Cy and an excess of NaPF$_6$ to a suspension of [RuCl(dppf)(Tp)] in MeOH resulted in the formation of [Ru(PH$_2$Cy)(dppf)(Tp)]PF$_6$. Attempts to synthesise this salt from a more generalisable route *via* [Ru(NCMe)(dppf)(Tp)]PF$_6$ were unsuccessful as the acetonitrile ligand was found to be relatively strongly bound.

Rather than yielding a phosphido complex, the isolated product following the deprotonation of [RuCl(PPh$_3$)(PH$_2$Cy)(Tp)] was the cyclometallated complex [Ru(PH$_2$Cy)(κ^2-C$_6$H$_4$PPh$_2$-2)(Tp)]. Based on previous reports, and the low conversion (*ca*. 6%) of [RuCl(PPh$_3$)$_2$(Tp)] to [RuH(PPh$_3$)$_2$(Tp)] and [RuH(H$_2$C=CHEt)(PPh$_3$)$_2$(Tp)] following the reaction with ^{n}BuLi, the formation of [Ru(PH$_2$Cy)(κ^2-C$_6$H$_4$PPh$_2$-2)(Tp)] likely occurs *via* the planar phosphido complex [Ru(PPh$_3$)(PHCy)(Tp)] followed by a rapid [2 + 2] cycloaddition. The proposed intermediate was never observed. The newly-formed four-membered ring is relatively robust; no reaction is observed with CO, PMe$_3$ or H$_2$O. Treatment with HCl does, however, restore the initial complex [RuCl(PPh$_3$)(PH$_2$Cy)(Tp)]. The cyclometallated complex [Ru(PH$_2$Cy)(κ^2-C$_6$H$_4$PPh$_2$-2)(Tp)] could be deprotonated with an additional equivalent of ^{n}BuLi to form [Ru(PHCy)(κ^2-C$_6$H$_4$PPh$_2$-2)(Tp)]$^-$. Unfortunately, this anionic phosphido complex proved extremely basic and could only be observed but not isolated.

It was anticipated that the deprotonation of the cationic cyclohexylphosphine complexes [Ru(PPh$_3$)(PH$_2$Cy)$_2$(Tp)]$^+$ and [Ru(PH$_2$Cy)(dppf)(Tp)]$^+$ would yield neutral phosphido complexes which might prove easier to manipulate. While the complexes [Ru(PPh$_3$)(PH$_2$Cy)(PHCy)(Tp)] and [Ru(PHCy)(dppf)(Tp)] could both be observed by ^{31}P NMR spectroscopy, they still proved

extremely basic and were reprotonated during attempts to purify them. The complex [Ru(PPh$_3$)(PH$_2$Cy)(PHCy)(Tp)] forms as a mixture of enantiomers of two diastereomers on account of the stereogenic ruthenium and phosphorus centres.

In an attempt to trap the extremely basic compound [Ru(PHCy)(dppf)(Tp)], its reaction with [AuCl(SMe$_2$)] was investigated. Initial observations indicated that the desired product, [Ru{PH(AuCl)Cy}(dppf)(Tp)], had formed. However, two different single crystals obtained from different solvent mixtures returned two different molecular structures. The first of these was of the expected product, [Ru{PH(AuCl)Cy}(dppf)(Tp)]. The second structure was of a molecule resulting from the dimerisation of [Ru{PH(AuCl)Cy}(dppf)(Tp)]: [{RuCl(Tp)}Au(μ-PHCy)(μ-*P,P'*-dppf)]$_2$. To form this dimer, the unusual opening of the bidentate coordination of dppf is required. Analysis of the crystals of the dimer by ^{31}P{^{1}H} NMR spectroscopy also revealed resonances consistent with the monomer [Ru{PH(AuCl)Cy}(dppf)(Tp)]. As a result, it is not clear if the dimerisation is a reversible phenomenon associated with the solid state, or if the determination of the structure was conducted on a crystal which was not representative of the entire mixture.

Generally, the complexes discussed in this chapter often behaved unexpectedly, frequently forming unusual products. The phosphido complexes which were observed were all extremely basic, making the investigation of their reactivity problematic. Therefore, in order to prioritise the overarching research goal of investigating primary phosphido complex reactivity, further studies were focused on obtaining phosphido complexes with reduced basicity which might be expected to be more amenable to study.

CHAPTER 3
Octahedral Ruthenium Complexes of Cyclohexylphosphine and Their Derivatives

Chapter 3: Octahedral Ruthenium Complexes of Cyclohexylphosphine and Their Derivatives

3.1 Introduction

Much of the difficulty in manipulating the phosphido complexes from the preceding chapter arose from the extremely reactive phosphorus lone pair, either directly or indirectly through its activation of co-ligands with respect to dissociation. In order to mitigate this basicity and nucleophilicity, complexes featuring the carbonyl ligand were targeted. It was believed that the π-acidic nature of a carbonyl co-ligand would draw electron density away from the phosphorus atom and confer stability to the desired complex.

The work of Roper proved particularly enlightening to the pursuit of carbonyl-containing phosphido complexes. The route began from the complexes $[OsH(Cl)(CO)(PPh_3)_2(PHRR')]$ (R = R' = H, Ph; R = H, R' = Ph) which, when treated with perchloric acid in the presence of acetonitrile, yielded the salts $[OsCl(NCMe)(CO)(PPh_3)_2(PHRR')]ClO_4$ (R = R' = H, Ph; R = H, R' = Ph). These acetonitrile complex cations served as key intermediates, readily undergoing ligand substitution with CO, PH_2Ph, AcO^-, $acac^-$, $Me_2NCS_2^-$, and NO_2^- (Scheme 3.1).[75-77, 148-150] A large number of complexes were readily synthesised, providing a platform for the subsequent phosphido chemistry.

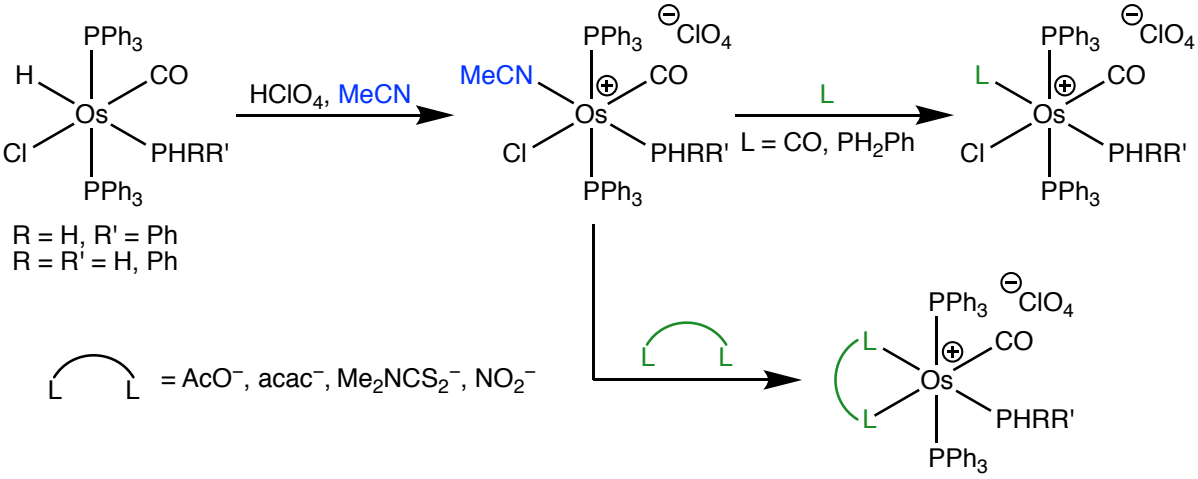

Scheme 3.1. Roper's synthesis of cationic phenylphosphine and diphenylphosphine complexes

3.2 Synthesis of Octahedral Complexes

Based on Roper's synthesis of cationic osmium phosphine complexes, a route was designed to generate cationic ruthenium complexes containing both cyclohexylphosphine and carbonyl ligands (Scheme 3.2). Beginning from the readily accessible complex $[RuH(Cl)(CO)(PPh_3)_3]$,[151] the labile PPh_3 *trans* to the hydride could be substituted for cyclohexylphosphine to obtain $[RuH(Cl)(CO)(PPh_3)_2(PH_2Cy)]$. Treatment of this new complex with a strong acid in the presence of acetonitrile is expected to cleave the Ru−H bond and yield the cationic complex $[RuCl(NCMe)(CO)(PPh_3)_2(PH_2Cy)]^+$. This cation contains labile acetonitrile, chloride and triphenylphosphine ligands, providing a convenient precursor to generate cyclohexylphosphine complexes with a variety of co-ligands.

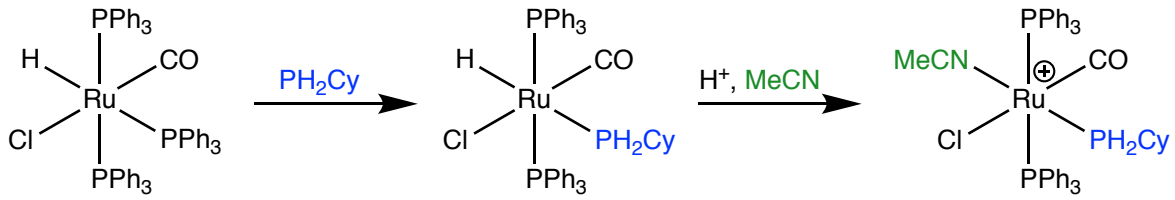

Scheme 3.2. Proposed synthetic route to $[RuCl(NCMe)(CO)(PPh_3)_2(PH_2Cy)]^+$

3.2.1 Synthesis of $[RuH(Cl)(CO)(PPh_3)_2(PH_2Cy)]$

Heating a suspension of $[RuH(Cl)(CO)(PPh_3)_3]$ in *n*-hexane under reflux with an excess of cyclohexylphosphine resulted in the decolourisation of the suspended pink solid. The colourless suspended solid was collected by vacuum filtration, and was found to be exclusively $[RuH(Cl)(CO)(PPh_3)_2(PH_2Cy)]$ (Scheme 3.3).

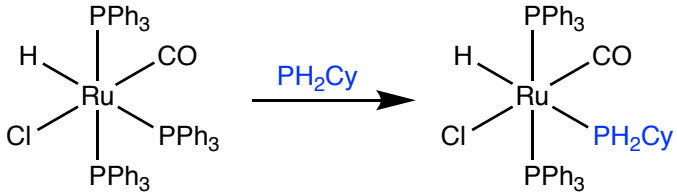

Scheme 3.3. Synthesis of $[RuH(Cl)(CO)(PPh_3)_2(PH_2Cy)]$

In comparison to $[RuH(Cl)(CO)(PPh_3)_3]$, the IR spectrum (KBr) for $[RuH(Cl)(CO)(PPh_3)_2(PH_2Cy)]$ contained new bands at 2923 and 2850 cm^{-1} for aliphatic CH groups as well as a new PH stretch band at 2299 cm^{-1} (only one band observed). Additionally, the ν_{CO} band was observed at 1945 cm^{-1}, at a higher frequency than that for $[RuH(Cl)(CO)(PPh_3)_3]$ (1925 cm^{-1}). Such a shift demonstrates the poorer electron-donating capacity of PH_2Cy compared to PPh_3, as is

expected for primary *versus* tertiary phosphines. The band for the RuH stretch of [RuH(Cl)(CO)(PPh_3)$_3$] appears at 2020 cm^{-1},[152] but no corresponding band was observed in the IR spectrum of [RuH(Cl)(CO)(PPh_3)$_2$(PH_2Cy)].

Two resonances were observed for the AX_2 system in the $^{31}P\{^1H\}$ NMR spectrum of [RuH(Cl)(CO)(PPh_3)$_2$(PH_2Cy)]: a doublet at δ_P 43.9 for the two equivalent, *trans*-disposed PPh_3 groups and a triplet at δ_P −22.0 for the PH_2Cy group. The PH_2Cy resonance also showed coupling to both the two P−H hydrogens and the Ru−H hydride in the ^{31}P NMR spectrum, giving rise to a triplet of doublets with $^1J_{PH}$ = 308 Hz (to P−H) and $^2J_{PH}$ = 112 Hz (to Ru−H). The large magnitude of the latter is indicative of coordination of PH_2Cy *trans* to the hydride ligand.

The ^1H NMR spectrum also supported the formation of the desired product. Multiplets were observed for both phenyl and cyclohexyl groups in their expected regions. The P−H protons resonated at 3.40 ppm, appearing as a doublet (J_{PH} = 308 Hz) on account of the one bond coupling to the phosphorus nucleus. A doublet of triplets at −5.27 ppm was assigned to the Ru-H hydride, with a larger doublet $^2J_{PH}$ of 112 Hz due to the *trans* position of the single PH_2Cy group compared to the smaller triplet $^2J_{PH}$ of 20 Hz for the two PPh_3 groups *cis* to the hydride. The Ru−H and P−H hydrogen atoms are three bonds apart, but no coupling was observed in the ^1H NMR spectrum. Presumably, the coupling constant was too small to be detected.

The $^{13}C\{^1H\}$ NMR data did not reveal any unusual features. The resonances for the *ipso*, *ortho* and *meta* carbons of the phenyl rings appeared as virtual triplets, typical for two *trans*-disposed triphenylphosphine groups. Four resonances were observed for the cyclohexyl carbons, indicative of the high symmetry of the molecule with a mirror plane bisecting the two PPh_3 groups. Lastly, the CO resonance appears as a doublet of triplets, showing coupling to the PH_2Cy and the two PPh_3 groups with $^2J_{PC}$ of 9 and 12 Hz respectively. The small coupling constants confirm the *cis* relationship between the CO and each of the three *mer*-disposed phosphine groups.

3.2.2 Synthesis of $[RuCl(NCMe)(CO)(PPh_3)_2(PH_2Cy)]^+$

The addition of acid (HPF_6, $HClO_4$ or HOTf) to $[RuH(Cl)(CO)(PPh_3)_2(PH_2Cy)]$ in a CH_2Cl_2/MeCN solution resulted in the evolution of H_2 gas and the formation of $[RuCl(NCMe)(CO)(PPh_3)_2(PH_2Cy)]X$ (X = PF_6, ClO_4, OTf) (Scheme 3.4). The product forms as a mixture of three isomers as observed by $^{31}P\{^1H\}$ NMR spectroscopy. These isomers appear as three separate pairs of coupled resonances: δ_P 19.6 and −1.9, δ_P 28.9 and −12.4, and δ_P 28.8 and −20.9. For each of these isomers the higher-frequency resonance is a doublet while the lower-frequency resonance is a triplet, which is consistent with expected *meridional* geometry of the phosphine groups. Further, each of the lower-frequency resonances appears as a triplet in the ^{31}P NMR spectrum, confirming their identification as PH_2Cy signals. Based on the $^{31}P\{^1H\}$ NMR data, the three isomers arise from different arrangements of the Cl, MeCN, CO and PH_2Cy ligands (Figure 3.1), although the exact assignment of isomers to resonances is not possible.

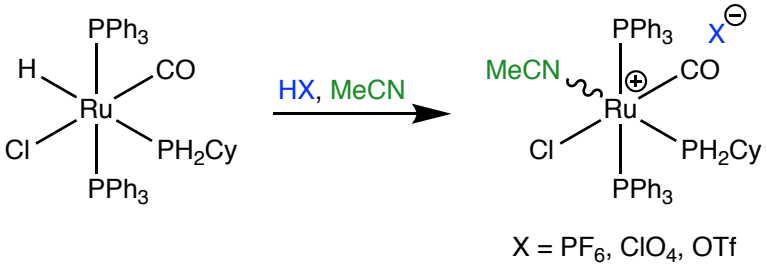

Scheme 3.4. Synthesis of $[RuCl(NCMe)(CO)(PPh_3)_2(PH_2Cy)]X$ (X = PF_6, ClO_4, OTf)

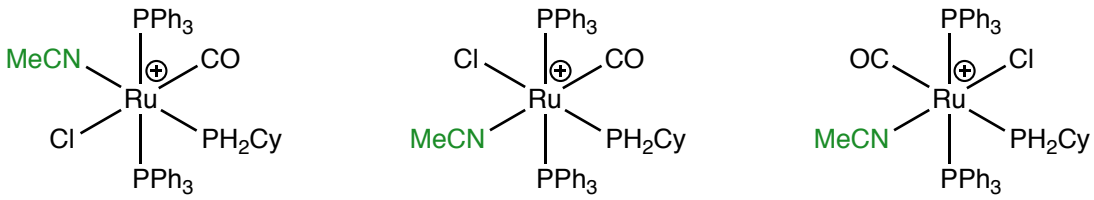

Figure 3.1. Isomers of $[RuCl(NCMe)(CO)(PPh_3)_2(PH_2Cy)]^+$

Crystals of one isomer of $[RuCl(NCMe)(CO)(PPh_3)_2(PH_2Cy)]ClO_4$ suitable for X-ray diffraction were grown from an MeCN solution. The molecular structure (Figure 3.2) confirms that the relative geometry of the phosphines (two *trans* PPh_3 groups with the PH_2Cy *cis* to these) is maintained. The geometric parameters of the structure are all within the expected ranges.[135]

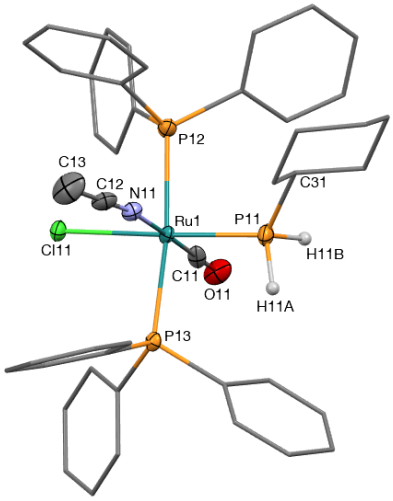

Figure 3.2. Molecular structure of one isomer of $[RuCl(NCMe)(CO)(PPh_3)_2(PH_2Cy)]^+$ in a crystal of $[RuCl(NCMe)(CO)(PPh_3)_2(PH_2Cy)]ClO_4.0.5(MeCN)$ (50% displacement ellipsoids, second independent molecule in cell, perchlorate anion, acetonitrile solvent and most H atoms omitted, phenyl and cyclohexyl rings simplified). Selected bond lengths (Å) and angles (°): Ru1−P11 2.3142(16), Ru1−P12 2.4088(16), Ru1−P13 2.4034(16), Ru1−Cl11 2.4299(15), Ru1−C11 1.831(6), Ru1−N11 2.096(5), P11−C31 1.839(8), O11−C11 1.158(8), P12−Ru1−P13 172.83(6), Ru1−P11−C31 122.2(3).

Importantly, the crystals contained a single isomer in which the Cl is *trans* to the PH_2Cy group. However, redissolving these crystals and acquiring the $^{31}P\{^1H\}$ NMR spectrum showed that a mixture of isomers was quickly re-established. These observations show that the MeCN is labile in solution, allowing for interconversion between the isomers.

Of the three counteranions used, triflate was chosen for future work. Overall, the choice of anion had little effect on the chemistry or on the distribution of isomers observed (Table 3.1). A major consideration was the safety of perchlorate salts, which are potentially explosive. Addtionally, hexafluorophosphates salts are known to hydrolyse,[153] leading to decomposition and inexact stoichiometries in further chemistry. Combining these two factors, triflate was deemed the most suitable anion.

Table 3.1. Relative proportion of each [RuCl(NCMe)(CO)(PPh_3)$_2$(PH_2Cy)]$^+$ isomer (δ_P) depending on counteranion

	δ_P PH_2Cy		
Anion	−1.9	−12.4	−20.9
PF_6^-	71	18	11
ClO_4^-	61	18	21
OTf^-	59	16	25

3.2.3 Reaction with CO

A considerable body of Roper's investigations into octahedral phosphido complexes involved two CO ligands. The second of the CO ligands was introduced *via* substitution of acetonitrile under *ca*. 2.7 atm of CO, and provides additional stability to the electron-rich phosphido complex through its π-acid properties. Using an analogous approach, bubbling CO through a solution of [RuCl(NCMe)(CO)(PPh_3)$_2$(PH_2Cy)]OTf, followed by recrystallisation from CH_2Cl_2 and isopropanol, gave [RuCl(CO)$_2$(PPh_3)$_2$(PH_2Cy)]OTf (Scheme 3.5) as a colourless solid in 84% yield.

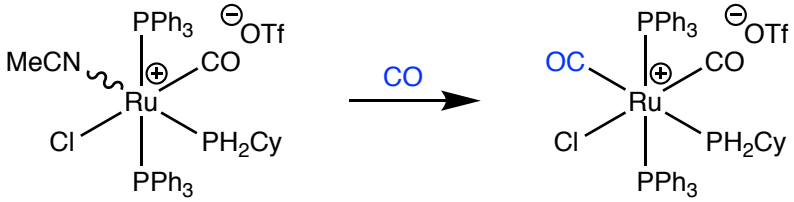

Scheme 3.5. Synthesis of [RuCl(CO)$_2$(PPh_3)$_2$(PH_2Cy)]OTf

The IR solution spectrum (CH_2Cl_2) revealed two CO bands at 2078 and 2018 cm^{-1}, at a higher wavenumber than the mixed isomers of the acetonitrile complex (1986, 1964 cm^{-1}). The higher wavenumber is indicative of the introduction of an additional π-acidic CO ligand, reducing the electron density at the metal centre. Additionally, the two bands observed in the CO region signify the presence of two *cis* CO ligands, and their symmetric and antisymmetric stretching modes.

The ^{1}H NMR spectrum for [RuCl(CO)$_2$(PPh$_3$)$_2$(PH$_2$Cy)]OTf displayed the expected multiplets for the phenyl and cyclohexyl groups. The P−H proton signals appeared as a doublet of doublet of triplets at δ_H 4.12, showing a large one bond ^{31}P–^{1}H coupling of 372 Hz, as well as smaller three bond coupling between the 1-cyclohexyl proton and the two PPh$_3$ groups (both 8 Hz).

Similarly, the ^{13}C{^{1}H} NMR spectrum showed all of the resonances expected for the phenyl and cyclohexyl groups. Two CO signals were observed, with one displaying a strong *trans* coupling ($^{2}J_{PC}$ = 97 Hz) to the phosphorus of the PH$_2$Cy ligand, and weaker *cis* coupling ($^{2}J_{PC}$ = 11 Hz) to those of the two PPh$_3$ groups. The other CO signal was also expected to resonate as a doublet of triplets with smaller *cis* $^{2}J_{PC}$, but the splitting of the signal was poorly resolved and coupling constants could not be extracted (^{13}C{^{1}H} NMR spectrum measured at 176.1 MHz).

The ^{31}P{^{1}H} NMR spectrum showed a doublet at 17.5 ppm for the PPh$_3$ groups and a triplet at −20.2 for the PH$_2$Cy group ($^{2}J_{PP}$ = 32 Hz). The $^{1}J_{PH}$ for the PH$_2$Cy triplet was measured to be 370 Hz in the ^{31}P NMR spectrum.

The structure of [RuCl(CO)$_2$(PPh$_3$)$_2$(PH$_2$Cy)]OTf was confirmed by X-ray crystallography (Figure 3.3). The ruthenium centre adopts an octahedral geometry with the PPh$_3$ groups *trans* to each other. The two CO groups are *cis* to each other, in agreement with the IR data. Interestingly, there is an increased amount of ruthenium-to-carbon bonding indicated by the shorter Ru−C (1.8901(18) *versus* 1.942(2) Å) and longer C−O (1.135(2) *versus* 1.121(2) Å) distances for the CO *trans* to Cl consistent with it being a stronger π-donor than PH$_2$Cy. Both the PH$_2$Cy hydrogen atoms were located in the Fourier difference map, and form an angle of 99.3(16)° at phosphorus.

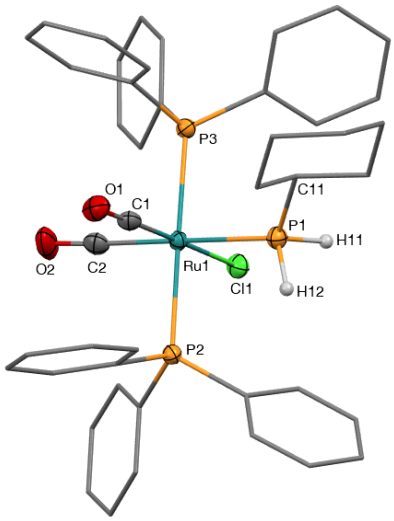

Figure 3.3. Molecular structure of $[RuCl(CO)_2(PPh_3)_2(PH_2Cy)]^+$ in a crystal of $[RuCl(CO)_2(PPh_3)_2(PH_2Cy)]OTf$ (50% displacement ellipsoids, triflate anion and most H atoms omitted, phenyl and cyclohexyl rings simplified). Selected bond lengths (Å) and angles (°): Ru1–P1 2.4079(4), Ru1–P2 2.4282(4), Ru1–P3 2.4239(4), Ru1–Cl1 2.4228(4), Ru1–C1 1.8901(18), Ru1–C2 1.942(2), P1–C11 1.8352(18), P1–H11 1.30(3), P1–H12 1.29(3), O1–C1 1.135(2), O2–C2 1.121(2), P2–Ru1–P3 177.450(14), Ru1–P1–C11 123.44(6), H11–P1–H12 99.3(16).

The formation of a single isomer of $[RuCl(CO)_2(PPh_3)_2(PH_2Cy)]OTf$ provides some interesting insights. Comparing and contrasting the complexes $[RuCl(CO)_2(PPh_3)_2(PH_2Cy)]OTf$ and $[RuCl(NCMe)(CO)(PPh_3)_2(PH_2Cy)]OTf$, the former has two π-acceptors and two donors in a plane while the latter as one π-acceptor and three donors. Thus, there is a thermodynamic preference to have the donors *trans* to the acceptors in $[RuCl(CO)_2(PPh_3)_2(PH_2Cy)]OTf$ and this is the isomer which is formed. In contrast, with three donors in $[RuCl(NCMe)(CO)(PPh_3)_2(PH_2Cy)]OTf$ there is no definitive driving force for a particular isomer so three different geometries are observed. The lability of MeCN *versus* CO allows for the conversion between the isomers. Indeed, the substitution of acetonitrile to form $[RuCl(CO)_2(PPh_3)_2(PH_2Cy)]OTf$ proceeds *via* a dissociative mechanism.[150] In the five coordinate intermediate the PH_2Cy group is bulkier than its co-equatorial Cl and CO ligands which may drive incoming ligands to the *trans* site. Additionally, based on the relative *trans* influence of the equatorial ligands (Cl < PH_2Cy < CO) the site *trans* to CO is the least favourable for incoming ligands and hence the formation of the *trans*-CO isomer is not observed.

3.2.4 Reaction with CNMes

Isocyanides (or isonitriles, C≡N−R) are isoelectronic to CO and also behave as neutral, two-electron ligands. In general, however, both the HOMO and LUMO of isocyanides tend to be higher in energy than in CO. Accordingly, isocyanides are considered to be better σ-donors but poorer π-acceptors, resulting in isocyanide complexes having more electron-rich metal centres than their CO counterparts.

Following the successful substitution of MeCN for CO in $[RuCl(NCMe)(CO)(PPh_3)_2(PH_2Cy)]OTf$, the analogous reaction with mesityl isocyanide (CNMes) was explored. Stirring a CH_2Cl_2 solution of $[RuCl(NCMe)(CO)(PPh_3)_2(PH_2Cy)]OTf$ with CNMes resulted in acetonitrile substitution to give $[RuCl(CO)(CNMes)(PPh_3)_2(PH_2Cy)]OTf$ (Scheme 3.6). Following recrystallisation, the product was isolated as a colourless solid in 61% yield.

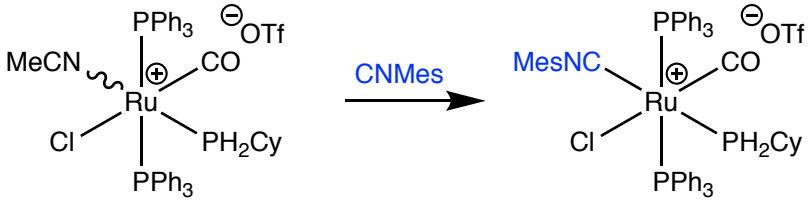

Scheme 3.6. Synthesis of $[RuCl(CO)(CNMes)(PPh_3)_2(PH_2Cy)]OTf$

The IR spectrum (CH_2Cl_2) of $[RuCl(CO)(CNMes)(PPh_3)_2(PH_2Cy)]OTf$ contained bands for both the CN and CO stretches at 2162 and 2004 cm^{-1}, respectively. Compared with free CNMes (ν_{CN} 2120 cm^{-1}) the CN stretch is higher, as has been previously observed for bound isocyanides.[154] Such increases are due to their poor π-acceptor properties, meaning that π retrodonation and subsequent weakening of the CN bond is much less pronounced than for CO. The CO stretch is lower than those observed for $[RuCl(CO)_2(PPh_3)_2(PH_2Cy)]OTf$ (2078 and 2018 cm^{-1} in CH_2Cl_2), which further illustrates the stronger σ-basic and weaker π-acidic properties of isocyanides *versus* CO.

The ^1H NMR spectrum of $[RuCl(CO)(CNMes)(PPh_3)_2(PH_2Cy)]OTf$ contained the expected multiplets for the cyclohexyl and aromatic protons. The methyl groups of the mesityl group were seen as two distinct singlets integrating in a 2:1 ratio, with the equivalent *ortho* methyl groups indicating that free rotation about the Ru−CN bond allows the group to traverse a geometry in which the Ru−PPh_3 vectors are co-planar with the mesityl ring. In contrast, the

most likely ground state structure without rotation would have the mesityl ring perpendicular to the Ru−PPh_3 vectors, resulting in inequivalent *ortho* methyl groups. A doublet of doublet of triplets at δ_H 3.97 was assigned to the P−H protons, showing one-bond coupling to phosphorus (372 Hz) as well as three-bond coupling to the two phosphorus nuclei of the PPh_3 groups ($^3J_{PH}$ = 6 Hz) and the proton at the 1 position of the cyclohexyl ring ($^3J_{HH}$ = 6 Hz).

A doublet at δ_P 20.5 for the PPh_3 groups and a triplet at δ_P −12.0 for the PH_2Cy group were observed in the $^{31}P\{^1H\}$ NMR spectrum. The $^2J_{PP}$ of 29 Hz was in the expected range for *cis* coupling between phosphorus nuclei at a Ru(II) centre. In the ^{31}P NMR experiment the PH_2Cy resonance appeared as a triplet with a measured $^1J_{PH}$ of 359 Hz.

In addition to the typical resonances for the PPh_3 and PH_2Cy groups in the $^{13}C\{^1H\}$ NMR spectrum, the four aromatic and two alkyl resonances for CNMes were also observed. Significant in the spectrum were the CO and CN resonances, appearing at δ_C 194.9 and 150.5 respectively. The CO resonance was observed as a doublet of triplets with coupling constants of 14 and 11 Hz. In contrast, the CN resonance was a doublet of broad (quadrupolar ^{14}N: I = 1) signals with $^2J_{PC}$ = 151 Hz. These data provide insight into the geometry at the metal centre, indicating that the CNMes is *trans* to the PH_2Cy whereas the CO is *cis* to all three ^{31}P nuclei. A smaller *cis* coupling between the C(N) and the two PPh_3 groups is also expected but could not be resolved in the spectrum. The geometry of the product further supports the previous assertion that the steric bulk of the PH_2Cy group drives incoming groups to the *trans* site at the metal.

3.2.5 Reaction with Diethyldithiocarbamate

Diethyldithiocarbamate is a strongly chelating ligand, and was used to introduce a bidentate ligand to the coordination sphere of the cyclohexylphosphine ruthenium complex. The addition of an EtOH/H_2O solution of $Na[S_2CNEt_2].2H_2O$ to a CH_2Cl_2 solution of $[RuCl(NCMe)(CO)(PPh_3)_2(PH_2Cy)]OTf$ yielded the chelated salt $[Ru(CO)(PPh_3)_2(PH_2Cy)(\kappa^2\text{-}S,S'\text{-}S_2CNEt_2)]OTf$ (Scheme 3.7).

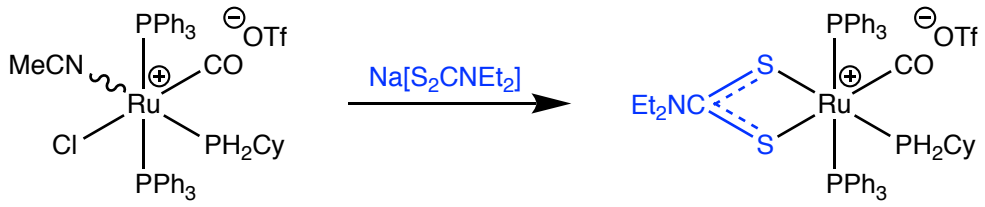

Scheme 3.7. Synthesis of [Ru(CO)(PPh$_3$)(PH$_2$Cy)(κ^2-S,S'-S$_2$CNEt$_2$)]OTf

The CO band in the IR spectrum (CH_2Cl_2) was at 1968 cm^{-1}, lower than the bands for both [RuCl(CO)$_2$(PPh$_3$)$_2$(PH$_2$Cy)]OTf and [RuCl(CNMes)(CO)(PPh$_3$)$_2$(PH$_2$Cy)]OTf. The higher electron density of the metal centre offers a comparison between the potent π-basic electron donating ability of the diethyldithiocarbamate ligand *cf*. the chloro ligand combined with either carbonyl or mesityl isocyanide.

In the ^{1}H NMR spectrum the PH hydrogens appear as a doublet of doublet of triplets, similar to the observations for the previously discussed complexes. The two ethyl groups are pseudo-*trans* to different groups at ruthenium and appear as two distinct A_3X_2 spin systems in the ^{1}H NMR spectrum. Two sets of ethyl signals are also observed in the ^{13}C{^{1}H} NMR spectrum.

The high frequency CS_2 resonance was observed at 202.0 ppm in the ^{13}C{^{1}H} NMR spectrum, but the signal for the CO group was not well resolved. A signal with a poor signal-to-noise ratio was observed at approximately 201.1 ppm which is in the expected range for a ruthenium(II) carbonyl resonance. The signal is expected to couple to the two PPh_3 groups as well as the PH_2Cy groups, resulting in a doublet of triplets. This multiplicity, combined with the generally poor signal-to-noise for carbonyls, may render the signal unobservable in a standard 1D ^{13}C NMR experiment within a reasonable timeframe. An attempt was made to observe the signal *via* the PH hydrogens in a 2D ^{1}H-^{13}C HMBC experiment, but no correlation was observed.

The characterisation of [Ru(CO)(PPh$_3$)$_2$(PH$_2$Cy)(κ^2-*S,S'*-S$_2$CNEt$_2$)]OTf included an X-ray crystallography study (Figure 3.4). As observed in the previous molecular structures, the Ru centre has an octahedral geometry with *trans* PPh_3 groups. The diethyldithiocarbamate ligand occupies two *cis* sites while CO and PH_2Cy complete the coordination sphere. Both Ru–S bonds are of comparable length (2.4440(7) and 2.4407(7) Å), implying that neither CO nor

PH_2Cy exhibits a strong *trans* influence relative to the other. The C_2NCS_2 core of the dieithyldithiocarbamate ligand is approximately planar, with angle sums of 360° at N and the CS_2 carbon, and C−N−C−S torsions of 6.2 and 6.7°.

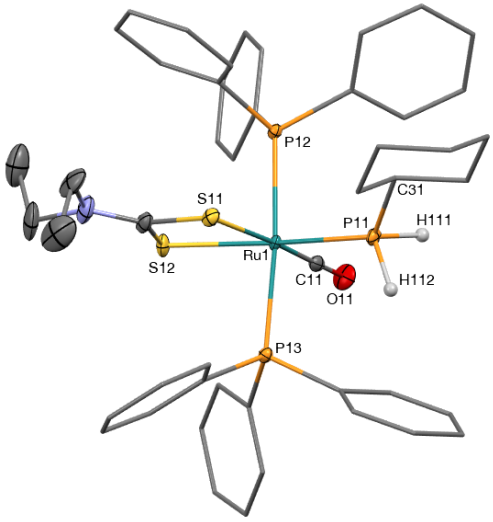

Figure 3.4. Molecular structure of $[Ru(CO)(PPh_3)_2(PH_2Cy)(\kappa^2\text{-}S,S'\text{-}S_2CNEt_2)]^+$ in a crystal of $[Ru(CO)(PPh_3)_2(PH_2Cy)(\kappa^2\text{-}S,S\text{-}S_2CNEt_2)]OTf.2(CHCl_3)$ (50% displacement ellipsoids, second independent molecule in cell, triflate anion, solvent molecules and most H atoms omitted, phenyl and cyclohexyl rings simplified). Selected bond lengths (Å) and angles (°): Ru1−P11 2.3298(7), Ru1−P12 2.4100(7), Ru1−P13 2.4031(7), Ru1−S11 2.4440(7), Ru1−S12 2.4407(7), Ru1−C11 1.864(3), P1−C31 1.835(3), P1−H111 1.28(4), P1−H12 1.32(4), O11−C11 1.156(4), P12−Ru1−P13 173.86(2), Ru1−P11−C31 125.29(9), H111−P11−H112 95(3).

3.2.6 Synthesis of $[Ru(CO)(PPh_3)(PH_2Cy)(Tp)]OTf$

The reaction of $[RuCl(NCMe)(CO)(PPh_3)_2(PH_2Cy)]OTf$ with the tridentate ligand Tp was also investigated. The expected product, $[Ru(CO)(PPh_3)(PH_2Cy)(Tp)]OTf$, is reminiscent of $[RuCl(PPh_3)(PH_2Cy)(Tp)]$ (see Section 2.2.1) with the key difference being the charge difference that attends including a carbonyl in place of a chloro ligand. Changing the ligand in this manner should increase the acidity of the P−H bond by making the complex cationic and by stabilising the electron density of the deprotonated product through the π−acidity of the carbonyl ligand.

Stirring a mixture of KTp and $[RuCl(NCMe)(CO)(PPh_3)_2(PH_2Cy)]OTf$ in THF gave a mixture of products as identified by $^{31}P\{^1H\}$ NMR spectroscopy. Triphenylphosphine was the major and expected by-product from the intended substitution. The desired product, $[Ru(CO)(PPh_3)(PH_2Cy)(Tp)]OTf$ (Scheme 3.8), was also identified by two doublets at δ_P 38.4

and −6.6 ($^2J_{PP}$ = 28 Hz) in the $^{31}P\{^1H\}$ NMR spectrum, for which the latter resonance appeared as a PH_2 triplet in the ^{31}P NMR with $^1J_{PH}$ = 358 Hz. Unfortunately, this product was never observed in more than 50% *in situ* yield with numerous (>17 $^{31}P\{^1H\}$ NMR resonances) unidentified side products. While purification was possible, low isolated yields (26%) prompted the exploration of alternative strategies.

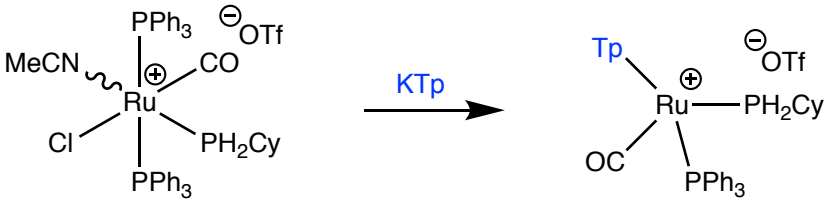

Scheme 3.8. Synthesis of [Ru(CO)(PPh₃)(PH₂Cy)(Tp)]OTf from [RuCl(NCMe)(CO)(PPh₃)₂(PH₂Cy)]OTf

The synthetic approach adopted (Scheme 3.9) was adapted from work by Gunnoe, who synthesised the aniline salt [Ru(NH_2Ph)(CO)(PPh_3)(Tp)]OTf from [Ru(OTf)(CO)(PPh_3)(Tp)].[120] Beginning from [RuH(Cl)(CO)(PPh_3)$_3$], the overall route involved coordination of Tp to form [RuH(CO)(PPh_3)(Tp)] followed by conversion to the chloride [RuCl(CO)(PPh_3)(Tp)].[128] Abstraction of chloride from this complex with AgOTf yielded [Ru(OTf)(CO)(PPh_3)(Tp)],[120] for which triflate substitution for PH_2Cy gave the target salt [Ru(CO)(PPh_3)(PH_2Cy)(Tp)]OTf. Furthermore, this process yielded microanalytically pure product with the final step occuring in 65% yield.

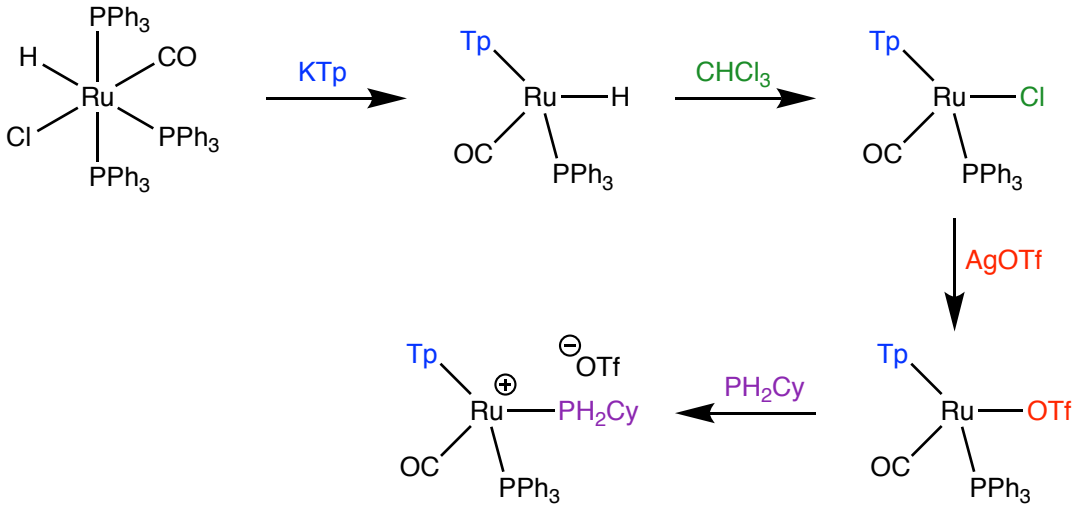

Scheme 3.9. Alternative synthesis of [Ru(CO)(PPh₃)(PH₂Cy)(Tp)]OTf

Despite returning high-purity product with a moderately-yielding final step, the above approach involved the time-consuming isolation of three intermediates so further optimisation was conducted. Inspired by work with metal hydrides and acids (*vide supra*), a one-pot procedure based on the addition of HOTf to [RuH(CO)(PPh_3)(Tp)], followed by addition of PH_2Cy was developed (Scheme 3.10). This method removed two synthetic steps and produced sufficiently pure (>95%) [Ru(CO)(PPh_3)(PH_2Cy)(Tp)]OTf in 85% yield on a two-gram scale.

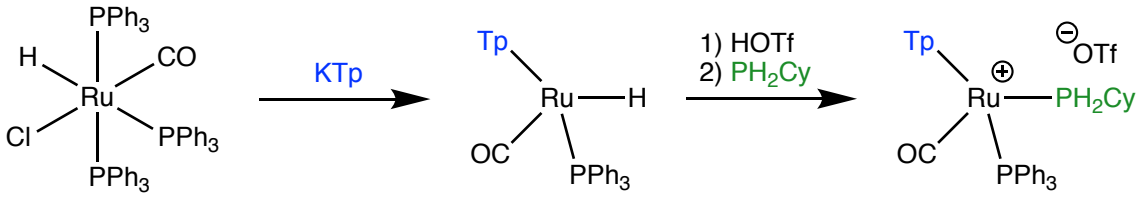

Scheme 3.10. Optimised synthesis of [Ru(CO)(PPh_3)(PH_2Cy)(Tp)]OTf

Weak ν_{BH} (2499 cm^{-1}) and ν_{PH} (2351 cm^{-1}) bands in the IR spectrum (CH_2Cl_2) of [Ru(CO)(PPh_3)(PH_2Cy)(Tp)]OTf showed the presence of Tp and PH_2Cy, respectively. The ν_{CO} band was observed at 1996 cm^{-1}. The ^1H NMR spectrum of [Ru(CO)(PPh_3)(PH_2Cy)(Tp)]OTf contained nine individual singlets in the range δ_H 7.85–6.03 for the Tp pyrazolyl rings, indicative of the asymmetric Ru centre. The asymmetry rendered the PH_2Cy hydrogens diastereotopic, and two individual resonances were observed at δ_H 4.56 and 3.88. One-bond phosphorus-hydrogen coupling constants of 364 and 357 Hz, respectively, could be measured for these resonances but finer couplings ($^2J_{HH}$, $^3J_{PH}$, $^3J_{HH}$) were not well-resolved. The triphenylphosphine hydrogen atoms were observed *via* three multiplets in the aromatic region at δ_H 7.51, 7.43 and 7.08, and the higher-order cyclohexyl spin system gave rise to multiplets in the range δ_H 2.20–0.87.

The most distinct feature of the $^{13}C\{^1H\}$ NMR spectrum was the CO signal at δ_C 200.9. The signal appears as a triplet but is actually a doublet of doublets, showing equal coupling values to the PPh_3 and PH_2Cy groups of $^2J_{PC}$ = 14 Hz. Resonances for PPh_3 were typical, and observed at δ_C 133.5 (d, J_{PC} = 11 Hz), 131.7 (s), 129.7 (d, $^1J_{PC}$ = 48 Hz) and 129.4 (d, J_{PC} = 11 Hz), in contrast to the virtual triplet resonances observed for the previous *trans*-Ru(PPh_3)$_2$ complexes. The asymmetry of the molecule resulted in the observation of nine pyrazolyl resonances and six individual resonances for the cyclohexyl ring.

The molecular structure of [Ru(CO)(PPh_3)(PH_2Cy)(Tp)]OTf is shown in Figure 3.5. As expected, the Tp ligand occupies three facial sites at the octahedral ruthenium centre. Triphenylphosphine, CO and PH_2Cy occupy the other three sites. Both PH_2Cy hydrogen atoms were located in the Fourier difference map, and all the geometric parameters of the structure fall within the expected ranges.

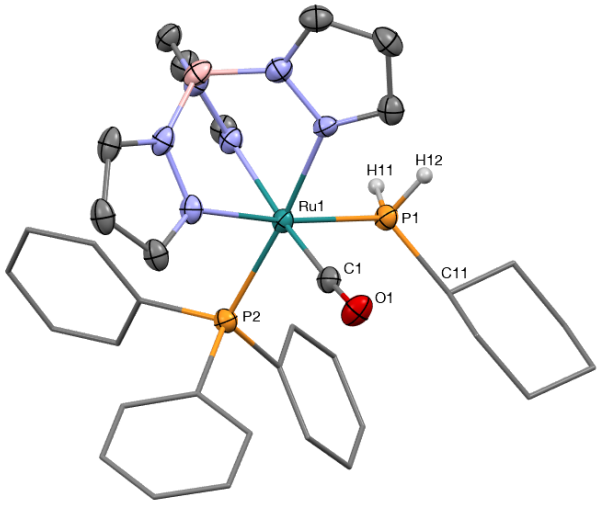

Figure 3.5. Molecular structure of S_{Ru}-[Ru(CO)(PPh_3)(PH_2Cy)(Tp)]$^+$ in a crystal of [Ru(CO)(PPh_3)(PH_2Cy)(Tp)]OTf.(CH_2Cl_2) (50% displacement ellipsoids, triflate anion, CH_2Cl_2 solvate and most H atoms omitted, phenyl and cyclohexyl rings simplified). Selected bond lengths (Å) and angles (°): Ru1–P1 2.3255(6), Ru1–P2 2.3645(7), Ru1–C1 1.853(3), P1–C11 1.841(2), O1–C1 1.151(3), P1–Ru1–P2 95.62(2), P1–Ru1–C1 93.12(7), P2–Ru1–C1 94.11(8). Molecule crystallised in the centrosymmetric $P2_1/c$ space group – enantiomer is present in the unit cell.

3.3 Deprotonation Reactions

In analogous conditions to Roper's deprotonation,[75-77, 149] the addition of DBU to a benzene suspension of [$RuCl(CO)_2(PPh_3)_2(PH_2Cy)$]OTf resulted in the immediate dissolution of solid and a colour change to red, which faded to orange. The IR spectrum (C_6H_6) of this mixture contained bands at 2033 (shoulder), 2022, 1968 and 1899 cm^{-1}. As expected for deprotonation, these bands are at lower frequency than those for the cationic starting material (2074, 2020 cm^{-1} in THF).

An aliquot of the reaction mixture taken for NMR spectroscopy showed a combination of products (Scheme 3.11). Seven $^{31}P\{^1H\}$ NMR resonances were observed, of which PPh_3 (δ_P −5.3) was the major product (41%). Also notable among these resonances was a broad singlet

at δ_P −50.7 which appeared as a doublet ($^1J_{PH}$ = 180 Hz) in the ^{31}P NMR spectrum. The far-low-frequency nature of this resonance as well as its coupling pattern suggest that the desired complex [RuCl(CO)$_2$(PPh$_3$)$_2$(PHCy)] has formed, albeit in relatively low proportions. Unfortunately, the PPh$_3$ resonance for this compound could not be unequivocally identified as there were three doublets which could reasonably correspond to [RuCl(CO)$_2$(PPh$_3$)$_2$(PHCy)] at δ_P 23.4 (J = 3 Hz), 23.2 (J = 8 Hz) and 20.7 (J = 25 Hz).

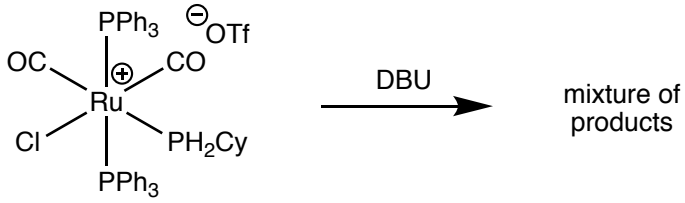

Scheme 3.11. Attempted deprotonation of [RuCl(CO)$_2$(PPh$_3$)$_2$(PH$_2$Cy)]OTf

The isolation of [RuCl(CO)$_2$(PPh$_3$)$_2$(PHCy)] was not achieved. Removing the solvent from the reaction mixture *in vacuo* and recording the ^{31}P{^{1}H} NMR spectrum of the residue showed an increased number of resonances (>18 in total). Furthermore, the addition of methanol to this residue resulted in the disappearance of resonances in the phosphido region of the ^{31}P{^{1}H} NMR spectrum, suggesting reprotonation. This is in direct contrast to Roper's osmium analogues which were recrystallised from benzene/methanol mixtures. Recrystallisations from combinations of benzene, n-hexane and diethyl ether did not result in any significant changes in the proportions of products.

The liberation of PPh$_3$ during the deprotonation reaction suggests that ligand substitution is occurring. There may be several factors contributing to this. The typically non-nuclephillic base, DBU, may be acting as a competitive ligand for PPh$_3$, although this seems unlikely. However, PPh$_3$ lability was generally not observed in the ligand substitutions previously described in this chapter, suggesting that additional processes must be occurring. One possibility is non-innocent behaviour of the phosphido lone pair in which access to the planar phosphido form labilises the co-ligands. In a non-polar solvent, such as benzene, the liberation of PPh$_3$ may be favoured over Cl. Furthermore, low-coordination complexes generated from ligand labilisation may combine with complexes bearing highly-nucleophilic phosphido groups to form a variety of phosphido-bridged oligomers, consistent with the increased number of resonances in the ^{31}P{^{1}H} NMR spectrum.

It was presumed that the involvement of multi-dentate ligands might prevent ligand substitution and add stability to the desired phosphido complex(es). The deprotonation of $[Ru(CO)(PPh_3)_2(PH_2Cy)(\kappa^2\text{-}S,S'\text{-}S_2CNEt_2)]OTf$ resulted in the formation of even more products (Scheme 3.12) than the same reaction with $[RuCl(CO)_2(PPh_3)_2(PH_2Cy)]OTf$. Again, PPh_3 was the major product, identified among more than thirty $^{31}P\{^1H\}$ NMR resonances. Deprotonating $[Ru(CO)(PPh_3)(PH_2Cy)(Tp)]OTf$, however, successfully yielded $[Ru(CO)(PPh_3)(PHCy)(Tp)]$ and its synthesis, properties and reactivity are described in the following two chapters.

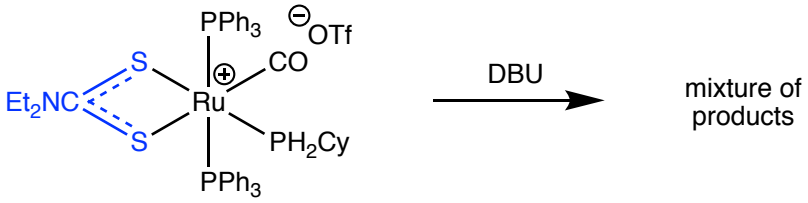

Scheme 3.12. Attempted deprotonation of $[Ru(CO)(PPh_3)_2(PH_2Cy)(\kappa^2\text{-}S,S'\text{-}S_2CNEt_2)]OTf$

3.4 Reaction with methoxide

As well as isolating nucleophilic phosphido complexes, Roper highlighted the ambiphilic potential of phosphido complexes by conducting the deprotonation in methanol (see Section 1.2.2). The polarity of methanol combined with the non-innocence of the phosphorus lone pair was believed to allow for the labilisation of the chloride *via* a planar phosphorus intermediate. The now-electrophilic planar phosphorus could then undergo nucleophilic addition by methanol/methoxide, generating complexes of the form $[Os(CO)_2(PPh_3)_2(PRR'\{OMe\})]$. Investigations were undertaken to explore the analogous chemistry with some of the ruthenium complexes described in this chapter.

3.4.1 Synthesis of $[Ru(CO)_2(PPh_3)_2\{PH(OMe)Cy\}]$

Addition of two equivalents of DBU to a methanol suspension of $[RuCl(CO)_2(PPh_3)_2(PH_2Cy)]OTf$ resulted in an immediate colour change from colourless to orange. After heating the mixture for 1 hour under reflux, $[Ru(CO)_2(PPh_3)_2(PH\{OMe\}Cy)]$ was isolated from the cooled mixture as an orange solid in 82% yield (Scheme 3.13).

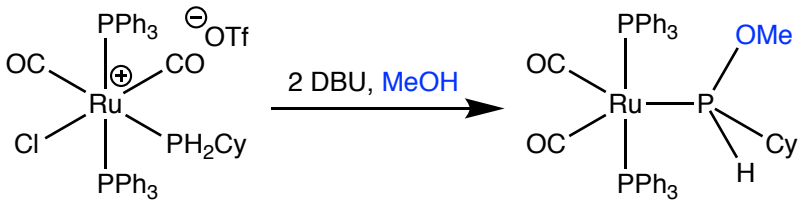

Scheme 3.13. Synthesis of [Ru(CO)$_2$(PPh$_3$)$_2${PH(OMe)Cy}]

Overall, the transformation results in a reduction of the metal centre from Ru(II) to Ru(0). This change is evident in the IR spectrum (THF) in which the CO bands appeared at 1911 and 1862 cm^{-1}, lower than the Ru(II) precursor (2074 and 2020 cm^{-1}). The presence of two CO bands indicates their *cis* geometry, giving rise to both symmetric and antisymmetric infrared-active modes.

The newly formed PH(OMe)Cy group was identified *via* a high frequency triplet at 158.5 ppm in the ^{31}P{^{1}H} NMR spectrum, with the resonance appearing as a PH doublet ($^1J_{PH}$ = 305 Hz) in the ^{31}P NMR experiment. This resonance had a $^2J_{PP}$ of 16 Hz to the PPh$_3$ groups, which suggests a *ca*. 90° relationship between the phosphine groups. The PH proton resonance appeared at 6.41 ppm in the ^{1}H NMR spectrum, and displayed the appropriate values for $^1J_{PH}$, $^3J_{PH}$ and $^3J_{HH}$. Both resonances appear at a higher frequency than those for the parent PH$_2$Cy group in [RuCl(CO)$_2$(PPh$_3$)$_2$(PH$_2$Cy)]$^+$, indicative of the introduction of the more electronegative OMe substituent. This OMe substituent could be seen in both the ^{1}H and ^{13}C{^{1}H} NMR spectra, with doublets at 3.03 ppm ($^3J_{PH}$ = 5 Hz) and 42.6 ppm ($^2J_{PC}$ = 25 Hz), respectively.

Formally, the PH(OMe)Cy group is asymmetric and renders both the PPh$_3$ groups and the CO groups each diastereotopic. Experimentally, however, a single doublet is seen for the PPh$_3$ groups at 54.9 ppm in the ^{31}P{^{1}H} NMR spectrum. Similarly, only one CO resonance at 216.1 ppm is seen in the ^{31}C{^{1}H} NMR spectrum. Coupling of this resonance to the PPh$_3$ groups was observed ($^2J_{PC}$ = 13 Hz), but coupling to the PH(OMe)Cy group was not resolved. A similar observation was made for the maleic anhydride complexes [M{η^2-C$_2$H$_2$(CO)$_2$O}(CO)$_2$(PPh$_3$)$_2$] (M = Ru, Os) in which the coupling of the maleic anhydride and CO ^{13}C NMR resonances to the axial PPh$_3$ was large while the coupling to the equatorial phosphine was relatively small (< 5Hz).[155]

The geometry of the metal fragment '$Ru(CO)_2(PPh_3)_2$' was utilised by Roper to compare the π-accepting capacity of the ligands ethylene, maleic anhydride and tetrafluoroethylene.[155] For stronger π-acceptors there would be fewer co-equatorial π-acid CO ligands to compete for electron density. As a result, there were two equatorial CO ligands with ethylene, one for maleic anhydride and none for tetrafluoroethylene. Therefore, based on the structure of $[Ru(CO)_2(PPh_3)_2\{PH(OMe)Cy\}]$ with two equatorial CO groups, the π-accepting capability of PH(OMe)Cy is less than maleic anhydride and comparable to ethylene. The calculated Tolman Electronic Parameter[132] for PH(OMe)Cy is 2072.2 *cf.* 2083.6 for ethylene.[156] Using this calculated Tolman Electronic Parameter, PH(OMe)Cy is less electron-donating than PCy_3 (2056.4) and PPh_3 (2068.9), but gives a more electron-rich metal centre than the $P(OMe)_3$ (2079.5) and the primary phosphine PH_2Ph (2077.0).[132]

3.4.2 Synthesis of $[Ru(CO)(CNMes)(PPh_3)_2\{PH(OMe)Cy\}]$

The reaction with methoxide was further explored with the mesityl isocyanide salt, $[RuCl(CO)(CNMes)(PPh_3)_2(PH_2Cy)]OTf$. The addition of two equivalents of DBU to a methanol solution of $[RuCl(CO)(CNMes)(PPh_3)_2(PH_2Cy)]OTf$ resulted in an immediate colour change to orange and precipitate formation. Over 20 minutes the precipitate dissolved and after 1.5 hours the mixture had faded to a pale yellow. Removal of the solvent from the reaction mixture returned an orange residue.

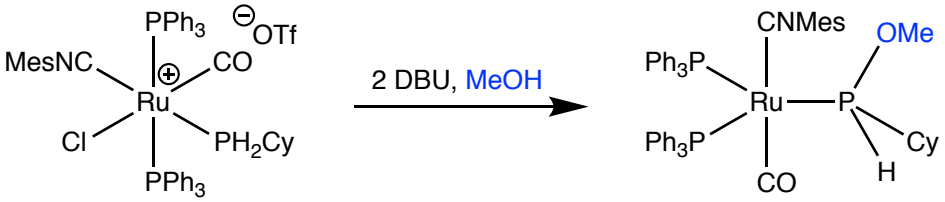

Scheme 3.14. Synthesis of $[Ru(CO)(CNMes)(PPh_3)_2\{PH(OMe)Cy\}]$

The $^{31}P\{^1H\}$ NMR spectrum of the residue showed a major product with a triplet at δ_P 160.1 and a doublet at δ_P 53.3 ($^2J_{PP}$ = 71 Hz). The triplet further split into a doublet with a $^1J_{PH}$ of 305 Hz in the absence of ^1H decoupling. These data are consistent with the formation of the desired product, $[Ru(CO)(CNMes)(PPh_3)_2\{PH(OMe)Cy\}]$ (Scheme 3.14). Interestingly, the $^2J_{PP}$ of 71 Hz suggests that the three phosphorus atoms occupy the equatorial sites of the trigonal bipyramid.

Table 3.2. $^{31}P\{^{1}H\}$ NMR data for two isomers of [Ru(CO)(CNMes)(PPh$_3$)$_2${PH(OMe)Cy}]

	PH(OMe)Cy		PPh_3		PPh_3	
Isomer	δ_P	$^2J_{PP}$ (Hz)	δ_P	$^2J_{PP}$ (Hz)	δ_P	$^2J_{PP}$ (Hz)
1	150.8	23 228	37.6	23 228	26.0	23 23
2	153.0	19 228	38.1	19 228	28.5	19 19

In the presence of methanol, [Ru(CO)(CNMes)(PPh$_3$)$_2${PH(OMe)Cy}] rearranges with a visible colour change. The $^{31}P\{^{1}H\}$ NMR data following rearrangement showed the presence of two major products, each with three resonances. These resonances were all doublet of doublets, with chemical shift and coupling constants summarised in Table 3.2. Based on the similarity of chemical shifts, coupling patterns and coupling constants the two isomers are likely very similar structures. The higher-frequency resonance is likely to be due to a PH(OMe)Cy ligand based on the chemical shift, and from the coupling constants it has an approximate 90° relationship to one PPh_3 group and a *trans* relationship to the other. From these data, the most likely structures are distorted square pyramids with *trans* CO and CNMes, and PH(OMe)Cy and PPh_3 groups (Scheme 3.15). In such a structure, the Ru centre is stereogenic. Combined with the stereogenic phosphorus atom in PH(OMe)Cy, this would generate two diastereomers which accounts for the observations from the $^{31}P\{^{1}H\}$ NMR data. While a trigonal bipyramidal structure is expected, deviations toward square pyramidal geometries are known for five-coordinate ruthenium(0) complexes.[157-158]

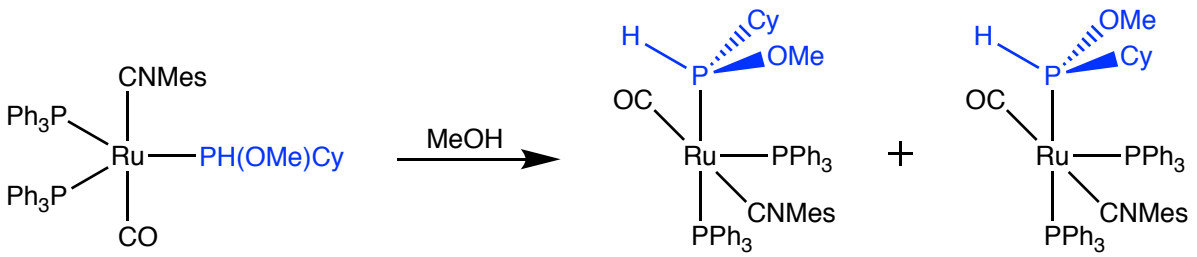

Scheme 3.15. Rearrangement of [Ru(CO)(CNMes)(PPh$_3$)$_2${PH(OMe)Cy}] in methanol

In comparison to $[Ru(CO)_2(PPh_3)_2\{PH(OMe)Cy\}]$, which could be filtered directly from the reaction mixture, the purification of $[Ru(CO)(CNMes)(PPh_3)_2\{PH(OMe)Cy\}]$ proved more difficult and was not achieved. Additionally, work with $[Ru(CO)(CNMes)(PPh_3)_2\{PH(OMe)Cy\}]$ would be further complicated by its isomerism in solution. Consequently, subsequent studies primarily focused on $[Ru(CO)_2(PPh_3)_2\{PH(OMe)Cy\}]$.

3.5 Reactivity of $[Ru(CO)_2(PPh_3)_2\{PH(OMe)Cy\}]$

Phosphines bearing both a P–H bond and a nucleofugic group (X = F, Cl, Br, I,[159-163] NR_2,[104, 161, 163-169] OR) are relatively rare within the literature. Such PHXR phosphines generally decompose with elimination of HX to form the cyclic oligomers $(PR)_n$.[170-171] Within the protective enclave of a metal complex, however, these complexes have been stabilised and isolated. A summary focusing on the chemistry of complexes with phosphines bearing both P–H and P–O bonds (excluding Roper's work, see Section 1.2.2) is given here.

The first report of the stabilisation of these phosphines was by Müller in 1975 (Scheme 3.16).[170] Treatment of the primary phosphine complex $[Mn(CO)_2(PH_2Ph)(Cp)]$ with NCl_2Cy gave a mixture of P-chlorinated products, $[Mn(CO)_2(PCl_2Ph)(Cp)]$ and $[Mn(CO)_2(PHClPh)(Cp)]$. The key step in these halogenation reactions was inferred to occur *via* a phosphinidene intermediate. While the latter complex could not be isolated, it did react with I_2 and THF to form a P–O bond-containing complex. Ring opening of the THF occurred to give the ω-iodobutoxy-substituted phosphine complex $[Mn(CO)_2\{PH(OCH_2CH_2CH_2CH_2I)Ph\}(Cp)]$.

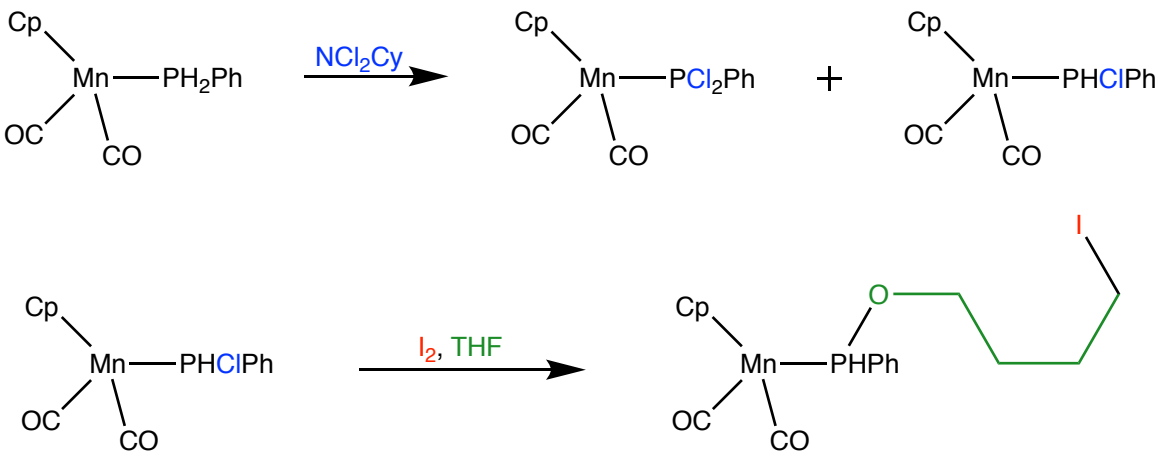

Scheme 3.16. First report of a complex bearing a phosphine with P–H and P–O bonds

A common route to these complexes is the reaction of a phosphinidene with an O–H bond. This approach was first demonstrated by Mathey through the treatment of a 7-phosphanorbornadiene complex with methanol to give the complex $[W(CO)_5\{PH(OMe)Ph\}]$.[171] The 7-phosphanorbornadiene complex undergoes thermolysis to form a transient phosphinidene intermediate which reacts with methanol to give the product $[W(CO)_5\{PH(OMe)Ph\}]$ (Scheme 3.17). Similar approaches have been utilised by Mathey,[172-173] Lammertsma,[174-175] and Ramos and Ruiz[176] to form complexes with PH(OR)R' phosphines.

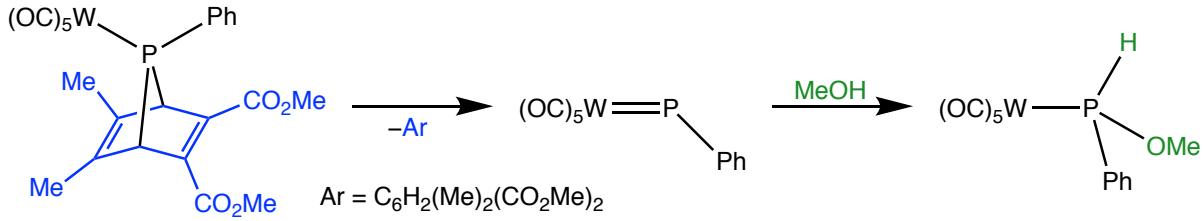

Scheme 3.17. Reaction of a phosphinidene complex with methanol

Notable work in this field has been conducted by Streubel. The 2*H*-azaphosphirene complex may lose benzonitrile to form the phosphinidene complex $[W(CO)_5\{PCH(SiMe_3)_2\}]$. This phosphinidene reacts with acetophenone or H_2O to form enol ether- and silyl ether-substituted phosphines, respectively. The phosphinidene intermediate also reacts with triethylammonium chloride to give the complex $[W(CO)_5(PHCl\{CH(SiMe_3)\})]$ (Scheme 3.18), which can undergo chlorine substitution to give even further oxygen-substituted phosphine complexes (Scheme 3.19).[177-179] Substitution at P–Cl bonds has also been utilised by others to form PH(OR)R' complexes.[180-182]

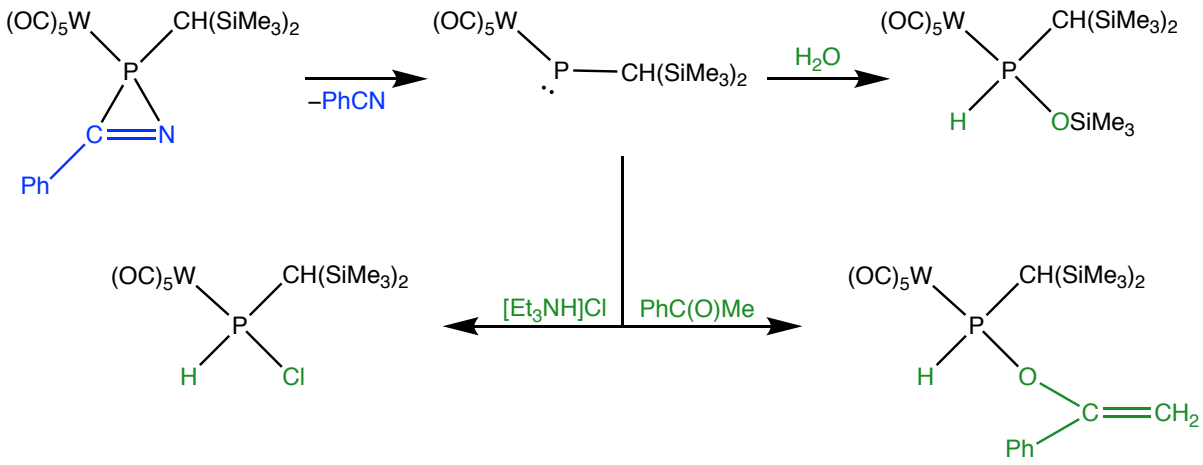

Scheme 3.18. Streubel's derivatives of a 2H-azaphosphirene complex

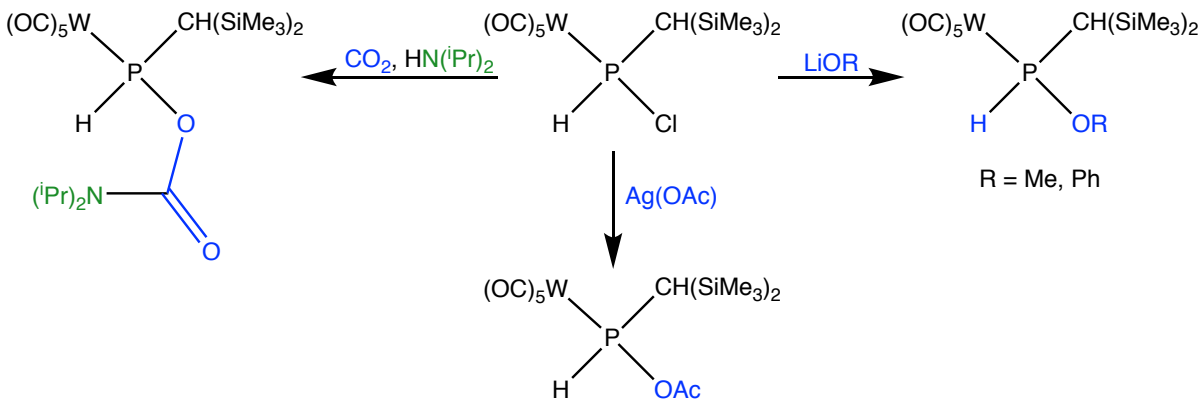

Scheme 3.19. Reactions of the P–Cl bond in [W(CO)$_5$(PHCl{CH(SiMe$_3$)$_2$})]

Another reported method to access phosphines with both P–H and P–O substituents is *via* protonation of an anionic complex already featuring a P–O bond (Scheme 3.20). One example of this was reported by Cowley,[183] in which the anion [Mo(CO)$_2${P(OMe)C(SiMe$_3$)$_2$}(Cp)]$^-$ is protonated by MeOH to form [Mo(CO)$_2${η^2-*P,C*-PH(OMe)C(SiMe$_3$)$_2$}(Cp)]. In another report by Schrock, the pincer complex anion [MoI(N)(κ^3-*P,C,P*-2,6-C$_6$H$_3$(OP^{t}Bu$_2$)$_2$)]$^-$ was treated with [Et$_3$NH]$^+$ to give a complex with a 3-centre-2-electron P–H–Mo bond.[184]

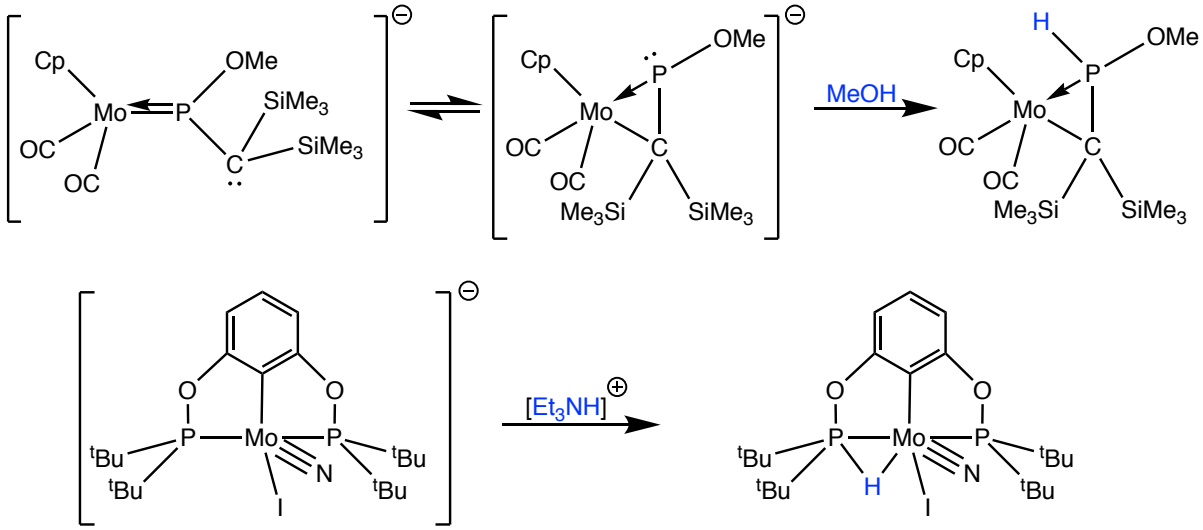

Scheme 3.20. Protonation of low-valent complexes to yield complexes with P–H and P–O bonds

Weber reported two complexes with a P–H and a P=O bond, with both complexes obtained from the hydrolysis of a phosphorus-element π bond. The complexes [Fe(CO)$_2${P=C(SiMe$_3$)$_2$}(Cp*)] and [Fe(CO)$_2$(P=PMes*)(Cp*)] both react with hexafluoropropane-2,2-diol dihydrate to give [Fe(CO)$_2${PH(O)CH(SiMe$_3$)$_2$}(Cp*)] and [Fe(CO)$_2${PH(O)PHMes*}], respectively (Scheme 3.21).[185]

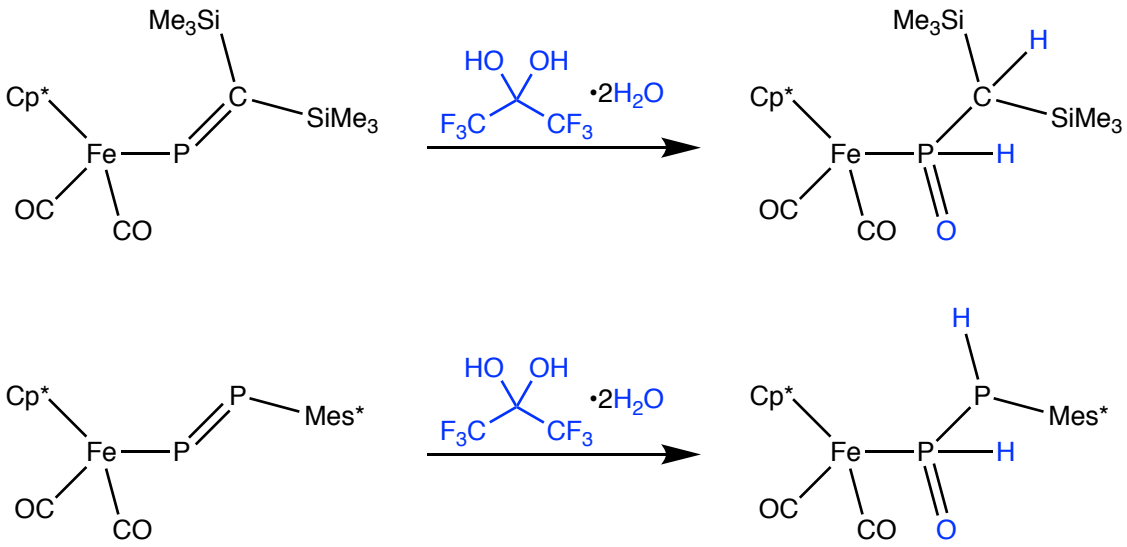

Scheme 3.21. Weber's formation of PH(O)R (R = $CH(SiMe_3)_2$, PHMes) complexes*

In nearly all of these reports the PH(OR)R' complex is treated as an endpoint and no further investigation into the reactivity of the complexes has been conducted. Only Streubel and Arduengo have reported further reactivity studies into these types of complexes.[186] The complexes $[W(CO)_5\{PH(OR)CH(SiMe_3)_2\}]$ (R = Me, Ph) may be deprotonated with an *N*-heterocyclic carbene or phosphazene to yield the phosphinidenoid anions $[W(CO)_5\{P(OR)CH(SiMe_3)_2\}]^-$ (R = Me, Ph) (Scheme 3.22).[186]

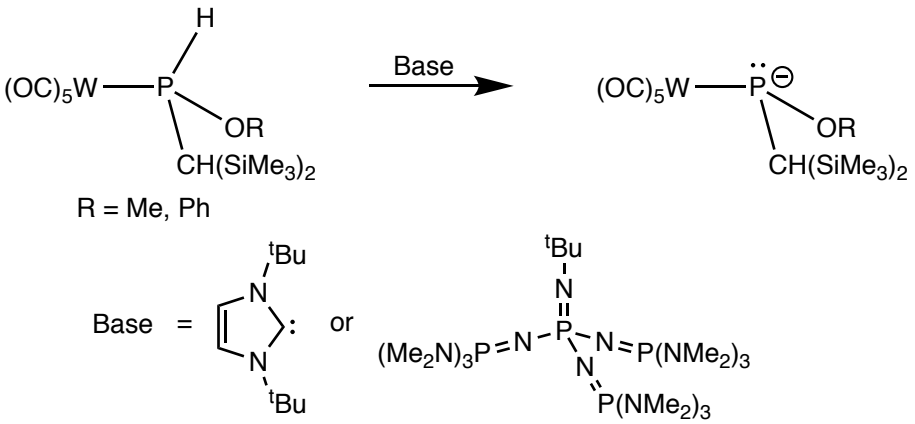

Scheme 3.22. Reactivity of a PH(OR)R' (R = Me, Ph; R' = $CH(SiMe_3)_2$) complex

Streubel extended deprotonation to the acetate-substituted complex $[W(CO)_5\{PH(OAc)CH(SiMe_3)_2\}]$. In the reaction with lithium diisopropylamide in the presence of 12-crown-4, the transient species $[Li(12\text{-crown-}4)][W(CO)_5\{P(OAc)CH(SiMe_3)_2\}]$ is formed. However, the final isolated product is the salt $[Li(12\text{-crown-}4)][W(CO)_5\{PH(O)CH(SiMe_3)_2\}]$, which can be considered to have a P=O bond with the oxygen atom coordinating to the

lithium ion (Scheme 3.23). The exact details of the loss of the acetyl group were not determined.[179]

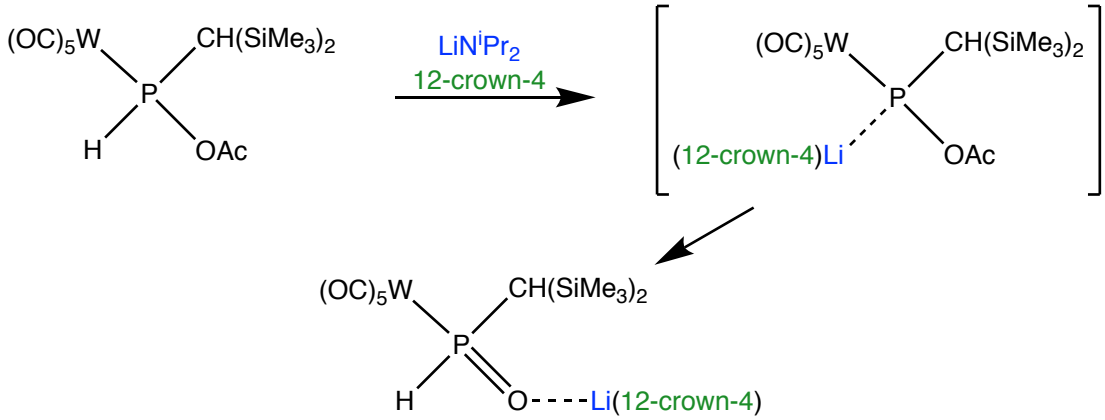

Scheme 3.23. Formation of [Li(12-crown-4)][W(CO)$_5${PH(O)CH(SiMe$_3$)$_2$}]

Considering the dearth of information in the literature, gaining further insight into the properties of these unusual ligands is desirable. The complex [Ru(CO)$_2$(PPh$_3$)$_2${PH(OMe)Cy}] contains several sites of potential reactivity: labile PPh$_3$ ligands, a zero-valent ruthenium centre and potentially reactive P−H and P−OMe bonds. Reactions were hence conducted to investigate each of these sites.

3.5.1 Reaction with CO

The first reaction of [Ru(CO)$_2$(PPh$_3$)$_2${PH(OMe)Cy}] investigated was ligand substitution with CO. While the two carbonyls are unlikely to be labile while bound to a Ru(0) centre, the reaction should provide insight into the comparative ligand capability of PPh$_3$ and PH(OMe)Cy.

Bubbling CO through a THF solution of [Ru(CO)$_2$(PPh$_3$)$_2${PH(OMe)Cy}] for 90 minutes followed by stirring the solution in the sealed flask for 16 hours resulted in the formation of [Ru(CO)$_3$(PPh$_3$){PH(OMe)Cy}] (Scheme 3.24) as the major product (43% by NMR). [Ru(CO)$_3$(PPh$_3$){PH(OMe)Cy}] was identified in the ^{31}P{^{1}H} NMR spectrum of the reaction mixture *via* two doublets at δ_P 155.0 and 53.2. The large $^2J_{PP}$ of 194 Hz indicates a *trans* relationship between the two phosphorus atoms. The resonance at δ_P 155.0 can be assigned to the PH(OMe)Cy group on account of its doublet of doublets pattern ($^1J_{PH}$ = 358 Hz, $^2J_{PP}$ = 194 Hz) in the ^{31}P NMR spectrum.

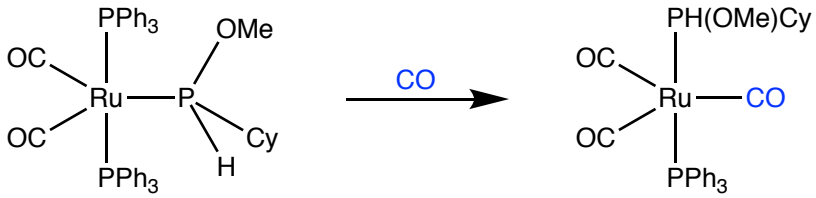

Scheme 3.24. Synthesis of [Ru(CO)$_3$(PPh$_3$){PH(OMe)Cy}]

The IR spectrum contained a single, high-intensity ν_{CO} band at 1906 cm^{-1}, which constitutes a shift to higher wavenumber than the precursor, [Ru(CO)$_2$(PPh$_3$)$_2$(PH(OMe)Cy}]. This shift is consistent with the introduction of an additional π-acidic CO ligand, which would reduce the electron density at the metal and consequently reduce the metal-to-carbonyl retrodonation. The appearance of a single ν_{CO} stretch and its high intensity indicate that the three carbonyl groups are coplanar,[187] consistent with the observation of *trans* phosphorus groups from the ^{31}P{^{1}H} NMR data. Such a geometry is common for [Ru(CO)$_3$(PR$_3$)$_2$] complexes, and likely arises from maximising the distance between the two phosphines whilst placing the π-acceptor ligands in the most π-basic equatorial sites.[188-189]

Several other products were observed in the ^{31}P{^{1}H} NMR spectrum of the reaction mixture. The most prominent two resonances were readily identified as PPh$_3$ and O=PPh$_3$, further confirming that phosphine substitution had occurred. The other products, comprising approximately 14% of the mixture, gave rise to singlet resonances at δ_P 55.7, 54.4, 46.8, 42.7 and 39.1. The product of PH(OMe)Cy substitution, [Ru(CO)$_3$(PPh$_3$)$_2$], is reported to give an ^{31}P{^{1}H} NMR shift at δ_P 57.4,[190] which is close to the resonance at δ_P 55.7. This resonance accounts for about 7% of the mixture. Another notable resonance was the singlet at δ_P 42.7, which appeared as a doublet with a remarkably large J_{PH} of 514 Hz in the absence of ^{1}H decoupling. The coupling pattern suggests that it may be a derivative of PH(OMe)Cy, while the extraordinarily large coupling constant is characteristic of low electron density at phosphorus.[138]

Purification of [Ru(CO)$_3$(PPh$_3$){PH(OMe)Cy}] was not satisfactorily achieved. The compound proved remarkably soluble in *n*-pentane, *n*-hexane, Et$_2$O, THF, benzene, toluene, methanol and ethanol. Recrystallisation from ethanol did yield a solid, but only in 8% yield and still *ca*. 30% impure by NMR. Leaving a 1:15 THF/*n*-hexane solution at −20°C resulted in the formation

of a yellow oil which could not be separated. Finally, column chromatography on silica with CH_2Cl_2/hexane as the eluent removed the majority of impurities. Unfortunately, the resonances at δ_P 55.7 and 39.1 were still present and comprised *ca*. 40% of the mixture.

3.5.2 Reaction with CNMes

Utilising the isocyanide/carbonyl analogy (Section 3.2.4), the next ligand substitution was attempted with CNMes. Stirring a mixture of CNMes and $[Ru(CO)_2(PPh_3)_2\{PH(OMe)Cy\}]$ for 25 hours resulted in the formation of $[Ru(CO)_2(CNMes)(PPh_3)\{PH(OMe)Cy\}]$ as the major product (Scheme 3.25). The complex $[Ru(CO)_2(CNMes)(PPh_3)\{PH(OMe)Cy\}]$ was identified by $^{31}P\{^1H\}$ NMR spectroscopy; the PPh_3 group appeared as a doublet at δ_P 56.1 while the PH(OMe)Cy group appeared as a doublet at δ_P 159.6, displaying a further doublet splitting ($^1J_{PH}$ = 347 Hz) in the absence of ^1H decoupling. Similarly to $[Ru(CO)_3(PPh_3)\{PH(OMe)Cy\}]$, the relatively large $^2J_{PP}$ of 188 Hz indicates a *trans* relationship between the two phosphorus atoms. The same NMR data were obtained from an NMR-scale reaction between $[Ru(CO)(CNMes)(PPh_3)_2\{PH(OMe)Cy\}]$ and CO, further corroborating the formation of $[Ru(CO)_2(CNMes)(PPh_3)\{PH(OMe)Cy\}]$.

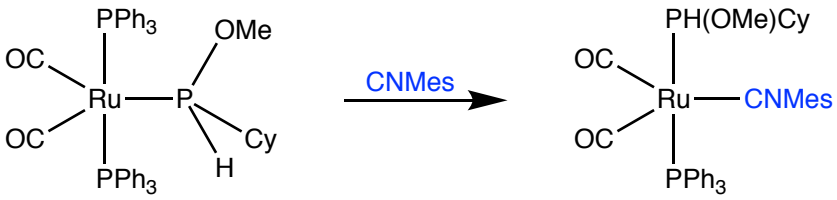

Scheme 3.25. Synthesis of $[Ru(CO)_2(CNMes)(PPh_3)\{PH(OMe)Cy\}]$

Infrared spectroscopy provided further structural information about $[Ru(CO)_2(CNMes)(PPh_3)\{PH(OMe)Cy\}]$. The presence of two ν_{CO} bands at 1911 and 1875 cm^{-1} indicated a *cis* relationship between the carbonyl groups, in good agreement with the geometry inferred from the $^{31}P\{^1H\}$ NMR data. These two disparate stretches also indicate the reduced symmetry of $[Ru(CO)_2(CNMes)(PPh_3)\{PH(OMe)Cy\}]$ *versus* $[Ru(CO)_3(PPh_3)\{PH(OMe)Cy\}]$. The introduction of CNMes was indicated *via* the ν_{CN} band at 2046 cm^{-1}.

Similarly to $[Ru(CO)_3(PPh_3)\{PH(OMe)Cy\}]$, the high solubility of $[Ru(CO)_2(CNMes)(PPh_3)\{PH(OMe)Cy\}]$ impeded its purification. Following a THF/hexane recrystallisation, the majority of $[Ru(CO)_2(CNMes)(PPh_3)\{PH(OMe)Cy\}]$ was found in the supernatant without increased purity. Analysis of the precipitate by $^{31}P\{^1H\}$ NMR spectroscopy revealed an increased number of resonances (>11 total). Placing a concentrated Et_2O solution of the reaction mixture in the freezer at −20°C only resulted in the formation of crystals of $[Ru(CO)_2(CNMes)(PPh_3)_2]$, which were identified by X-ray crystallography. This compound gives rise to a $^{31}P\{^1H\}$ NMR resonance at δ_P 60.5,[154] and only comprised <1% of the reaction mixture.

3.5.3 Reaction with dppe

Following the observed substitution of PPh_3 for CO and CNMes, substitution with the bidentate ligand dppe was investigated. Stirring a THF solution of $[Ru(CO)_2(PPh_3)_2\{PH(OMe)Cy\}]$ and dppe for 22 hours resulted in the formation of $[Ru(CO)_2\{PH(OMe)Cy\}(dppe)]$ as the major product. This product was identified in the $^{31}P\{^1H\}$ NMR spectrum of the reaction mixture by a doublet at δ_P 73.5 and a triplet at δ_P 163.5 ($^2J_{PP}$ = 86 Hz). The resonance at δ_P 163.5 was assigned to the PH(OMe)Cy group as it appears as a PH doublet ($^1J_{PH}$ = 342 Hz) in the ^{31}P NMR spectrum. Based on these data, the two phosphorus atoms of the dppe group are in equivalent (or time-averaged) environments. Furthermore, the coupling constant between these atoms and the PH(OMe)Cy group suggests that the three phosphorus groups are co-equatorial, leaving the CO ligands to take the axial positions.

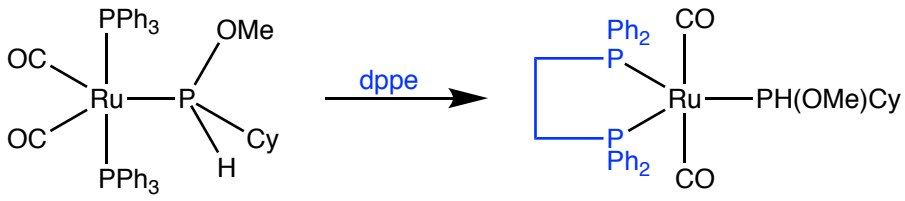

Scheme 3.26. Synthesis of $[Ru(CO)_2\{PH(OMe)Cy\}(dppe)]$

The IR spectrum of $[Ru(CO)_2\{PH(OMe)Cy\}(dppe)]$ contained two ν_{CO} bands at 1914 and 1857 cm^{-1}, with the very small change (ν_{CO} $[Ru(CO)_2(PPh_3)_2\{PH(OMe)Cy\}]$: 1911, 1862 cm^{-1}) indicative of the similar electronic properties of PPh_3 and dppe. The presence of two distinct ν_{CO} bands in the IR spectrum disagrees with the geometry deduced from the $^{31}P\{^1H\}$ NMR

data. For geometry with *trans* CO groups in the apical positions only a single stretch is expected, as the symmetric CO stretch is centrosymmetric and IR inactive. Thus, the geometry must include *cis* CO groups. A possible geometry that matches the observed data is a distorted square pyramid with PH(OMe)Cy in the apical position. Such a geometry contains *cis* CO ligands as inferred from the IR data and could allow for the increased $^{2}J_{PP}$ if the distortion increases the P−Ru−PH(OMe)Cy angles over 90°.

Several other resonances were observed in the $^{31}P\{^{1}H\}$ NMR spectrum of the crude product. The most prominent of these was the signal for PPh_3, which is expected as a by-product of the reaction. Approximately 4 resonances were observed in the range 150-160 ppm, which is the range observed for PH(OMe)Cy complexes. These resonances may therefore represent either different isomers of $[Ru(CO)_2\{PH(OMe)Cy\}(dppe)]$ or products of different substitution reactions. There were >13 resonances in the range 25-65 ppm, which has generally been the range observed for triaryl phosphine groups. One possible side product of the reaction is $[Ru(CO)_2(PPh_3)(dppe)]$, but the resonances for this complex[191] were not observed. Unfortunately, the signal-to-noise ratio of these other signals precluded more in-depth analysis.

Purification of $[Ru(CO)_2\{PH(OMe)Cy\}(dppe)]$ could not be achieved. Recrystallisations from MeOH, EtOH, *n*-hexane and Et_2O were attempted, all without significant improvement of the purity of $[Ru(CO)_2\{PH(OMe)Cy\}(dppe)]$. Yields from these recrystallisations were also relatively low, limiting the practicality of multiple recrystallisations. Overall, the solubility of $[Ru(CO)_2\{PH(OMe)Cy\}(dppe)]$ was generally high and matched that of the side products, preventing the isolation of the pure compound.

3.5.4 Reaction with Air

As a solid, $[Ru(CO)_2(PPh_3)_2\{PH(OMe)Cy\}]$ is not air stable, and decomposes to form the bidentate carbonate complex $[Ru(CO)(PPh_3)_2\{PH(OMe)Cy\}(\kappa^2\text{-}O_2CO)]$ (Scheme 3.27). Infrared ν_{CO} bands for $[Ru(CO)(PPh_3)_2\{PH(OMe)Cy\}(\kappa^2\text{-}O_2CO)]$ (*vide infra*) were observed after one month of standing the solid sample in air. Close monitoring of the oxidation was not conducted, but the process was complete after seven months.

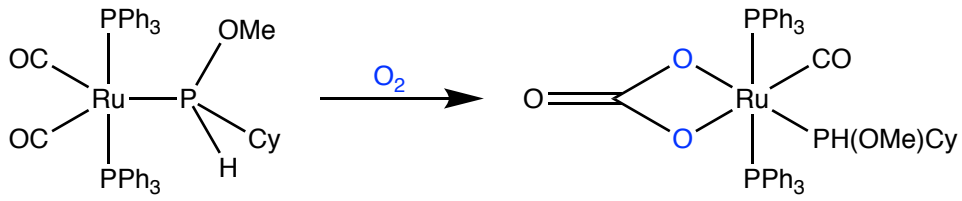

Scheme 3.27. Oxidation of $[Ru(CO)_2(PPh_3)_2\{PH(OMe)Cy\}]$ with O_2

Attempts were made to accelerate the oxidation of $[Ru(CO)_2(PPh_3)_2\{PH(OMe)Cy\}]$. Heating an aerobic *n*-heptane suspension of $[Ru(CO)_2(PPh_3)_2\{PH(OMe)Cy\}]$ under reflux resulted in the formation of $[Ru(CO)(PPh_3)_2\{PH(OMe)Cy\}(\kappa^2\text{-}O_2CO)]$. However, after 24 hours of heating the reaction had only reached 75% completion, as estimated by IR spectroscopy. A sample of $[Ru(CO)_2(PPh_3)_2\{PH(OMe)Cy\}]$ dissolved in CD_2Cl_2 was also observed to decompose by $^{31}P\{^1H\}$ NMR spectroscopy. After 23 hours, no more resonances for $[Ru(CO)_2(PPh_3)_2\{PH(OMe)Cy\}]$ were observed. In addition to the product, however, significant amounts of $O{=}PPh_3$ and PPh_3 were present. The simplest way to obtain $[Ru(CO)(PPh_3)_2\{PH(OMe)Cy\}(\kappa^2\text{-}O_2CO)]$ for characterisation was to use the solid-state sample which had already undergone oxidation.

The formation of $[Ru(CO)(PPh_3)_2\{PH(OMe)Cy\}(\kappa^2\text{-}O_2CO)]$ was established by solid-state IR spectroscopy. A single metal ν_{CO} band was seen at 1942 cm^{-1}, with the higher frequency compared to $[Ru(CO)_2(PPh_3)_2\{PH(OMe)Cy\}]$ (1913, 1859 cm^{-1}) indicative of oxidation at ruthenium. Additionally, the formation of the carbonate ligand was indicated by an absorption at 1657 cm^{-1}, within the typical ν_{CO} range for the C=O bond of bidentate carbonato ligands.[192]

In the $^{31}P\{^1H\}$ NMR spectrum, the PH(OMe)Cy group appeared as overlapping doublet of doublets at δ_P 164.2. A doublet splitting with $^1J_{PH}$ = 356 Hz was seen for this resonance in the ^{31}P NMR spectrum. The two PPh_3 groups are diastereotopic and, on account of their strongly-coupled *trans* arrangement, appear as two higher-order roofed doublet of doublets (Figure 3.6). These resonances appear at δ_P 32.5 and 29.9 ($\Delta\nu$ = 428.0 Hz) with $^2J_{PP}$ of 340 Hz (*trans*), and 23 and 26 Hz (*cis*).

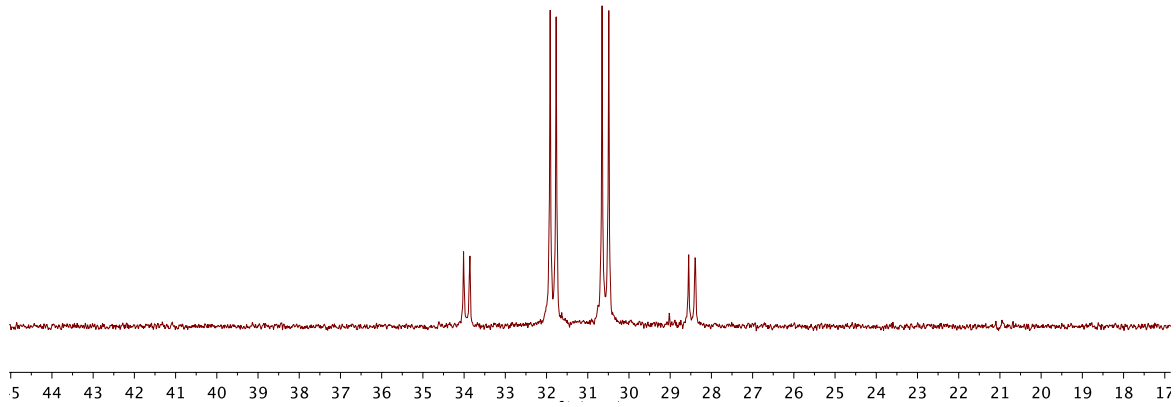

Figure 3.6. Triphenylphosphine $^{31}P\{^{1}H\}$ NMR resonances of [Ru(CO)(PPh$_3$)$_2${PH(OMe)Cy}(κ^2-O$_2$CO)]

The $^{13}C\{^{1}H\}$ NMR data were consistent with the expected structure of [Ru(CO)(PPh$_3$)$_2${PH(OMe)Cy}(κ^2-O$_2$CO)]. Two sets of resonances were observed for the inequivalent PPh$_3$ groups. A single CO signal was seen at δ_C 202.8, although the signal-to-noise ratio was too low to accurately determine coupling information. Additionally, a singlet was seen at δ_C 164.2 which corresponded to the newly-formed carbonate ligand. As expected, six distinct resonances were observed for the cyclohexyl ring. Interestingly, the cyclohexyl CH (δ_C 44.0) and OMe (δ_C 62.4) resonances both appeared at a higher frequency compared to [Ru(CO)$_2$(PPh$_3$)$_2${PH(OMe)Cy}] (δ_C 29.4 and 42.6, respectively).

No unexpected observations were made in the ^{1}H NMR spectrum. Multiplets were present for the PPh$_3$ groups and the Cy group. A doublet ($^{3}J_{PH}$ = 11 Hz) at δ_H 3.24 was seen for the methyl hydrogens. The P−H hydrogen atom resonance appeared as a doublet at δ_H 5.77. A $^{1}J_{PH}$ of 353 Hz was measured, but the smaller couplings could not be resolved.

The molecular structure of [Ru(CO)(PPh$_3$)$_2${PH(OMe)Cy}(κ^2-O$_2$CO)] was determined by X-ray crystallography. In the molecular structure (Figure 3.7), the ruthenium centre adopts an octahedral geometry with *trans* PPh$_3$ groups and a bidentate carbonate ligand, as inferred from spectroscopic data. The formation of the PH(OMe)Cy group from the previous step is also confirmed, although the OMe group is disordered (one position shown). As expected, the sum of angles about the carbonate carbon is 360°, indicating the planarity of the ligand. The carbonate C−O bond lengths show one double bond (1.227(6) Å) and two longer bonds (1.324(6) and1.328(6) Å) for the delocalised π system. Interestingly, the Ru−O distances are

different by 0.036 Å (12 e.s.d.). This disparity arises from the different *trans* ligands and indicates that PH(OMe)Cy exerts a stronger *trans* influence than CO, or that the *trans* disposition of π-donor (O) and π-acceptor (CO) enhances the metal-oxygen bond.

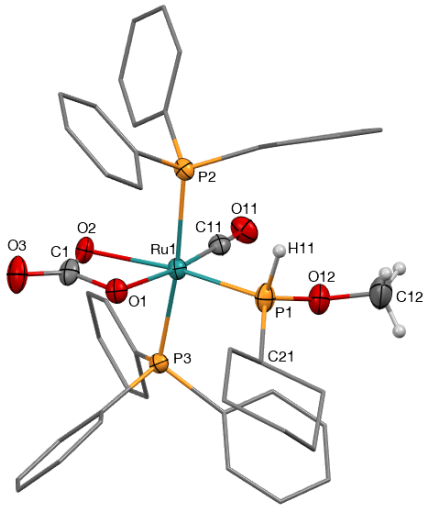

Figure 3.7. Molecular structure of S_P-[Ru(CO)(PPh_3)$_2${PH(OMe)Cy}(κ^2-O_2CO)] in a crystal of [Ru(CO)(PPh_3)$_2${PH(OMe)Cy}(κ^2-O_2CO)].2(CH_2Cl_2) (50% displacement ellipsoids, minor disordered OMe fragment, CH_2Cl solvent molecules and most H atoms omitted, phenyl and cyclohexyl rings simplified). Selected bond lengths (Å) and angles (°): Ru1–P1 2.2682(14), Ru1–P2 2.3793(14), Ru1–P3 2.4026(14), Ru1–O1 2.095(3), Ru1–O2 2.131(3), Ru1–C11 1.858(5), P1–C21 1.791(8), O1–C1 1.324(6), O2–C1 1.328(6), O3–C1 1.227(6), O11–C11 1.142(6), P2–Ru1–P3 171.30(5), O1–Ru1–O2 62.57(14), Ru1–P1–C21 115.3(3), Ru1–P1–O12 113.3(2). Molecule crystallised in the centrosymmetric P–1 space group – enantiomer is present in the unit cell.

The complex [Ru(CO)(PPh_3)$_2${PH(OMe)Cy}(κ^2-O_2CO)] bears some resemblance to [OsCl(NO)(PPh_3)$_2$(κ^2-O_2CO)], a complex reported by Roper.[193] Both compounds result from the oxidation of a coordinatively-saturated, zero-valent Group 8 metal carbonyl complex and in Roper's case, the initial complex is [OsCl(NO)(CO)(PPh_3)$_2$]. Roper was also able to isolate the intermediate peroxycarbonyl complex [OsCl(NO)(PPh_3)$_2${κ^2-*C,O*-C(O)O_2}] (Scheme 3.28) which demonstrates the initial site of reaction with O_2 is not the saturated metal, but rather the metal-carbon bond in a [2 + 2] manner. It is likely that the oxidation of [Ru(CO)$_2$(PPh_3)$_2${PH(OMe)Cy}] to [Ru(CO)(PPh_3)$_2${PH(OMe)Cy}(κ^2-O_2CO)] follows the same pathway.

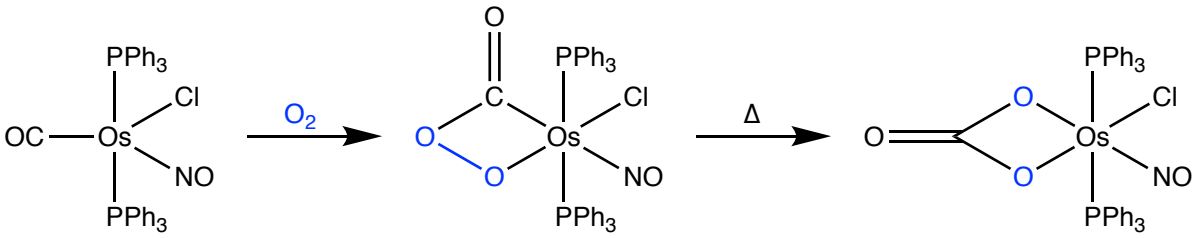

Scheme 3.28. Roper's synthesis of [OsCl(NO)(PPh$_3$)$_2$(κ^2-O$_2$CO)][193]

3.5.5 Reaction with ^{n}BuLi

In an attempt to explore the reactivity of the P–H bond in [Ru(CO)$_2$(PPh$_3$)$_2${PH(OMe)Cy}], its reaction with ^{n}BuLi was explored. Deprotonation had previously been reported by Streubel and Arduengo (*vide supra*).[186] The addition of ^{n}BuLi to a solution of [Ru(CO)$_2$(PPh$_3$)$_2${PH(OMe)Cy}] resulted in an yellow-to-red colour change. However, despite the presence of new bands in the IR spectrum (2003, 1996, 1967, 1935 and 1916 cm^{-1}), ^{31}P{^{1}H} NMR spectroscopy revealed [Ru(CO)$_2$(PPh$_3$)$_2${PH(OMe)Cy}] (58%) and PPh$_3$ (18%) to be the major species present (Scheme 3.29).

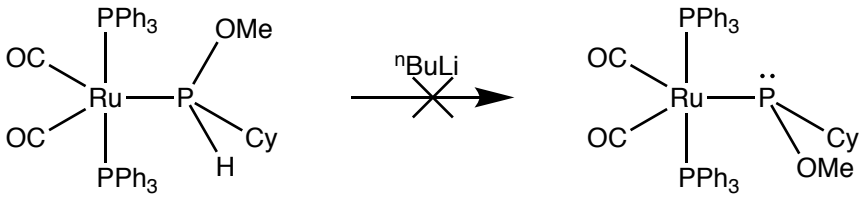

Scheme 3.29. Attempted deprotonation of [Ru(CO)$_2$(PPh$_3$)$_2${PH(OMe)Cy}]

To further investigate the possibility that [Ru(CO)$_2$(PPh$_3$)$_2${PH(OMe)Cy}] is to some extent deprotonated, but the deprotonated product is not observed, the experiment was repeated followed by the addition of D$_2$O to the mixture. No evidence of deuterium incorporation was observed, and [Ru(CO)$_2$(PPh$_3$)$_2${PH(OMe)Cy}] was again seen as the major product (Scheme 3.30). Therefore, the Ru(0) centre does not appear to render the P–H bond sufficiently acidic to be deprotonated with ^{n}BuLi.

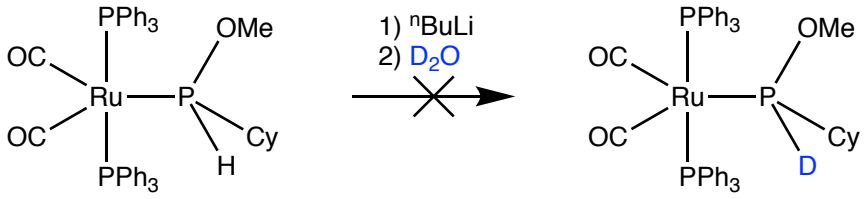

Scheme 3.30. Attempted deuterium incorporation into [Ru(CO)$_2$(PPh$_3$)$_2${PH(OMe)Cy}]

3.5.6 Reaction with Phenylacetylene

The complex $[Ru(CO)_2(PPh_3)_2\{PH(OMe)Cy\}]$ contains a potentially reactive Ru(0) centre. To probe this reactivity, its reaction with phenylacetylene (HC≡CPh) was investigated. Terminal acetylenes have previously been shown to oxidatively add to Ru(0) centres,[158, 194] and it was expected that the same process could occur with $[Ru(CO)_2(PPh_3)_2\{PH(OMe)Cy\}]$ following ligand dissociation.

Phenylacetylene reacts slowly with $[Ru(CO)_2(PPh_3)_2\{PH(OMe)Cy\}]$. The reaction was monitored by $^{31}P\{^1H\}$ NMR spectroscopy, and was determined to be complete after 5 days stirring at room temperature. As well as liberated PPh_3, there were two major products in the $^{31}P\{^1H\}$ NMR spectrum giving rise to doublet pairs at δ_P 150.8 and 40.7, and δ_P 150.1 and 40.9. Each of the doublets displayed a $^2J_{PP}$ of 273 Hz and the coupled pairs were assigned based on relative intensities. The high frequency resonances at δ_P 150.8 and 150.1 fall in the typical range previously observed for PH(OMe)Cy ligands and their identity was confirmed by further P−H doublet splitting in the ^{31}P NMR spectrum, with $^1J_{PH}$ of 377 and 381 Hz, respectively.

Based on the $^{31}P\{^1H\}$ NMR data, two isomers of $[RuH(C{\equiv}CPh)(CO)_2(PPh_3)\{PH(OMe)Cy\}]$ would appear to have formed (Scheme 3.31). The extremely large $^2J_{PP}$ for both isomers indicates that the phosphine groups are *trans* to each other. Therefore, the only remaining geometric variability is in the plane containing the two carbonyl ligands, the hydride and the acetylide ligand. It therefore follows that the two isomers observed must involve either *cis* or *trans* CO groups, as depicted in Scheme 3.31.

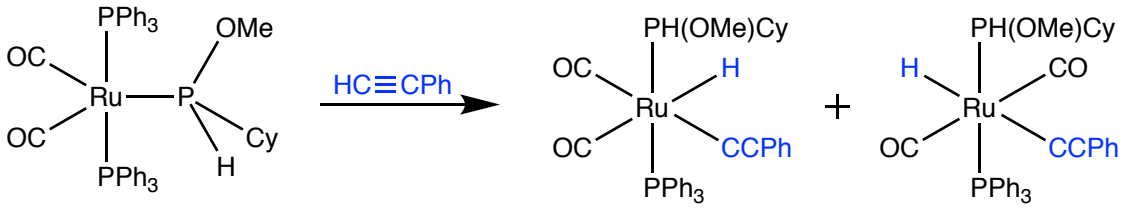

Scheme 3.31. Reaction of $[Ru(CO)_2(PPh_3)_2\{PH(OMe)Cy\}]$ with phenylacetylene

It should be noted that both the PH(OMe)Cy phosphorus atom and the ruthenium centre are stereogenic in the *cis*-CO isomer of [RuH(C≡CPh)(CO)$_2$(PPh$_3$){PH(OMe)Cy}]. Accordingly, there should be two sets of diastereomers for the *cis*-CO isomer (Figure 3.8). The existence of these isomers is observed in the ^{1}H NMR spectrum of the crude product. While impurities obfuscated the standard region of the spectrum, three low frequency hydride doublet of doublets could be seen at δ_H −5.80, −5.81 and −6.06 (Figure 3.9). All three resonances displayed two separate $^2J_{PH}$ of 20 and 24 Hz, which is typical of a *cis* relationship between the P and H atoms. The overlapping signals at δ_H −5.80 and −5.81 are indicative of two very similar environments, leading to their assignment to the two *cis*-CO diastereomers of [RuH(C≡CPh)(CO)$_2$(PPh$_3$){PH(OMe)Cy}].

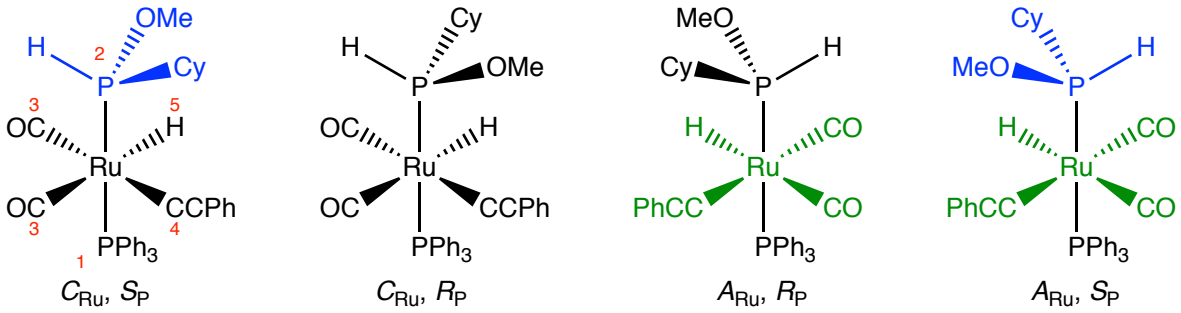

Figure 3.8. Stereoisomers of the cis-CO isomer of [RuH(C≡CPh)(CO)$_2$(PPh$_3$){PH(OMe)Cy}] with stereochemical descriptors.[195] The Cahn-Ingold-Prelog priorities are provided in red.

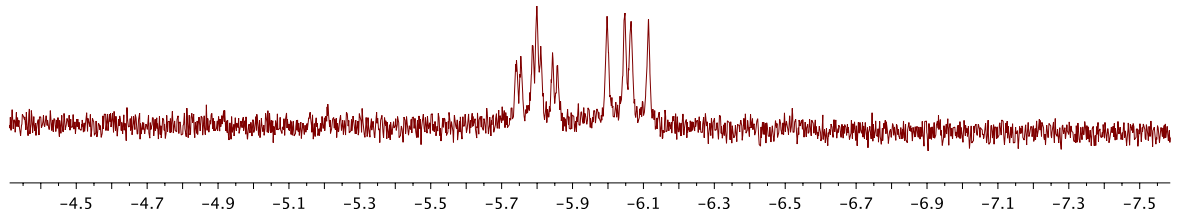

Figure 3.9. Hydride region of the crude ^{1}H NMR spectrum of [RuH(C≡CPh)(CO)$_2$(PPh$_3$){PH(OMe)Cy}]

The IR spectrum (THF) of the mixture contained three ν_{CO} bands at 2032, 1983 and 1945 cm^{-1}. These absorptions are all at higher frequency than in [Ru(CO)$_2$(PPh$_3$)$_2$(PH(OMe)Cy}] (ν_{CO} = 1911, 1862 cm^{-1} in THF), which is a good indication that oxidative addition has occurred to form a less electron-rich metal centre. While not providing definitive proof, the number of ν_{CO} stretches does agree with the formation of *cis* and *trans* isomers deduced from the NMR data. The *cis* isomer should provide two ν_{CO} stretches while only one should be observed for

the *trans* isomer. The *cis*-CO isomer of [RuH(C≡CC$_6$H$_4$Me-4)(CO)$_2$(PPh$_3$)$_2$], obtained from the reaction of [Ru(CO)$_2$](PPh$_3$)$_3$] with 4-ethynyltoluene has ν_{CO} absorptions at 2033 and 1982 cm^{-1} and it may therefore be assumed that the two highest frequency absorptions correspond to the *cis*-CO isomer while the third absorption (1945 cm^{-1}) corresponds to the *trans*-CO isomer.[196]

The formation of [RuH(C≡CPh)(CO)$_2$(PPh$_3$){PH(OMe)Cy}] did not proceed cleanly. While the two isomers of [RuH(C≡CPh)(CO)$_2$(PPh$_3$){PH(OMe)Cy}] were the major products, they only constituted approximately 42% of the mixture (excluding PPh$_3$), as estimated by ^{31}P{^{1}H} NMR spectroscopy. More than 20 resonances appeared in the range 12-56 ppm amongst which only the signal for O=PPh$_3$ could be identified. Similarly to the other derivatives of [Ru(CO)$_2$(PPh$_3$)$_2$}{PH(OMe)Cy}], purification by recrystallisation was not successfully achieved and no further studies were conducted on [RuH(C≡CPh)(CO)$_2$(PPh$_3$){PH(OMe)Cy}].

3.5.7 Reaction with HBF$_4$

A common reaction for low oxidation state metals centres is protonation to yield a hydride complex. This potential reactivity was investigated for [Ru(CO)$_2$(PPh$_3$)$_2$}{PH(OMe)Cy}] *via* its reaction with HBF$_4$. Decolourisation occurred upon the addition of HBF$_4$ to a solution of [Ru(CO)$_2$(PPh$_3$)$_2$}{PH(OMe)Cy}]. The IR spectrum of the mixture contained two ν_{CO} bands at 2069 and 2009 cm^{-1}. These absorptions are at a higher frequency than for [Ru(CO)$_2$(PPh$_3$)$_2$}{PH(OMe)Cy}], supporting the formation of a cationic complex with reduced electron density at the metal centre. No bands attributable to a RuH stretching mode were observed.

The ^{31}P{^{1}H} NMR spectrum of the reaction mixture revealed a large number of products (Scheme 3.32). There were five resonances (δ_P 194.1, 188.7, 146.6, 144.4 and 140.0) in the appropriate high frequency range for a PH(OMe)Cy complex which all showed P−H coupling. Ten resonances appeared in the typical range for PPh$_3$ ligands of 25-42 ppm.

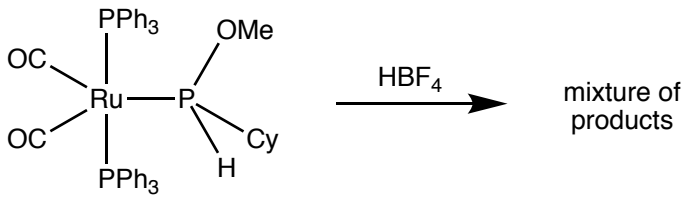

Scheme 3.32. Reaction of $[Ru(CO)_2(PPh_3)_2\{PH(OMe)Cy\}]$ with HBF_4

Low frequency resonances were observed in the ^1H NMR spectrum (Figure 3.10), suggesting the formation of hydride complexes. However, at least four resonances were observed of which only two were sufficiently well-resolved to extract coupling data.

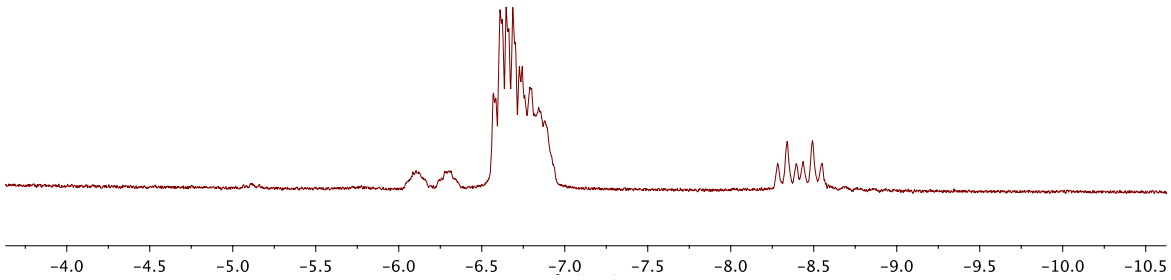

Figure 3.10. Hydride region of the ^1H NMR spectrum following the reaction between HBF_4 and $[Ru(CO)_2(PPh_3)_2\{PH(OMe)Cy\}]$

Neither the ^1H nor $^{31}P\{^1H\}$ NMR data could be readily deconvoluted. The likely cause of such a mixture is multiple isomers of the desired cation, $[RuH(CO)_2(PPh_3)_2\{PH(OMe)Cy\}]^+$, leading to multiple hydride and PH(OMe)Cy resonances in their respective spectra. Furthermore, the chirality of the PH(OMe)Cy ligand results in diastereomers for some geometries. It was evident that purification of such a mixture was unlikely, and different reactivity investigations were pursued.

3.5.8 Reaction with HCl and Synthesis of $[RuCl_2(CO)(PPh_3)_2(PH_2Cy)]$

While HBF_4 is a Brønsted-Lowry acid with a weakly-coordinating conjugate base, HCl provides a coordinating Cl^- anion. The presence of Cl^- provides the potential for different chemistry, and so the protonation of $[Ru(CO)_2(PPh_3)_2\{PH(OMe)Cy\}]$ with HCl was investigated.

The addition of four equivalents of ethereal HCl to a solution of $[Ru(CO)_2(PPh_3)_2\{PH(OMe)Cy\}]$ resulted in immediate decolourisation. Several bands were observed in the ν_{CO} region of the IR spectrum of the reaction mixture, indicating that a mixture of products had formed (Scheme 3.33). The two strongest absorptions were at 2003 and 1992 cm^{-1}, with minor bands

at 2082, 2060 and 1968 cm^{-1}. Based on the intensity and position of the bands at 2082 and 2060 cm^{-1} they could potentially be due to RuH stretching modes. Each of the bands is at a higher frequency than those for $[Ru(CO)_2(PPh_3)_2\{PH(OMe)Cy\}]$, so if they are due to ν_{CO} modes then they suggest that a cationic complex has formed. However, the positions of the bands are different than those observed for the reaction with HBF_4, indicating that different products have formed with the two different acids.

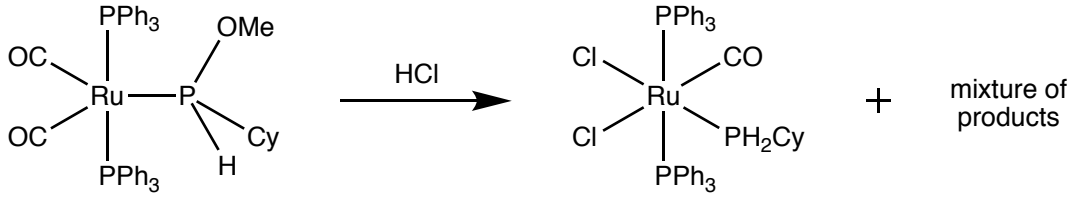

Scheme 3.33. Reaction of $[Ru(CO)_2(PPh_3)_2\{PH(OMe)Cy\}]$ with HCl

The NMR data also showed a mixture of products. By $^{31}P\{^1H\}$ NMR spectroscopy, the major product (40%) gave rise to a triplet at δ_P 168.6 and a doublet at δ_P 19.7 ($^2J_{PP}$ = 25 Hz). The resonance at δ_P 168.6 was confirmed to be due to a PH(OMe)Cy group by its doublet splitting in the ^{31}P NMR experiment with a $^1J_{PH}$ of 360 Hz. No other PH(OMe)Cy resonances were observed. There were *ca*. 11 other $^{31}P\{^1H\}$ NMR resonances in the range 10-45 ppm constituting the rest of the mixture. Notably, the reaction of $[Ru(CO)_2(PPh_3)_2\{PH(OMe)Cy\}]$ with HCl gave products with different $^{31}P\{^1H\}$ NMR data to the reaction with HBF_4.

Four hydride resonances were observed in the ^1H NMR spectrum. Three of these (δ_H −4.10, −6.79 and −13.37) were triplets, which do not match the splitting for the expected product $[RuH(CO)_2(PPh_3)_2\{PH(OMe)Cy\}]^+$. However, the strongest resonance at δ_H −6.86 showed a doublet of triplets pattern, as anticipated for coupling to one PH(OMe)Cy and two PPh_3 groups. As seen with the $^{31}P\{^1H\}$ NMR data, the ^1H NMR data were different between the HCl and HBF_4 reactions.

In order to identify the products of the reaction between $[Ru(CO)_2(PPh_3)_2\{PH(OMe)Cy\}]$ and HCl, crystals suitable for X-ray diffraction were grown. The crystals were identified to be $[RuCl_2(CO)(PPh_3)_2(PH_2Cy)]$ (Figure 3.11). The structural parameters of $[RuCl_2(CO)(PPh_3)_2(PH_2Cy)]$ reassuringly fall within standard ranges[135, 197] and conform with

previously discussed octahedral PH_2Cy ruthenium complexes. Notable within the structure is the absence of a hydride ligand at the coordinatively-saturated Ru centre and the absence of a methoxide substituent on the phosphorus atom. Instead, chlorides have coordinated at the metal centre, while the P−O bond has been replaced by a P−H bond.

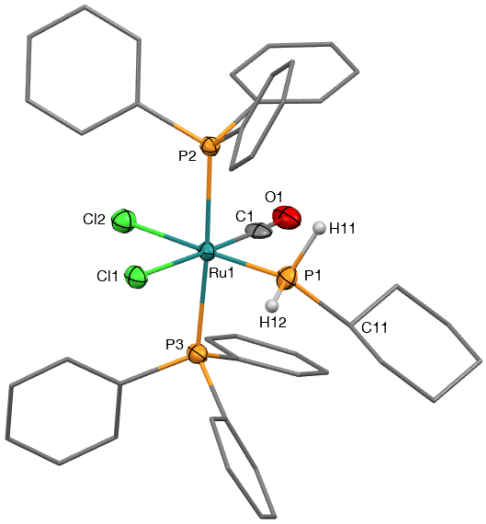

Figure 3.11. Molecular structure of $[RuCl_2(CO)(PPh_3)_2(PH_2Cy)]$ in a crystal of $[RuCl_2(CO)(PPh_3)_2(PH_2Cy)].3(CH_2Cl_2)$ (50% displacement ellipsoids, CH_2Cl_2 solvent molecules and most H atoms omitted, phenyl and cyclohexyl rings simplified). Selected bond lengths (Å) and angles (°): Ru1−P1 2.276(2), Ru1−P2 2.409(2), Ru1−P3 2.413(2), Ru1−Cl1 2.4628(18), Ru1−Cl2 2.467(2), Ru1−C1 1.861(8), P1−C11 1.830(8), P1−H11 1.39(7), P1−H12 1.37(7), O1−C1 1.128(8), P2−Ru1−P3 174.84(8), Cl1−Ru1−Cl2 93.50(7), Ru1−P11−C11 121.7(3), H111−P11−H112 100(4).

After obtaining the molecular structure of $[RuCl_2(CO)(PPh_3)_2(PH_2Cy)]$, its unequivocal synthesis was pursued for full characterisation. Roper reported the synthesis of the analogous complex $[OsCl_2(CO)(PPh_3)_2(PH_2Ph)]$ from $[OsH(Cl)(CO)(PPh_3)_2(PH_2Ph)]$ and HCl,[149] and a similar approach was used to obtain the target complex. Effervescence was observed upon the addition of ethereal HCl to a solution of $[RuH(Cl)(CO)(PPh_3)_2(PH_2Cy)]$. Following the removal of volatiles and recrystallisation, $[RuCl_2(CO)(PPh_3)_2(PH_2Cy)]$ was obtained in 98% yield (Scheme 3.34).

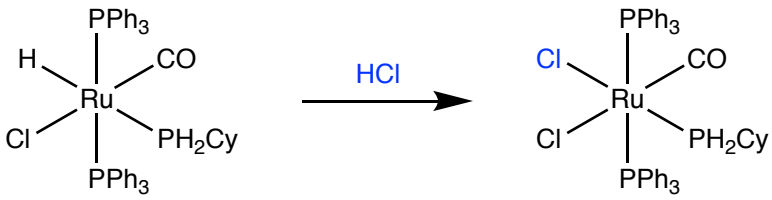

Scheme 3.34. Synthesis of $[RuCl_2(CO)(PPh_3)_2(PH_2Cy)]$ from $[RuH(Cl)(CO)(PPh_3)_2(PH_2Cy)]$

The NMR data were consistent with the formation of $[RuCl_2(CO)(PPh_3)_2(PH_2Cy)]$. The $^{31}P\{^1H\}$ NMR spectrum contained a doublet for the PPh_3 groups at δ_P 21.0, which coupled ($^2J_{PP}$ = 24 Hz) to a triplet at δ_P 11.7 for the PH_2Cy group. A triplet pattern with a $^1J_{PH}$ of 364 Hz was seen for the PH_2Cy group in the ^{31}P NMR spectrum. All of the expected phenyl and cyclohexyl resonances were observed in the ^1H NMR spectrum, as were the P–H hydrogen atoms at δ_H 3.54. The appearance of a single signal for the phosphorus-bound H atoms indicates the high symmetry within the molecule. This symmetry is also evident in the $^{13}C\{^1H\}$ NMR spectrum, in which only four cyclohexyl resonances are observed. Carbonyl and phenyl resonances were also present in the $^{13}C\{^1H\}$ NMR spectrum.

Curiously, two ν_{CO} bands were seen in the solution IR spectrum (THF: 1984, 1961 cm^{-1}; CH_2Cl_2: 1977, 1963 cm^{-1}). Roper reported that $[OsCl_2(CO)(PPh_3)_2(PH_2Cy)]$ formed as a mixture of *cis* and *trans* isomers based on the number ν_{CO} and ν_{OsCl} bands in the IR spectrum.[149] In the absence of far-infrared data,[§] a definitive observation of isomers for $[RuCl_2(CO)(PPh_3)_2(PH_2Cy)]$ cannot be made. However, only a single compound is seen by NMR spectroscopy. Furthermore, the interchange between octahedral isomers is usually slow, and would be expected to be observed in an NMR experiment. Therefore, a more plausible explanation for the two IR bands for $[RuCl_2(CO)(PPh_3)_2(PH_2Cy)]$ is the presence of rotamers caused by hindered rotation about the Ru–PH_2Cy bond. Such an interconversion would not be observed by IR spectroscopy due to the short timescale, but would be fast on the NMR timescale.

Following the full spectroscopic characterisation of $[RuCl_2(CO)(PPh_3)_2(PH_2Cy)]$, the data from the reaction between $[Ru(CO)_2(PPh_3)_2\{PH(OMe)Cy\}]$ and HCl were re-examined. The ν_{CO} bands for $[RuCl_2(CO)(PPh_3)_2(PH_2Cy)]$ (THF: 1984, 1961 cm^{-1}) were not observed in the IR spectrum of the reaction mixture (2082, 2060, 2003, 1992 and 1968 cm^{-1}). However, the resonances for $[RuCl_2(CO)(PPh_3)_2(PH_2Cy)]$ were seen in the $^{31}P\{^1H\}$ NMR spectrum and comprised approximately 9% of the mixture. The identity of the major product of the reaction

[§] An instrument with far-infrared capability is not currently accessible

is still uncertain and it is unclear if it is an intermediate on the pathway towards $[RuCl_2(CO)(PPh_3)_2(PH_2Cy)]$ or if it is a completely separate product.

The formation of $[RuCl_2(CO)(PPh_3)_2(PH_2Cy)]$ from $[Ru(CO)_2(PPh_3)\{PH(OMe)Cy\}]$ involves activation of the P–OMe bond. A plausible mechanism (Scheme 3.35) involves initial protonation of the metal centre, followed by substitution of a CO ligand for chloride. This substitution is facilitated by the cationic nature of $[RuH(CO)_2(PPh_3)_2\{PH(OMe)Cy\}]^+$ rendering one of its two π-acidic carbonyls labile. The methoxide group may then be protonated, allowing the extrusion of methanol with the formation of a phosphenium intermediate. Finally, chloride addition to the Ru centre and hydride migration to the electrophilic phosphenium group results in the formation of $[RuCl_2(CO)(PPh_3)_2(PH_2Cy)]$.

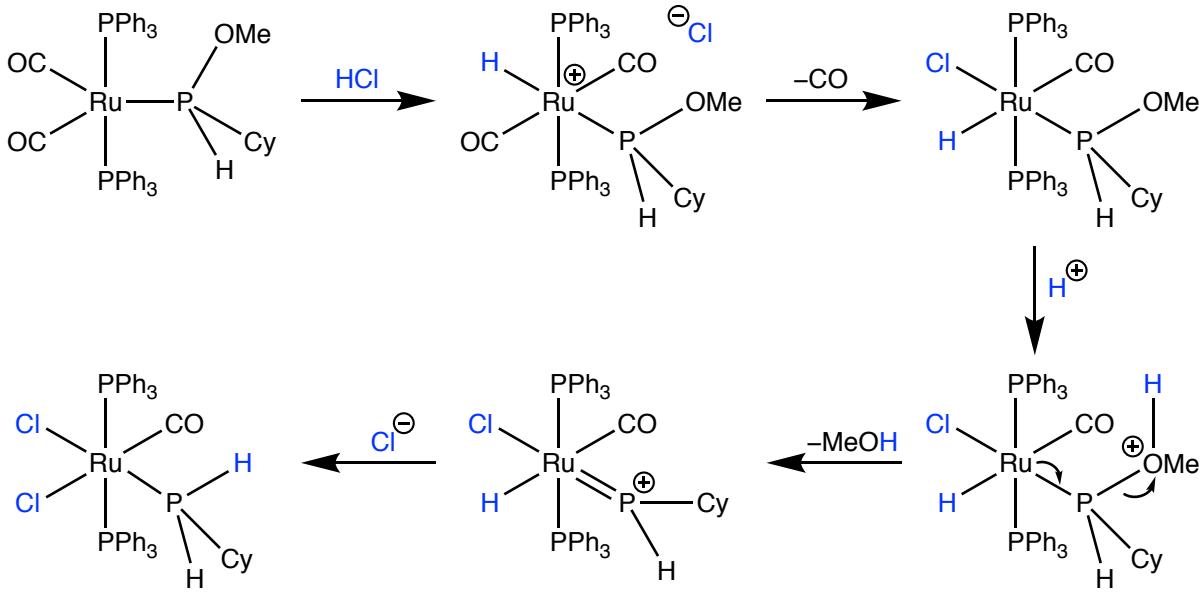

Scheme 3.35. Potential mechanism for transformation of $[Ru(CO)_2(PPh_3)_2\{PH(OMe)Cy\}]$ to $[RuCl_2(CO)(PPh_3)_2(PH_2Cy)]$

3.6 Summary and Future Work

The octahedral ruthenium cyclohexylphosphine complex $[RuH(Cl)(CO)(PPh_3)_2(PH_2Cy)]$ was synthesised by substitution of PPh_3 from $[RuH(Cl)(CO)(PPh_3)_3]$. Treatment of the cyclohexylphosphine complex with acid (HPF_6, $HClO_4$ or HOTf) in the presence of acetonitrile gave the cation $[RuCl(NCMe)(CO)(PPh_3)_2(PH_2Cy)]^+$. This cation is isolated as a mixture of three interconverting isomers and features a labile acetonitrile ligand. The labile acetonitrile, in

combination with the chloride and triphenylphosphine ligands, provides a pathway to many more cyclohexylphosphine ruthenium complexes. Triflate was determined to be the most suitable anion for further work.

The utility of the acetonitrile-substituted cation was demonstrated by ligand substitutions with CO, CNMes, S_2CNEt_2 and Tp to form $[RuCl(CO)_2(PPh_3)_2(PH_2Cy)]OTf$, $[RuCl(CO)(CNMes)(PPh_3)_2(PH_2Cy)]OTf$, $[Ru(CO)(PPh_3)_2(PH_2Cy)(\kappa^2\text{-}S,S\text{-}S_2CNEt_2)]OTf$ and $[Ru(CO)(PPh_3)(PH_2Cy)(Tp)]OTf$, respectively. The salt $[Ru(CO)(PPh_3)(PH_2Cy)(Tp)]OTf$ could be accessed *via* two alternative routes, both beginning from $[RuH(CO)(PPh_3)(Tp)]$.

Deprotonation of the primary phosphine in the cationic complexes $[RuCl(CO)_2(PPh_3)_2(PH_2Cy)]^+$ and $[Ru(CO)(PPh_3)_2(PH_2Cy)(\kappa^2\text{-}S,S\text{-}S_2CNEt_2)]^+$ both yielded mixtures of complexes in which liberated PPh_3 was the major product. It is believed that a phosphido complex is formed, but the phosphorus lone pair labilises its co-ligands which leads to the formation of oligomers. The deprotonation of $[Ru(CO)(PPh_3)(PH_2Cy)(Tp)]OTf$ successfully yielded the phosphido complex $[Ru(CO)(PPh_3)(PHCy)(Tp)]$ and its synthesis, properties and reactivity are discussed in the subsequent two chapters.

Both $[RuCl(CO)_2(PPh_3)_2(PH_2Cy)]OTf$ and $[RuCl(CO)(CNMes)(PPh_3)_2(PH_2Cy)]OTf$ react with methoxide to form $[Ru(CO)_2(PPh_3)_2\{PH(OMe)Cy\}]$ and $[Ru(CO)(CNMes)(PPh_3)_2\{PH(OMe)Cy\}]$, respectively. The latter forms several isomers, rearranging based on the presence of MeOH in the solution. The complex $[Ru(CO)_2(PPh_3)_2\{PH(OMe)Cy\}]$ contains the unusual PH(OMe)Cy ligand, and further studies were conducted on the complex to gain an understanding of its properties. The P−H bond was not sufficiently acidic to react with ^{n}BuLi. The substitution of PPh_3, as opposed to PH(OMe)Cy, occurred in ligand substitution reactions with CO, CNMes and dppe. These reactions indicate that the PH(OMe)Cy ligand is more strongly bound to the ruthenium centre in $[Ru(CO)_2(PPh_3)_2\{PH(OMe)Cy\}]$ than PPh_3. A similar observation was made in the reaction with phenylacetylene, in which the loss of a PPh_3 group revealed a vacant site for oxidative addition.

Reactivity at the Ru(0) centre was further demonstrated by the aerobic decomposition of $[Ru(CO)_2(PPh_3)_2\{PH(OMe)Cy\}]$, which reacted with O_2 to form the carbonate complex $[Ru(CO)(PPh_3)_2\{PH(OMe)Cy\}(\kappa^2\text{-}O_2CO)]$. The metal centre was also protonated by HBF_4 to form a mixture of hydride complexes which could not be separated. A different hydride complex was observed following the reaction with HCl, which contained a coordinating counteranion. The presence of the coordinating Cl^- ion led to the formation of $[RuCl_2(CO)(PPh_3)_2(PH_2Cy)]$ *via* activation of the P−O bond. This complex could also be formed *via* a more direct, though mechanistically less intriguing, route by treating $[RuH(Cl)(CO)(PPh_3)(PH_2Cy)]$ with HCl. The complex $[RuCl_2(CO)(PPh_3)_2(PH_2Cy)]$, with two chloride and two PPh_3 ligands, also provides a pathway to generate new ruthenium cyclohexylphosphine complexes.

CHAPTER 4
Synthesis, Properties and Reactivity of a Primary Phosphido Complex

Chapter 4: Synthesis, Properties and Reactivity of a Primary Phosphido Complex

As mentioned in the previous chapter, the deprotonation of [Ru(CO)(PPh_3)(PH_2Cy)(Tp)]OTf successfully yielded a phosphido complex. The formation of [Ru(CO)(PPh_3)(PHCy)(Tp)] and its properties are discussed in this chapter. Studies into the reactivity of [Ru(CO)(PPh_3)(PHCy)(Tp)] are also presented, although details of its reactions with chalcogenide sources are reserved for Chapter 5.

4.1 Synthesis of a Primary Phosphido Complex

Treatment of [Ru(CO)(PPh_3)(PH_2Cy)(Tp)]OTf with DBU or KH yielded the novel phosphido complex [Ru(CO)(PPh_3)(PHCy)(Tp)]. Addition of excess DBU, KH or ^{n}BuLi to [Ru(CO)(PPh_3)(PHCy)(Tp)] did not, however, result in further deprotonation to form an anionic phosphinidene complex (Scheme 4.1).

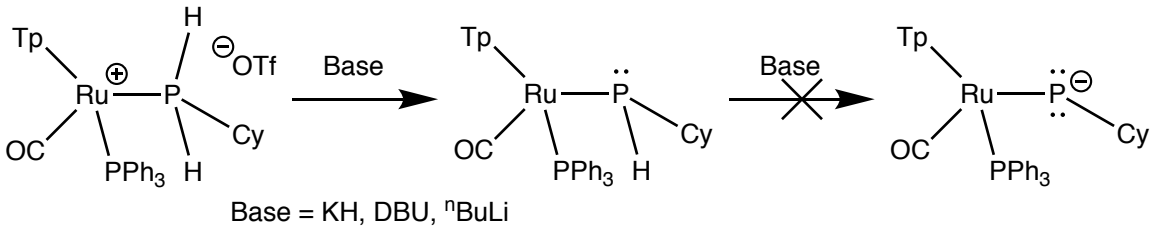

Scheme 4.1. Deprotonation of [Ru(CO)(PPh_3)(PH_2Cy)(Tp)]OTf

The formation of [Ru(CO)(PPh_3)(PHCy)(Tp)] was observed by solution IR spectroscopy (THF). The product gave rise to a single CO band at 1931 cm^{-1}, at a lower wave number than the starting material (1985 cm^{-1}). Such a shift is consistent with an increase of metal π-basicity due to the transformation from a cationic to a neutral complex.

Phosphorus-31 NMR spectroscopy also confirmed the formation of [Ru(CO)(PPh_3)(PHCy)(Tp)]. Two diastereomers were observed in the $^{31}P\{^1H\}$ NMR spectrum, with two doublets at δ_P 48.8 ($^2J_{PP}$ = 7 Hz) and 47.0 ($^2J_{PP}$ = 4 Hz) corresponding to PPh_3 groups and two broad singlets at −19.8 and −34.2 for the cyclohexylphosphido ligand (Figure 4.1). Based on the integration of the PHCy resonances, the two isomers were present in a 7:3 (δ_P −19.8:−34.2) ratio. The low frequency shifts of the cyclohexylphosphine resonances and their appearance as doublets

($^1J_{PH}$ = 167 Hz and 177 Hz, respectively) in the ^{31}P NMR spectrum both support deprotonation at phosphorus to generate PHCy groups. Additionally, the reduction in both J_{PP} and J_{PH} are indicative of the reduction in phosphorus coordination number and the attendant redistribution of s-orbital character into the phosphorus lone pair.[146]

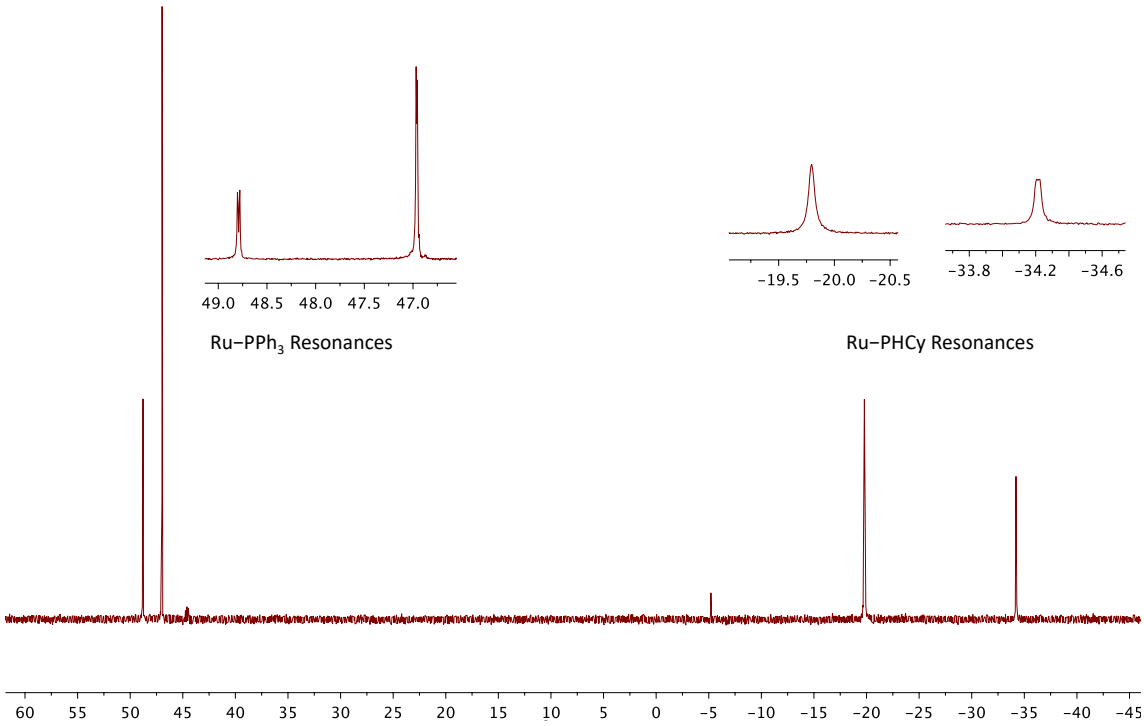

Figure 4.1. The $^{31}P\{^1H\}$ NMR spectrum of two diastereomers of [Ru(CO)(PPh$_3$)(PHCy)(Tp)]

Despite numerous attempts and strategies, a pure solid sample of [Ru(CO)(PPh$_3$)(PHCy)(Tp)] could not be isolated. In contrast to Roper's complexes,[75-77, 149] the addition of alcohols (MeOH, EtOH or ^{i}PrOH) resulted in reprotonation of the phosphido complex, precluding their use to remove ionic side products. This would imply that the pK_a of [Ru(CO)(PPh$_3$)(PH$_2$Cy)(Tp)]$^+$ in DMSO is greater than 30.3, the reported value for ^{i}PrOH.[198] When KH was used as a base the excess could be conveniently removed by cannula filtration. The solvent was then removed from the filtrate and the residue extracted with toluene to sequester the desired neutral product. Unfortunately, its purity as a result of these manipulations was reduced compared to the reaction mixture as observed by $^{31}P\{^1H\}$ NMR spectroscopy. Furthermore, attempts to grow single crystals to determine the molecular structure of [Ru(CO)(PPh$_3$)(PHCy)(Tp)] only resulted in crystals of [Ru(CO)(PPh$_3$){PH(O)Cy}(Tp)], the synthesis and molecular structure of which is discussed in

Section 5.2.1. All subsequent studies involving [Ru(CO)(PPh_3)(PHCy)(Tp)] were conducted with the compound freshly generated *in situ*.

4.1.1 Dynamic Behaviour of [Ru(CO)(PPh_3)(PHCy)(Tp)]

The presence of two diastereomers arises from the presence of both stereogenic ruthenium and phosphorus centres within the molecule. Interconversion between the two isomers should be possible by phosphorus inversion (Scheme 4.2) and, as discussed in Section 1.2.2, phosphido complexes have a lower barrier for this process than free phosphines. The variable temperature NMR behaviour of [Ru(CO)(PPh_3)(PHCy)(Tp)] was therefore investigated in order to gain further insight into the kinetics of phosphorus inversion.

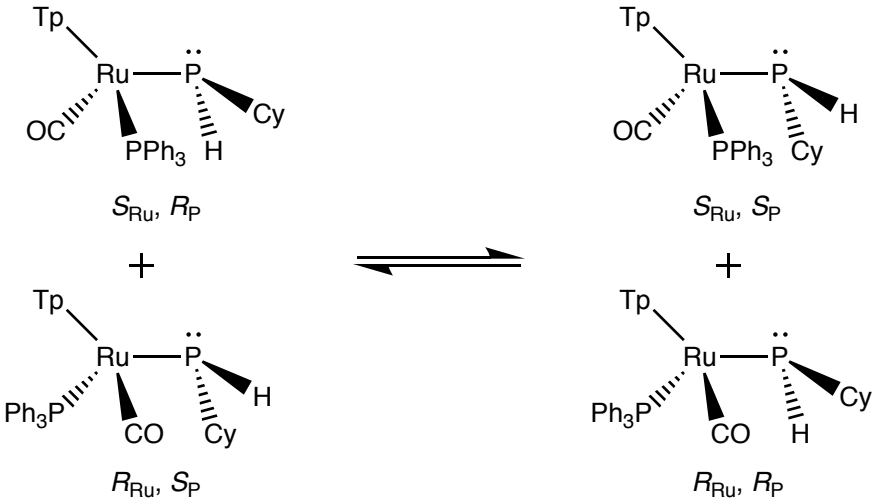

Scheme 4.2. Interconversion between diastereomers of [Ru(CO)(PPh_3)(PHCy)(Tp)]

Since two distinct sets of $^{31}P\{^1H\}$ NMR resonances were seen for [Ru(CO)(PPh_3)(PHCy)(Tp)] at room temperature it was reasoned that the system was in slow exchange. A sample of the phosphido complex was dissolved in toluene-d_8 and heated from 298 K to 373 K, with spectra recorded at 10 K increments up to 368 K and at 373 K (Figure 4.2). Coalescence was not observed over this temperature range, with the highest temperature corresponding to an estimated energy barrier of 63.6 kJ mol^{-1}. Theoretically, choosing a higher-boiling solvent such as DMF or DMSO would allow sufficiently high temperatures to observe fast exchange. These solvents were, however, eschewed for their potential reactivity with the phosphido complex.

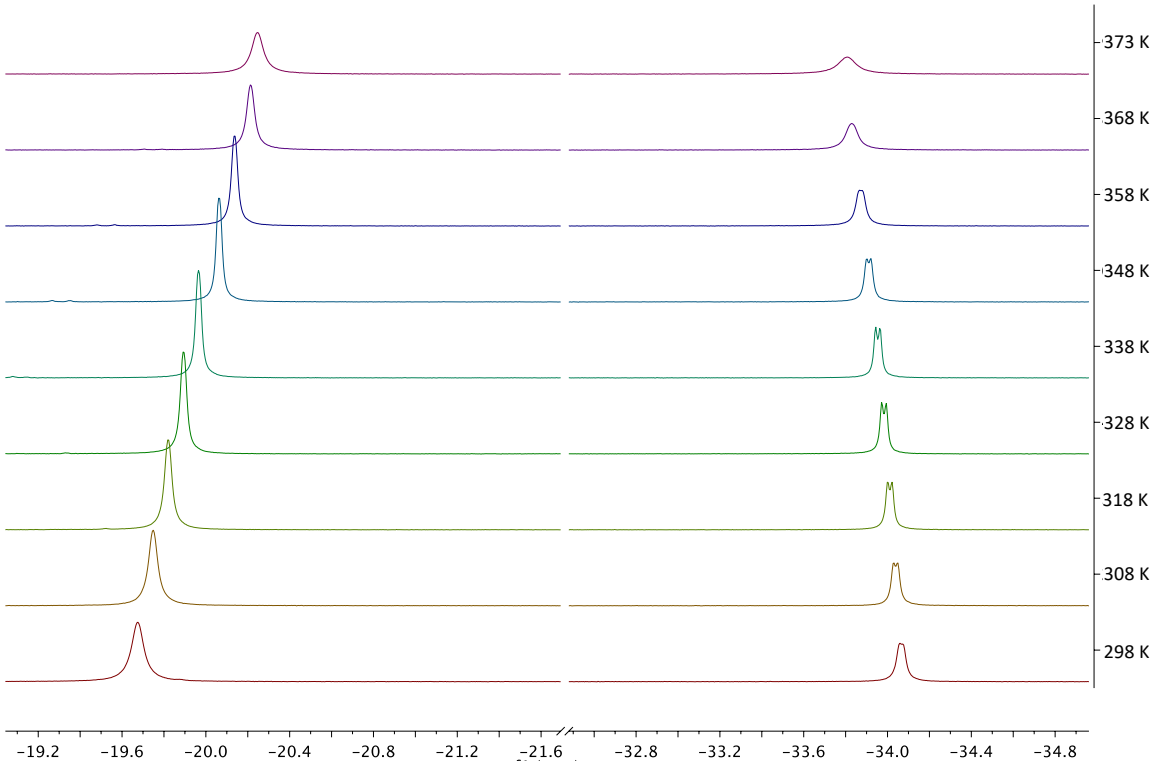

Figure 4.2. Variable (high) temperature behaviour of PHCy $^{31}P\{^{1}H\}$ NMR resonances in [Ru(CO)(PPh$_3$)(PHCy)(Tp)]

To further investigate the behaviour of [Ru(CO)(PPh$_3$)(PHCy)(Tp)], the $^{31}P\{^{1}H\}$ NMR behaviour of a toluene-d_8 solution was monitored over the temperature range 188−298 K (Figure 4.3). Broadening of the signals was observed over the range 218−278 K with the signals appearing to sharpen below this temperature. Closer inspection of the 188 K spectrum revealed a weak resonance at δ_P −21.9 in addition to a more intense resonance at δ_P −19.5 indicating that the original resonance at δ_P −19.8 had split into two unequally-populated states (Figure 4.4). It was reasoned that the observed kinetic process was rotation about the Ru−P bond leading to the resolution of different rotamers of the two diastereomers of [Ru(CO)(PPh$_3$)(PHCy)(Tp)]. This process is lower in energy than phosphorus inversion for late transition metal complexes.[90] Based on a coalescence temperature of 248(5) K, a barrier to rotation could be estimated[199] to be $\Delta G^{\ddagger}$ = 45.2(9) kJ mol^{-1} (See Section A.1). The barrier to rotation is higher than the range calculated (8.8−36.0 kJ mol^{-1}) for the complexes [Fe(CO)$_2$(PR$_2$)(Cp)],[90] which likely arises from the presence of bulkier PPh$_3$ and Tp coligands in the ruthenium complex *versus* CO and Cp in the modelled complex.

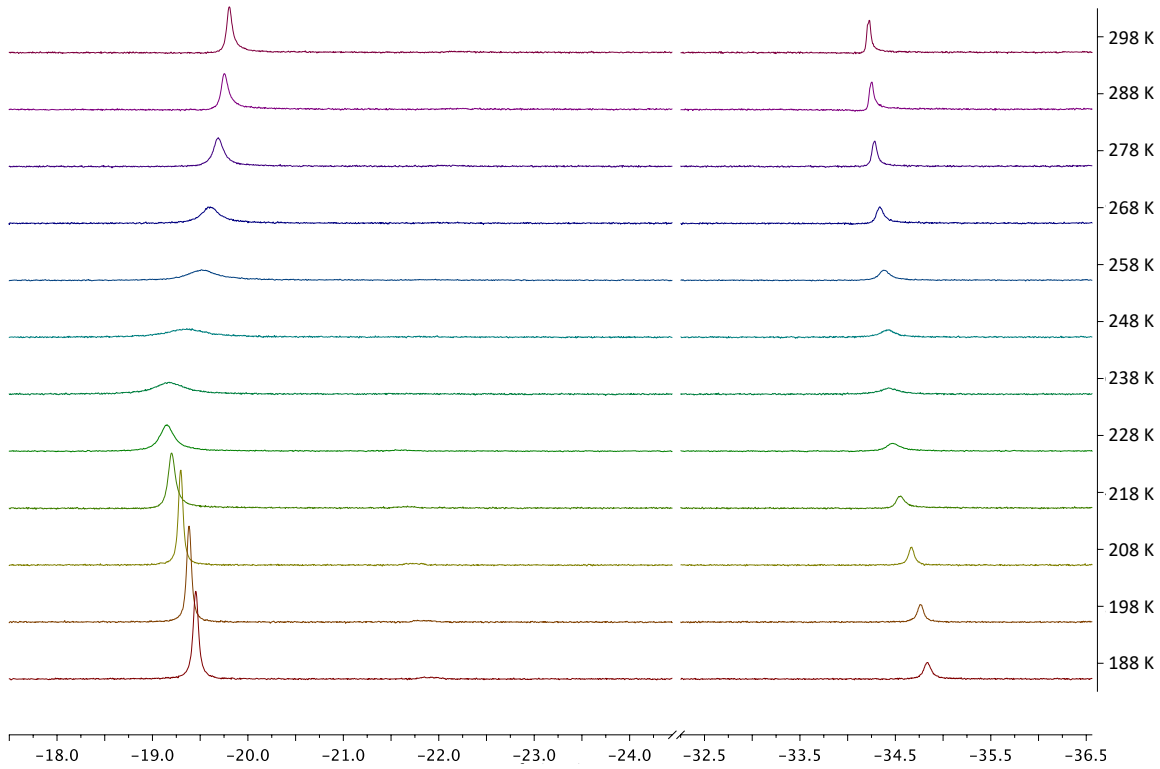

Figure 4.3. Variable (low) temperature behaviour of PHCy $^{31}P\{^{1}H\}$ NMR resonances in [Ru(CO)(PPh$_3$)(PHCy)(Tp)]

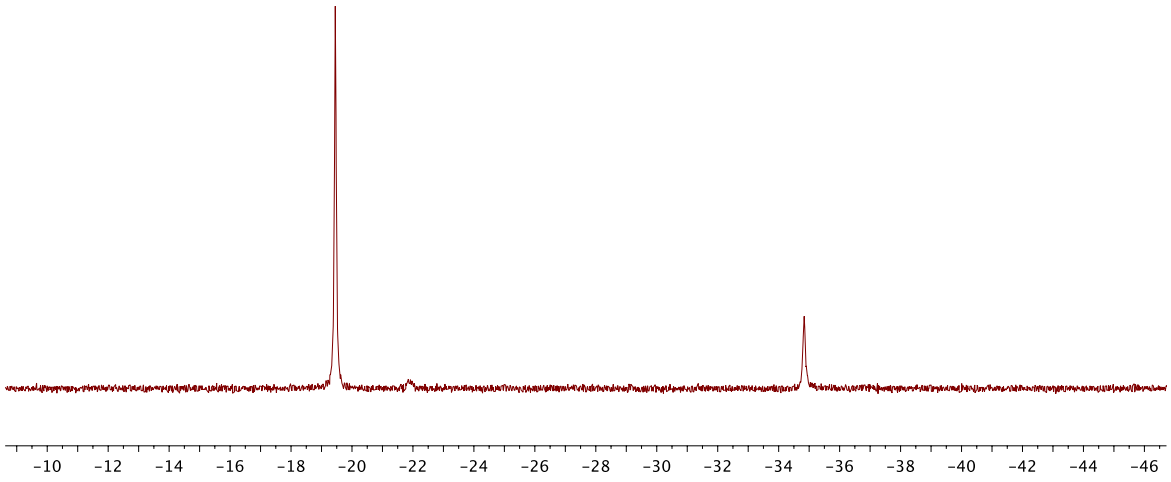

Figure 4.4. $^{31}P\{^{1}H\}$ NMR Spectrum of [Ru(CO)(PPh$_3$)(PHCy)(Tp)] at 188 K

A notable observation was that at 298 K the two stereoisomers of [Ru(CO)(PPh$_3$)(PHCy)(Tp)] were present in a 7:3 ratio. The unequal populations of the two isomers at equilibrium indicate that one diastereomer is more energetically favourable than the other. Crucially, the equilibrium constant at any given temperature is linked to the difference in thermodynamic

parameters between the two states in equilibrium. Having measured spectra over a range of temperatures, equilibrium constants at each temperature were calculated and values of $|\Delta H|$ = 3.23(15) kJ mol^{-1} and $|\Delta S|$ = 4.06(51) J mol^{-1} extracted (see Section A.2).

A convolution of unequal populations, a competing Ru–P rotation process and only observing the system in slow exchange precluded the use of traditional 1D NMR methods[199] to obtain kinetic data for phosphorus inversion in [Ru(CO)(PPh_3)(PHCy)(Tp)]. Instead 2D Exchange Spectroscopy (EXSY) was utilised,[200**] a method which monitors magnetisation transfer between sites through the appearance of cross peaks.

A noteworthy observation from the EXSY experiments was the presence of cross peaks between resonances for the two diastereomers (Figure 4.5). These cross peaks provided confirmation that exchange between the two isomers was occurring. Prior to this experiment no direct evidence had been obtained with the system only ever being observed in slow exchange.

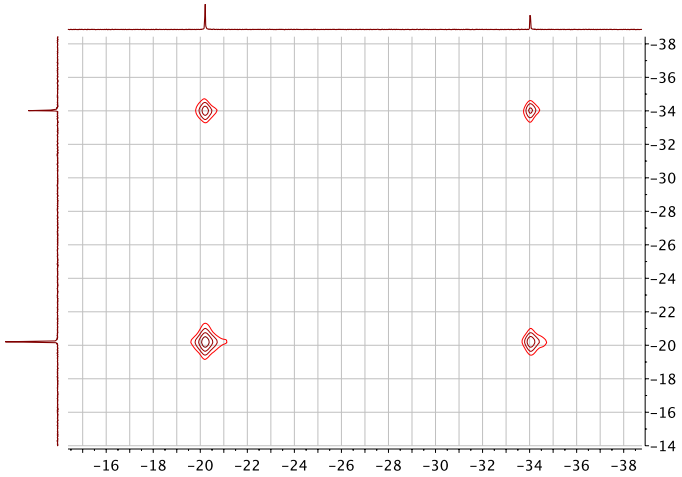

Figure 4.5. 2D-EXSY spectrum of [Ru(CO)(PPh_3)(PHCy)(Tp)]

From the EXSY experiments, a barrier to phosphorus inversion of $\Delta G^{\ddagger}$ = 84.9(9) kJ mol^{-1} was obtained (see Section A.3). The value is at least 25 kJ mol^{-1} higher than those reported for the other primary phosphido complexes [Re(NO)(PPh_3)(PHPh)(Cp)] and [Fe(PHPh){1,2-C_6H_4($PMePh_2$)}(Cp)] (Table 4.1). The barrier is also higher than that calculated for

** Experiments were conducted with assistance from Mr H. W. Orton and Prof. G. Otting

[Fe(PHPh)(CO)$_2$(Cp)] but in good agreement with the value for [Fe(PMe$_2$)(CO)$_2$(Cp)]. This agreement is consistent with Marynick's suggestion[90] that aromatic substituents may assist in stabilising the trigonal planar transition state, and provides a reasonable explanation as to why [Ru(CO)(PPh$_3$)(PHCy)(Tp)] has a higher barrier to phosphorus inversion than other (aromatic-substituted) primary phosphido complexes.

Table 4.1. Phosphorus inversion barriers for various phosphido complexes

Complex	Barrier (kJ mol^{-1})	Method
[Re(NO)(PPh$_3$)(P{*p*-tol}$_2$)(Cp)][83]	55.6(8)	Experimental
[Re(NO)(PPh$_3$)(PHPh)(Cp)][89]	48.1(4)	Experimental
[Fe(PHPh){1,2-C$_6$H$_4$(PMePh)$_2$}(Cp)][91]	60(4)	Experimental
[Fe(PHPh)(CO)$_2$(Cp)][90]	68.6	Computational
[Fe(PMe$_2$)(CO)$_2$(Cp)][90]	85.8	Computational

4.2 Potential Non-Innocent Behaviour of Phosphorus Lone Pair

As mentioned in Section 1.2.2, the phosphorus lone pair in phosphido complexes has potential non-innocent behaviour and may have an impact on the lability of co-ligands (Scheme 4.3). In order to investigate this possibility with [Ru(CO)(PPh$_3$)(PHCy)(Tp)], ligand substitution reactions with PMe$_2$Ph and CO were attempted. After 72 hours, no change was observed by ^{31}P{^{1}H} NMR spectroscopy upon stirring a solution of [Ru(CO)(PPh$_3$)(PHCy)(Tp)] with excess PMe$_2$Ph. In the case of CO, after bubbling CO gas through a THF solution of [Ru(CO)(PPh$_3$)(PHCy)(Tp)] and stirring at room temperature for 72 hours the relative proportion of PPh$_3$ determined by ^{31}P{^{1}H} NMR spectroscopy increased from 4% to 17%. However, there was no concommitant appearance of other signals in the spectrum. Furthermore, no distinct bis-carbonyl bands were observed in the IR spectrum of the mixture. From these data it can be inferred that ligand substitution is not likely to be occuring (Scheme 4.4), and that the rate of substitution processes is not significantly accelerated by the presence of the phosphorus lone pair.

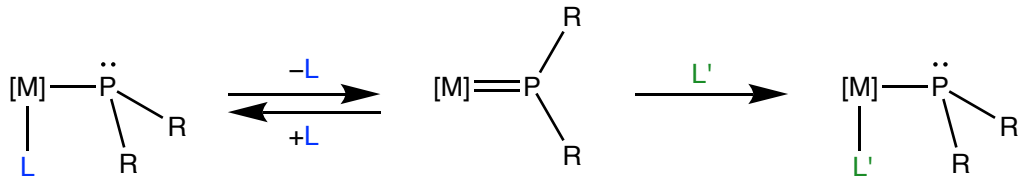

Scheme 4.3. Non-innocent behaviour of the phosphido lone pair

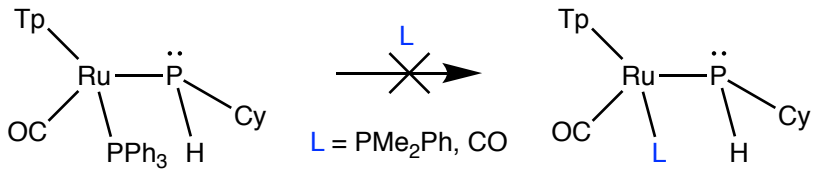

Scheme 4.4. Attempted ligand substitution of [Ru(CO)(PPh$_3$)(PHCy)(Tp)]

4.3 Methylation of [Ru(CO)(PPh$_3$)(PHCy)(Tp)]

Methylation of metal phosphido complexes has been widely reported[75, 80, 83, 91, 201-202] (see Sections 1.2.2 and 1.2.3). Treatment of a THF solution of [Ru(CO)(PHCy)(PPh$_3$)(Tp)] with iodomethane (Scheme 4.5) resulted in decolourisation and the observation of a single ν_{CO} band at 1975cm^{-1} in the IR spectrum of the reaction mixture. The increase in wavenumber of the ν_{CO} band (from 1931 cm^{-1}) was consistent with the alkylation of the phosphido complex and the formation of a cationic complex. The presence of three products giving rise to six doublet resonances was observed by $^{31}P\{^1H\}$ NMR spectroscopy ($CDCl_3$): two diastereomers of the expected cationic salt [Ru(CO)(PHMeCy)(PPh$_3$)(Tp)]OTf (δ_P 38.3 and 13.5; 38.0 and 16.1) as well as the dimethylated product [Ru(CO)(PMe$_2$Cy)(PPh$_3$)(Tp)]OTf (δ_P 34.5 and 11.0). The presence of the compounds was further evident from ESI-MS data, which contained isotopic distributions for both mono- and dimethylated products.

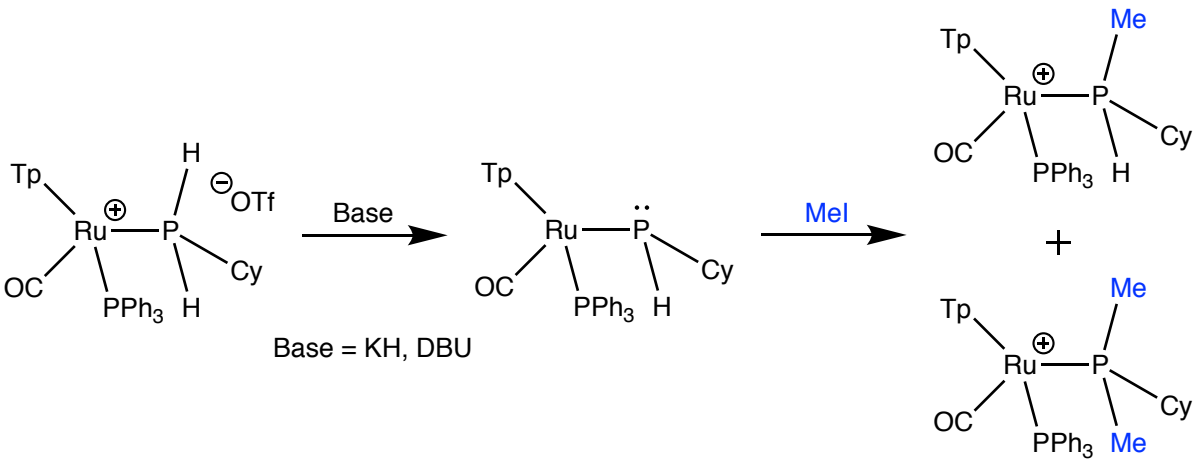

Scheme 4.5. Methylation of [Ru(CO)(PPh$_3$)(PHCy)(Tp)]

Despite numerous attempts at both varying reaction conditions and recrystallising the mixture, the diastereomeric monomethylated complexes could not be isolated free from the dimethylated product. The dimethylated product was observed in yields up to 30%, depending on reaction conditions. With removal of excess KH by filtration through diatomaceous earth and careful stoichiometric addition of MeI, the dimethylated complex still comprised 3% of the isolated product, as measured by $^{31}P\{^{1}H\}$ NMR spectroscopy. Given the similarity of the mono− and dimethylated complexes, their solubilities did not differ sufficiently to allow for fractional crystallisation, and their cationic nature precluded chromatographic separation.

To form the dimethylated product, [Ru(CO)(PHMeCy)(PPh_3)(Tp)]OTf would need to be deprotonated, followed by methylation of the resultant phosphido complex [Ru(CO)(PMeCy)(PPh_3)(Tp)] to give [Ru(CO)(PMe_2Cy)(PPh_3)(Tp)] (Scheme 4.6, right). The formation of the dimethylated product, even after removal of excess KH, implies the presence of another base in solution. The phosphido complex [Ru(CO)(PHCy)(PPh_3)(Tp)] appears to be the most likely candidate, establishing an acid-base equilibrium with $[Ru(CO)(PH_2Cy)(PPh_3)(Tp)]^+$ in solution. Within this process is the counter-intuitive implication that [Ru(CO)(PHCy)(PPh_3)(Tp)] acts as a Brønsted-Lowry base to yield the higher-substituted, more basic [Ru(CO)(PMeCy)(PPh_3)(Tp)] (Scheme 4.6). Given the distribution of products, it can be presumed that the acid-base equilibrium lies far to the left, in agreement with conventional reasoning.

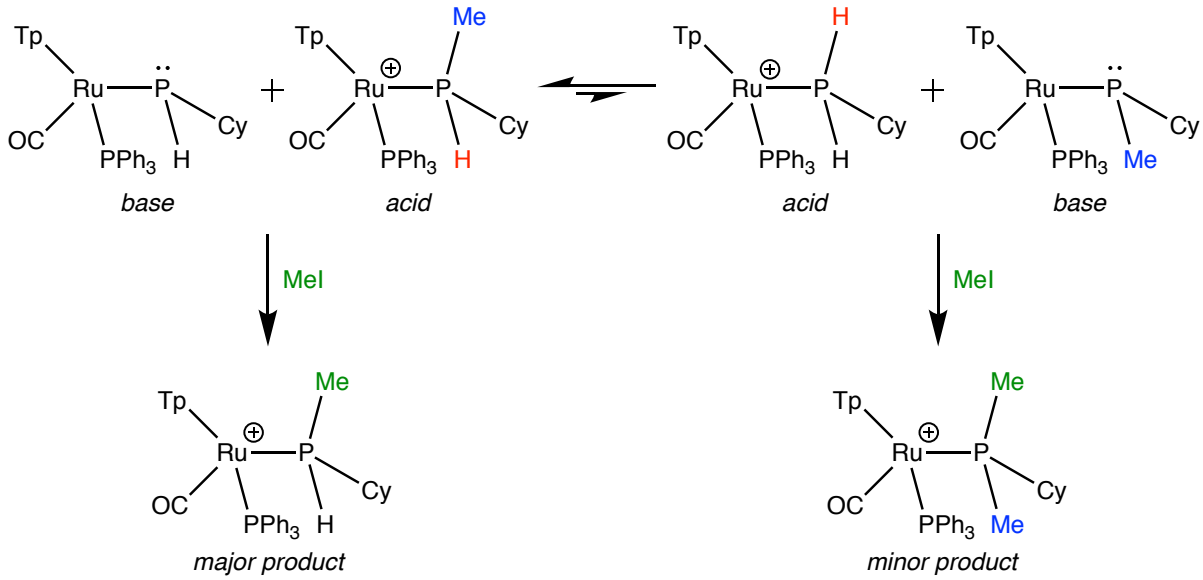

Scheme 4.6. Formation of dimethylated product

The dimethylated product could be obtained by deprotonating [Ru(CO)(PHMeCy)(PPh_3)(Tp)]OTf followed by reaction with MeI, or by directly treating [Ru(CO)(PH_2Cy)(PPh_3)(Tp)]OTf with excess KH and MeI (Scheme 4.7). While the latter is the simpler, preferred method, the former is remarkable in that it produces the intermediate phosphido complex [Ru(CO)(PMeCy)(PPh_3)(Tp)]. This intermediate was only observed spectroscopically.

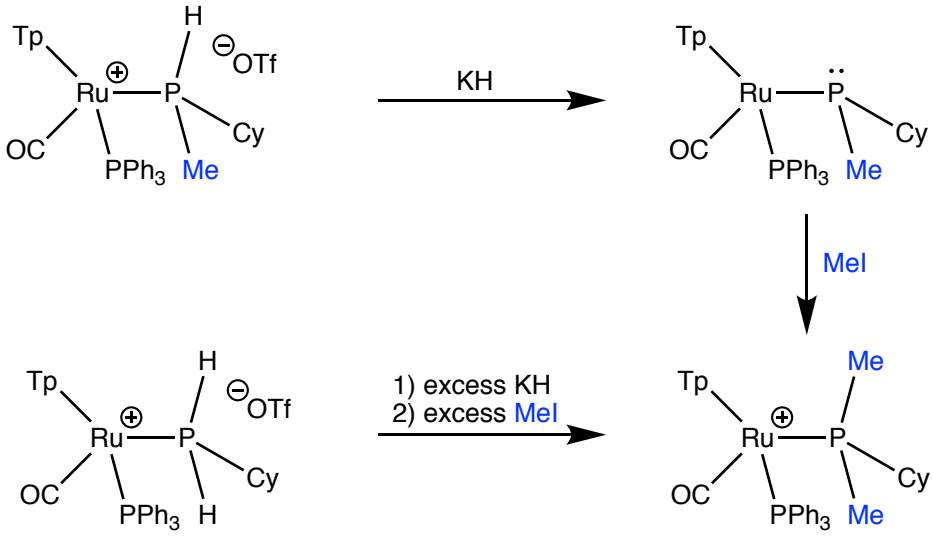

Scheme 4.7. Synthesis of [Ru(CO)(PPh_3)(PMe_2Cy)(Tp)]$^+$

Deprotonation to give [Ru(CO)(PMeCy)(PPh_3)(Tp)] resulted in a ν_{CO} band with a lower frequency at 1926 cm^{-1} in the IR spectrum (THF), as expected on moving from a cationic to a neutral species. Two diastereomers were observed in the $^{31}P\{^1H\}$ NMR spectrum (C_6D_6), one

giving rise to doublets at δ_P 47.8 and 9.2 ($^2J_{PP}$ = 8 Hz) and the other to doublets at δ_P 45.9 and 13.3 ($^2J_{PP}$ = 13 Hz). The $^{31}P\{^1H\}$ NMR chemical shifts of the two isomers are within 10 ppm of those for [Ru(CO)(PHMeCy)(PPh_3)(Tp)]OTf. Given the relatively small differences, and the fact that the spectra for the two compounds were measured in different solvents (C_6D_6 for the neutral, highly basic [Ru(CO)(PMeCy)(PPh_3)(Tp)] and $CDCl_3$ for the salt [Ru(CO)(PHMeCy)(PPh_3)(Tp)]OTf), it would be imprudent to draw conclusions from the change in chemical shifts. Coupling constants are less dependent on solvent choice, and the substantial reduction in $^2J_{PP}$ is consistent with the trend observed for the formation of [Ru(CO)(PHCy)(PPh_3)(Tp)].

The salt [Ru(CO)(PMe_2Cy)(PPh_3)(Tp)]OTf gave rise to a single ν_{CO} IR band (THF) at 1984 cm^{-1}, as expected, to a higher frequency than the absorption for [Ru(CO)(PMeCy)(PPh_3)(Tp)]. The ν_{CO} value is higher than observed for [Ru(CO)(PHMeCy)(PPh_3)(Tp)]OTf and roughly equal to [Ru(CO)(PH_2Cy)(PPh_3)(Tp)]OTf, which is unusual since one might expect these to monotonically follow the Tolman electronic parameters for PH_2Cy > PHMeCy > PMe_2Cy. [132] Conventional reasoning dictates that an increasing degree of alkyl substitution leads to a more electron-donating phosphorus atom, in turn leading to a decrease in ν_{CO} for any CO co-ligands. As such, the ν_{CO} value for the complexes should decrease in the order PH_2Cy > PHMeCy > PMe_2Cy. The reason for the observed deviation is not known, although it is clear factors other than ligand σ-basicity (*e.g.* hyperconjugation of the methyl C−H bonds) must apply.

As with observations for previous PH_2Cy complexes the two methyl groups are diastereotopic, as confirmed by the distinct resonances observed for the two groups in both the ^1H (δ_H 1.02 and 0.54) and $^{13}C\{^1H\}$ (δ_C 10.7 and 10.1) NMR spectra. These resonances all appeared as doublets as a result of coupling to the ^{31}P nucleus. The remaining NMR data were unremarkable and consistent with those previously observed and discussed for the ancilliary Tp, CO, PPh_3 and PCy groups.

4.4 Formation and Reactivity of a BH_3 Adduct

Amine-borane adducts are archetypal Lewis acid-base pairs and they have recently enjoyed a reinvigorated interest due to their potential for hydrogen storage,[203-204] as well as their use as precursors for new boron- and nitrogen-based materials.[204-205] Phosphine-boranes are also well-known, albeit with comparatively fewer studies than the lighter amine-boranes. The disparity in popularity between the two is likely due to the notorious pyrophoric and malodorous natures of primary and secondary phosphines, particularly if the ultimate goal is dehydrocoupling. Furthermore, the heavier molecular weight of phosphorus *versus* nitrogen leads to a reduced weight percentage of hydrogen in the case of potential hydrogen storage materials. Nevertheless, phosphine-boranes have played an important role as phosphine precursors and monomers for phosphinoborane formation. Additional interest has also arisen in their use as transition metal ligands, and as Frustrated Lewis Pairs in the case of sterically cumbersome substituents which prevent formal adduct formation.[206]

4.4.1 Synthesis of $[Ru(CO)(PPh_3)\{PH(BH_3)Cy\}(Tp)]$

A common route to the preparation of phosphine-borane adducts is the treatment of either $BH_3{\cdot}SMe_2$ or $BH_3{\cdot}THF$ with the desired phosphine precursor. Indeed, this route was utilised in early preparations of transition metal phosphine-boranes[87, 207-208] (*e.g.* $[Fe(CO)_2\{P(BH_3)Ph_2\}(Cp)]$, Scheme 4.8) and the extension of this reactivity to the present system was investigated.

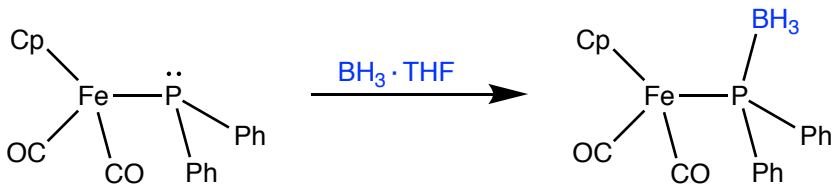

Scheme 4.8. Common route to phosphine-borane adducts

Treatment of a THF solution of $[Ru(CO)(PPh_3)(PHCy)(Tp)]$ with $BH_3{\cdot}SMe_2$ (Scheme 4.9) resulted in a colour change from yellow to colourless. Infrared spectroscopy (THF) of the reaction mixture revealed two ν_{CO} bands at 1983 and 1958 cm^{-1}. Both bands have shifted to a higher wavenumber, which is consistent with the reduced electron density at the metal

centre in the desired product, [Ru(CO)(PPh$_3$){PH(BH$_3$)Cy}(Tp)], than in the phosphido complex precursor (ν_{CO} 1931 cm^{-1} in THF).

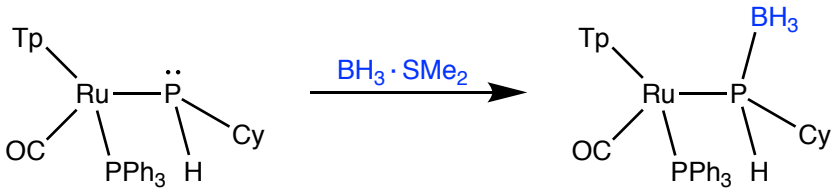

Scheme 4.9. Reaction of [Ru(CO)(PPh$_3$)(PHCy)(Tp)] with BH$_3$·SMe$_2$

Resonances due to two diastereomeric products were seen in the $^{31}P\{^1H\}$ NMR spectrum of the reaction mixture. One product gave rise to a doublet at 43.2 ppm ($^2J_{PP}$ = 23 Hz) and a broad singlet at −4.8 ppm, while the other corresponded to a doublet at 44.2 ppm ($^2J_{PP}$ = 21 Hz) and a broad singlet at –1.2 ppm. The signal broadening is typical of coupling to quadrupolar boron (^{10}B and ^{11}B), and these resonances were assigned to PH(BH$_3$)Cy groups. These resonances appeared as doublets in the ^{31}P NMR spectrum with $^1J_{PH}$ of 309 and 293, Hz respectively, further supporting their assignment.

The two products were observed in approximately equal amounts, and are likely two diastereomers of the desired product, [Ru(CO)(PPh$_3$){PH(BH$_3$)Cy}(Tp)]. As the intermediate phosphido complex exists as two diastereomers, either isomer may react with BH$_3$·SMe$_2$ to give two isomers of the borane adduct. The two diastereomeric precursors need not have identical nucleophilicities such that the relative proportions of the two product diastereomers (*ca*. 1:1) may be different to those of the equilibrating precursors (*ca*. 7:3). The formulation of the two isomers is further supported by the similar ^1H and $^{31}P\{^1H\}$ NMR shifts of the two products.

Some unusual phenomena were observed in the ESI-MS data. The molecular ion was observed as the [M + Na]$^+$ adduct at *m/z* 757.2, which is common using this ionisation technique. Unusual, however, were the two base peaks at *m/z* 721.2 and 737.2. The former may correspond to a [M – BH$_3$ + H]$^+$ ion. Although this is the same mass as the starting material, [Ru(CO)(PPh$_3$)(PH$_2$Cy)(Tp)]$^+$, no starting material was detected in the sample by NMR spectroscopy and the purification should have removed such ionic materials. Therefore,

a reasonable assumption is that the loss of BH_3 occurs during the relatively high-energy mass spectrometry experiment. The peak at *m/z* 737.2 is three mass units higher than expected for the [Ru(CO)(PPh_3){PH(BH_3)Cy}(Tp)] molecular ion (*m/z* 734.2). Again considering potential events during the mass spectrometry experiment, a possibility is that BH_3 is lost followed by oxidation to form the phosphine oxide. Thus, the peak at *m/z* 737.2 may correspond to the $[M - BH_3 + O + H]^+$ ion. For both base peaks, the high-resolution data and isotopic distributions are in good agreement with those calculated for the proposed structures.

The use of alkali metal borohydrides in the synthesis of amine-boranes is well established, and this method has been successfully extended to phosphine-boranes.[206] Among the established routes, the most expedient involves the direct reaction of $NaBH_4$ with the desired phosphine and a proton source to return the phosphine-borane in high yields (Scheme 4.10).[209] Given the presence of an acidic P−H bond within the cationic precursor, a more direct route to the borane adduct was investigated (Scheme 4.11).

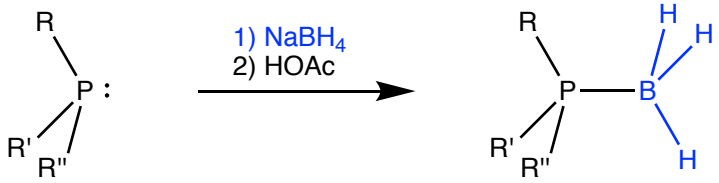

Scheme 4.10. Synthesis of phosphine-boranes from $NaBH_4$ and acetic acid

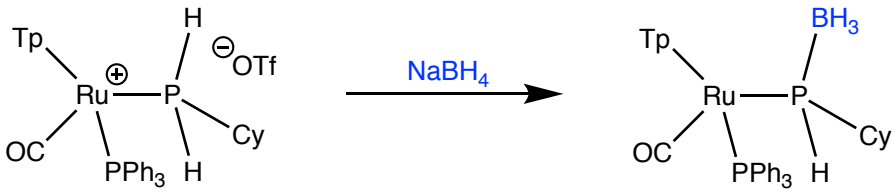

Scheme 4.11. Synthesis of [Ru(CO)(PPh_3){PH(BH_3)Cy}(Tp)] using $NaBH_4$

Initially, toluene was chosen as the solvent for the reaction to allow for the simple removal of ionic by-products. Stirring a suspension of [Ru(CO)(PPh_3)(PH_2Cy)(Tp)]OTf and $NaBH_4$ in toluene at room temperature for two hours did not result in the appearance of any ν_{CO} bands in the IR spectrum of the supernatant solution. However, after heating the mixture under reflux for one hour a weak band at 1985 cm^{-1} had developed. Heating was continued up to a total of seventeen hours and a strong ν_{CO} band was observed. Following filtration and recrystallisation, the product was obtained as a white solid in 33% yield.

Curiously, the product only consisted of one diastereomer (δ_P 43.2 and −4.8). Importantly, by circumventing the formation of the phosphido complex, an intermediate with freely interconverting diastereomers would appear to have been avoided. As a corollary, there is also no path between the two isomers of the borane adduct unless reversible dissociation of BH_3 ensues. Finally, whether the selectivity between the two diasteromers is kinetic or thermodynamic in nature has not been established, and this will be discussed further in this section.

While only a single isomer formed, which simplified both characterisation and subsequent investigations, the yield for the reaction remained low. A major impediment to yield optimisation was the heterogeneous reaction conditions which did not allow for the monitoring of starting material consumption. Additionally, the high temperatures used may have readily led to product decomposition or the loss of borane gas before adduct formation. Considering these two factors, a solvent that would allow for a homogeneous reaction at mild temperatures was sought.

Effervescence was observed upon stirring a THF solution of [Ru(CO)(PPh_3)(PH_2Cy)(Tp)]OTf and $NaBH_4$. While IR spectroscopy was inconclusive in monitoring the reaction (ν_{CO} 1985 and 1983 cm^{-1} for starting material and product, respectively), $^{31}P\{^1H\}$ NMR spectroscopy could be used to monitor the reaction. After 18 hours stirring at room temperature the $^{31}P\{^1H\}$ NMR spectrum of the mixture showed no resonances due to [Ru(CO)(PPh_3)(PH_2Cy)(Tp)]OTf. Following workup and recrystallisation, pure [Ru(CO)(PPh_3){PH(BH_3)Cy}(Tp)] was obtained in an improved 50% yield, in a 93:7 ratio of major and minor isomers. While selectivity between the two diastereomers is reduced, this method is preferred as a result of the higher yield.

Given that selectivity between the diastereomers of [Ru(CO)(PPh_3){PH(BH_3)Cy}(Tp)] is observed at room temperature, it is implicit that the major diastereomer is the kinetic product. However, since the selectivity is even greater at elevated temperatures it also follows that the major product is also the thermodynamic product.

The installation of the BH_3 group was apparent in the ^1H NMR spectrum; two broad resonances appeared at δ_H 4.83 and 4.64 for the Tp B−H and BH_3 groups, although the exact assignment could not be made. These two groups also arose as two resonances in the $^{11}B\{^1H\}$ NMR spectrum at δ_B −3.74 (Tp) and −33.85 (BH_3). The P−B connectivity was confirmed, as previously mentioned, by the broad resonance at δ_P −4.8 in the $^{31}P\{^1H\}$ NMR spectrum, typical for coupling to quadrupolar boron nuclei.

The molecular structure was confirmed by an X-ray diffraction experiment, with the molecular geometry shown in Figure 4.6. The formation of the P−B bond is clear with a P−B length of 1.904(10) Å. This length is marginally shorter (6 e.s.d.) than the P−B length of 1.965(5) Å reported for the only other structurally-characterised ruthenium phosphine-borane complex, $[Ru(CO)_2\{P(BH_3)Ph_2\}(Cp)]$.[210] Indeed, the value is below (albeit with a relatively large e.s.d.) the reported range 1.923−1.981 Å for terminal transition metal phosphine-borane complexes, suggesting a strong P−B bond. The Ru−P bond length of 2.345(2) Å is shorter than the value of 2.3760(11) Å reported for $[Ru(CO)_2\{P(BH_3)Ph_2\}(Cp)]$. Presumably, this reflects reduced substitution at phosphorus, as the same trend is observed between $[Fe(CO)_2\{PH(BH_3)Ph\}(Cp)]$ and $[Fe(CO)_2\{P(BH_3)Ph_2\}(Cp)]$.[211]

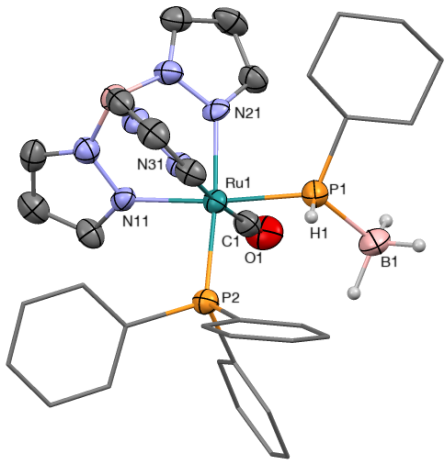

Figure 4.6. Molecular structure of S_{Ru},S_P-[Ru(CO)(PPh$_3$){PH(BH$_3$)Cy}(Tp)] in a crystal of [Ru(CO)(PPh$_3$){PH(BH$_3$)Cy}(Tp)].(CHCl$_3$) (50% displacement ellipsoids, solvent and most H atoms omitted, phenyl and cyclohexyl rings simplified). Selected bond lengths (Å) and angles (°): Ru1−P1 2.345(2), Ru1−P2 2.3565(18), Ru1−C1 1.862(8), P1−B1 1.904(10), P1−C11 1.851(8), P1−H1 1.30(2), O1−C1 1.119(9), P1−Ru1−P2 91.88(7), P1−Ru1−C1 88.7(2), P2−Ru1−C1 94.9(2). Molecule crystallised in the centrosymmetric Pbca *space group – enantiomer, but not diastereomers, present in unit cell.*

It is noteworthy that the crystal was obtained from a pure sample of the major diastereomer, allowing the relative stereochemistry to be assigned. The molecule crystallised in the centrosymmetric *Pbca* space group, indicating that it was a mixture of enantiomers and precluding the assignment of absolute stereochemistry. Using established conventions,[212] the isolated isomer can be identified as S^*_{Ru}, S^*_{P}.

4.4.2 Attempted Reactions at the P–H Bond

As noted previously, deprotonation of the phosphido complex [Ru(CO)(PPh_3)(PHCy)(Tp)] to yield an anionic phosphinidene complex was unsuccessful. It was reasoned that borane, as a Lewis acid, would withdraw electron density from the P–H bond and increase its acidity. Deprotonation of borane adducts of primary or secondary phosphines is a well-established protocol of considerable synthetic utility.[206] Thus, deprotonation of the borane complex might be expected to lead to a borane-protected phosphinidene complex. However, no reaction between the borane complex and KH or ^{n}BuLi was observed (Scheme 4.12).

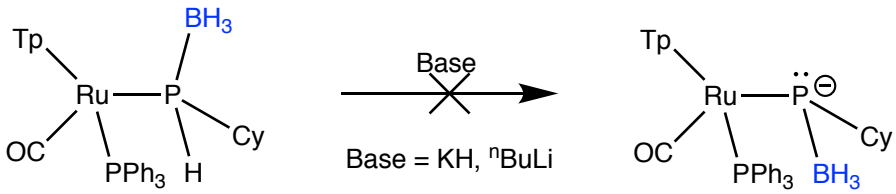

Scheme 4.12. Attempted deprotonation of [Ru(CO)(PPh_3){PH(BH_3)Cy}(Tp)]

Given the failure of deprotonation, the reaction with the hydride-abstracting reagent [CPh_3]PF_6 was explored (Scheme 4.13). It was postulated that the P–H bond would have some hydridic character (rather than acidic) and that a cationic phosphenium complex might form. Such hydridic character has been reported for P–H bonds[213] and hydride extraction in metal phosphorus complexes has been utilised to access dimetallaphosphacumulenes.[214] Addition of [CPh_3]PF_6 to a CH_2Cl_2 solution of [Ru(CO)(PPh_3){PH(BH_3)Cy}(Tp)] resulted in an immediate disappearance of the yellow colour of [CPh_3]PF_6. IR and $^{31}P\{^1H\}$ spectroscopy of the reaction mixture showed [Ru(CO)(PPh_3)(PH_2Cy)(Tp)]$^+$ as the only product.

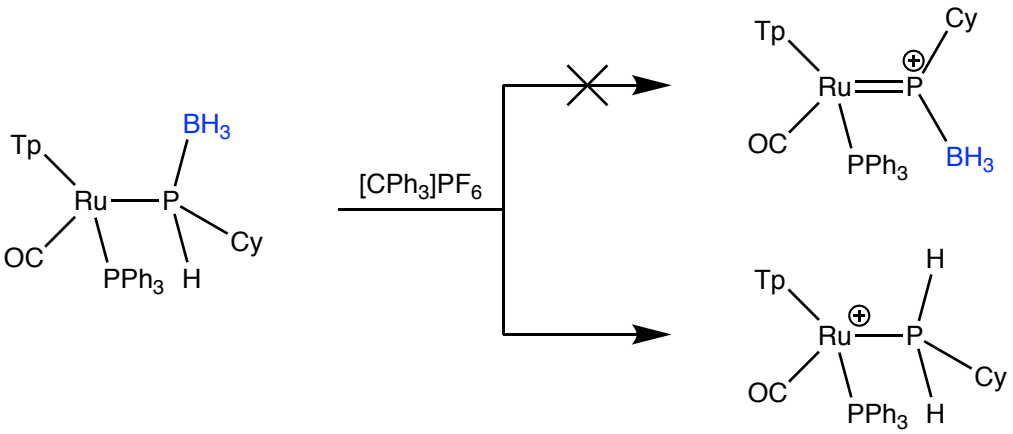

Scheme 4.13. Reaction of [Ru(CO)(PPh$_3$){PH(BH$_3$)Cy}(Tp)] with [CPh$_3$]PF$_6$

While the exact mechanism of this reaction was not explored in detail, previous studies on amine- and phosphine-boranes have demonstrated hydridic reactivity at boron over the Group 15 element.[206] As such, hydride abstraction may be expected to competitively occur at boron rather than phosphorus. The removal of electron density may then disrupt the Lewis pair formation (perhaps BF_4^-/F^- mediated), generating a phosphido complex which can be reprotonated. Boron-11 NMR spectroscopy of the mixture revealed a sharp singlet at δ_B −0.7 in addition to the Tp resonance (δ_B −4.1). The sharp shape of the ^{11}B NMR resonance suggests a homoleptically-substituted boron atom in a symmetrical electrical field and the absence of B–H coupling excludes BH_3 and BH_4^-. Unfortunately, the chemical shift did not correspond to any immediately obvious possible products (BF_4^-: δ_B −1.6, pentet ;BCl_4^-: δ_B 6.7; $B(OH)_4^-$: δ_B 1.1).[215]

4.4.3 Attempted Deprotection With Amines

Another common reaction of phosphine-boranes is their deprotection with amines. In these reactions an equilibrium is established between the amine-borane and phosphine-borane adducts, with the position contingent on the relative energies of the two pairs (Scheme 4.14).[206] Notably, the strength of adduct formation is often Lewis acid-dependent and does not necessarily correlate to the strength of the Lewis base. In the case of BH_3, displacement reactions have shown a preference for P-bound over N-bound adducts.[216-217] Nevertheless, phosphines have successfully been obtained from phosphine boranes in good yield (and with good stereoselectivity).[218] As such, the reaction with amines was sought as a potential alternative route to the phosphido complex.

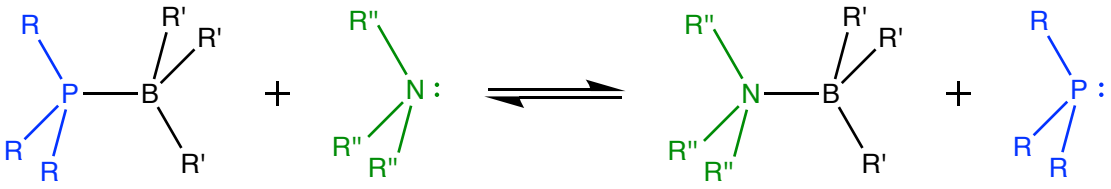

Scheme 4.14. Deprotection of phosphine-boranes with amines

The treatment of [Ru(CO)(PPh$_3$){PH(BH$_3$)Cy}(Tp)] with an excess of NHEt$_2$, NEt$_3$ or pyridine at room temperature failed to show any evidence of phosphido complex formation or starting material consumption (Scheme 4.15). With either NEt$_3$ or pyridine, heating the toluene-d_8 solution at 100°C for 2 hours resulted in a number (*ca*. 5) of new ^{31}P{^{1}H} NMR resonances while the starting material was still present in *ca*. 80%. After 20 hours the starting material was *ca*. 90% consumed with >9 new resonances appearing. The majority of these did not show any ^{31}P–^{31}P coupling and were not identified, except for a resonance at δ_P 66.5 which corresponds to [RuH(CO)(PPh$_3$)(Tp)].[128] This compound was the major product in each case (*ca*. 25–35%).

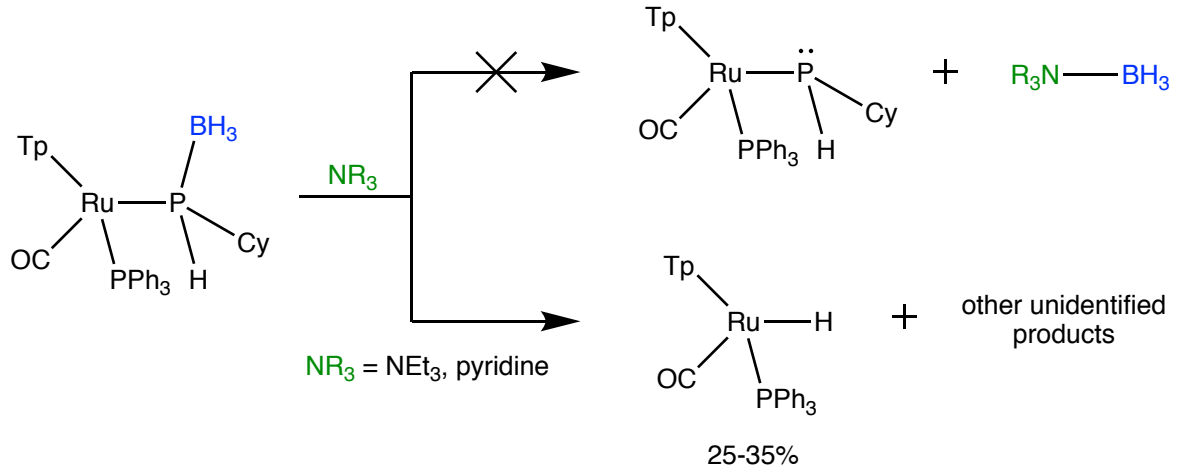

Scheme 4.15. Reaction of [Ru(CO)(PPh$_3$){PH(BH$_3$)Cy}(Tp)] with amines

Remarkable about the formation of [RuH(CO)(PPh$_3$)(Tp)] is the loss of the cyclohexylphosphine moiety. The exact mechanism is unknown, but the following experiments were conducted in attempts to elucidate more information about the process. Firstly, heating a toluene-d_8 solution of [Ru(CO)(PPh$_3$){PH(BH$_3$)Cy}(Tp)] in the absence of amine gave no change by ^{31}P{^{1}H} NMR, establishing the important role of the amine (Scheme 4.16).

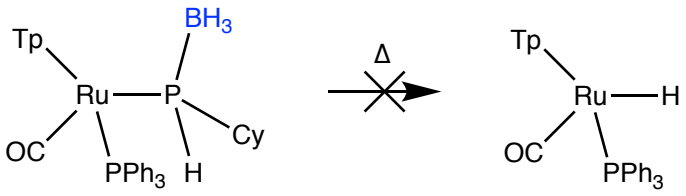

Scheme 4.16. Heating of [Ru(CO)(PPh₃){PH(BH₃)Cy}(Tp)]

There is the possibility that pyridine-borane (Py-BH_3) is formed and that it is the active species in the formation of [RuH(CO)(PPh_3)(Tp)]. Heating a mixture of [Ru(CO)(PPh_3){PH(BH_3)Cy}(Tp)] and pyridine-borane in toluene-d_8 for 17 hours resulted in only 5% conversion to [RuH(CO)(PPh_3)(Tp)] (Scheme 4.17), with unchanged [Ru(CO)(PPh_3){PH(BH_3)Cy}(Tp)] being the only other compound observed to be present by $^{31}P\{^1H\}$ NMR spectroscopy. The low conversion compared to the direct reaction with an amine after a similar reaction time demonstrates that the key step is not between the starting material and an amine borane. Instead, a more active 'free' amine is required.

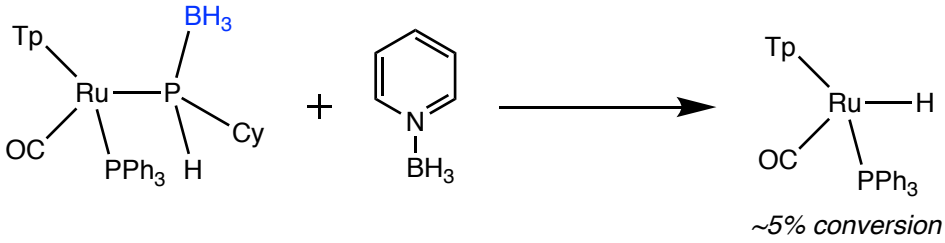

Scheme 4.17. Reaction of [Ru(CO)(PPh₃){PH(BH₃)Cy}(Tp)] with pyridine-borane

Finally, the reaction between the phosphido complex [Ru(CO)(PPh_3)(PHCy)(Tp)] and pyridine-borane was investigated (Scheme 4.18). Importantly, this would model the two major products had deprotection with amine been successful. Addition of pyridine-borane to a THF solution of [Ru(CO)(PPh_3)(PHCy)(Tp)] resulted in no visible changes after 30 minutes stirring at room temperature. After heating under reflux for 1.5 hours, the mixture had turned colourless. A $^{31}P\{^1H\}$ NMR spectrum of the mixture showed that [Ru(CO)(PPh_3){PH(BH_3)Cy}(Tp)] was the major product (93%) of the reaction, while a small amount (7%) of [RuH(CO)(PPh_3)(Tp)] had formed. While not providing any conclusive evidence as to the significant formation of [RuH(CO)(PPh_3)(Tp)], the reaction did demonstrate the extreme nucleophilicity of [Ru(CO)(PPh_3)(PHCy)(Tp)] such that the conditions required for

removal of BH_3 from the phosphido-borane complex [Ru(CO)(PPh_3){PH(BH_3)Cy}(Tp)] were incompatible with the stability of the resulting species.

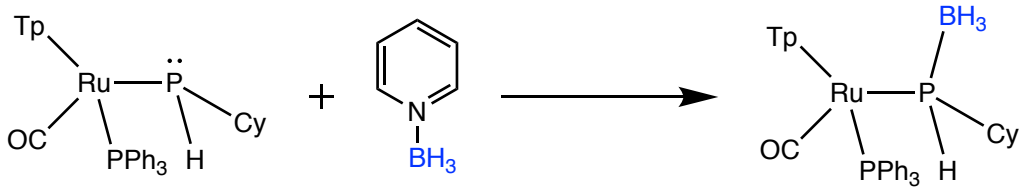

Scheme 4.18. Reaction of [Ru(CO)(PPh_3)(PHCy)(Tp)] with pyridine-borane

4.5 Attempted Synthesis of a B_3H_7 complex

Motivated by the successful use of BH_4^- in combination with a cationic primary phosphine complex to deliver borane, other potential borohydride reagents to create intriguing phosphineborane connectivities were investigated. The chosen reagent was the triboronate anion *nido*-$B_3H_8^-$. The structure of $B_3H_8^-$ contains a tetrahedral BH_4^- unit, of which two H atoms engage in 3-centre-2-electron bonding with a B_2H_4 unit (Figure 4.7 a). The triboronate anion has been used as a bidentate or tridentate ligand towards transition metals (Figure 4.7 b).[125, 219-237] Importantly, the reaction with HCl or HBr produced the halogenated species $B_3H_7X^-$ (X = Cl, Br).[238] Such reactivity demonstrates the hydridic nature of the B–H bonds and intimates that the molecule may behave similarly to BH_4^- in the formation of phosphine boranes. The degradation of tetraborane (B_4H_{10}) by phosphines PHRR' (R = R' = H, Me; R = H, R' = Me) affords the neutral monophosphine adducts B_3H_7(PHRR') (Figure 4.8a),[239] while the cation $[B_3H_6(PMe_3)_2]^+$ has two phosphine-coordinated boron centres (Figure 4.8b).[240] Thus, phosphide trapping by the $B_3H_n^{x+}$ (n = 7, x = 0; n = 6, x = 1) would seem plausible.

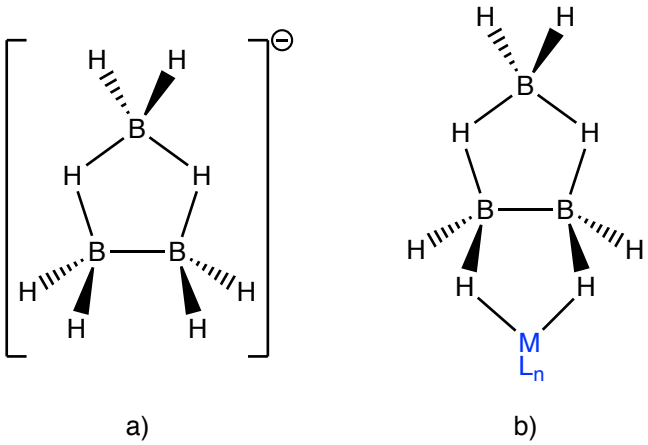

Figure 4.7. a) Structure of $B_3H_8^-$ b) Bidentate coordination of $B_3H_8^-$

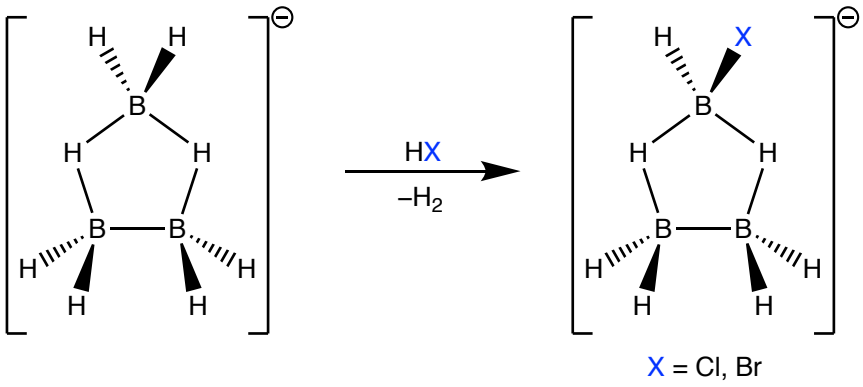

Scheme 4.19. Synthesis of $B_3H_7X^-$ (X = Cl, Br) from $B_3H_8^-$

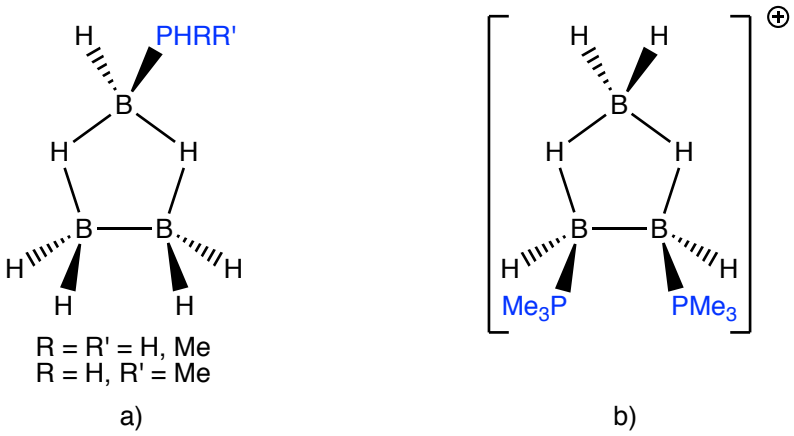

Figure 4.8. Phosphine adducts of the triboronate anion

Mixing [Ru(CO)(PPh_3)(PH_2Cy)(Tp)]OTf and [NBu_4][B_3H_8] in THF at room temperature for up to 14 days did not result in any reaction as observed by $^{31}P\{^1H\}$ NMR spectroscopy. Using more vigorous conditions (refluxing THF or toluene) only resulted in the formation of [Ru(CO)(PPh_3){$PH(BH_3)Cy$}(Tp)] (Scheme 4.20), as evidenced by IR, ^1H, $^{31}P\{^1H\}$ and $^{11}B\{^1H\}$

NMR spectroscopy and, most importantly, ESI-MS. The experiments show that the hydridic reactivity of $B_3H_8^-$ is significantly reduced compared to BH_4^-, and that the B_3 core is not stable at elevated temperatures. Scrambling and cluster degradation of triboronate scaffolds by phosphines is well-documented.[239-240]

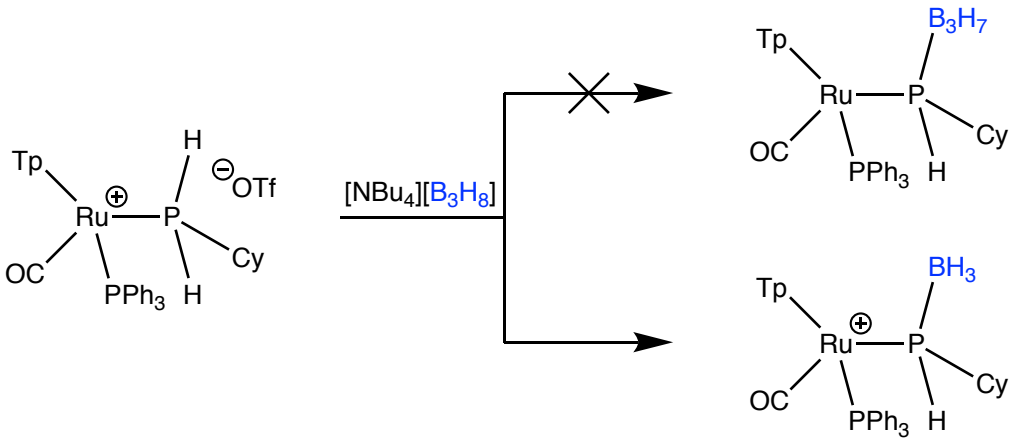

Scheme 4.20. Reaction of [Ru(CO)(PPh$_3$)(PH$_2$Cy)(Tp)]OTf with [NBu$_4$][B$_3$H$_8$]

4.6 Formation and Reactivity of CS_2 Adduct

Phosphine-carbon disulfide adducts have been known to chemists for over a century.[241] The adduct $Cy_3P.CS_2$ is commonly used as an air stable source of air-sensitive PCy_3, with the volatile CS_2 being removed *in situ* prior to use. $Cy_3P.CS_2$ and other phosphine-carbon disulfide adducts have also been used as bidentate ligands, in a manner analogous to the previously discussed dithiocarbamates.[242-245]

The first reaction between a phosphido complex and CS_2 was reported by Lappert.[246] CS_2 inserted into the M–P bond of the phosphido complexes $[Zr(Cp)_2(PR_2)X]$ (R = $SiMe_3$; X = Cl, Me) to yield a new complex bearing the $S_2C–PR_2$ ligand in a κ^2-*S,S'* binding mode (Scheme 4.21, top).

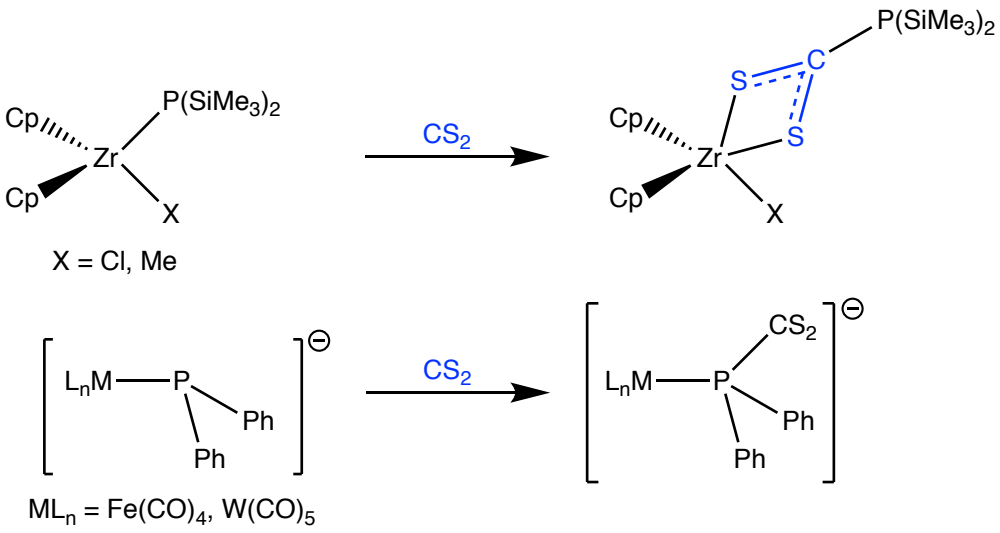

Scheme 4.21. Reactivity of metal phosphido complexes with CS_2

In contrast to Lappert's work, the complexes $[Fe(CO)_4(PPh_2)]^-$ and $[W(CO)_5(PPh_2)]^-$ both react with CS_2 to yield a monodentate, P-bound $(S_2C–PPh_2)^-$ ligand (Scheme 4.21, bottom).[247-248] For these cases the reactivity is similar to a conventional phosphine with a nucleophilic lone pair at phosphorus. The origin of the different phosphido reactivities is uncertain. Although Petz suggested that two K···S interactions in the molecular structure of [K(18-crown-6)][$Fe(CO)_4(PPh_2)$] restricted the insertion of CS_2 into the Fe–P bond, this link between solid-state structure and solution-phase reactivity is tenuous. The coordinative saturation at iron (*cf*. Lappert's zirconium example) may be more relevant. Additionally, $[W(CO)_5(PPh_2CS_2)]^-$ could also be synthesised from the direct reaction of $(PPh_2CS_2)^-$ and $[W(CO)_5(NCMe)]$[249] indicating a thermodynamic preference for the phosphorus-based coordination of $(PPh_2CS_2)^-$.

Lin carried out further studies into the reactivity of the $[W(CO)_5\{PPh_2(CS_2)\}]^-$ anion (Scheme 4.22).[249] Notably, the nucleophilicity of the S atom was amply demonstrated; the reaction with alkyl and acyl halides resulted in nucleophilic substitution by sulfur, while the addition of $[Re(CO)_5Br]$ gave the dinuclear species $[(OC)_5W(\mu\text{-}PPh_2CS_2)Re(CO)_5]$. The nucleophilic reactivity was extended towards the α,ω-alkyl iodides $I(CH_2)_nI$ (n = 1, 2, 3) as well as oxalyl bromide to give bridged dinuclear complexes. Finally, heating of $[W(CO)_5\{PPh_2(CS_2)\}]^-$ resulted in decarbonylation and a new complex featuring the PPh_2CS_2 ligand in a κ^2-*P,S* binding mode.

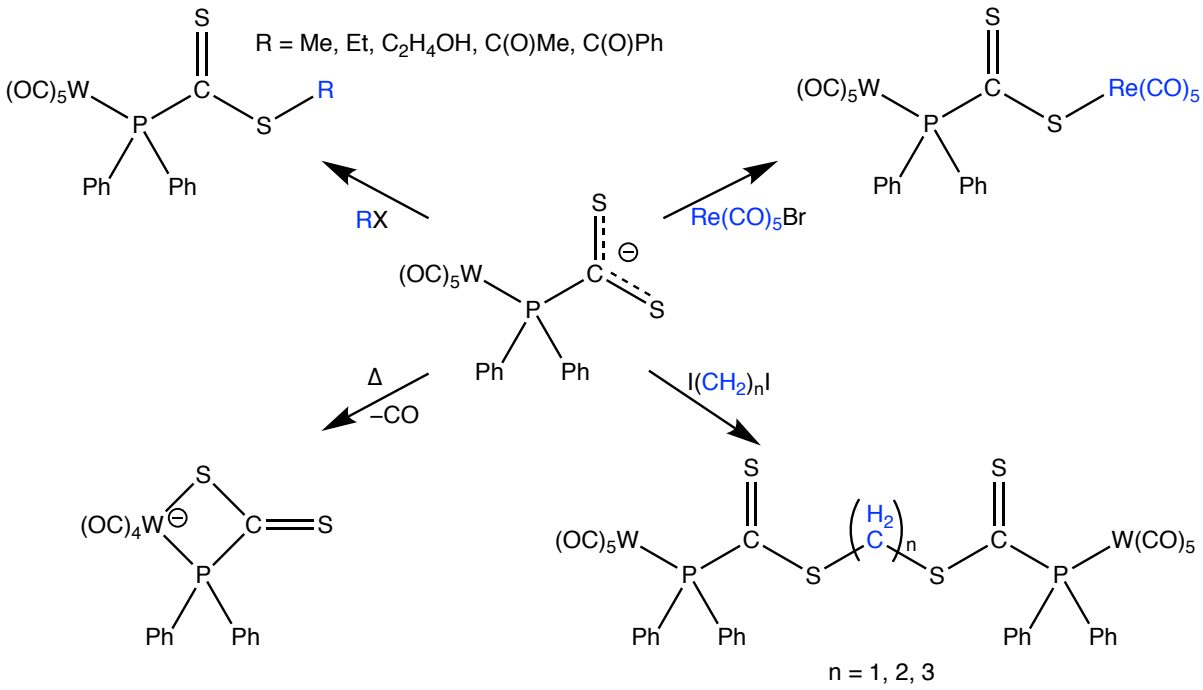

Scheme 4.22. Reactivity of $[W(CO)_5\{PPh_2(CS_2)\}]^-$

Formation of a CS_2 adduct of a primary phosphido complex sets the stage for some additional potentially curious intramolecular activity. The formal valence bond description of the adduct is zwitterionic,[250] with the negative and positive charge delocalised within the CS_2 and the metal phosphido fragments, respectively. Given this valence bond form, the potential for tautomerisation between a dithiocarboxylate phosphine and a dithiocarboxylic acid phosphido complex exists (Scheme 4.23).

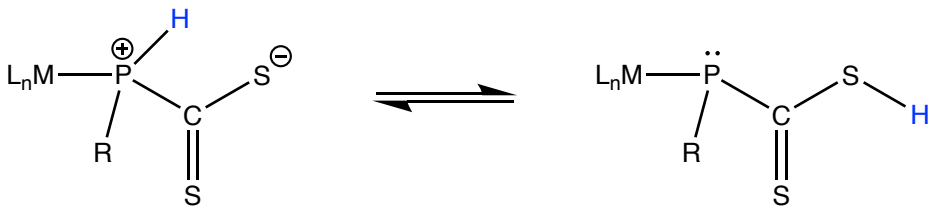

Scheme 4.23. Potential tautomerisation in a primary phosphido CS_2 adduct

4.6.1 Reaction of [Ru(CO)(PPh$_3$)(PHCy)(Tp)] with CS$_2$

Addition of CS_2 to a THF solution of the phosphido complex resulted in a colour change to red, and solution IR spectroscopy of the reaction mixture revealed ν_{CO} bands at 2005 and 1996 cm^{-1}. The increase in wavenumber of ν_{CO} is consistent with the zwitterionic valence bond form and the localisation of positive charge within the metal phosphido fragment. The presence of two ν_{CO} bands suggests the presence of an isomer in which one of the sulfur atoms may be close enough to the CO group to interact as part of a six-membered ring.

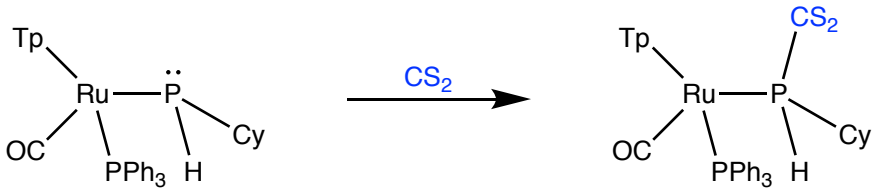

Scheme 4.24. Reaction of [Ru(CO)(PPh$_3$)(PHCy)(Tp)] with CS$_2$

The $^{31}P\{^1H\}$ NMR spectrum of the reaction mixture contained two doublets corresponding to the product at 78.3 and 40.6 ppm ($^2J_{PP}$ = 27 Hz), with no other resonances observed. The coupling between the two $^{31}P\{^1H\}$ NMR resonances indicates that the product is [Ru(CO)(PPh$_3$){PH(CS$_2$)Cy}(Tp)] (Scheme 4.24), the result of direct P–C bond formation rather than insertion into the Ru–P bond. Importantly, the high frequency resonance appeared as a doublet with a large $^1J_{PH}$ of 322 Hz in the ^{31}P NMR spectrum, ruling out the existence of an observable P(CS$_2$H)Cy tautomer in solution.

While no other products were observed in the $^{31}P\{^1H\}$ NMR spectrum of the reaction mixture, following removal of the solvent *in vacuo* during workup a number of new resonances appeared. The desired product was still present (*ca*. 50%) as well as the phosphido complex (*ca*. 25%) and *ca*. nine other unidentified $^{31}P\{^1H\}$ NMR resonances. These observations suggest that the addition of CS_2 is a reversible process (hence only one diastereomer observed on the ^{31}P NMR timescale) and that CS_2 is subsequently removed under reduced pressure. The volatility of CS_2 (b.p. 46.3°C) impeded attempts to isolate [Ru(CO)(PPh$_3$){PH(CS$_2$)Cy}(Tp)] and a bulk sample sufficiently pure for full characterisation could not be obtained.

Nevertheless, crystals of [Ru(CO)(PPh_3){PH(CS_2)Cy}(Tp)] suitable for X-ray diffraction were grown from a CH_2Cl_2 solution of the complex. The molecule crystallised in the centrosymmetric *P*−1 space group, indicating that a mixture of enantiomers are present. The molecular structure (Figure 4.9) clearly shows the formation of the P−CS_2 bond with a P1−C11 bond length of 1.868(6) Å, comparable with the corresponding bond lengths of 1.879(11) Å in [NEt_4][W(CO)$_5${PPh_2(CS_2)}][248] and 1.866(4) Å in [K(18-crown-6)][Fe(CO)$_4${PPh_2(CS_2)}].[247] Importantly, H11 was located in the Fourier difference map, confirming the P−H connectivity inferred from the NMR data. The position of this H atom was not independently refined. Additionally, the geometry about C11 is planar with an angle sum 360°, consistent with the delocalised π bond within the CS_2 fragment.

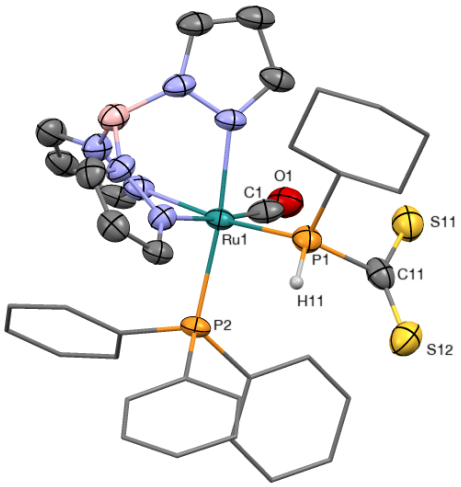

Figure 4.9. Molecular structure of S_{Ru},R_P-[Ru(CO)(PPh_3){PH(CS_2)Cy}(Tp)] in a crystal of [Ru(CO)(PPh_3){PH(CS_2)Cy}(Tp)].(CH_2Cl_2) (50% displacement ellipsoids, CH_2Cl_2 solvent molecule and most H atoms omitted, phenyl and cyclohexyl rings simplified). Selected bond lengths (Å) and angles (°): Ru1−P1 2.3448(15), Ru1−P2 2.3684(12), Ru1−C1 1.882(6), P1−C11 1.868(6), P1−C21 1.860(5), P1−H11 1.44(7), O1−C1 1.126(7), P1−Ru1−P2 95.17(5), P1−Ru1−C1 96.21(19), P2−Ru1−C1 93.29(17), S11−C11−S12 132.9(4). Molecule crystallised in the centrosymmetric P−1 space group – enantiomer, but not diastereomers, present in the unit cell.

Curiously, the C11−S11 and C11−S12 bond lengths have different (21 e.s.d.) values of 1.715(6) and 1.587(7) Å, respectively. While the disparity may suggest a dithiocarboxylic acid (CS_2H) moiety with one C=S and one C−S bond (*cf*. 1.7361(19) and 1.633(2) Å for Mes*CS_2H[251]), no H atom could be found in the Fourier difference map nor was there any residual electron density for a requisite counteranion. Upon closer inspection the C11 ellipsoid is elongated along the direction of the S12 bond which may contribute to the disparity in C−S bond lengths. Attempts

to model the CS_2 group over two positions, however, did not yield a more precise structural model.

4.6.2 Attempted Intramolecular Reactivity of [Ru(CO)(PPh_3){PH(CS_2)Cy}(Tp)]

The phosphoniodithiocarboxylate product contains both CO and PPh_3, both of which might conceivably be labilised to encourage bidentate coordination of the PH(CS_2)Cy ligand (Scheme 4.25).[252-253] Such reactivity involving labile co-ligands was reported by Lin.[249] Heating of a THF solution of the product at reflux showed no change by IR or $^{31}P\{^1H\}$ NMR spectroscopy after 16 hours. After 5 days of heating, the only change observed was the development of a band at 1931 cm^{-1} in the IR spectrum of the mixture due to the phosphido complex. The appearance of this band is indicative of the reversible nature of CS_2 adduct formation, with volatile CS_2 slowly evaporating after prolonged heating.

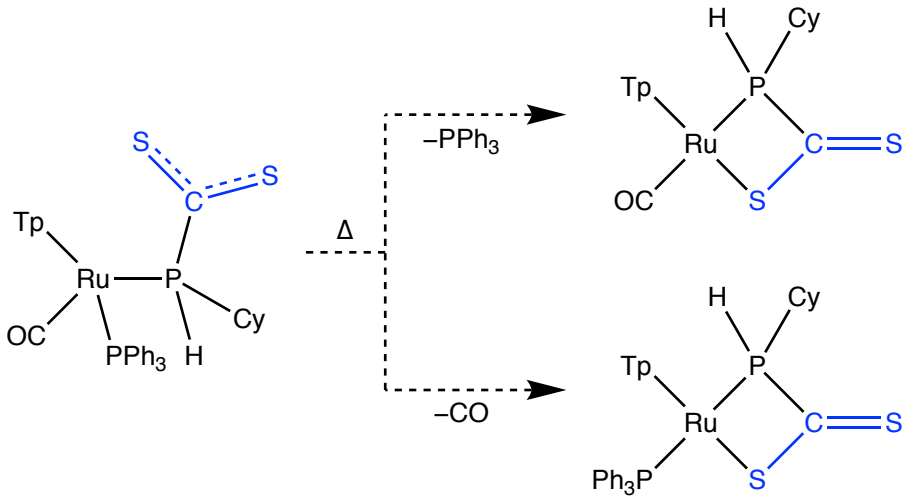

Scheme 4.25. Potential intramolecular reactivity of [Ru(CO)(PPh_3){PH(CS_2)Cy}(Tp)]

4.6.3 Methylation of CS_2 complex

While a bulk sample of synthetically pure [Ru(CO)(PPh_3){PH(CS_2)Cy}(Tp)] could not be obtained, solutions of the complex could be generated *in situ* to explore its reactivity. Iodomethane was chosen for this study, in an effort to synthesise [Ru(CO)(PPh_3){PH(CS_2Me)Cy}(Tp)]OTf and emulate the reactivity reported by Lin.

Upon addition of MeI to a freshly-generated THF solution of [Ru(CO)(PPh_3){PH(CS_2)Cy}(Tp)] (Scheme 4.26) the mixture immediately turned from red to purple before changing back to

red over 5 minutes. After 2 hours, IR spectroscopy of the reaction mixture revealed a single ν_{CO} band at 1997 cm^{-1} while the $^{31}P\{^{1}H\}$ NMR spectrum contained two doublets at δ_P 61.7 and 34.7 ($^{2}J_{PP}$ = 26 Hz). The former of these resonances was assigned as the PHCy moiety, appearing as a doublet ($^{1}J_{PH}$ = 345 Hz) in the ^{31}P NMR spectrum. This resonance shifted to lower frequency by *ca.* 17 ppm as a result of the reaction with MeI.

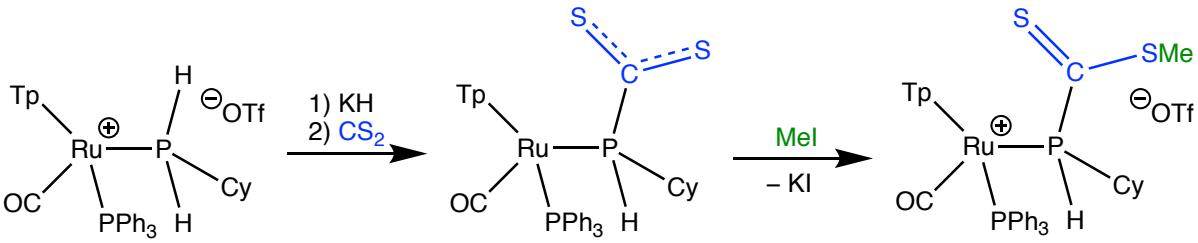

Scheme 4.26. Synthesis of [Ru(CO)(PPh₃){PH(CS₂Me)Cy}(Tp)]⁺

Workup consisted of removal of the THF *in vacuo*, extraction of the residue with CH_2Cl_2 and filtration to remove potassium iodide. Following crystallisation from a CH_2Cl_2/Et_2O mixture, the triflate salt of the desired product was obtained as a microanalytically-pure orange solid in 40% yield. The synthesis is conducted in one vessel beginning with [Ru(CO)(PPh₃)(PH₂Cy)(Tp)]OTf, and this is the source of the triflate anion. Notably, the precursor could not be isolated due to the reversible nature of CS_2 adduct formation and the volatility of CS_2. Methylation at sulfur prevents the loss of CS_2 and results in a conveniently isolable salt.

In the $^{13}C\{^{1}H\}$ NMR spectrum the CS_2 group was observed as a high frequency doublet at δ_C 232.4 with a $^{1}J_{PC}$ of 23 Hz. Methylation was confirmed by the presence of a singlet in the $^{13}C\{^{1}H\}$ NMR spectrum at δ_C 21.6 and a corresponding ^{1}H NMR singlet at δ_H 2.67. The remaining $^{13}C\{^{1}H\}$ and ^{1}H NMR resonances were all consistent with previous observations for the 'Ru(CO)(PPh₃)(PHCy)(Tp)' framework without any notable deviations.

Crystals of [Ru(CO)(PPh₃){PH(CS₂Me)Cy}(Tp)]OTf suitable for X-ray diffraction were grown by vapour diffusion of Et_2O into a CH_2Cl_2 solution of the compound. The molecular structure (Figure 4.10) confirms the addition of a methyl group to one sulfur atom of the CS_2 group, as well as the preservation of the P–H connectivity. Both the disparate (14 e.s.d.) C–S bond

lengths of 1.704(5) and 1.633(5) Å and the planar geometry about C2 (angle sum 360°) concur with a dithioester-type description of the CS_2Me group.

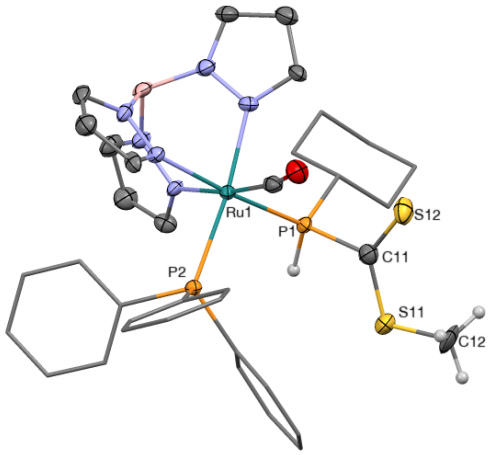

Figure 4.10. Molecular structure of R_{Ru},S_P-[Ru(CO)(PPh$_3$){PH(CS$_2$Me)Cy}(Tp)]$^+$ in a crystal of [Ru(CO)(PPh$_3$){PH(CS$_2$Me)Cy}(Tp)]OTf.(CH$_2$Cl$_2$)(C$_4$H$_{10}$O) (50% displacement ellipsoids, triflate counteranion, CH$_2$Cl$_2$ and Et$_2$O solvent molecules and most H atoms omitted, phenyl and cyclohexyl rings simplified). Selected bond lengths (Å) and angles (°): Ru1−P1 2.3375(11), Ru1−P2 2.3867(11), Ru1−C1 1.860(5), P1−C11 1.850(5), S11−C11 1.705(5), S11−C12 1.791(6), S12−C11 1.633(5), O1−C1 1.160(6), P1−Ru1−P2 94.88(4), P1−Ru1−C1 94.39(15), P2−Ru1−C1 95.03(15), S11−C11−S12 128.8(3). Molecule crystallised in the non-centrosymmetric P2$_1$ space group.

Intriguingly, [Ru(CO)(PPh$_3$){PH(CS$_2$Me)Cy}(Tp)]OTf crystallised in the non-centrosymmetric space group $P2_1$, meaning that the absolute stereochemistry within the observed structure could be assigned as R_{Ru}, S_P. The enantiopurity of the compound within this crystal raised the possibility that its formation had been stereoselective. However, the specific rotation of the bulk sample was $[\alpha]_D^{20}$ (CHCl$_3$) −0.86, corresponding to a racemic mixture. As such, the observed enantiopurity of the molecular structure within the selected crystal is likely to be a phenomenon associated with crystallisation and crystal packing, *i.e.*, crystals of the S_{Ru}, R_P isomer are likely to be equally present.

4.6.4 Deprotonation of Methylated Complex

As with [Ru(CO)(PPh$_3$)(PHMeCy)(Tp)]OTf, [Ru(CO)(PPh$_3$){PH(CS$_2$Me)Cy}(Tp)]OTf is a P-functionalised product which is cationic and contains a potentially acidic P–H bond. The possibility of deprotonation of [Ru(CO)(PPh$_3$){PH(CS$_2$Me)Cy}(Tp)]OTf to form [Ru(CO)(PPh$_3$){P(CS$_2$Me)Cy}(Tp)] (Scheme 4.27) was therefore explored. A mixture of [Ru(CO)(PPh$_3$){PH(CS$_2$Me)Cy}(Tp)]OTf and KH in THF immediately turned a deep purple

colour. The IR spectrum of the mixture showed the expected shift of ν_{CO} to a lower wavenumber from 1997 to 1961 cm^{-1}. Change was also observed in the $^{31}P\{^{1}H\}$ NMR spectrum with two resonances observed at δ_P 81.1 and 38.8. Neither resonance showed any one-bond $^{31}P–^{1}H$ coupling, indicating the absence of P–H bonds. Additionally, the $^{2}J_{PP}$ splittings were too small to be resolved, consistent with observations for the other observed phosphido complexes discussed above.

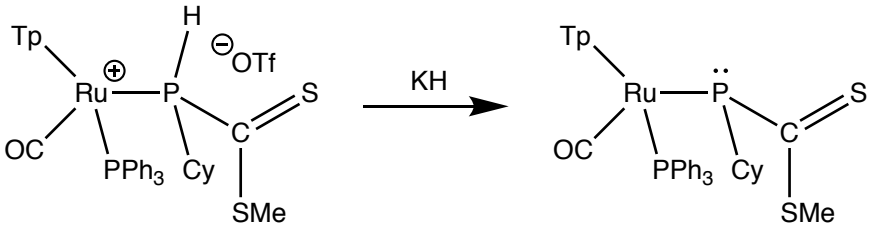

Scheme 4.27. Deprotonation of [Ru(CO)(PPh$_3$){PH(CS$_2$Me)Cy}(Tp)]OTf

After stirring the mixture at room temperature for 3 hours a colour change to orange was observed. Three new IR ν_{CO} absorptions were seen at 1957, 1927 and 1902 cm^{-1}, indicating that the putative product [Ru(CO)(PPh$_3$){P(CS$_2$Me)}(Tp)] was unstable and decomposed to form multiple unidentified products. After 24 hours the $^{31}P\{^{1}H\}$ NMR spectrum no longer contained the resonances attributed to [Ru(CO)(PPh$_3$){P(CS$_2$Me)Cy}(Tp)], instead showing a doublet (J = 31 Hz) at δ_P 102.8 and singlets at δ_P 43.4, 42.5 and 42.3. Following these observations, the phosphido complex [Ru(CO)(PPh$_3$){P(CS$_2$Me)Cy}(Tp)] was deemed to be unstable and its isolation and characterisation was not pursued further. Instead an investigation into its *in situ* reactivity was conducted.

4.6.5 Methylation of [Ru(CO)(PPh$_3$){P(CS$_2$Me)Cy}(Tp)]

Methylation of [Ru(CO)(PPh$_3$){P(CS$_2$Me)Cy}(Tp)] raises the interesting question of competition between either P or S nucleophilic sites (Scheme 4.28). Addition of MeI to a mixture of [Ru(CO)(PPh$_3$){P(CS$_2$Me)Cy}(Tp)] (generated *in situ* from [Ru(CO)(PPh$_3$){PH(CS$_2$Me)Cy}(Tp)]OTf and KH) resulted in an colour change to orange. Cannula filtration to remove KH and the removal of solvent returned an orange residue which contained four compounds observed by $^{31}P\{^{1}H\}$ NMR spectroscopy. These molecules gave rise to doublets at δ_P 106.1 and 38.9 ($^{2}J_{PP}$ = 31 Hz, 36%), 100.9 and 37.2 ($^{2}J_{PP}$ = 31 Hz, 47%), 60.0

and 29.9 ($^2J_{PP}$ = 26Hz, 7%), and 58.7 and 37.6 ($^2J_{PP}$ = 26 Hz, 10%).[††] None of the resonances displayed any one-bond H coupling in the ^{31}P NMR spectrum, implying the absence of P–H bonds.

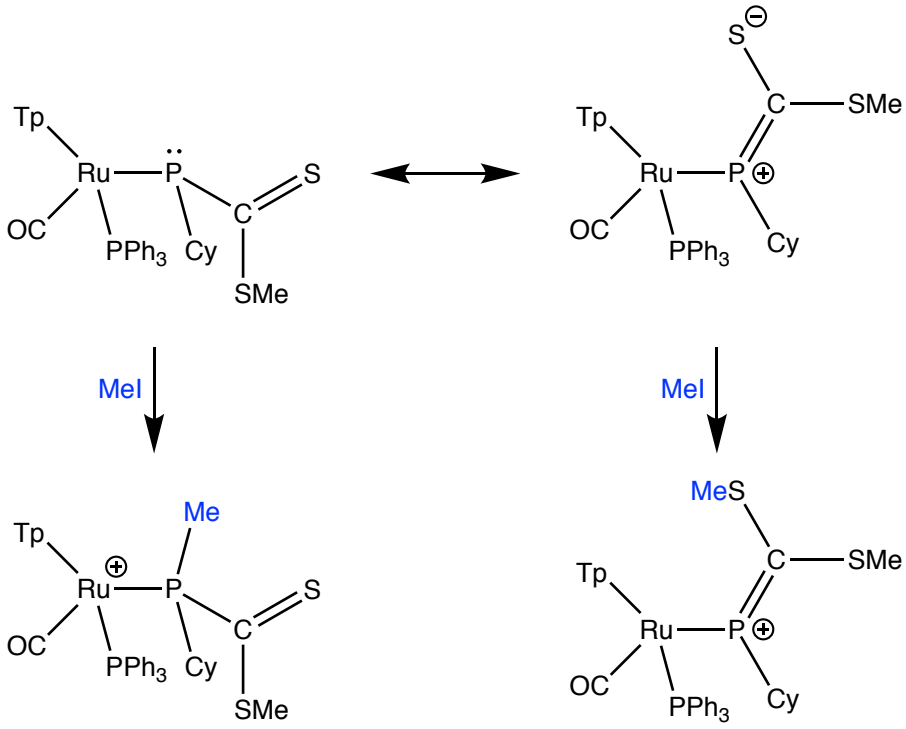

Scheme 4.28. Potential sites of methylation in [Ru(CO)(PPh$_3$){P(CS$_2$Me)Cy}(Tp)]

Further insight was gained *via* a 2D ^{31}P–^{1}H HSQC NMR experiment (Figure 4.11). The four low frequency resonances displayed correlations to ^{1}H nuclei in the aromatic region (not pictured), suggesting that they arise from PPh$_3$ groups. Of the four high frequency resonances, those for the two major products (δ_P 106.1 and 100.9) each showed correlations to two ^{1}H environments. In contrast, those for the minor products (δ_P 60.0 and 58.7) show correlation to only one ^{1}H nucleus. From this information it may be inferred that methylation has occurred at phosphorus in the major product, giving rise to two diastereomers of [Ru(CO)(PPh$_3$){PMe(CS$_2$Me)Cy}(Tp)]$^+$. Thus, the two ^{31}P–^{1}H correlations are to cyclohexyl and methyl groups.

[††] Correlations between resonances were confirmed by a 2D ^{31}P-^{31}P ADEQUATE NMR experiment conducted with the assistance of Mr R. Y. Kong and Prof. G. Otting

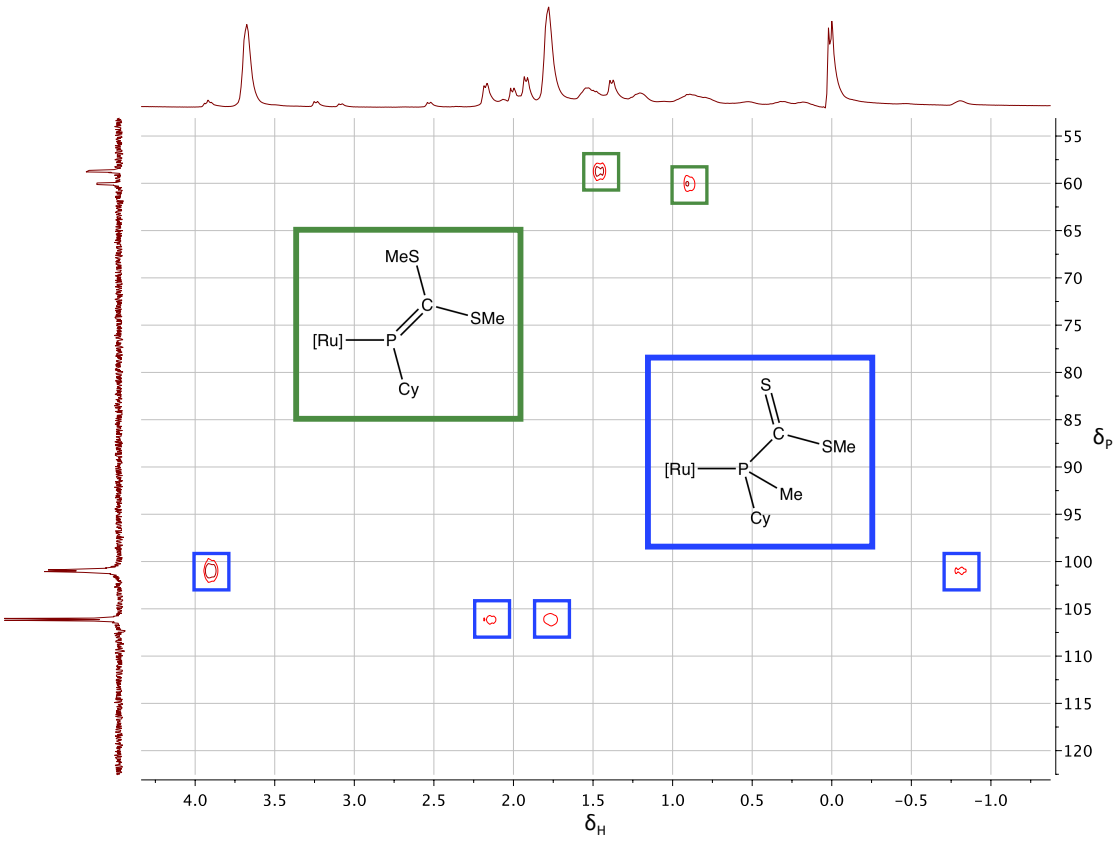

Figure 4.11. 2D $^{31}P–^{1}H$ HSQC NMR spectrum of residue following addition of MeI to [Ru(CO)(PPh$_3$){P(CS$_2$Me)Cy}(Tp)] (proposed assignments are colour-coded)

The identities of the minor products are more uncertain. Significantly, ESI-MS of the mixture showed only isotopic distributions due to [Ru(CO)(PPh$_3$){PMe(CS$_2$Me)Cy}(Tp)]$^+$ and its H$_2$O adduct, suggesting that the minor product is of the same elemental composition as the major product. Consequently, it is postulated that the minor product is [Ru(CO)(PPh$_3$){P(CS$_2$Me$_2$)Cy}(Tp)]$^+$, the result of S-methylation. The presence of two sets of ^{31}P NMR resonances for this product is unusual, however, as there is a single Ru stereocentre within the molecule which would give rise to two NMR-identical enantiomers. A tentative suggestion is that there are two rotamers present, with increased steric bulk from the methyl group and a rigid, planar (π-acidic) phosphorus atom leading to a greatly increased barrier to Ru–P rotation. As discussed in Sections 1.2.2 and 1.2.3, *N*-heterocyclic carbene-stabilised phosphinidenes (NHC=PR) represent a field of intense current study.[66, 110-113, 254-255] As such, comparable complexes of CyP=C(SMe)$_2$ would seem entirely reasonable. Furthermore, the π-acidity of phosphaalkenes R–P=CH^{t}Bu (R = H, Me, AuPPh$_3$) κ^1-*P* bound to ruthenium has been

noted[67, 256] and this retrodonation would contribute an electronic component to any rotation barrier about the Ru−P bond.

Attempts to separate the compounds for further spectroscopic analysis have been unsuccessful so far, as have efforts to obtain X-ray-diffraction-quality crystals. Subsequent studies in this area would focus on these aspects, as well as further expanding on the competing P *versus* S reactivity.

4.7 Summary and Future Work

The deprotonation of [Ru(CO)(PPh_3)(PH_2Cy)(Tp)]OTf with DBU, KH or ^{n}BuLi yielded the primary phosphido complex [Ru(CO)(PPh_3)(PHCy)(Tp)], with no further deprotonation to form a phosphinidene-type complex occurring. While the complex could not be directly isolated, it could be cleanly generated *in situ* for further studies. [Ru(CO)(PPh_3)(PHCy)(Tp)] was obtained as a mixture of diastereomers, on account of its stereogenic Ru and P centres. These diastereomers interchange *via* phosphorus inversion with a measured barrier of $\Delta G^{\ddagger}$ = 84.9(9) kJ mol^{-1}, higher than other reported primary phosphido complexes but in good agreement with the calculated barrier for [Fe(PMe_2)$(CO)_2$(Cp)]. A dynamic process involving restricted Ru−P bond rotation was also observed at low temperatures, with a measured barrier of $\Delta G^{\ddagger}$ = 45.2 kJ mol^{-1}.

The reactivity of [Ru(CO)(PPh_3)(PHCy)(Tp)], generated *in situ*, with a variety of electrophiles was explored. In the reaction with MeI, [Ru(CO)(PPh_3)(PHCy)(Tp)] produced two diastereomers of the expected product [Ru(CO)(PPh_3)(PHMeCy)(Tp)]OTf as well as small amounts of [Ru(CO)(PPh_3)(PMe_2Cy)(Tp)]OTf. These compounds could not be separated, but [Ru(CO)(PPh_3)(PMe_2Cy)(Tp)]OTf could be directly synthesised *via* two different methods.

Addition of $BH_3{\cdot}SMe_2$ to [Ru(CO)(PPh_3)(PHCy)(Tp)] yielded [Ru(CO)(PPh_3){PH(BH_3)Cy}(Tp)] which could also be synthesised from [Ru(CO)(PPh_3)(PH_2Cy)(Tp)]OTf and $NaBH_4$. While it was postulated that coordination to a Lewis Acid may make the P−H bond more acidic, no deprotonation with KH or ^{n}BuLi was observed. The reaction with $[CPh_3]PF_6$ resulted in the breaking of the Lewis Pair and reformation of [Ru(CO)(PPh_3)(PH_2Cy)(Tp)]$^+$. It is expected that

the first step of this process involves hydridic reactivity of the BH_3 group, something that may be explored further in the future. Attempts to remove the BH_3 group with amines to return the free phosphido complex were unsuccessful, indicating a remarkably strong P−B bond.

The complex [Ru(CO)(PPh_3)(PHCy)(Tp)] reversibly forms the adduct [Ru(CO)(PPh_3){PH(CS_2)Cy}(Tp)] upon addition of CS_2. The reversibility is arrested by the addition of MeI, with methylation occuring regioselectively at sulfur to give the cationic complex [Ru(CO)(PPh_3){PH(CS_2Me)Cy}(Tp)]OTf. Deprotonation of the salt [Ru(CO)(PPh_3){PH(CS_2Me)Cy}(Tp)]OTf led to the formation of [Ru(CO)(PPh_3){P(CS_2Me)Cy}(Tp)] which was observed by IR and $^{31}P\{^1H\}$ NMR spectroscopy. Methylation of this thioester-substituted phosphido complex appeared to result in a mixture of P-methylated and S-methylated products, an interesting occurrence of dichotomous reactivity. The nature of this dichotomy provides a potentially interesting avenue for future investigations.

CHAPTER 5
Phosphine Chalcogenide Complexes Derived From [Ru(CO)(PPh$_3$)(PHCy)(Tp)]

Chapter 5: Phosphine Chalcogenide Complexes Derived From [Ru(CO)(PPh$_3$)(PHCy)(Tp)]

5.1 Introduction

Compounds which contain phosphorus−chalcogen bonds are ubiquitous throughout synthetic chemistry. While providing interesting chemistry in their own right they have also found diverse applications such as organic reagents, pesticides, lubricant and plastic additives, and precursors for thin film and quantum dot growth.[257] In these compounds, the phosphorus-chalcogen bond strength decreases down the group in the order O > S > Se > Te. It is this trend that underpins the synthetic utility of Lawesson[258] and Woollins[259] reagents, $Ar_2P_2E_n$ (Ar = 4-C_6H_4OMe, Ph; E = S, Se; n = 2, 3) in oxygen-chalcogen exchange processes. It also explains why, at least historically, similarly effective tellurium-based reagents have yet to emerge, providing a challenge for the future. The decreasing bond strength gives rise to a decrease in thermal and hydrolytic stability. Consequently, the number of known compounds featuring a phosphorus-chalcogen bond decreases for the heavier chalcogens.

Phosphine chalcogenides (Figure 5.1a) and their role as ligands are of specific interest to this chapter. Tertiary phosphine chalcogenides bind to metals *via* the chalcogen atom, which provide the only lone pairs available for bonding.[257] Such coordination may occur in either monodentate (Figure 5.1b) or bridging (Figure 5.1c) fashion.

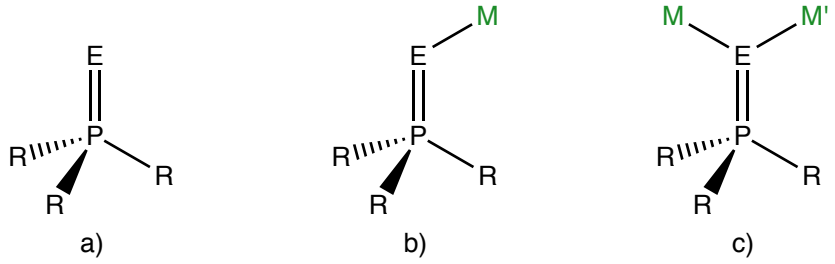

Figure 5.1. Tertiary phosphine chalcogenides and their metal coordination modes

More interesting are less substituted phosphine chalcogenides, for which tautomerisation (Figure 5.2a, b) allows for two possible binding modes.[260] These modes involve coordination *via* the chalcogen atom (similar to tertiary phosphine chalcogenides, Figure 5.2c) or, alternatively, through phosphorus in the chalcogenophosphinous acid tautomeric form (Figure 5.2d). For secondary phosphine sulfides, coordination through phosphorus is

generally preferred whereas chalcogen coordination is the more common mode for secondary phosphine selenides.[257] Phosphorus-bound phosphine selenide complexes are often unstable with respect to extrusion of elemental selenium.[257]

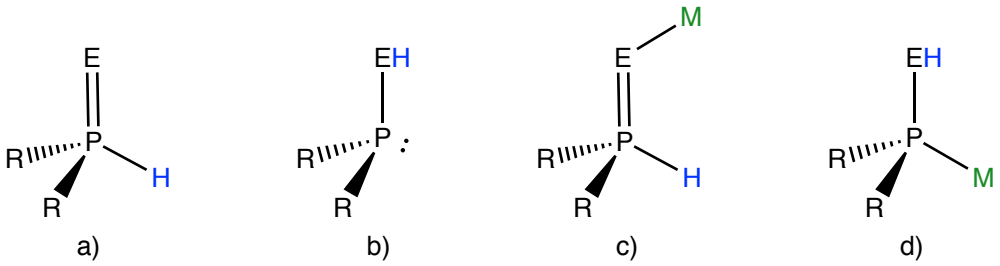

Figure 5.2. Tautomers and coordination modes of less substituted phosphine chalcogenides

Deprotonation of lower-substituted phosphine chalcogenides further increases the range of potential binding modes. Similar to tautomerisation in secondary phosphine chalcogenides, the resonance forms of the chalcogenophosphinite anion (Figure 5.3a, b) explain either phosphorus (Figure 5.3c) or chalcogen (Figure 5.3d) coordination. The more common of the two modes is phosphorus coordination, and this form is what is observed throughout this chapter. Other interesting coordination modes exploit the two possible coordination modes of the chalcogenophosphinite anion, including a *dihapto* mode (3 valence electron donation, Figure 5.3e) and the possibility of bridging two similar or, indeed, disparate metal centres (Figure 5.3f).[257, 260]

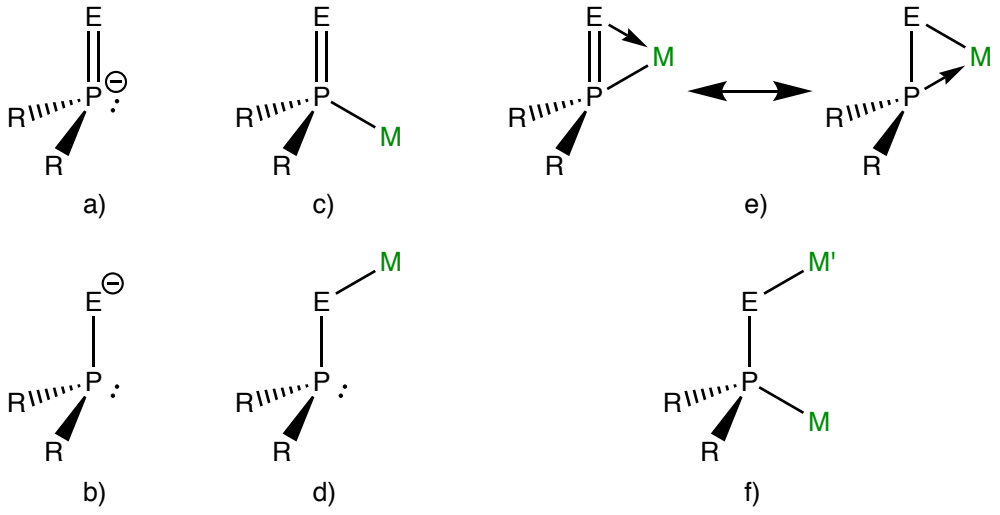

Figure 5.3. Resonance forms and coordination modes of the chalcogenophosphinite anion

The reaction of terminal phosphido complexes with chalcogen sources generally results in complexes bearing the P-bound chalcogenophosphinite ligand (Figure 5.3c). As discussed in Section 1.2.1, this approach was first demonstrated by Dobbie with the phosphido complex

$[Fe(CO)_2\{P(CF_3)_2\}(Cp)]$ (Scheme 5.1).[68] Addition of chalcogen sources to this phosphido complex resulted in the formation of the phosphine chalcogenide complexes $[Fe(CO)_2\{P(E)(CF_3)_2\}(Cp)]$ (E = O, S, Se). Subsequent studies by Malisch,[87, 181, 207, 261-262] Roper,[77, 263-264] Gladysz[83] and Morris[265] have all yielded similar phosphine chalcogenide complexes.

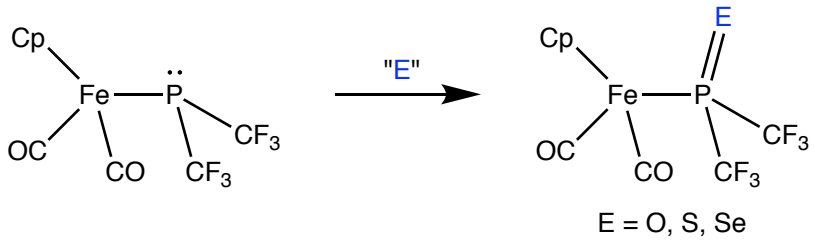

Scheme 5.1. Reaction of $[Fe(CO)_2\{P(CF_3)_2\}(Cp)]$ with chalcogen sources

In cases where there is a vacant coordination site at the metal a *dihapto* coordination is adopted (Scheme 5.2). Malisch demonstrated this reactivity with the complexes $[W(CO)_2(P^tBu_2)(Cp)]$ and $[Fe(CO)(PMes_2)(Cp)]$, which respectively form the complexes $[W(CO)_2(\eta^2\text{-}P,E\text{-}EP^tBu_2)(Cp)]$ and $[Fe(CO)(\eta^2\text{-}P,E\text{-}EPMes_2)(Cp)]$ (E = S, Se) when treated with elemental sulfur or selenium.[266-267] The *dihapto* coordination mode may also be accessed by generating a vacant coordination site after the formation of the phosphine chalcogenide. This was the case for the cations $[Os(CO)_2(PPh_3)_2(\eta^2\text{-}P,E\text{-}EPH_2)]^+$ (E = S, Se), which were respectively obtained from $[Os(OAc)(CO)_2(PPh_3)_2\{PH_2(E)\}]$ (E = S, Se) following removal of the acetate ligand by protonation.[263-264]

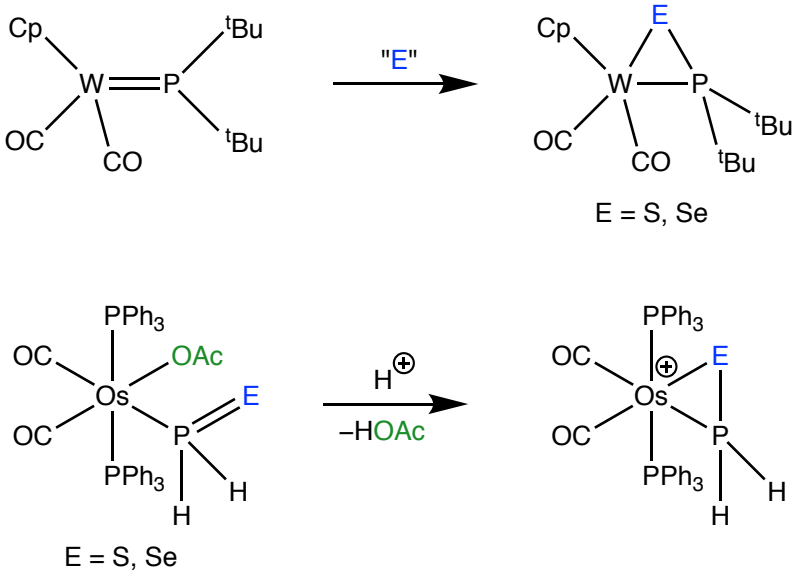

Scheme 5.2. Formation of η^2 phosphine chalcogenide complexes

Excluding the examples involving oxygen discussed in Section 3.5, complexes containing a phosphorus atom bonded to a metal, a chalcogen and a hydrogen atom remain rare.[77, 172, 180, 263-264, 268-279] Of these limited examples, studies which have explicitly explored reactions with the P–H bond are even fewer. The aforementioned cations $[Os(CO)_2(PPh_3)_2(\eta^2\text{-}P,E\text{-}EPH_2)]^+$ (E = S, Se) may be reversibly deprotonated to form $[Os(CO)_2(PPh_3)_2(\eta^2\text{-}P,E\text{-}EPH)]$ (E = S, Se) which contain the unusual thioxophosphane (S=PH) and selenoxophosphane (Se=PH) ligands, respectively. These ligands could be methylated at phosphorus to produce the cations $[Os(CO)_2(PPh_3)_2(\eta^2\text{-}P,E\text{-}EPHMe)]^+$ (E = S, Se) and the sulfur-containing product could be deprotonated to form $[Os(CO)_2(PPh_3)_2(\eta^2\text{-}P,S\text{-}SPMe)]$. Curiously, the S=PMe ligand has a profound impact on the lability of its co-ligands and protonation yields the isomer of $[Os(CO)_2(PPh_3)_2(\eta^2\text{-}P,S\text{-}SPHMe)]^+$ containing *cis* PPh_3 and CO ligands. In contrast, methylation gives $[Os(CO)_2(PPh_3)_2(\eta^2\text{-}P,S\text{-}SPMe_2)]^+$ which has *trans*-disposed PPh_3 ligands. Importantly, the dimethylated product is the result of functionalising both P–H bonds in the parent cation, $[Os(CO)_2(PPh_3)_2(\eta^2\text{-}P,S\text{-}SPH_2)]^+$ (Scheme 5.3).[264]

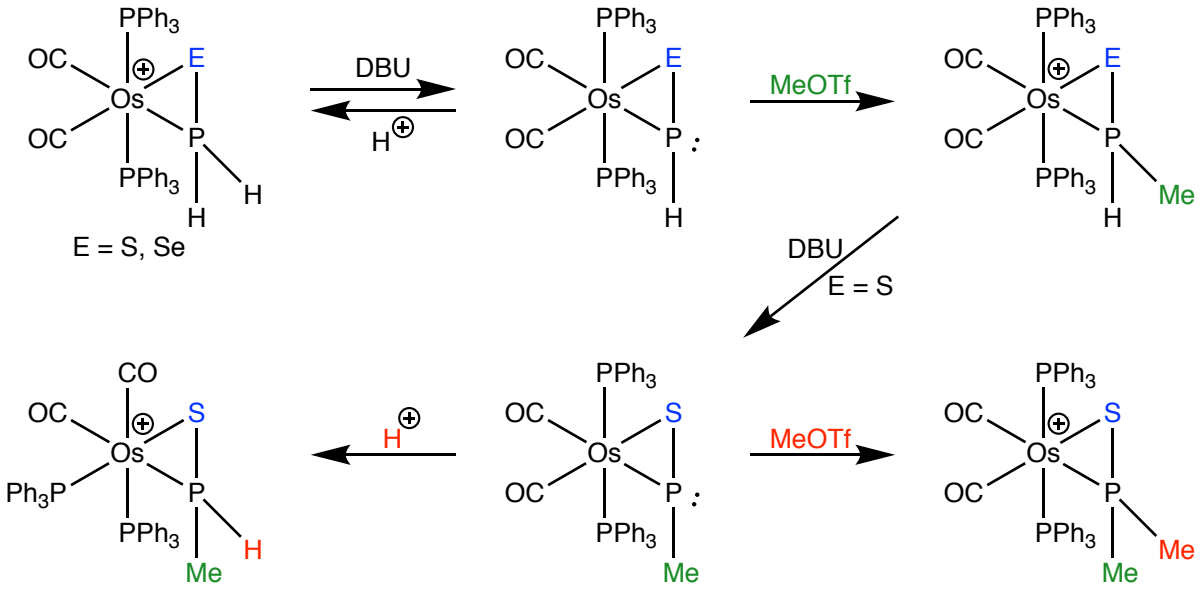

Scheme 5.3. Reactivity of $[Os(CO)_2(PPh_3)_2(\eta^2\text{-}P,E\text{-}EPH_2)]^+$ (E = S, Se)

Malisch conducted the only other investigation which illustrated the functionality of the P–H bond in phosphine chalcogenide complexes (Scheme 5.4).[272] The P–H bond in $[W(CO)_2(\eta^2\text{-}P,S\text{-}SPH^tBu)(Cp)]$ was converted to a P–Cl bond with CCl_4, resulting in the formation of $[W(CO)_2(\eta^2\text{-}P,S\text{-}SPCl^tBu)(Cp)]$. Additionally, the selenium analogue $[W(CO)_2(\eta^2\text{-}P,Se\text{-}SePH^tBu)(Cp)]$ reacted with ethyldiazoacetate to form $[W(CO)_2\{\eta^2\text{-}P,Se\text{-}$

SeP^{t}Bu(N$_2$CH$_2$CO$_2$Et)}(Cp)], the product of P−H insertion. A subsequent 1,3-hydrogen shift occurs, resulting in [W(CO)$_2${η^2-*P,Se*-SeP^{t}Bu(NH−N=CHCO$_2$Et)}(Cp)].

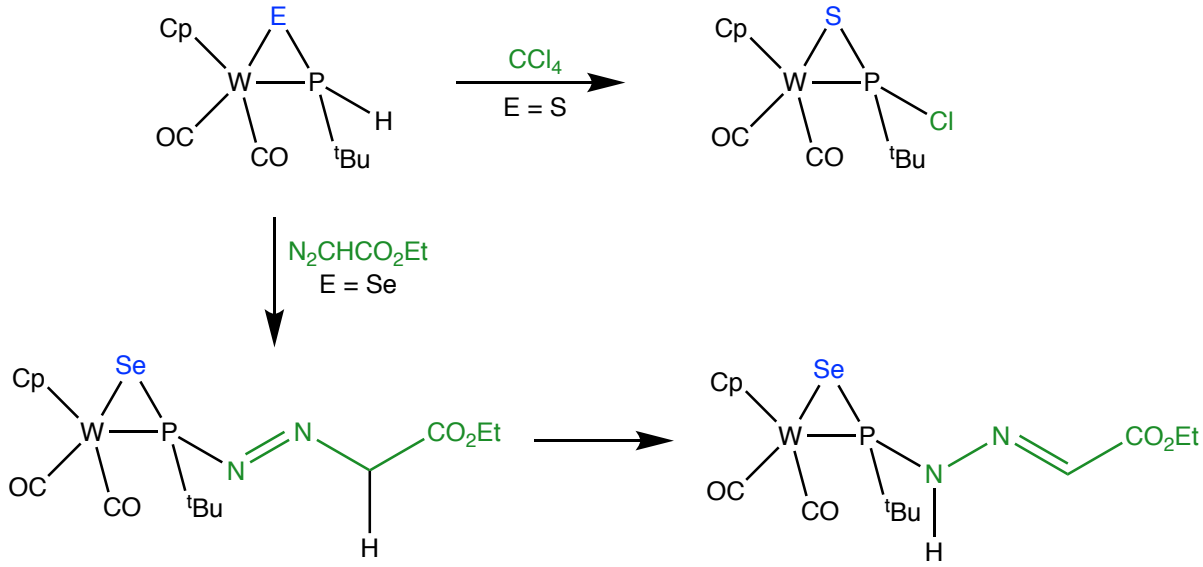

Scheme 5.4. P−H reactivity of [W(CO)$_2$(η^2-P,E-EPH^{t}Bu)(Cp)] (E = S, Se)

Considering the relative scarcity of complexes containing a phosphorus atom bonded to a metal, a chalcogen and a hydrogen atom, the work described in this chapter aims to synthesise complexes containing this unusual bonding motif. The reactivity of these complexes will be further investigated, with a key goal to map the functionality of the P−H bond. There is currently a dearth of studies in this area, and it has the potential to yield unique phosphorus-based connectivities.

5.2 Synthesis of Chalcogenide Complexes

5.2.1 Synthesis of [Ru(CO)(PPh$_3$){PH(O)Cy}(Tp)]

As mentioned in Section 4.1, attempts to obtain crystals of [Ru(CO)(PPh$_3$)(PHCy)(Tp)] instead yielded the oxidised product [Ru(CO)(PPh$_3$){PH(O)Cy}(Tp)]. The molecular structure of [Ru(CO)(PPh$_3$){PH(O)Cy}(Tp)] is shown in Figure 5.4. The formation of a P=O bond is clear and the P−O distance of 1.516(4) Å sits within the range expected for a double bond.[197] Interestingly, the PH(O)Cy ligand exhibits a notable *trans* influence compared to its PPh$_3$ and CO co-ligands; the Ru−N(pyrazolyl) bond lengths are 2.214(4) (Ru1−N51; *trans* to PH(O)Cy), 2.142(5) (Ru1−N61; *trans* to PPh$_3$; >14 e.s.d. difference) and 2.144(4) Å (Ru1−N71; *trans* to CO; >17 e.s.d. difference). Although free rotation about the Ru1−P1 bond is to be expected in

solution, in the solid state the adopted conformation places the bulky cyclohexyl group between two of the pyrazolyl groups to minimise inter-ligand non-bonding interactions. Otherwise, the remaining structural features are unremarkable.

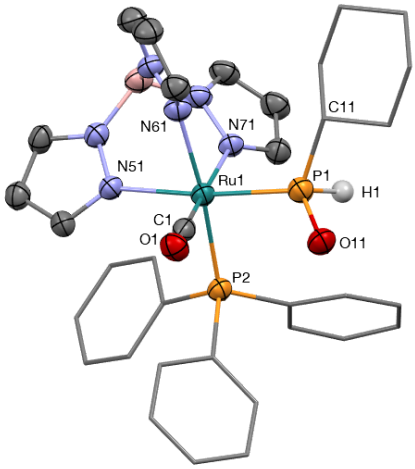

Figure 5.4. Molecular structure of S_{Ru},S_P-[Ru(CO)(PPh$_3$){PH(O)Cy}(Tp)] in a crystal (50% displacement ellipsoids, most H atoms omitted, phenyl and cyclohexyl rings simplified). Selected bond lengths (Å) and angles (°): Ru1–P1 2.3111(15), Ru1–P2 2.3679(14), Ru1–N51 2.214(4), Ru1–N61 2.142(5), Ru1–N71 2.144(4), Ru1–C1 1.850(6), P1–O11 1.516(4), P1–H1 1.37(7), P1–C11 1.832(6), O1–C1 1.148(7), P1–Ru1–P2 92.42(5), P1–Ru1–C1 85.61(16), P2–Ru1–C1 92.45(16). Molecule crystallised in the centrosymmetric R*–3 space group – enantiomer, but not diastereomers, present in unit cell.*

Prompted by the adventitious isolation of its single crystals, attempts were made to directly and intentionally synthesise [Ru(CO)(PPh$_3$){PH(O)Cy}(Tp)] *via* the oxidation of [Ru(CO)(PPh$_3$)(PHCy)(Tp)]. Given the water-sensitivity of [Ru(CO)(PPh$_3$)(PHCy)(Tp)], common oxidising agents which are commercially available as aqueous solutions such as H_2O_2 and *meta*-chloroperoxybenzoic acid were unsuitable. As such, iodosobenzene was chosen as the oxidising agent. This reagent has previously been used to successfully oxidise the phosphido complexes [Re(NO)(PPh$_3$)(PR$_2$)(Cp)] (R = Ph, ^{t}Bu) to the phosphorus oxides [Re(NO)(PPh$_3$){P(O)R$_2$}(Cp)] (R = Ph, ^{t}Bu).[83]

After 16 hours stirring at room temperature, the consumption of solid PhIO was observed in a mixture of [Ru(CO)(PPh$_3$)(PHCy)(Tp)] and PhIO in THF. The IR spectrum of the mixture included a ν_{CO} band at 1973 cm^{-1} as well as a shoulder at 1949 cm^{-1}, at higher frequency than the precursor phosphido complex (1931cm^{-1}). An aliquot taken for NMR spectroscopy contained four ^{31}P{^{1}H} NMR doublets at δ_P 97.0, 90.4, 46.8 and 44.4 ($^2J_{PP}$ = 32 Hz) as well as singlets at δ_P 43.8 and 25.2. The four doublets likely arise from two diastereomers of the

desired product [Ru(CO)(PPh$_3$){PH(O)Cy}(Tp)] (Scheme 5.5) while the resonance at δ_P 25.2 conceivably arises from the presence of O=PPh$_3$ (δ_P 26.1 in benzene, 24.9 in CCl_4).[280] The signal-to-noise ratio in the (non-^{1}H decoupled) ^{31}P NMR spectrum was too poor to obtain satisfactory data.

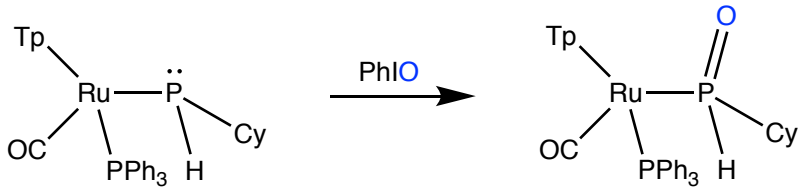

Scheme 5.5. Oxidation of [Ru(CO)(PPh$_3$)(PHCy)(Tp)] with iodosobenzene

In an attempt to work up the reaction, volatiles were removed *in vacuo* and the residue dissolved in toluene and filtered through diatomaceous earth to remove ionic by-products. Removal of toluene from the filtrate yielded a residue for which the ^{31}P{^{1}H} NMR spectrum contained the aforementioned resonances as well singlets at δ_P −5.3 (PPh$_3$) and 30.2 and doublets at δ_P 119.8 and 44.9 ($^2J_{PP}$ = 36 Hz). Importantly, the resonances at δ_P 97.0 and 90.4 were doublets in the ^{31}P NMR spectrum with $^1J_{PH}$ = 337 and 345 Hz, respectively. The appearance and $^1J_{PH}$ of these signals are consistent with PH(O)Cy groups. Thus, the two diastereomers of [Ru(CO)(PPh$_3$){PH(O)Cy}(Tp)] comprised 27% (δ_P 97.0) and 33% (δ_P 90.4) of the mixture, as estimated by ^{31}P{^{1}H} NMR spectroscopy. The presence of these diastereomers within the mixture was further confirmed by the presence of an $[M + H]^+$ isotopic distribution in the ESI-MS of the mixture.

Recrystallisation of the residue to yield [Ru(CO)(PPh$_3$){PH(O)Cy}(Tp)] has been unsuccessful so far. No precipitate formed upon addition of Et_2O to a concentrated CH_2Cl_2 solution of the residue. Concentration of a CH_2Cl_2/MeOH solution of the residue on a rotary evaporator similarly failed to yield any precipitate. Following the same process with CH_2Cl_2 and *n*-hexane as the solvents returned an oil which could be separated from the supernatant. However, aside from the absence of PPh$_3$, the ratio of products remained unchanged in this oil.

A major impediment to the isolation of [Ru(CO)(PPh$_3$){PH(O)Cy}(Tp)] may be its low purity from the reaction mixture. Even accounting both diastereomers together the desired product comprises 60% of the crude reaction mixture, immediately compromising the prospects of

fractional recrystallisation (including *via* the same method used to obtain the X-ray-quality single crystal: vapour diffusion of *n*-pentane into a toluene soution over 71 days). A more astute approach may be to further refine the reaction conditions or to investigate alternative oxidation reagents, although exhaustively exploring all possibilities may still prove unsuccessful.

5.2.2 Synthesis of [Ru(CO)(PPh$_3$){PH(S)Cy}(Tp)]

Addition of elemental sulfur to a solution of [Ru(CO)(PPh$_3$)(PHCy)(Tp)] resulted in the formation of [Ru(CO)(PPh$_3$){PH(S)Cy}(Tp)] (Scheme 5.6). Following workup and recrystallisation the product was isolated as a colourless solid in 59% yield.

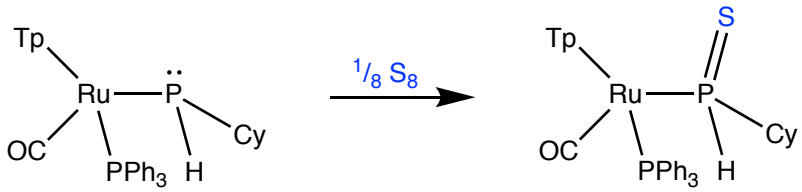

Scheme 5.6. Reaction of [Ru(CO)(PPh$_3$)(PHCy)(Tp)] with elemental sulfur

The IR spectrum (THF) of the compound contained a ν_{CO} band at 1989 cm^{-1}, consistent with oxidation at phosphorus and reduced electron density at the Ru centre. The retention of the P–H bond could also be confirmed *via* a ν_{PH} band at 2234 cm^{-1}.

Oxidation by sulfur results in a shift to higher frequency of the PHCy $^{31}P\{^1H\}$ NMR resonance to δ_P 51.2. This resonance is a doublet as a result of coupling to the PPh$_3$ resonance at δ_P 42.2 ($^2J_{PP}$ = 28Hz). Additionally, the PHCy resonance appears as a doublet in the ^{31}P NMR spectrum with a $^1J_{PH}$ of 337 Hz in accordance with the presence of one P–H bond.

The ^1H NMR spectrum of the product contained all of the resonances expected for phenyl, Tp and cyclohexyl groups. In addition, the P–H hydrogen atom was observed as a doublet of doublet of doublets, displaying strong one-bond coupling to phosphorus (343 Hz) as well as three-bond coupling constants to phosphorus and hydrogen (8 Hz and 6 Hz respectively). The two different ^3J were assigned based on a 1D $^1H\{^{31}P\}$ NMR experiment.

In the $^{13}C\{^1H\}$ NMR spectrum the carbonyl resonance appeared as a doublet of doublets at δ_C 202.2, with equivalent *cis* $^2J_{PC}$ of 13 Hz to the PPh_3 and PH(S)Cy nuclei. Six distinct resonances are also observed for the cyclohexyl ring, indicative of the asymmetry of the molecule both at phosphorus and at ruthenium; the 2, 3, 4 and 5 positions of the ring are all chemically inequivalent.

A minor stereoisomer is also observed during syntheses of [Ru(CO)(PPh_3){PH(S)Cy}(Tp)]. The minor isomer gives rise to an IR ν_{CO} band at 1956 cm^{-1} as well as $^{31}P\{^1H\}$ NMR doublets at δ_P 56.0 and 42.9 ($^2J_{PP}$ = 26 Hz). The former resonance is due to the PH(S)Cy group, appearing in the ^{31}P NMR spectrum as a doublet with $^1J_{PH}$ = 351 Hz. Samples typically comprised <10% of this minor isomer.

The characterisation of [Ru(CO)(PPh_3){PH(S)Cy}(Tp)] included an X-ray crystallographic analysis, and the results are summarised in Figure 5.5. The formation of the P=S bond is immediately apparent and the P−S distance of 2.0183(16) Å is in good agreement with the P−S bond length of 2.011(2) Å reported for [Ru(PPh_3)$_2${PH_2(S)}(Cp)].[276] The P−H H atom was located in the Fourier difference map, confirming the formation of the PH(S)Cy ligand. Similarly to [Ru(CO)(PPh_3){PH(O)Cy}(Tp)], the PH(S)Cy ligand exhibits a greater *trans* influence than its co-ligands; the Ru−N51 (*trans*-PH(S)Cy) length of 2.176(4) Å is longer than both the Ru−N61 (*trans*-PPh_3) distance of 2.134(4) Å (>10 e.s.d.) and the Ru−N71 (*trans*-CO) length of 2.149(4) Å (>6 e.s.d.). These differences are less pronounced than observed for [Ru(CO)(PPh_3){PH(O)Cy}(Tp)].

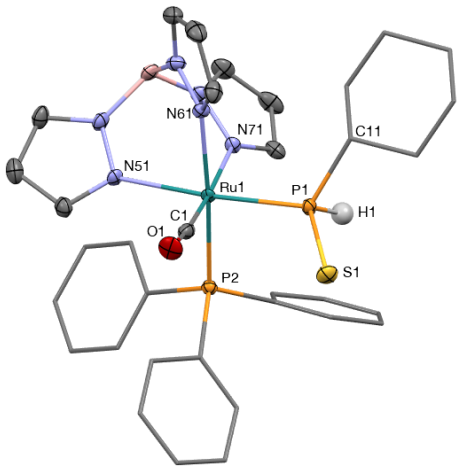

Figure 5.5. Molecular structure of S_{Ru},S_P-[Ru(CO)(PPh$_3$){PH(S)Cy}(Tp)] in a crystal of [Ru(CO)(PPh$_3$){PH(S)Cy}(Tp)].2(CH$_4$O) (50% displacement ellipsoids, MeOH solvent molecules and most H atoms omitted , phenyl and cyclohexyl rings simplified). Selected bond lengths (Å) and angles (°): Ru1−P1 2.3317(11), Ru1−P2 2.3691(11), Ru1−N51 2.176(4), Ru1−N61 2.134(4), Ru1−N71 2.149(4), Ru1−C1 1.843(5), S1−P1 2.0183(16), P1−H1 1.33(8), P1−C11 1.858(5), O1−C1 1.149(6), P1−Ru1−P2 91.86(2), P1−Ru1−C1 89.04(14), P2−Ru1−C1 94.31(14). Molecule crystallised in the centrosymmetric Pbca *space group – enantiomer, but not diastereomers, present in unit cell.*

The formation of the P=S bond in [Ru(CO)(PPh$_3$){PH(S)Cy}(Tp)] results in reduced electron density at the phosphorus atom, potentially acidifying the P−H bond. However, no reaction was observed between [Ru(CO)(PPh$_3$){PH(S)Cy}(Tp)] and DBU or ^{n}BuLi (Scheme 5.7).

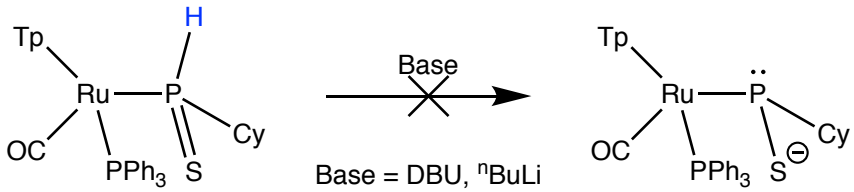

Scheme 5.7. Attempted deprotonation of [Ru(CO)(PPh$_3$){PH(S)Cy}(Tp)]

5.2.3 Synthesis of [Ru(CO)(PPh$_3$){PH(Se)Cy}(Tp)]

Following the successful synthesis of [Ru(CO)(PPh$_3$){PH(S)Cy}(Tp)], the approach was extended further down Group 16 to selenium. Addition of elemental selenium to a THF solution of [Ru(CO)(PPh$_3$)(PHCy)(Tp)] resulted in the decolourisation of the mixture to pale yellow as well as the disappearance of the insoluble dark solid selenium. The IR spectrum of the solution contained two ν_{CO} bands at 1993 (very strong) and 1960 cm^{-1} (medium). The ν_{BH} and ν_{PH} absorptions appeared at 2487 and 2250 cm^{-1}, respectively.

After the removal of solvent, the major compound (*ca*. 85%) was identified as [Ru(CO)(PPh$_3$){PH(Se)Cy}(Tp)] (Scheme 5.8) by $^{31}P\{^1H\}$ NMR spectroscopy. This complex gave rise to two doublet resonances at δ_P 41.1 and 19.9 with the $^2J_{PP}$ of 28 Hz consistent with the *cis*-disposed phosphorus atoms. The latter resonance appeared as a doublet ($^1J_{PH}$ = 335 Hz) in the ^{31}P NMR spectrum as a result of the single P−H bond. Additionally, this resonance also displayed ^{77}Se satellites (I = ½, 7.6% natural abundance, $^1J_{Pse}$ = 497 Hz), confirming the formation of a phosphorus-selenium bond (Figure 5.6, *purple*). Although the $^1J_{PSe}$ is significantly lower than that reported for [Fe(CO)$_2${P(Se)(O^{i}Pr)$_2$}(Cp)] (712.9 Hz),[281] it is in good agreement with the coupling constant reported for [OsCl(CO)$_2$(PPh$_3$)$_2${PH$_2$(Se)}] (517 Hz).[264]

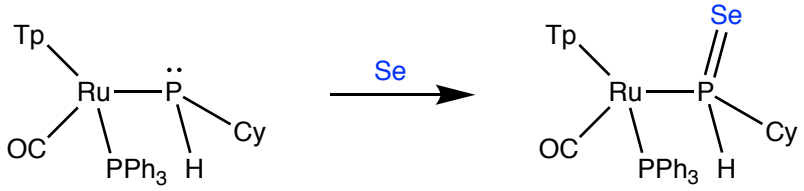

Scheme 5.8. Reaction of [Ru(CO)(PPh$_3$)(PHCy)(Tp)] with elemental selenium

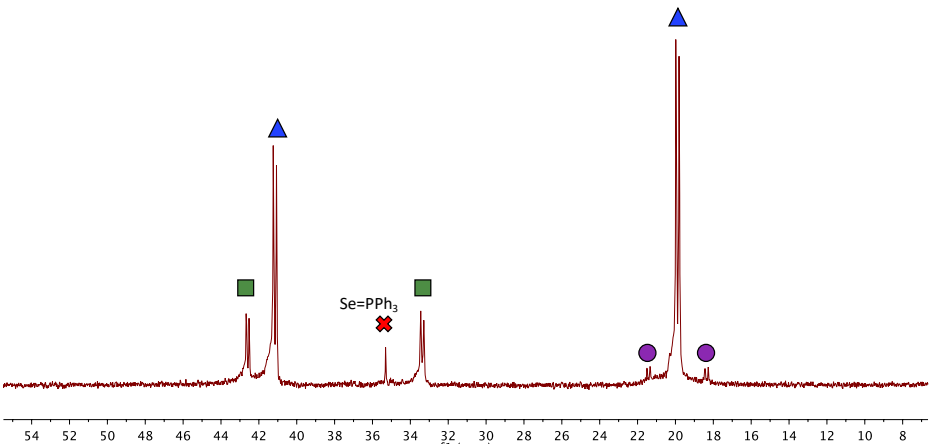

Figure 5.6. $^{31}P\{^1H\}$ NMR spectrum of [Ru(CO)(PPh$_3$){PH(Se)Cy}(Tp)] (blue), showing minor diastereomer (green) and ^{77}Se satellites (purple)

In addition to the major product, a number of minor products were observed in the crude $^{31}P\{^1H\}$ NMR spectrum of the reaction mixture. In particular, one complex comprising *ca*. 10% of the entire mixture gave rise to mutually coupled doublet resonances (Figure 5.6, *green*) at δ_P 42.6 and 33.4 ($^2J_{PP}$ = 24 Hz). The latter resonance (P−H) displayed coupling ($^1J_{PH}$ = 357 Hz) in the ^{31}P NMR spectrum. The minor product would appear to be a diastereomer of the major product, [Ru(CO)(PPh$_3$){PH(Se)Cy}(Tp)], and likely also gives rise to the ν_{CO} band observed at

1960 cm^{-1}. Upon recrystallisation, the proportion of the minor diastereomer was reduced to <5% and no further investigations into its identity were conducted.

The ^{1}H and ^{13}C{^{1}H} NMR data were unremarkable and contained the expected resonances for the Tp, CO and PHCy groups. While ^{77}Se satellites are expected for the P–H resonance (δ_H 4.48, splitting of $^{2}J_{SeH}$ expected), they could not be unequivocally identified in the baseline of the ^{1}H NMR spectrum.

While [Ru(CO)(PPh$_3$){PH(S)Cy}(Tp)] is stable in the solid state over several months, partial decomposition of solid [Ru(CO)(PPh$_3$){PH(Se)Cy}(Tp)] was noted after 2 weeks in air. Complete decomposition was observed after 5 weeks. No compounds were detected by ^{31}P NMR spectroscopy. Secondary phosphine selenides are unstable due to the ready separation of elemental selenium,[260] and this is the most likely decomposition pathway for [Ru(CO)(PPh$_3$){PH(Se)Cy}(Tp)]. Theoretically, this should result in the formation of either [Ru(CO)(PPh$_3$)(PHCy)(Tp)] or, if exposed to water, [Ru(CO)(PPh$_3$)(PH$_2$Cy)(Tp)]$^{+}$. However, given the absence of ^{31}P NMR resonances the fate of these phosphorus-containing fragments remains unknown.

5.2.4 Synthesis of [Ru(CO)(PPh$_3$){PH(Te)Cy}(Tp)]

Tellurium was the final chalcogen for which addition to the phosphido complex was investigated. Following the addition of elemental Te to a solution of [Ru(CO)(PPh$_3$)(PHCy)(Tp)], the formation of a grey solid was observed after 1 hour. The two ν_{CO} bands at 1994 cm^{-1} and 1936 cm^{-1} in the IR spectrum of the supernatant solution were at higher frequency than [Ru(CO)(PPh$_3$)(PHCy)(Tp)] (ν_{CO} 1931 cm^{-1}) which is consistent with previous observations upon chalcogen addition.

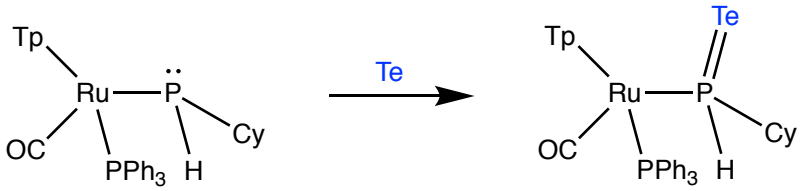

Scheme 5.9. Reaction of [Ru(CO)(PPh$_3$)(PHCy)(Tp)] with elemental tellurium

The ^{31}P NMR data provided more evidence for the formation of [Ru(CO)(PPh$_3$){PH(Te)Cy}(Tp)]. In the ^{31}P{^{1}H} NMR spectrum, the major product gave rise to doublets at δ_P 39.7 and −61.9 ($^2J_{PP}$ = 25 Hz). The low frequency resonance is due to the PH(Te)Cy group, and appears as a P−H doublet ($^1J_{PH}$ = 317 Hz) in the ^{31}P NMR spectrum. No satellites due to the *I* = ½ nuclei ^{123}Te (0.89% abundance) or ^{125}Te (7.07% abundance) were observed, likely as a result of a low signal-to-noise ratio.

The complex [Ru(CO)(PPh$_3$){PH(Te)Cy}(Tp)] is unstable, and it decomposed during the attempted workup. Volatiles were removed from the reaction mixture *in vacuo*, toluene added to the resultant residue and the orange supernatant obtained *via* cannula filtration. An orange residue was obtained following the removal of solvent from the filtrate, of which the ^{31}P{^{1}H} NMR spectrum contained more than 8 resonances. Two of these at δ_P 39.1 and −61.9 could be attributed to [Ru(CO)(PPh$_3$){PH(Te)Cy}(Tp)]. The other major products were PPh$_3$ and two broad resonances at δ_P 120.3 and 48.0. At this stage, it was estimated that approximately 50% of the sample had decomposed. Complete decomposition was observed after 24 hours, and the resonances observed in the ^{31}P{^{1}H} NMR spectrum were for PPh$_3$ as well as the two resonances at δ_P 120.3 and 48.0 previously mentioned. The latter two resonances could not be identified, and it is not clear if they are coupled or due to separate compounds – no correlation was observed in the 2D ^{31}P–^{31}P ADEQUATE NMR experiment.

There are a few possibilities for the decomposition of [Ru(CO)(PPh$_3$){PH(Te)Cy}(Tp)] and some which can be excluded, such as the reversible extrusion of tellurium to regenerate [Ru(CO)(PPh$_3$)(PHCy)(Tp)] or [Ru(CO)(PPh$_3$)(PH$_2$Cy)(Tp)]$^+$. As discussed in Section 5.1, phosphorus-chalcogen bonds decrease in stability going down the group and P−Te bonds are often unstable with respect to dismutation to form Te−Te and P−P products.[282] Given the presence of free PPh$_3$ after decomposition, another possibility is the displacement of PPh$_3$ to form an η^2-*P,Te* complex (Scheme 5.10). Such a rearrangement would be the first observation of labile co-ligands for this complex (see Sections 4.2 and 4.6.2).

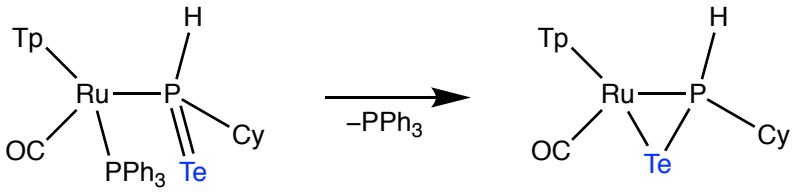

Scheme 5.10. Potential η^2 coordination of phosphine telluride

5.2.5 Comparison of Spectral Data for Chalcogenide Complexes

While not all of the complexes were directly isolated, sufficient data have been obtained to make some comparisons between the phosphine chalcogenide complexes [Ru(CO)(PPh$_3$){PH(E)Cy}(Tp)] (E = O, S, Se, Te) (Table 5.1). The most significant trend is the decrease in δ_P of the PH(E)Cy group going down the group. This trend follows the decreasing electronegativity of heavier chalcogens, and suggests a progressive increase of electron density at phosphorus. A similar, though less pronounced, trend is evident for the simple phosphine chalcogenides E=PCy$_3$ (δ_P: E = S: 62.4, Se: 59.1, Te: 29.2).[283,‡‡] Both $^1J_{PH}$ and $^2J_{PP}$ decrease going down the group, although the relative magnitude of this decrease is negligible. Finally, an increase in ν_{CO} is observed moving down the group, suggesting that the σ-donating ability of the phosphine decreases with heavier chalcogens. Alternatively, it may imply that the P–E π* and/or σ* orbital has π-symmetry with respect to the Ru–P vector. As the effective orbital overlap between P and E decreases down the chalcogen group the antibonding orbital would decrease in energy, serving to increase the π-acidity of the ligand.

Table 5.1. Comparison of spectral data for the phosphine chalcogenide complexes [Ru(CO)(PPh3){PH(E)Cy}(Tp)] (E = O, S, Se, Te)

Chalcogen	ν_{CO} (cm^{-1})	δ_P PH(E)Cy	$^1J_{PH}$ (Hz)	$^2J_{PP}$ (Hz)
O	1973	97.0	337	32
S	1989	51.2	337	28
Se	1993	19.9	335	28
Te[a]	1994	−61.9	317	25

[a] Tentative assignment, compound not isolated

‡‡ O=PCy$_3$ does not fit this trend, δ_P = 48.3.[284]

5.3 Nucleophilic Reactivity of Chalcogenide Complexes

Roper has demonstrated the nucleophilic reactivity of transition metal phosphine chalcogenide complexes at the chalcogen atom (Scheme 5.11).[77] The complex $[OsCl(CO)_2(PPh_3)_2\{PH_2(S)\}]$ could be reversibly protonated as observed by *in situ* ^1H NMR experiments. This nucleophilic reactivity was extended to include methylation, yielding the cation $[Os(Cl)(CO)_2(PPh_3)_2\{PH_2(SMe)\}]^+$ which contains the unusual S-methyl thiophosphinite ligand. The P–H bond of this cationic complex could then be deprotonated to afford the methylthiophosphido complex $[OsCl(CO)_2(PPh_3)_2\{PH(SMe)\}]$. This complex was air stable, similar to Roper's other complexes, and was demonstrated to display nucleophilic character at phosphorus through electrophilic methylation and acylation reactions.

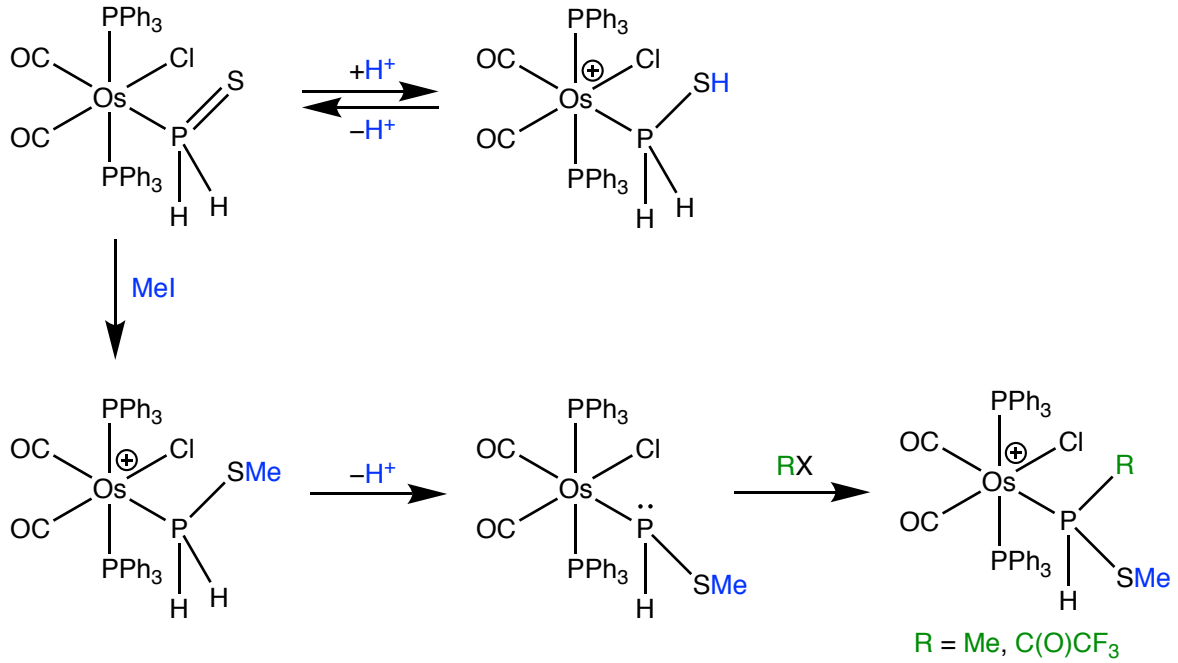

Scheme 5.11. Reactivity of $[OsCl(CO)_2(PPh_3)_2\{PH_2(S)\}]$

The nucleophilic reactivity of transition metal phosphine chalcogenide complexes has been further illustrated by Stoppioni (Scheme 5.12). The cation $[Ru(PPh_3)_2\{PH_2(SH)\}(Cp)]^+$ can be reversibly deprotonated, the isolable intermediate being $[Ru(PPh_3)_2\{PH_2(S)\}(Cp)]$.[276] The complex $[Ru(PPh_3)_2\{PH_2(S)\}(Cp)]$ could also be methylated with MeOTf to give the salt $[Ru(PPh_3)_2\{PH_2(SMe)\}(Cp)]OTf$. In addition to Stoppioni's work, the methylation of iron phosphine selenide complexes has been reported by Leong and Liu.[285] The complexes $[Fe(CO)_2\{P(Se)(OR)_2\}(Cp)]$ (R = ^{i}Pr, ^{n}Pr, Et) are methylated by $[OMe_3]BF_4$ to give the salts $[Fe(CO)_2\{P(SeMe)(OR)_2\}(Cp)]BF_4$ (Scheme 5.13), providing an example of Se nucleophilicity.

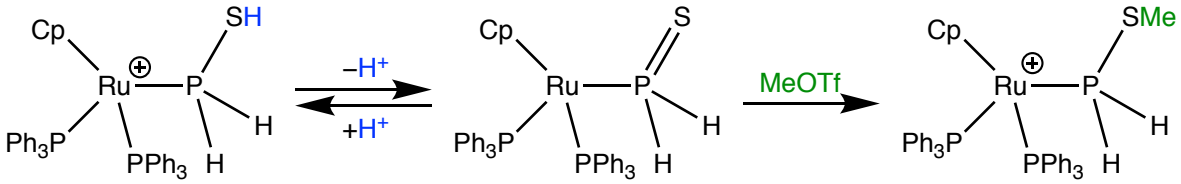

Scheme 5.12. Synthesis and reactivity of [Ru(PPh3)2{PH2(S)}(Cp)]

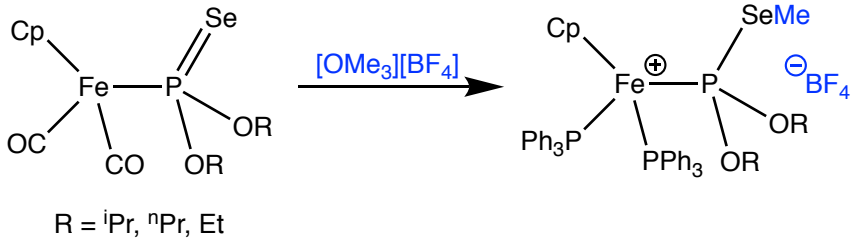

Scheme 5.13. Nucleophilic reactivity of [Fe(CO)2{P(OR)2(Se)}(Cp)] (R = iPr, nPr, Et) complexes

5.3.1 Synthesis of [Ru(CO)(PPh3){PH(SH)Cy}(Tp)]OTf

The first investigation into the nucleophilic reactivity of primary phosphine chalcogenide complexes involved the use of HOTf. Addition of HOTf to a THF solution of [Ru(CO)(PPh3){PH(S)Cy}(Tp)] resulted in a shift of the ν_{CO} frequency from 1989 to 1998 cm^{-1} as expected for the formation of a cationic complex. The product, [Ru(CO)(PPh3){PH(SH)Cy}(Tp)]OTf (Scheme 5.14), was obtained in 50% yield following the removal of volatiles and ultrasonic trituration of the residue in Et_2O.

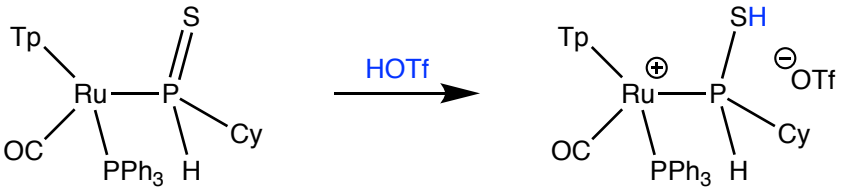

Scheme 5.14. Reaction of [Ru(CO)(PPh3){PH(S)Cy}(Tp)] with triflic acid

The $^{31}P\{^1H\}$ NMR spectrum of [Ru(CO)(PPh3){PH(SH)Cy}(Tp)]OTf showed a shift to lower frequency for both resonances: δ_P 42.2 to 36.3 for the PPh_3 group and δ_P 51.2 to 44.2 for the PHCy resonance. The value of $^2J_{PP}$ remained essentially unchanged (28 Hz for [Ru(CO)(PPh3){PH(S)Cy}(Tp)] and 29 Hz for [Ru(CO)(PPh3){PH(SH)Cy}(Tp)]OTf) whereas $^1J_{PH}$ was seen to increase from 337 to 371 Hz. Increases in $^1J_{PH}$ indicated a reduction in electron density at phosphorus,[138] consistent with the disruption of the P=S π bond.

The protonation at sulfur was observed by ^{1}H NMR spectroscopy with the emergence of a broad singlet at δ_H 3.24. Importantly, a correlation between this resonance and the PHCy resonance at δ_P 44.2 was observed in a 2D ^{1}H–^{31}P HSQC NMR experiment, supporting the formation of the PH(SH)Cy group. The other ^{1}H and ^{13}C{^{1}H} NMR data were relatively unchanged compared to [Ru(CO)(PPh$_3$){PH(S)Cy}(Tp)].

X-ray crystallography confirmed the formation of [Ru(CO)(PPh$_3$){PH(SH)Cy}(Tp)]OTf and the results are summarised in Figure 5.7. Of immediate significance to the characterisation of the product are the P−H and S−H hydrogen atoms, which were located in the Fourier difference map and have had their positions freely refined. As expected, the P−S bond length of 2.1002(9) Å is also appreciably longer than in [Ru(CO)(PPh$_3$){PH(S)Cy}(Tp)] (2.0183(16) Å), signifying the change from a formal double to a single P−S bond. In comparison to [Ru(CO)(PPh$_3$){PH(S)Cy}(Tp)], the Ru1−P1 bond length for [Ru(CO)(PPh$_3$){PH(SH)Cy}(Tp)]OTf is shorter (2.331(11) Å *versus* 2.3203(6) Å) while the Ru1−P2 bond length is longer (2.3691(11) Å *versus* 2.3914(6) Å). The same trend was observed between [Ru(PPh$_3$){PH$_2$(S)}(Cp)][276] and [Ru(PPh$_3$){PH$_2$(SH)}(Cp)]OTf.[274]

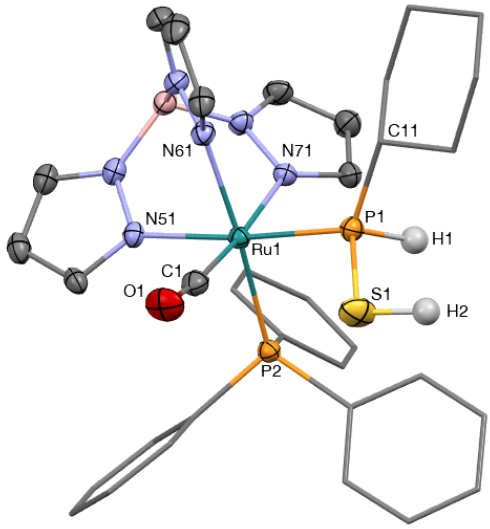

Figure 5.7. Molecular structure of S_{Ru},S_P-[Ru(CO)(PPh$_3$){PH(SH)Cy}(Tp)]$^+$ in a crystal of [Ru(CO)(PPh$_3$){PH(SH)Cy}(Tp)]OTf (50% displacement ellipsoids, triflate counteranion and most H atoms omitted, phenyl and cyclohexyl rings simplified). Selected bond lengths (Å) and angles (°): Ru1−P1 2.3203(6), Ru1−P2 2.3914(6), Ru1−N51 2.1442(19), Ru1−N61 2.123(2), Ru1−N71 2.1357(19), Ru1−C1 1.865(3), S1−P1 2.1002(9), S1−H1 1.25(3), P1−H1 1.39(3), P1−C11 1.835(3), O1−C1 1.142(3), P1−Ru1−P2 95.07(2), P1−Ru1−C1 91.07(8), P2−Ru1−C1 95.41(8), P1−S1−H1 96.6(15). Molecule crystallised in the centrosymmetric I2/a space group – enantiomer, but not diastereomers, present in unit cell.

The ligand PH(SH)Cy exerts a notably larger (10 e.s.d.) *trans* influence than PPh_3, the respective *trans* Ru−N bonds being 2.1442(19) Å and 2.123(2) Å. The Ru−N distance *trans* to the CO group is 2.1357(19) and sits within the bounds of statistical variation (4.5 e.s.d.) to the corresponding bond length *trans* to PH(SH)Cy.

The salt [Ru(CO)(PPh_3){PH(SH)Cy}(Tp)]OTf contains two potential sites for deprotonation: the P−H or the S−H bond. The reaction of [Ru(CO)(PPh_3){PH(SH)Cy}(Tp)]OTf with KH resulted in the reformation of [Ru(CO)(PPh_3){PH(S)Cy}(Tp)] *i.e. ultimately* S−H deprotonation. This result is expected given the initial formation and structure of [Ru(CO)(PPh_3){PH(S)Cy}(Tp)]. If P−H deprotonation had occurred it would imply that the sulfur atom is more basic than the phosphorus atom, and correspondingly [Ru(CO)(PPh_3){PH(S)Cy}(Tp)] should readily tautomerise to [Ru(CO)(PPh_3){P(SH)Cy}(Tp)], which is not observed.

5.3.2 Synthesis of [Ru(CO)(PPh_3){PH(SMe)Cy}(Tp)]OTf

Following the successful protonation of [Ru(CO)(PPh_3){PH(S)Cy}(Tp)] to form [Ru(CO)(PPh_3){PH(SH)Cy}(Tp)]OTf, the next step was to determine if the reactivity could be extended to other electrophiles. As previously discussed, Roper reported methylation at the sulfur site of [$OsCl(CO)_2(PPh_3)_2${$PH_2(S)$}] and this reaction was chosen for investigation.[77] Methyl triflate reacted with [Ru(CO)(PPh_3){PH(S)Cy}(Tp)] in benzene to form [Ru(CO)(PPh_3){PH(SMe)Cy}(Tp)]OTf (Scheme 5.15), which precipitated as a colourless solid. The air-stable product was collected by vacuum filtration and obtained in 58% yield.

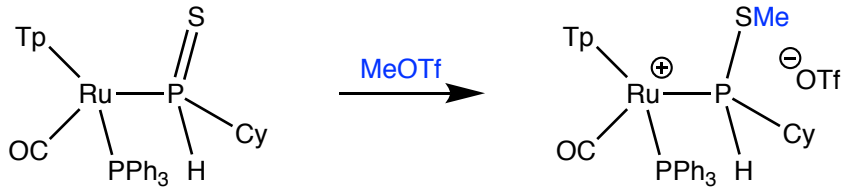

Scheme 5.15. Reaction of [Ru(CO)(PPh_3){PH(S)Cy}(Tp)] with methyl triflate

The ν_{CO} band for [Ru(CO)(PPh_3){PH(SMe)Cy}(Tp)]OTf appeared at 1992 cm^{-1} in the IR spectrum (THF). As expected for a cationic complex, this value is higher than that for neutral [Ru(CO)(PPh_3){PH(S)Cy}(Tp)] (ν_{CO} 1989 cm^{-1}). However, the ν_{CO} band for [Ru(CO)(PPh_3){PH(SH)Cy}(Tp)]OTf (1998 cm^{-1}) is higher still, suggesting that PH(SH)Cy is a poorer net donor than PH(SMe)Cy. In the solid-state (ATR) IR spectrum a new, very strong

absorbance appeared at 637 cm^{-1} compared to the IR spectrum for [Ru(CO)(PPh$_3$){PH(S)Cy}(Tp)]. The position of this band[286] and its absence from the spectrum for [Ru(CO)(PPh$_3$){PH(S)Cy}(Tp)] suggest that it is a ν_{CS} mode due to the newly-formed S−Me bond.

The methyl group was observed in the ^{1}H NMR spectrum as a doublet at δ_H 2.04 with $^3J_{PH}$ = 7Hz. This assignment was further confirmed by the observation of a cross peak in a 2D ^{1}H–^{31}P HSQC experiment as well as the absence of coupling in a ^{1}H{^{31}P} NMR experiment. The ^{13}C{^{1}H} NMR resonance for the methyl group was also a doublet ($^2J_{PC}$ = 7 Hz), appearing at δ_C 21.8. The remaining ^{1}H and ^{13}C{^{1}H} NMR data are consistent with previous observations.

Methylation at sulfur results in a shift to higher frequency of the PHCy ^{31}P{^{1}H} NMR resonance from δ_P 51.2 to 66.8. Curiously, this shift is in the opposite direction to that for protonation. A small shift to lower frequency of the PPh$_3$ resonance to δ_P 36.2 was observed and this is essentially the same as the value observed in [Ru(CO)(PPh$_3$){PH(SH)Cy}(Tp)]$^+$ (δ_P 36.3). The $^2J_{PP}$ of 29 Hz is relatively unchanged while $^1J_{PH}$ has increased to 371 Hz, the same as measured for the protonated cation [Ru(CO)(PPh$_3$){PH(SH)Cy}(Tp)]$^+$.

Crystals of [Ru(CO)(PPh$_3$){PH(SMe)Cy}(Tp)]OTf suitable for an X-ray diffraction study were grown by vapour diffusion of *n*-hexane into a CH_2Cl_2 solution of the salt and the results are summarised in Figure 5.8. Formation of a S−C bond is clear, and the corresponding bond length of 1.829(4) Å is comparable to the average C(sp^3)−S distance of 1.817(13) Å.[197] The P−S distance has elongated to 2.0955(12) Å which is within statistical variation (4 e.s.d.) of the corresponding distance in [Ru(CO)(PPh$_3$){PH(SH)Cy}(Tp)]OTf and signifies an essentially single P−S bond.

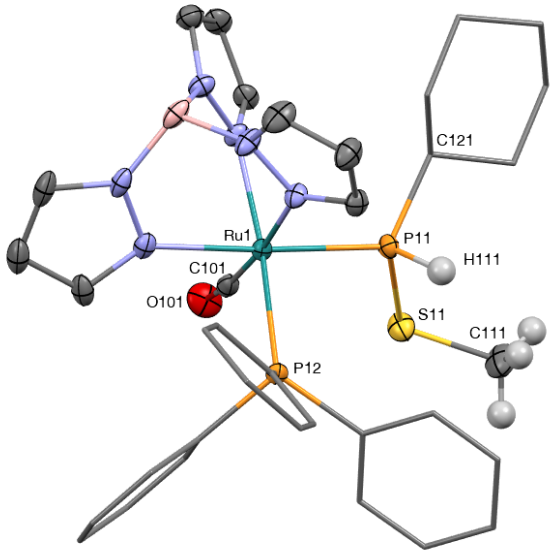

Figure 5.8. Molecular structure of R_{Ru},S_P-[Ru(CO)(PPh$_3$){PH(SMe)Cy}(Tp)]$^+$ in a crystal of [Ru(CO)(PPh$_3$){PH(SMe)Cy}(Tp)]OTf.(CH_2Cl_2) (50% displacement ellipsoids, second independent molecule in cell, triflate counteranions, two CH_2Cl_2 solvates and most H atoms omitted, phenyl and cyclohexyl rings simplified). Selected bond lengths (Å) and angles (°): Ru1–P11 2.3284(9), Ru1–P12 2.3740(8), Ru1–C101 1.860(4), P11–S11 2.0955(12), S11–C111 1.829(4), P11–H111 1.31(4), P11–C121 1.840(4), O101–C101 1.149(5), P11–Ru1–P12 93.19(3), P11–Ru1–C101 90.72(11), P12–Ru1–C101 95.78(11), P11–S11–C111 105.93(15). Molecule crystallised in the centrosymmetric P2$_1$/c space group – enantiomer, but not diastereomers, present in unit cell.

The Ru–PHCy bond length in [Ru(CO)(PPh$_3$){PH(SMe)Cy}(Tp)]OTf (2.3284(9) Å) is longer than in [Ru(CO)(PPh$_3$){PH(SH)Cy}(Tp)]OTf (2.3203(6) Å). This may potentially arise from the increased steric bulk of the additional methyl group, although the fact that this group points away from the metal centre reduces the likelihood of this cause. Intriguingly, the Ru–PPh$_3$ distance of 2.3740(8) Å in the methylated complex is much shorter than in the protonated complex (2.3914(6) Å).

5.3.3 Synthesis of [Ru(CO)(PPh$_3$){PH(SeMe)Cy}(Tp)]OTf

Given the successful methylation of [Ru(CO)(PPh$_3$){PH(S)Cy}(Tp)], investigations were undertaken to ascertain if the reactivity extended to the selenium analogue. The addition of methyl triflate to a benzene solution of [Ru(CO)(PPh$_3$){PH(Se)Cy}(Tp)] resulted in the formation of [Ru(CO)(PPh$_3$){PH(SeMe)Cy}(Tp)]OTf as a colourless precipitate in 53% yield (Scheme 5.16). The ν_{CO} band for [Ru(CO)(PPh$_3$){PH(SeMe)Cy}(Tp)]OTf appeared at 1986 cm^{-1} in the IR spectrum (THF). Curiously, this is *lower* than the ν_{CO} stretch for the neutral precursor,

[Ru(CO)(PPh$_3$){PH(Se)Cy}(Tp)] (1993 cm^{-1}). The shift to lower frequency is unexpected for a neutral-to-cationic transformation, but perhaps indicates that the positive charge is not localised on the metal centre in [Ru(CO)(PPh$_3$){PH(SeMe)Cy}(Tp)]OTf.

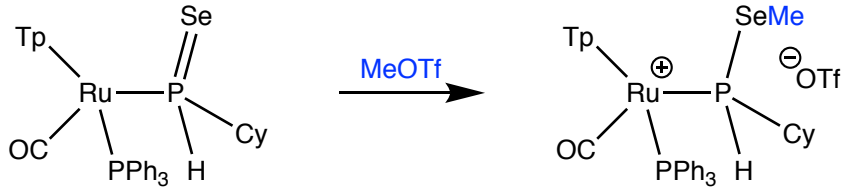

Scheme 5.16. Reaction of [Ru(CO)(PPh$_3$){PH(Se)Cy}(Tp)] with methyl triflate

Methylation was evident in the $^{31}P\{^1H\}$ NMR spectrum of the product due to a shift to higher frequency of the PSe signal from 19.9 to 46.3 ppm. This resonance was easily identifiable due to the ^{77}Se satellites with a $^1J_{PSe}$ of 318 Hz. The value of $^1J_{PSe}$ is greatly reduced compared to [Ru(CO)(PPh$_3$){PH(Se)Cy}(Tp)] ($^1J_{PSe}$ = 497 Hz), indicative of the increase in coordination number at selenium and the consequent decrease of selenium s-character in the P–Se bond. Finally, the resonance appeared as a doublet ($^1J_{PH}$ = 371 Hz) in the ^{31}P NMR spectrum, confirming the P–H connectivity.

The introduction of the methyl group was also observed in the ^1H and $^{13}C\{^1H\}$ NMR spectra *via* doublets appearing at δ_H 2.04 ($^3J_{PH}$ = 7 Hz) and δ_C 12.6 ($^2J_{PC}$ = 5 Hz), respectively. Selenium-77 satellites could not be identified for either resonance in their respective spectra. Interestingly, the $^{13}C\{^1H\}$ NMR signal for the methyl group is at a lower frequency compared to that of [Ru(CO)(PPh$_3$){PH(SMe)Cy}(Tp)]OTf (Me δ_C 21.8) which is the same trend observed for the ^{31}P NMR resonances of the two complexes as well as [Ru(CO)(PPh$_3$){PH(Se)Cy}(Tp)] and [Ru(CO)(PPh$_3$){PH(S)Cy}(Tp)]. As discussed in Section 5.2.5, this trend plausibly arises from the modest electonegativity difference between S and Se. Otherwise, the features of the ^1H and $^{13}C\{^1H\}$ NMR spectra were unremarkable.

X-ray diffraction quality crystals of [Ru(CO)(PPh$_3$){PH(SeMe)Cy}(Tp)]OTf were grown by vapour diffusion of *n*-hexane into a chloroform solution of [Ru(CO)(PPh$_3$){PH(SeMe)Cy}(Tp)]OTf and the results of the study are shown in Figure 5.9. Both the Ru–PHCy (2.3383(11) Å) and Ru–PPh$_3$ (2.3915(11) Å) bond lengths are longer than in the corresponding sulfur complex [Ru(CO)(PPh$_3$){PH(SMe)Cy}(Tp)]OTf (2.3284(9) and 2.3740(8) Å,

respectively). The P−Se (2.2240(13) Å) and Se−C (1.945(6) Å) bonds fall within their expected ranges[197] and, as expected for the larger chalcogen, are longer than the P−S (2.0955(12) Å) and S−C (1.829(4) Å) distances. Finally, the P−E−C (E = S: 105.93(15)°; E = Se: 103.29(19)°) is smaller for selenium, a phenomenon arising due to the increased p character of bonds in heavy elements.

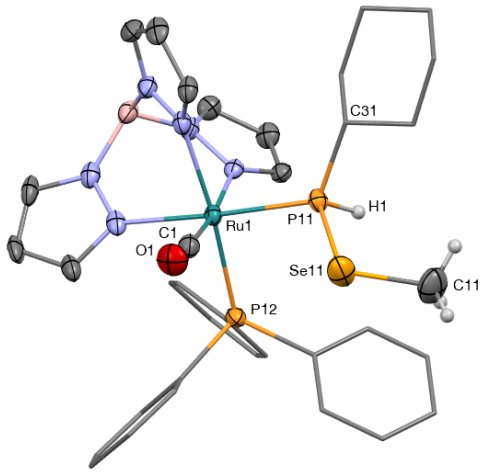

Figure 5.9. Molecular structure of S_{Ru},S_P-[Ru(CO)(PPh$_3$){PH(SeMe)Cy}(Tp)]$^+$ in a crystal of [Ru(CO)(PPh$_3$){PH(SeMe)Cy}(Tp)]OTf.(CHCl$_3$) (50% displacement ellipsoids, second independent molecule in cell, triflate counteranions, two chloroform solvates and most H atoms omitted, phenyl and cyclohexyl rings simplified). Selected bond lengths (Å) and angles (°): Ru1−P11 2.3383(11), Ru1−P12 2.3915(11), Ru1−C1 1.872(5), P11−Se11 2.2240(13), Se11−C11 1.945(6), P11−H1 1.15(5), P11−C31 1.841(5), O1−C1 1.132(6), P11−Ru1−P12 93.28(4), P11−Ru1−C1 90.78(15), P12−Ru1−C1 95.97(15), P11−Se11−C11 103.29(19). Molecule crystallised in the non-centrosymmetric Cc *space group – enantiomer not present in unit cell. The second independent molecule in the cell is the S_{Ru},R_P diastereomer.*

5.4 Deprotonation and Subsequent Reactivity of [Ru(CO)(PPh$_3$){PH(SMe)Cy}(Tp)]OTf

5.4.1 Formation and Decomposition of [Ru(CO)(PPh$_3$){P(SMe)Cy}(Tp)]OTf

Similarly to Roper's cationic complex [Os(Cl)(CO)$_2$(PPh$_3$)$_2${PH$_2$(SMe)}]$^+$, the cation [Ru(CO)(PPh$_3$){PH(SMe)Cy}(Tp)]$^+$ only contains a P−H group as a functionalisable H atom. Additionally, its cationic nature should render the P−H bond more acidic than in [Ru(CO)(PPh$_3$){PH(S)Cy}(Tp)]. Treatment of the colourless salt [Ru(CO)(PPh$_3$){PH(SMe)Cy}(Tp)]OTf with KH in THF resulted in effervescence and a colour change to yellow. Infrared spectroscopy of the mixture after 30 minutes stirring at room temperature revealed two ν_{CO} bands at 1950 and 1935 cm^{-1}. Both bands appear at lower

frequency than in the precursor [Ru(CO)(PPh$_3$){PH(SMe)Cy}(Tp)]OTf, consistent with deprotonation having occurred to form [Ru(CO)(PPh$_3$){P(SMe)Cy}(Tp)] (Scheme 5.17).

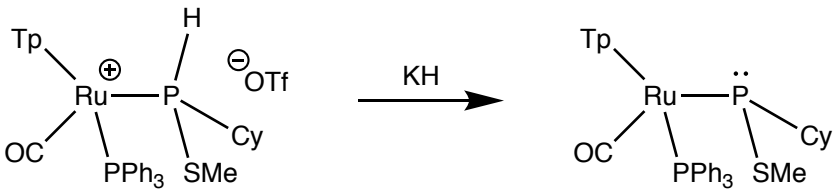

Scheme 5.17. Deprotonation of [Ru(CO)(PPh$_3$){PH(SMe)Cy}(Tp)]OTf

Cannula filtration, removal of the solvent from the filtrate *in vacuo* and NMR spectroscopic investigation of the resultant residue gave further insight into the nature of the products. Four doublet resonances were present in the $^{31}P\{^1H\}$ NMR spectrum, consistent with the formation of two diastereomers of [Ru(CO)(PPh$_3$){P(SMe)Cy}(Tp)]. The resonances were approximately equal by integration and appeared at δ_P 126.4 and 43.2 ($^2J_{PP}$ = 18 Hz) for one isomer and δ_P 90.5 and 43.8 ($^2J_{PP}$ = 8 Hz) for the other. None of the resonances displayed any one-bond P−H coupling in the ^{31}P NMR spectrum, confirming the absence of a P−H bond following deprotonation.

While the majority of the ^1H NMR data were unremarkable, two SMe doublets at δ_H 1.98 ($^3J_{PH}$ = 8 Hz) and 1.83 ($^3J_{PH}$ = 8 Hz) were notable. These resonances correlated to the ^{31}P NMR signals at δ_P 90.5 and 126.4, respectively, in a 2D ^1H–^{31}P HSQC experiment, confirming the preservation of the P−S−Me connectivity. Furthermore, the 2D experiment allowed the assignment of the high frequency $^{31}P\{^1H\}$ NMR signals to P(SMe)Cy groups.

The shift to higher frequency of the P(SMe)Cy resonance following deprotonation is remarkable, as this transformation is expected to result in a shift to lower frequency due to the increased electron density at phosphorus. A high frequency ^{31}P NMR shift was observed following the stepwise deprotonation of the phosphido-bridged bimetallic complex [Ni$_2$(μ−PHMes)$_2$(Cp)$_2$],[287] but reasonable explanations for this observation have not been found.[138]

Attempts to isolate pure [Ru(CO)(PPh$_3$){P(SMe)Cy}(Tp)] were unsuccessful. Extraction of the reaction mixture with toluene separated [Ru(CO)(PPh$_3$){P(SMe)Cy}(Tp)] from ionic by-

products. However, decomposition was observed during recrystallisation attempts. No [Ru(CO)(PPh$_3$){P(SMe)Cy}(Tp)] was detected by $^{31}P\{^1H\}$ NMR spectroscopy after 5 days of monitoring a sample in a NMR tube sealed under argon.

The $^{31}P\{^1H\}$ NMR spectrum following the decomposition of [Ru(CO)(PPh$_3$){P(SMe)Cy}(Tp)] contained five major resonances (~98%) along with five minor resonances (<2%). Among the major resonances, the predominant product (~63%) gave rise to two broad resonances at δ_P 119.9 and 48.0. The other major resonances were two doublets (~29%) at δ_P 105.1 and 41.1 (J_{PP} = 18 Hz) as well as a singlet at δ_P 24.5 (~6%).

Identification of one major decomposition product was achieved by X-ray crystallography. A single crystal obtained from the decomposed NMR sample yielded the molecular structure of [Ru(CO)(PPh$_3$){P(O)(OH)Cy}(Tp)] (Figure 5.10). The structure contains two crystallographically independent molecules in the asymmetric unit cell and includes several disordered sites. Among these sites was disorder in both O=P−OH systems, showing the presence of two tautomers within the crystal. The P−O bond lengths (*e.g.* 1.514(10) and 1.62(6) Å) were indicative of the mixed double and single bonds, falling within the expected range for each type.[197] Additionally, the P(O)(OH)Cy groups exhibit hydrogen bonding with symmetry-generated molecules within the unit cell (Figure 5.11); the H···A distances within these groups fall in the range 1.52−1.60 Å. There have been four other reports involving structurally-characterised complexes of P(O)(OH)R ligands,[288-291] and solid-state H-bonding was also observed for the molecule [IrH{P(O)(OH)Ph}(cod)(L^2)] (cod = 1,4-cyclooctadiene, L^2 = κ^2-*N,C'*-2-(2-phenylene)-4,4-dimethyl-5-hydrooxazole).[288] The D···A distances of 2.525(17) and 2.512(17) Å in the iridium complex are comparable to the range of D···A distances 2.43(4)−2.59(4) Å observed for [Ru(CO)(PPh$_3$){P(O)(OH)Cy}(Tp)].

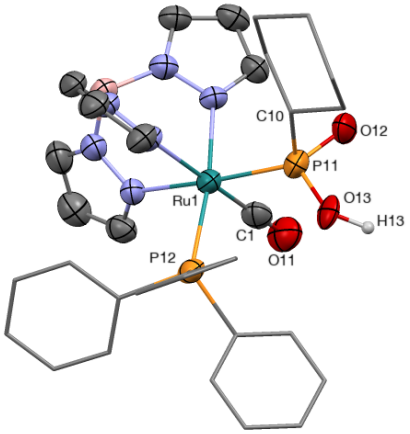

Figure 5.10. Molecular structure of S_{Ru}-[Ru(CO)(PPh$_3$){P(O)(OH)Cy}(Tp)] in a crystal (50% displacement ellipsoids, second independent molecule in cell, minor disordered components and most H atoms omitted, phenyl and cyclohexyl rings simplified). Selected bond lengths (Å) and angles (°): Ru1–P11 2.319(6), Ru1–P12 2.354(5), Ru1–C1 1.85(2), P11–O12 1.514(10), P11–O13 1.62(6), P11–C10 1.82(3), O11–C1 1.14(3), P11–Ru1–P12 94.9(2), P11–Ru1–C1 83.4(7), P12–Ru1–C1 92.8(6), O12–P11–O13 106(7). Molecule crystallised in the centrosymmetric P–1 space group – enantiomer is present in unit cell.

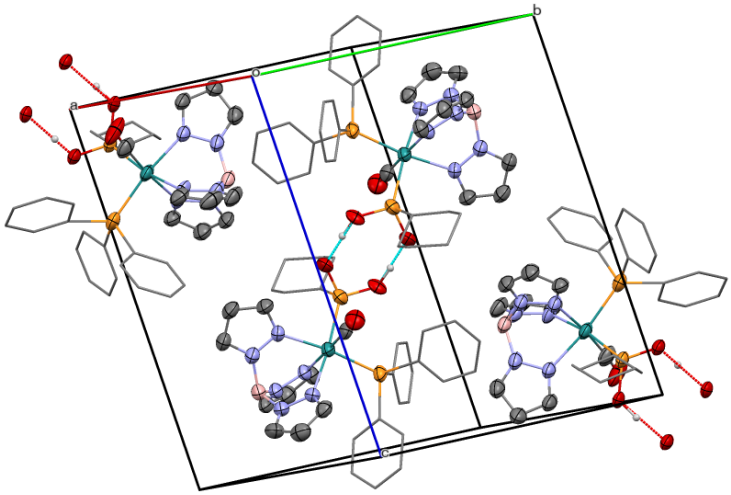

Figure 5.11. Hydrogen bonding between molecules of [Ru(CO)(PPh$_3$){P(O)(OH)Cy}(Tp)] in the unit cell.

The formation of [Ru(CO)(PPh$_3$){P(O)(OH)Cy}(Tp)] is due to a combination of hydrolysis of the P–S bond and oxidation of phosphorus. These processes are most likely due to the presence of adventitious moisture and air, respectively. The hydrolysis of P–S bonds is well known[1] and has been reported for σ^3,λ^3-phosphorus centres such as the cyclic phosphonodithioate PhP{SCH(CO_2Et)CH(CO_2Et)S}.[292-293] Furthermore, the lability of phosphorus-chalcogen bonds

is well known and is key to the mechanisms-of-action of Lawesson's[258] and Woollin's[259] reagents.

To further investigate the formation of [Ru(CO)(PPh$_3$){P(O)(OH)Cy}(Tp)], the aerobic reaction between [Ru(CO)(PPh$_3$){PH(SMe)Cy}(Tp)]OTf and KOH in THF was conducted. After 24 hours, the ^{31}P{^{1}H} NMR spectrum of the reaction mixture contained doublets at δ_P 117.7, 107.4, 46.3 40.4 and 40.1. Each signal displayed a J_{PP} of 32 Hz, but a 2D ^{31}P–^{31}P ADEQUATE NMR experiment showed that the coupled pairs of signals were δ_P 117.7 and 40.1, and δ_P 107.4 and 40.4. At first inspection, these resonances do not agree with those observed in the initial decomposition of [Ru(CO)(PPh$_3$){PH(SMe)Cy}(Tp)]OTf. As observed in the solid state structure, however, the expected product [Ru(CO)(PPh$_3$){P(O)(OH)Cy}(Tp)] is capable of H-bonding which can cause variation in the ^{31}P{^{1}H} NMR shifts of such molecules.[138, 294] It is then reasonable to assume that [Ru(CO)(PPh$_3$){P(O)(OH)Cy}(Tp)] has formed, although the assignment of its NMR shifts are still unclear.

Attempts to purify [Ru(CO)(PPh$_3$){P(O)(OH)Cy}(Tp)] were unsuccessful. The solvent was removed from the residue *in vacuo*, followed by extraction of the residue with toluene and filtration through diatomaceous earth to remove ionic by-products. At this stage, the ^{31}P{^{1}H} NMR spectrum of the mixture showed additional resonances at δ_P 29.1 and 121.5. The former resonance is presumed to be O=PPh$_3$, while the latter was a doublet with J_{PP} = 32 Hz and was presumed to be coupled to the resonance at δ_P 46.3. The signal at δ_P 121.5 is assumed to be have been unobserved in the previously-discussed NMR spectrum of the crude mixture which had a relatively poor signal-to-noise ratio. The mixture was soluble in EtOH and Et_2O. Attempts to crystallise the product from these solvents, as well as toluene/*n*-hexane and CH_2Cl_2/*n*-hexane mixtures, at −20°C did not yield any precipitate. As such, the isolation and spectral characterisation of [Ru(CO)(PPh$_3$){P(O)(OH)Cy}(Tp)] could not be completed.

5.4.2 Reaction with Iodomethane

Adding iodomethane to a freshly-generated solution of [Ru(CO)(PPh$_3$){P(SMe)Cy}(Tp)] resulted in the formation of two diastereomers of the P-methylated product

[Ru(CO)(PPh$_3$){P(Me)(SMe)Cy}(Tp)]OTf (Scheme 5.18). The cationic nature of the product was evident from the shift to higher frequency of the ν_{CO} band from 1950 cm^{-1} to 1996 cm^{-1}.

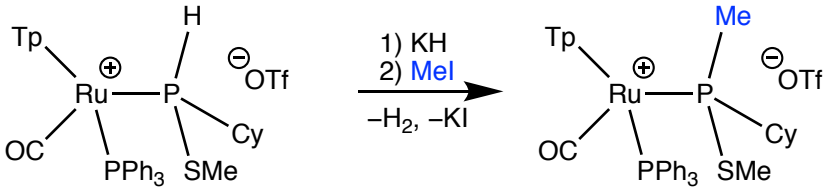

Scheme 5.18. Synthesis of [Ru(CO)(PPh$_3$){P(SMe)MeCy}(Tp)]OTf

Methylation at phosphorus resulted in a shift to lower frequency of the P(SMe)Cy ^{31}P{^{1}H} NMR resonances to δ_P 57.6 and 51.8 (from δ_P 126.4 and 90.5). These signals were doublets ($^2J_{PP}$ = 28 Hz), coupling to PPh$_3$ resonances at δ_P 35.0 and 32.6, respectively, based on relative integrations. Furthermore, each of the P(SMe)Cy resonances displayed correlations to two methyl groups in a 2D ^{31}P–^{1}H HSQC NMR experiment, indicating the introduction of a methyl group. These methyl groups appeared at δ_H 1.81 and 1.39 for the resonance at δ_P 57.6, and at δ_H 2.21 and 0.64 for the resonance at δ_P 51.8. Each of these four methyl signals appeared as doublets with J_{PH} = 8 Hz with no difference in observed $^2J_{PH}$ and $^3J_{PH}$ to distinguish between PMe and SMe groups.

The characterisation of [Ru(CO)(PPh$_3$){P(Me)(SMe)Cy}(Tp)]$^+$ included ESI-MS data, with the [M]$^+$ ion being observed at *m/z* 781.2. In the high-resolution spectrum, the measured *m/z* of 781.1758 exactly matched the calculated value of *m/z* 781.1758 for its expected formula, $C_{36}H_{42}BN_6OP_2RuS$.

Attempts at purification to obtain a bulk sample of [Ru(CO)(PPh$_3$){P(Me)(SMe)Cy}(Tp)]$^+$ were not successful. To work up the reaction, the reaction mixture was freed of volatiles and the resultant residue dissolved in CH_2Cl_2. This mixture was filtered through diatomaceous earth with the intention of removing KI. Removal of solvent from the filtrate gave a yellow residue which was subjected to various recrystallisation procedures. Evaporation of solvent from a CH_2Cl_2/MeOH mixture on a rotary evaporator failed to yield any precipitate. Following the same procedure using a CH_2Cl_2/hexane or a CH_2Cl_2/Et_2O mixture yielded an oil. In the latter case, however, the high viscosity of the oil allowed its separation from the supernatant. Unfortunately, the purity of [Ru(CO)(PPh$_3$){P(Me)(SMe)Cy}(Tp)]$^+$ within this oil had not

improved. Finally, a concentrated ^{i}PrOH solution placed in a −20°C freezer yielded an oil which could not be separated.

While bulk purification of [Ru(CO)(PPh$_3$){P(Me)(SMe)Cy}(Tp)]$^+$ could not be achieved, crystals of [Ru(CO)(PPh$_3$){P(Me)(SMe)Cy}(Tp)]$^+$ suitable for X-ray diffraction were obtained *via* evaporation of solvent from the supernatant CH_2Cl_2/Et_2O mixture. The molecular structure of [Ru(CO)(PPh$_3$){P(Me)(SMe)Cy}(Tp)]$^+$ (Figure 5.12) confirms the P-methylation, with a P−C bond length of 1.911(5) Å. Compared to the closely-related structure of [Ru(CO)(PPh$_3$){PH(SMe)Cy}(Tp)]$^+$, the P−S bond length of 2.069(2) Å is slightly shorter ([Ru(CO)(PPh$_3$){PH(SMe)Cy}(Tp)]$^+$ 2.0955(12) Å, 13 e.s.d.). Both the Ru−PCy and Ru−PPh$_3$ bond lengths are longer (Ru−PCy: 2.3574(14) *versus* 2.3284(9), 20 e.s.d.; Ru−PPh$_3$: 2.3918(14) *versus* 2.3740(8) Å, 12 e.s.d.), a phenomenon likely arising from the increased bulk of the methyl group compared to hydrogen. Otherwise, no significant deviations between the two structures were observed.

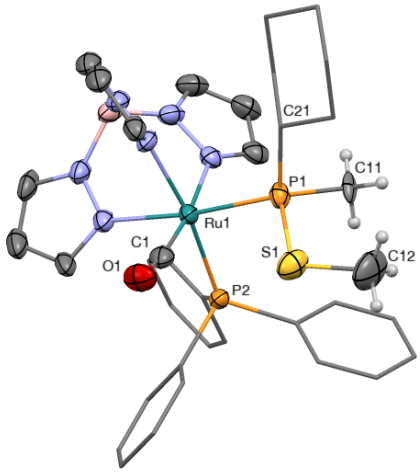

Figure 5.12. Molecular structure of S_{Ru},S_P-[Ru(CO)(PPh$_3$){P(Me)(SMe)Cy}(Tp)]$^+$ in a crystal of [Ru(CO)(PPh$_3$){P(Me)(SMe)Cy}(Tp)][OTf]$_{0.74}$I$_{0.26}$.(CHCl$_3$)(C$_4$H$_{10}$O) (50% displacement ellipsoids, triflate and iodide counteranions, solvent molecules and most H atoms omitted, phenyl and cyclohexyl rings simplified). Selected bond lengths (Å) and angles (°): Ru1−P1 2.3574(14), Ru1−P2 2.3918(14, Ru1−C1 1.862(8), P1−S1 2.069(2), P1−C11 1.911(5), P1−C21 1.844(6), S1−C12 1.806(9), O1−C1 1.151(9), P1−Ru1−P2 96.53(5), P1−Ru1−C1 92.2(2), P2−Ru1−C1 94.69(19), P1−S1−C12 108.7(4). Molecule crystallised in the centrosymmetric Pbcn *space group – enantiomer, but not diastereomers, present in unit cell.*

Disorder was observed in the counteranion of the crystal structure. The anionic site was observed to be a mixture of OTf$^-$ and I$^-$, in a 74:26 ratio, respectively. The co-crystallisation of different anions indicates that the attempt to remove KI at an earlier stage was unsuccessful.

In the future, MeOTf could be used as the methylating agent to prevent anion mixing. However, this approach may also create difficulty in separating the two salts KOTf and [Ru(CO)(PPh$_3$){P(Me)(SMe)Cy}(Tp)]OTf.

5.4.3 Reaction with BH$_3$·SMe$_2$

To continue exploring the phosphido-type reactivity of [Ru(CO)(PPh$_3$){P(SMe)Cy}(Tp)], its reaction with BH$_3$·SMe$_2$ was conducted. Addition of BH$_3$·SMe$_2$ to a solution of [Ru(CO)(PPh$_3$){P(SMe)Cy}(Tp)] resulted in an immediate decolourisation. The IR spectrum of the mixture contained a single ν_{CO} absorption at 1978 cm^{-1} and the shift to higher frequency is consistent with previous observations upon coordination of BH$_3$.

The $^{31}P\{^1H\}$ NMR spectrum of the mixture showed [Ru(CO)(PPh$_3$){P(BH$_3$)(SMe)Cy}(Tp)] to be the major (*ca.* 93%) product (Scheme 5.19), forming as a mixture of two diastereomers in a 5:2 ratio. The major diastereomer gives rise to a boron-broadened singlet at δ_P 56.5 and a PPh$_3$ doublet ($^2J_{PP}$ = 23 Hz) at δ_P 44.6, while the minor isomer has the P(BH$_3$)(SMe)Cy resonance and PPh$_3$ doublet ($^2J_{PP}$ = 24 Hz) at δ_P 54.9 and 44.0, respectively.

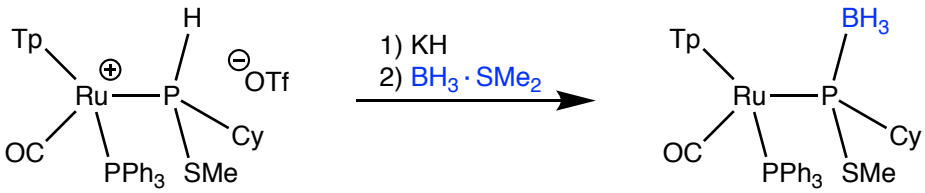

Scheme 5.19. Synthesis of [Ru(CO)(PPh$_3$){P(BH$_3$)(SMe)Cy}(Tp)]

Similar behaviour to the phosphido-borane complex, [Ru(CO)(PPh$_3$){PH(BH$_3$)Cy}(Tp)], was displayed by [Ru(CO)(PPh$_3$){P(BH$_3$)(SMe)Cy}(Tp)] in the ESI-MS experiment. A peak at *m/z* 767.2 corresponded to the [M – BH$_3$ + H]$^+$ ion and the [M – BH$_3$ + O + H]$^+$ ion was accounted for by a peak at *m/z* 783.2. Both peaks also matched their expected calculated values in the high-resolution mass spectrum as well as showing the same isotopic distribution.

5.4.4 Reaction with Elemental Sulfur

The final reagent chosen for the investigation of the reactivity of [Ru(CO)(PPh$_3$){P(SMe)Cy}(Tp)] was elemental sulfur. The reaction between elemental sulfur and [Ru(CO)(PPh$_3$){P(SMe)Cy}(Tp)] resulted in decolourisation of the mixture over 10

minutes, and the formation of the sulfur-oxidised product [Ru(CO)(PPh$_3$){P(S)(SMe)Cy}(Tp)] (Scheme 5.20). As with the other products derived from [Ru(CO)(PPh$_3$){P(SMe)Cy}(Tp)], [Ru(CO)(PPh$_3$){P(S)(SMe)Cy}(Tp)] formed as two diastereomers which gave rise to ν_{CO} bands at 1983 and 1968 cm^{-1} in the IR spectrum.

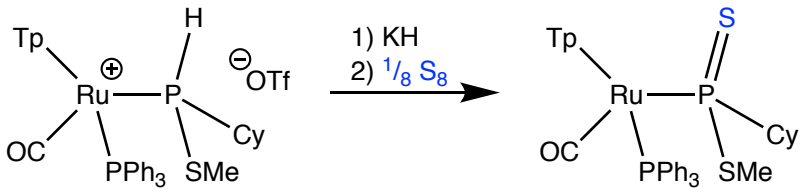

Scheme 5.20. Synthesis of [Ru(CO)(PPh$_3$){P(S)(SMe)Cy}(Tp)]

Nuclear magnetic resonance spectroscopy gave further insight into the formation of [Ru(CO)(PPh$_3$){P(S)(SMe)Cy}(Tp)]. The two diastereomers formed in a 1:1 ratio and together comprised 88% of the reaction mixture, as estimated by $^{31}P\{^1H\}$ NMR spectroscopy. These diastereomers each gave rise to a pair of doublets in the $^{31}P\{^1H\}$ NMR spectrum; the P(S)(SMe)Cy groups appeared at δ_P 101.8 and 99.2 while the PPh$_3$ resonances were present as overlapping signals at δ_P 42.2. Each of the signals had a $^2J_{PP}$ of 28 Hz which, along with the similar signal intensities, precluded the definitive assignment of doublet pairs.

5.5 Summary and Future Work

The reaction of [Ru(CO)(PPh$_3$)(PHCy)(Tp)] with a variety of chalcogen sources was investigated. While the four species [Ru(CO)(PPh$_3$){PH(E)Cy}(Tp)] (E = O, S, Se, Te) were all formed and observed, only the sulfur and selenium complexes could be isolated. Oxidation of phosphorus with sulfur could potentially acidify the P–H bond in [Ru(CO)(PPh$_3$){PH(S)Cy}(Tp)] relative to [Ru(CO)(PPh$_3$)(PHCy)(Tp)], but no reaction was observed in the presence of base.

The chalcogen atom in the complexes [Ru(CO)(PPh$_3$){PH(E)Cy}(Tp)] (E = S, Se) was found to be nucleophilic. Protonation of the sulfur complex yielded [Ru(CO)(PPh$_3$){PH(SH)Cy}(Tp)]OTf and methylation of both complexes resulted in the formation of [Ru(CO)(PPh$_3$){PH(EMe)Cy}(Tp)]OTf (E = S, Se). All three salts were structurally characterised.

The formation of [Ru(CO)(PPh$_3$){PH(SMe)Cy}(Tp)]OTf provided access to the new thioether-substituted phosphido complex [Ru(CO)(PPh$_3$){P(SMe)Cy}(Tp)] *via* deprotonation. This

complex decomposes to form [Ru(CO)(PPh$_3$){P(O)(OH)Cy}(Tp)] in the presence of adventitious H_2O and air. The phosphido atom is nucleophilic, undergoing methylation, borane adduct formation and sulfur oxidation to form [Ru(CO)(PPh$_3$){PMe(SMe)Cy}(Tp)]$^+$, [Ru(CO)(PPh$_3$){P(SMe)(BH$_3$)Cy}(Tp)] and [Ru(CO)(PPh$_3$){P(S)(SMe)Cy}(Tp)], respectively. This reactivity provides access to new compounds and demonstrates a viable pathway to more chalcogen-substituted phosphorus architectures in the future.

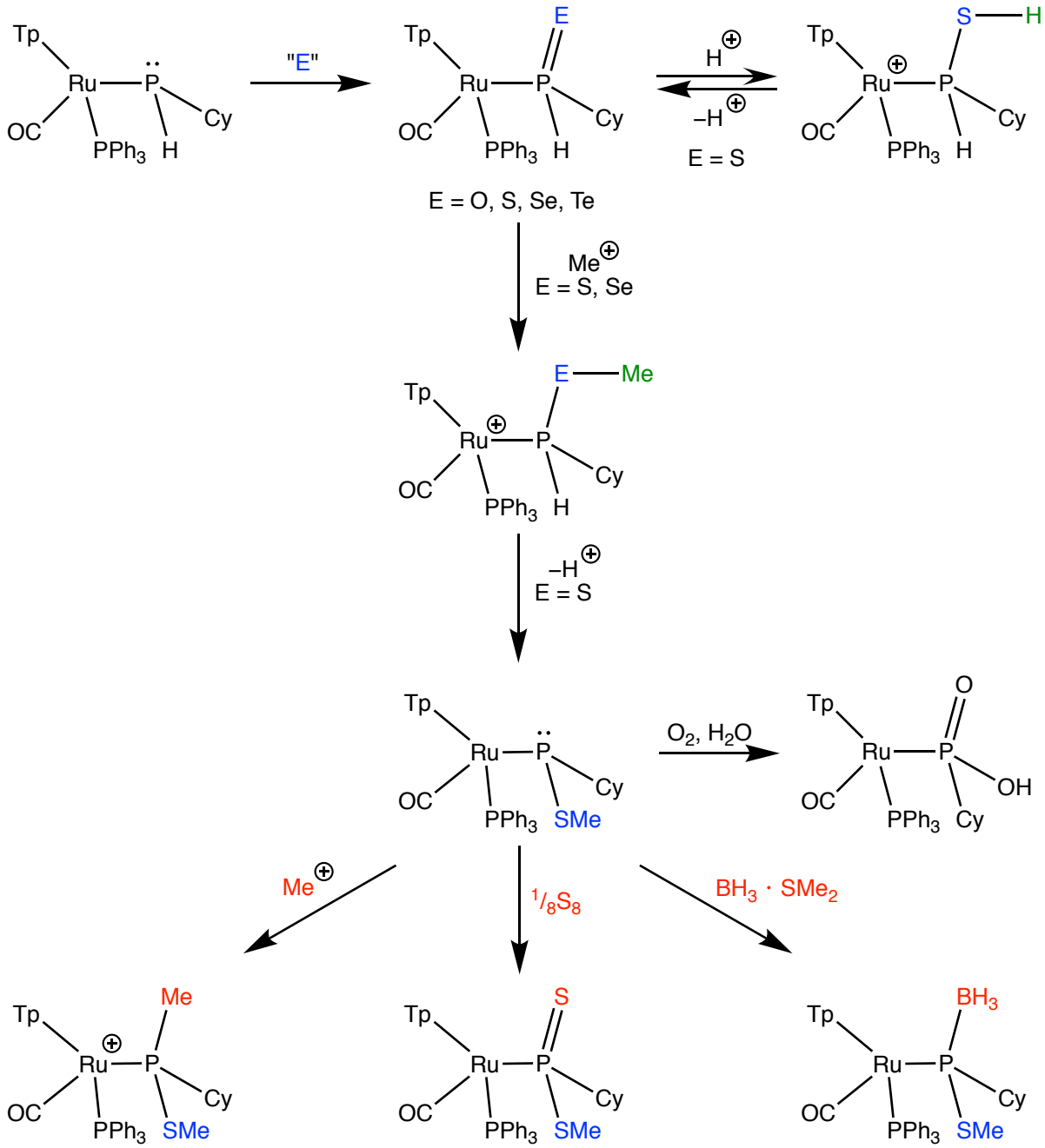

Scheme 5.21. Summary of reactivity discussed in this chapter

CHAPTER 6
Conclusions

Chapter 6: Conclusions

A range of ruthenium complexes bearing cyclohexylphosphine as a ligand have been synthesised. Broadly, these complexes have all been derived by exploiting the substitution reactivity of $[RuCl(PPh_3)_2(Tp)]$, $[RuH(Cl)(CO)(PPh_3)_3]$ and $[RuH(CO)(PPh_3)(Tp)]$. The deprotonation of these complexes to form new terminal phosphido complexes was then explored.

The phosphido complexes bearing a Tp ligand but no π-acidic CO group were found to be highly basic and reactive. Consequently, a variety of unintended reactions were observed upon deprotonation of the primary phosphine complex precursor, such as cyclometallation ($[RuCl(PPh_3)(PH_2Cy)(Tp)]$), reprotonation due to high basicity ($[Ru(PPh_3)(PH_2Cy)_2(Tp)]^+$) or rearrangement of the products ($[Ru(PH_2Cy)(dppf)(Tp)]^+$; dimerisation of $[Ru\{PH(AuCl)Cy\}(dppf)(Tp)]^+$). The unpredictable nature of these results led to the exploration of alternative primary phosphine complexes to serve as phosphido complex precursors.

Cyclohexylphosphine complexes bearing a CO ligand were synthesised with the expectation that the π-acidic group would mitigate the high reactivity of the phosphido lone pair upon deprotonation. However, in the absence of the tridentate Tp ligand, these phosphido complexes were found to be unstable with respect to the loss of co-ligands (particularly PPh_3). The lability of the co-ligands could be exploited to obtain complexes bearing the unusual PH(OMe)Cy ligand, which is unstable in its free form. The reactivity of $[Ru(CO)_2(PPh_3)_2\{PH(OMe)Cy\}]$ was investigated. Triphenylphosphine is more labile than PH(OMe)Cy and is preferentially displaced in ligand substitution reactions. The Ru(0) centre is reactive – evidence for oxidative addition and metal protonation was observed, and the complex oxidises when stored in air. Finally, elimination of methanol from the PH(OMe)Cy ligand led to the formation of $[RuCl_2(CO)(PPh_3)_2(PH_2Cy)]$.

Combining the steric and kinetic stabilisation of the Tp ligand with the electron-withdrawing capacity of CO led to the synthesis of the new phosphido complex $[Ru(CO)(PPh_3)(PHCy)(Tp)]$. While this complex could not be isolated, it could be readily generated *in situ* for further study. The dynamic behaviour of $[Ru(CO)(PPh_3)(PHCy)(Tp)]$ was investigated through variable

temperature NMR spectroscopy, and the phosphorus inversion barrier of the PHCy group was found to be higher than other experimentally-observed transition metal phosphido complexes, but still within the expected computationally-calculated range.

The utility of [Ru(CO)(PPh_3)(PHCy)(Tp)] as a synthetic precursor was explored through its reactions with electrophiles such as MeI, BH_3 and CS_2. Additionally, the reaction of [Ru(CO)(PPh_3)(PHCy)(Tp)] with an appropriate chalcogen source produced the phosphine chalcogenide complexes [Ru(CO)(PPh_3){PH(E)Cy}(Tp)] (E = O, S, Se, Te). Of the chalcogenide complexes, only the sulfide and selenide derivatives could be isolated and fully characterised. For the sulfide and selenide complexes, the chalcogen was shown to be nucleophilic through reactions with triflic acid and methyl triflate. The P−H bond in cationic complexes derived from [Ru(CO)(PPh_3)(PHCy)(Tp)] (such as $[Ru(CO)(PPh_3)(PHMeCy)(Tp)]^+$, $[Ru(CO)(PPh_3)\{PH(CS_2Me)Cy\}(Tp)]^+$ and $[Ru(CO)(PPh_3)\{PH(SMe)Cy\}(Tp)]^+$) was generally acidic, leading to new phosphido complexes upon deprotonation. The stability of the new phosphido complexes was varied, but allowed access to rarely-seen phosphorus architectures through their reactions with electrophiles.

Overall, a library of cyclohexylphosphine ruthenium complexes has been created. Factors which contribute to the stability of their corresponding phosphido complexes have also been determined. The augmented reactivity of phosphido complexes has been employed to obtain unusual phosphorus-based structures derived from cyclohexylphosphine, demonstrating the synthetic utility of combining the functionalisable potential of primary phosphines with the unique properties of terminal phosphido complexes.

CHAPTER 7
Experimental

Chapter 7: Experimental

7.1 General Procedures

Unless otherwise stated, all manipulations were conducted at room temperature under a dry, oxygen-free N_2 atmosphere using standard Schlenk, vacuum-line, or inert atmosphere (argon) glovebox techniques. Solvents were purified by distillation from an appropriate drying agent (ethers, paraffins and arenes from sodium benzophenone ketyl; halocarbons and acetonitrile from CaH_2; alcohols from magnesium turnings) under a N_2 atmosphere.

The following compounds were prepared according to published procedures: KTp,[295] [RuCl(PPh_3)$_2$(Tp)],[126] [RuCl(dppf)(Tp)],[134] [AuCl(SMe_2)],[296] [RuH(Cl)(CO)(PPh_3)$_3$],[151] CNMes,[154] [Ru(OTf)(CO)(PPh_3)(Tp)],[120] [RuH(CO)(PPh_3)(Tp)],[128] [CPh_3]PF_6,[297] $PyBH_3$,[298] [NBu_4][B_3H_8],[151] and PhIO.[299] All other reagents were obtained from commercial sources and purified as necessary.

Solution and KBr IR spectra were recorded on a Perkin-Elmer Spectrum One FT-IR spectrometer. All other IR spectra were recorded on a Perkin-Elmer Spectrum Two FT-IR spectrometer with a diamond plate Attenuated Total Reflectance (ATR) sampling attachment. Only the bands associated with chromophores of interest are reported, and the strengths of their IR absorptions are denoted by the abbreviations vs (very strong), s (strong), m (medium), w (weak), sh (shoulder) and br (broad).

Nuclear magnetic resonance spectra were recorded on Varian Mercury 300 (^{1}H at 300.1 MHz, ^{31}P at 121.5 MHz), Bruker Avance 400 (^{1}H at 400.1 MHz, ^{13}C at 100.6 MHz, ^{11}B at 128.4 MHz, ^{31}P at 162.0 MHz), Bruker Avance 600 (^{1}H at 600.0 MHz, ^{13}C at 150.9 MHz), Bruker Avance 700 (^{1}H at 700.1 MHz, ^{13}C at 176.1 MHz, ^{31}P at 283.4 MHz) or Bruker Avance 800 (^{1}H at 800.1 MHz, ^{13}C at 201.2 MHz) spectrometers. Chemical shifts (δ) are reported in ppm and are referenced to tetramethylsilane using the residual protio solvent peak (^{1}H), tetramethylsilane using the solvent peak (^{13}C), external 85% H_3PO_4 (^{31}P) or external BF_3.Et_2O (^{11}B). The multiplicities of NMR signals are denoted s (singlet), d (doublet), t (triplet), q (quartet), m (multiplet), t^v (virtual triplet), br (broad), app (apparent) and combinations thereof for more highly coupled

systems. Where applicable, the stated multiplicities are of the primary resonance exclusive of heteronuclear satellites. For cases where virtual coupling is present the apparent *J* value is indicated. In some cases, distinct peaks were observed in the ^{1}H and $^{13}C\{^{1}H\}$ NMR spectra, but to the level of accuracy that is reportable (*i.e.* 2 decimal places for ^{1}H NMR, 1 decimal place for ^{13}C NMR) they are reported as having the same chemical shift. The abbreviation 'pz' denotes signals due to the pyrazolyl ring. Whilst $^{13}C\{^{1}H\}$ signals for carbon nuclei of PPh and PCy groups could be routinely observed, their narrow spectral range and comparable J_{PC} values often precluded unequivocal assignment in which case plausible, but not definitive, assignments are provided. The PH_2 and PH ^{1}H NMR signals were often poorly resolved or exhibited second-order coupling effects. In these cases the appearance of the signal is provided and the apparent *J* values are indicated.

Electrospray Ionisation Mass Spectrometry (ESI-MS) was conducted by staff at the Australian National University Joint Mass Spectrometry Facility. Data were acquired on Waters LCT Premier, Orbitrap Elite or Orbitrap Q Exactive machines with MeCN or MeOH as the matrix.

Elemental microanalytical data were obtained from the Elemental Analysis Service at the London Metropolitan University. All samples for microanalysis were washed with *n*-hexane and *n*-pentane, followed by drying *in vacuo* for extended periods of time. While due care was taken to package sensitive samples under an inert atmosphere, there was no guarantee of the condition of the analytes upon arrival at the service. Where satisfactory elemental microanalytical data could not be obtained the results are presented for reference.

Optical rotation was measured on a Rudolph Research Analytical Autopol 1 polarimeter with a 100 mm path length cell.

Data for X-ray crystallography were collected using Agilent SuperNova CCD or Agilent Xcalibur CCD diffractometers, or at the Australian Synchrotron.[§§] Structures were solved and refined

[§§] The assistance of Dr Nicholas White and Dr Stephanie Boer for the acquisition of synchrotron-derived data is gratefully acknowledged.

by the author using the *CRYSTALS*[300] or *Olex2*[301] software packages. The advice of Dr Anthony Willis, Dr Jas Ward, Dr Nicholas White, Dr Benjamin Frogley and Dr Michael Gardiner for the solutions of some structures is gratefully acknowledged.

7.2 Complexes Derived from [RuCl(PPh$_3$)$_2$(Tp)]

Synthesis of [RuCl(PPh$_3$)(PH$_2$Cy)(Tp)]

Cyclohexylphosphine (0.32 mL, 2.4 mmol) was added to a suspension of [RuCl(PPh$_3$)$_2$(Tp)] (2.00 g, 2.29 mmol) in toluene (100 mL). The mixture was stirred for 20 days and the yellow solution freed of volatiles *in vacuo*. *n*-Hexane was added and the flask was placed in an ultrasonic bath for 5 minutes. The product was collected as a yellow powder by vacuum filtration, washing with Et$_2$O (2 × 40 mL). The product is stable in air in the short term, but should be kept under an inert atmosphere for long term storage. A microanalytically pure sample was obtained after recrystallisation from CH$_2$Cl$_2$/EtOH.

Yield: 1.39g (83%). IR (ATR) ν/cm^{-1}: 3054 w, 2935 w, 2917 w, 2842 w (CH), 2455 m (BH), 2352 w, 2302 m (PH). ^{1}H NMR (CDCl$_3$, 400.1 MHz, 298 K) δ/ppm: 8.01, 7.69, 7.66, 7.63, 6.96, 6.62, 6.18, 5.88, 5.73 (s × 9, 9 × 1H, J_{HH} not resolved, Hpz), 7.33–7.23 (m, 15H, C$_6$H$_5$), 4.32 (d, 1H, $^1J_{PH}$ = 328 Hz, $^2J_{HH}$ not resolved, PH), 3.89 (d, 1H, $^1J_{PH}$ = 328 Hz, $^2J_{HH}$ not resolved, PH), 1.54–0.59 (m, 11H, C$_6$H$_{11}$). ^{13}C{^{1}H} NMR (CDCl$_3$, 100.6 MHz, 300 K) δ/ppm: 146.3, 144.2, 142.4 (s × 3, 3 × C^3(pz)), 136.0, (s, C^5(pz)), 135.1 – 134.7 (range for overlapping signals, 2 × C^5(pz) + *ipso*-PC$_6$H$_5$), 134.3 (d, J_{PC} = 9 Hz, *o/m*-PC$_6$H$_5$), 129.2 (s, *p*-PC$_6$H$_5$), 127.8 (d, J_{PC} = 9 Hz, *o/m*-PC$_6$H$_5$), 105.7 C^4(pz)), 105.3 (C^4(pz)), 33.5 (d, $^3J_{PC}$ = 6 Hz, 3,5-C$_6$H$_{11}$), 28.3 (d, $^1J_{PC}$ = 26 Hz, 1-C$_6$H$_{11}$), 27.3, 27.1 (d × 2, $^2J_{PC}$ = 10 Hz, 2,6-C$_6$H$_{11}$), 25.9 (s, 4-C$_6$H$_{11}$). ^{31}P {^{1}H} NMR (CDCl$_3$, 162.0 MHz, 300 K) δ/ppm: 49.3 (d, $^2J_{PP}$ = 32 Hz, PPh$_3$), 15.1 (d, $^2J_{PP}$ = 32 Hz, PH$_2$Cy). ^{31}P NMR (CDCl$_3$, 162.0 MHz, 300 K) δ/ppm: 49.4 (app s, PPh$_3$), 15.3 (app t, $^1J_{PH}$ = 327 Hz, PH$_2$Cy). ESI-MS (+, MeCN) *m/z*: 734.2 [M + MeCN – Cl]$^+$, 693.2 [M – Cl]$^+$. Accurate mass: found 734.2036 [M + MeCN – Cl]$^+$, Calcd. for C$_{35}$H$_{41}$^{11}BN$_7$P$_2$^{102}Ru 734.2036; found 693.1768 [M – Cl]$^+$, Calcd. for C$_{33}$H$_{38}$^{11}BN$_6$P$_2$^{102}Ru 693.1770. Anal. Found: C, 54.39; H, 5.29; N, 11.36 %. Calcd. For C$_{33}$H$_{38}$BClN$_6$P$_2$Ru: C, 54.45; H, 5.26; N, 11.54 %.

Formation of [RuCl(PH_2Cy)$_2$(Tp)]

A solution of PH_2Cy (0.31 mL, 2.34 mmol) and [RuCl(PPh_3)$_2$(Tp)] (1.00 g, 1.15 mmol) in toluene (80 mL) was stirred for 5 days. At this point, an aliquot taken for $^{31}P\{^1H\}$ NMR spectroscopy indicated that the species present in solution were [RuCl(PPh_3)(PH_2Cy)(Tp)], PPh_3 and PH_2Cy. A reflux condenser was attached to the flask and the mixture heated under reflux with stirring for 96 hours, after which only a small amount (<3%) of [RuCl(PPh_3)(PH_2Cy)(Tp)] was detected. The mixture was freed of volatiles *in vacuo* and the residue treated to ultrasonic trituration in Et_2O. The product was collected as a yellow solid by vacuum filtration. The product was contaminated by approximately 6% [RuCl(PPh_3)(PH_2Cy)(Tp)] and conditions for its removal were not identified.

Yield: 0.274 g (41%). ^1H NMR (C_6D_6, 400.1 MHz, 298 K) δ/ppm: 8.16 (s, 2H, Hpz), 7.58 (br s, 1H, Hpz), 7.52 (s, 2H, Hpz), 7.45 (s, 1H, Hpz), 6.00 (s, 2H, Hpz), 5.86 (s, 1H, Hpz), 4.62 (br d, 2H, $^1J_{PH}$ = 324 Hz, PH), 4.30 (br d, 2H, $^1J_{PH}$ = 316 Hz, PH), 1.95–0.90 (m, 22H, C_6H_{11}). $^{13}C\{^1H\}$ NMR (C_6D_6, 100.62 MHz, 300 K) δ/ppm: 143.7 (s, C^3(pz)), 143.1 (s, C^3(pz)), 136.1 (s, C^5(pz)), 134.8 (s, C^5(pz)), 105.8 (s, C^4(pz)), 105.8 (s, C^4(pz)), 33.2 (d, $^1J_{PC}$ = 37 Hz, 1-C_6H_{11}), 29.9 (d, $^2J_{PC}$ = 15 Hz, 2,6-C_6H_{11}), 29.8 (d, $^2J_{PC}$ = 13 Hz, 2,6-C_6H_{11}), 27.3, 27.2 (d × 2, $^2J_{PC}$ = 5 Hz, 3,5-C_6H_{11}), 26.1 (s, 4-C_6H_{11}). $^{31}P\{^1H\}$ NMR (C_6D_6, 162.0 MHz, 300 K) δ/ppm: 9.56 (s, PH_2Cy). ^{31}P NMR (C_6D_6, 162.0 MHz, 300 K) δ/ppm: 9.56 (app t, $^1J_{PH}$ = 326 Hz, PH_2Cy). ESI-MS (+, MeCN) *m/z*: 582.1 $[M]^+$. Accurate mass: found 582.1303 $[M]^+$, Calcd. for $C_{21}H_{36}{}^{11}B^{35}ClN_6P_2{}^{102}Ru$ 582.1302.

Synthesis of [Ru(PPh_3)(PH_2Cy)$_2$(Tp)]PF_6

Cyclohexylphosphine (0.22 mL, 1.7 mmol) was added to a mixture of [RuCl(PPh_3)$_2$(Tp)] (0.728g, 0.833 mmol), $NaPF_6$ (0.211g, 1.26 mmol) and MeOH (20 mL). The mixture was stirred at room temperature for 4 days over which the mixture changed from yellow suspension to colourless solution. Volatiles were removed *in vacuo* and the remainder of the procedure conducted in air. The colourless residue was dissolved in CH_2Cl_2 (35 mL) and filtered through diatomaceous earth. The filtrate was freed of volatiles on a rotary evaporator and the residue placed in an ultrasonic bath with Et_2O, forming a colourless powder that was collected by vacuum filtration. Crystals suitable for X-ray diffraction were grown *via* vapour diffusion of Et_2O into a CH_2Cl_2 solution of the product. As discussed in Section 2.2.3, the crystals were a

mixture of $[Ru(PPh_3)(PH_2Cy)_2(Tp)]PF_6$ and the chlorotris(pyrazolyl)borate complex $[Ru(PPh_3)(PH_2Cy)_2(^{Cl}Tp)]PF_6$.

Yield: 0.593g (75%). IR (ATR) ν/cm^{-1}: 2929 w, 2917 sh, 2858 sh, 2849 w (CH), 2497 w (BH), 2354 w (PH). ^{1}H NMR ($CDCl_3$, 600.0 MHz, 298 K) δ/ppm: 7.90 (s, 1H, J_{HH} not resolved, Hpz), 7.86 (s, 2H, J_{HH} not resolved, Hpz), 7.74 (s, 1H, J_{HH} not resolved, Hpz), 7.43–7.02 (m, 15H + 2H, C_6H_5 + Hpz), 6.29 (s, 1H, J_{HH} not resolved, Hpz), 6.06 (s, 2H, J_{HH} not resolved, Hpz), 4.41 (d, 2H, $^1J_{PH}$ = 354 Hz, finer coupling not resolved, PH), 3.72 (d, 2H, $^1J_{PH}$ = 348 Hz, finer coupling not resolved, PH), 1.45–0.60 (m, 11H, C_6H_{11}). ^{13}C{^{1}H} NMR ($CDCl_3$, 150.9 MHz, 298 K) δ/ppm: 144.3 (s, C^3(pz)), 143.8 (s, C^3(pz)), 136.8 (s, C^4(pz)), 136.7 (s, C^4(pz)), 133.8 (d, J_{PC} = 9 Hz, *o/m*-P(C_6H_5)), 132.7 (d, $^1J_{PC}$ = 44 Hz, *ipso*-P(C_6H_5)), 130.7 (s, *p*-(PC_6H_5)), 128.6 (d, J_{PC} = 9 Hz, *o/m*-P(C_6H_5)), 106.6 (s, C^5(pz)), 106.4 (s, C^5(pz)), 32.1 (s, 3,5-C_6H_{11}), 32.0 (s, 3,5-C_6H_{11}), 29.8 (t^v, J_{PC} = 14 Hz, 1-C_6H_{11}), 27.1 (t^v, J_{PC} = 5 Hz, 2,6-C_6H_{11}), 26.8 (t^v, J_{PC} = 5 Hz, 2,6-C_6H_{11}), 25.4 (s, 4-C_6H_{11}). ^{31}P {^{1}H} NMR ($CDCl_3$, 162.0 MHz, 300 K) δ/ppm: 44.9 (t, $^2J_{PP}$ = 29 Hz, PPh_3), 3.8 (d, $^2J_{PP}$ = 29 Hz, PH_2Cy), –143.4 (sep, $^1J_{PF}$ = 713 Hz, PF_6). ^{31}P NMR ($CDCl_3$, 162.0 MHz, 300 K) δ/ppm: 44.9 (br s, PPh_3), 3.8 (ddt, $^1J_{PH}$ = 337 Hz, $^2J_{PH}$ = $^2J_{PP}$ = 26 Hz, PH_2Cy), –143.4 (sep, $^1J_{PF}$ = 713 Hz, PF_6). ESI-MS (+, MeCN) *m/z*: 809.3 $[M]^+$. Accurate mass: found 809.2525 $[M]^+$, Calcd. for $C_{39}H_{51}{}^{11}BN_6P_3{}^{102}Ru$ 809.2525. Anal. Found: C, 49.08; H, 5.34; N, 8.80 %. Calcd. For $C_{39}H_{51}BF_6N_6P_4Ru$: C, 49.12; H, 5.39; N, 8.81 %. Crystal data for $[C_{39}H_{50.89}BCl_{0.11}N_6P_3Ru][PF_6]$: M_W = 957.31, triclinic, *P*–1, *a* = 10.3638(3) Å, *b* = 13.8127(5) Å, *c* = 15.0143(5) Å, *α* = 85.745(3) °, *β* = 82.688(3)°, *γ* = 83.692(3)°, *V* = 2114.99(12) Å^3, *Z* = 2, ρ_{cacld} = 1.503 Mg m^{-3}, *μ*(Mo Kα) = 0.59 mm^{-1}, *T* = 150 K, colourless prism, 0.15 × 0.11 × 0.04 mm, 37770 measured reflections, 10393 independent (R_{int} = 0.043), F^2 refinement, *R* = 0.041, *wR* = 0.087 for 8258 reflections (*I* > *2σ(I)*, $2\vartheta_{max}$ = 59.4°), 536 parameters with 0 restraints.

NMR data for $[Ru(PPh_3)(PH_2Cy)_2(^{Cl}Tp)]PF_6$

^{31}P {^{1}H} NMR ($CDCl_3$, 162.0 MHz, 300 K) δ/ppm: 44.1 (t, $^2J_{PP}$ = 29 Hz, PPh_3), 3.3 (d, $^2J_{PP}$ = 29 Hz, PH_2Cy), –143.4 (sep, $^1J_{PF}$ = 713 Hz, PF_6).

^{31}P NMR: obscured by resonances for $[Ru(PPh_3)(PH_2Cy)_2(Tp)]PF_6$

Synthesis of [Ru(dppf)(PH_2Cy)(Tp)]PF_6

Cyclohexylphosphine (0.25 mL, 0.96M in *n*-hexane, 0.24 mmol) was added to a mixture of [RuCl(dppf)(Tp)] (0.200g, 0.221 mmol), $NaPF_6$ (0.045g, 0.268 mmol) and MeOH (10 mL). The mixture was stirred for 2 days after which no more solid was observed in the flask. Volatiles were removed *in vacuo* and the remainder of the procedure was conducted in air. The yellow residue was dissolved in CH_2Cl_2 (10 mL) and filtered through diatomaceous earth. The filtrate was freed of volatiles on a rotary evaporator and the residue placed in an ultrasonic bath with Et_2O (15 mL), forming a yellow powder that was collected by vacuum filtration. Crystals suitable for X-ray diffraction were grown by liquid diffusion of Et_2O into a CH_2Cl_2 solution of the product.

Yield: 0.127g (61%). IR (ATR) ν/cm^{-1}: 2931 w, 2924 w, 2915 w, 2848 w (CH), 2527 w (BH), 2334 w (PH). ^{1}H NMR ($CDCl_3$, 800.1 MHz, 298 K) δ/ppm: 8.77 (s, 2H, Hpz), 8.20 (s, 1H, Hpz), 7.92–7.09 (m, 20 H, PPh_2), 6.79 (s, 2H, Hpz), 6.29 (s, 1H, Hpz), 6.03 (s, 2H, Hpz), 5.33 (s, 1H, Hpz), 4.90 (br s, BH), 4.44, 4.21, 3.98 (s × 3, 8H, C_5H_4), 3.08 (d, 2H, $^1J_{PH}$ = 344 Hz, PH), 1.25–0.11 (m, 11H, C_6H_{11}). ^{13}C{^{1}H} NMR ($CDCl_3$, 100.6 MHz, 300 K) δ/ppm: 148.0 (s, C^3(pz)), 144.8, (s, 2 × C^3(pz)), 137.9 (s, C^5(pz)), 137.6 (s, 2 × C^5(pz)), 134.9 (s, *o/m*-PC_6H_5), 132.9 (s, *o/m*-PC_6H_5), 130.5 (s, *p*-PC_6H_5), 130.0 (s, *p*-PC_6H_5), 129.0 (s, *o/m*-PC_6H_5), 127.3 (s, *o/m*-PC_6H_5), 107.4 (s, C^4(pz)), 106.7 (s, 2 × C^4(pz)), 87.8 (t^v, J_{PC} = 24 Hz, 1-C_5H_4), 74.1, 72.0, 70.6 (s × 3, 3 × C_5H_4), 31.8 (s, 3,5-C_6H_{11}), 29.3 (d, $^1J_{PC}$ = 27 Hz, 1-C_6H_{11}), 26.6 (d, $^2J_{PC}$ = 10 Hz, 2,6-C_6H_{11}), 25.1 (s, 4-C_6H_{11}), *ipso* carbons not seen, fifth ferrocenyl carbon likely obscured by solvent. ^{31}P {^{1}H} NMR ($CDCl_3$, 162.0 MHz, 300 K) δ/ppm: 41.6 (d, $^2J_{PP}$ = 28 Hz, dppf), 19.8 (t, $^2J_{PP}$ = 28 Hz, PH_2Cy), –143.4 (sep, $^1J_{PF}$ = 713 Hz, PF_6). ^{31}P NMR ($CDCl_3$, 162.0 MHz, 300 K) δ/ppm: 41.6 (d, $^2J_{PP}$ = 28 Hz, dppf), 19.8 (app t, $^1J_{PH}$ = 340 Hz, PH_2Cy), –143.4 (sep, $^1J_{PF}$ = 713 Hz, PF_6). ESI-MS (+, MeCN) *m/z*: 985.2 [M]$^+$. Accurate mass: found 985.1871 [M]$^+$, Calcd. for $C_{49}H_{51}{}^{11}BN_6P_3{}^{56}Fe^{102}Ru$ 985.1874. Anal. Found: C, 51.94; H, 4.64; N, 7.31%. Calcd. For $C_{49}H_{51}BF_6FeN_6P_4Ru$: C, 52.10; H, 4.55; N, 7.44. Crystal data for $[C_{49}H_{51}BFeN_6P_3Ru][PF_6]$: M_W = 1129.59, monoclinic, $P2_1/n$, a = 16.8780(1) Å, b = 15.7177(1) Å, c = 19.3807(2) Å, β = 109.4522(9)°, V = 4847.90(7) Å^3, Z = 4, ρ_{calcd} = 1.548 Mg m^{-3}, μ(Cu Kα) = 6.73 mm^{-1}, T = 150 K, yellow block, 0.10 × 0.07 × 0.04 mm, 76916 measured reflections, 9571 independent (R_{int} = 0.045), F^2 refinement, R = 0.025, wR = 0.058 for 8683 reflections ($I > 2\sigma(I)$, $2\vartheta_{max}$ = 144.8°), 656 parameters with 24 restraints.

Synthesis of [Ru(NCMe)(dppf)(Tp)]PF_6

A mixture of $AgPF_6$ (0.270 g, 0.107 mmol) and [RuCl(dppf)(Tp)] (0.965 g, 0.107 mmol) was stirred in MeCN (80 mL) for 16 hours. Over this period, a colourless precipitate formed. The supernatant was separated by cannula filtration then freed of volatiles *in vacuo*. Nuclear magnetic resonance spectroscopy of the yellow residue showed the major component to be [Ru(NCMe)(dppf)(Tp)]PF_6. Additionally, exposure of the NMR sample to air over 19 hours did not result in any change so the rest of the procedure was conducted under aerobic conditions. The residue was dissolved in MeCN (30 mL), and the volume reduced to *ca*. 5 mL on a rotary evaporator. Diethyl ether (50 mL) was added, and the product collected as a yellow microcrystalline solid by vacuum filtration. Crystals suitable for X-ray diffraction were grown by slow evaporation of solvent from a MeCN/C_6H_6 solution of the product.

Yield: 0.849 g (75%). IR (ATR) ν/cm^{-1}: 3147 w, 3131 w, 3113 w, 3046 w, 2928 (CH), 2561 w (BH), 2278 w (CN). ^{1}H NMR (CD_3CN, 400.1 MHz, 298 K) δ/ppm: 8.29 (s, 2H, pz), 8.22 (s, 1H, pz), 7.97–6.92 (m, 20H, PPh_2), 6.86 (s, 2H, pz), 6.20 (s, 2H, pz), 6.04 (s, 1H, pz), 5.22 (s, 1H, pz), 4.50, 4.35, 4.19 (s × 3, C_5H_4), MeCN signal obscured by CD_3CN. $^{13}C\{^1H\}$ NMR (CD_3CN, 100.62 MHz, 300 K) δ/ppm: 150.1 (s, C^3(pz)), 144.7 (s, 2 × C^3(pz)), 139.2 (s, C^5(pz)), 138.1 (s, 2 × C^5(pz)), 135.9 (t^v, J_{PC} = 5 Hz, *o/m*-PC_6H_5), 135.3 (t^v, J_{PC} = 20 Hz, *ipso*-PC_6H_5), 143.3 (t^v, J_{PC} = 4 Hz, *o/m*-PC_6H_5), 143.2 (t^v, J_{PC} = 21 Hz, *ipso*-PC_6H_5), 131.1 (s, *p*-PC_6H_5), 131.0 (s, *p*-C_6H_5), 129.2 (t^v, J_{PC} = 5 Hz, *o/m*-PC_6H_5), 128.3 (t^v, J_{PC} = 5 Hz, *o/m*-PC_6H_5), 89.5 (t^v, J_{PC} = 25 Hz, 1-C_5H_4), 76.8 (t^v, J_{PC} = 5 Hz, C_5H_4), 74.8 (t^v, J_{PC} = 2 Hz, C_5H_4), 72.7 (t^v, J_{PC} = 2 Hz, C_5H_4), 70.8 (t^v, J_{PC} = 2 Hz, C_5H_4), MeCN signal obscured by CD_3CN. $^{31}P\{^1H\}$ NMR (CD_3CN, 162.0 MHz, 300 K) δ/ppm: 45.2 (s, dppf), –144.6 (sep, $^1J_{PF}$ = 706 Hz, PF_6). ESI-MS (+, MeCN) *m/z*: 910.1 $[M]^+$. Accurate mass: found 910.1398 $[M]^+$, Calcd. for $C_{45}H_{41}{}^{11}BN_7P_2{}^{56}Fe^{102}Ru$ 910.1385. Crystal data for $[C_{45}H_{41}BFeN_7P_2Ru][PF_6].(CH_3CN)$: M_W = 1095.56, monoclinic, $P2_1/n$, a = 16.6573(4) Å, b = 14.6728(3) Å, c = 19.8809(5) Å, β = 109.064(3)°, V = 4592.6(2) Å^3, Z = 4, ρ_{calcd} = 1.548 Mg m^{-3}, μ(Mo, Kα) = 0.82 mm^{-1}, T = 150 K, yellow block, 0.25 × 0.17 × 0.06 mm, 29156 measured reflections, 9706 independent (R_{int} = 0.036), F^2 refinement, R = 0.040, wR = 0.092 for 8033 reflections ($I > 2\sigma(I)$, $2\vartheta_{max}$ = 56.8°), 604 parameters with 0 restraints.

Formation of [Ru(PH_2Cy)(κ^2–$C_6H_4PPh_2$–2)(Tp)]

A THF (30 mL) solution of [RuCl(PPh_3)(PH_2Cy)(Tp)] (0.246g, 0.338 mmol) was added *via* cannula to a suspension of KH (0.047g, 1.17 mmol) in THF (10 mL). After two days of stirring no resonances due to the starting material were observed in the $^{31}P\{^1H\}$ NMR spectrum of the yellow suspension. The supernatant was removed *via* cannula filtration and freed of volatiles *in vacuo*. The product appeared to have formed quantitively by $^{31}P\{^1H\}$ NMR spectroscopy of the residue. All purification attempts were unsuccessful due to the slow decomposition of the product, evident by a colour change to blue as well as an increased number of resonances in the $^{31}P\{^1H\}$ NMR spectrum.

^1H NMR (C_6D_6, 600.0 MHz, 298 K) δ/ppm: 7.83, 7.76, 7.70 (s × 3, 3 × 1H, J_{HH} not resolved, Hpz), 7.61−6.71 (m + s × 3, 17H, 2 × C_6H_5 + 3 × Hpz), 7.53 (m, 1H, 3-C_6H_4, observed via 2D), 7.30 (m, 1H, 6-C_6H_4, observed *via* 2D ^1H–^{13}C HSQC and HMBC), 7.15 (m, 1H, 5-C_6H_4, observed *via* 2D ^1H–^{13}C HSQC and HMBC), 7.09 (m, 1H, 4-C_6H_4, observed *via* 2D ^1H–^{13}C HSQC and HMBC), 6.14, 6.06, 5.47 (s × 3, 3 × 1H, J_{HH} not resolved, Hpz), 4.37 (d, finer coupling not resolved, 1H, $^1J_{PH}$ = 312 Hz, PH), 4.12 (d, finer coupling not resolved, 1H, $^1J_{PH}$ = 318 Hz, PH), 1.34–0.62 (m, 11H, C_6H_{11}). $^{13}C\{^1H\}$ NMR (C_6D_6, 150.9 MHz, 298 K) δ/ppm: 173.9 (dd, $^2J_{PC}$ = 12.8 Hz, $^2J_{PC}$ = 12.8 Hz, 1-C_6H_4), 153.3 (d, $^1J_{PC}$ = 44 Hz, 2-C_6H_4), 143.9, 143.4, 142.5 (s × 3, C^3(pz)), 138.2 (d, $^1J_{PC}$ = 35 Hz, *ipso*-PC_6H_5), 136.4 (d, J = 15 Hz, unknown), 135.1, 135.0, 134.6 (s × 3, C^4(pz)), 134.0 (d, $^2J_{PC}$ = 7.5 Hz, 3-C_6H_4), 131.8 (d, J = 11 Hz, unknown), 129.3 (d, J = 17 Hz, unknown), 128.4 (obscured by solvent, observed by 2D ^1H–^{13}C HSQC and HMBC, 5-C_6H_4), 125.4 (s, 6-C_6H_4), 121.6 (d, $^3J_{PC}$ = 8 Hz, 4-C_6H_4), 33.3 (d, J_{PC} = 5 Hz, 3,5-C_6H_{11}), 32.8 (d, J_{PC} = 3 Hz, 3,5-C_6H_{11}), 31.0 (d, $^1J_{PC}$ = 27 Hz, 1-C_6H_{11}), 27.4 (d, J_{PC} = 9 Hz, 2,6-C_6H_{11}), 27.3 (d, J_{PC} = 11 Hz, 2,6-C_6H_{11}), 26.1 (s, 4-C_6H_{11}). $^{31}P\{^1H\}$ NMR ($CDCl_3$, 162.0 MHz, 298 K) δ/ppm: 16.9 (d, $^2J_{PP}$ = 36 Hz, PH_2Cy), −4.8 (d, $^2J_{PP}$ = 36 Hz, $C_6H_4PPh_2$). ^{31}P NMR ($CDCl_3$, 162.0 MHz, 298 K) δ/ppm: 16.9 (app t, $^1J_{PH}$ = 316 Hz, PH_2Cy), −4.8 (br s, $C_6H_4PPh_2$). ESI-MS (+, MeCN) *m/z*: 693.2 $[M + H]^+$. Accurate mass: found 693.1764 $[M + H]^+$, Calcd. for $C_{33}H_{38}BN_6P_2Ru$ 693.1783.

Reaction of [RuCl(PPh$_3$)$_2$(Tp)] with ^{n}BuLi

A solution of [RuCl(PPh$_3$)$_2$(Tp)] (0.150 g, 0.172 mmol) in THF (10 mL) was cooled in a water/ice bath and ^{n}BuLi (0.13 mL, 1.6 M in hexanes, 0.208 mmol) was added, resulting in a colour change to orange. The mixture was stirred for 5 minutes before the water/ice bath was removed and the mixture allowed to warm to room temperature over 25 minutes. Volatiles were removed *in vacuo* and the resulting orange residue analysed by ^{31}P{^{1}H} NMR spectroscopy. The major components were [RuCl(PPh$_3$)$_2$(Tp)] (*ca*. 68%) and PPh$_3$ (*ca*. 12%). Resonances attributable to [RuH(PPh$_3$)$_2$(Tp)][144] (*ca*. 2%) and RuH(H$_2$C=CHEt)(PPh$_3$)$_2$(Tp)] (*ca*. 4%) were also observed, and these data and the associated ^{1}H NMR hydride resonance are listed below.

Data for [RuH(PPh$_3$)$_2$(Tp)]

^{1}H NMR (C$_6$D$_6$, 400.1 MHz, 298 K) δ/ppm: −13.16 (t, $^2J_{PH}$ = 28 Hz, RuH).

^{31}P {^{1}H} NMR (C$_6$D$_6$, 162.0 MHz, 300 K) δ/ppm: 67.4 (s, PPh$_3$).

Data for RuH(H$_2$C=CHEt)(PPh$_3$)$_2$(Tp)]

^{1}H NMR (C$_6$D$_6$, 400.1 MHz, 298 K) δ/ppm: −13.66 (dd, $^2J_{PH}$ = 24 Hz, $^2J_{PH}$ = 38 Hz, RuH).

^{31}P {^{1}H} NMR (C$_6$D$_6$, 162.0 MHz, 300 K) δ/ppm: 69.2 (d, $^2J_{PP}$ = 32 Hz, PPh$_3$), −4.8 (d, $^2J_{PP}$ = 32 Hz, PPh$_3$).

Reaction of [Ru(PH$_2$Cy)(κ^2–C$_6$H$_4$PPh$_2$–2)(Tp)] with HCl

Using a syringe, a drop of HCl (1 M in Et$_2$O) was added to an NMR tube containing a sample of [Ru(PH$_2$Cy)(κ^2–C$_6$H$_4$PPh$_2$–2)(Tp)] in C$_6$D$_6$. No visible change was observed, but ^{31}P{^{1}H} and ^{31}P NMR spectroscopy showed that the only product was [RuCl(PPh$_3$)(PH$_2$Cy)(Tp)].

Reaction of [Ru(PH$_2$Cy)(κ^2–C$_6$H$_4$PPh$_2$–2)(Tp)] with CO

An NMR sample of [Ru(PH$_2$Cy)(κ^2–C$_6$H$_4$PPh$_2$–2)(Tp)] in C$_6$D$_6$ was subjected to three freeze-pump-thaw cycles before being placed under an atmosphere of CO. The reaction was monitored for 16 hours, over which no change was observed by ^{31}P{^{1}H} NMR spectroscopy.

Reaction of [Ru(PH_2Cy)(κ^2–$C_6H_4PPh_2$–2)(Tp)] with PMe_3

A solution of [RuCl(PPh_3)(PH_2Cy)(Tp)] (0.150 g, 0.206 mmol) in THF (15 mL) was added to a suspension of KH (0.029 g, 0.723 mmol) in THF (10 mL). The mixture was stirred for 7 hours, then subjected to cannula filtration. Trimethylphosphine (0.27 mL, 0.79 M in hexanes, 0.213 mmol) was added to the filtrate and the mixture stirred. The reaction was monitored by $^{31}P\{^1H\}$ spectroscopy, and no PMe_3 substitution was observed after 13 days and the major component of the mixture was [Ru(PH_2Cy)(κ^2–$C_6H_4PPh_2$–2)(Tp)].

Formation of [Ru(PHCy)(κ^2–$C_6H_4PPh_2$–2)(Tp)]$^-$

n-Butyllithium (0.26 mL, 1.6 M in hexanes, 0.416 mmol) was added to a solution of [RuCl(PPh_3)(PH_2Cy)(Tp)] (0.148 g, 0.203 mmol) in THF (10 mL). A colour change to orange resulted and the mixture was stirred for 3 hours. An aliquot taken for NMR spectroscopy at this point showed resonances for [Ru(PHCy)(κ^2-$C_6H_4PPh_2$-2)(Tp)]$^-$ comprising 55% of the mixture. Three other resonances were observed at δ_P 13.8, −7.1 and −32.9.

$^{31}P\{^1H\}$ NMR (THF, 121.5 MHz, 298 K) δ/ppm: −2.8 (d, $^2J_{PP}$ = 18 Hz, $C_6H_4PPh_2$), −48.8 (d, $^2J_{PP}$ = 18 Hz, PHCy). ^{31}P NMR (THF, 121.5 MHz, 298 K) δ/ppm: −2.8 (br s, $C_6H_4PPh_2$), −48.8 (d, $^1J_{PH}$ = 182 Hz, PHCy).

Formation of [Ru(PPh_3)(PH_2Cy)(PHCy)(Tp)]

n-Butyllithium (0.07 mL, 1.6 M in hexanes, 0.112 mmol) was added to a solution of [Ru(PPh_3)(PH_2Cy)$_2$(Tp)]PF_6 (0.101 g, 0.106 mmol) in THF (10 mL). The mixture immediately turned yellow and was stirred for 5.5 hours before it was freed of volatiles *in vacuo*. At this point an NMR sample of the residue was taken for which the major product [Ru(PPh_3)(PH_2Cy)(PHCy)(Tp)] was identified by its resonances listed below. The residue was then extracted with toluene and insoluble material removed by cannula filtration. Freeing the filtrate of volatiles *in vacuo* followed by NMR analysis of the resultant residue showed that it now contained the starting material [Ru(PPh_3)(PH_2Cy)$_2$(Tp)]PF_6 as the major product.

In a separate experiment, a sample of [Ru(PPh_3)(PH_2Cy)(PHCy)(Tp)] was kept under an atmosphere of N_2 in the solid state. After 20 hours its reprotonation to form [Ru(PPh_3)(PH_2Cy)$_2$(Tp)]PF_6 was complete.

$^{31}P\{^1H\}$ NMR (C_6D_6, 162.0 MHz, 300 K) δ/ppm: 55.2 (d, $^2J_{PP}$ = 36 Hz, PPh_3) 48.6 (br s, $^2J_{PP}$ = 31 Hz, PPh_3), 23.8 (dd, $^2J_{PP}$ = 24 Hz, $^2J_{PP}$ = 29 Hz, PH_2Cy), 11.5 (t, $^2J_{PP}$ = 16 Hz, PH_2Cy), –17.0 (app s, $^2J_{PP}$ not resolved, PHCy), –32.0 (dd, $^2J_{PP}$ = 34 Hz, PHCy). ^{31}P NMR (C_6D_6, 162.0 MHz, 300 K) δ/ppm: 55.2 (br s, PPh_3), 48.6 (br s, PPh_3), 23.8 (t, $^1J_{PH}$ = 326 Hz, PH_2Cy), 11.5 (t, $^1J_{PH}$ = 322 Hz, PH_2Cy), –17.0 (d, $^1J_{PH}$ = 172 Hz, PHCy), –32.0 (dd, $^1J_{PH}$ = 174 Hz, $^2J_{PP}$ = 32 Hz, PHCy).

Attempted synthesis of [Ru{PH(AuCl)Cy}(dppf)(Tp)PF_6

Tetrahydrofuran (12 mL) was added to a mixture of [Ru(PH_2Cy)(dppf)(Tp)]PF_6 (0.100g, 0.0885 mmol) and KH (0.017g, 0.42 mmol). The mixture was stirred for 3 days before the supernatant was separated by cannula filtration directly into a flask containing AuCl(SMe_2) (0.042g, 0.143 mmol) with an immediate colour change to black. The mixture was freed of volatiles *in vacuo* and the black residue was found to contain [Ru{PH(AuCl)Cy}(dppf)(Tp)] as the major product (*ca*. 80% by $^{31}P\{^1H\}$ NMR spectroscopy). Toluene (10 mL) was added to the residue and cannula filtration of the mixture yielded a yellow solution from which the volatiles were removed *in vacuo*. Phosphorus-31 NMR spectroscopy of the resulting yellow residue showed that *ca*. 10% of [Ru{PH(AuCl)Cy}(dppf)(Tp)] had decomposed with the appearance of *ca*. 8 new resonances

From the yellow residue, crystals suitable for X-ray diffraction studies were grown *via* two different methods: diffusion of *n*-hexane into a CH_2Cl_2 solution, and diffusion of *n*-hexane into a C_6D_6 solution of the residue. These mixtures yielded two different molecular structures: [Ru{PH(AuCl)Cy}(dppf)(Tp)] and [{RuCl(Tp)}Au(μ-PHCy)(μ-*P,P'*-dppf)]$_2$, respectively. Both sets of crystal data are provided.

$^{31}P\{^1H\}$ NMR (C_6D_6, 162.0 MHz, 300 K) δ/ppm: 37.7 (dd, $^2J_{PP}$ = 24 Hz, $^2J_{PP}$ = 29 Hz PPh_2), 33.2 (dd, $^2J_{PP}$ = 29 Hz, $^2J_{PP}$ = 29 Hz, PPh_2), –10.0 (dd, $^2J_{PP}$ = 24 Hz, $^2J_{PP}$ = 29 Hz, PH{AuCl}Cy). ^{31}P NMR (C_6D_6, 162.0 MHz, 300 K) δ/ppm: 37.7 (br s, PPh_2), 33.2 (br s, PPh_2), –10.0 (d, $^1J_{PH}$ = 300 Hz,

PH{AuCl}Cy). ESI-MS (+, MeCN) *m/z*: 1222.2 [M – Cl + MeCN]$^+$. Accurate mass: found 1222.1733 [M – Cl + MeCN]$^+$, Calcd. for $C_{51}H_{53}{}^{11}BN_7P_3{}^{56}Fe^{102}Ru^{197}Au$ 1222.1727. Crystal data for [$C_{49}H_{50}AuBClFeN_6P_3Ru$]: M_W = 1216.04, monoclinic, $P2_1/n$, a = 15.0055(2) Å, b = 15.7441(1) Å, c = 24.1683(3) Å, β = 102.8310(11)°, V = 5567.14(11) Å^3, Z = 4, ρ_{calcd} = 1.451 Mg m^{-3}, μ(Cu Kα) = 10.62 mm^{-1}, T = 150 K, yellow prism, 0.21 × 0.14 × 0.12 mm, 92613 measured reflections, 11259 independent (R_{int} = 0.038), F^2 refinement, R = 0.045, wR = 0.114 for 10464 reflections ($I > 2\sigma(I)$, $2\vartheta_{max}$ = 148.2°), 568 parameters with 0 restraints.

Crystal data for dimer

Crystal data for ($C_{49}H_{50}AuBClFeN_6P_3Ru$).2($C_6H_6$): M_W = 1372.27, triclinic, $P\bar{1}$, a = 14.2018(3) Å, b = 14.8058(3) Å, c = 16.4376(3) Å, α = 66.0678(17)°, β = 74.8849(16)°, γ = 69.9048(18)°, V = 2937.03(11) Å^3, Z = 2, ρ_{calcd} = 1.552 Mg m^{-3}, μ(Cu Kα) = 10.14 mm^{-1}, T = 150 K, yellow block, 0.10 × 0.10 × 0.06 mm, 57773 measured reflections, 11576 independent (R_{int} = 0.029), F^2 refinement, R = 0.023, wR = 0.060 for 10797 reflections ($I > 2\sigma(I)$, $2\vartheta_{max}$ = 144.8°), 679 parameters with 36 restraints.

7.3 Octahedral Ruthenium Complexes of Cyclohexylphosphine and Their Derivatives

Synthesis of [RuH(Cl)(CO)(PPh_3)$_2$(PH_2Cy)]

A mixture of [RuH(Cl)(CO)(PPh_3)$_3$] (4.428g, 4.65 mmol), PH_2Cy (0.62 mL, 4.67 mmol) and *n*-hexane (50 mL) was stirred while heating under reflux for 1.5 hours. The colourless suspension was allowed to cool and the solid collected by vacuum filtration, washing with petroleum spirits (40-60), EtOH, then petroleum spirits (40-60).

Yield: 3.516g (94%). IR (KBr) ν/cm^{-1}: 3054 m (aromatic CH), 2923 w, 2850 w (CH), 2299 w (PH), 1945 vs (CO). IR (THF) ν/cm^{-1}: 1947 vs (CO). ^{1}H NMR ($CDCl_3$, 400.1 MHz, 298 K) δ/ppm: 7.77 (m, 12H, C_6H_5), 7.36 (m, 18H, C_6H_5), 3.40 (d, 2H, $^1J_{PH}$ = 308 Hz, PH_2), 1.60–0.87 (m, 11H, C_6H_{11}), −5.27 (dt, cis $^2J_{PH}$ = 20 Hz, trans $^2J_{PH}$ = 112 Hz, Ru−H). ^{13}C{^{1}H} NMR ($CDCl_3$, 176.1 MHz, 298 K) δ/ppm: 202.3 (dt, $^2J_{PC}$ = 12 Hz, $^2J_{PC}$ = 9 Hz, CO), 135.2 (t^v, $^1J_{PC}$ = 21 Hz, *ipso*-C_6H_5), 134.2 (t^v, $^1J_{PC}$ = 5 Hz, *o/m*-C_6H_5), 129.7 (s, *p*-C_6H_5), 128.1 (t^v, $^1J_{PC}$ = 5 Hz, *o/m*-C_6H_5), 33.9 (d, $^3J_{PC}$ = 4 Hz, 3,5-C_6H_{11}), 31.6 (d, $^1J_{PC}$ = 21 Hz, 1-C_6H_{11}), 27.2 (d, $^2J_{PC}$ = 9 Hz, 2,6-C_6H_{11}), 25.7 (s, 4-C_6H_{11}). ^{31}P {^{1}H} NMR ($CDCl_3$, 162.0 MHz, 300 K) δ/ppm: 43.9 (d, $^2J_{PP}$ = 16 Hz, 2 × PPh_3), −22.0 (t, $^2J_{PP}$ = 16 Hz,

PH_2Cy). ^{31}P NMR ($CDCl_3$, 162.0 MHz, 300 K) δ/ppm: 43.9 (br s, 2 × PPh_3), −22.0 (dt, $^2J_{PH}$ = 112 Hz, $^1J_{PH}$ = 308 Hz, PH_2Cy). ESI-MS (+, MeCN) *m/z*: 805.1 $[M - H]^+$. Accurate mass: found 805.1259 $[M – H]^+$, Calcd. for $C_{43}H_{43}OP_3{}^{35}Cl^{102}Ru$ 805.1259. ESI-MS (+, MeCN) *m/z*: 807.1 $[M - H]^+$. Accurate mass: found 807.1238 $[M – H]^+$, Calcd. for $C_{43}H_{43}OP_3{}^{37}Cl^{102}Ru$ 807.1229. Anal. Found: C, 64.13; H, 5,58 %. Calcd. For $C_{43}H_{44}ClOP_3Ru$: C, 64.06; H, 5.50 %.

Synthesis of $[RuCl(NCMe)(CO)(PPh_3)_2(PH_2Cy)]PF_6$

A solution of HPF_6 (0.46 mL, 60% *w/v* aqueous solution, 0.185 mmol) in MeCN (30 mL) was added to a solution of $[RuH(Cl)(CO)(PPh_3)_2(PH_2Cy)]$ (1.50g, 0.186 mmol) in CH_2Cl_2 (50 mL) resulting in gas evolution. After 15 hours of stirring the mixture was freed of volatiles *in vacuo* and the rest of the procedure was conducted in air. The residue was recrystallised from $MeCN/Et_2O$ to yield the product as a colourless solid.

Yield 1.70g (92% assuming a PF_6^- anion). IR (KBr) ν/cm^{-1}: 3058 m (aromatic CH), 2929 m, 2852 m (CH), 2320 w, 2320 w (CN), 2290 w (PH), 1978 vs (CO). IR (CH_2Cl_2) ν/cm^{-1}: 1986 s, 1964 sh (CO). IR (THF) ν/cm^{-1}: 1983 sh, 1961 s (CO). ESI-MS (+, MeCN) *m/z*: 846.2 $[M]^+$. Accurate mass: found 846.1530 $[M]^+$, Calcd. for $C_{45}H_{46}NOP_3{}^{35}Cl^{102}Ru$ 846.1524.

Isomer 1 (71%)

^1H NMR (CD_3CN, 400.1 MHz, 298 K) δ/ppm: 4.35 (d overlapping dd, 2H, $^1J_{PH}$ = 372 Hz, $^2J_{PH}$ = 4 Hz, PH_2). ^{31}P $\{^1H\}$ NMR (CD_3CN, 162.0 MHz, 300 K) δ/ppm: 19.6 (d, $^2J_{PP}$ = 15 Hz, PPh_3), −1.8 (t, $^2J_{PP}$ = 15 Hz, PH_2Cy). ^{31}P NMR (CD_3CN, 162.0 MHz, 300 K) δ/ppm: 19.6 (br s, PPh_3), −1.8 (t, $^1J_{PH}$ = 368 Hz, PH_2Cy).

Isomer 2 (18%)

^1H NMR (CD_3CN, 400.1 MHz, 298 K) δ/ppm: 3.78 (d overlapping dd, 2H, $^1J_{PH}$ = 368 Hz, $^2J_{PH}$ = 4 Hz, PH_2). ^{31}P $\{^1H\}$ NMR (CD_3CN, 162.0 MHz, 300 K) δ/ppm: 28.9 (d, $^2J_{PP}$ = 23 Hz, PPh_3), −12.4 (t, $^2J_{PP}$ = 23 Hz, PH_2Cy). ^{31}P NMR (CD_3CN, 162.0 MHz, 300 K) δ/ppm: 28.9 (br s, PPh_3), −12.4 (t, $^1J_{PH}$ = 368 Hz, PH_2Cy).

Isomer 3 (11%)

^{31}P {^{1}H} NMR (CD_3CN, 162.0 MHz, 300 K) δ/ppm: PPh_3 resonance coincident with Isomer 2, −20.9 (t, $^{2}J_{PP}$ = 26 Hz, PH_2Cy).

Synthesis of [RuCl(NCMe)(CO)(PPh_3)$_2$(PH_2Cy)]ClO_4

Caution: perchlorate salts are potentially heat and friction sensitive and explosive

A solution of $HClO_4$ (0.18 mL, 70% w/v aqueous solution, 1.25 mmol) in MeCN (25 mL) was added to a solution of [RuH(Cl)(CO)(PPh_3)$_2$(PH_2Cy)] (1.00 g, 1.24 mmol) in CH_2Cl_2 (50 mL), resulting in gas evolution. The mixture was stirred for 35 minutes then freed of volatiles *in vacuo*. In air, the resulting residue was subjected to ultrasonic trituration in Et_2O to give the product as a white solid. Crystals suitable for X-ray diffraction were grown by slow evaporation of solvent from a concentrated MeCN solution of the compound.

Yield: 1.15 g (98%). Crystal data for $[C_{45}H_{46}ClNOP_3Ru][ClO_4].0.5(C_2H_3N)$: M_w = 966.23, orthorhombic, $Pca2_1$, a = 23.0601(3) Å, b = 10.1663(1) Å, c = 38.8976(5) Å, V = 9118.99(19) Å^3, Z = 8, ρ_{calcd} = 1.408 Mg m^{-3}, μ(Mo, Kα) = 0.61 mm^{-1}, T = 150 K, colourless block, 0.83 × 0.80 × 0.46 mm, 182594 measured reflections, 18531 independent (R_{int} = 0.057), F^2 refinement, R = 0.041, wR = 0.084 for 16972 reflections ($I > 2\sigma(I)$, $2\vartheta_{max}$ = 59.0°), 1035 parameters with 10 restraints.

Isomer 1 (61%)

^{31}P {^{1}H} NMR (CD_3CN, 162.0 MHz, 300 K) δ/ppm: 19.6 (d, $^{2}J_{PP}$ = 30 Hz, PPh_3), −1.9 (t, $^{2}J_{PP}$ = 30 Hz, PH_2Cy). ^{31}P NMR (CD_3CN, 162.0 MHz, 300 K) δ/ppm: 19.6 (s, PPh_3), −1.9 (t, $^{1}J_{PH}$ = 371 Hz, PH_2Cy).

Isomer 2 (18%)

^{31}P {^{1}H} NMR (CD_3CN, 162.0 MHz, 300 K) δ/ppm: 28.9 (d, $^{2}J_{PP}$ = 23 Hz, PPh_3), −12.4 (t, $^{2}J_{PP}$ = 23 Hz, PH_2Cy). ^{31}P NMR (CD_3CN, 162.0 MHz, 300 K) δ/ppm: 28.9 (s, PPh_3), −12.4 (t, $^{1}J_{PH}$ = 377 Hz, PH_2Cy).

Isomer 3 (21%)

^{31}P {^{1}H} NMR (CD_3CN, 162.0 MHz, 300 K) δ/ppm: 28.8 (d, $^{2}J_{PP}$ = 26 Hz, PPh_3), −20.9 (t, $^{2}J_{PP}$ = 26 Hz, PH_2Cy). ^{31}P NMR (CD_3CN, 162.0 MHz, 300 K) δ/ppm: 28.8 (s, PPh_3), −20.9 (t, $^{1}J_{PH}$ = 374 Hz, PH_2Cy).

Synthesis of [RuCl(NCMe)(CO)(PPh_3)$_2$(PH_2Cy)]OTf

A solution of HOTf (0.43 mL, 4.86 mmol) in MeCN (30 mL) was added to a solution of [RuH(Cl)(CO)(PPh_3)$_2$(PH_2Cy)] (3.897 g, 4.834 mmol) in CH_2Cl_2 (50 mL), resulting in gas evolution. The mixture was stirred for 1 hour. In air, the mixture was transferred to a round bottom flask and freed of volatiles on a rotary evaporator. Subjecting the resulting residue to ultrasonic trituration in Et_2O (125 mL) and collecting the colourless solid by vacuum filtration gave the product as a white solid.

Yield: 4.294 g (89%). IR (ATR) ν/cm^{-1}: 3064 w, 3051 w, 2933 w, 2920 w, 2853 w (CH), 2323 w, 2295 w (PH or CN). ESI-MS (+, MeCN) *m/z*: 846.2 $[M]^+$. Accurate mass: found 846.1521 $[M]^+$, Calcd. for $C_{45}H_{46}{}^{14}NOP_3{}^{35}Cl{}^{102}Ru$ 846.1524. Anal. Found: C, 55.44; H, 4.61; N, 1.47 %. Calcd. For $C_{46}H_{46}ClF_3NO_4P_3RuS$: C, 55.51; H, 4.66; N, 1.41 %.

Isomer 1 (59%)

^{31}P {^{1}H} NMR (CD_3CN, 162.0 MHz, 300 K) δ/ppm: 19.6 (d, $^{2}J_{PP}$ = 31 Hz, PPh_3), −1.8 (t, $^{2}J_{PP}$ = 31 Hz, PH_2Cy). ^{31}P NMR (CD_3CN, 162.0 MHz, 300 K) δ/ppm: 19.6 (s, PPh_3), −1.8 (t, $^{1}J_{PH}$ = 371 Hz, PH_2Cy).

Isomer 2 (16%)

^{31}P {^{1}H} NMR (CD_3CN, 162.0 MHz, 300 K) δ/ppm: 28.9 (d, $^{2}J_{PP}$ = 23 Hz, PPh_3), −12.4 (t, $^{2}J_{PP}$ = 23 Hz, PH_2Cy). ^{31}P NMR (CD_3CN, 162.0 MHz, 300 K) δ/ppm: 28.9 (s, PPh_3), −12.4 (t, $^{1}J_{PH}$ = 369 Hz, PH_2Cy).

Isomer 3 (25%)

^{31}P {^{1}H} NMR (CD_3CN, 162.0 MHz, 300 K) δ/ppm: 28.8 (d, $^{2}J_{PP}$ = 26 Hz, PPh_3), −20.8 (t, $^{2}J_{PP}$ = 26 Hz, PH_2Cy). ^{31}P NMR (CD_3CN, 162.0 MHz, 300 K) δ/ppm: 28.8 (s, PPh_3), −20.8 (t, $^{1}J_{PH}$ = 381 Hz, PH_2Cy).

Synthesis of $[RuCl(CO)_2(PPh_3)_2(PH_2Cy)]OTf$

This procedure was conducted under aerobic conditions. Carbon monoxide gas was bubbled through a solution of $[RuCl(NCMe)(CO)(PH_2Cy)(PPh_3)_2]OTf$ (1.50 g, 1.51 mmol) in CH_2Cl_2 (100 mL) for 3 hours. The mixture was freed of volatiles on a rotary evaporator and the colourless residue recrystallised from CH_2Cl_2/^{i}PrOH to yield the product as a colourless powder. Crystals suitable for X-ray diffraction were grown by vapour diffusion of Et_2O into a CH_2Cl_2 solution of the product at −10°C.

Yield: 1.25 g (84%). IR (KBr) ν/cm^{-1}: 3078 w, 3060 w (aromatic CH), 2931 w, 2854 w (aliphatic CH), 2071 vs, 2020 vs (CO). IR (CH_2Cl_2) ν/cm^{-1}: 2078 vs, 2018 vs (CO). IR (THF) ν/cm^{-1}: 2074 vs, 2020 vs (CO). ^{1}H NMR ($CDCl_3$, 400.1 MHz, 298 K) δ/ppm: 7.73−7.49 (m, 30 H, C_6H_5), 4.12 (ddt, $^{1}J_{PH}$ = 372 Hz, $^{3}J_{PH}$ = 8 Hz, $^{3}J_{HH}$ = 8 Hz, 2 H, PH_2), 1.57−0.86 (m, 11 H, C_6H_{11}). $^{13}C\{^{1}H\}$ NMR ($CDCl_3$, 176.1 MHz, 300 K) δ/ppm: 190.9 (m, CO), 190.5 (dt, $^{2}J_{PC}$ = 97 Hz, $^{2}J_{PC}$ = 11 Hz, CO), 133.6 (t^{v}, J_{PC} = 5 Hz, o/m-C_6H_5), 132.2 (s, *p*-C_6H_5), 130.2 (t^{v}, $^{1}J_{PC}$ = 25 Hz, *ipso*-C_6H_5), 129.6 (t^{v}, J_{PC} = 5 Hz, o/m-C_6H_5), 32.9 (d, $^{3}J_{PC}$ = 5 Hz, 3,5-C_6H_{11}), 30.9 (d, $^{1}J_{PC}$ = 26 Hz, 1-C_6H_{11}), 26.8 (d, $^{2}J_{PC}$ = 12 Hz, 2,6-C_6H_{11}), 24.6 (s, 4-C_6H_{11}). ^{31}P {^{1}H} NMR ($CDCl_3$, 162.0 MHz, 300 K) δ/ppm: 17.5 (d, $^{2}J_{PP}$ = 32 Hz, PPh_3), −18.4 (t, $^{2}J_{PP}$ = 32 Hz, PH_2Cy). ^{31}P NMR ($CDCl_3$, 162.0 MHz, 300 K) δ/ppm: 17.5 (d, $^{2}J_{PP}$ = 32 Hz, PPh_3), −20.2 (dt, $^{2}J_{PP}$ = 32 Hz, $^{1}J_{PH}$ = 370 Hz, PH_2Cy). ESI-MS (+, MeCN) *m/z*: 805.1 $[M - CO]^+$. Accurate mass: found 805.1272 $[M - CO]^+$, Calcd. for $C_{43}H_{43}OP_3{}^{35}Cl^{102}Ru$ 805.1259. Anal. Found: C, 54.93; H, 4.51 %. Calcd. For $C_{45}H_{43}ClF_3O_5P_3RuS$: C, 55.02; H, 4.41 %. Crystal data for $[C_{44}H_{43}ClO_2P_3Ru][CF_3SO_3]$: M_w = 982.34, monoclinic $P2_1/c$, a = 11.2204(2) Å, b = 25.2977(4) Å, c = 16.7686(3) Å, β = 99.3034(16)°, V = 4697.16(14) Å^3, Z = 4, ρ_{calcd} = 1.389 Mg m^{-3}, μ(Cu, Kα) = 5.06 mm^{-1}, T = 150 K, colourless block, 0.13 × 0.07 × 0.05 mm, 51547 measured reflections, 9175 independent (R_{int} = 0.028), F^2 refinement, R = 0.025, wR = 0.06 for 8578 reflections ($I > 2\sigma(I)$, $2\vartheta_{max}$ = 144.2°), 538 parameters with 0 restraints.

Synthesis of [RuCl(CO)(CNMes)(PPh_3)$_2$(PH_2Cy)]OTf

Dichloromethane (40 mL) was added to a mixture of [Ru(MeCN)(Cl)(CO)(PH_2Cy)(PPh_3)$_2$]OTf (1.002g, 1.01 mmol) and CNMes (0.146g, 1.01 mmol), immediately forming a brown mixture. The mixture was stirred for 2.5 hours after which the solution IR spectrum showed the formation of bands due to the desired product. The mixture was freed of volatiles *in vacuo* and the residue recrystallised from CH_2Cl_2/^{i}PrOH to give the product as a white powder.

Yield: 0.679g (61%). IR (KBr) ν/cm^{-1}: 3058 w (aromatic CH), 2930 w, 2853 w (aliphatic CH), 2164 s (CN), 1997 vs (CO). IR (CH_2Cl_2) ν/cm^{-1}: 2162 s (CN), 2001 vs (CO). IR (THF) ν/cm^{-1}: 2161 s (CN), 2004 vs (CO). ^{1}H NMR ($CDCl_3$, 400.1 MHz, 298 K) δ/ppm: 7.68−7.38 (m, 30 H, C_6H_5), 6.82 (s, 2 H, $C_6H_2Me_3$), 3.97 (ddt, $^1J_{PH}$ = 360 Hz, $^3J_{PH}$ = $^3J_{HH}$ = 6 Hz, 2 H, PH_2), 2.27 (s, 3H, 4-MeC_6H_2), 1.86 (s, 6H, 2,6-MeC_6H_2), 1.63−0.90 (m, 11 H, C_6H_{11}). ^{13}C{^{1}H} NMR ($CDCl_3$, 176.1 MHz, 300 K) δ/ppm: 194.9 (dt, $^2J_{PC}$ = 14 Hz, $^2J_{PC}$ = 11 Hz, CO), 150.5 (br d, $^2J_{PC}$ = 109 Hz, CNMes), 140.9 (s, 4-Mes), 134.9 (s, 2,6-Mes), 133.7 (t^v, J_{PC} = 5 Hz, o/m-PC_6H_5), 131.7 (s, *p*-C_6H_5), 130.9 (t^v, $^1J_{PC}$ = 24 Hz, i-PC_6H_5), 129.1 (s, 3,5-Mes), 129.1 (t^v, J_{PC} = 5 Hz, o/m-PC_6H_5), 123.2 (s, 1-Mes), 33.1 (d, $^3J_{PC}$ = 5 Hz, 3,5-C_6H_{11}), 31.5 (d, $^1J_{PC}$ = 26 Hz, 1-C_6H_{11}), 26.8 (d, $^1J_{PC}$ = 11 Hz, 2,6-C_6H_{11}), 24.9 (s, 4-C_6H_{11}), 21.4 (s, 4-MeC_6H_2), 18.2 (s, 2,6-MeC_6H_2). ^{31}P {^{1}H} NMR ($CDCl_3$, 162.0 MHz, 300 K) δ/ppm: 20.5 (d, $^2J_{PP}$ = 29 Hz, PPh_3), −12.0 (t, $^2J_{PP}$ = 29 Hz, PH_2Cy). ^{31}P NMR ($CDCl_3$, 162.0 MHz, 300 K) δ/ppm: 20.5 (d, $^2J_{PP}$ = 32 Hz, PPh_3), −12.0 (t, $^1J_{PH}$ = 359 Hz, PH_2Cy). ESI-MS (+, MeCN) *m/z*: 950.2 [M]$^+$. Accurate mass: found 950.2150 [M]$^+$, Calcd. for $C_{53}H_{54}{}^{35}Cl{}^{14}NOP_3{}^{102}Ru$ 950.2150. Anal. Found: C, 58.89; H, 5.02; N, 1.36 %. Calcd. For $C_{54}H_{54}ClF_3NO_4P_3RuS$: C, 58.99; H, 4.95; N, 1.27 %.

Synthesis of [Ru(CO)(PPh_3)$_2$(PH_2Cy)(κ^2-*S,S'*-S_2CNEt_2)]OTf

A solution of Na[S_2CNEt_2] (0.286 g, 1.67 mmol) in EtOH (8 mL) and H_2O (4 mL) was added to a CH_2Cl_2 (50 mL) solution of [RuCl(NCMe)(CO)(PPh_3)$_2$(PH_2Cy)]OTf (1.50 g, 1.51 mmol). The mixture immediately turned yellow and was stirred for 2 hours. At this point, the mixture was exposed to air and transferred to a round-bottom flask. The volume was reduced to *ca.* 10 mL on a rotary evaporator and the yellow precipitate collected by vacuum filtration. This solid was further recrystallised from a CH_2Cl_2/EtOH mixture on a rotary evaporator, giving the product as a yellow microcrystalline powder. A small amount of microanalytically pure

product was obtained by further recrystallisation of the product from CH_2Cl_2/Et_2O. Crystals suitable for X-ray diffraction were grown by liquid diffusion of Et_2O into a $CHCl_3$ solution of the product at −10°C.

Yield: 0.940 g (58%). IR (KBr) ν/cm^{-1}: 3057 w (aromatic CH), 2931 w, 2853 w (aliphatic CH), 2346 w (PH), 1961 vs (CO). IR (THF) ν/cm^{-1}: 2344 w (PH), 1964 vs (CO). ^{1}H NMR ($CDCl_3$, 700.1 MHz, 298 K) δ/ppm: 7.52−7.47 (m, 30H, C_6H_5), 3.79 (d overlapping dd, 2H, $^1J_{PH}$ = 356 Hz, $^3J_{PH}$ = 4.0 Hz, PH_2), 2.91 (q, $^3J_{HH}$ = 8 Hz, N$\underline{CH_2}$CH$_3$), 2.62 (q, $^3J_{HH}$ = 8 Hz, N$\underline{CH_2}$CH$_3$), 1.55–0.82 (m, 11H, C_6H_{11}), 0.68 (t, $^3J_{HH}$ = 8 Hz, NCH$_2\underline{CH_3}$), 0.51 (t, $^3J_{HH}$ = 8 Hz, NCH$_2\underline{CH_3}$). ^{13}C{^{1}H} NMR ($CDCl_3$, 176.1 MHz, 298 K) δ/ppm: 202.0 (s, CS_2), 201.1 (m, CO), 134.5 (t^v, J_{PC} = 5 Hz, o/m-PC_6H_5), 131.1 (s, *p*-PC_6H_5), 130.2 (t^v, $^1J_{PC}$ = 23 Hz, *ipso*-PC_6H_5), 128.6 (t^v, J_{PC} = 5 Hz, o/m-PC_6H_5), 44.2, 43.9 (s × 2, NCH_2), 33.8 (s, C_6H_{11}), 33.0 (d, $^1J_{PC}$ = 30 Hz, 1-C_6H_{11}), 26.9 (d, $^2J_{PC}$ = 11 Hz, 2,6-C_6H_{11}), 25.1 (s, 4-C_6H_{11}), 12.5, 11.8 (s × 2, CH_3). ^{31}P {^{1}H} NMR ($CDCl_3$, 162.0 MHz, 300 K) δ/ppm: 36.1 (d, $^2J_{PP}$ = 23 Hz, PPh_3), −16.6 (t, $^2J_{PP}$ = 23 Hz, PH_2Cy). ^{31}P NMR ($CDCl_3$, 162.0 MHz, 300 K) δ/ppm: 36.1 (br s, PPh_3), −16.6 (t, $^1J_{PH}$ = 348 Hz, PH_2Cy). ESI-MS (+, MeCN) *m/z*: 918.2 [M]$^+$. Accurate mass: found 918.1822 [M]$^+$, Calcd. for $C_{48}H_{53}ONPS_2{}^{102}Ru$ 918.1825. Anal. Found: C, 55.35; H, 4.87; N, 1.36 %. Calcd. For $C_{49}H_{53}F_3NO_4P_3RuS_3$: C, 55.15; H, 5.01; N, 1.31 %. Crystal data for $[C_{48}H_{53}NOP_3RuS_2][CF_3SO_3].2(CHCl_3)$: M_w = 1305.91, triclinic, *P*–1, *a* = 12.1992(1) Å, *b* = 19.2851(3) Å, *c* = 25.2199(3) Å, *α* = 100.2487(12)°, *β* = 95.3343(9)°, *γ* = 96.3096(10)°, *V* = 5764.74(13) Å^3, *Z* = 4, ρ_{calcd} = 1.505 Mg m^{-3}, *μ*(Cu, K*α*) = 7.01 mm^{-1}, *T* = 150 K, colourless needle, 0.55 × 0.22 × 0.14 mm, 102090 measured reflections, 23259 independent (R_{int} = 0.036), F^2 refinement, *R* = 0.044, *wR* = 0.124 for 21525 reflections (*I* > 2*σ*(*I*), $2\vartheta_{max}$ = 143.8°), 1309 parameters with 18 restraints.

Synthesis of [Ru(CO)(PPh$_3$)(PH$_2$Cy)(Tp)]OTf

From [RuCl(NCMe)(CO)(PH$_2$Cy)(PPh$_3$)$_2$]OTf

A mixture of [RuCl(NCMe)(CO)(PH_2Cy)(PPh_3)$_2$]OTf (1.000 g, 1.00 mmol) and KTp (0.255 g, 1.01 mmol) was stirred in THF (50 mL). After 2 hours, the solution IR spectrum of the mixture no longer contained bands for [RuCl(NCMe)(CO)(PH_2Cy)(PPh_3)$_2$]OTf and a fine colourless precipitate had formed. The supernatant was separated *via* cannula filtration and freed of

volatiles *in vacuo*. In air, the residue was subjected to ultrasonic trituration in Et_2O (10 mL) and the colourless solid was collected by vacuum filtration.

Yield: 0.229 g (26%).

From [Ru(OTf)(CO)(PPh_3)(Tp)]

This method is preferred for obtaining microanalytically-pure product. A mixture of [Ru(OTf)(CO)(PPh_3)(Tp)] (0.300 g, 0.398 mmol) and PH_2Cy (0.26 mL, 2.0 mmol) in THF (15 mL) was heated under reflux with stirring for 15 hours. The mixture was allowed to cool to room temperature, then freed of volatiles *in vacuo*. From this point, the procedure was conducted under aerobic conditions. The residue was subjected to ultrasonic trituration in Et_2O (20 mL) and the product collected as a colourless powder.

Yield: 0.228 g (65%).

From [RuH(CO)(PPh_3)(Tp)], HOTf and PH_2Cy

This method is best suited for larger-scale syntheses and the product is sufficiently pure for subsequent synthetic manipulations. Triflic acid (0.32 mL, 3.62 mmol) was added to a solution of [RuH(CO)(PPh_3)(Tp)] (2.00 g, 3.30 mmol) in THF (80 ml). Effervescence was observed and the mixture was stirred for 30 minutes. Cyclohexylphosphine (0.77 mL, 5.80 mmol) was then added and the mixture heated under reflux with stirring for 16 hours. The mixture was allowed to cool to room temperature and freed of volatiles *in vacuo*. From this point the procedure was conducted under aerobic conditions. The residue was subjected to ultrasonic trituration in Et_2O (50 mL) and the product collected as a colourless solid by vacuum filtration.

Yield: 2.449 g (85%).

Crystals suitable for X-ray diffraction were grown by vapour diffusion of Et_2O into a CH_2Cl_2 solution of the product at −15°C.

IR (KBr) ν/cm^{-1}: 3117 w, 3064 w (aromatic CH), 2937 w, 2853 w (aliphatic CH), 2523 w (BH), 2328 w (PH), 1984 vs (CO). IR (CH_2Cl_2) ν/cm^{-1}: 3131 w, 3063 w (aromatic CH), 2937 w, 2857 w (aliphatic CH), 2499 w (BH), 2351 w (PH), 1996 vs (CO). IR (THF) ν/cm^{-1}: 2494 w (BH), 1985 vs (CO). ^{1}H NMR ($CDCl_3$, 700.22 MHz, 298 K) δ/ppm: 7.85, 7.84, 7.83, 7.73, 7.67, 6.45, 6.32, 6.14, 6.03 (s x 9, 9 × 1H, J_{HH} not resolved, pz), 7.51, 7.43, 7.08 (m × 3, 15H, C_6H_5), 4.61 (br s, 1H, BH), 4.56 (d app t, 1H, $^1J_{PH}$ = 364 Hz, J = 7 Hz, PH), 3.88 (d app quintet, 1H, $^1J_{PH}$ = 357 Hz, J = 7 Hz, PH), 2.20–0.87 (m, 11H, C_6H_{11}). ^{13}C{^{1}H} NMR ($CDCl_3$, 176.1 MHz, 298 K) δ/ppm: 200.9 (dd, $^2J_{PC}$ = 14 Hz, CO), 145.2, 144.4, 144.0 (s × 3, 3 × C^3(pz)), 137.4, 137.3, 136.9 (s × 3, 3 × C^5(pz)), 133.5 (d, J_{PC} = 11 Hz, o/m-PC_6H_5), 131.7 (s, *p*-PC_6H_5), 129.7 (d, $^1J_{PC}$ = 48 Hz, *ipso*-PC_6H_5), 129.4 (d, J_{PC} = 11 Hz, o/m-PC_6H_5), 107.7, 107.6, 107.1 (s × 3, 3 × C^4(pz)), 33.1 (d, $^3J_{PC}$ = 7 Hz, 3,5-C_6H_{11}), 31.7 (d, $^3J_{PC}$ = 4 Hz, 3,5-C_6H_{11}), 30.2 (d, $^1J_{PC}$ = 31.7 Hz, 1-C_6H_{11}), 26.9 (d, $^2J_{PC}$ = 7 Hz, 2,6-C_6H_{11}), 26.8 (d, $^2J_{PC}$ = 7 Hz, 2,6-C_6H_{11}), 25.2 (s, 4-C_6H_{11}). ^{31}P {^{1}H} NMR ($CDCl_3$, 162.0 MHz, 300 K) δ/ppm: 38.4 (d, $^2J_{PP}$ = 28 Hz, PPh_3), −6.6 (d, $^2J_{PP}$ = 28 Hz, PH_2Cy). ^{31}P NMR ($CDCl_3$, 162.0 MHz, 300 K) δ/ppm: 38.4 (br s, PPh_3), −6.6 (app t, $^1J_{PH}$ = 358 Hz, PH_2Cy). ESI-MS (+, MeCN) *m/z*: 721.2 [M]$^+$. Accurate mass: found 721.1710 [M]$^+$, Calcd for $C_{34}H_{38}{}^{11}BON_6P_2{}^{102}Ru$ 721.1713. Anal. Found: C, 48.23; H, 4.50; N, 9.55 %. Calcd. For $C_{35}H_{38}BF_3N_6O_4P_2RuS$: C, 48.34; H, 4.40; N, 9.66 %. Crystal data for $[C_{34}H_{38}BON_6P_2Ru][CF_3O_3S].(CH_2Cl_2)$: M_w = 954.54, monoclinic, $P2_1/c$, a = 13.3148(2) Å, b = 15.2137(2) Å, c = 20.0334(2) Å, β = 91.1333(12)°, V = 4055.30(4) Å^3, Z = 4, ρ_{calcd} = 1.583 Mg m^{-3}, μ(Cu, Kα) = 6.09 mm^{-1}, T = 150 K, colourless plate, 0.15 × 0.10 × 0.03 mm, 22624 measured reflections, 7851 independent (R_{int} = 0.031), F^2 refinement, R = 0.034, wR = 0.091 for 6770 reflections ($I > 2\sigma(I)$, $2\vartheta_{max}$ = 144°), 505 parameters with 0 restraints.

Reaction of $[RuCl(CO)_2(PPh_3)_2(PH_2Cy)]OTf$ with DBU

1,8-Diazabicyclo[5.4.0]undec-7-ene (0.08 mL, 0.535 mmol) was added to a suspension of $[RuCl(CO)_2(PPh_3)_2(PH_2Cy)]OTF$ (0.500 g, 0.509 mmol) in benzene (20 mL). An immediate colour change to red occurred concurrently with the dissolution of all solids. After 45 minutes of stirring the colour had faded to orange. The spectral data provided below were acquired from aliquots taken at this time. Stirring was continued for a total time of 2 hours, followed by the removal of volatiles *in vacuo*. The addition of methanol to this residue resulted in the disappearance of the low frequency phosphido ^{31}P{^{1}H} NMR resonances. Attempts to

recrystallise the residue from combinations of benzene, *n*-hexane and diethyl ether did not result in any appreciable change in the proportions of the products.

IR (C_6H_6) ν/cm^{-1}: 2033 sh, 2022 s, 1968 vs, 1899 m (CO). $^{31}P\{^1H\}$ NMR (C_6D_6, 162.0 MHz, 300 K) δ/ppm: 55.7 (s), 23.4 (d, J = 3 Hz), 23.2 (d, J = 8 Hz), 20.7 (d, J = 26 Hz), 12.0 (t, J = 24 Hz), –5.31 (s), −50.7 (br s). ^{31}P NMR (C_6D_6, 162.0 MHz, 300 K) δ/ppm: 55.7 (br s), 23.3 (br s), 20.7 (br s), –5.3 (br s), −50.7 (d, $^1J_{PH}$ = 180 Hz, PHCy).

Reaction of [Ru(CO)(PPh$_3$)$_2$(PH$_2$Cy)(κ^2-*S,S'*-S$_2$CNEt$_2$)]OTf with DBU

1,8-Diazabicyclo[5.4.0]undec-7-ene (0.05 mL, 0.334 mmol) was added to a suspension of [Ru(CO)(PPh$_3$)$_2$(PH$_2$Cy)(κ^2-*S,S'*-S$_2$CNEt$_2$)]OTf (0.300 g, 0.281 mmol) in benzene (10 mL). An immediate colour change to red was observed, and the mixture faded to yellow over 10 minutes. Stirring was continued for 2 hours, after which no solid was observed in the mixture. Volatiles were removed *in vacuo*, and $^{31}P\{^1H\}$ NMR analysis of the residue revealed over 30 resonances. Amongst these, PPh$_3$ was the major product.

Synthesis of [Ru(CO)$_2$(PPh$_3$)$_2${PH(OMe)Cy}]

1,8-Diazabicyclo[5.4.0]undec-7-ene (0.55 mL, 3.68 mmol) was added to a suspension of [RuCl(CO)$_2$(PPh$_3$)$_2$(PH$_2$Cy)]OTf (1.63 g, 1.66 mmol) in MeOH (25 mL). The mixture immediately turned orange, and was heated under reflux with stirring for 1 hour. Upon cooling to room temperature, the suspended orange product was collected by vacuum filtration and washed with methanol, ethanol and *n*-pentane.

Yield: 1.124g (82%). IR (KBr) ν/cm^{-1}: 3053 w, 2925 w, 2850 w (CH), 2234 w (PH), 1921 m, 1913 s, 1859 vs (CO), 1029 m (PO). IR (THF) ν/cm^{-1}: 1911 s, 1862 vs (CO). ^1H NMR (C_6D_6, 400.1 MHz, 298 K) δ/ppm: 7.82−6.96 (m, 30H PPh$_3$), 6.41 (dddd, 1H, $^1J_{PH}$ = 308 Hz, 2 × $^3J_{PH}$ = 8 Hz, $^3J_{HH}$ = 4 Hz, PH), 3.03 (d, 3H, $^3J_{PH}$ = 5 Hz, OMe), 2.27−0.91 (m, 11H, C_6H_{11}). $^{13}C\{^1H\}$ NMR (C_6D_6, 176.1 MHz, 298 K) δ/ppm: 216.1 (t, $^2J_{PC}$ = 13 Hz, CO), 138.9 (dt^v, $^vJ_{PC}$ = 21 Hz, $^3J_{PC}$ = 4 Hz, *ipso*-C_6H_5), 134.3 (t^v, J_{PC} = 6 Hz, o/m-C_6H_{11}), 129.3 (s, *p*-C_6H_{11}), o/m-C_6H_{11} obscured by solvent, 42.6 (d, $^2J_{PC}$ = 25 Hz, OCH_3), 29.4 (d, $^1J_{PC}$ = 81 Hz, 1-C_6H_{11}), 27.3 (d, $^3J_{PC}$ = 2 Hz, 3,5-C_6H_{11}), 27.3 (d, $^2J_{PC}$ = 7 Hz, 2,6-C_6H_{11}), 26.8 (s, 4-C_6H_{11}). $^{31}P\{^1H\}$ NMR (C_6D_6, 162.0 MHz, 300 K) δ/ppm: 158.5 (t, $^2J_{PP}$

= 16 Hz, PH(OMe)Cy), 54.9 (d, $^{2}J_{PP}$ = 16 Hz, PPh_3). ^{31}P NMR (C_6D_6, 162.0 MHz, 300 K) δ/ppm: 158.5 (d, $^{1}J_{PH}$ = 305 Hz, PH(OMe)Cy), 54.9 (br s, PPh_3). ESI-MS (+, MeCN) *m/z*: 829.2 $[M + H]^+$. Accurate mass: found 829.1702 $[M + H]^+$, Calcd for $C_{45}H_{46}O_3P_3{}^{102}Ru$ 829.1703. Anal. Found: C, 65.31; H, 5.63%. Calcd. For $C_{45}H_{45}O_3P_3Ru$: C, 65.29; H, 5.48.

Formation of [Ru(CO)(CNMes)(PPh_3)$_2${PH(OMe)Cy}]

1,8-Diazabicyclo[5.4.0]undec-7-ene (0.10 mL, 0.585 mmol) was added to a solution of [RuCl(CO)(CNMes)(PPh_3)$_2$(PH_2Cy)]OTf (0.300 g, 0.273 mmol) in MeOH (15 mL), causing an immediate colour change to orange and precipitate formation. After 20 minutes of stirring the precipitate dissolved and after 1.5 hours the mixture had faded to a pale yellow colour. Removal of volatiles *in vacuo* resulted in a reversion to orange, and a residue with the following NMR data:

^{31}P{^{1}H} NMR (C_6D_6, 162.0 MHz, 300 K) δ/ppm: 160.1 (t, $^{2}J_{PP}$ = 71 Hz, PH(OMe)Cy), 53.3 (d, $^{2}J_{PP}$ = 71 Hz, PPh_3). ^{31}P NMR (C_6D_6, 162.0 MHz, 300 K) δ/ppm: 160.1 (dt, $^{2}J_{PP}$ = 71 Hz, $^{1}J_{PH}$ = 305 Hz, PH(OMe)Cy), 53.3 (d, $^{2}J_{PP}$ = 71 Hz, PPh_3).

The presence of methanol causes a colour change to yellow and rearrangement to two new isomers with the following NMR data:

Isomer 1

^{31}P{^{1}H} NMR (C_6D_6, 162.0 MHz, 300 K) δ/ppm: 150.8 (dd, $^{2}J_{PP}$ = 23 Hz, $^{2}J_{PP}$ = 228 Hz, PH(OMe)Cy), 37.6 (d, $^{2}J_{PP}$ = 23 Hz, $^{2}J_{PP}$ = 228 Hz, PPh_3), 26.0 (dd, $^{2}J_{PP}$ = 23 Hz, $^{2}J_{PP}$ = 23 Hz, PPh_3).

Isomer 2

^{31}P{^{1}H} NMR (C_6D_6, 162.0 MHz, 300 K) δ/ppm: 153.0 (dd, $^{2}J_{PP}$ = 19 Hz, $^{2}J_{PP}$ = 228 Hz, PH(OMe)Cy), 38.1 (dd, $^{2}J_{PP}$ = 19 Hz, $^{2}J_{PP}$ = 228 Hz, PPh_3), 28.5 (dd, $^{2}J_{PP}$ = 19 Hz, $^{2}J_{PP}$ = 19 Hz, PPh_3).

Formation of $[Ru(CO)_3(PPh_3)\{PH(OMe)Cy\}]$

Carbon monoxide gas was bubbled through a solution of $[Ru(CO)_2(PPh_3)_2\{PH(OMe)Cy\}]$ (0.150 g, 0.181 mmol) in THF (10 mL) for 45 minutes. The IR spectrum of the mixture at this time showed the ν_{CO} bands for $[Ru(CO)_2(PPh_3)_2\{PH(OMe)Cy\}]$ (1911, 1861 cm^{-1}) as well as the development of a new ν_{CO} absorption at 1907 cm^{-1}. Carbon monoxide gas was passed through the solution for a further 45 minutes. The flask was then sealed and stirred for 16 hours, after which there was no $[Ru(CO)_2(PPh_3)_2\{PH(OMe)Cy\}]$ detected by IR spectroscopy. The mixture was freed of volatiles *in vacuo*. Analysis of the yellow residue by $^{31}P\{^1H\}$ NMR spectroscopy showed that $[Ru(CO)_3(PPh_3)\{PH(OMe)Cy\}]$ and PPh_3 were the major products. The residue was highly soluble in *n*-pentane, *n*-hexane, Et_2O, THF, benzene, toluene and methanol, and concentrating solutions of these solvents did not yield any precipitate. High solubility in ethanol was also observed, but a precipitate formed upon reducing the volume to *ca*. 2 mL *in vacuo*. After isolating the precipitate by cannula filtration, $^{31}P\{^1H\}$ NMR spectroscopy showed that it was still *ca*. 30% impure. Purification of the residue was also attempted by column chromatography on silica with 2:1 CH_2Cl_2/*n*-hexane as the eluent. The first band contained only PPh_3, while the product was collected as the second, yellow band. While a number of impurities had been removed, $^{31}P\{^1H\}$ NMR spectroscopy of this fraction also showed two resonances at δ_P 55.7 and 39.1 which were estimated to comprise *ca*. 40% of the mixture.

IR (THF) ν/cm^{-1}: 1906 vs (CO). $^{31}P\{^1H\}$ NMR (C_6D_6, 162.0 MHz, 300 K) δ/ppm: 155.0 (d, $^2J_{PP}$ = 194 Hz, PH(OMe)Cy), 53.2 (d, $^2J_{PP}$ = 194 Hz, PPh_3). ^{31}P NMR (C_6D_6, 162.0 MHz, 300 K) δ/ppm: 155.0 (dd, $^1J_{PH}$ = 358 Hz, $^2J_{PP}$ = 194 Hz, PH(OMe)Cy), 53.2 (d, $^2J_{PP}$ = 194 Hz, PPh_3). ESI-MS (+, MeCN) *m/z*: 595.1 $[M + H]^+$. Accurate mass: found 595.0742 $[M + H]^+$, Calcd. for $C_{28}H_{31}O_4{}^{31}P_2{}^{102}Ru$ 595.0741.

Formation of $[Ru(CO)_2(CNMes)(PPh_3)\{PH(OMe)Cy\}]$

From $[Ru(CO)(CNMes)(PPh_3)_2\{PH(OMe)Cy\}]$

An NMR sample of $[Ru(CO)(CNMes)(PPh_3)_2\{PH(OMe)Cy\}]$ in C_6D_6 was subjected to three freeze-pump-thaw cycles before being placed under an atmosphere of CO. The reaction was monitored for 18 hours, after which no $^{31}P\{^1H\}$ NMR resonances for

[Ru(CO)(CNMes)(PPh_3)$_2${PH(OMe)Cy}] were observed. Signals for PPh_3 and [Ru(CO)$_2$(CNMes)(PPh_3){PH(OMe)Cy}] were present, amongst others.

From [Ru(CO)$_2$(PPh_3)$_2${PH(OMe)Cy}]

Mesityl isocyanide (0.043 g, 0.296 mmol) and [Ru(CO)$_2$(PPh_3)$_2${PH(OMe)Cy}] (0.200 g, 0.242 mmol) were dissolved in THF (10 mL). The reaction was monitored by $^{31}P\{^1H\}$ NMR spectroscopy and after 25 hours of stirring no signals for [Ru(CO)$_2$(PPh_3)$_2${PH(OMe)Cy}] were observed. The signals for [Ru(CO)$_2$(CNMes)(PPh_3){PH(OMe)Cy}] and PPh_3 represented the major products in addition to some minor components (<5%). The volume of solvent was reduced to *ca*. 1 mL *in vacuo*, *n*-hexane (9 mL) was added and the flask placed in a −20°C freezer. A yellow precipitate formed overnight and the mixture was subjected to cannula filtration, with the filtrate freed of volatiles *in vacuo*. Analysis of both fractions by NMR spectroscopy showed that the precipitate had an increased number of resonances, while the bulk of [Ru(CO)$_2$(CNMes)(PPh_3){PH(OMe)Cy}] was contained in the filtrate. No separation of components from the filtrate *via* thin-layer chromatography was observed when using CH_2Cl_2 or THF as the mobile phase. Ultimately, the residue obtained from the filtrate was dissolved in Et_2O (15 mL) and placed in a −20°C freezer. After several weeks only crystals of [Ru(CO)$_2$(CNMes)(PPh_3)$_2$] formed which were characterised by X-ray crystallography.

IR (THF) ν/cm^{-1}: 2046 (CNMes), 1911 vs, 1875 vs (CO). $^{31}P\{^1H\}$ NMR (C_6D_6, 162.0 MHz, 300 K) δ/ppm: 159.6 (d, $^2J_{PP}$ = 188 Hz, PH(OMe)Cy), 56.1 (d, $^2J_{PP}$ = 188 Hz, PPh_3). ^{31}P NMR (C_6D_6, 162.0 MHz, 300 K) δ/ppm: 159.6 (dd, $^1J_{PH}$ = 347 Hz, $^2J_{PP}$ = 188 Hz, PH(OMe)Cy), 56.1 (d, $^2J_{PP}$ = 188 Hz, PPh_3).

Crystal data for [Ru(CO)$_2$(CNMes)(PPh_3)$_2$]

Crystal data for [$C_{48}H_{41}NO_2P_2Ru$]: M_w = 826.88, triclinic, *P*−1, *a* = 11.5539(2) Å, *b* = 11.7273(3) Å, *c* = 16.2669(3) Å, *α* = 93.1308(18)°, *β* = 102.3482(17)°, *γ* = 108.2973(19)°, *V* = 2026.56(4) Å^3, *Z* = 2, ρ_{calcd} = 1.355 Mg m^{-3}, μ(Cu, K*α*) = 4.18 mm^{-1}, *T* = 150 K, yellow block, 0.16 × 0.10 × 0.06 mm, 33291 measured reflections, 8187 independent (R_{int} = 0.034), F^2 refinement, *R* = 0.038, *wR* = 0.104 for 7564 reflections (*I* > 2*σ*(*I*), $2\vartheta_{max}$ = 147.6°), 487 parameters with 0 restraints.

Formation of [Ru(CO)$_2${PH(OMe)Cy}(dppe)]

1,2-bis(diphenylphosphino)ethane (0.147 g, 0.369 mmol) and [Ru(CO)$_2$(PPh$_3$)$_2${PH(OMe)Cy}] (0.202 g, 0.244 mmol) were dissolved in THF (15 mL) and stirred. The reaction was monitored by ^{31}P{^{1}H} NMR spectroscopy and after 22 hours no resonances for [Ru(CO)$_2$(PPh$_3$)$_2${PH(OMe)Cy}] were observed. Volatiles were removed *in vacuo*, and ^{31}P{^{1}H} NMR spectroscopy revealed [Ru(CO)$_2$(dppe){PH(OMe)Cy}] and PPh$_3$ to be the major products. Recrystallisation from concentrated solutions of MeOH, EtOH, Et$_2$O and *n*-hexane all did not significantly improve the purity of the product.

IR (THF) ν/cm^{-1}: 1914 s, 1858 vs (CO). ^{31}P{^{1}H} NMR (C$_6$D$_6$, 162.0 MHz, 300 K) δ/ppm: 163.5 (d, $^2J_{PP}$ = 86 Hz, PH(OMe)Cy), 73.5 (d, $^2J_{PP}$ = 86 Hz, dppe). ^{31}P NMR (C$_6$D$_6$, 162.0 MHz, 300 K) δ/ppm: 163.5 (dd, $^1J_{PH}$ = 342 Hz, $^2J_{PP}$ = 86 Hz, PH(OMe)Cy), 73.5 (d, $^2J_{PP}$ = 86 Hz, dppe).

Formation of [Ru(CO)(PPh$_3$)$_2${PH(OMe)Cy}(κ^2-O$_2$CO)]

A solid sample of [Ru(CO)$_2$(PPh$_3$)$_2${PH(OMe)Cy}] was allowed to stand in air for 7 months. At this point, the solid had turned brown and the IR spectrum showed the presence of a new ν_{CO} band at 1657 cm^{-1}. The sample used for analysis was recrystallised from a mixture of CH$_2$Cl$_2$ and *n*-hexane on a rotary evaporator. Crystals suitable for X-ray diffraction were grown by vapour diffusion of *n*-hexane into a CH$_2$Cl$_2$ solution of the compound.

IR (ATR) ν/cm^{-1}: 3052 w, 2926 w, 2854 w (CH), 2274 w (PH), 1942 vs (CO), 1657 vs (CO). ^{1}H NMR (C$_6$D$_6$, 400.1 MHz, 298 K) δ/ppm: 7.57−7.37 (m, 30H, PPh$_3$), 5.77 (br d, 1H, $^1J_{PH}$ = 353 Hz, PH), 3.24 (d, 3H, $^3J_{PH}$ = 11 Hz, OMe), 1.94−0.75 (m, 11H, Cy). ^{13}C{^{1}H} NMR (C$_6$D$_6$, 201.2 MHz, 298 K) δ/ppm: 202.8 (coupling not resolved, CO), 164.2 (s, CO$_3$), 134.8 (d, J_{PC} = 10 Hz, o/m-C$_6$H$_5$), 134.6 (d, J_{PC} = 10 Hz, o/m-C$_6$H$_5$), 131.1 (d, $^1J_{PC}$ = 42 Hz, *ipso*-C$_6$H$_5$), 130.6 (s, *p*-C$_6$H$_5$), 130.4 (s, *p*-C$_6$H$_5$), 128.4 (d, J_{PC} = 10 Hz, o/m-C$_6$H$_5$), 128.1 (d, J_{PC} = 10 Hz, o/m-C$_6$H$_5$), 62.4 (d, $^2J_{PC}$ = 16 Hz, OCH$_3$), 44.0 (d, $^1J_{PC}$ = 24 Hz, 1-C$_6$H$_{11}$), 28.4 (d, $^3J_{PC}$ = 4 Hz, 3,5-C$_6$H$_{11}$), 28.1 (s, 3,5-C$_6$H$_{11}$), 26.6 (d, $^2J_{PC}$ = 10 Hz, 2,6-C$_6$H$_{11}$), 26.5 (d, $^2J_{PC}$ = 14 Hz, 2,6-C$_6$H$_{11}$), 25.8 (s, 4-C$_6$H$_{11}$). ^{31}P{^{1}H} NMR (CDCl$_3$, 162.0 MHz, 298 K) δ/ppm: 164.2 (dd, $^2J_{PP}$ ≈ 24 Hz, PH(OMe)Cy), 32.5[***] (dd, $^2J_{PP}$ = 23

[***] Chemical shifts and coupling constants were determined by treating the resonance as an ABX spin system.

Hz, $^2J_{PP}$ = 340 Hz, PPh_3), 29.9*** (dd, $^2J_{PP}$ = 26 Hz, $^2J_{PP}$ = 340 Hz, PPh_3). ^{31}P NMR ($CDCl_3$, 162.0 MHz, 298 K) δ/ppm: 164.2 (d, $^1J_{PH}$ = 356 Hz PH(OMe)Cy), 32.5 (d, $^2J_{PP}$ = 340 Hz, PPh_3), 29.9 (dd, $^2J_{PP}$ = 340 Hz, PPh_3). ESI-MS (+, MeCN) *m/z*: 861.2 $[M + H]^+$. Accurate mass: found 861.1578 $[M + H]^+$, Calcd. for $C_{45}H_{46}O_5P_3Ru$ 861.1598. Anal. Found: C, 61.43; H, 4.55%. Calcd. For $C_{45}H_{45}O_5P_3Ru$: C, 62.86; H, 5.28 (satisfactory data not acquired). Crystal data for $[C_{45}H_{45}O_5P_3Ru].2(CH_2Cl_2)$: M_w = 1029.70, triclinic, *P*−1, *a* = 11.9551(4) Å, *b* = 13.2531(4) Å, *c* = 17.9666(6) Å, *α* = 99.701(3)°, *β* = 109.416(3)°, *γ* = 107.375(3)°, *V* = 2446.26(17) Å^3, *Z* = 2, ρ_{calcd} = 1.398 Mg m^{-3}, μ(Mo, K*α*) = 0.68 mm^{-1}, *T* = 150 K, colourless prism, 0.31 × 0.18 × 0.13 mm, 43818 measured reflections, 12291 independent (R_{int} = 0.050), F^2 refinement, *R* = 0.071, *wR* = 0.206 for 8989 reflections (*I* > *2σ(I)*, $2\vartheta_{max}$ = 60.2°), 551 parameters with 42 restraints.

Attempted deprotonation of $[Ru(CO)_2(PPh_3)_2\{PH(OMe)Cy\}]$

A solution of $[Ru(CO)_2(PPh_3)_2\{PH(OMe)Cy\}]$ (0.200 g, 0.242 mmol) in THF (10 mL) was cooled to −78°C in a dry ice/acetone bath. *n*-Butyllithium (0.17 mL, 1.6 M in hexanes, 0.272 mmol) was added to the mixture, causing a colour change to orange. Stirring was continued for 1 hour before the cooling bath was removed and the mixture allowed to warm to room temperature. During warming the mixture turned a deep red, and the IR spectrum (THF) showed new bands at 2003 m, 1996 m, 1967 s, 1935 s and 1916 s cm^{-1} along with starting material bands at 1911 s and 1861 vs cm^{-1}. The $^{31}P\{^1H\}$ NMR spectrum showed that $[Ru(CO)_2(PPh_3)_2\{PH(OMe)Cy\}]$ was the major product (58%). PPh_3 was also present (18%) along with four resonances in the range 40-50 ppm.

In a confirmatory experiment, the above addition of ^{n}BuLi was conducted followed by the immediate addition of D_2O. No deuterium incorporation was observed in the $^{31}P\{^1H\}$ NMR spectrum of the product.

Attempted synthesis of $[RuH(C{\equiv}CPh)(CO)_2(PPh_3)\{PH(OMe)Cy\}]$

Phenylacetylene (0.25 mL, 0.25 mmol) was added to a solution of $[Ru(CO)_2(PPh_3)_2\{PH(OMe)Cy\}]$ (0.200 g, 0.241 mmol). The mixture was stirred and monitored by $^{31}P\{^1H\}$ NMR spectroscopy. After 5 days, no more $[Ru(CO)_2(PPh_3)_2\{PH(OMe)Cy\}]$ was observed and the mixture was freed of volatiles *in vacuo*. The two major products, expected

to be two isomers of [RuH(C≡CPh)(CO)$_2$(PPh$_3$){PH(OMe)Cy}], constituted around 42% of the products observed. Purification could not be achieved, and limited spectral data are reported below.

Combined $^{31}P\{^1H\}$ and ^{31}P NMR data

$^{31}P\{^1H\}$ NMR (C_6D_6, 162.0 MHz, 300 K) δ/ppm: 150.8 (d, $^2J_{PP}$ = 273 Hz, PH(OMe)Cy), 150.1 (d, $^2J_{PP}$ = 273 Hz, PH(OMe)Cy), 40.9 (d, $^2J_{PP}$ = 273 Hz, PPh$_3$), 40.7 (d, $^2J_{PP}$ = 273 Hz, PPh$_3$). ^{31}P NMR (C_6D_6, 162.0 MHz, 300 K) δ/ppm: 150.8 (dd, $^1J_{PH}$ = 377 Hz, $^2J_{PP}$ = 273 Hz, PH(OMe)Cy), 150.1 (dd, $^1J_{PH}$ = 381 Hz, $^2J_{PP}$ = 273 Hz, PH(OMe)Cy), 40.9 (d, $^2J_{PP}$ = 273 Hz, PPh$_3$), 40.7 (d, $^2J_{PP}$ = 273 Hz, PPh$_3$).

cis-*Isomer*

IR (THF) ν/cm^{-1}: 2032 s, 1983 s (CO). ^1H NMR (C_6D_6, 400.1 MHz, 298 K) δ/ppm: –5.80 (dd, $^2J_{PH}$ = 20 Hz, $^2J_{PH}$ = 24 Hz, RuH), –5.81 (dd, $^2J_{PH}$ = 20 Hz, $^2J_{PH}$ = 24 Hz, RuH).

trans-*Isomer*

IR (THF) ν/cm^{-1}: 1945 m (CO). ^1H NMR (C_6D_6, 400.1 MHz, 298 K) δ/ppm: –6.06 (dd, $^2J_{PH}$ = 20 Hz, $^2J_{PH}$ = 24 Hz, RuH).

Reaction of [Ru(CO)$_2$(PPh$_3$)$_2$\{PH(OMe)Cy\}] with HBF$_4$.Et$_2$O

Tetrafluoroboric acid diethyl etherate (0.1 mL, 0.679 mmol) was added to a solution of [Ru(CO)$_2$(PPh$_3$)$_2$\{PH(OMe)Cy\}] (0.250 g, 0.302 mmol) in THF (15 mL). The mixture immediately turned colourless. After 15 minutes of stirring at room temperature the IR spectrum of the mixture showed new ν_{CO} bands at 2069 and 2009 cm^{-1}. The mixture was freed of volatiles *in vacuo*, and NMR spectroscopy was conducted on the resulting colourless residue. Multiple compounds were observed (data provided below) and further purification was not attempted.

IR (THF) ν/cm^{-1}: 2069 m, 2009 vs (CO). ^1H NMR (CD_3CN, 400.1 MHz, 298 K) δ/ppm: −6.20 (br d, *J* = 72 Hz), −6.65 (m), −6.80 (m), −8.42 (dt, *J* = 60 Hz, *J* = 24 Hz). $^{31}P\{^1H\}$ NMR (CD_3CN, 162.0 MHz, 300 K) δ/ppm: 194.1 (t, $^2J_{PP}$ = 37 Hz, PH(OMe)Cy), 188.7 (t, $^2J_{PP}$ = 37 Hz, PH(OMe)Cy),

146.6 (dd, $^2J_{PP}$ = 193 Hz, $^2J_{PP}$ = 21 Hz, PH(OMe)Cy), 144.4 (t, $^2J_{PP}$ = 36 Hz, PH(OMe)Cy), 140.0 (m, coupling not resolved), 41.6 (d, *J* = 36 Hz), 40.5 (d, *J* = 36 Hz), 39.7 (d, *J* = 36 Hz), 38.9 (d, *J* = 36 Hz), 38.5 (d, *J* = 36 Hz), 38.2 (d, *J* = 37 Hz), 37.5 (m), 37.1 (d, *J* = 36 Hz), 34.2 (dd, $^2J_{PP}$ = 193 Hz, $^2J_{PP}$ = 18 Hz), 25.2 (t, *J* = 36 Hz). ^{31}P NMR (CD_3CN, 162.0 MHz, 300 K) δ/ppm: 194.1 (d, $^1J_{PH}$ = 389 Hz, PPh_3), 188.7 (d, $^1J_{PH}$ = 398 Hz, PH(OMe)Cy) 146.6 (dd, $^2J_{PP}$ = 193 Hz, $^1J_{PH}$ = 373 Hz, PH(OMeCy), 144.4 (t, $^1J_{PH}$ = 366 Hz, PH(OMe)Cy), 140.0 (d, $^1J_{PH}$ = 350 Hz), 41.6 (s), 40.5 (s), 39.7 (s), 38.9 (s), 38.5 (s), 38.2 (s), 37.5 (s), 37.1 (s), 34.2 (d, $^2J_{PP}$ = 193 Hz), 25.2 (d, *J* = 57 Hz).

Reaction of $[Ru(CO)_2(PPh_3)_2\{PH(OMe)Cy\}]$ with HCl

Hydrochloric acid (0.2 mL, 1.0 M in Et_2O, 0.20 mmol) was added to a solution of $[Ru(CO)_2(PPh_3)_2\{PH(OMe)Cy\}]$ (0.041 g, 49.5 µmol) in THF (5 mL) with immediate decolourisation of the mixture. After 15 minutes stirring the IR spectrum of the mixture showed the presence of multiple new ν_{CO} absorptions (*vide infra*). Volatiles were removed *in vacuo*, and NMR spectroscopy of the resulting residue showed a mixture of products. The low frequency ^{1}H NMR data are provided below, as are the $^{31}P\{^1H\}$ and ^{31}P NMR data for the major product. Crystals suitable for X-ray crystallography were grown by vapour diffusion of *n*-hexane into a CH_2Cl_2 solution of the residue at −10°C. The molecular structure was determined to be $[RuCl_2(CO)(PPh_3)_2(PH_2Cy)]$, and the crystal data are provided under the relevant heading below.

IR (THF) ν/cm^{-1}: 2082 w, 2060 m, 2003 vs, 1992 vs, 1968 m (CO). ^{1}H NMR (C_6D_6, 400.1 MHz, 300 K) δ/ppm: –4.10 (t, *J* = 20 Hz), –6.79 (t, *J* = 16 Hz), – 6.86 (dt, *J* = 32 Hz, *J* = 20 Hz), –13.37 (t, *J* = 16 Hz). $^{31}P\{^1H\}$ NMR (C_6D_6, 162.0 MHz, 300 K) δ/ppm: 168.6 (t, $^2J_{PP}$ = 25 Hz, PH(OMe)Cy), 19.7 (d, $^2J_{PP}$ = 25 Hz, PPh_3). ^{31}P NMR (C_6D_6, 162.0 MHz, 300 K) δ/ppm: 168.6 (d, $^1J_{PH}$ = 360 Hz, PH(OMe)Cy), 19.7 (br s, PPh_3).

Synthesis of $[RuCl_2(CO)(PPh_3)_2(PH_2Cy)]$

Hydrochloric acid (4.00 mL, 1.0 M in Et_2O, 4.0 mmol) was added to a solution of $[RuH(Cl)(CO)(PPh_3)_2(PH_2Cy)]$ (3.00 g, 3.72 mmol) in CH_2Cl_2 (70 mL). Effervescence was observed, and the mixture was stirred for 1.5 hours. The mixture was freed of volatiles *in vacuo*, and the resulting residue recrystallised from a mixture of CH_2Cl_2 and EtOH on a rotary

evaporator. The product was collected as a colourless solid by vacuum filtration, washing with EtOH and petroleum spirits (40-60).

Yield: 3.061 g (98%). IR (CH_2Cl_2) ν/cm^{-1}: 1977 vs, 1963 sh (CO). IR (THF) ν/cm^{-1}: 1984 vs, 1961 vs (CO). ^{1}H NMR ($CDCl_3$, 700.1 MHz, 298 K): 7.96, 7.36 (m × 2, 30 H, PPh_3), 3.54 (ddt, 2H, $^1J_{PH}$ = 357 Hz, $^3J_{PH}$ = $^3J_{HH}$ = 5 Hz, PH_2), 1.54-0.55 (m, 11H, C_6H_{11}). ^{13}C{^{1}H} NMR (C_6D_6, 176.1 MHz, 298 K) δ/ppm: 216.1 (dt, 2 × $^2J_{PC}$ = 13 Hz, CO), 134.9 (t^v, J_{PC} = 5 Hz, o/m-C_6H_5), 133.1 (t^v, $^1J_{PC}$ = 23 Hz, *ipso*-C_6H_{11}), 130.0 (s, *p*-C_6H_{11}), 128.1 (t^v, J_{PC} = 5 Hz, o/m-C_6H_{11}), 33.0 (d, $^1J_{PC}$ = 32 Hz, 1-C_6H_{11}), 32.6 (d, $^3J_{PC}$ = 5 Hz, 3,5-C_6H_{11}), 27.0 (d, $^2J_{PC}$ = 11 Hz, 2,6-C_6H_{11}), 25.4 (s, 4-C_6H_{11}). ^{31}P{^{1}H} NMR ($CDCl_3$, 162.0 MHz, 300 K) δ/ppm: 21.0 (d, $^2J_{PP}$ = 24 Hz, PPh_3), 11.7 (t, $^2J_{PP}$ = 24 Hz, PH_2Cy). ^{31}P NMR ($CDCl_3$, 162.0 MHz, 300 K) δ/ppm: 21.0 (br s, PPh_3), 11.7 (t, $^1J_{PH}$ = 364 Hz, PH_2Cy). ESI-MS (+, MeCN) *m/z*: 805.1 [M – Cl]$^+$. Accurate mass: found 805.1250 [M − Cl]$^+$, Calcd. for $C_{43}H_{43}ClOP_3Ru$ 805.1253. Anal. Found: C, 61.35; H, 5.23 %. Calcd. For $C_{43}H_{43}Cl_2OP_3Ru$: C, 61.43; H, 5.16 %. Crystal data for $[C_{43}H_{43}Cl_2OP_3Ru].3(CH_2Cl_2)$: M_w = 1095.51, monoclinic, $P2_1/c$, a = 10.2649(9) Å, b = 18.9106(14) Å, c = 25.4783(17) Å, V = 4862.5(3) Å^3, Z = 4, ρ_{calcd} = 1.496 Mg m^{-3}, μ(Mo, Kα) = 0.90 mm^{-1}, T = 150 K, colourless block, 0.14 × 0.11 × 0.06 mm, 48790 measured reflections, 12154 independent (R_{int} = 0.123), F^2 refinement, R = 0.067, wR = 0.127 for 5122 reflections ($I > 2\sigma(I)$, $2\vartheta_{max}$ = 60.2°), 566 parameters with 118 restraints.

7.4 Synthesis, Properties and Reactivity of a Primary Phosphido Complex

Formation of [Ru(CO)(PPh_3)(PHCy)(Tp)]

With DBU as base

1,8-Diazabicyclo(5.4.0)undec-7-ene (0.04 mL, 0.27 mmol) was added to a solution of [Ru(CO)(PPh_3)(PH_2Cy)(Tp)]OTf (0.202 g, 0.232 mmol) in THF (10 mL). The mixture immediately turned red, changing to yellow over a few seconds. After 5 minutes of stirring the IR spectrum of the mixture showed a new ν_{CO} band at 1931 cm^{-1}, and no ν_{CO} absorptions for [Ru(CO)(PPh_3)(PH_2Cy)(Tp)]OTf. The mixture was freed of volatiles *in vacuo*, and NMR spectroscopy of the yellow residue revealed the resonances listed below. The residue was redissolved in THF, and the volume reduced to *ca*. 1 mL *in vacuo*. *n*-Hexane (5 mL) was added, immediately resulting in the formation of a white precipitate. The supernatant was obtained *via* cannula filtration and freed of volatiles *in vacuo*. Nuclear magnetic resonance

spectroscopy of this yellow residue showed that [Ru(CO)(PPh_3)(PHCy)(Tp)] was the major product, contaminated with a small amount (< 1%) of PPh_3. After storage of this residue under an inert N_2 atmosphere for 17 days, however, 12 new $^{31}P\{^1H\}$ NMR resonances were observed. There was also an increase in the proportion of PPh_3 to *ca*. 10%. The addition of MeOH to an NMR sample acquired from this procedure resulted in the disappearance of the $^{31}P\{^1H\}$ NMR signals for [Ru(CO)(PPh_3)(PHCy)(Tp)] and the appearance of those for [Ru(CO)(PPh_3)(PH_2Cy)(Tp)]$^+$.

With KH as base

Tetrahydrofuran (10 mL) was added to a mixture of [Ru(CO)(PPh_3)(PH_2Cy)(Tp)]OTf (0.200 g, 0.230 mmol) and KH (0.018 g, 0.45 mmol). The mixture was stirred for 30 minutes, as it became a yellow solution with a colourless suspended solid. At this point the only ν_{CO} in the IR spectrum of the supernatant was that for [Ru(CO)(PPh_3)(PHCy)(Tp)]. Cannula filtration of the mixture yielded a clear yellow solution which was freed of volatiles *in vacuo*. Analysis of the yellow residue by NMR spectroscopy showed the appropriate resonances for [Ru(CO)(PPh_3)(PHCy)(Tp)]. The residue was extracted with toluene, and the insoluble colourless solids removed by cannula filtration. Removal of volatiles from the filtrate *in vacuo* yielded a residue for which the $^{31}P\{^1H\}$ NMR spectrum showed an increased number of resonances compared to the one acquired prior to toluene extraction.

With ^{n}BuLi as base

n-Butyllithium (0.30 mL, 0.48 mmol) was added to a solution of [Ru(CO)(PPh_3)(PH_2Cy)(Tp)]OTf (0.200 g, 0.230 mmol) in THF (10 mL). The mixture immediately turned orange. Aliquots of the mixture taken for IR and NMR spectroscopy revealed data consistent with the formation of [Ru(CO)(PPh_3)(PHCy)(Tp)].

IR (THF) ν/cm^{-1}: 2476 w (BH), 2231 w (PH), 1931 s (CO).

Diastereomer 1

$^{31}P\{^1H\}$ NMR (C_6D_6, 283.45 MHz, 298 K) δ/ppm: 48.8 (d, $^2J_{PP}$ = 7 Hz, PPh_3), –34.2 (br s, PHCy).

^{31}P NMR (C_6D_6, 162.0 MHz, 300 K) δ/ppm: 48.8 (br s, PPh_3), –34.2 (d, $^1J_{PH}$ = 177 Hz, PHCy).

Diastereomer 2

$^{31}P\{^{1}H\}$ NMR (C_6D_6, 283.45 MHz, 298 K) δ/ppm: 47.0 (d, $^{2}J_{PP}$ = 4 Hz, PPh_3), –19.8 (br s, PHCy).

^{31}P NMR (C_6D_6, 162.0 MHz, 300 K) δ/ppm: 47.0 (br s, PPh_3), –19.8 (d, $^{1}J_{PH}$ = 167 Hz, PHCy).

Reaction of [Ru(CO)(PPh_3)(PHCy)(Tp)] with PMe_2Ph

A mixture of [Ru(CO)(PPh_3)(PH_2Cy)(Tp)]OTf (0.030 g, 34 μmol) and PMe_2Ph (0.02 mL, 0.14 mmol) in THF (3 mL) was stirred for 2 hours. No change was observed by $^{31}P\{^{1}H\}$ NMR spectroscopy. Potassium hydride (0.019 g, 0.47 mmol) was added and the mixture began to turn yellow. After 45 minutes, a $^{31}P\{^{1}H\}$ NMR spectrum of the mixture showed only resonances for [Ru(CO)(PPh_3)(PHCy)(Tp)] (*vide supra*) and PMe_2Ph (δ_P −46.5). After 72 hours of stirring the $^{31}P\{^{1}H\}$ NMR spectrum showed the same three major resonances, along with the development of one for PPh_3 (δ_P −5.5). No other significant signals were observed.

Reaction of [Ru(CO)(PPh_3)(PHCy)(Tp)] with CO

Tetrahydrofuran (3 mL) was added to a mixture of [Ru(CO)(PPh_3)(PH_2Cy)(Tp)]OTf (0.032 g, 37 μmol) and KH (0.018 g, 0.45 mmol). The yellow mixture was stirred for 30 minutes, then CO gas bubbled through the mixture for 20 minutes. The flask was then sealed and stirred for a further 20 minutes before an aliquot was taken for NMR analysis. The $^{31}P\{^{1}H\}$ NMR spectrum showed only resonances for [Ru(CO)(PPh_3)(PH_2Cy)(Tp)] (*vide supra*). Carbon monoxide gas was bubbled through the mixture for a further 20 minutes, the flask sealed and stirring continued for a total time of 19 hours. After this time, the $^{31}P\{^{1}H\}$ NMR spectrum showed the development of the PPh_3 signal (δ_P −5.5) from *ca*. 4% to *ca*. 17% of the mixture. No other new resonances had appeared, however.

Formation of [Ru(CO)(PPh_3)(PHMeCy)(Tp)]OTf

Tetrahydrofuran (10 mL) was added to a mixture of [Ru(CO)(PPh_3)(PH_2Cy)(Tp)]OTf (0.200 g, 0.230 mmol) and KH (0.023 g, 0.573 mmol). The resultant yellow mixture was stirred for 1 hour then filtered through diatomaceous earth. The flask and diatomaceous earth were further washed with THF (2 × 20 mL). Iodomethane (0.24 mL, 1.0 M in hexanes, 0.24 mmol) was added to the combined filtrates, immediately turning the mixture colourless. The mixture was stirred for a further 20 minutes, followed by the removal of volatiles *in vacuo*. From this

point the procedure was conducted in air. Recrystallisation of the colourless residue from a mixture of CH_2Cl_2 and ^{i}PrOH on a rotary evaporator resulted in the formation of an oil. The addition of *n*-hexane to a concentrated THF solution of the residue resulted in the formation of a solid which was collected by vacuum filtration. This solid was estimated to contain *ca*. 95% [Ru(CO)(PPh_3)(PHMeCy)(Tp)]OTf by $^{31}P\{^{1}H\}$ NMR spectroscopy.

Yield: 0.007 g (3% assuming formation of pure product)
IR (THF) ν/cm^{-1}: 2493 w (BH), 1975 vs (CO). ESI-MS (+, MeCN) *m/z*: 735.2 $[M]^+$. Accurate mass: found 735.1895 $[M]^+$, Calcd. for $C_{35}H_{40}{}^{11}BN_6OP_2{}^{102}Ru$ 735.1875

The following NMR data were assigned to different diastereomers based on the relative intensity of the signals:

Diastereomer 1
$^{31}P\{^{1}H\}$ NMR ($CDCl_3$, 162.0 MHz, 300 K) δ/ppm: 38.3 (d, $^{2}J_{PP}$ = 28 Hz, PPh_3), 13.5 (d, $^{2}J_{PP}$ = 28 Hz, PHMeCy).

Diastereomer 2
$^{31}P\{^{1}H\}$ NMR ($CDCl_3$, 162.0 MHz, 300 K) δ/ppm: 38.0 (d, $^{2}J_{PP}$ = 28 Hz, PPh_3), 16.1 (d, $^{2}J_{PP}$ = 28 Hz, PHMeCy).

Formation of [Ru(CO)(PPh_3)(PMeCy)(Tp)]

Tetrahydrofuran (10 mL) was added to a mixture of [Ru(CO)(PPh_3)(PHMeCy)(Tp)]OTf (0.100 g, 0.115 mmol) and KH (0.030 g, 0.75 mmol). The resulting yellow mixture was stirred for 45 minutes before IR and NMR spectroscopy were performed.

IR (THF) ν/cm^{-1}: 2477 w (BH), 1926 vs (CO)

Diastereomer 1
$^{31}P\{^{1}H\}$ NMR (C_6D_6, 162.0 MHz, 300 K) δ/ppm: 47.8 (d, $^{2}J_{PP}$ = 8 Hz, PPh_3), 9.2 (d, $^{2}J_{PP}$ = 8 Hz, PHMeCy).

Diastereomer 2

$^{31}P\{^{1}H\}$ NMR (C_6D_6, 162.0 MHz, 300 K) δ/ppm: 45.9 (d, $^{2}J_{PP}$ = 13 Hz, PPh_3), 13.3 (d, $^{2}J_{PP}$ = 13 Hz, PHMeCy).

Synthesis of [Ru(CO)(PPh_3)(PMe_2Cy)(Tp)]OTf

Tetrahydrofuran (10 mL) was added to a mixture of [Ru(CO)(PPh_3)(PH_2Cy)(Tp)]OTf (0.200g, 0.230 mmol) and KH (0.035g 0.873 mmol). After stirring the resultant mixture for 20 minutes MeI (0.05 mL, 0.803 mmol) was added, turning the yellow mixture colourless. Stirring was continued for 1 hour, during which a colourless precipitate formed. The mixture was freed of volatiles *in vacuo* and the rest of the process was carried out in air. The colourless residue was dissolved in CH_2Cl_2 (30 mL) and filtered through diatomaceous earth. Dichloromethane was removed from the filtrate on a rotary evaporator and the residue was recrystallised on a rotary evaporator from a THF/*n*-hexane mixture. The product was a colourless solid.

Yield: 0.107g (52%). IR (THF) ν/cm^{-1}: 2494 w (BH), 1984 vs (CO). ^{1}H NMR ($CDCl_3$, 700.2 MHz, 298 K) δ/ppm: 8.05, 7.73, 7.56, 6.48, 6.38, 6.35, 5.94 (s x 7, 7 × 1H, J_{HH} not resolved, Hpz), 7.80 (s × 2, 2 × 1H, J_{HH} not resolved, Hpz), 7.50−7.09 (m, 15H, PC_6H_5), 1.98–0.88 (m, 11H, C_6H_{11}), 1.02 (d, 3H, $^{2}J_{PH}$ = 7 Hz, PMe_2), 0.54 (d, 3H, $^{2}J_{PH}$ = 7 Hz, PMe_2). $^{31}P\{^{1}H\}$ NMR ($CDCl_3$, 162.0 MHz, 300 K) δ/ppm: 34.5 (d, $^{2}J_{PP}$ = 28 Hz, PPh_3), 11.0 (d, $^{2}J_{PP}$ = 28 Hz, PMe_2Cy). $^{13}C\{^{1}H\}$ NMR ($CDCl_3$, 176.1 MHz, 298 K) δ/ppm: 202.4 (dd,2 × $^{2}J_{PC}$ = 14 Hz, CO), 145.4, 144.8, 144.7 (s × 3, 3 × C^{3}(pz)), 137.9, 137.6, 137.5 (s × 3, 3 × C^{5}(pz)), 134.1 (d, J_{PC} = 9 Hz, o/m-PC_6H_5), 131.7 (d, $^{1}J_{PC}$ = 46 Hz, *ipso*-PC_6H_5), 131.6 (s, *p*-PC_6H_5), 129.1 (d, J_{PC} = 9 Hz, o/m-PC_6H_5), 108.2, 107.5, 107.2 (s × 3, 3 × C^{4}(pz)), 38.1 (d, $^{1}J_{PC}$ = 28 Hz, 1-C_6H_{11}), 27.9 (d, $^{3}J_{PC}$ = 2 Hz, 3,5-C_6H_{11}) 27.0 (d, $^{2}J_{PC}$ = 11 Hz, 2,6-C_6H_{11}), 26.9 (d, $^{2}J_{PC}$ = 11 Hz, 2,6-C_6H_{11}), 26.4 (d, $^{3}J_{PC}$ = 5 Hz, 3,5-C_6H_{11}), 25.9 (s, 4-C_6H_{11}), 10.7 (d, $^{1}J_{PC}$ = 30 Hz, PMe), 10.1 (d, $^{1}J_{PC}$ = 32 Hz, PMe). ESI-MS (+, MeCN) *m/z*: 749.2 $[M]^+$. Accurate mass: found 749.2025 $[M]^+$, Calcd. for $C_{36}H_{42}{}^{11}BN_6OP_2{}^{102}Ru$ 749.2032. Anal. Found: C, 48.84; H, 4.82; N, 9.57%. Calcd. For $C_{37}H_{42}BF_3N_6O_4P_2RuS$: C, 49.51; H, 4.72; N, 9.36 (satisfactory data not acquired).

Synthesis of [Ru(CO)(PPh_3){PH(BH_3)Cy}(Tp)]

With $BH_3.SMe_2$ as the borane source

Tetrahydrofuran (10 mL) was added to a mixture of [Ru(CO)(PPh_3)(PH_2Cy)(Tp)]OTf (0.200 g, 0.230 mmol) and KH (0.018 g, 0.49 mmol). The yellow mixture was stirred for 15 minutes before it was subjected to cannula filtration. Borane dimethylsulfide complex (0.03 mL, 0.32 mmol) was added to the filtrate resulting in immediate decolourisation. After 2 hours of stirring the IR spectrum of the mixture contained two ν_{CO} bands at 1983 and 1958 cm^{-1}. The volume was reduced to *ca*. 2 mL *in vacuo* and *n*-hexane (10 mL) was added, resulting in the precipitation of a colourless solid. Cannula filtration of the mixture yielded a colourless solution which was freed of volatiles *in vacuo*. Analysis of the mixture by $^{31}P\{^1H\}$ and ^{31}P NMR spectroscopy showed the presence of two diastereomers.

With $NaBH_4$ as the borane source and toluene as the solvent

A suspension of [Ru(CO)(PPh_3)(PH_2Cy)(Tp)]OTf (0.75 g, 0.861 mmol) and $NaBH_4$ (0.035 g, 0.925 mmol) in toluene (50 mL) was heated under reflux with stirring for 16 hours. The mixture was allowed to cool to room temperature, *n*-hexane (40 mL) added and the mixture filtered through diatomaceous earth. Volatiles were removed from the filtrate on a rotary evaporator and the resultant colourless residue triturated with MeOH in an ultrasonic bath. The colourless product was collected by vacuum filtration. Crystals suitable for X-ray diffraction were grown by vapour diffusion of *n*-hexane into a $CHCl_3$ solution of the compound at −10°C.

Yield 0.152 g (24 %).

With $NaBH_4$ as the borane source and THF as the solvent

A mixture of [Ru(CO)(PPh_3)(PH_2Cy)(Tp)]OTf (1.00 g, 1.15 mmol) and $NaBH_4$ (0.101 g, 2.67 mmol) was stirred in THF (60 mL). Effervescence was observed at the beginning of the reaction. The mixture was stirred for 18 hours, after which the $^{31}P\{^1H\}$ NMR spectrum showed no resonances for [Ru(CO)(PPh_3)(PH_2Cy)(Tp)]OTf. Volatiles were removed from the mixture *in vacuo*. From this point the procedure was conducted in air. Toluene (100 mL) was added to the residue and the mixture filtered through diatomaceous earth. This process was repeated and the combined filtrates were freed of volatiles on a rotary evaporator. The resulting

residue was recrystallised from a mixture of CH_2Cl_2 and MeOH on a rotary evaporator. The product was collected as a colourless solid by vacuum filtration, washing with MeOH, EtOH, petroleum spirits (40-60) then *n*-pentane.

Yield: 0.421 g (50 %).

IR (CH_2Cl_2) ν/cm^{-1}: 2923 w, 2850 w (aliphatic CH), 2490 w (BH), 2348 w (PH), 1977 vs (CO). IR (THF) ν/cm^{-1}: 1983 vs (CO). IR (Toluene) ν/cm^{-1}: 2481 w (BH), 2361 w (PH), 1985 vs (CO). ^{1}H NMR ($CDCl_3$, 700.2 MHz, 298 K) δ/ppm: 8.14, 7.99, 7.24, 7.02, 6.35, 6.24, 5.99 (s x 7, 7 × 1H, J_{HH} not resolved, Hpz), 7.79 (s, 2H, J_{HH} not resolved, Hpz), 7.53, 7.43, 7.02 (m × 3, 15H, PC_6H_5), 4.83 (br s, BH or BH_3), 4.64 (br s, BH or BH_3), 2.83 (ddd, 1H, $^{1}J_{PH}$ = 343 Hz, J = 7 Hz, J = 14 Hz, PH), 1.97–0.41 (m, 11H, C_6H_{11}). ^{13}C{^{1}H} NMR ($CDCl_3$, 201.3 MHz, 298 K) δ/ppm: 203.2 (dd, $^{2}J_{PC}$ = 14 Hz, CO), 145.3, 144.4, 144.2 (s × 3, 3 × C^{3}(pz)), 136.3, 135.4, 135.3 (s × 3, 3 × C^{5}(pz)), 134.3 (d, J_{PC} = 8 Hz, o/m-PC_6H_5), 131.9 (d, $^{1}J_{PC}$ = 44 Hz, *ipso*-PC_6H_5) 130.3 (s, *p*-PC_6H_5), 128.1 (d, J_{PC} = 14 Hz, o/m-PC_6H_5), 106.0 (s, 2 × C^{4}(pz)), 105.7 (s, C^{4}(pz)), 33.8 (d, $^{1}J_{PC}$ = 20 Hz, 1-C_6H_{11}), 32.0 (d, J_{PC} = 6 Hz, 2,3,5,6-C_6H_{11}) 31.7 (s, 3,4,5-C_6H_{11}), 28.0 (d, J_{PC} = 8 Hz, 2,3,5,6-C_6H_{11}), 27.7 (2, J_{PC} = 12 Hz, 2,3,5,6-C_6H_{11}), 26.3 (s, 3,4,5-C_6H_{11}). ^{11}B{^{1}H} NMR ($CDCl_3$, 128.4 MHz, 300 K): –3.74 (Tp), –33.85 (BH_3). ^{31}P{^{1}H} NMR ($CDCl_3$, 283.4 MHz, 298 K) δ/ppm: 43.4 (d, $^{2}J_{PP}$ = 23 Hz, PPh_3), –4.8 (br s, PH{BH_3}Cy). ^{31}P NMR ($CDCl_3$, 283.4 MHz, 298 K) δ/ppm: 43.2 (br s, PPh_3), – 4.8 (br d, $^{1}J_{PH}$ = 309 Hz, PPh_3). ESI-MS (+, MeCN) *m/z*: 727.2 [M – BH_3 + H]$^{+}$, 737.2 [M – BH_3 + O + H]$^{+}$, 757.2 [M + Na]$^{+}$. Accurate mass: found 721.1721 [M – BH_3 + H]$^{+}$, Calcd. for $C_{34}H_{38}{}^{11}BN_6OP_2{}^{102}Ru$ 721.1719; found 737.1670 [M – BH_3 + O + H]$^{+}$, Calcd. for $C_{34}H_{38}{}^{11}B_2N_6O_2P_2{}^{102}Ru$ 737.1668; found 757.1874 [M + Na]$^{+}$, Calcd. for $C_{34}H_{40}{}^{11}B_2N_6NaOP_2{}^{102}Ru$ 757.1866. Anal. Found: C, 55.39; H, 5.68; N, 11.27%. Calcd. For $C_{34}H_{40}B_2N_6OP_2Ru$: C, 55.68; H, 5.50; N, 11.56. Crystal data for [$C_{34}H_{40}B_2N_6OP_2Ru$].($CHCl_3$): M_w = 852.75, orthorhombic, *Pbca*, a = 19.9543(6) Å, b = 10.1541(2) Å, c = 38.1601(13) Å, V = 7731.9(3) Å^{3}, Z = 8, ρ_{calcd} = 1.465 Mg m^{-3}, μ(Cu, Kα) = 6.27 mm^{-1}, T = 150 K, colourless plate, 0.19 × 0.09 × 0.03 mm, 35604 measured reflections, 7528 independent (R_{int} = 0.057), F^2 refinement, R = 0.084, wR = 0.179 for 6318 reflections ($I > 2\sigma(I)$, $2\vartheta_{max}$ = 144.2°), 438 parameters with 72 restraints.

Data for second siastereomer

IR (THF) ν/cm^{-1}: 1958 s (CO). $^{11}B\{^1H\}$ NMR ($CDCl_3$, 128.4 MHz, 300 K): –3.74 (Tp), –35.99 (BH_3). $^{31}P\{^1H\}$ NMR ($CDCl_3$, 162.0 MHz, 298 K) δ/ppm: 44.2 (d, $^2J_{PP}$ = 21 Hz, PPh_3), –1.2 (br s, PH{BH_3}Cy). ^{31}P NMR ($CDCl_3$, 162.0 MHz, 298 K) δ/ppm: 44.2 (br s, PPh_3), –1.2 (br d, $^1J_{PH}$ = 293 Hz, PPh_3).

Reaction of [Ru(CO)(PPh_3){PH(BH_3)Cy}(Tp)] with KH

A mixture of [Ru(CO)(PPh_3){PH(BH_3)Cy}(Tp)] (0.020 g, 27.3 μmol), KH (0.005 g, 0.1 mmol) and THF (5 mL) was stirred for 24 hours. No visual change was observed during this time and no change occurred in the IR spectrum of the mixture.

Reaction of [Ru(CO)(PPh_3){PH(BH_3)Cy}(Tp)] with ^{n}BuLi

n-Butyllithium (0.1 mL, 1.6 M in hexanes, 0.16 mmol) was added to a solution of [Ru(CO)(PPh_3){PH(BH_3)Cy}(Tp)] (0.020 g, 27.3 μmol) in THF (3 mL). There was a colour change to pale yellow, but no change was observed by IR or NMR spectroscopy.

Reaction of [Ru(CO)(PPh_3){PH(BH_3)Cy}(Tp)] with $[CPh_3]PF_6$

Dichloromethane (5 mL) was added to a mixture of [Ru(CO)(PPh_3){PH(BH_3)Cy}(Tp)] (0.050 g, 68 μmol) and $[CPh_3]PF_6$ (0.027 g, 70 μmol). The mixture was initially yellow, but turned colourless within a few seconds. Infrared spectroscopy of the mixture after 5 minutes stirring showed a ν_{CO} band at 1996 cm^{-1}, which corresponds to [Ru(CO)(PPh_3)(PH_2Cy)(Tp)]$^+$. The mixture was freed of volatiles *in vacuo* and NMR spectroscopy was conducted on the resultant residue. The $^{31}P\{^1H\}$ and ^{31}P NMR data confirmed the presence of [Ru(CO)(PPh_3)(PH_2Cy)(Tp)]$^+$.

^{11}B NMR ($CDCl_3$, 128.4 MHz, 298 K): −0.7 (s), −4.1 (br s, Tp).

Reaction of [Ru(CO)(PPh_3){PH(BH_3)Cy}(Tp)] with NEt_3

Triethylamine (*ca*. 4 drops) was added to a NMR tube containing a sample of [Ru(CO)(PPh_3){PH(BH_3)Cy}(Tp)] in toluene-d_8. The tube was then heated to 100°C. After 2 hours the mixture still contained *ca*. 90% [Ru(CO)(PPh_3){PH(BH_3)Cy}(Tp)], as estimated by $^{31}P\{^1H\}$ NMR spectroscopy. About 70% of the starting material had been consumed after 20

hours of heating, along with the appearance of more than 9 new $^{31}P\{^{1}H\}$ NMR signals. After 48 hours of heating, over 90% of the starting material had been consumed. The $^{31}P\{^{1}H\}$ NMR resonances which could be identified were those at δ_P 66.5 ([RuH(CO)(PPh_3)(Tp)]) and −5.2 (PPh_3) . The former resonance was estimated to comprise *ca*. 24% of the mixture.

$^{11}B\{^{1}H\}$ NMR (toluene-d_8, 128.4 MHz, 300 K): 1.6 (br s), –3.3 (br s), –10.7 (s). $^{31}P\{^{1}H\}$ NMR (toluene-d_8, 162.0 MHz, 298 K) δ/ppm: 173.7 (d, *J* = 37 Hz), 66.5 (s, [RuH(CO)(PPh_3)(Tp)]), 49.0 (d, *J* = 34 Hz), 48.1 (d, *J* = 36 Hz), 47.0 (s), 44.2 (d, *J* = 23 Hz, [Ru(CO)(PPh_3){PH(BH_3)Cy}(Tp)]), 43.5 (s), 43.0 (s), 42.8 (s), 41.3 (s), 41.2 (s), 40.0 (s), 1.49 (br s, [Ru(CO)(PPh_3){PH(BH_3)Cy}(Tp)]), −5.2 (s, PPh_3).

Reaction of [Ru(CO)(PPh_3){PH(BH_3)Cy}(Tp)] with pyridine

Pyridine (*ca*. 4 drops) was added to a NMR tube containing a sample of [Ru(CO)(PPh_3){PH(BH_3)Cy}(Tp)] in toluene-d_8. The tube was then heated to 100°C. After 2 hours the mixture still contained *ca*. 90% [Ru(CO)(PPh_3){PH(BH_3)Cy}(Tp)], as estimated by $^{31}P\{^{1}H\}$ NMR spectroscopy. About 70% of the starting material had been consumed after 20 hours of heating, along with the appearance of more than 12 new $^{31}P\{^{1}H\}$ NMR signals. After 48 hours of heating no signals for the starting material were detected. Among the new $^{31}P\{^{1}H\}$ NMR resonances, those at δ_P 66.5 ([RuH(CO)(PPh_3)(Tp)]), 24.5 (O=PPh_3) and −5.2 (PPh_3) could be identified. These components comprised *ca*. 32%, 23% and 9% of the mixture, respectively.

$^{11}B\{^{1}H\}$ NMR (toluene-d_8, 128.4 MHz, 300 K): –3.3 (br s), –12.2 (s), −32.2 (br s). $^{31}P\{^{1}H\}$ NMR (toluene-d_8, 162.0 MHz, 298 K) δ/ppm: 66.5 (s, [RuH(CO)(PPh_3)(Tp)]), 48.7 (s), 46.6 (d, *J* = 37 Hz), 42.9 (s), 42.6 (s), 41.2 (s), 40.7 (s), 40.3 (s), 38.0 (s), 37.5 (s), 35.4 (s), 24.5 (s, O=PPh_3), –5.5 (s, PPh_3).

Reaction of [Ru(CO)(PPh_3){PH(BH_3)Cy}(Tp)] with heat

An NMR tube containing a solution of [Ru(CO)(PPh_3){PH(BH_3)Cy}(Tp)] in toluene-d_8 was heated at 100°C for 72 hours. No change was observed visually, or by $^{31}P\{^{1}H\}$ or $^{11}B\{^{1}H\}$ NMR spectroscopy.

Reaction of [Ru(CO)(PPh_3){PH(BH_3)Cy}(Tp)] with borane pyridine complex

Borane pyridine complex (*ca*. 3 drops) was added to a NMR tube containing a sample of [Ru(CO)(PPh_3){PH(BH_3)Cy}(Tp)] in toluene-d_8. The tube was then heated to 100°C for 17 hours. A small amount of colourless precipitate had formed in the tube and the mixture had turned a faint yellow colour. A small amount (*ca*. 5%) of [RuH(CO)(PPh_3)(Tp)] had formed, as estimated by $^{31}P\{^1H\}$ NMR spectroscopy. The complex [Ru(CO)(PPh_3){PH(BH_3)Cy}(Tp)] was the only other compound observed.

Reaction of [Ru(CO)(PPh_3)(PHCy)(Tp)] with borane pyridine complex

Tetrahydrofuran (6 mL) was added to a mixture of [Ru(CO)(PPh_3)(PH_2Cy)(Tp)]OTf (0.050 g, 57.4 μmol) and KH (0.018 g, 0.49 mmol). The yellow mixture was stirred for 30 minutes before it was subjected to cannula filtration. Borane pyridine complex (0.03 mL, 0.30 mmol) was added to filtrate, and no visible change occurred after stirring the mixture for 30 minutes. The mixture was heated under reflux with stirring for 1.5 hours, during which it turned colourless. The major product was [Ru(CO)(PPh_3){PH(BH_3)Cy}(Tp)], as determined by $^{31}P\{^1H\}$ NMR spectroscopy, while a small amount (*ca*. 5%) of [RuH(CO)(PPh_3)(Tp)] was also observed.

Attempted synthesis of [Ru(CO)(PPh_3){PH(B_3H_7)Cy}(Tp)]

A mixture of [Ru(CO)(PPh_3)(PH_2Cy)(Tp)]OTf (0.200 g, 0.230 mmol) and [NBu_4][B_3H_8] (0.066 g, 0.233 mmol) in THF (10 mL) was stirred for 14 days. No change was observed by $^{31}P\{^1H\}$ NMR spectroscopy. The mixture was heated under reflux for 4 hours, after which the major product observed by $^{31}P\{^1H\}$ NMR spectroscopy was [Ru(CO)(PPh_3){PH(BH_3)Cy}(Tp)]. When toluene is used as the solvent the same observation (formation of [Ru(CO)(PPh_3){PH(BH_3)Cy}(Tp)] after heating under reflux) occurs.

IR (THF) ν/cm^{-1}: 2481 w (BH), 2361 w (PH), 1985 vs (CO).

Formation of [Ru(CO)(PPh_3){PH(CS_2)Cy}(Tp)]

Tetrahydrofuran (10 mL) was added to a mixture of [Ru(CO)(PH_2Cy)(PPh_3)(Tp)]OTf (0.100 g, 0.115 mmol) and KH (0.018 g, 0.32 mmol). The yellow mixture was stirred for 30 minutes before being subjected to cannula filtration. Carbon disulfide (0.02 mL, 0.331 mmol) was

added to filtrate, turning it a deep red. After 15 minutes, IR and $^{31}P\{^{1}H\}$ NMR spectroscopy suggested [Ru(CO)(PPh_3)(PH{CS_2}Cy)(Tp)] as the single product. The mixture was freed of volatiles *in vacuo* and $^{31}P\{^{1}H\}$ NMR spectroscopy of the residue revealed the presence of at least 10 resonances, including the desired product (*ca*. 50%) and [Ru(CO)(PHCy)(PPh_3)(Tp)] (*ca*. 25 %). Vapour diffusion of *n*-hexane into a CH_2Cl_2 extract of this residue at −10°C yielded a crystal suitable for X-ray diffraction, but a bulk sample could not be obtained due to the reversibility of adduct formation.

IR (THF) ν/cm^{-1}: 2490 w (BH), 2170 w (PH), 2005 vs, 1996 vs (CO). $^{31}P\{^{1}H\}$ NMR (C_6D_6, 162.0 MHz, 300 K) δ/ppm: 78.3 (d, $^{2}J_{PP}$ = 27 Hz, PH(CS_2)Cy), 40.6 (d, $^{2}J_{PP}$ = 27 Hz, PPh_3). ^{31}P NMR (C_6D_6, 162.0 MHz, 300 K) δ/ppm: 78.3 (d, $^{1}J_{PH}$ = 322 Hz, PH(CS_2)Cy), 40.6 (br s, PPh_3). Crystal data for [$C_{35}H_{37}BN_6OP_2RuS_2$].($CH_2Cl_2$): M_w = 880.61, triclinic, *P*−1, a = 10.9830(5) Å, b = 11.3277(5) Å, c = 16.6020(7) Å, α = 87.908(3)°, β = 82.851(4)°, γ = 72.224(4)°, V = 1951.59(8) Å^3, Z = 2, ρ_{calcd} = 1.498 Mg m^{-3}, μ(Cu, Kα) = 6.59 mm^{-1}, T = 150 K, red plate, 0.08 × 0.04 × 0.02 mm, 23428 measured reflections, 7878 independent (R_{int} = 0.050), F^2 refinement, R = 0.060, wR = 0.169 for 6516 reflections ($I > 2\sigma(I)$, $2\vartheta_{max}$ = 149.2°), 473 parameters with 13 restraints.

Reaction of [Ru(CO)(PPh_3){PH(CS_2)Cy}(Tp)] with heat

Tetrahydrofuran (6 mL) was added to a mixture of [Ru(CO)(PH_2Cy)(PPh_3)(Tp)]OTf (0.050 g, 57 μmol) and KH (0.013 g, 0.449 mmol). The yellow mixture was stirred for 20 minutes before being subjected to cannula filtration. Carbon disulfide (0.02 mL, 0.0331 mmol) was added to filtrate, turning it a deep red. The mixture was then heated under reflux with stirring for 16 hours, after which no changed was observed by IR or $^{31}P\{^{1}H\}$ NMR spectroscopy. Heating was continued up to a total time of 5 days, after which the only change was the development of a ν_{CO} band for [Ru(CO)(PPh_3)(PHCy)(Tp)] at 1931 cm^{-1} in the IR spectrum.

Synthesis of [Ru(CO)(PPh_3){PH(CS_2Me)Cy}(Tp)]OTf

Tetrahydrofuran (10 mL) was added to a mixture of [Ru(CO)(PH_2Cy)(PPh_3)(Tp)]OTf (0.200g, 0.230 mmol) and KH (0.022g, 0.548 mmol). The yellow mixture was stirred for 20 minutes before being subjected to cannula filtration. Carbon disulfide (0.02 mL, 0.331 mmol) was added to filtrate, turning a deep red. Stirring was continued for 5 minutes and a *n*-hexane

solution of MeI (0.26 mL, 1.0 M, 0.26 mmol) was added. The mixture initially turned purple and faded to red as the mixture was stirred for a further 2 hours. Volatiles were removed *in vacuo*, CH_2Cl_2 (10 mL) added to the residue and the mixture filtered through diatomaceous earth in air. The filtrate was concentrated to *ca.* 1 mL on a rotary evaporator. The product was precipitated by the addition of Et_2O and collected as an orange solid by vacuum filtration. Crystals suitable for X-ray diffraction were grown by vapour diffusion of Et_2O into a CH_2Cl_2 solution of the compound at −15°C.

Yield: 0.088g (40%). IR (THF) ν/cm^{-1}: 2493 w (BH), 2171 w (PH), 1997 vs (CO). ^{1}H NMR ($CDCl_3$, 700.2 MHz, 298 K) δ/ppm: 8.23, 7.91, 7.82, 7.77, 7.58, 6.33, 6.32, 6.24, 5.97 (s x 9, 9 × 1H, J_{HH} not resolved, Hpz), 7.50, 7.40, 6.95 (m × 3, 15H, PC_6H_5), 4.66 (br s, 1H, BH), 2.83 (d app quartet, 1H, $^1J_{PH}$ = 294 Hz, J = 7 Hz, PH), 2.67 (s, 3H, SMe), 2.15 – −0.04 (m, 11H, C_6H_{11}). ^{13}C{^{1}H} NMR ($CDCl_3$, 176.1 MHz, 298 K) δ/ppm: 232.4 (d, $^1J_{PC}$ = 23 Hz, PCS_2), 201.7 (dd, $^2J_{PC}$ = 11 Hz, CO), 147.2, 145.8, 144.7 (s × 3, 3 × C^3(pz)), 137.6, 137.5, 137.0 (s × 3, 3 × C^5(pz)), 134.1 (d, J_{PC} = 9 Hz, o/m-PC_6H_5), 131.7 (s, *p*-PC_6H_5), 129.3 (d, J_{PC} = 9 Hz, o/m-PC_6H_5), 129.3 (d, $^1J_{PC}$ = 48 Hz, *ipso*-PC_6H_5), 108.0 (s, C^4(pz)), 107.3 (s, 2 × C^4(pz)), 38.7 (d, J_{PC} = 25 Hz, 1,2,6-C_6H_{11}), 30.9 (d, J_{PC} = 9 Hz, 1,2,3-C_6H_{11}) 27.4 (s, 3,4,5-C_6H_{11}), 27.4 (d, J_{PC} = 23 Hz, 1,2,6-C_6H_{11}), 26.4 (s, 3,4,5-C_6H_{11}), 25.1 (s, 3,4,5-C_6H_{11}), 21.6 (s, SMe). ^{31}P{^{1}H} NMR ($CDCl_3$, 283.45 MHz, 298 K) δ/ppm: 61.7 (d, $^2J_{PP}$ = 26 Hz, PH(CS_2Me)Cy), 34.7 (d, $^2J_{PP}$ = 26 Hz, PPh_3). ^{31}P NMR ($CDCl_3$, 162.0 MHz, 300 K) δ/ppm: 61.7 (d, $^1J_{PH}$ = 345 Hz, PH(CS_2Me)Cy), 34.7 (br s, PPh_3). ESI-MS (+, MeCN) *m/z*: 811.1 [M]$^+$. Accurate mass: found 811.1317 [M]$^+$, Calcd. for $C_{36}H_{40}{}^{11}BN_6OP_2{}^{102}RuS_2$ 811.1317. Anal. Found: C, 46.20; H, 4.28; N, 8.67%. Calcd. For $C_{37}H_{40}BF_3N_6O_4P_2RuS_3$: C, 46.30; H, 4.20; N, 8.76. $[\alpha]_D$ –0.86° (c 1.05 g mL^{-1}, $CHCl_3$). Crystal data for $[C_{36}H_{40}BN_6OP_2RuS_2][CF_3O_3S].(CH_2Cl_2)(C_4H_{10}O)$: M_w = 1118.84, monoclinic, *P2$_1$*, a = 9.6004(1) Å, b = 23.4491(3) Å, c = 11.2941(2) Å, β = 101.5502(13)°, V = 2491.05(6) Å^3, Z = 2, ρ_{calcd} = 1.492 Mg m^{-3}, μ(Cu, Kα) = 5.83 mm^{-1}, T = 150 K, pale purple irregular, 0.36 × 0.20 × 0.14 mm, 33195 measured reflections, 9908 independent (R_{int} = 0.035), F^2 refinement, R = 0.041, wR = 0.110 for 9858 reflections ($I > 2\sigma(I)$, $2\vartheta_{max}$ = 149.2°), 590 parameters with 2 restraints, Flack parameter = −0.003(3).

Formation of [Ru(CO)(PPh$_3$){P(CS$_2$Me)Cy}(Tp)]

Tetrahydrofuran (1.5 mL) was added to a mixture of [Ru(CO)(PPh$_3$){PH(CS$_2$Me)Cy}(Tp)]OTf (0.020 g, 21 μmol) and KH (0.008 g, 0.20 mmol). The mixture immediately turned purple and the IR spectrum after 20 minutes of stirring contained a new ν_{CO} band at 1961 cm^{-1}. Additionally, the $^{31}P\{^1H\}$ NMR spectrum contained the resonances listed below. After stirring the mixture for 3 hours a colour change to orange was observed. The IR spectrum contained new absorptions, and after 24 hours the $^{31}P\{^1H\}$ NMR spectrum contained new resonances but no longer showed the signals attributed to [Ru(CO)(PPh$_3$){P(CS$_2$Me)Cy}(Tp)].

IR (THF) ν/cm^{-1}: 2486 w (BH), 1961 vs (CO). $^{31}P\{^1H\}$ NMR (C_6D_6, 162.0 MHz, 298 K): 81.1 (s, $^2J_{PP}$ not resolved, P(CS$_2$Me)Cy), 38.8 (s, $^2J_{PP}$ not resolved, PPh$_3$).

Data acquired following decomposition of product

IR (THF) ν/cm^{-1}: 2477 w (BH), 1957 vs, 1927 s, 1902 m (CO). $^{31}P\{^1H\}$ NMR (C_6D_6, 162.0 MHz, 298 K): 102.8 (d, *J* = 31 Hz),[†††] 43.4 (s), 42.5 (s), 42.3 (s).

Reaction of [Ru(CO)(PPh$_3$){P(CS$_2$Me)Cy}(Tp)] with MeI

Tetrahydrofuran (5 mL) was added to a mixture of [Ru(CO)(PPh$_3$){PH(CS$_2$Me)Cy}(Tp)]OTf (0.040 g, 42 μmol) and KH (0.008 g, 0.20 mmol). The purple mixture was stirred for 10 minutes before MeI (0.03 mL, 0.48 mmol) was added. A colour change to orange resulted, and the mixture was stirred for a further 10 minutes before it was subjected to cannula filtration. The filtrate was freed of volatiles *in vacuo*, and NMR and ESI-MS analysis was conducted on the resulting orange residue. The molecular ion in the mass spectrometry data is presumed to be either [Ru(CO)(PPh$_3$){P(CS$_2$Me$_2$)Cy}(Tp)]$^+$ or [Ru(CO)(PPh$_3$){P(CS$_2$Me)MeCy}(Tp)]$^+$, both of which have the same molecular formula.

IR (THF) ν/cm^{-1}: 2483 w (BH), 1995 m (CO), 1965 sh (CO), 1949 vs (CO). $^{31}P\{^1H\}$ NMR ($CDCl_3$, 162.0 MHz, 298 K): 81.1 (s, $^2J_{PP}$ not resolved, P(CS$_2$Me)Cy), 38.8 (s, $^2J_{PP}$ not resolved, PPh$_3$). ESI-MS (+, MeCN) *m/z*: 825.1 [M]$^+$, 843.2 [M + H$_2$O]$^+$. Accurate mass: found 825.1463 [M]$^+$,

[†††] This resonance may also be two individual singlets of equal intensity at δ_P 102.9 and 102.7

Calcd. for $C_{37}H_{42}BN_6OP_2RuS_2$ 825.1468; Accurate mass: found 843.1554 $[M + H_2O]^+$, Calcd. for $C_{37}H_{44}BN_6O_2P_2RuS_2$ 843.1587.

7.5 Phosphine Chalcogenide Complexes Derived From [Ru(CO)(PPh_3)(PHCy)(Tp)]

Formation of [Ru(CO)(PPh_3){PH(O)Cy}(Tp)]

Tetrahydrofuran (25 mL) was added to a mixture of [Ru(CO)(PH_2Cy)(PPh_3)(Tp)]OTf (0.300 g, 0.345 mmol) and KH (0.025 g, 0.623 mmol). The yellow mixture was stirred for 30 minutes after which the supernatant was isolated by cannula filtration. Iodosyl benzene (0.078 g, 0.355 mmol) was added to the filtrate and the mixture stirred for 16 hours over which the mixture turned from yellow to brown. The mixture was freed of volatiles *in vacuo* and the rest of the procedure was carried out in air. The residue was taken up in toluene (20 mL) and filtered through diatomaceous earth. Solvent was removed from the filtrate on a rotary evaporator, and NMR spectroscopy was conducted on the residue. Recrystallisation of the residue from CH_2Cl_2/MeOH or CH_2Cl_2/Et_2O mixtures failed to yield any precipitate. Recrystallisation from CH_2Cl_2/*n*-hexane gave an oil, but the purity of [Ru(CO)(PPh_3){PH(O)Cy}(Tp)] within this oil was not increased.

A crystal of [Ru(CO)(PPh_3){PH(O)Cy}(Tp)] suitable for X-ray diffraction was grown by liquid diffusion of *n*-pentane into a toluene solution of [Ru(CO)(PPh_3)(PHCy)(Tp)] at −20°C over 71 days.

IR (THF) ν/cm^{-1}: 2487 w (BH), 1973 vs (CO), 1949 sh (CO). $^{31}P\{^1H\}$ NMR ($CDCl_3$, 162.0 MHz, 300 K) δ/ppm: 97.0 (d, $^2J_{PP}$ = 32 Hz, PH(O)Cy), 44.4 (d, $^2J_{PP}$ = 32 Hz, PPh_3). ^{31}P NMR ($CDCl_3$, 162.0 MHz, 298 K) δ/ppm: 97.0 (d,$^1J_{PH}$ = 337 Hz, PH(O)Cy), 44.4 (br s, PPh_3). ESI-MS (+, MeCN) *m/z*: 737.2 $[M + H]^+$. Accurate mass: found 737.1688 $[M + H]^+$, Calcd. for $C_{34}H_{38}{}^{11}BN_6O_2{}^{31}P_2{}^{102}Ru$ 737.1668. Crystal data for $[C_{34}H_{37}BN_6O_2P_2Ru]$: M_w = 735.53, trigonal, *R*-3, *a* = 44.774(6) Å, *c* = 9.5300(19) Å, *V* = 16545(3) $Å^3$, *Z* = 18, ρ_{calcd} = 1.329 Mg m^{-3}, μ(synchrotron, λ = 0.71073 Å) = 0.55 mm^{-1}, *T* = 100 K, colourless block, 0.03 × 0.02 × 0.01 mm, 10485 measured reflections, 10485 independent (R_{int} = 0.145), F^2 refinement, *R* = 0.066, *wR* = 0.210 for 6705 reflections ($I > 2\sigma(I)$, $2\vartheta_{max}$ = 63.6°), 421 parameters with 0 restraints.

Minor Diastereomer

$^{31}P\{^{1}H\}$ NMR ($CDCl_3$, 162.0 MHz, 300 K) δ/ppm: 90.4 (d, $^{2}J_{PP}$ = 32 Hz, PH(O)Cy), 46.8 (d, $^{2}J_{PP}$ = 32 Hz, PPh_3). ^{31}P NMR ($CDCl_3$, 162.0 MHz, 298 K) δ/ppm: 90.4 (d,$^{1}J_{PH}$ = 345 Hz, PH(O)Cy), 46.8 (br s, PPh_3).

Synthesis of [Ru(CO)(PPh_3){PH(S)Cy}(Tp)]

Tetrahydrofuran (70 mL) was added to a mixture of [Ru(CO)(PH_2Cy)(PPh_3)(Tp)]OTf (1.50 g, 1.72 mmol) and KH (0.093 g, 2.32 mmol). The yellow mixture was stirred for 45 minutes after which the supernatant was isolated by cannula filtration. Elemental sulfur (0.057 g, 1.8 mg-atom) was added to the filtrate and stirring continued for 15 minutes over which the mixture turned pale yellow. The mixture was freed of volatiles *in vacuo* and the rest of the procedure was carried out in air. The residue was taken up in toluene (100 mL) and filtered through diatomaceous earth. Solvent was removed from the filtrate on a rotary evaporator, and the residue recrystallised from a CH_2Cl_2/MeOH mixture to yield the product as a white solid. Crystals suitable for X-ray diffraction were grown by vapour diffusion of MeOH into a CH_2Cl_2 solution of the product at −10°C.

Yield: 0.767 g (59%). IR (ATR) ν/cm^{-1}: 2925 w, 2848 w (CH), 2486 w (BH), 1973 vs (CO). IR (THF) ν/cm^{-1}: 2487 w (BH), 2234 w (PH), 1989 vs (CO). ^{1}H NMR ($CDCl_3$, 700.2 MHz, 298 K) δ/ppm: 8.59, 7.82, 6.96, 6.71, 6.21, 6.05, 5.85 (s x 7, 7 × 1H, J_{HH} not resolved, Hpz), 7.64 (s × 2, 2 × 1H, J_{HH} not resolved, Hpz), 7.40−7.30 (m, 15H, PC_6H_5), 5.42 (ddd, 1H, $^{1}J_{PH}$ = 343 Hz, $^{3}J_{PH}$ = 8 Hz, $^{3}J_{HH}$ = 6 Hz, PH), 4.56 (br s, BH), 1.70–0.22 (m, 11H, C_6H_{11}). $^{13}C\{^{1}H\}$ NMR ($CDCl_3$, 176.1 MHz, 298 K) δ/ppm: 202.2 (dd, $^{2}J_{PC}$ = 13 Hz, CO), 145.4 (s,C^3(pz)), 144.4 (s × 2, 2 × C^3(pz)), 136.5, 135.7, 135.5 (s × 3, 3 × C^5(pz)), 134.4 (d, J_{PC} = 11 Hz, o/m-PC_6H_5), 131.9 (d, $^{1}J_{PC}$ = 44 Hz, *ipso*-PC_6H_5), 130.4 (s, *p*-PC_6H_5), 128.2 (d, J_{PC} = 11 Hz, o/m-PC_6H_5), 106.1, 105.9, 105.7 (s × 3, 3 × C^4(pz)), 40.7 (d, $^{1}J_{PC}$ = 25 Hz, 1-C_6H_{11}), 29.6 (d, $^{3}J_{PC}$ = 4 Hz, 3,5-C_6H_{11}) 28.6 (d, $^{3}J_{PC}$ = 4 Hz, 3,5-C_6H_{11}), 27.4 (d, $^{2}J_{PC}$ = 12 Hz, 2,6-C_6H_{11}), 27.1 (d, $^{2}J_{PC}$ = 11 Hz, 2,6-C_6H_{11}), 26.0 (s, 4-C_6H_{11}). $^{31}P\{^{1}H\}$ NMR ($CDCl_3$, 162.0 MHz, 300 K) δ/ppm: 51.2 (d, $^{2}J_{PP}$ = 28 Hz, PH(S)Cy), 42.2 (d, $^{2}J_{PP}$ = 28 Hz, PPh_3). ^{31}P NMR ($CDCl_3$, 162.0 MHz, 298 K) δ/ppm: 51.2 (dd,$^{1}J_{PH}$ = 337 Hz, $^{2}J_{PP}$ = 28 Hz, PH(S)Cy), 42.2 (br s, PPh_3). ESI-MS (+, MeCN) *m/z*: 753.1 $[M + H]^+$. Accurate mass: found 753.1449 $[M + H]^+$, Calcd. for $C_{34}H_{38}{}^{11}BN_6OP_2{}^{102}RuS$ 753.1440. Anal. Found: C, 54.16; H, 5.18; N, 11.18%. Calcd. For $C_{34}H_{37}BN_6OP_2RuS$: C, 54.33; H, 4.96; N, 11.18. Crystal data for

$[C_{34}H_{37}BN_6OP_2RuS].2(CH_4O)$: M_w = 815.69, orthorhombic, *Pbca*, a = 19.5948(1) Å, b = 10.1385(1) Å, c = 37.6063(2) Å, V = 7470.94(4) Å^3, Z = 8, ρ_{calcd} = 1.450 Mg m^{-3}, μ(Cu, Kα) = 5.09 mm^{-1}, T = 150 K, colourless block, 0.55 × 0.16 × 0.07 mm, 131620 measured reflections, 7564 independent (R_{int} = 0.064), F^2 refinement, R = 0.063, wR = 0.164 for 7248 reflections ($I > 2\sigma(I)$, $2\vartheta_{max}$ = 147.6°), 457 parameters with 2 restraints.

Data for minor Diastereomer

Typically present as 8-10% of the product.

IR (THF) ν/cm^{-1}: 1956 s (CO). $^{31}P\{^1H\}$ NMR ($CDCl_3$, 162.0 MHz, 300 K) δ/ppm: 56.0 (d, $^2J_{PP}$ = 26 Hz, PH(S)Cy), 42.9 (d, $^2J_{PP}$ = 26 Hz, PPh_3). ^{31}P NMR ($CDCl_3$, 162.0 MHz, 298 K) δ/ppm: 56.0 (dd,$^1J_{PH}$ = 351 Hz, $^2J_{PP}$ = 28 Hz, PH(S)Cy), 42.9 (br s, PPh_3).

Attempted Deprotonation of [Ru(CO)(PPh_3){PH(S)Cy}(Tp)]

Base (DBU, 0.01 mL, 67 µmol; or ^{n}BuLi, 0.05 mL, 1.6 M in hexanes, 80 µmol) was added to a solution of [Ru(CO)(PPh_3){PH(S)Cy}(Tp)] (0.050 g, 67 µmol) in THF (5 mL). After 30 minutes of stirring, no visible change was observed and there was no change in the IR or $^{31}P\{^1H\}$ NMR spectrum of the mixture.

Synthesis of [Ru(CO)(PPh_3){PH(Se)Cy}(Tp)]

Tetrahydrofuran (30 mL) was added to a mixture of [Ru(CO)(PH_2Cy)(PPh_3)(Tp)]OTf (0.500 g, 0.574 mmol) and KH (0.034 g, 0.848 mmol). The yellow mixture was stirred for 45 minutes after which the supernatant was isolated by cannula filtration. Elemental selenium (0.046 g, 0.58 mg-atom) was added to the filtrate and stirring continued for 2 hours over which the mixture turned pale yellow and the black selenium dissolved completely. The mixture was freed of volatiles *in vacuo* and the rest of the procedure was carried out in air. The residue was taken up in toluene (50 mL) and filtered through diatomaceous earth. Solvent was removed from the filtrate on a rotary evaporator, and the residue recrystallised from a CH_2Cl_2/MeOH mixture to yield the product as a pale yellow solid.

Yield 0.238g (52%). IR (THF) ν/cm^{-1}: 2487 w (BH), 2250 w (PH), 1993 vs (CO). ^{1}H NMR ($CDCl_3$, 400.1 MHz, 298 K) δ/ppm: 8.63, 7.83, 6.99, 6.72, 6.22, 6.06, 5.85 (s x 7, 7 × 1H, J_{HH} not resolved, Hpz), 7.64 (s, 2H, J_{HH} not resolved, Hpz), 7.40–7.30 (m, 15H, PC_6H_5), 4.48 (ddd, 1H, $^{1}J_{PH}$ = 336 Hz, ^{3}J = 4 Hz, ^{3}J = 8 Hz, PH), 1.74–0.17 (m, 11H, C_6H_{11}). $^{13}C\{^{1}H\}$ NMR ($CDCl_3$, 150.9 MHz, 298 K) δ/ppm: 202.6 (dd, $^{2}J_{PC}$ = 14.3 Hz, CO) 145.3 (s, C^3(pz)), 144.5 (s, C^3(pz)), 144.4 (s, C^3(pz)), 136.5 (s, C^4(pz)), 135.8 (s, C^4(pz)), 135.6 (s, C^4(pz)), 134.4 (d, J_{PC} = 9 Hz, o/m-PC_6H_5), 131.8 (d, $^{1}J_{PC}$ = 45 Hz, *ipso*-PC_6H_5), 130.5 (s, *p*-PC_6H_5), 128.3 (d, J_{PC} = 9 Hz, o/m-PC_6H_5), 106.2 (s, C^5(pz)), 105.9 (s, C^5(pz)), 105.8 (s, C^5(pz)), 38.5 (d, $^{1}J_{PC}$ = 20 Hz, 1-C_6H_{11}), 30.9 (d, $^{3}J_{PC}$ = 5 Hz, 3,5-C_6H_{11}), 29.9 (d, $^{3}J_{PC}$ = 2 Hz, 3,5-C_6H_{11}), 27.6 (d, $^{2}J_{PC}$ = 12 Hz, 2,6-C_6H_{11}), 27.2 (d, $^{2}J_{PC}$ = 12 Hz, 2,6-C_6H_{11}), 26.1 (s, 4-C_6H_{11}). $^{31}P\{^{1}H\}$ NMR ($CDCl_3$, 162.0 MHz, 300 K) δ/ppm: 41.1 (d, $^{2}J_{PP}$ = 28 Hz, PPh_3), 19.9 (d, $^{2}J_{PP}$ = 28 Hz, $^{1}J_{PSe}$ = 497 Hz, PH(Se)Cy). ^{31}P NMR ($CDCl_3$, 162.0 MHz, 298 K) δ/ppm: 41.1 (br s, PPh_3), 19.9 (dd, $^{2}J_{PP}$ = 28 Hz, $^{1}J_{PH}$ = 335 Hz, PH(S)Cy). ESI-MS (+, MeCN) *m/z*: 801.1 $[M + H]^+$, 823.1 $[M + Na]^+$. Accurate mass: found 801.0889 $[M + H]^+$, Calcd. for $C_{34}H_{38}{}^{11}BN_6OP_2{}^{102}Ru^{80}Se$ 801.0884; found 823.0726, Calcd. for $C_{34}H_{37}{}^{11}BN_6{}^{23}NaOP_2{}^{102}Ru^{80}Se$ 801.0884. Anal. Found: C, 50.85; H, 4.60; N, 10.48%. Calcd. For $C_{34}H_{37}BN_6OP_2RuSe$: C, 51.14; H, 4.67; N, 10.53.

Minor Diastereomer

IR (THF) ν/cm^{-1}: 1960 s (CO). $^{31}P\{^{1}H\}$ NMR ($CDCl_3$, 162.0 MHz, 300 K) δ/ppm: 42.6 (d, $^{2}J_{PP}$ = 24 Hz, PPh_3), 33.4 (d, $^{2}J_{PP}$ = 24 Hz, PH(Se)Cy). ^{31}P NMR ($CDCl_3$, 162.0 MHz, 300 K) δ/ppm: 42.6 (br s, PPh_3), 33.4 (d, $^{1}J_{PH}$ = 357 Hz, PH(Se)Cy).

Formation of [Ru(CO)(PPh_3){PH(Te)Cy}(Tp)]

Tetrahydrofuran (10 mL) was added to a mixture of [Ru(CO)(PH_2Cy)(PPh_3)(Tp)]OTf (0.100 g, 0.115 mmol) and KH (0.018 g, 0.449 mmol). The yellow mixture was stirred for 30 minutes after which the supernatant was isolated by cannula filtration. Elemental tellurium (0.018 g, 0.14 mg-atom) was added to the filtrate and the mixture stirred for 2 hours by which time the tellurium had dissolved. At this point, aliquots of the mixture were taken for IR and ^{31}P NMR spectroscopy. The mixture was freed of volatiles *in vacuo* and toluene (40 mL) added to the resultant orange residue. Cannula filtration yielded a clear orange liquid which was freed of volatiles *in vacuo*. Nuclear magnetic resonance spectroscopy of the residue showed that *ca*.

50% of the desired complex had decomposed. Monitoring this sample showed complete decomposition to a complex mixture of products after 24 hours.

IR (THF) ν/cm^{-1}: 2483 w (BH), 1994 vs (CO). $^{31}P\{^{1}H\}$ NMR (C_6D_6, 162.0 MHz, 300 K) δ/ppm: 39.7 (d, $^{2}J_{PP}$ = 25 Hz, PPh_3), –61.9 (d, $^{2}J_{PP}$ = 25 Hz, PH(Te)Cy). ^{31}P NMR (C_6D_6, 162.0 MHz, 300 K) δ/ppm: 39.7 (br s, PPh_3), –61.9 (d, $^{1}J_{PH}$ = 317 Hz, PH(Te)Cy).

Synthesis of [Ru(CO)(PPh_3){PH(SH)Cy}(Tp)]OTf

Triflic acid (0.02 mL, 0.226 mmol) was added to a solution of [Ru(CO)(PPh_3){PH(S)Cy}(Tp)] (0.050 g, 0.067 mmol) in THF (5 mL). After 30 minutes of stirring IR spectroscopy revealed only a single CO band corresponding to the product (1997 cm^{-1}). The THF was removed under reduced pressure and the yellow residue subjected to ultrasonic trituration in Et_2O (30 mL). The product was collected as a colourless solid by vacuum filtration. Crystals suitable for X-ray diffraction and elemental analysis were obtain by vapour diffusion of *n*-hexane into a CH_2Cl_2 solution of the product at 25°C.

Yield: 0.030 g (50%). IR (THF) ν/cm^{-1}: 2493 w (BH), 1998 vs (CO). ^{1}H NMR ($CDCl_3$, 700.2 MHz, 298 K) δ/ppm: 7.94, 7.93, 7.78, 7.76, 7.22, 6.61, 6.33, 6.21, 5.96 (s x 9, 9 × 1H, J_{HH} not resolved, Hpz), 7.51, 7.41, 7.10 (m × 3, 15H, PC_6H_5), 5.03 (ddd, 1H, $^{1}J_{PH}$ = 364 Hz, *J* = 3 Hz, *J* = 9 Hz, PH), 3.83 (br s, BH), 3.24 (br s, SH), 1.97– –0.29 (m, 11H, C_6H_{11}). $^{13}C\{^{1}H\}$ NMR ($CDCl_3$, 176.1 MHz, 298 K) δ/ppm: 200.5 (dd, $^{2}J_{PC}$ = 13 Hz, CO), 145.4, 145.3, 144.8 (s × 3, 3 × C^3(pz)), 137.8, 137.1, 137.0 (s × 3, 3 × C^5(pz)), 133.8 (d, J_{PC} = 9 Hz, o/m-PC_6H_5), 131.7 (s, *p*-PC_6H_5), 129.2 (d, J_{PC} = 11 Hz, o/m-PC_6H_5), 129.1 (d, $^{1}J_{PC}$ = 48 Hz, *ipso*-PC_6H_5), 107.6, 107.4, 107.2 (s × 3, 3 × C^4(pz)), 38.2 (d, $^{2}J_{PC}$ = 19 Hz, 1-C_6H_{11}), 29.9 (d, $^{2}J_{PC}$ = 7 Hz, 2,6-C_6H_{11}) 27.7 (s, 3,4,5-C_6H_{11}), 27.0 (d, $^{2}J_{PC}$ = 16 Hz, 2,6-C_6H_{11}), 26.8 (d, $^{3}J_{PC}$ = 11 Hz, 3,5-C_6H_{11}), 25.2 (s, 3,4,5-C_6H_{11}). $^{31}P\{^{1}H\}$ NMR ($CDCl_3$, 162.0 MHz, 300 K) δ/ppm: 44.2 (d, $^{2}J_{PP}$ = 29 Hz, PH(SH)Cy), 36.3 (d, $^{2}J_{PP}$ = 29 Hz, PPh_3). ^{31}P NMR ($CDCl_3$, 162.0 MHz, 298 K) δ/ppm: 44.2 ($^{1}J_{PH}$ = 371 Hz, $^{2}J_{PP}$ = 29 Hz, PH(SH)Cy), 36.3 (br s, PPh_3). ESI-MS (+, MeCN) *m/z*: 753.1 $[M]^+$. Accurate mass: found 753.1432 $[M]^+$, Calcd. for $C_{34}H_{38}{}^{11}BN_6OP_2{}^{102}RuS$ 753.1440. Anal. Found: C, 46.53; H, 4.19; N, 9.19 %. Calcd. For $C_{35}H_{38}BF_3N_6O_4P_2RuS_2$: C, 46.64; H, 4.25; N, 9.32 %. Crystal data for $[C_{34}H_{38}BN_6OP_2RuS][CF_3O_3S]$: M_w = 901.68, monoclinic, *I2/a*, *a* = 20.5298(5) Å, *b* = 9.5759(4) Å,

c = 40.1943(18) Å, β = 98.953(3)°, V = 7805.6(3) Å^3, Z = 8, ρ_{calcd} = 1.534 Mg m^{-3}, μ(Cu, Kα) = 5.55 mm^{-1}, T = 150 K, colourless block, 0.08 × 0.06 × 0.04 mm, 20922 measured reflections, 7495 independent (R_{int} = 0.028), F^2 refinement, R = 0.029, wR = 0.068 for 6734 reflections ($I > 2\sigma(I)$, $2\vartheta_{max}$ = 144.2°), 493 parameters with 0 restraints.

Deprotonation of [Ru(CO)(PPh$_3$){PH(SH)Cy}(Tp)]OTf

Tetrahydrofuran (1 mL) was added to a mixture of [Ru(CO)(PPh$_3$){PH(SH)Cy}(Tp)]OTf (0.005 g, 5.5 µmol) and KH (0.009 g, 0.22 mmol). A pale yellow mixture formed and effervescence was observed. After 40 minutes of stirring IR and ^{31}P{^{1}H} NMR spectroscopy both showed that the major component was [Ru(CO)(PPh$_3$){PH(S)Cy}(Tp)].

Synthesis of [Ru(CO)(PPh$_3$){PH(SMe)Cy}(Tp)]OTf

Methyl triflate (0.042 mL, 0.348 mmol) was added to a solution of [Ru(CO)(PPh$_3$){PH(S)Cy}(Tp)] (0.278g, 0.370 mmol) in benzene (20 mL). The mixture was stirred for 1 hour after which the product had precipitated as a colourless solid. The product was collected by vacuum filtration in air and washed with benzene and diethyl ether. Crystals suitable for X-ray diffraction were grown by vapour diffusion of *n*-hexane into a CH_2Cl_2 solution of the compound at 25°C.

Yield: 0.194g (58%). IR (THF) ν/cm^{-1}: 1992 vs (CO). IR (ATR) ν/cm^{-1}: 3054 w, 2902 w, 2848 w (CH), 1983 s (CO), 637 vs (CS). ^{1}H NMR ($CDCl_3$, 700.2 MHz, 298 K) δ/ppm: 7.90, 7.80, 7.76, 6.41, 6.32, 6.29, 6.00 (s x 7, 7 × 1H, J_{HH} not resolved, Hpz), 7.82 (s, 2H, J_{HH} not resolved, Hpz), 7.49, 7.42, 7.09 (m × 3, 15H, PC_6H_5), 5.20 (ddd, 1H, $^1J_{PH}$ = 378 Hz, J = 4 Hz, J = 4 Hz, PH), 4.66 (br s, BH), 2.04 (d, 3H, $^3J_{PH}$ = 7 Hz, SMe), 1.82–0.03 (m, 11H, C_6H_{11}). ^{13}C{^{1}H} NMR ($CDCl_3$, 176.1 MHz, 298 K) δ/ppm: 200.7 (dd, $^2J_{PC}$ = 16 Hz, CO), 146.7, 145.1, 144.2 (s × 3, 3 × C^3(pz)), 137.5, 137.3, 137.0 (s × 3, 3 × C^5(pz)), 134.0 (d, J_{PC} = 11 Hz, o/m-PC_6H_5), 131.6 (s, *p*-PC_6H_5), 129.7 (d, $^1J_{PC}$ = 48 Hz, *ipso*-PC_6H_5), 129.1 (d, J_{PC} = 11 Hz, o/m-PC_6H_5), 108.1 (s, C^4(pz)), 107.11, 107.07 (s × 2, 2 × C^4(pz)), 40.5 (d, $^1J_{PC}$ = 19 Hz, 1-C_6H_{11}), 30.1 (d, $^2J_{PC}$ = 7 Hz, 2,6-C_6H_{11}) 28.4 (s, 3,4,5-C_6H_{11}), 27.1 (d, $^2J_{PC}$ = 5 Hz, 2,6-C_6H_{11}), 27.0 (s, 3,4,5-C_6H_{11}), 24.9 (s, 3,4,5-C_6H_{11}), 21.8 (d, $^2J_{PC}$ = 7 Hz, SMe). ^{31}P{^{1}H} NMR ($CDCl_3$, 162.0 MHz, 300 K) δ/ppm: 66.8 (d, $^2J_{PP}$ = 29 Hz, PH(SMe)Cy), 36.2 (d, $^2J_{PP}$ = 29 Hz, , PPh_3). ^{31}P NMR ($CDCl_3$, 162.0 MHz, 298 K) δ/ppm: 66.8 (d, $^1J_{PH}$ = 371 Hz,

PH(SMe)Cy), 36.2 (br s, PPh_3). ESI-MS (+, MeCN) *m/z*: 767.2 $[M]^+$. Accurate mass: found 767.1609 $[M]^+$, Calcd. for $C_{35}H_{40}{}^{11}BN_6OP_2{}^{102}RuS$ 767.1591. Anal. Found: C, 47.10; H, 4.47; N, 9.05%. Calcd. For $C_{35}H_{40}BF_3N_6O_4P_2RuS_2$: C, 47.22; H, 4.40; N, 9.18. Crystal data for $[C_{35}H_{40}BN_6OP_2RuS][CF_3O_3S].(CH_2Cl_2)$: M_w = 1000.64, monoclinic, $P2_1/c$, a = 24.1178(2) Å, b = 37.5559(4) Å, c = 9.6253(1) Å, β = 91.3470(9)°, V = 8715.86(9) Å^3, Z = 8, ρ_{calcd} = 1.525 Mg m^{-3}, μ(Cu, Kα) = 6.13 mm^{-1}, T = 150 K, colourless needle, 0.13 × 0.04 × 0.03 mm, 64169 measured reflections, 17228 independent (R_{int} = 0.043), F^2 refinement, R = 0.045, wR = 0.107 for 14860 reflections ($I > 2\sigma(I)$, $2\vartheta_{max}$ = 147.4°), 1057 parameters with 0 restraints.

Synthesis of [Ru(CO)(PPh_3){PH(SeMe)Cy}(Tp)]OTf

Methyl triflate (18 µL, 0.16 mmol) was added to a solution of [Ru(CO)(PPh_3){PH(Se)Cy}(Tp)] (0.060 g, 0.0751 mmol) in benzene (8.0 mL). The mixture slowly decolourised with the formation of a colourless precipitate over 5 minutes and stirring was continued for 3 hours. At this point the flask was opened to air and the precipitate collected by vacuum filtration, washing with Et_2O (3 × 10 mL) and *n*-pentane (2 × 10 mL). Crystals suitable for X-ray diffraction were grown by vapour diffusion of *n*-hexane into a $CHCl_3$ solution of the compound at −10°C.

Yield: 0.039 g (53%). IR (THF) ν/cm^{-1}: 2495 w (BH), 1986 vs (CO). ^{1}H NMR ($CDCl_3$, 600.0 MHz, 298 K) δ/ppm: 7.93, 7.83, 7.69, 6.44, 6.33, 6.27, 6.01 (s x 7, 7 × 1H, J_{HH} not resolved, Hpz), 7.78 (s, 2H, J_{HH} not resolved, Hpz), 7.51, 7.41, 7.10 (m × 3, 15H, PC_6H_5), 4.73 (ddd, 1H, $^1J_{PH}$ = 366 Hz, J = 3 Hz, J = 7 Hz, PH), 4.66 (br s, BH), 2.04 (d, 3H, $^3J_{PH}$ = 7 Hz, Se satellites not observed, SeMe), 1.86–0.02 (m, 11H, C_6H_{11}). ^{13}C{^{1}H} NMR ($CDCl_3$, 150.9 MHz, 298 K) δ/ppm: 201.0 (dd, 2 × $^2J_{PC}$ = 12.8 Hz, CO), 146.2, 145.1, 144.5 (s × 3, 3 × C^3(pz)), 137.7, 137.4, 137.1 (s × 3, 3 × C^5(pz)), 134.0 (d, J_{PC} = 11 Hz, o/m-PC_6H_5), 131.7 (s, *p*-PC_6H_5), 129.5 (d, $^1J_{PC}$ = 47 Hz, *ipso*-PC_6H_5), 129.1 (d, J_{PC} = 11 Hz, o/m-PC_6H_5), 107.9 (s, C^4(pz)), 107.2 (s, 2 × C^4(pz)), 39.2 (d, $^1J_{PC}$ = 15 Hz, 1-C_6H_{11}), 31.1 (d, $^2J_{PC}$ = 6 Hz, 2,6-C_6H_{11}), 29.5 (s, 3,5-C_6H_{11}), 27.2 (d, $^2J_{PC}$ = 6 Hz, 2,6-C_6H_{11}), 27.1 (d, $^3J_{PC}$ = 3 Hz, 3,5-C_6H_{11}), 25.0 (s, 4-C_6H_{11}), 12.6 (d, $^2J_{PC}$ = 5 Hz, SeMe). ^{31}P{^{1}H} NMR ($CDCl_3$, 162.0 MHz, 298 K) δ/ppm: 46.3 (d, $^2J_{PP}$ = 28 Hz, $^1J_{PSe}$ = 318 Hz, PH{SeMe}Cy), 35.9 (d, $^2J_{PP}$ = 28 Hz, PPh_3). ^{31}P NMR ($CDCl_3$, 162.0 MHz, 298 K) δ/ppm: 46.3 (d, $^1J_{PH}$ = 371 Hz, PH(SeMe)Cy), 35.9 (br s, PPh_3). ESI-MS (+, MeCN) *m/z*: 815.1 $[M]^+$. Accurate mass: found 815.1046 $[M]^+$, Calcd. for $C_{35}H_{40}{}^{11}BN_6OP_2{}^{102}Ru^{80}Se$ 815.1041. Anal. Found: C, 44.80; H, 4.06; N, 8.62%. Calcd.

For $C_{36}H_{40}BF_3N_6O_4P_2RuSSe$: C, 44.92; H, 4.19; N, 8.73. Crystal data for $[C_{35}H_{40}BN_6OP_2RuSe][CF_3O_3S].(CHCl_3)$: M_w = 1081.98, monoclinic, *Cc*, a = 37.9374(5) Å, b = 9.5647(1) Å, c = 25.2710(3) Å, β = 100.8862(12)°, V = 9004.81(19) Å^3, Z = 8, ρ_{calcd} = 1.596 Mg m^{-3}, μ(Mo, Kα) = 1.51 mm^{-1}, T = 150 K, colourless block, 0.18 × 0.15 × 0.05 mm, 76758 measured reflections, 21445 independent (R_{int} = 0.051), F^2 refinement, R = 0.047, wR = 0.100 for 18483 reflections ($I > 2\sigma(I)$, $2\vartheta_{max}$ = 59.6°), 1070 parameters with 38 restraints, Flack parameter = 0.205(3).

Formation of [Ru(CO)(PPh$_3$){P(SMe)Cy}(Tp)]

Tetrahydrofuran (3 mL) was added to a mixture of [Ru(CO)(PPh$_3$){PH(SMe)Cy}(Tp)]OTf (5 mg, 5.5 µmol) and KH (5 mg, 0.12 mmol). Effervescence was observed and the mixture turned yellow. After stirring for 30 minutes the IR spectrum of the mixture showed two new ν_{CO} bands at 1950 and 1935 cm^{-1}. The mixture was freed of volatiles *in vacuo* and the resulting residue was analysed by NMR spectroscopy. An approximately 1:1 mixture of diastereomers of [Ru(CO)(PPh$_3$){P(SMe)Cy}(Tp)] was observed. A NMR sample of the residue in toluene-d_8 was monitored over 5 days, after which no more resonances for [Ru(CO)(PPh$_3$){P(SMe)Cy}(Tp)] were observed. Crystals suitable for X-ray crystallography were grown from this sample and were determined to be [Ru(CO)(PPh$_3$){P(O)(OH)Cy}(Tp)] (crystal data provided below). Notably, the precursor [Ru(CO)(PPh$_3$){PH(SMe)Cy}(Tp)]OTf does not decompose under the same conditions.

Data for mixture of diastereomers

IR (THF) ν/cm^{-1}: 2476 w (BH) 1950 vs, 1935 w (CO). ^{1}H NMR (C_6D_6, 400.1 MHz, 298 K) δ/ppm: 8.27, 8.20, 8.04, 7.85, 7.53, 7.33, 7.27, 6.72, 6.64, 5.91, 5.84, 5.74 (s × 12, 12 × 1H, Hpz), 7.47–6.97 (m, PPh$_3$), 5.62 (s, 2H, pzH), 2.94 – –0.14 (m, Cy), 1.98 (d, $^3J_{PH}$ = 8 Hz, 2D correlation to δ_P 90.5, SMe), 1.83 (d, $^3J_{PH}$ = 8 Hz, 2D correlation to δ_P 126.4, SMe). ^{31}P{^{1}H} NMR (C_6D_6, 162.0 MHZ, 298 K) δ/ppm: 126.4 (d, $^2J_{PP}$ = 18 Hz, P(SMe)Cy), 90.5 (d, $^2J_{PP}$ = 8 Hz, P(SMe)Cy), 43.8 (d, $^2J_{PP}$ = 8 Hz, PPh$_3$), 43.2 (d, $^2J_{PP}$ = 18 Hz, PPh$_3$).

NMR data following decomposition

$^{31}P\{^{1}H\}$ NMR (toluene-d_8, 283.4 MHz, 298 K) δ/ppm: 119.9 (br s), 113.5 (d, J = 31 Hz), 105.1 (d, J = 18 Hz), 71.4 (s), 56.7 (s), 48.0 (br s), 45.3 (s), 43.3 (d, J = 26 Hz), 41.1 (d, J = 18 Hz), 24.5 (s).

Crystal data for [Ru(CO)(PPh₃){P(O)(OH)Cy}(Tp)]

Crystal data for $[C_{34}H_{37}BN_6O_3P_2Ru]$: M_w = 751.53, triclinic, $P\bar{1}$, a = 15.6048(10) Å, b = 16.2656(11), c = 17.1335(9) Å, α = 70.628(5)°, β = 75.178(5)°, γ = 72.736(6)°, V = 3857.6(4) Å^3, Z = 4, ρ_{calcd} = 1.294 Mg m^{-3}, μ(Cu, Kα) = 4.39 mm^{-1}, T = 150 K, colourless prism, 0.13 × 0.11 × 0.05 mm, 26727 measured reflections, 15090 independent (R_{int} = 0.041), F^2 refinement, R = 0.073, wR = 0.195 for 11068 reflections ($I > 2\sigma(I)$, $2\vartheta_{max}$ = 147.6°), 1005 parameters with 344 restraints.

Attempted Synthesis of [Ru(CO)(PPh₃){P(O)(OH)Cy}(Tp)]

This procedure was conducted under aerobic conditions. A mixture of [Ru(CO)(PPh$_3$){PH(SMe)Cy}(Tp)]OTf (0.050 g, 55 µmol), KOH (0.022 g, 0.39 mmol) and THF (5 mL) was stirred for 24 hours. At this point the mixture had turned yellow and an aliquot was taken for NMR spectroscopy. The mixture was freed of volatiles on a rotary evaporator and toluene (20 mL) was added to the resulting residue. The suspension was filtered through diatomaceous earth and the filtrate freed of volatiles on a rotary evaporator. A $^{31}P\{^{1}H\}$ NMR spectrum of the residue was acquired, and the development of new resonances at δ_P 121.5 and 29.1 (O=PPh$_3$) was observed. The residue was soluble in EtOH and Et$_2$O. Attempts to crystallise the product from these solvents, as well as toluene/*n*-hexane and CH_2Cl_2/*n*-hexane mixtures, at −20°C did not yield any precipitate.

Compound 1

$^{31}P\{^{1}H\}$ NMR ($CDCl_3$, 162.0 MHZ, 300 K) δ/ppm: 117.7 (d, $^2J_{PP}$ = 32 Hz), 40.1 (d, $^2J_{PP}$ = 32 Hz).

Compound 2

$^{31}P\{^{1}H\}$ NMR ($CDCl_3$, 162.0 MHZ, 300 K) δ/ppm: 107.4 (d, $^2J_{PP}$ = 32 Hz), 40.4 (d, $^2J_{PP}$ = 32 Hz).

Compound 3

$^{31}P\{^{1}H\}$ NMR ($CDCl_3$, 162.0 MHZ, 300 K) δ/ppm: 121.5 (d, $^{2}J_{PP}$ = 32 Hz), 46.3 (d, $^{2}J_{PP}$ = 32 Hz).

Formation of [Ru(CO)(PPh_3){PMe(SMe)Cy}(Tp)]

Tetrahydrofuran (10 mL) was added to a mixture of [Ru(CO)(PPh_3){PH(SMe)Cy}(Tp)]OTf (0.100 g, 0.109 mmol) and KH (0.017 g, 0.424 mmol). The yellow mixture was stirred for 30 minutes before being subjected to cannula filtration. Iodomethane (0.02 mL, 0.32 mmol) was added to filtrate resulting in decolourisation and the formation of a colourless precipitate after 10 minutes. Stirring was continued for 22 hours, after which the IR spectrum of the mixture showed a new ν_{CO} band at 1996 cm^{-1} and did not contain the ν_{CO} bands for [Ru(CO)(PPh_3){P(SMe)Cy}(Tp)] (1950, 1935 cm^{-1}). The mixture was freed of volatiles *in vacuo*, and the rest of the procedure was conducted in aerobic conditions. Dichloromethane (20 mL) was added to the residue and the resulting mixture filtered through diatomaceous earth. The filtrate was then freed of volatiles on a rotary evaporator. Attempted recrystallisation of the residue from CH_2Cl_2/MeOH and CH_2Cl_2/Et_2O solvent mixtures on a rotary evaporator both yielded oils. In the latter case the oil could be separated from the supernatant, but the purity of the product was not improved. A concentrated ^{i}PrOH solution of the residue placed in a −20°C freezer yielded an oil which could not be separated. Crystals suitable for an X-ray diffraction experiment were grown by slow evaporation of solvent from a CH_2Cl_2/Et_2O solution of the residue but a bulk sample of pure compound could not be obtained. The NMR data for the crude sample are provided below and the $^{31}P\{^{1}H\}$ NMR resonances are paired based on the relative intensities of the signals.

IR (THF) ν/cm^{-1}: 2492 w (BH), 1996 vs (CO). ^{1}H NMR ($CDCl_3$, 400.1 MHz, 298 K) δ/ppm: 8.07, 8.00, 7.89, 7.81, 7.77, 7.73, 7.59 (s × 7, Hpz), 7.50−7.10 (m, PPh_3), 6.58, 6.45, 6.37, 6.32, 6.25, 5.95, 5.86 (s × 7, Hpz), 2.21 (d, J_{PH} = 8 Hz, 2D correlation to δ_P 51.8), 2.02−0.27 (m, C_6H_{11}), 1.81 (d, J_{PH} = 8 Hz, 2D correlation to δ_P 57.6), 1.39 (d, J_{PH} = 8 Hz, 2D correlation to δ_P 57.6), 0.64 (d, J_{PH} = 8 Hz, 2D correlation to δ_P 51.8). $^{31}P\{^{1}H\}$ NMR ($CDCl_3$, 162.0 MHZ, 300 K) δ/ppm: 57.6 (d, $^{2}J_{PP}$ = 28 Hz, PMe(SMe)Cy, diastereomer 1), 51.8 (d, $^{2}J_{PP}$ = 28 Hz, PMe(SMe)Cy, diastereomer 2), 35.0 (d, $^{2}J_{PP}$ = 28 Hz, PPh_3, diastereomer 1), 32.6 (d, $^{2}J_{PP}$ = 28 Hz, PPh_3, diastereomer 2). ESI-MS (+, MeCN) *m/z*: 781.2 $[M]^+$. Accurate mass: found 781.1758 $[M]^+$, Calcd. for

$C_{36}H_{42}BN_6OP_2RuS$ 781.1758. Crystal data for $[C_{36}H_{42}BN_6OP_2RuS][CF_3O_3S]_{0.74}I_{0.26}.(CHCl_3)(C_4H_{10}O)$: M_w = 1080.40, orthorhombic, *Pbcn*, a = 38.5769(5) Å, b = 10.7484(2) Å, c = 22.7303(4) Å, V = 9424.9(3) Å^3, Z = 8, ρ_{calcd} = 1.523 Mg m^{-3}, μ(Cu, Kα) = 7.41 mm^{-1}, T = 150 K, yellow irregular, 0.24 × 0.11 × 0.09 mm, 26871 measured reflections, 8943 independent (R_{int} = 0.035), F^2 refinement, R = 0.071, wR = 0.199 for 7929 reflections ($I > 2\sigma(I)$, $2\vartheta_{max}$ = 142.0°), 574 parameters with 19 restraints.

Formation of [Ru(CO)(PPh$_3$){P(BH$_3$)(SMe)Cy}(Tp)]

Tetrahydrofuran (6 mL) was added to a mixture of [Ru(CO)(PPh$_3$){PH(SMe)Cy}(Tp)]OTf (0.050 g, 55 µmol) and KH (0.017 g, 0.42 mmol). The yellow mixture was stirred for 30 minutes before being subjected to cannula filtration. Borane dimethylsulfide complex (0.10 mL, 1.1 mmol) was added to the filtrate, immediately turning it colourless. Stirring was continued for 10 minutes, after which the IR spectrum of the mixture contained a single ν_{CO} band at 1978 cm^{-1}. The mixture was freed of volatiles *in vacuo*, resulting in a residue with the NMR data provided below. The rest of the procedure was conducted in air. Toluene (20 mL) was added to the residue, the mixture filtered through diatomaceous earth and the filtrate freed of volatiles on a rotary evaporator. The residue was dissolved in MeOH (10 mL) and the volume reduced to dryness on a rotary evaporator yielded an oil without any solid formation. The residue was then dissolved in Et_2O (15 mL) and *n*-hexane (15 mL) added. Reducing the volume of this residue on a rotary evaporator produced a colourless precipitate which was collected by vacuum filtration (8 mg). This solid did not contain the desired product, as determined by $^{31}P\{^1H\}$ NMR spectroscopy. Instead, the removal of volatiles from the filtrate yielded a solid residue which appeared to contain pure [Ru(CO)(PPh$_3$){P(BH$_3$)(SMe)Cy}(Tp)] by $^{31}P\{^1H\}$ NMR spectroscopy. The solid residue was used to obtain microanalytical data.

IR (THF) ν/cm^{-1}: 1978 vs (CO). ^1H NMR ($CDCl_3$, 400.1 MHz, 298 K) δ/ppm: 8.10, 8.06 (s × 2, Hpz), 7.51−7.14 (m, PPh$_3$), 6.85, 6.85, 6.12, 6.07, 5.75, 5.67, 5.64 (s × 7, Hpz), 1.88 − −0.46 (m, C_6H_{11}), SMe resonances were assigned to diastereomers based on signal intensity and are listed below. ESI-MS (+, MeCN) *m/z*: 767.2 [M – BH$_3$ + H]$^+$, 783.2 [M – BH$_3$ + O + H]$^+$. Accurate mass: found 767.1599 [M – BH$_3$ + H]$^+$, Calcd. for $C_{35}H_{40}{}^{11}BN_6OP_2{}^{102}RuS$ 767.1596; found 783.1580 [M – BH$_3$ + O + H]$^+$, Calcd. for $C_{35}H_{40}{}^{11}BN_6O_2P_2{}^{102}RuS$ 783.1545. Anal. Found: C,

50.72; H, 5.53; N, 8.83%. Calcd. For $C_{35}H_{42}B_2N_6OP_2RuS$: C, 53.93; H, 5.43; N, 10.78 (satisfactory data not obtained).

Diastereomer 1

^{1}H NMR ($CDCl_3$, 400.1 MHz, 298 K) δ/ppm: 2.04 (d, $^3J_{PH}$ = 8 Hz, SMe).

$^{31}P\{^1H\}$ NMR ($CDCl_3$, 162.0 MHZ, 300 K) δ/ppm: 56.5 (br s, $P(BH_3)$(SMe)Cy), 44.6 (d, $^2J_{PP}$ = 23 Hz, PPh_3).

Diastereomer 2

^{1}H NMR ($CDCl_3$, 400.1 MHz, 298 K) δ/ppm: 2.50 (d, $^3J_{PH}$ = 8 Hz, SMe).

$^{31}P\{^1H\}$ NMR ($CDCl_3$, 162.0 MHZ, 300 K) δ/ppm: 54.9 (br s, $P(BH_3)$(SMe)Cy), 44.0 (d, $^2J_{PP}$ = 24 Hz, PPh_3).

Formation of [Ru(CO)(PPh_3)(P{SMe}(S)Cy)(Tp)]

Tetrahydrofuran (7 mL) was added to a mixture of [Ru(CO)(PPh_3){PH(SMe)Cy}(Tp)]OTf (0.050 g, 55 μmol) and KH (0.017 g, 0.424 mmol). The yellow mixture was stirred for 30 minutes before being subjected to cannula filtration. Elemental sulfur (0.003 g, 0.09 mg-atom) was added to the filtrate, resulting in a slight decolourisation. Stirring was continued for 10 minutes, after which the IR spectrum of the mixture contained ν_{CO} bands at 1983 and 1968 cm^{-1}. The mixture was freed of volatiles *in vacuo*, resulting in a residue with the NMR and ESI-MS data provided below.

IR (THF) ν/cm^{-1}: 2485 w (BH), 1983 s (CO), 1968 vs (CO). ^{1}H NMR ($CDCl_3$, 400.1 MHz, 298 K) δ/ppm: 8.31, 7.86, 7.79 (s × 3), 7.46−7.04 (m, PPh_3), 6.85, 6.02, 5.61, 5.56, 5.52 (s × 5), 2.34 (d, ^2J = 8 Hz, SMe), 1.82 (d, ^2J = 4 Hz, SMe), 1.41 − −0.83 (m, C_6H_{11}). $^{31}P\{^1H\}$ NMR ($CDCl_3$, 162.0 MHZ, 300 K) δ/ppm: 101.8 (d, $^2J_{PP}$ = 28 Hz, P(S)(SMe)Cy), 99.2 (d, $^2J_{PP}$ = 28 Hz, P(S)(SMe)Cy), 42.21 (d, $^2J_{PP}$ = 28 Hz, PPh_3), 42.18 (d, $^2J_{PP}$ = 28 Hz, PPh_3). ESI-MS (+, MeCN) *m/z*: 799.1 $[M + H]^+$. Accurate mass: found 799.1320 $[M + H]^+$, Calcd. for $C_{35}H_{40}{}^{11}BN_6OP_2{}^{102}RuS_2$ 799.1317.

CHAPTER 8
References

Chapter 8: References

1. Phosphorus. In *Chemistry of the Elements*, 2nd ed.; Greenwood, N. N.; Earnshaw, A., Eds. Butterworth-Heinemann: Oxford, 1997; pp 473.
2. Clarke, M. L.; Frew, J. J. R., Ligand electronic effects in homogeneous catalysis using transition metal complexes of phosphine ligands. In *Organometallic Chemistry: Volume 35*, The Royal Society of Chemistry: Cambridge, United Kingdom, 2009; Vol. 35, pp 19.
3. Woltermann, C. J., *PharmaChem*, **2002**, *1*, 11.
4. Grubbs, R. H., *Angew. Chem. Int. Ed.*, **2006**, *45*, 3760.
5. Noyori, R., *Angew. Chem. Int. Ed.*, **2002**, *41*, 2008.
6. Knowles, W. S., *Angew. Chem. Int. Ed.*, **2002**, *41*, 1998.
7. Brynda, M., *Coord. Chem. Rev.*, **2005**, *249*, 2013.
8. Fleming, J. T.; Higham, L. J., *Coord. Chem. Rev.*, **2015**, *297-298*, 127.
9. González-Blanco, Ò.; Branchadell, V., *Organometallics*, **1997**, *16*, 5556.
10. Drago, R. S., *Organometallics*, **1995**, *14*, 3408.
11. Li, C.; Ogasawara, M.; Nolan, S. P.; Caulton, K. G., *Organometallics*, **1996**, *15*, 4900.
12. Hiney, R. M.; Higham, L. J.; Müller-Bunz, H.; Gilheany, D. G., *Angew. Chem. Int. Ed.*, **2006**, *45*, 7248.
13. Stewart, B.; Harriman, A.; Higham, L. J., *Organometallics*, **2011**, *30*, 5338.
14. Spang, C.; Edelmann, F. T.; Noltemeyer, M.; Roesky, H. W., *Chem. Ber.*, **1989**, *122*, 1247.
15. Goodwin, N. J.; Henderson, W.; Nicholson, B. K., *Chem. Commun.*, **1997**, 31.
16. Goodwin, N. J.; Henderson, W.; Nicholson, B. K.; Fawcett, J.; R. Russell, D., *J. Chem. Soc., Dalton Trans.*, **1999**, 1785.
17. Henderson, W.; Alley, S. R., *J. Organomet. Chem.*, **2002**, *656*, 120.
18. Katti, K. V.; Pillarsetty, N.; Raghuraman, K., New Vistas in Chemistry and Applications of Primary Phosphines. In *New Aspects in Phosphorus Chemistry III*, Majoral, J.-P., Ed. Springer Berlin Heidelberg: Berlin, Heidelberg, 2003; pp 121.
19. Cowley, A. H.; Barron, A. R., *Acc. Chem. Res.*, **1988**, *21*, 81.
20. Hitchcock, P. B.; Lappert, M. F.; Leung, W.-P., *J. Chem. Soc., Chem. Commun.*, **1987**, 1282.
21. Cummins, C. C.; Schrock, R. R.; Davis, W. M., *Angew. Chem. Int. Ed.*, **1993**, *32*, 756.
22. Zanetti, N. C.; Schrock, R. R.; Davis, W. M., *Angew. Chem. Int. Ed.*, **1995**, *34*, 2044.
23. Laplaza, C. E.; Davis, W. M.; Cummins, C. C., *Angew. Chem. Int. Ed.*, **1995**, *34*, 2042.
24. Mösch-Zanetti, N. C.; Schrock, R. R.; Davis, W. M.; Wanninger, K.; Seidel, S. W.; O'Donoghue, M. B., *J. Am. Chem. Soc.*, **1997**, *119*, 11037.
25. Bonanno, J. B.; Wolczanski, P. T.; Lobkovsky, E. B., *J. Am. Chem. Soc.*, **1994**, *116*, 11159.
26. Termaten, A. T.; Nijbacker, T.; Schakel, M.; Lutz, M.; Spek, A. L.; Lammertsma, K., *Organometallics*, **2002**, *21*, 3196.
27. Glueck, D. S.; Wu, J.; Hollander, F. J.; Bergman, R. G., *J. Am. Chem. Soc.*, **1991**, *113*, 2041.
28. Termaten, A. T.; Aktas, H.; Schakel, M.; Ehlers, A. W.; Lutz, M.; Spek, A. L.; Lammertsma, K., *Organometallics*, **2003**, *22*, 1827.
29. Termaten, A. T.; Nijbacker, T.; Schakel, M.; Lutz, M.; Spek, A. L.; Lammertsma, K., *Chem. Eur. J.*, **2003**, *9*, 2200.

30. Basuli, F.; Tomaszewski, J.; Huffman, J. C.; Mindiola, D. J., *J. Am. Chem. Soc.*, **2003**, *125*, 10170.
31. Basuli, F.; Bailey, B. C.; Huffman, J. C.; Baik, M.-H.; Mindiola, D. J., *J. Am. Chem. Soc.*, **2004**, *126*, 1924.
32. Searles, K.; Carroll, P. J.; Mindiola, D. J., *Organometallics*, **2015**, *34*, 4641.
33. Hey, E.; Bott, S. G.; Atwood, J. L., *Chem. Ber.*, **1988**, *121*, 561.
34. Issleib, K.; Häckert, H., *Z. Naturforsch., B.*, **1966**, *21*, 519.
35. Benac, B. L.; Jones, R. A., *Polyhedron*, **1989**, *8*, 1774.
36. Hou, Z.; Breen, T. L.; Stephan, D. W., *Organometallics*, **1993**, *12*, 3158.
37. Ho, J.; Breen, T. L.; Ozarowski, A.; Stephan, D. W., *Inorg. Chem.*, **1994**, *33*, 865.
38. Ho, J.; Rousseau, R.; Stephan, D. W., *Organometallics*, **1994**, *13*, 1918.
39. Etkin, N.; Fermin, M. C.; Stephan, D. W., *J. Am. Chem. Soc.*, **1997**, *119*, 2954.
40. Masuda, J. D.; Hoskin, A. J.; Graham, T. W.; Beddie, C.; Fermin, M. C.; Etkin, N.; Stephan, D. W., *Chem. Eur. J.*, **2006**, *12*, 8696.
41. Roering, A. J.; MacMillan, S. N.; Tanski, J. M.; Waterman, R., *Inorg. Chem.*, **2007**, *46*, 6855.
42. Waterman, R., *Organometallics*, **2007**, *26*, 2492.
43. Huttner, G.; Müller, H. D.; Friedrich, P.; Kölle, U., *Chem. Ber.*, **1977**, *110*, 1254.
44. Pringle, P. G.; Smith, M. B., *J. Chem. Soc., Chem. Commun.*, **1990**, 1701.
45. Hoye, P. A. T.; Pringle, P. G.; Smith, M. B.; Worboys, K., *J. Chem. Soc., Dalton Trans.*, **1993**, 269.
46. Wicht, D. K.; Kourkine, I. V.; Lew, B. M.; Nthenge, J. M.; Glueck, D. S., *J. Am. Chem. Soc.*, **1997**, *119*, 5039.
47. Wicht, D. K.; Kourkine, I. V.; Kovacik, I.; Glueck, D. S.; Concolino, T. E.; Yap, G. P. A.; Incarvito, C. D.; Rheingold, A. L., *Organometallics*, **1999**, *18*, 5381.
48. Zhao, G.; Basuli, F.; Kilgore, U. J.; Fan, H.; Aneetha, H.; Huffman, J. C.; Wu, G.; Mindiola, D. J., *J. Am. Chem. Soc.*, **2006**, *128*, 13575.
49. Bange, C. A.; Ghebreab, M. B.; Ficks, A.; Mucha, N. T.; Higham, L.; Waterman, R., *Dalton Trans.*, **2016**, *45*, 1863.
50. Boni, G.; Kubicki, M. M.; Moïse, C., Group 5 and 6 Bimetallic Complexes with Phosphido Bridges: Syntheses and Some Structural Features. In *Metal Clusters in Chemistry*, Braunstein, P.; Oro, L. A.; Raithby, P. R., Eds. Wiley-VCH: Weinheim, 1999; pp 110.
51. Comte, V.; Blacque, O.; Moïse, C.; Kubicki, M. M., *Phosphorus, Sulfur, Silicon Relat. Elem.*, **1999**, *144*, 721.
52. Mealli, C.; Ienco, A.; Galindo, A.; Carreño, E. P., *Inorg. Chem.*, **1999**, *38*, 4620.
53. Böttcher, H.-C.; Graf, M.; Wagner, C., *Phosphorus, Sulfur, Silicon Relat. Elem.*, **2001**, *169*, 185.
54. Piero, M., *Eur. J. Inorg. Chem.*, **2008**, *2008*, 4835.
55. Bender, R.; Welter, R.; Braunstein, P., *Inorg. Chim. Acta*, **2015**, *424*, 20.
56. Cooke, M.; Green, M.; Kirkpatrick, D., *J. Chem. Soc. A.*, **1968**, 1507.
57. Green, M.; Taunton-Rigby, A.; Stone, F. G. A., *J. Chem. Soc. A.*, **1969**, 1875.
58. Gross, E.; Jörg, K.; Fiederling, K.; Göttlein, A.; Malisch, W.; Boese, R., *Angew. Chem. Int. Ed.*, **1984**, *23*, 738.
59. Jörg, K.; Malisch, W.; Reich, W.; Meyer, A.; Schubert, U., *Angew. Chem. Int. Ed.*, **1986**, *25*, 92.

60. Haines, R. J.; Nolte, C. R., *J. Organomet. Chem.*, **1972**, *36*, 163.
61. Schunn, R. A., *Inorg. Chem.*, **1973**, *12*, 1573.
62. Ellis, J. W.; Harrison, K. N.; Hoye, P. A. T.; Orpen, A. G.; Pringle, P. G.; Smith, M. B., *Inorg. Chem.*, **1992**, *31*, 3026.
63. Glueck, D. S., *Synlett*, **2007**, *2007*, 2627.
64. Burn, M. J.; Fickes, M. G.; Hollander, F. J.; Bergman, R. G., *Organometallics*, **1995**, *14*, 137.
65. Arduengo III, A. J.; Carmalt, C. J.; Clyburne, J. A. C.; Cowley, A. H.; Pyati, R., *Chem. Commun.*, **1997**, 981.
66. Larocque, T. G.; Lavoie, G. G., *New J. Chem.*, **2014**, *38*, 499.
67. Bedford, R. B.; Hill, A. F.; Jones, C.; White, A. J. P.; Wilton-Ely, J. D. E. T., *J. Chem. Soc., Dalton Trans.*, **1997**, 139.
68. Dobbie, R. C.; Mason, P. R., *J. Chem. Soc., Dalton Trans.*, **1973**, 1124.
69. Cullen, W. R.; Hayter, R. G., *J. Am. Chem. Soc.*, **1964**, *86*, 1030.
70. Vaughan, G. A.; Hillhouse, G. L.; Rheingold, A. L., *Organometallics*, **1989**, *8*, 1760.
71. Hillhouse, G. L.; Bercaw, J. E., *Organometallics*, **1982**, *1*, 1025.
72. Hillhouse, G. L.; Bercaw, J. E., *J. Am. Chem. Soc.*, **1984**, *106*, 5472.
73. Hillhouse, G. L.; Bulls, A. R.; Santarsiero, B. D.; Bercaw, J. E., *Organometallics*, **1988**, *7*, 1309.
74. Caulton, K. G., *New J. Chem.*, **1994**, *18*, 25.
75. Bohle, D. S.; Jones, T. C.; Rickard, C. E. F.; Roper, W. R., *J. Chem. Soc., Chem. Commun.*, **1984**, 865.
76. Bohle, D. S.; Jones, T. C.; Rickard, C. E. F.; Roper, W. R., *Organometallics*, **1986**, *5*, 1612.
77. Bohle, D. S.; Clark, G. R.; Rickard, C. E. F.; Roper, W. R., *J. Organomet. Chem.*, **1990**, *393*, 243.
78. Cowley, A. H.; Kemp, R. A., *Chem. Rev.*, **1985**, *85*, 367.
79. Gudat, D., *Coord. Chem. Rev.*, **1997**, *163*, 71.
80. Derrah, E. J.; Pantazis, D. A.; McDonald, R.; Rosenberg, L., *Organometallics*, **2007**, *26*, 1473.
81. Rosenberg, L., *Coord. Chem. Rev.*, **2012**, *256*, 606.
82. Buhro, W. E.; Georgiou, S.; Hutchinson, J. P.; Gladysz, J. A., *J. Am. Chem. Soc.*, **1985**, *107*, 3346.
83. Buhro, W. E.; Zwick, B. D.; Georgiou, S.; Hutchinson, J. P.; Gladysz, J. A., *J. Am. Chem. Soc.*, **1988**, *110*, 2427.
84. Eichenseher, S.; Delacroix, O.; Kromm, K.; Hampel, F.; Gladysz, J. A., *Organometallics*, **2005**, *24*, 245.
85. Giner Planas, J.; Hampel, F.; Gladysz, J. A., *Chem. Eur. J.*, **2005**, *11*, 1402.
86. Giner Planas, J.; Gladysz, J. A., *Inorg. Chem.*, **2002**, *41*, 6947.
87. Malisch, W.; Maisch, R.; Meyer, A.; Greissinger, D.; Gross, E.; Colquhoun, I. J.; McFarlane, W., *Phosphorus Sulfur*, **1983**, *18*, 299.
88. Mislow, K., *Trans. N. Y. Acad. Sci.*, **1973**, *35*, 227.
89. Buhro, W. E.; Gladysz, J. A., *Inorg. Chem.*, **1985**, *24*, 3505.
90. Rogers, J. R.; Wagner, T. P. S.; Marynick, D. S., *Inorg. Chem.*, **1994**, *33*, 3104.
91. Crisp, G. T.; Salem, G.; Stephens, F. S.; Wild, S. B., *J. Chem. Soc., Chem. Commun.*, **1987**, 600.
92. Salem, G.; Wild, S. B., *J. Chem. Soc., Chem. Commun.*, **1987**, 1378.

93. Crisp, G. T.; Salem, G.; Wild, S. B.; Stephens, F. S., *Organometallics*, **1989**, *8*, 2360.
94. Chan, V. S.; Stewart, I. C.; Bergman, R. G.; Toste, F. D., *J. Am. Chem. Soc.*, **2006**, *128*, 2786.
95. Chan, V. S.; Chiu, M.; Bergman, R. G.; Toste, F. D., *J. Am. Chem. Soc.*, **2009**, *131*, 6021.
96. Rocklage, S. M.; Schrock, R. R.; Churchill, M. R.; Wasserman, H. J., *Organometallics*, **1982**, *1*, 1332.
97. Bohle, D. S.; Clark, G. R.; Rickard, C. E. F.; Roper, W. R., *J. Organomet. Chem.*, **1988**, *353*, 355.
98. Malisch, W.; Hirth, U. A.; Bright, T. A.; Käb, H.; Ertel, T. S.; Hückmann, S.; Bertagnolli, H., *Angew. Chem. Int. Ed.*, **1992**, *31*, 1525.
99. Breen, T. L.; Stephan, D. W., *J. Am. Chem. Soc.*, **1995**, *117*, 11914.
100. Hou, Z.; Stephan, D. W., *J. Am. Chem. Soc.*, **1992**, *114*, 10088.
101. MacMillan, S. N.; Tanski, J. M.; Waterman, R., *Chem. Commun.*, **2007**, 4172.
102. Malisch, W.; Thirase, K.; Reising, J., *Z. Naturforsch., B.*, **1998**, *53*, 1084.
103. Malisch, W.; Thirase, K.; Reising, J., *J. Organomet. Chem.*, **1998**, *568*, 247.
104. Malisch, W.; Thirase, K.; Rehmann, F. J.; Reising, J.; Gunzelmann, N., *Eur. J. Inorg. Chem.*, **1998**, *1998*, 1589.
105. Melenkivitz, R.; Mindiola, D. J.; Hillhouse, G. L., *J. Am. Chem. Soc.*, **2002**, *124*, 3846.
106. Iluc, V. M.; Hillhouse, G. L., *J. Am. Chem. Soc.*, **2010**, *132*, 15148.
107. Rankin, M. A.; Cummins, C. C., *Dalton Trans.*, **2012**, *41*, 9615.
108. Zhou, J.; Li, T.; Maron, L.; Leng, X.; Chen, Y., *Organometallics*, **2015**, *34*, 470.
109. Lv, Y.; Zhou, J.; Leng, X.; Chen, Y., *New J. Chem.*, **2015**, *39*, 7582.
110. Hansen, K.; Szilvási, T.; Blom, B.; Inoue, S.; Epping, J.; Driess, M., *J. Am. Chem. Soc.*, **2013**, *135*, 11795.
111. Tondreau, A. M.; Benkő, Z.; Harmer, J. R.; Grützmacher, H., *Chem. Sci.*, **2014**, *5*, 1545.
112. Doddi, A.; Bockfeld, D.; Bannenberg, T.; Jones, P. G.; Tamm, M., *Angew. Chem. Int. Ed.*, **2014**, *53*, 13568.
113. Lemp, O.; von Hänisch, C., *Phosphorus, Sulfur, Silicon Relat. Elem.*, **2016**, *191*, 659.
114. Hickey, A. K.; Munoz, S. B.; Lutz, S. A.; Pink, M.; Chen, C.-H.; Smith, J. M., *Chem. Commun.*, **2017**, *53*, 412.
115. Becker, E.; Pavlik, S.; Kirchner, K., *Adv. Organomet. Chem.*, **2008**, *56*, 155.
116. Caldwell, L. M., *Adv. Organomet. Chem.*, **2008**, *56*, 1.
117. Crossley, I. R., *Adv. Organomet. Chem.*, **2008**, *56*, 199.
118. Lail, M.; Pittard, K. A.; Gunnoe, T. B., *Adv. Organomet. Chem.*, **2008**, *56*, 95.
119. Jayaprakash, K. N.; Conner, D.; Gunnoe, T. B., *Organometallics*, **2001**, *20*, 5254.
120. Jayaprakash, K. N.; Gunnoe, T. B.; Boyle, P. D., *Inorg. Chem.*, **2001**, *40*, 6481.
121. Conner, D.; Jayaprakash, K. N.; Gunnoe, T. B.; Boyle, P. D., *Organometallics*, **2002**, *21*, 5265.
122. Conner, D.; Jayaprakash, K. N.; Gunnoe, T. B.; Boyle, P. D., *Inorg. Chem.*, **2002**, *41*, 3042.
123. Jayaprakash, K. N.; Gillepsie, A. M.; Gunnoe, T. B.; White, D. P., *Chem. Commun.*, **2002**, 372.
124. Conner, D.; Jayaprakash, K. N.; Wells, M. B.; Manzer, S.; Gunnoe, T. B.; Boyle, P. D., *Inorg. Chem.*, **2003**, *42*, 4759.
125. Alcock, N. W.; Burns, I. D.; Claire, K. S.; Hill, A. F., *Inorg. Chem.*, **1992**, *31*, 2906.

126. Hill, A. F.; Wilton-Ely, J. D. E. T.; Rauchfuss, T. B.; Schwartz, D. E., *Inorg. Synth.*, **2002**, *33*, 206.
127. Mislow, K.; Raban, M., *Top. Stereochem.*, **1967**, *1*, 1.
128. Sun, N.-Y.; Simpson, S. J., *J. Organomet. Chem.*, **1992**, *434*, 341.
129. Falivene, L.; Cao, Z.; Petta, A.; Serra, L.; Poater, A.; Oliva, R.; Scarano, V.; Cavallo, L., *Nat. Chem.*, **2019**, *11*, 872.
130. Bancroft, G. M.; Libbey, E. T., *Can. J. Chem.*, **1973**, *51*, 1482.
131. Musher, J. I.; Corey, E. J., *Tetrahedron*, **1962**, *18*, 791.
132. Tolman, C. A., *Chem. Rev.*, **1977**, *77*, 313.
133. Foley, N. A.; Abernethy, R. J.; Gunnoe, T. B.; Hill, A. F.; Boyle, P. D.; Sabat, M., *Organometallics*, **2009**, *28*, 374.
134. Buriez, B.; Burns, I. D.; Hill, A. F.; White, A. J. P.; Williams, D. J.; Wilton-Ely, J. D. E. T., *Organometallics*, **1999**, *18*, 1504.
135. Orpen, A. G.; Brammer, L.; Allen, F. H.; Kennard, O.; Watson, D. G.; Taylor, R., *J. Chem. Soc., Dalton Trans.*, **1989**, S1.
136. Rüba, E.; Simanko, W.; Mereiter, K.; Schmid, R.; Kirchner, K., *Inorg. Chem.*, **2000**, *39*, 382.
137. Mohr, F.; Privér, S. H.; Bhargava, S. K.; Bennett, M. A., *Coord. Chem. Rev.*, **2006**, *250*, 1851.
138. Kühl, O., *Phosphorus-31 NMR Spectroscopy: A Concise Introduction for the Synthetic Organic and Organometallic Chemist*. 1 ed.; Springer-Verlag: Berlin; Heidelberg, 2008.
139. Belli, R. G.; Wu, Y.; Ji, H.; Joshi, A.; Yunker, L. P. E.; McIndoe, J. S.; Rosenberg, L., *Inorg. Chem.*, **2019**, *58*, 747.
140. Derrah, E. J.; McDonald, R.; Rosenberg, L., *Chem. Commun.*, **2010**, *46*, 4592.
141. Derrah, E. J.; Pantazis, D. A.; McDonald, R.; Rosenberg, L., *Angew. Chem. Int. Ed.*, **2010**, *49*, 3367.
142. Waterman, R., *Organometallics*, **2013**, *32*, 7249.
143. Chan, W.-C.; Lau, C.-P.; Chen, Y.-Z.; Fang, Y.-Q.; Ng, S.-M.; Jia, G., *Organometallics*, **1997**, *16*, 34.
144. Tenorio, M. J.; Tenorio, M. A. J.; Puerta, M. C.; Valerga, P., *Inorg. Chim. Acta*, **1997**, *259*, 77.
145. Klein, H. F.; Schneider, S.; He, M.; Floerke, U.; Haupt, H. J., *Eur. J. Inorg. Chem.*, **2000**, *2000*, 2295.
146. Deeming, A. J.; Doherty, S.; Marshall, J. E.; Powell, J. L.; Senior, A. M., *J. Chem. Soc., Dalton Trans.*, **1993**, 1093.
147. Basolo, F.; Burmeister, J. L., *On Being Well-coordinated: A Half-century of Research on Transition Metal Complexes : Selected Papers of Fred Basolo*. World Scientific: Singapore, 2003.
148. Bohle, D. S.; Rickard, C. E. F.; Roper, W. R., *J. Chem. Soc., Chem. Commun.*, **1985**, 1594.
149. Bohle, D. S.; Roper, W. R., *Organometallics*, **1986**, *5*, 1607.
150. Bohle, D. S.; Clark, G. R.; Rickard, C. E. F.; Roper, W. R.; Taylor, M. J., *J. Organomet. Chem.*, **1988**, *348*, 385.
151. Hill, A. F.; Woollins, J. D., Preparation of $[Bu_4N][B_3H_8]$ and the Formation of $RuH[B_3H_8](CO)(PPh_3)_2$. In *Inorganic Experiments*, 3rd ed.; Woollins, J. D., Ed. Wiley-VCH Verlag GmbH: Weinheim, 2010; pp 405.
152. Vaska, L.; DiLuzio, J. W., *J. Am. Chem. Soc.*, **1961**, *83*, 1262.

153. Fernandez-Galan, R.; Manzano, B. R.; Otero, A.; Lanfranchi, M.; Pellinghelli, M. A., *Inorg. Chem.*, **1994**, *33*, 2309.
154. Caldwell, L. M. Ph.D. Thesis. Australian National University, 2006.
155. Burrell, A. K.; Clark, G. R.; Rickard, C. E. F.; Roper, W. R.; Ware, D. C., *J. Organomet. Chem.*, **1990**, *398*, 133.
156. Perrin, L.; Clot, E.; Eisenstein, O.; Loch, J.; Crabtree, R. H., *Inorg. Chem.*, **2001**, *40*, 5806.
157. Hiraki, K.; Kira, S.-i.; Kawano, H., *Bull. Chem. Soc. Jpn.*, **1997**, *70*, 1583.
158. Ogasawara, M.; Macgregor, S. A.; Streib, W. E.; Folting, K.; Eisenstein, O.; Caulton, K. G., *J. Am. Chem. Soc.*, **1996**, *118*, 10189.
159. Bedford, R. B.; Hibbs, D. E.; Hill, A. F.; Hursthouse, M. B.; Malik, K. M. A.; Jones, C., *Chem. Commun.*, **1996**, 1895.
160. Khan, A. A.; Wismach, C.; Jones, P. G.; Streubel, R., *Chem. Commun.*, **2003**, 2892.
161. Streubel, R.; Özbolat-Schön, A.; von Frantzius, G.; Lee, H.; Schnakenburg, G.; Gudat, D., *Inorg. Chem.*, **2013**, *52*, 3313.
162. Greenacre, V. K.; Day, I. J.; Crossley, I. R., *Organometallics*, **2017**, *36*, 435.
163. Streubel, R.; Schmer, A.; Kyri, A. W.; Schnakenburg, G., *Organometallics*, **2017**, *36*, 1488.
164. King, R. B.; Wu, F. J.; Sadanani, N. D.; Holt, E. M., *Inorg. Chem.*, **1985**, *24*, 4449.
165. Reisacher, H.-U.; Duesler, E. N.; Paine, R. T., *J. Organomet. Chem.*, **1998**, *564*, 13.
166. Streubel, R.; Priemer, S.; Ruthe, F.; Jones, P. G., *Eur. J. Inorg. Chem.*, **2000**, *2000*, 1253.
167. Duan, L.; Schnakenburg, G.; Daniels, J.; Streubel, R., *Eur. J. Inorg. Chem.*, **2012**, *2012*, 2314.
168. Mao, Y.; Wang, Z.; Ganguly, R.; Mathey, F., *Organometallics*, **2012**, *31*, 4786.
169. Schmer, A.; Terschüren, T.; Schnakenburg, G.; Espinosa Ferao, A.; Streubel, R., *Eur. J. Inorg. Chem.*, **2019**, *2019*, 1604.
170. Huttner, G.; Müller, H. D., *Angew. Chem. Int. Ed.*, **1975**, *14*, 571.
171. Marinetti, A.; Mathey, F.; Fischer, J.; Mitschler, A., *J. Am. Chem. Soc.*, **1982**, *104*, 4484.
172. Marinetti, A.; Mathey, F., *Organometallics*, **1982**, *1*, 1488.
173. Marinetti, A.; Mathey, F., *Organometallics*, **1984**, *3*, 456.
174. Borst, M. L. G.; Bulo, R. E.; Winkel, C. W.; Gibney, D. J.; Ehlers, A. W.; Schakel, M.; Lutz, M.; Spek, A. L.; Lammertsma, K., *J. Am. Chem. Soc.*, **2005**, *127*, 5800.
175. Jansen, H.; Samuels, M. C.; Couzijn, E. P. A.; Slootweg, J. C.; Ehlers, A. W.; Chen, P.; Lammertsma, K., *Chem. Eur. J.*, **2010**, *16*, 1454.
176. Alvarez, M. A.; García, M. E.; García-Vivó, D.; Ramos, A.; Ruiz, M. A., *Inorg. Chem.*, **2012**, *51*, 3698.
177. Nesterov, V.; Duan, L.; Schnakenburg, G.; Streubel, R., *Eur. J. Inorg. Chem.*, **2011**, *2011*, 567.
178. Schulten, C.; von Frantzius, G.; Schnakenburg, G.; Espinosa, A.; Streubel, R., *Chem. Sci.*, **2012**, *3*, 3526.
179. Duan, L.; Schnakenburg, G.; Streubel, R., *Organometallics*, **2011**, *30*, 3246.
180. Ebsworth, E. A. V.; Gould, R. O.; McManus, N. T.; Pilkington, N. J.; Rankin, D. W. H., *J. Chem. Soc., Dalton Trans.*, **1984**, 2561.
181. Malish, W.; Angerer, W.; Cowley, A. H.; Norman, N. C., *J. Chem. Soc., Chem. Commun.*, **1985**, 1811.
182. Challet, S.; Lebanc, J. C.; Moïse, C., *Phosphorus, Sulfur, Silicon Relat. Elem.*, **1994**, *97*, 95.

183. Carrano, C. J.; Cowley, A. H.; Nunn, C. M.; Pakulski, M.; Quashie, S., *J. Chem. Soc., Chem. Commun.*, **1988**, 170.
184. Hebden, T. J.; Schrock, R. R.; Takase, M. K.; Müller, P., *Chem. Commun.*, **2012**, *48*, 1851.
185. Weber, L.; Buchwald, S.; Rühlicke, A.; Stammler, H. G.; Neumann, B., *Z. Anorg. Allg. Chem.*, **1993**, *619*, 934.
186. Duan, L.; Nesterov, V.; Runyon, J. W.; Schnakenburg, G.; Arduengo III, A. J.; Streubel, R., *Aust. J. Chem.*, **2011**, *64*, 1583.
187. Haines, L. M.; Stiddard, M. H. B., Vibrational Spectra of Transition Metal Carbonyl Complexes. In *Adv. Inorg. Radiochem.*, Emeléus, H. J.; Sharpe, A. G., Eds. Academic Press: New York, 1970; Vol. 12, pp 53.
188. Collman, J. P.; Roper, W. R., *J. Am. Chem. Soc.*, **1965**, *87*, 4008.
189. Jeschke, J.; Korb, M.; Rüffer, T.; Gäbler, C.; Lang, H., *Adv. Synth. Catal.*, **2015**, *357*, 4069.
190. Hill, A. F.; Neumann, H.; Wagler, J., *Organometallics*, **2010**, *29*, 1026.
191. Anillo, A.; Obeso-Rosete, R.; Pellinghelli, M. A.; Tiripicchio, A., *J. Chem. Soc., Dalton Trans.*, **1991**, 2019.
192. Nakamoto, K., *Infrared and Raman Spectra of Inorganic and Coordination Compounds, Part B: Applications in Coordination, Organometallic and Bioinorganic Chemistry*. 2nd ed.; John Wiley & Sons, Inc.: Hoboken, New Jersey, 2009.
193. Clark, G. R.; Laing, K. R.; Roper, W. R.; Wright, A. H., *Inorg. Chim. Acta*, **2004**, *357*, 1767.
194. Sentets, S.; Rodriguez Martinez, M. d. C.; Vendier, L.; Donnadieu, B.; Huc, V.; Lugan, N.; Lavigne, G., *J. Am. Chem. Soc.*, **2005**, *127*, 14554.
195. Connelly, N. G.; Damhus, T.; Hartshorn, R. M.; Hutton, A. T., *Nomenclature of Inorganic Chemistry: IUPAC Recommendations 2005*. Royal Society of Chemistry: Cambridge, UK, 2005.
196. Thompsett, A. R. Ph.D. Thesis. Imperial College of Science, Technology and Medicine, 1998.
197. Allen, F. H.; Kennard, O.; Watson, D. G.; Brammer, L.; Orpen, A. G.; Taylor, R., *J. Chem. Soc., Perkin Trans. 2*, **1987**, S1.
198. Olmstead, W. N.; Margolin, Z.; Bordwell, F. G., *J. Org. Chem.*, **1980**, *45*, 3295.
199. Sandstrom, J., *Dynamic NMR Spectroscopy*. Academic Press: London ; New York, 1982.
200. Perrin, C. L.; Dwyer, T. J., *Chem. Rev.*, **1990**, *90*, 935.
201. Treichel, P. M.; Douglas, W. M.; Dean, W. K., *Inorg. Chem.*, **1972**, *11*, 1615.
202. Malisch, W.; Meyer, A., *J. Organomet. Chem.*, **1980**, *198*, C29.
203. Boom, D. H. A.; Jupp, A. R.; Slootweg, J. C., *Chem. Eur. J.*, **2019**, *25*, 9133.
204. Han, D.; Anke, F.; Trose, M.; Beweries, T., *Coord. Chem. Rev.*, **2019**, *380*, 260.
205. Colebatch, A. L.; Weller, A. S., *Chem. Eur. J.*, **2019**, *25*, 1379.
206. Staubitz, A.; Robertson, A. P. M.; Sloan, M. E.; Manners, I., *Chem. Rev.*, **2010**, *110*, 4023.
207. Angerer, W.; Sheldrick, W. S.; Malisch, W., *Chem. Ber.*, **1985**, *118*, 1261.
208. Maisch, R.; Ott, E.; Buchner, W.; Malisch, W.; Colquhoun, I. J.; McFarlane, W., *J. Organomet. Chem.*, **1985**, *286*, c31.
209. McNulty, J.; Zhou, Y., *Tetrahedron Lett.*, **2004**, *45*, 407.
210. Lee, K.; Clark, T. J.; Lough, A. J.; Manners, I., *Dalton Trans.*, **2008**, 2732.
211. Schäfer, A.; Jurca, T.; Turner, J.; Vance, J. R.; Lee, K.; Du, V. A.; Haddow, M. F.; Whittell, G. R.; Manners, I., *Angew. Chem. Int. Ed.*, **2015**, *54*, 4836.

212. Stanley, K.; Baird, M. C., *J. Am. Chem. Soc.*, **1975**, *97*, 6598.
213. Gudat, D.; Haghverdi, A.; Nieger, M., *Angew. Chem. Int. Ed.*, **2000**, *39*, 3084.
214. Strube, A.; Heuser, J.; Huttner, G.; Lang, H., *J. Organomet. Chem.*, **1988**, *356*, C9.
215. Hermanek, S., *Chem. Rev.*, **1992**, *92*, 325.
216. Graham, W. A. G.; Stone, F. G. A., *J. Inorg. Nucl. Chem.*, **1956**, *3*, 164.
217. Parry, R. W.; Bissot, T. C., *J. Am. Chem. Soc.*, **1956**, *78*, 1524.
218. Imamoto, T.; Oshiki, T.; Onozawa, T.; Kusumoto, T.; Sato, K., *J. Am. Chem. Soc.*, **1990**, *112*, 5244.
219. Lippard, S. J.; Melmed, K. M., *Inorg. Chem.*, **1969**, *8*, 2755.
220. Greenwood, N. N.; Kennedy, J. D.; Reed, D., *J. Chem. Soc., Dalton Trans.*, **1980**, 196.
221. Greenwood, N. N.; Kennedy, J. D.; Thornton-Pett, M.; Woollins, J. D., *J. Chem. Soc., Dalton Trans.*, **1985**, 2397.
222. Grebenik, P. D.; Leach, J. B.; Green, M. L. H.; Walker, N. M., *J. Organomet. Chem.*, **1988**, *345*, C31.
223. Grebenik, P. D.; Leach, J. B.; Pounds, J. M.; Green, M. L. H.; Mountford, P., *J. Organomet. Chem.*, **1990**, *382*, C1.
224. Burns, I. D.; Hill, A. F.; Thompsett, A. R.; Alcock, N. W.; Claire, K. S., *J. Organomet. Chem.*, **1992**, *425*, C8.
225. Bown, M.; Ingham, S. L.; Norris, G. E.; Waters, J. M., *Acta Crystallogr. Sect. C: Cryst. Struct. Commun.*, **1995**, *51*, 1503.
226. Aldridge, S.; Downs, A. J.; Parsons, S., *Chem. Commun.*, **1996**, 2055.
227. Burns, I. D.; Hill, A. F.; Williams, D. J., *Inorg. Chem.*, **1996**, *35*, 2685.
228. Dyson, P. J.; Hill, A. F.; Hulkes, A. G.; White, A. J. P.; Williams, D. J., *Angew. Chem. Int. Ed.*, **1998**, *37*, 1430.
229. Ghosh, S.; Beatty, A. M.; Fehlner, T. P., *Collect. Czech. Chem. Commun.*, **2002**, *67*, 808.
230. Beckett, M. A.; Brassington, D. S.; Coles, S. J.; Gelbrich, T.; Hursthouse, M. B., *Polyhedron*, **2003**, *22*, 1627.
231. Goedde, D. M.; Girolami, G. S., *J. Am. Chem. Soc.*, **2004**, *126*, 12230.
232. Kim, D. Y.; Girolami, G. S., *J. Am. Chem. Soc.*, **2006**, *128*, 10969.
233. Green, M. L. H.; Leach, J. B.; Kelland, M. A., *Organometallics*, **2007**, *26*, 4031.
234. Kim, D. Y.; You, Y.; Girolami, G. S., *J. Organomet. Chem.*, **2008**, *693*, 981.
235. Geetharani, K.; Bose, S. K.; Pramanik, G.; Saha, T. K.; Ramkumar, V.; Ghosh, S., *Eur. J. Inorg. Chem.*, **2009**, *2009*, 1483.
236. Hill, A. F.; Lee, S. B.; Park, J.; Shang, R.; Willis, A. C., *Organometallics*, **2010**, *29*, 5661.
237. Ramalakshmi, R.; Bhattacharyya, M.; Rao, C. E.; Ghosh, S., *J. Organomet. Chem.*, **2015**, *792*, 31.
238. Ryschkewitsch, G. E.; Miller, V. H., *J. Am. Chem. Soc.*, **1975**, *97*, 6258.
239. Bishop, V. L.; Kodama, G., *Inorg. Chem.*, **1981**, *20*, 2724.
240. Kameda, M.; Kodama, G., *Inorg. Chem.*, **1984**, *23*, 3710.
241. Hofmann, A. W., *Ber. Dtsch. Chem. Ges.*, **1880**, *13*, 1732.
242. Galindo, A.; Miguel, D.; Perez, J., *Coord. Chem. Rev.*, **1999**, *193-195*, 643.
243. Leung, W.-H.; Chan, E. Y. Y.; Lam, T. C. H.; Williams, I. D., *J. Organomet. Chem.*, **2000**, *608*, 139.
244. Lo, Y.-H.; Fong, Y.-H.; Tong, H.-C.; Liang, Y.-R.; Kuo, T.-S.; Huang, C.-C., *Inorg. Chem. Commun.*, **2010**, *13*, 331.

245. Ghiassi, K. B.; Walters, D. T.; Aristov, M. M.; Loewen, N. D.; Berben, L. A.; Rivera, M.; Olmstead, M. M.; Balch, A. L., *Inorg. Chem.*, **2015**, *54*, 4565.
246. Hey, E.; Lappert, M. F.; Atwood, J. L.; Bott, S. G., *J. Chem. Soc., Chem. Commun.*, **1987**, 421.
247. Petz, W.; Weller, F., *J. Chem. Soc., Chem. Commun.*, **1995**, 1049.
248. Yih, K.-H.; Lin, Y.-C.; Cheng, M.-C.; Wang, Y., *J. Chem. Soc., Chem. Commun.*, **1993**, 1380.
249. Yih, K.-H.; Lin, Y.-C.; Cheng, M.-C.; Wang, Y., *J. Chem. Soc., Dalton Trans.*, **1995**, 1305.
250. Butler, I. S.; Svedman, J., *Spectrochim. Acta, Part A*, **1979**, *35*, 425.
251. Grote, J.; Friedrich, F.; Berthold, K.; Hericks, L.; Neumann, B.; Stammler, H.-G.; Mitzel, N. W., *Chem. Eur. J.*, **2018**, *24*, 2626.
252. Moers, F. G.; Thewissen, D. H. M. W.; Steggerda, J. J., *J. Inorg. Nucl. Chem.*, **1977**, *39*, 1321.
253. Dakternieks, D.; Hoskins, B. F.; Tiekink, E. R. T., *Aust. J. Chem.*, **1984**, *37*, 197.
254. Back, O.; Henry-Ellinger, M.; Martin, C. D.; Martin, D.; Bertrand, G., *Angew. Chem. Int. Ed.*, **2013**, *52*, 2939.
255. Bispinghoff, M.; Grützmacher, H., *Chimia*, **2016**, *70*, 279.
256. Bedford, R. B.; Hill, A. F.; Jones, C.; White, A. J. P.; Williams, D. J.; Wilton-Ely, J. D. E. T., *Chem. Commun.*, **1997**, 179.
257. Davies, R.; Patel, L., Chalcogen–Phosphorus (and Heavier Congener) Compounds. In *Handbook of Chalcogen Chemistry: New Perspectives in Sulfur, Selenium and Tellurium (2)*, The Royal Society of Chemistry: Cambridge, United Kingdom, 2013; Vol. 1, pp 238.
258. Jesberger, M.; Davis, T. P.; Barner, L., *Synthesis*, **2003**, *2003*, 1929.
259. Woollins, J. D., *Synlett*, **2012**, *2012*, 1154.
260. Walther, B., *Coord. Chem. Rev.*, **1984**, *60*, 67.
261. Malisch, W.; Alsmann, R., *Angew. Chem. Int. Ed.*, **1976**, *15*, 769.
262. Malisch, W.; Hindahl, K.; Grün, K.; Adam, W.; Prechtl, F.; Sheldrick, W. S., *J. Organomet. Chem.*, **1996**, *509*, 209.
263. Bohle, D. S.; Rickard, C. E. F.; Roper, W. R., *Angew. Chem. Int. Ed.*, **1988**, *27*, 302.
264. Bohle, D. S.; Rickard, C. E. F.; Roper, W. R.; Schwerdtfeger, P., *Organometallics*, **1990**, *9*, 2068.
265. Sues, P. E.; Forbes, M. W.; Lough, A. J.; Morris, R. H., *Dalton Trans.*, **2014**, *43*, 4137.
266. Malisch, W.; Jörg, K.; Hofmockel, U.; Scmeusser, M.; Schemm, R.; Sheldrick, W. S., *Phosphorus Sulfur*, **1987**, *30*, 205.
267. Malisch, W.; Märkl, M.; Amann, S.; Hirth, U.; Schmeußer, M., *Phosphorus, Sulfur, Silicon Relat. Elem.*, **1990**, *49-50*, 441.
268. Ebsworth, E. A. V.; Gould, R. O.; McManus, N. T.; Rankin, D. W. H.; Walkinshaw, M. D.; Whitelock, J. D., *J. Organomet. Chem.*, **1983**, *249*, 227.
269. Ebsworth, E. A. V.; Gould, R. O.; Mayo, R. A.; Walkinshaw, M., *J. Chem. Soc., Dalton Trans.*, **1987**, 2831.
270. Frank, L.-R.; Evertz, K.; Zsolnai, L.; Huttner, G., *J. Organomet. Chem.*, **1987**, *335*, 179.
271. Weber, L.; Misiak, H.; Stammler, H. G.; Neumann, B., *Chem. Ber.*, **1995**, *128*, 441.
272. Malisch, W.; Grün, K.; Hirth, U.-A.; Noltemeyer, M., *J. Organomet. Chem.*, **1996**, *513*, 31.
273. Weng, Z.; Leong, W. K.; Vittal, J. J.; Goh, L. Y., *Organometallics*, **2003**, *22*, 1645.

274. Barbaro, P.; Di Vaira, M.; Peruzzini, M.; Seniori Costantini, S.; Stoppioni, P., *Chem. Eur. J.*, **2007**, *13*, 6682.
275. Graham, T. W.; Udachin, K. A.; Zgierski, M. Z.; Carty, A. J., *Can. J. Chem.*, **2007**, *85*, 885.
276. Vaira, M. D.; Peruzzini, M.; Costantini, S. S.; Stoppioni, P., *J. Organomet. Chem.*, **2008**, *693*, 3011.
277. Wong, R. C. S.; Ooi, M. L., *Inorg. Chim. Acta*, **2011**, *366*, 350.
278. Alvarez, B.; Alvarez, M. A.; Amor, I.; García, M. E.; García-Vivó, D.; Suárez, J.; Ruiz, M. A., *Inorg. Chem.*, **2012**, *51*, 7810.
279. Alvarez, B.; Alvarez, M. A.; Amor, I.; García, M. E.; García-Vivó, D.; Suárez, J.; Ruiz, M. A., *Eur. J. Inorg. Chem.*, **2014**, *2014*, 1706.
280. Maciel, G. E.; James, R. V., *Inorg. Chem.*, **1964**, *3*, 1650.
281. Liu, C. W.; Chen, J.-M.; Santra, B. K.; Wen, S.-Y.; Liaw, B.-J.; Wang, J.-C., *Inorg. Chem.*, **2006**, *45*, 8820.
282. Du Mont, W.-W.; Hensel, R.; Kubiniok, S.; Lange, L., Organic compounds containing bonds between Se or Te with P, As, Sb and Bi. In *Organic Selenium and Tellurium Compounds*, Patai, S., Ed. John Wiley & Sons Ltd: Avon, United Kingdom, 1987; Vol. 2.
283. McDonough, J. E.; Mendiratta, A.; Curley, J. J.; Fortman, G. C.; Fantasia, S.; Cummins, C. C.; Rybak-Akimova, E. V.; Nolan, S. P.; Hoff, C. D., *Inorg. Chem.*, **2008**, *47*, 2133.
284. Caraballo, R.; Rahm, M.; Vongvilai, P.; Brinck, T.; Ramström, O., *Chem. Commun.*, **2008**, 6603.
285. Chiou, L.-S.; Fang, C.-S.; Sarkar, B.; Liu, L.-K.; Leong, M. K.; Liu, C. W., *Organometallics*, **2009**, *28*, 4958.
286. Lambert, J. B.; Shurvell, H. F.; Lightner, D. A.; Cooks, R. G., *Organic Structural Spectroscopy*. Prentice-Hall, Inc.: New Jersey, 1998.
287. Maslennikov, S. V.; Glueck, D. S.; Yap, G. P. A.; Rheingold, A. L., *Organometallics*, **1996**, *15*, 2483.
288. Liniger, M.; Gschwend, B.; Neuburger, M.; Schaffner, S.; Pfaltz, A., *Organometallics*, **2010**, *29*, 5953.
289. Nesterov, V.; Schwieger, S.; Schnakenburg, G.; Grimme, S.; Streubel, R., *Organometallics*, **2012**, *31*, 3457.
290. Allefeld, N.; Kurscheid, B.; Neumann, B.; Stammler, H.-G.; Ignat'ev, N.; Hoge, B., *Chem. Eur. J.*, **2015**, *21*, 13666.
291. Hu, C.-Y.; Chen, Y.-Q.; Lin, G.-Y.; Huang, M.-K.; Chang, Y.-C.; Hong, F.-E., *Eur. J. Inorg. Chem.*, **2016**, *2016*, 3131.
292. Kim, S.; Mimikakis, J. L.; Roundhill, D. M., *Phosphorus, Sulfur, Silicon Relat. Elem.*, **1992**, *68*, 119.
293. Kim, S.; Roundhill, D. M., *Phosphorus, Sulfur, Silicon Relat. Elem.*, **1992**, *70*, 3.
294. Golubev, N. S.; Asfin, R. E.; Smirnov, S. N.; Tolstoi, P. M., *Russ. J. Gen. Chem.*, **2006**, *76*, 915.
295. Trofimenko, S., *J. Am. Chem. Soc.*, **1967**, *89*, 3170.
296. Al-Sa'Ady, A. K.; McAuliffe, C. A.; Parish, R. V.; Sandbank, J. A.; Potts, R. A.; Schneider, W. F., *Inorg. Synth.*, **1985**, 191.
297. Forschner, T. C.; Cutler, A. R.; Goodson, P. A.; Casey, C. P.; Beck, W.; Sünkel, K. H., *Inorg. Synth.*, **1989**, 231.
298. Ramachandran, P. V.; Kulkarni, A. S., *Inorg. Chem.*, **2015**, *54*, 5618.
299. Saltzman, H.; Sharefkin, J. G., *Org. Synth.*, **1963**, *43*, 60.

300. Betteridge, P. W.; Carruthers, J. R.; Cooper, R. I.; Prout, K.; Watkin, D. J., *J. Appl. Crystallogr.*, **2003**, *36*, 1487.
301. Dolomanov, O. V.; Bourhis, L. J.; Gildea, R. J.; Howard, J. A. K.; Puschmann, H., *J. Appl. Crystallogr.*, **2009**, *42*, 339.

APPENDIX A
Calculation of Thermodynamic and Kinetic Parameters for [Ru(CO)(PPh$_3$)(PHCy)(Tp)]

Appendix A: Calculation of Thermodynamic and Kinetic Parameters for [Ru(CO)(PPh$_3$)(PHCy)(Tp)]

A.1 Rotation Barrier About the Ru–PHCy Bond

The Gibbs energy of activation barrier ($\Delta G^{\ddagger}$) for a dynamic process at the coalescence temperature (T_c) can be *estimated* in units of kJ mol^{-1} from the equation:[1]

$$\Delta G^{\ddagger} = 1.914 \times 10^{-2} \times T_c \times \left[9.972 \times \log\left(\frac{T_c}{\Delta\nu}\right)\right]$$

Where Δν is the difference (in Hz) between the NMR signals for the two exchanging sites.

For rotation about the Ru–PHCy bond in [Ru(CO)(PPh$_3$)(PHCy)(Tp)], coalescence was observed at 248(5) K and the difference between the two sites was 710.5 Hz. The error in the final value was calculated by obtaining difference between $\Delta G^{\ddagger}$, and the corresponding value when the maximum and minimum T_c values (*i.e.* 253 K and 243 K) are used. This process returned the final value of $\Delta G^{\ddagger}$ = 45.2(9) kJ mol^{-1}.

A.2 Difference in Thermodynamic Parameters Between the Two Diastereomers

The equilibrium constant, K_{eq}, at each temperature can be calculated from the ratio between the integrals of the the $^{31}P\{^1H\}$ NMR signals for the two isomers. For this process the signals for the PHCy groups at δ_P −19.8 and −34.2 were used. The linear form of the van't Hoff equation relates the natural logarithm of the equilibrium constant to the inverse of the temperature:

$$\ln K_{eq} = -\frac{\Delta H}{R} \cdot \frac{1}{T} + \frac{\Delta S}{R}$$

Thus, by plotting ln K_{eq} against $\frac{1}{T}$, the enthalphy and entropy difference between the two equilibriating species can be calculated from the slope and the intercept of the graph, respectively, using the universal gas constant, R. The data are contained in Table A.1 and the van't Hoff plot is shown in Figure A.1. After applying a linear least-squares regression to these

data the equation of the line-of-best-fit was calculated to be y = 387.95x – 0.4885. The error in the slope and intercept were also calculated by the least-squares method to be 18.16 and 0.0608, respectively. Therefore, the experimental values for the difference between the two diastereomers are:

$$|\Delta H| = 3.23(15) \text{ kJ mol}^{-1}$$

$$|\Delta S| = 4.06(51) \text{ J mol}^{-1}$$

Table A.1. Integration Data Obtained from Variable Temperature NMR Experiments on [Ru(CO)(PPh₃)(PHCy)(Tp)]

T (K)	1/T ($\times 10^{-3}$ K^{-1})	Integral δ_P −19.8	Integral δ_P −34.2	K_{eq}	ln K_{eq}
238	4.202	10089	3059	3.298	1.1934
248	4.032	9087	3167	2.869	1.0541
258	3.876	8356	3048	2.741	1.0085
268	3.731	8785	3485	2.521	0.9246
278	3.597	8988	3923	2.291	0.8290
288	3.472	8019	3338	2.402	0.8764
298	3.356	115647	49500	2.336	0.8486
308	3.247	110562	50329	2.197	0.7870
318	3.145	108532	50377	2.154	0.7675
328	3.049	103501	50957	2.031	0.7086
338	2.959	99956	51421	1.944	0.6647
348	2.874	95473	52009	1.836	0.6074
358	2.793	92954	51519	1.804	0.5902
368	2.717	83302	47943	1.738	0.5525
373	2.681	82995	47779	1.737	0.5522

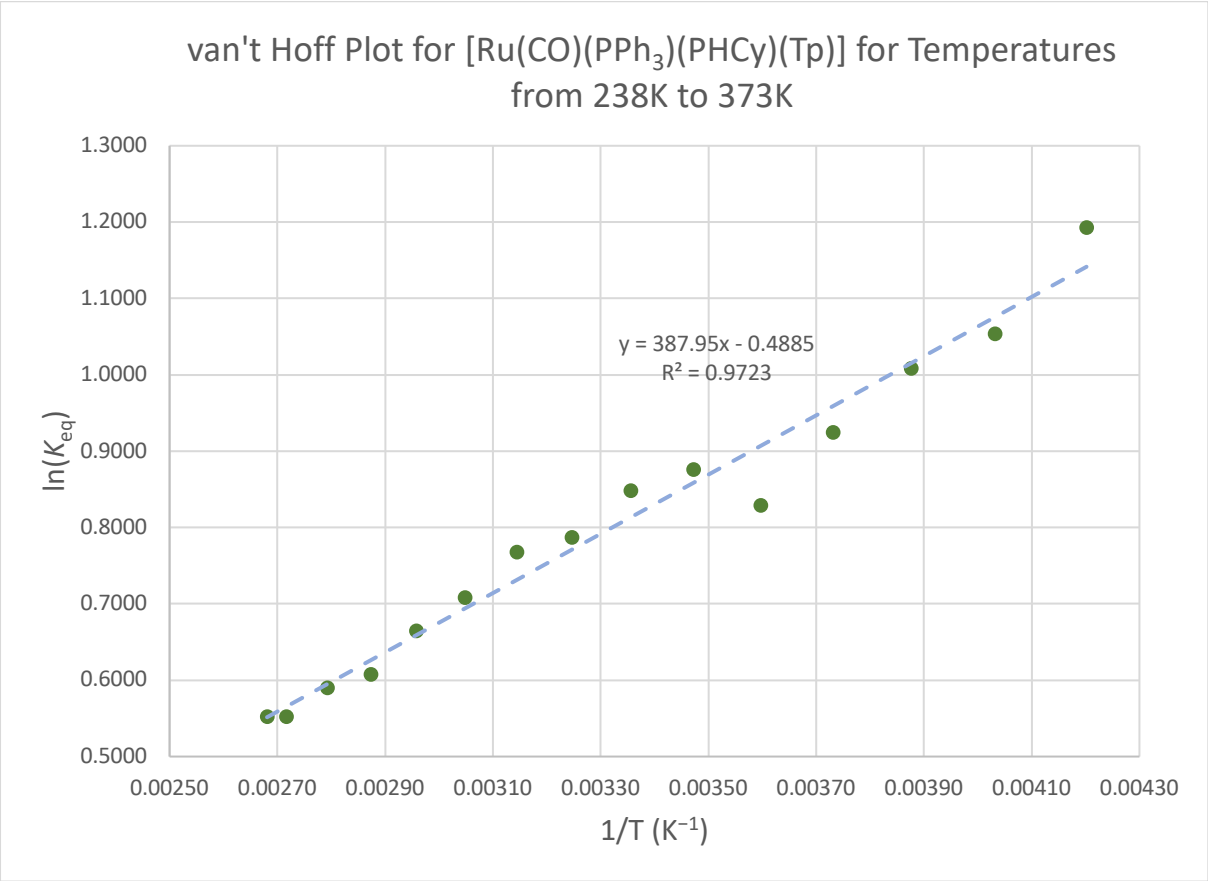

Figure A.1. van't Hoff Plot for [Ru(CO)(PPh$_3$)(PHCy)(Tp)]

A.3 Calculation of Parameters Associated with Phosphorus Inversion

A.3.1 The 2D Exchange Spectroscopy (EXSY) Experiment

A 2D Exchange Spectroscopy[2-3] (EXSY) experiment was conducted to determine the value of the phosphorus inversion barrier in [Ru(CO)(PPh$_3$)(PHCy)(Tp)]. The EXSY experiment monitors the transfer of magnetisation from one state to the other *via* the appearance of cross peaks. To obtain kinetic data from an EXSY experiment, two spectra are acquired. These spectra utilise identical pulse sequences and only differ in the 'mixing time', which is the period during which magnetisation transfer takes place. One experiment is conducted with an effective mixing time of zero so that no change occurs in the system (and therefore no cross peaks appear). The second experiment is conducted with a user-defined mixing time. The choice of mixing time is important, as a short mixing time does not allow sufficient magnetisation transfer to occur while a long mixing time begins to allow processes other than the target kinetic process (*e.g.* spin-lattice relaxation) to affect the measurements. By comparing the

proportion of the four peaks (*i.e.* the integrals) with those from the zero mixing time experiment the rate constants for the forward (k_1) and reverse (k_{-1}) reactions are obtained through linear algebra. The *overall* rate constant (k) is the sum of k_1 and k_{-1}. The EXSY experiment can be conducted at different temperatures to obtain a range of values for k, from which an average value can be calculated.

A.3.2 Calculation of $\Delta G^{\ddagger}$

For this experiment a mixing time of 0.2 s was chosen, and the measurements were taken at temperatures of 338, 343 and 348 K. The rate constants were obtained by processing the integration data with the software program *EXSYCalc*[4] and the results are summarised in Table A.2. The Gibbs energy of activation barrier, $\Delta G^{\ddagger}$, was then be calculated based on the Eyring equation:

$$\Delta G^{\ddagger} = RT\left[\ln\left(\frac{k_b T}{h}\right) - \ln(k)\right]$$

Where R is the universal gas constant, k_b is the Boltzmann constant, h is Planck's constant, k is the rate constant and T is the temperature at which the experiment was conducted.

*Table A.2. Rate constants (*k*) and Gibbs energy activation barriers ($\Delta G^{\ddagger}$) obtained from EXSY experiments*

Temperature (K)	k (s^{-1})	$\Delta G^{\ddagger}$ (kJ mol^{-1})
338	1.54	84.4
343	1.02	84.3
348	0.363	86.0

From these data an average value of $\Delta G^{\ddagger}$ = 84.9 kJ mol^{-1} was obtained with a standard deviation of 0.9 kJ mol^{-1}.

A.3.3 Eyring Plot

The values for $\Delta H^{\ddagger}$ and $\Delta S^{\ddagger}$ can be obtained from the Eyring plot (Figure A.2), which is obtained by plotting $\ln\left(\frac{k}{T}\right)$ against $\frac{1}{T}$. The equation of the line then matches the form:

$$\ln\frac{k}{T} = \frac{-\Delta H^{\ddagger}}{R}\frac{1}{T} + \ln\frac{k_b}{h} + \frac{\Delta S^{\ddagger}}{R}$$

Where k is the rate constant, T is the temperature, $\Delta H^{\ddagger}$ is the enthalpy of activation, R is the universal gas constant, k_b is the Boltzmann constant, h is Planck's constant and $\Delta S^{\ddagger}$ is the entropy of activation.

The following equations may then be used to calculate $\Delta H^{\ddagger}$ and $\Delta S^{\ddagger}$:

$$slope = \frac{-\Delta H^{\ddagger}}{R}$$

$$intercept = \ln\frac{k_b}{h} + \frac{\Delta S^{\ddagger}}{R}$$

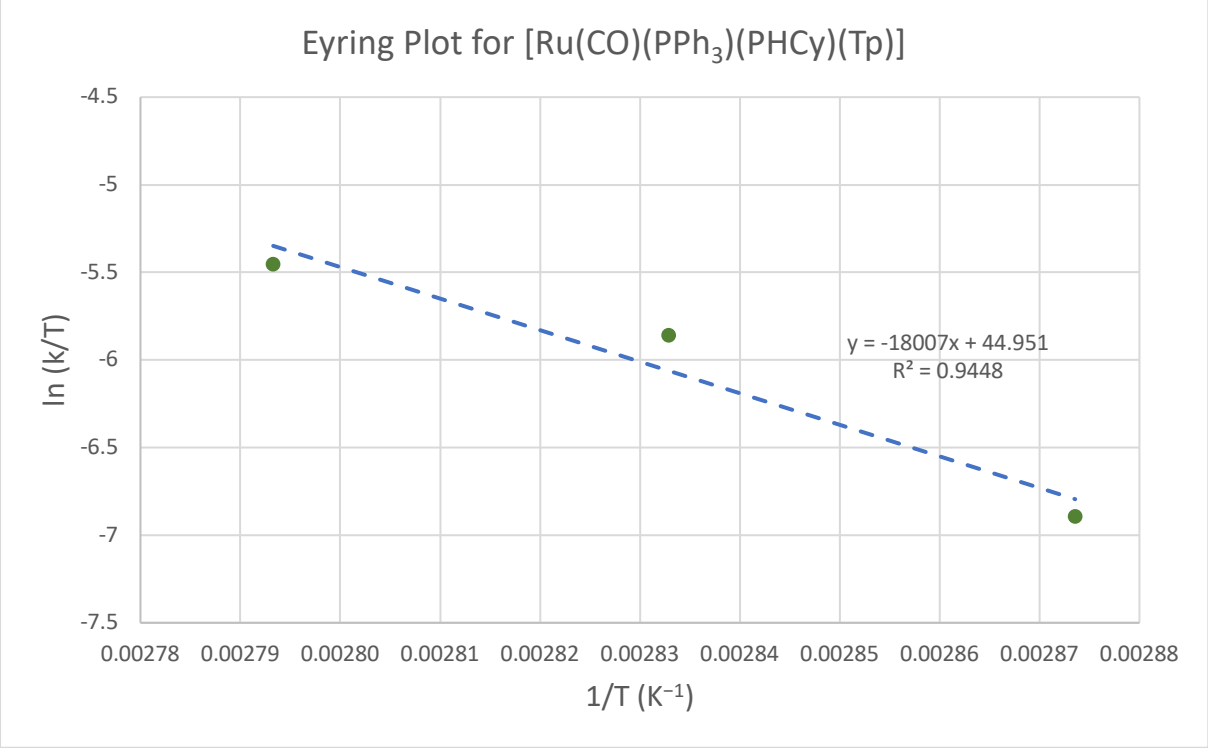

Figure A.2. Eyring plot for [Ru(CO)(PPh₃)(PHCy)(Tp)]

The line-of-best-fit had a slope of −18007(4400) and an intercept of 44(12). From these, the following values were calculated:

$$\Delta H^{\ddagger} = 149(36) \text{ kJ mol}^{-1}$$

$$\Delta S^{\ddagger} = 176(28) \text{ J mol}^{-1}$$

A.3.4 Arrhenius Plot

The Arrhenius plot (Figure A.3) is obtained by plotting ln *k* against $\frac{1}{T}$, and the equation of the line matches the form:

$$\ln k = -\frac{E_a}{R}\left(\frac{1}{T}\right) + \ln A$$

Where *k* is the rate constant, E_a is the activation energy, *R* is the universal gas constant, *T* is the temperature and *A* is the Arrhenius pre-exponential factor.

The following equations may then be used to calculate E_a and *A*:

$$slope = -\frac{E_a}{R}$$

$$intercept = \ln A$$

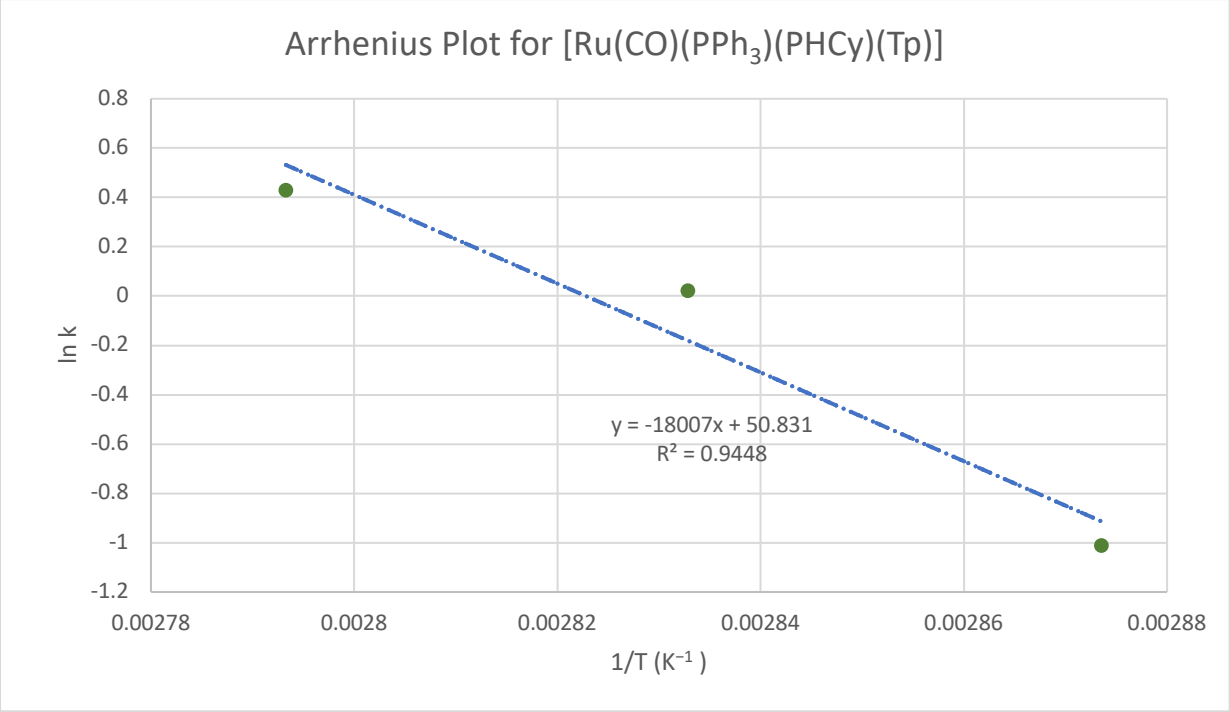

Figure A.3. Arrhenius plot for [Ru(CO)(PPh₃)(PHCy)(Tp)]

The line-of-best-fit had a slope of −18000(4300) and an intercept of 50(12). From these the following values were calculated:

$$E_a = 149(36) \text{ kJ mol}$$

$$A = 1.19 \times 10^{22}$$

n.b. the value for *A* has an associated error of 1.4×10^{23}, an order of magnitude larger than the value for *A*. The large value arises from a high fractional error in the intercept (*ca*. 20%) and the exponential function used to obtain *A*. It would be nonsensical to quote a value with such a high e.s.d., but it is provided here for transparency.

A.4 References

1. Sandstrom, J., *Dynamic NMR Spectroscopy*. Academic Press: London ; New York, 1982.
2. Jeener, J.; Meier, B. H.; Bachmann, P.; Ernst, R. R., *J. Chem. Phys.*, **1979**, *71*, 4546.
3. Perrin, C. L.; Dwyer, T. J., *Chem. Rev.*, **1990**, *90*, 935.
4. Cobas, J. C.; Martin-Pastor, M. *EXSYCalc*, 1.0; Mestrelab Research: 2007.